

DYES AND PIGMENTS

New Research

Arnold R. Lang
Editor

NOVA

A microscopic image showing a textured surface with various colors. The top half is predominantly blue with some yellow and red speckles. The bottom half is mostly yellow with some red and blue speckles. The texture appears fibrous or crystalline.

DYES AND PIGMENTS: NEW RESEARCH

No part of this digital document may be reproduced, stored in a retrieval system or transmitted in any form or by any means. The publisher has taken reasonable care in the preparation of this digital document, but makes no expressed or implied warranty of any kind and assumes no responsibility for any errors or omissions. No liability is assumed for incidental or consequential damages in connection with or arising out of information contained herein. This digital document is sold with the clear understanding that the publisher is not engaged in rendering legal, medical or any other professional services.

**DYES AND PIGMENTS:
NEW RESEARCH**

ARNOLD R. LANG
EDITOR

Nova Science Publishers, Inc.
New York

Copyright © 2009 by Nova Science Publishers, Inc.

All rights reserved. No part of this book may be reproduced, stored in a retrieval system or transmitted in any form or by any means: electronic, electrostatic, magnetic, tape, mechanical photocopying, recording or otherwise without the written permission of the Publisher.

For permission to use material from this book please contact us:

Telephone 631-231-7269; Fax 631-231-8175

Web Site: <http://www.novapublishers.com>

NOTICE TO THE READER

The Publisher has taken reasonable care in the preparation of this book, but makes no expressed or implied warranty of any kind and assumes no responsibility for any errors or omissions. No liability is assumed for incidental or consequential damages in connection with or arising out of information contained in this book. The Publisher shall not be liable for any special, consequential, or exemplary damages resulting, in whole or in part, from the readers' use of, or reliance upon, this material. Any parts of this book based on government reports are so indicated and copyright is claimed for those parts to the extent applicable to compilations of such works.

Independent verification should be sought for any data, advice or recommendations contained in this book. In addition, no responsibility is assumed by the publisher for any injury and/or damage to persons or property arising from any methods, products, instructions, ideas or otherwise contained in this publication.

This publication is designed to provide accurate and authoritative information with regard to the subject matter covered herein. It is sold with the clear understanding that the Publisher is not engaged in rendering legal or any other professional services. If legal or any other expert assistance is required, the services of a competent person should be sought. FROM A DECLARATION OF PARTICIPANTS JOINTLY ADOPTED BY A COMMITTEE OF THE AMERICAN BAR ASSOCIATION AND A COMMITTEE OF PUBLISHERS.

LIBRARY OF CONGRESS CATALOGING-IN-PUBLICATION DATA

Dyes & pigments : new research / [edited by] Arnold R. Lang.

p. cm.

ISBN 978-1-60876-195-1 (E-Book)

1. Dyes and dyeing. 2. Pigments. I. Lang, Arnold R. II. Title: Dyes and pigments.

TP910.D96 2008

667'.2--dc22

2008031082

Published by Nova Science Publishers, Inc. ✦ New York

CONTENTS

Preface		vii
Chapter 1	Photodynamic Therapy <i>Petr Zimcik and Miroslav Miletin</i>	1
Chapter 2	Phthalocyanine to Use Photosensitizer for Photodynamic Therapy of Cancer <i>Keiichi Skamoto and Eiko Ohno-Okumura</i>	63
Chapter 3	Dyes, Pigments and Supercritical Fluids: Selection of Emerging Applications <i>M. D. Gordillo, C. Pereyra and E. J. Martínez de la Ossa</i>	97
Chapter 4	Photo-Controlled Molecular Switches Based on Photochromic Spirooxazine Dyes <i>Sung-Hoon Kim and Sheng Wang</i>	111
Chapter 5	Combined Sonohomogeneous and Heterogeneous Oxidation of Dyes for Wastewater Treatment <i>Ewere Odaro and Shaobin Wang</i>	143
Chapter 6	Decoloration of Textile Wastewaters <i>Julija Volmajer Valh and Alenka Majcen Le Marechal</i>	175
Chapter 7	Non-conventional Sorbents for the Dye Removal from Waters: Mechanisms and Selected Applications <i>Pavel Janoš</i>	201
Chapter 8	Irradiation Treatment of Azo Dyes in Aqueous Solution <i>László Wojnárovits and Erzsébet Takács</i>	225
Chapter 9	Application of Advanced Oxidation Processes (AOP) to Dye Degradation - An Overview <i>M. A. Rauf and S. Salman Ashraf</i>	259
Chapter 10	First Steps to a Deductive Classification System of Colorants from the Point of View of Structural Chemistry <i>G. Lincke</i>	291

Chapter 11	Removal of Dyes from Solution on Clay Surfaces - An Overview <i>M. A. Rauf</i>	309
Chapter 12	The Beauty of Colors: The Yellow Flavonols in Science and Art <i>Aldo Romani</i>	331
Chapter 13	Inorganic Pigments to Colour Ceramic Materials: State of the Art and Future Trends <i>Federica Bondioli</i>	351
Chapter 14	Synthesis and Characterization of Several Series of Substituted Metallophthalocyanines <i>Fangdi Cong, Xiguang Du, Jianxin Li, Dongliang Tian and Wenjuan Duan</i>	369
Chapter 15	Dyes and Pigments with Ecologically More Tolerant Application <i>T. N. Konstantinova and P. P. Miladinova</i>	383
Chapter 16	Enhanced Anthraquinone Dye Production in Plant Cell Cultures of Rubiaceae Species: Emerging Role of Signaling Pathways <i>Norbert Orbán, Imre Boldizsár and Károly Bóka</i>	403
Short Commentary		421
	The Use of Solid Media for Bacterial Growth in Degradation of Dyes <i>Carlos Costa, Blanca E. Barragán and M. Carmen Márquez</i>	421
Index		433

PREFACE

Chapter 1 - Photodynamic therapy (PDT) is a cancer treatment based on activation of a drug by light. The drug, called photosensitizer, absorbs the energy of light of the proper wavelength and transfers it to surrounding molecules, mainly oxygen, forming reactive oxygen forms like radicals and singlet oxygen. These highly reactive species are responsible for destruction of targeted cells. Besides the direct effect on the cells, vascular shutdown develops as well and immune response is activated, both being important for long-term control over the tumor. Most of the photosensitizers are recruited from the group of porphyrins and related compounds like chlorins, bacteriochlorins, porphycenes, texaphyrins, and phthalocyanines. However, other dyes also entered the trials for photodynamic evaluation, e.g. some tricyclic dyes or hypericine. We discuss in this chapter, the history, photophysical and photochemical principles of PDT, as well as the biological effects of the photosensitizers. The main structural groups of photosensitizers are discussed and the most important drugs, either approved or in trials are described. Also, other approaches closely connected with PDT (catalytic therapy, sonodynamic therapy, photothermal therapy, and photochemical internalisation) are mentioned in this chapter.

Chapter 2 - Phthalocyanine analogues containing alkyl-substituted benzenoid rings and pyridine rings are interesting compounds, because quaternation of the pyridine nitrogen is expected to form cationic amphiphilic compounds.

Non peripheral long alkyl substituted zinc phthalocyanine derivatives, zinc bis(1,4-didecylbenzo)-bis(3,4-pyrido)porphyrzine and zinc bis(1,4-didecylbenzo)-bis(2,3-pyrido)porphyrzine were reacted with dimethyl sulfate and monochloroacetic acid to give their quaternary products. Also the zinc phthalocyanine derivatives reacted with diethyl sulfate to afford the sufo-substituted products. All reacted compounds showed amphiphilic character.

Regio isomers of zinc bis(1,4-didecylbenzo)-bis(3,4-pyrido)porphyrzine were also quaternized with dimethyl sulfate.

Identical peaks in cyclic voltammograms appeared for these products before and after quaternization.

Zinc bis(1,4-didecylbenzo)-bis(2,3-pyrido)porphyrzine was evaluated the the photodynamic therapy of cancer efficacy by cancer cell culture.

The light exposed dimethyl sulfate quaternized zinc bis(1,4-didecylbenzo)-bis(2,3-pyrido) porphyrzines in IU-002 cells produces cell disruption that can be detected as a decrease as fluorescence.

Chapter 3 - The textile industry uses large amounts of water in its dyeing processes. Due to environmental problems the supercritical dyeing process has been developed. In this process supercritical carbon dioxide is used as the solvent for dyes.

On the other hand, pigments, used in the formulation of paints, inks, toners and photographic emulsions can be micronized by supercritical antisolvent process. Their production in form of micrometric particles with controlled particle size distribution can largely improve their characteristics.

For these reason, in the last years, supercritical fluids more and more have been proved as environmentally benign media for dyeing processes and as antisolvent to control the formation of micrometric particles.

The physico-chemical properties of supercritical fluids are halfway between those of gases and liquids; more these properties can be easily modified by a simple variation of pressure or/and temperature. Therefore, supercritical fluids can be used to develop solventless or solvent reduced processes and their mass transfer properties are useful to produce micronized particles with controlled size and distribution.

In this field, the publications appeared over the past years could be reviewed under two groupings, one involving the measurements of solubilities of dyes in supercritical carbon dioxide, with and without co-solvent, and supercritical CO₂ dyeing of fibre, and the other involving the micronization of dyes with narrow particle size distribution using a supercritical antisolvent process. In the following, a lot of recent papers will be cited, which should give an overview of actual results on solubility and precipitation of dyes in supercritical carbon dioxide.

Chapter 4 - Photochromism refers to a reversible phototransformation of a chemical species between two forms having different absorption spectra. Photochromic compounds reversibly change not only the absorption spectra but also their geometrical and electronic structures. The molecular structure changes induce physical property changes of the molecules, such as fluorescence, refractive index, polarizability, electrical conductivity, and magnetism. When such photochromophores are incorporated into functional molecules, such as polymers, host molecules, conductive molecules, liquid crystals, the properties can be switched by photo irradiation. Among of all kinds of photochromic compounds, the spirooxazine dyes (SPO) are well-known photochromic compounds that show their high fatigue resistance and excellent photostability, which is one of the most promising candidates for applications in molecular electronics such as optical memory, molecular switching devices. In this review, we describe the recent development of spirooxazine dye as photo-controlled molecular switches in molecular materials, especially photochromism of spirooxazine in single crystal phase, spirooxazine dye polymer materials as fluorescence molecular switches, electrical conductivity switches, and viscosity switches, liquid crystal switches, gel switches and so on. In addition, layer by layer self-assemble spirooxazine dye in supermolecular chemistry as a photoswitching unit is described. We mainly present specific examples from our own research, which highlight our research group's contribution.

Chapter 5 - Dyestuff in water introduces several environmental problems and should be removed for clean water system. Fenton oxidation can be as an effective technique for the water treatment. In this report, homogeneous and heterogeneous catalysis in Fenton oxidation was examined for two dyes with acidic (Naphthol blue-black, NBB) and basic (Methylene Blue, MB) properties. The behaviour of these dyes under different experimental conditions (temperature, pH, peroxide concentration, Fe concentration) was studied using Fenton (Fe²⁺)

and Fenton-like (Fe^{3+}) reactions for the following processes: 1) normal Fenton oxidation, 2) Fenton oxidation combined with sonication effect, 3) Fenton oxidation combined with a solid catalyst (activated carbon). The main Fenton oxidation reactants, Fe^{2+} , Fe^{3+} and H_2O_2 were used in small quantities in order to observe closely the reaction kinetics for decolourisation of these dyes. It was found that both sonication and heterogeneous catalysis offer improvements to the Fenton oxidation under optimised conditions, with Fe^{2+} being faster than Fe^{3+} initially but Fe^{3+} ending up with a higher overall efficiency. 90-95% decolourisation was achieved in some optimised runs after 2 hours; however the general decolourisation was completed for all batch runs after a period of 24 hours, except in conditions where the reaction did not proceed at all. Chemical oxygen demand (COD) removal also occurred during the decolourisation process of both dyes, in maximum efficiencies of about 80% after 48 hours. Methylene blue also showed greater decolourisation efficiency in comparison with Naphthol blue-black for most of the experimental runs under the same experimental conditions. The reaction kinetics was mainly pseudo-first order for majority of the homogeneous reaction, as determined by non-linear regression or a combination of first order kinetics for heterogeneous reactions.

Chapter 6 - Water is an important natural resource for sustainable ecosystems, human life and economical development. The control of water pollution has become of increasing importance in recent years. Dyes make the world more beautiful through colored products, but cause a lot of problems in the environment. For decoloration and degradation of textile wastewater many applicable methods have been developed, but because of the composition complexity of the textile wastewater the use of universal procedures seems to be impossible. So, there is a need to find an efficient and cost-effective wastewater treatment for the decoloration of textile wastewaters. In this chapter a survey of the most widely used and, according to many researches, the most promising textile wastewater decoloration methods are presented.

Chapter 7 - Synthetic dyes that are extensively used in various industrial branches represent a serious environmental problem when they are emitted into the effluents as they are hardly biodegradable in conventional wastewater treatment plants. Therefore, alternative methods for decolouration of the wastewaters are developed, among them adsorption on solid sorbents is one of the most effective ones. Because the conventional sorbents such as activated carbon are rather expensive for large-scale applications, various low-cost materials have been tested as alternative non-conventional sorbents for the dye removal from waters. Numerous natural materials (zeolites, clays), industrial wastes (fly ash, iron slag), agrowastes or biosorbents exhibit a sufficient ability to retain various kinds of dyes from aqueous solutions and are available (locally and sometimes also globally) in great quantities and at low prices, and thus they can be used potentially for the treatment of the dye-containing effluents. A brief review of the non-conventional sorbents for the dye removal is given in this article together with selected applications. It should be emphasized that the dye sorption onto non-conventional sorbents is a rather complex process in which several mechanisms may be effective simultaneously. Effects of principal operational parameters on the dye sorption are discussed in the article, such as an effect of pH (governing both the dissociation/protonation of the active groups on the sorbent surface as well as side equilibria in solution), the presence of inorganic salts or surfactants. Basic equations describing the sorption equilibria (sorption isotherms) are presented. The results of kinetic measurements that allowed (in some cases) to identify a rate-limiting step of the overall sorption process are also mentioned in this chapter.

Chapter 8 - Laboratory investigations, pilot-plant experiments and an industrially established technology illustrated that electron beam (EB) treatment can efficiently destroy textile dyes in aqueous solutions. This treatment belongs to the class of Advanced Oxidation Processes (AOP): here also, as in most of AOP principally $\bullet\text{OH}$ radicals induce the chemical transformations. The final result of the treatment depends on the absorbed radiation energy (dose); with sufficient dose mineralization can be achieved. Major benefits of EB treatment with respect to the conventional methods are: no usage of chemical additives, room temperature operation, penetration in the bulk of water even in case of turbidity, production of high concentrations of oxidizing radicals in a fraction of a second and simultaneous disinfection.

The book chapter summarizes the radiation sources and the experimental techniques used for studying the reactions of dyes in irradiated systems (e.g. pulse radiolysis, gamma radiolysis, UV-VIS spectroscopy), describes the decomposition of water under the effect of ionizing radiation, characterizes the reactive intermediates formed (hydroxyl radical, hydrogen atom, hydrated electron), and discusses their reactions with dye molecules. An essential part of the chapter is the description of the kinetics and mechanism of azo dye decomposition. At the beginning of the treatment the water radicals reacting with the dye cause destruction of the highly conjugated electronic system resulting in decoloration. The decoloration is followed by a step-by-step degradation, destruction of the aromatic rings, ring-opening, fragmentation to smaller molecular mass aldehydes, ketones, carboxylic acids, etc. When oxygen is present compounds with progressively higher oxygen-to-carbon ratio are involved in the conversion of an organic molecule to CO_2 and H_2O . The individual reactions are detailed on the examples of several dye molecules.

Pilot plant experiments on dye containing industrial wastewater have proven that combining conventional treatments with the EB based technology results in a considerable improvement of the treatment efficiency. Considerable reduction of chemical additive consumption, and also reduction in retention time were observed, with an increase in removal efficiencies as indicated by reduction in Total Organic Carbon content, TOC, Chemical Oxygen Demand, COD and Biological Oxygen Demand, BOD. Based on the pilot-plant experiments a full-scale plant for recycling EB-treated textile wastewater went into operation just at the end of 2005 in Daegu, Republic of Korea.

Chapter 9 - Advanced oxidation Processes (AOP's) are novel methods for water treatment and are extremely useful in the case of substances resistant to conventional technologies. Organic dyes are a group of those chemicals of special interest which have drawn considerable attention in many industrial processes. However due to their high toxicity and low biodegradability, various approaches have been forwarded concerning the degradation of these dyes by means of AOP's. In this work, an overview of such work is presented and the following approaches are presented: processes based on hydrogen peroxide ($\text{H}_2\text{O}_2 + \text{UV}$, Fenton, photo-Fenton and Fenton-like processes), photolysis, photocatalysis and processes based on ozone (O_3 , $\text{O}_3 + \text{UV}$ and $\text{O}_3 + \text{catalyst}$). Degradation is reviewed and the different mechanistic degradation pathways are taken into account.

Chapter 10 - Beginning with well known building blocks and putting them together by using noncovalent bonds of the type 1) intermolecular H-bonds and 2) intramolecular $\pi \dots \pi$ -bonds and 3) inorganic metal-complexes, the deductive classification system of colorants is

derived. The building blocks are called 1) 'chromogens' and 2) 'tetrahedral' respectively 'octahedral' metal-complexes.

There are three 'classes' of colorants: 1) 0.4 nm structures, 2) sheets structures, 3) 3-dimensional networks.

The dichotomy soluble-insoluble is due to quality and number of bonds between the building blocks, forming the crystal lattices of colorants. A view on their entirety and characteristics is opened.

This paper makes use of the stack principle of organic molecules of dyestuffs in order to create the deductive classification system of colorants. Important but nevertheless in the second position in the order of rank are solubility/insolubility, stability, counteractions of light with colorants (absorption/reflexion). The author hopes for intriguing queries by colour chemists.

The author is of the opinion that the deductive classification of colorants points to an axiomatic wording. Perhaps therefore colorants become more understandable and interesting for students of chemistry?

Chapter 11 - Organic dyes are a group of those chemicals of special interest which have drawn considerable attention in many industrial processes. However due to their high toxicity and low biodegradability, various approaches such as adsorption, coagulation, sedimentation, membrane-filtration processes (nano-filtration), reverse osmosis, electro dialysis, advanced oxidation processes etc. have been forwarded concerning the removal of these dyes from solution. Adsorption is a well known equilibrium separation process and is an effective method for water decontamination applications. It is well-known that natural materials, waste materials from industry and agriculture and biosorbents can be obtained and employed as inexpensive sorbents. Some of the reported sorbents include commercially activated carbon, clay materials (bentonite, kaolinite), zeolites, siliceous material (silica beads, alunite, perlite) and polymeric materials as low cost adsorbents for dye removal. This overview focuses on using adsorption method to remove dyes from solution and the literature findings of such studies on various types of clays are presented.

Chapter 12 - Dyes extracted from plants have been used for centuries for coloring materials. In this paper, typical behaviors of some naturally occurring colorants belonging to the class of flavonoids are presented. Their structures derive from that of flavone (2-phenylbenzopyrone), which is colorless, whereas hydroxy derivatives absorb UV and blue light, so appearing yellow colored. Current interest in flavonoids is mainly due to their varied biological activity in medicine, but also to their use as colored components in works of art (tapestries, carpets, miniatures).

The color of hydroxy-substituted flavonoids (flavonols) can be markedly modified by changing the pH or bonding with different metal ions, therefore, it critically depends on the acidity and the presence of metals in the environment. The absorption and emission spectra generally shift to the red by increasing the pH, due to stabilization of anionic forms. The number and sequence of acid-base dissociation steps depend on the number and position of the hydroxy-substituents. These aspects will be illustrated here with some significant examples concerning two naturally occurring colorants, old fustic and weld, and their main chemical components (morin, apigenin and luteolin). Absorption and fluorescence spectra recorded in solution provide the base for developing scientific investigations on the colorants spread on paper as watercolors or used in mordant dyeing of textiles.

Chapter 13 - Inorganic natural and synthetic pigments produced and marketed as fine powders are an integral part of many decorative and protective coatings and are used for the mass coloration of many ceramic materials, including glazes, ceramic bodies, and porcelain enamels. In all these applications, pigments are dispersed (they do not dissolve) in the media, forming a heterogeneous mixture. In conclusion, powders used for colouring ceramics must show thermal and chemical stability at high temperature and must be inert to the action of molten glass (frits or sintering aids). These requirements limit ceramic pigments to a very small number of refractory systems which are fully reacted and relatively inert to the matrix in which they are dispersed. This need for great chemical and thermal stability has dominated research and development in recent years. In this chapter the state of the art will be reported focusing in particular on the specific systems used in this industrial field. The advantages and the limitations of different colours will be underlined with particular emphasis on the current problems and on the possible way to solve them.

Chapter 14 - The twenty-four substituted metallophthalocyanines were synthesized, in two steps, from 4-nitrophthalonitrile or 3-nitrophthalonitrile, and characterized by MS, ^1H NMR, UV-vis, IR and element analysis. The results showed that they all were consistent with proposed structures. They behaved excellent solubility in some organic solvents, but the stability of them in solution was not good as in solid state. According to the scopes of red shift, the impact of metals, substituents and substitution positions on Q-bands could be displayed as follow: $\text{Mn} > \text{Zn} \approx \text{Cu} > \text{Ni} \approx \text{Co}$; 2-isopropyl-5-methylphenoxy 4-tert-butylphenoxy quinolin-8-yloxy 2-methoxyethoxy; non-periphery > periphery. The research displayed that the alternative ways to control the Q bands of Pc compounds to have a big change were to alter the chemical value of metal in the center of Pc ring, replace the atom banding directly with Pc ring or its chemical circumstance, and change the substitution position of substituent on Pc ring (periphery or non-periphery).

Chapter 15 - A review of the basic ecological problems related to the application of dyes and pigments for textile, foods and polymers is presented. A modern approach for solving the problems is shown. Along with a review of the synthesis and application of functional dyes and pigments already reported, in this paper we present a synthesis of 20 new bifunctional azo- and anthraquinone dyes-triazine derivatives. Six of them are metallized (Cu, Cr^{III} and Co^{III}) dyes and two of them contain a tetramethylpiperidine (TMP) stabilizer fragment in their molecule. In a color assessment of the new dyes, the percentage of exhaustion and fixation to cotton was found to be with 10-15 % higher compared to those of the model ones.

The photo degradation of 10 fluorescent naphthalimide dyes, synthesized before, was investigated and the structure-stability dependence was determined.

The copolymers of acryl amide and five fluorescent 9-phenylxanthene dyes derivatives, allylic ether-esters were obtained. The percentage of the chemical bound in the polymer dye was found to be 45-80, providing an intensive, stable to wet treatment and solvent's color and fluorescence, thus making the dyes suitable for ecologically tolerant application in food and cosmetics.

The photo stability of the triazine azodyes with a TMP fragment in the molecule was 25-30 % higher than those of the similar bifunctional azodyes without TMP. Their polymers of acrylonitrile were obtained and it was found that they have a good stabilizing effect on the photo degradation of the copolymer thus making these dyes suitable for "one-step" coloration and stabilization of materials with more tolerant ecological behavior.

Chapter 16 - Synthetic and natural analogues of 9,10-anthracenedione are well-known and widely used substances in the food and dye industries. Beyond their dyeing ability some anthraquinones are used as medicines as they exhibit beneficial effects in mammals and humans; moreover, anthracycline antibiotics have been applied therapeutically in the case of several malignant diseases. Total synthesis of anthraquinone derivatives using organic chemical methods is common; however, sophisticated biotechnological techniques provide alternatives for synthesis and overcome some environmental and economical concerns. The most frequently studied plant cell culture systems originate from members of the *Rubiaceae* family because these cell cultures are capable of producing high amounts of anthraquinone derivatives. Several methods to enhance the dye yield in order to obtain the best results have been and are still being used on a small-scale prior to applying them in large-scale industrial production. Numerous factors regulate the biosynthesis of anthraquinones in cell cultures like compartmentation, environmental stimuli (e.g. light, precursors) and endogenous (metabolic and developmental) factors. Since major points of the anthraquinone biosynthesis regulation are known in the *Rubiaceae* family, various possibilities have been raised to exploit these findings. Formation of hairy root and other transgenic cell cultures have proved to be useful tools to increase the anthraquinone production capacity; moreover, newer approaches (DNA and protein microarrays, proteomics) are promising techniques to define biosynthetic pathways to elucidate the unknown and rate limiting steps. Another effective approach to dye production enhancement in plant cell cultures is elicitation: exogenous stimuli induced gene activation. Various elicitors have been introduced during the past two decades affecting anthraquinone yields of measured cell cultures; however, the background of the influence on physiological events caused by elicitors is not fully understood. Elicitors are recognized by plant receptor(s) localized in the plasma membrane or cytoplasm. After elicitor signal perception, plant receptors activate effectors and signal transduction leads to the modulation of genes via second messengers. Altered gene expression might manifest itself in heightened production of anthraquinone derivatives. An increasing knowledge of plant signal transduction enables us to choose a suitable elicitor, which activates/modulates the desired pathways for anthraquinone production leading to a more selective production of the needed compounds. This commentary summarizes results of the latest studies on elicitor induced signal transduction leading to anthraquinone production in plant cell cultures and discusses other relevant techniques on a comparative basis. Furthermore, major problems and a future outlook are also debated.

Short Commentary - Dyes are normally difficult to eliminate from effluents by conventional biological wastewater treatments. There are many references in which it is proven a poor removal by activated sludge or other systems in wastewater treatment plants. Their xenobiotic nature and their low concentration in residual streams (20 – 200 mg/l) make them to be difficult substrates for bacterial growth. Actually it is not clear the role they play in biological systems. Under anaerobic environment, it seems they act as electron acceptors in organic matter biodegradation. Under aerobic environment, it seems that a few number of microorganisms are able to use them as electron donors, in the presence of oxygen. Combined anaerobic-aerobic processes have efficiency on dye removal due to the first step in dye degradation, the breakdown of the azo bond, is assumed to be done under anaerobic conditions.

The use of solid supports for bacteria which utilize azo dyes is an attractive alternative for remove them from residual streams. These supports need to have two characteristics: an

adequate texture for bacterial growth (particle and porous size) and affinity for dye. Under this situation, dye is adsorbed and concentrated on solid surface and bacteria can grow and degrade it on the surface of the solid. The surface of the solid seems to be a good environment for dye degradation, because oxygen concentration can be low inside the porous structure and microaerophilic conditions can be established, therefore cleavage of the azo bond can be performed easily. Several solids can be used on this purpose: activated carbon, bentonite and kaolin, for example. The solid used has to be investigated in terms of texture of the surface, growth of microorganisms and dye degradation.

Chapter 1

PHOTODYNAMIC THERAPY

Petr Zimcik and Miroslav Miletin*

Department of Pharmaceutical Chemistry and Drug Control,
Faculty of Pharmacy in Hradec Kralove, Charles University in Prague,
Heyrovského 1203, 500 05 Hradec Kralove, Czech Republic

ABSTRACT

Photodynamic therapy (PDT) is a cancer treatment based on activation of a drug by light. The drug, called photosensitizer, absorbs the energy of light of the proper wavelength and transfers it to surrounding molecules, mainly oxygen, forming reactive oxygen forms like radicals and singlet oxygen. These highly reactive species are responsible for destruction of targeted cells. Besides the direct effect on the cells, vascular shutdown develops as well and immune response is activated, both being important for long-term control over the tumor. Most of the photosensitizers are recruited from the group of porphyrins and related compounds like chlorins, bacteriochlorins, porphycenes, texaphyrins, and phthalocyanines. However, other dyes also entered the trials for photodynamic evaluation, e.g. some tricyclic dyes or hypericine. We discuss in this chapter, the history, photophysical and photochemical principles of PDT, as well as the biological effects of the photosensitizers. The main structural groups of photosensitizers are discussed and the most important drugs, either approved or in trials are described. Also, other approaches closely connected with PDT (catalytic therapy, sonodynamic therapy, photothermal therapy, and photochemical internalisation) are mentioned in this chapter.

HISTORY OF PDT

The sun's radiation is one of the essential prerequisites for existence of life on Earth, the visible light being the most important part of the sun's radiation spectrum. Photosynthesis, realized by chlorophyll, an essential natural dye built on a tetrapyrrolic porphyrin molecule,

* E-mail: petr.zimcik@faf.cuni.cz, tel.:+420 49 5067257, fax: +420 49 5067167.

employs the visible light to transfer the sun's light energy into the energy of organic bonds thus building basic conditions for the actual terrestrial life existence. However, the porphyrin skeleton is a nature's patent, enabling more than just the transfer of energy for life.

Human beings, since the ancient civilizations including the Egyptian, Indian and Chinese cultures, realized the potential of light for treatment of some skin disorders like vitiligo, psoriasis, and also saw its importance for mental health [1]. The ancient Mediterranean civilizations extended this knowledge: the heliotherapy was introduced by ancient Greeks (Herodotus) for health renovation, and they used the light for treatment of many diseases [2]. However, people always realized both positive effects of the sun's radiation and its damaging potential. It was probably one of the reasons for light skin to be considered a sign of higher society and therefore people protected their skin against radiation [3-5].

There are two basic ways people have used light therapeutically:

Phototherapy, which usually does not require oxygen or any drug, could be defined as an exposure to non-ionizing radiation to treat a disease. It may be realized by an exposure to visible light, UVB or UVA radiation, or their combination [6, 7]. It was widely practiced hundreds of years B.C. in Ayurvedic medicine. Today it is employed in several medical areas, particularly in dermatology and psychiatry for the treatment of internal depressions, sleeping changes, the circadian rhythm, regulation and some other disorders.

Photochemotherapy is a therapeutic technique employing a photosensitizing chemical substance that is subsequently activated by a non-ionizing radiation [6]. Also, this type of treatment we could observe in ancient civilizations where naturally occurring plant ingredients psoralens were used by Egyptians to treat a wide spectrum of skin diseases [8]. Also, in the Indian Ayurvedic medicine system the psoralen/light combination was being used already around 1400 B.C. [9], and it was rediscovered again about 30 years ago [10].

Photodynamic therapy is usually considered as a type of photochemotherapy, which requires oxygen as the third component, along with a photosensitizer and light, necessary to be effective.

In the course of the 19th century, a lot of important work for the future development of PDT was done on exploring the structure, function and properties of the blood-red dye hem, a structural base of future clinically important photosensitizers. Among others, several German scientists [11-13] reported the removal of iron from hem and the resulting changes of such a modified molecule, which was called hematoporphyrin. The onset of fluorescence was also noted, but still not appreciated. An important step in phototherapy development was the treatment of smallpox using red light and of cutaneous tuberculosis with ultraviolet light, reported in 1901 by Danish physician Niels Finsen [14], who was awarded the Nobel Prize in 1903 for this discovery.

The milestone of photodynamic therapy was the concept of cell death induced by the interaction of chemicals and light, formulated by Oscar Raab, a medical student at Hermann von Tappeiner in Germany. More than 100 years ago, in 1900, he reported the lethal effect of acridine red and light simultaneously acting on the paramecium *Infusoria* [15], while both agents alone were harmless. This accidental famous discovery happened thanks to a flash during a thunderstorm, when the ambient lighting was very low. Around the same time as Raab's discovery, a French neurologist, Prime, reported photosensibilisation in sun-exposed areas in an epileptic patient treated with parental eosin [16].

Employing the above findings, von Tappeiner and the dermatologist Jesionek, at Munich Dermatological Clinic in 1903, performed a topical treatment of skin tumors by eosin and

white light [17]. Subsequently (1904), von Tappeiner and Jodlbauer evidenced the oxygen as an integral part in photosensitization reactions. They also established the term “photodynamic action” (1907) [18, 19].

Concurrently with this crucial improvement in the understanding of the photodynamic action mechanisms, scientists recalled the fluorescence of heme derivatives described almost half a century ago and started a period of exploration of photodynamic properties and potential clinical use of hematoporphyrin derivatives. In 1908-1911 Hausmann reported on fluorescence and photosensitized cell destruction with hematoporphyrin [20, 21]. The consideration of porphyrins as photodynamic agents arose from an explanation of porphyria, an inborn error of heme synthesis and metabolism in the 1900s. This type of disease is accompanied by considerable photosensitivity. The patients with porphyria were found to produce various porphyrins in abundance, among them some behaving as endogenous photosensitizers which accumulate in many tissues, particularly in the skin. This results in an unintended PDT when exposed to light. In the early to mid 1900s, Fisher did much of the work in the field of porphyrin metabolism [22] and treatment of porphyrias for which he was awarded the Nobel Prize in 1943. He revealed the potency of porphyrins for PDT, however, he did not use them for clinical PDT. This step was done by Meyer-Betz in 1913, when he intentionally applied himself a potential effective dose of hematoporphyrin and after light exposure experienced the first intentional porphyrin-based PDT reaction [23]. Unfortunately, the clinical significance of this risky experiment was not appreciated for several decades.

In 1924, French physician Policard noted enhanced tumor fluorescence when exposed to a Woods lamp, which indicated possible selective localization of endogenous porphyrins to tumor tissue [24]. After more than 20 years, Figge et al. [25] and Rasmussen-Taxdal et al. [26] paid attention to the selectivity of porphyrin tumor localization, and they could confirm the observations of Policard. In the 1950s, Schwartz and Lipson continued in the work of Fisher and Meyer-Betz to develop more refined and more active forms of hematoporphyrin, which was called Hematoporphyrin Derivative (HpD), and employed it at first only for fluorescent diagnosis of human tumors [27-29].

Experimental studies performed in the 1970s confirmed the hypothesis of von Tappeiner and Jodlbauer that singlet oxygen is the main cytotoxic agent in the photodynamic treatment [30]. Utilizing the above knowledge and experience, Dougherty appreciated the relatively high singlet oxygen quantum yield of HpD after absorption in the Q-band region of spectrum and he used the HpD/red light combination for treatment of 25 patients suffering from several types of both primary and secondary skin tumors with considerable effects [31]. In this key study, of the 113 cancer lesions 98 were cured completely, 13 responded partially, and only two were resistant to the PDT. The success of Dougherty was followed by more clinical studies of PDT treatment, performed mainly with HpD, e.g. for treatment of lung [32], esophageal [33], colon [34] cancer, cerebral glioma [35], and other brain tumors [36].

Their discoveries and experience started an era of modern PDT development realized by the introduction of HpD as standard medicinal preparation Photofrin[®] into clinical use by QLT PhotoTherapeutics in 1993, even if it still was not a structurally uniform and defined product.

PHOTOPHYSICS AND PHOTOCHEMISTRY IN PDT

Actually, the mechanism of action of PDT is nothing else than transfer of absorbed energy from photosensitizer to various substrates, oxygen being the most important, with subsequent formation of highly reactive cytotoxic species. The energy absorbed after illumination with light of appropriate wavelength excites the sensitizer from ground singlet state (S_0) to excited singlet state (S_1). Excited singlet state is only short-lived with lifetimes in nanosecond range and that is why it does not cause any PDT-important interactions with surrounding molecules. The deactivation (Figure 1) of singlet excited state is done *via* either radiative emission (fluorescence) or non-radiative decay (internal conversion). The energy dissipates also through non-radiative intersystem crossing to excited triplet state (T_1) with somewhat lower energy than S_1 . This process is accompanied by change of the spin of one of the outermost electrons.

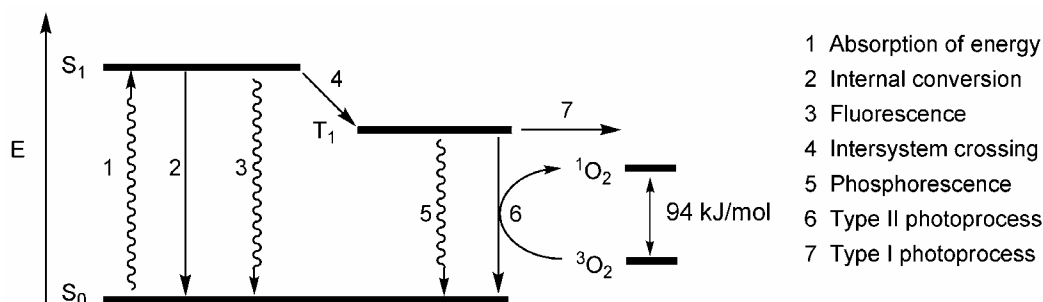


Figure 1. Modified Jablonski diagram.

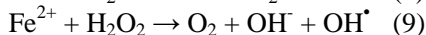
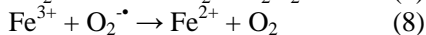
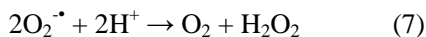
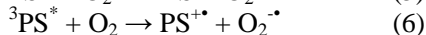
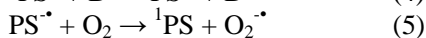
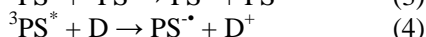
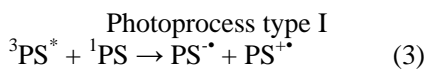
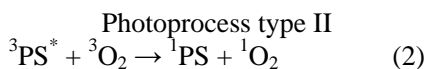
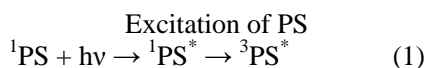


Figure 2. Basic reactions occurring during PDT.

The emission of photon in the form of fluorescence can be utilized for detection purposes. It helps to observe the distribution of photosensitizer both *in vitro* and *in vivo* and enables monitoring of its pharmacokinetic after *in vivo* application. The emitted fluorescence can be also useful diagnostic tool in approach called photodetection or photodiagnosis [37,

38]. The final effect of the photosensitizer is not to kill the cancer cells but to visualize them only and therefore high fluorescence quantum yields (Φ_F) are advantageous in this application. On the other hand, the fluorescence and intersystem crossing are competitive ways of excited singlet state relaxation. Very strong fluorescence of photosensitizer decreases its feasibility to be transformed to the excited triplet state which is the most important for production of cytotoxic species and consequently for photodynamic action. That is why some strong fluorescent dyes were structurally modified to improve their photodynamic properties and they were introduced to PDT trials. An addition of heavy atoms such as bromine to rhodamines [39], dyes with high Φ_F , serves as typical example. The “heavy atom effect” increased their singlet oxygen quantum yield (Φ_Δ) on the account of Φ_F .

The collisions of photosensitizer with solvent molecules result in deactivation of the excited singlet state and the energy is lost in the form of heat (internal conversion). As it is also a competitive process to intersystem crossing, it decreases the photodynamic effect. This relaxation way was, however, also studied as a cancer treatment possibility and termed photothermal therapy [40]. The temperature in local environment of the sensitized cells can reach very high values for short time causing disruption and death of targeted cells.

Despite the fact that the intersystem crossing to T_1 state is a spin-forbidden pathway, the efficient photosensitizers undergo this process with high probability. Energy from this state can be released through a triplet-singlet emission of the photon known as phosphorescence or through energy transfer to surrounding molecules in triplet state. Once the photosensitizer gets into the triplet state, its deactivation is relatively long, again due to spin-forbidden transitions $T_1 \rightarrow S_0$ with lifetimes in the micro- to millisecond range. A long time of triplet state relaxation enables interaction of excited photosensitizer with other molecules in the triplet state and allows energy transfer to them. The quenching of triplet excited state can be distinguished to be photoprocess type I or photoprocess type II (Figure 1). A type I mechanism involves hydrogen atom extraction or electron transfer between excited state of photosensitizer and some surrounding molecules leading to production of radicals. The energy transfer between triplet states of photosensitizer and oxygen results in the type II mechanism and formation of singlet oxygen. Both photoprocesses occur usually simultaneously and it depends on oxygen concentration, type of PS and polarity of the environment which of them prevails in the photooxidative damage of the cells. However, the photoprocess type II that produces highly reactive singlet oxygen is generally accepted to be the main reason for cells destruction.

Photoprocess Type II

Singlet oxygen produced by photoprocess type II (Figure 2, Eq. 2) is highly reactive species and most of the effects of PDT are related to oxidative damage caused by this active molecule. Good overview of its properties and characteristic can be found e.g. in the work of Lang *et al.* [41]. Ground state oxygen is in the triplet state (3O_2)(Figure 3). This is not very common feature for molecules and that is why only limited number of them (e.g. also vitamin A and nitric oxide) can also react in type II photoreactions [42] because the energy transfer proceeds only between species of the same multiplicity. Excitation of ground state triplet oxygen leads to change of the spin of one of the outermost electrons and thus to singlet oxygen (1O_2)(Figure 3). One of the important characteristics of photosensitizers is therefore

their singlet oxygen quantum yield (Φ_{Δ}) that can be defined as number of singlet oxygen molecules formed per absorbed energy quantum. Typical values for PS range from 0.2 to 0.8, the higher the better.

Singlet oxygen is short-lived species with lifetime in water 3-4 μs [43, 44] which even decreases to approximately 0.2 μs in cells due to its high reactivity with biological substrates [45]. However, the observed low lifetimes in biological media may be more or less caused by problems with detection of $^1\text{O}_2$ in this environment. Recently, a lifetime 3 μs which is very close to $^1\text{O}_2$ lifetime in water was measured in viable cells [46]. The singlet oxygen lifetime increases in organic solvents and reaches value e.g. 19 μs in octanol [44] or 50-100 μs in lipids [47]. As a consequence of its general short lifetime it can diffuse to distance only about 10 nm [47] (or according to other authors to 45 nm [48]). For comparison, plasma membrane thickness is 7-10 nm, human cells diameter ranges from 10 to 100 μm . It is therefore obvious that the effect of singlet oxygen is strictly limited to the place of origin and shall not affect any surrounding cells.

Photoprocess Type I

Photoprocess type I (Figure 2) is based on electron transfer to excited photosensitizer and involves production of reactive oxygen species (ROS) including mainly superoxide anion ($\text{O}_2^{\cdot-}$), hydrogen peroxide (H_2O_2) and hydroxyl radical (OH^{\cdot}). The excited photosensitizer ($^3\text{PS}^*$) can react with photosensitizer in the ground state (^1PS) producing reduced anion ($\text{PS}^{\cdot-}$) and oxidized cation ($\text{PS}^{\cdot+}$) radicals (Eq. 3). Many surrounding electron-donating molecules (D) (e.g. NADH, vitamin C, cysteine, guanine) can also reduce $^3\text{PS}^*$ leading to $\text{PS}^{\cdot-}$ and oxidized substrate (D^+) (Eq. 4). Photosensitizer anion radical ($\text{PS}^{\cdot-}$) undergoes electron-exchange reaction with oxygen (Eq. 5) to produce superoxide anion ($\text{O}_2^{\cdot-}$). Though the excited photosensitizer ($^3\text{PS}^*$) can also theoretically yield superoxide anion directly through electron transfer (Eq. 6), it has been shown that competitive energy transfer leading to singlet oxygen (Eq. 2) is more favorable [49]. Superoxide anion is reactive species and can inactivate several enzymes but its most important role is in production of hydrogen peroxide (Eq. 7), reduction of Fe^{3+} (Eq. 8) and subsequent formation of hydroxyl radical in Fenton reaction (Eq. 9). This highly reactive radical can add to an organic substrate (e.g. fatty acids, phenylalanine, nucleic acids) disturbing thus its biological functions.

Despite the predominant influence of type II reaction in the photodynamic action, both reactions usually occur at the same time. Photoprocess type II is favored in oxygenated tissues and due to longer singlet oxygen lifetimes also in more lipophilic environment. On the other hand, the balance shifts toward the type I reactions under hypoxic conditions and these reactions substantially contribute to the photodamage of the membrane components in tissues with low oxygen concentration. They are also preferred in more polar environment where the radicals should be stabilized.

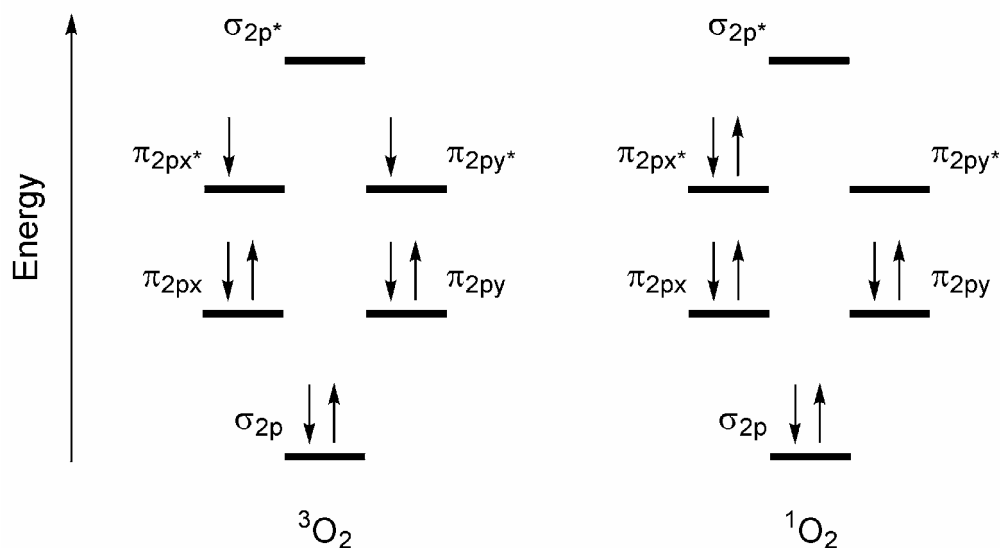


Figure 3. Molecular orbital diagrams of singlet ($^1\text{O}_2$) and triplet ($^3\text{O}_2$) state of oxygen.

Although some photoreactions can occur under hypoxic conditions, the presence of oxygen is an absolute requirement for successful photodynamic activity. The photodynamic effect is directly proportional to the concentration of oxygen in tissues and no cancer cells are killed under anoxic conditions [50]. The possible oxygen depletion from human tissues may occur due to two main reasons. The first one is a fast consumption of oxygen in photoreactions after illumination of targeted area. It means that the photodynamic effect may limit itself in further cell killing. This problem can be bypassed using lower light fluence rates when the oxygen is not consumed so rapidly. As a consequence, much better clinical results are obtained for the same fluence but lower fluence rates [51]. The second reason arises from low oxygen level in the target tissue. Tumor cells generally are poorly supplied with blood leading to local hypoxia. Moreover, the photodynamic effect causes vascular damage leading to even lower supply. This effect limits the use of PDT in solid tumors where hypoxia must be considered. On the other hand, PDT-induced vascular shutdown is one of the important effects leading to final control over tumor.

BIOLOGICAL RESPONSE

The death of each cell that accumulated enough of the photosensitizer and was illuminated is not the sole effect responsible for regression of the tumor. Three main mechanisms by which PDT mediates the tumor destruction were described. The direct lethal effect of singlet oxygen and other ROS on cells is the first one. PDT-mediated vascular shutdown leading to low nourishment supply and tumor infarction is also very important pathway. Finally, PDT can activate immune response against tumor cells.

Direct Effect

Since the active radius of toxic species produced by PDT is limited, the cell death is a consequence of the damage of subcellular structures. The absorbed photosensitizers are located inside the cell mainly in lysosomes [52-54] and also in mitochondria [55-57]. Some examples are described for photosensitizers (especially temoporfine) present also in endoplasmic reticulum or Golgi apparatus [57-59]. Plasma membrane is a relatively uncommon target in PDT [60] and photosensitizers are localized within it usually only during first minutes of incubation [61]. The fragmentation of DNA after PDT treatment is suggested to be rather a consequence of induced apoptotic response than a contribution of direct PDT effect on cell nucleus [42].

However, it is sometimes impossible to appoint only one target organelle responsible for cell death. The photosensitizer localization can change over time of incubation [61, 62], some of them allocate in various organelles [63], they can redistribute after illumination and thus affect more intracellular targets [64, 65], or they can be found diffused in cytoplasm indicating no distinct subcellular localization [66, 67]. Generally, photosensitizers which are hydrophobic and have two or less negative charges can diffuse across plasma membrane and then relocate to other intracellular membranes. Those which are less hydrophobic and have more than two negative charges tend to be too polar to cross the membrane by passive diffusion and therefore are taken up by endocytosis and they are found in lysosomes [68]. Endocytosis is also important uptake mechanism for aggregated photosensitizers. The cationic dyes are known to accumulate in mitochondria [55, 69, 70] and belong to the most phototoxic ones. Mitochondria are the source of ATP production therefore their injury will lead to energy imbalance. The membrane-bound mitochondrial proteins were found to be more susceptible to photodamage than those located in their matrix or in cytosol [71] due to longer singlet oxygen lifetime in hydrophobic environment. Moreover, mitochondrial way is believed to be the most important in induction of apoptosis after PDT [42, 72, 73].

Vascular Effects

Damage of vasculature of targeted area strongly contributes to final control over the tumor. The viability of tumor depends on the supply of oxygen and other nutrients by blood vessels. The destruction of delivery ways will lead to local hypoxia, anoxia and lack of available nutrients. The basic mechanism of action depends on the photosensitizer used. Porfimer sodium and hydrophobic phthalocyanines induces vessel constriction [74-76], trombus formation was observed after treatment with talaporfin [77] and disulfonated phthalocyanines caused only vascular leakage [74]. The vessel constriction is connected with release of eicosanoids and can be inhibited using indomethacin (inhibitor of cyclooxygenase) [78]. The mechanism may have also a biphasic character as shown for indium pyropheorbide [79]. The acute vascular effects were characteristic of vasoconstriction; however, the long-term vascular shutdown was mediated by thrombus formation.

The highest vascular effect of PDT occurs usually when activation is performed shortly after photosensitizer injection, while direct effect becomes more important when delayed times are used. Vascular targeting of PDT may be of higher effectiveness or even higher selectivity than direct effect and that is why this regimen is currently used for age-related

macular degeneration (AMD) treatment in clinic [80] and experimentally for tumor destruction [81, 82]. Especially for drugs with low selectivity to tumor cells or which are rapidly excreted from the body, this approach may be the primary effect responsible for the cure [77, 83, 84].

Immune Response

Activation of immune response in the targeted area after PDT is perhaps not the primary reason leading to cells death but it may help in long-term control over the tumor. In experiments with normal and immunodeficient mice, the long-term control has been observed only for normal mice although the short-term effects were comparable [85]. The mechanism of activation comprises release of cytokines, inflammatory and chemotactic signals from treated tissues followed by invasions of neutrophils, mast cells, monocytes and macrophages [86]. Several other studies confirmed that tumor-specific response may be developed [42, 87] and on this ground the pretreatment with immunostimulants seems to bring benefits for PDT [88]. Suggestion that tumor-specific immunity is developed after PDT can be considered in development of vaccination using PDT-influenced tumor cell lysates [89].

PHOTOSENSITIZERS' PROPERTIES

Photosensitizers (PS) are the main components of PDT treatment. Their structure determines the photophysical as well as pharmacokinetic properties and as a consequence leads to different efficacy, tumor selectivity, application methods, irradiation schemes and side effects (especially long-term phototoxicity).

UV-vis absorption spectrum of each photosensitizer is perhaps the most important photophysical property. The transmittance of biological tissues is relatively low at lower wavelengths and increases at longer wavelengths. Endogenous chromophores in human body (hemoglobin, oxyhemoglobin and melanin) are responsible for light absorption up to approximately 630 nm and light penetration through tissues in range of only millimeters. Melanin absorption is important even at wavelengths around 700 nm and that is why especially highly melanotic tumors require photosensitizers with absorption at longer wavelengths. The IR radiation at wavelengths higher than 1000 nm is absorbed by water. The optical window of tissues opens therefore between 630 and 1000 nm. Nevertheless, absorption above 800 nm may not be suitable for singlet oxygen production. The energy difference between $^1\text{O}_2$ and $^3\text{O}_2$ (ΔE_Δ) is 94 kJ mol^{-1} so the energy of the photosensitizers excited triplet state (ΔE_t) must be larger. As ΔE_t decreases with increasing wavelength it may not be sufficient for excitation of $^3\text{O}_2$ to $^1\text{O}_2$. The optimal range of absorption for ideal photosensitizer is therefore 680-800 nm.

Similarly to all dyes, the photosensitizers undergo also a photobleaching. This is a process when the macrocycle loses its absorption as a result of self-destruction after illumination. The stability of photosensitizer on light decreases generally with absorption at higher wavelengths. Such low stability may be a limitation during use in therapy but also an

advantage, since the photosensitizer is then excreted from the body faster and it may reduce long-term photosensitivity.

The ideal photosensitizer for PDT would have the following characteristics:

- *Be chemically pure and of known composition.* The porfimer sodium (a hematoporphyrin derivative), which was the first compound approved in clinical practice, consists of a number of different dimers, trimers and other oligomers. Also sulfonated aluminium phthalocyanine (known as Photosens) is a mixture of several phthalocyanine macrocycles with different degree of sulfonation and position of sulfo group.
- *Have low dark toxicity of both photosensitizer and its degradation products.*
- *Be preferentially retained in target tissues.* High tumor-to-healthy tissues ratio is advantage and decreases the systemic toxicity. However, the low selectivity can be bypassed by special irradiation schemes as in the case of talaporfin.
- *Be rapidly excreted from the body.* As the photosensitizer tends to cumulate in skin, it causes prolonged photosensitivity (almost 2 months for porfimer) and patients must avoid the contact with direct sunlight for several weeks. Therefore the use of hydrophilic, rapidly eliminated PS seems to be more advantageous even at the expense of lower selectivity.
- *Have the high singlet oxygen quantum yields.* Since the production of singlet oxygen is crucial for PDT, the quantum yields should be as high as possible. For PS in clinical practice or in trials it ranges from 0.2 to 0.8.
- *Absorb strongly at longer wavelengths.* As mentioned above, the optimal wavelengths for absorption ranges from 680 nm to 800 nm. Moreover, high extinction coefficients (ϵ) at illumination wavelength allow reduction of PS dose while preserving the amount of produced toxic species.
- *Be available.*

According to above mentioned criteria, the available photosensitizers can be divided into three generations. Compounds involved in the first generation absorb usually at low wavelengths (about 630 nm) with low extinction coefficient ($\epsilon \sim 3000 \text{ M}^{-1} \text{ cm}^{-1}$), have low tumor/skin ratio and are retained in cutaneous tissues for several months. Actually, the only representatives of this generation are porfimer sodium and similar hematoporphyrin derivatives.

The second generation of PS is excited using light at longer wavelengths, mainly from 670 to 800 nm, which penetrates up to 2-3 cm. Also their absorption is much stronger ($\epsilon \sim 50000\text{-}300000 \text{ M}^{-1} \text{ cm}^{-1}$) which allows reduction of PS amount required for certain therapeutic effect. The interpretations of dose-response relationships are easier because they are not mixtures of compounds as in the case of porfimer. The selectivity of tumor targeting is, however, still not fully satisfying. That is why, the combination of the second generation PS with targeting moieties (monoclonal antibodies, steroids, nucleotides etc.) is under development and sometimes called the third generation of PS.

STRUCTURES OF PHOTSENSITIZERS

Tetrapyrrolic compounds based on [18]annulene structure are among the most useful PS for PDT. The basic structure of porphyrin consists of four pyrrol units linked by methine bridges to make a ring. The porphyrin ring is an aromatic system containing 22 π -electrons, but only 18 of them are involved in delocalization (Figure 4). It obeys Huckel's rule of aromaticity $4n+2$ π -electrons. The pyrrol rings in porphyrin are named A, B, C and D, the carbons forming methine bridges (position 5, 10, 15 and 20) are called *meso* carbons. Reduction of one double bond not involved in [18]annulene ring leads to chlorins, reduction of another double bond gives rise to bacteriochlorins. Pheophorbides and bacteriopheophorbides can be considered as members of chlorin or bacteriochlorin family, respectively, with ethylene bridge between *meso* carbon and adjacent pyrrol unit. [18]annulene ring can be found also in the structure of compounds derived from porphyrin – texaphyrins and porphycenes. Isosteric replacement of *meso* carbons in porphyrin with nitrogens and condensation of benzene rings to each of pyrrol units leads to well known group of synthetic dyes phthalocyanines.

All porphyrin-like compounds have two important absorption bands – Soret band (known as B-band) around 400 nm and a Q-band in area 600-800 nm. The Q-band is important for PDT since it lays in area used for excitation. Porphyrins absorb at $\lambda_{\max} \sim 630$ nm with only weak extinction coefficient. Reduction of double bonds in porphyrin's pyrrol rings causes bathochromic shift and strengthens the absorption at Q-band. Thus, chlorins absorb at $\lambda_{\max} \sim 650-690$ nm with $\epsilon \sim 40000 \text{ M}^{-1} \text{ cm}^{-1}$ and bacteriochlorins at $\lambda_{\max} \sim 740-800$ nm with $\epsilon \sim 50000 \text{ M}^{-1} \text{ cm}^{-1}$ depending on the substitution of the ring (see Figure 5¹ for comparison [90]).

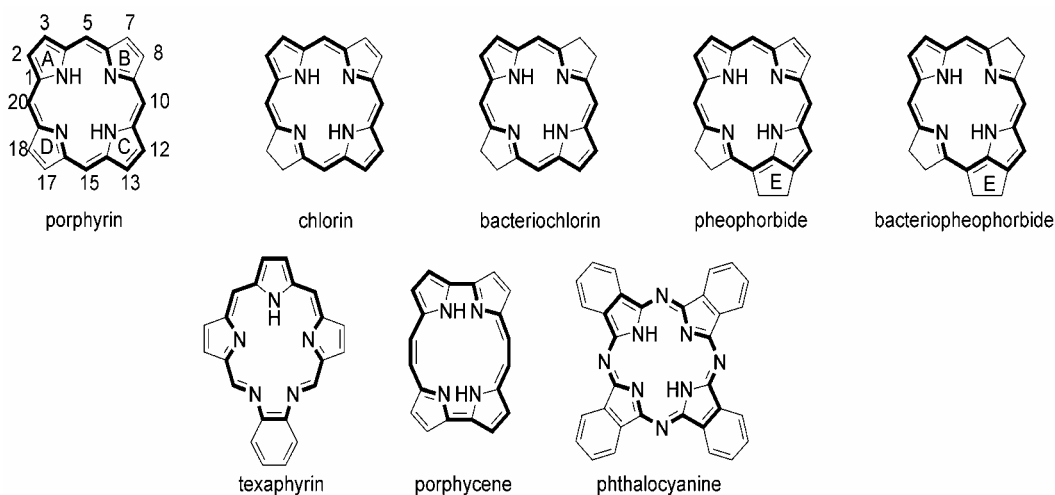


Figure 4. Basic structures of porphyrinoid photosensitizers.

¹ Reprinted with permission from ref [90]. Copyright (2006) American Chemical Society.

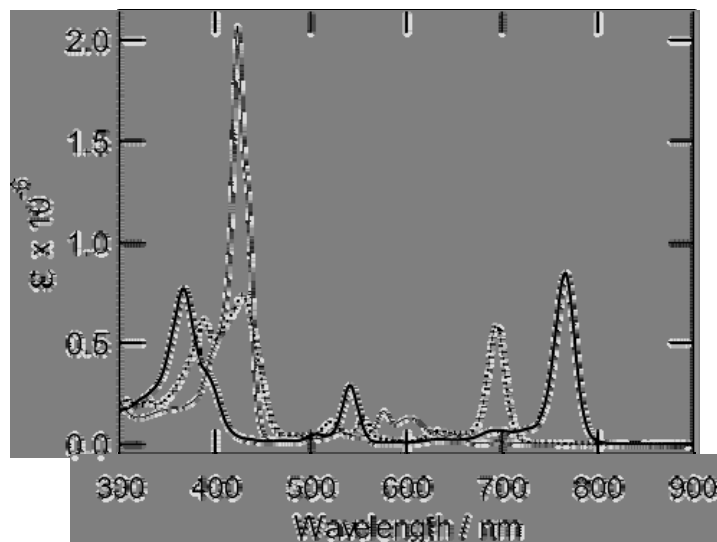


Figure 5. UV-vis absorption spectra of porphyrin (thin line), chlorin (dotted line) and bacteriochlorin (thick line) of the same peripheral substitution and at the same concentration.

Whole macrocyclic system of phthalocyanines is aromatic and conjugated and this substantially changes photophysical properties especially in the Q-band area. The band is shifted to higher wavelengths (λ_{\max} =650-700 nm) and is very strong (ϵ up to 200000 M⁻¹ cm⁻¹). B-band absorption, on the other hand, is only weak. Enlargement of phthalocyanine ring for next benzene rings lead to naphthalocyanines (Nc) with even more red-shifted Q-band (λ_{\max} =760-810 nm) and ϵ over 250000 M⁻¹ cm⁻¹.

In following paragraphs, we will concentrate on the photosensitizers which have been already approved in clinical practice, are undergoing clinical trials or are prospective in future PDT treatment. The compounds are divided according to their structures into porphyrins, chlorins and bacteriochlorins, phthalocyanines, tricyclic dyes and other photosensitizers. Since the compounds were developed or investigated often by different research groups, they received a lot of names including several abbreviations. For instance, mono-*L*-aspartyl chlorin e6 is also known as talaporfin, Npe6, LS11, MACE or Laserphyrin[®] and can be also mentioned as a part of Litx[™] technology. Where possible, we will prefer use of the international nonproprietary names (INN) which are recommended by WHO for drugs.

PORPHYRINS

Porfimer Sodium

Other names used: hematoporphyrin derivative, HpD, Photofrin, Photogem, Photosan.

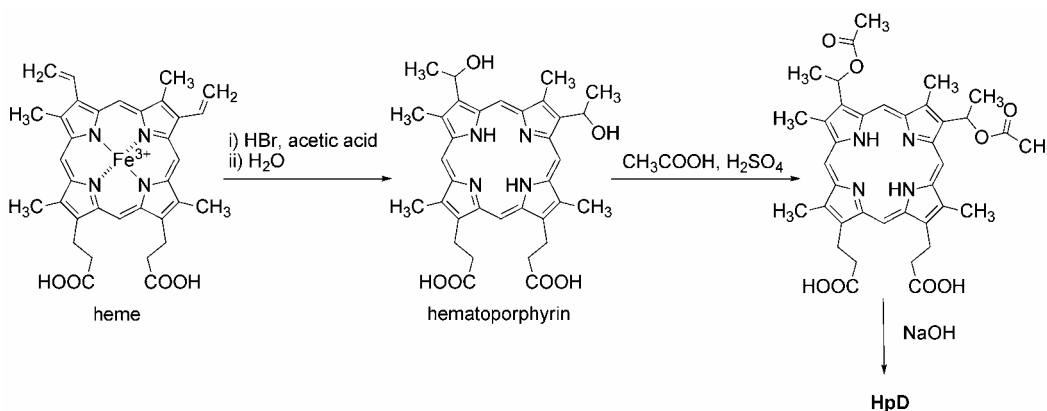
Porfimer sodium is an INN name for mix of compounds which are named hematoporphyrin derivative (HpD). In fact, this is not a single compound but a mixture of monomers, dimers and oligomers with not exactly defined proportions of the constituents. Hematoporphyrin (Hp) itself is a potent photosensitizers but it is lack of selectivity to tumor tissues. It was found that oligomeric fractions that arise during isolation of Hp from blood

[91] are responsible for the selective accumulation and therefore these fractions were synthetically enriched to form HpD and later concentrated using gel permeation chromatography.

Heme is a red blood dye responsible for oxygen transport *in vivo* and is photodynamically inactive. It is demetallated using HBr in acetic acid (Scheme 1), the vinyl groups are hydrobrominated at the same time and subsequently hydrolyzed in water medium to yield Hp [92]. Treatment of Hp with sulphuric acid in acetic acid leads to acetylation of free hydroxy groups. Their subsequent hydrolysis with NaOH and neutralization gives a mixture known as HpD. During this process a lot of linkages either ether, ester or direct C-C bonds arises and oligomer fraction is enriched. The removal of acetyl group by NaOH may lead also to elimination and some vinyl groups on periphery may be restored [93]. An example of tetramer combining some of the possible connections and peripheral substitutions in HpD is shown on (Figure 6). The crude mixture was purified by HPLC or gel permeation chromatography to enrich the oligomeric fractions which are responsible for increased tumor uptake and such HpD was used in clinical tests and later introduced to clinical practice as porfimer sodium.

The maximum wavelength of HpD absorption is at 630 nm, its ϵ at this wavelength reaches only $3000 \text{ M}^{-1} \text{ cm}^{-1}$ and as a consequence large doses of photosensitizer and light are needed for therapeutic effect. Porfimer sodium is water soluble and applied in the form of *i.v.* injections at the dose 2 mg/kg. Its half-life ranges from 17-22 days. The best tumor uptake is reached after 45-50 hours when the targeted area is irradiated. Next irradiation can be done after 90-120 hours. If necessary, second PDT-cycle (including drug administration) can be performed after 30 days. Porfimer is retained in skin for at least 6-8 weeks causing long-term phototoxicity.

The HpD enriched for its oligomeric fractions is approved as porfimer sodium. However, a lot of other HpD of different origin were prepared and the composition may vary. For example, three different HpD forms from a various manufacturers are investigated in China (BeijingHpD, YangzhouHpD, Photocarcinorin) and they have been shown to be of different composition [94]. HpD developed by different technology has been investigated also in Russia and approved for clinical use under the name Photogem[®] in 1996 [95]. The clinical results obtained for such preparations are therefore very hard to correlate correctly.



Scheme 1. Preparation of HpD.

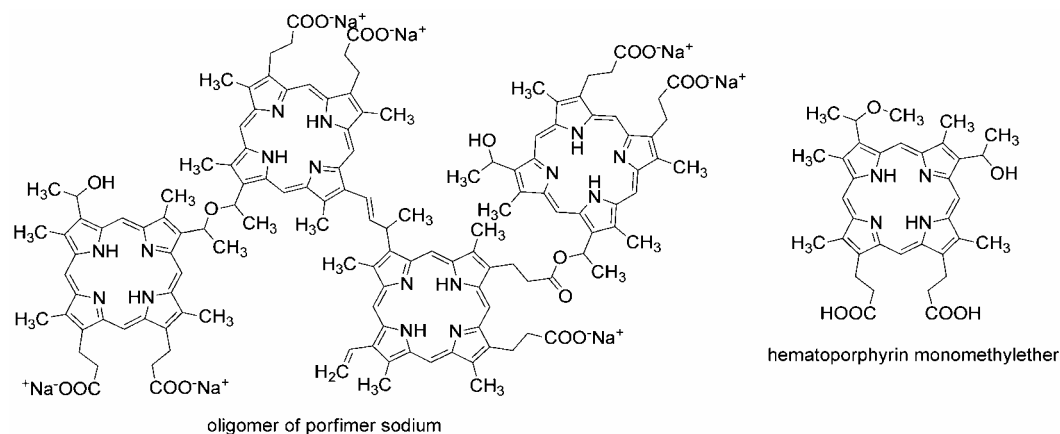


Figure 6. Example of one of porfimer oligomers and structure of hematoporphyrin monomethylether.

Porfimer sodium was developed by QLT, Inc. and as the first photosensitizer approved in clinical practice for PDT in Canada (Photofrin[®]) in 1993 for the treatment of superficial bladder cancer. A lot of other approvals have been received since that time also in other countries for treatment of advanced stage esophageal cancer, advanced non-small-cell lung cancer, early-stage lung cancer, cervical cancer, gastric cancer and Barret's esophagus [96]. However, since the porfimer sodium is the first and the best known photosensitizer, a lot of other clinical trials for new cancer treatment are under run [97]. For instance, head and neck cancers [98] brain and central nervous system tumors [99, 100] and cholangiocarcinoma [101, 102] have been shown to respond to the porfimer sodium-PDT treatment. The worldwide rights to Photofrin[®] were sold to Axcan Pharma, Inc. in 2000.

Hematoporphyrin Monomethylether

Other names: HMME, Herimether, PsD-044.

Hematoporphyrin monomethyl ether (Figure 6) is a name for two positional isomers – 3- or 8-methoxyethyl-8- or 3-hydroxyethyldeuteroporphyrin IX. It was synthesized in China and clinical studies have demonstrated that, compared to HpD, it has advantages of stronger photodynamic effect, higher tumor selectivity, lower toxicity and shorter skin photosensitivity [94]. It has been successfully used for treatment of port-wine stains, cancer of gastrointestinal tract and gliomas [103].

5-aminolevulinic Acid

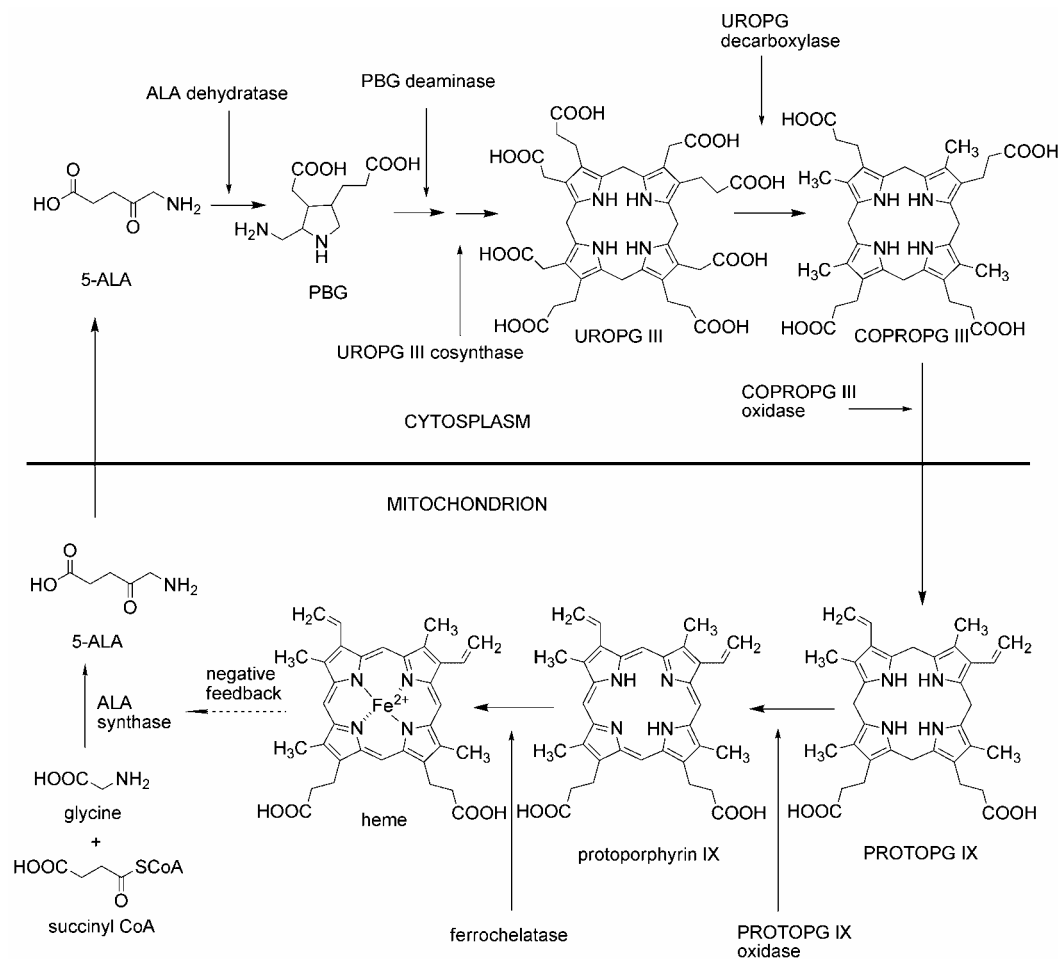
Chemical name: 5-amino-4-oxo-pentanoic acid

Other names: δ -aminolevulinic acid, 5-aminolaevulinic acid, ALA, 5-ALA

5-aminolevulinic acid (5-ALA) is the first compound in the porphyrin synthesis pathway (Scheme 2), leading in the end to hemoglobin in mammals. In eukaryotic cells it is produced by the enzyme ALA synthetase from glycine and succinyl CoA. 5-ALA biosynthesis in plants, algae and most of bacteria starts from glutamic acid and glutamate-1-semialdehyde.

There are two rate-limiting steps in the heme biosynthesis in eukaryotic cells: synthesis of 5-ALA and conversion of PpIX to heme by the enzyme ferrochelatase [104].

As a PDT tool, 5-ALA is a prodrug in the sense of Albert's [105] concept. The 5-ALA molecule itself is non-active. If produced naturally in cells, it is fluently converted to porphobilinogen (PBG), and then up to heme through several biosynthetic steps. The concentration of heme works as a feedback control mechanism, inhibiting the endogenous 5-ALA formation, so no biosynthesis intermediate is accumulated under physiological conditions. When exogenous 5-ALA is supplied, the biosynthesis runs relatively quickly to the protoporphyrin IX (PpIX), the last intermediate, which normally incorporates an iron ion to form the heme molecule. However, since this step is a bottleneck of the heme biosynthesis, in the case of exogenous 5-ALA supply the PpIX is accumulated in cells in high concentration depending on the 5-ALA availability, because of limited capacity of the ferrochelatase [106, 107]. In contrast to heme, which is not photoactive, the PpIX oxygen quantum yield is about 0.56, which is quite sufficient for effective PDT [108].



Scheme 2. Pathway of heme biosynthesis.

The fundamentals for employment of 5-ALA in photodynamic therapy were put in 1987 by Malik and Lugaci [109], who first used 5-ALA induced PpIX and light for *in vitro* cells inactivation, and by Peng et al. [110, 111], who described endogenous porphyrin synthesis 24 hr after intra-peritoneal injection of 5-ALA in tumor-bearing mice. However, for these successful 5-ALA applications, previous improvements in knowledge about porphyrin biosynthesis and metabolism were necessary. Research of porphyria brought important new information in this field in 1980s, when e.g. Sandberg and Romslo found the phototoxic efficacy of protoporphyrin IX was much higher than that of coproporphyrin and uroporphyrin [112]. In another important finding the same authors revealed the efficiency of PpIX was strongly dependent on subcellular localization of the porphyrins. While PpIX was localized and exerted its damaging power mainly in the mitochondria, uroporphyrin was concentrated in lysosomes and after irradiation it caused release and inactivation of lysosomal enzymes. The higher efficacy of PpIX localized in mitochondria corresponded with the previously described importance of oxygen in the PDT [113, 114].

5-ALA was introduced into human PDT by Kennedy and Pottier in 1990-1992 [115, 116]. They described photosensitivity at patients with superficial skin disorders after exogenous administration of 5-ALA in an aqueous solution and they confirmed that the photosensitivity was caused by PpIX.

Considering the routine human applications of PDT, 5-ALA and its derivatives perform majority of the clinical cases nowadays. Of them, vast majority is realized in dermatology as topical PDT. Beyond the officially approved applications (Bowen's disease, actinic keratosis and basal cell carcinoma) [117, 118], both 5-ALA and its ester derivatives are examined in many other experimental topical therapeutic and diagnostic applications, e.g. superficial fungal infections [119, 120], acne [121-123], psoriasis [124, 125], warts [126] and other skin viral infections [127, 128]. For these applications, 5-ALA possesses both excellent advantages but also some drawbacks.

The main advantages of the 5-ALA PDT include:

1. The natural character of both the (pro)drug and active metabolite is a good premise for low toxicity of this photodynamic therapeutic system.
2. Relatively short and low skin photosensitization, since the PpIX is not too much accumulated in the skin and the tissue levels are at the standard value in about 24 to 48 hrs [129].
3. The relative selectivity caused by various reasons, e.g.:
 - more expressed porphobilinogen deaminase at some types of tumors enhances the PpIX biosynthesis in tumor cells compared to the normal cells [130-132]
 - lower ferrochelatase activity at some cancer cells [131-134] decreases the PpIX to heme conversion and increases the PpIX accumulation
 - limited availability of iron atoms in rapidly proliferating cancer tissues also contributes to slower PpIX to heme conversion [135].

The main drawbacks of the 5-ALA mediated PDT are:

1. The strong hydrophilicity of the 5-ALA, which considerably limits its penetration especially through the upper layer of skin, stratum corneum, and through cell membranes. Therefore, only very superficial changes can be treated [136, 137].
2. The instability of 5-ALA, especially in solutions buffered to the physiological pH value.
3. Absorption maximum of the highest PpIX Q-band at approx. 630 nm, which also limits the use of 5-ALA mediated PDT to superficial skin disorders only and disables it from use on pigmented skin defects, because of the endogenous porphyrins and melanins absorption, reaching up to approx. 700 nm.

Despite of these problems, 5-ALA itself is used relatively frequently in human PDT. Officially it is approved for topical treatment of actinic keratoses of head and scalp since 1999 (USA, Levulan[®] Kerastick[®], DUSA Pharmaceuticals). Since 2000 it is also registered as the medicinal preparation Alasens [138] in Russia, as the hydrochloride in powder form for dissolution before application.

A big effort exists in the scientific community to resolve the above mentioned 5-ALA drawbacks, and in some cases this effort was at least partially successful. The 5-ALA hydrophilicity can be overwhelmed to some extent by either chemical modifications or technological formulation methods.

Chemical modifications intended to enhance the 5-ALA penetration through skin and membranes should consider the mechanism of its action, i.e. the amino and carbonyl groups of its molecule are included in the subsequent steps of the hem biosynthesis cycle. Therefore, to maintain its biological activity, these moieties usually should stay free and available for enzymatic condensation. Several studies described formation of *N*-derivatives of 5-ALA, mainly of simple amide or peptide type. Simple amide derivatives were usually not active, probably because of low ability of cells to cleave the amide bond [139-143]. Some peptide derivatives were more successful [141, 142], however, the doses of such compounds to achieve equivalent PpIX biosynthesis compared to 5-ALA were high.

Even if the carboxy group is not directly included in the metabolic bio-condensation, only carboxylic acid precursors are usually considered to be suitable for PDT. Of the chemical modifications described until now, the esterification has shown to be the most successful in enhancing the lipophilicity and penetration while maintaining the activity [137, 144]. A number of 5-ALA esters was synthesized, including both non-branched and branched aliphatic esters [139, 145], alicyclic and aromatic esters (all of them including halogenated derivatives [146]), ethylene glycol esters, nitrophenyl esters, thioesters [147], dendron and dendrimer esters. Despite of the number of compounds, only two ester derivatives were introduced into clinical use until now. The methyl ester (Metvix[®], Photocure ASA, Oslo, Norway) is officially approved for treatment of actinic keratoses and hexyl ester (Hexvix[®], Photocure ASA, Oslo, Norway) for photodiagnostic use.

Even if the esterification of 5-ALA has shown to enhance penetration through cell membranes and the influx into the cells, the positive effect on the PpIX formation in cells compared to free 5-ALA occurs only in low concentrations. Another factors, especially the rate of the ester hydrolysis and the porphobilinogen deaminase and uroporphyrinogen II cosynthase activity seem to be the limiting for PpIX synthesis [135, 140, 148, 149] in the concentrations above approx. 3-5 mM. Since the concentrations currently used in the dermatologic therapeutic applications are in the range of 16-20 per cent (w/w) (about 1M or

more), the formation of 5-ALA esters as pro-prodrugs with enhanced penetration is probably not the main advantage of this modification. Nevertheless, until now there seems to be no clear evidence that 5-ALA esters are biologically active only after the hydrolysis, since in some cases formation of PpIX esters and diesters was observed and they shown spectral properties analogous to the ones of PpIX itself [150-152]. Taylor et al. also showed that exposition of 5-ALA and its ethyl ester mixture to the 5-ALA dehydratase, the second enzyme in the hem biosynthesis pathway, resulted in a mixture of porphobilinogen as the main product and its ester as the by-product [153].

Unlike the topical use, the concentrations of 5-ALA and its derivatives in body fluids and tissues after systemic administration are much lower and enhanced cell influx enabled by esterification may play an important role. For example, the porphyrin synthesis from 5-ALA hexyl ester was found to be several times higher than that from 5-ALA at 0.05 mM concentration in experiments performed at the murine mammary adenocarcinoma M3 derived LM3 cell line [154]. The low plasmatic concentrations sufficient for high PpIX fluorescence localized with relatively high selectivity in cancer tissue favor the 5-ALA hexylester as the photodiagnostic tool (Hexvix[®], Photocure ASA, Oslo, Norway), actually approved for detection of bladder cancer.

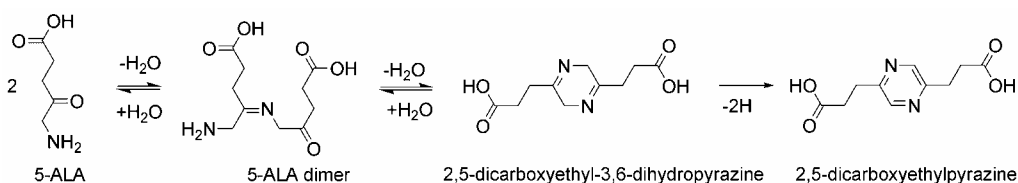
For the topical applications, the advantage of ester derivatives seems to be more important as a factor influencing the selectivity of subsequent photodynamic treatment. It was shown that the porphyrin synthesis from 5-ALA esters is much more localized in the cancer tissue than in the surrounding normal cells [155-157]. The reason could be the higher activity of esterases in some cancer or another abnormal cells, as already noted above. The differences in PpIX ratio in normal skin and actinic keratoses were observed by Fritsch et al. [158] also in isolated human skin. Another condition contributing to the higher ratio of PpIX concentrations between the place of application and surrounding tissue at 5-ALA esters could be the higher partitioning and subsequent sequestration of the esters within the stratum corneum, while the free 5-ALA can diffuse to surrounding tissues through vascular networks more easily thanks to its hydrophilicity [159].

Another advantage of 5-ALA methyl ester mediated topical PDT over the 5-ALA treatment is less pain accompanying the treatment procedure. This phenomenon is probably attributable to different cell uptake mechanisms of these two 5-ALA application forms. While 5-ALA cellular uptake very probably at least partly employs a Na⁺ and Cl⁻ dependent active transport mechanism [160, 161], the uptake mechanism of its methyl ester is independent on the Cl⁻. On the other hand, it can be inhibited by amino acids of low polarity (e.g. alanine, methionine, tryptophan) [162].

The second main shortage of the 5-ALA mediated PDT is the drug insufficient stability. It depends strongly on the pH value, on the drug concentration, and temperature of the solution. The main reaction causing the decrease of free 5-ALA molecules number available for PDT is dimerization. 5-ALA belongs among the α -amino ketones which under neutral and alkaline condition readily dimerize and subsequently cyclize to dihydropyrazine derivatives [163](Scheme 3). In the case of 5-ALA, the formation of mainly 2,5-dicarboxyethyl-3,6-dihydropyrazine [164-166] *via* an open-chain ketimine 5-ALA dimer was observed. Porphobilinogen [167] and pseudoporphobilinogen [165, 167] were described to arise as minor side-products. Similarly to biosynthetic steps to subsequent hem intermediates, the amino and carbonyl groups are included in the dimerization reaction [167]. In the presence of oxygen, the dihydropyrazine derivative is further oxidized to the 2,5-dicarboxyethylpyrazine

[165, 168]. The speed of dimerization reaction depends mainly on the pH value. While solutions of 5-ALA with pH under 2 are stable, at pH 7.4 almost complete degradation could occur in several hours. Similarly, at 0.3 g/ml solution the decrease of concentration is more than four times higher during 45 min test period than at a 0.1 g/ml solution at pH 5.5 [167].

Since the 5-ALA instability is caused by similar mechanism, as are the ones which 5-ALA undergoes in the first steps of hem biosynthesis, it is not easy to stabilize the molecule against these undesirable changes. Some attempts to protect the amino moiety via formation of amides were performed, however, they usually resulted in biologically inactive derivatives, as already mentioned above. As a result, a theoretically possible way to stabilize the 5-ALA solutions is to keep the pH at very low value, which is unfortunately unsuitable for clinical human application. The other way is to prepare the solution *in-situ* just before application. This approach is employed at the both the clinically used preparations Levulan[®] Kerastick[®] (DUSA Pharmaceuticals, Inc.) and Alasens. Another possible approach is a development of formulations avoiding direct contact of 5-ALA or its derivatives with water. The literature concerning such formulations is outside the scope of this review.



Scheme 3. Reaction mechanism of 5-ALA instability.

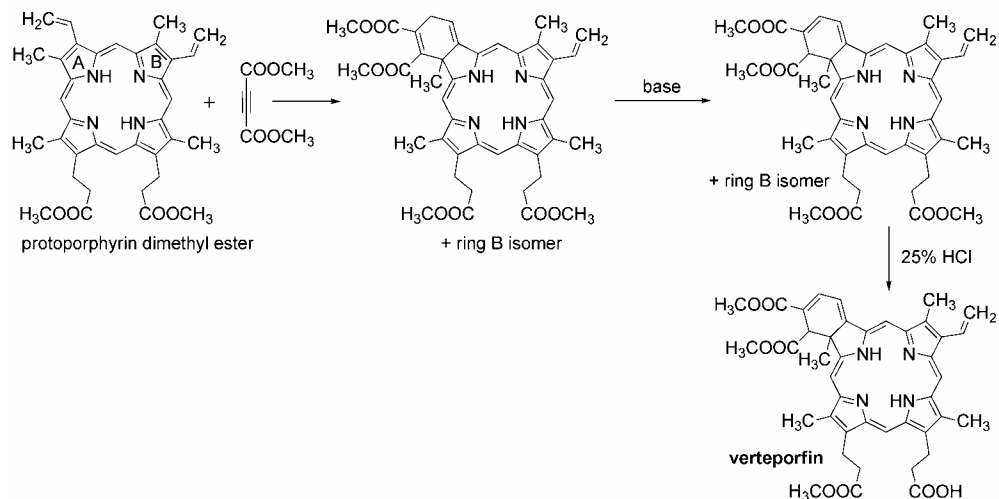
CHLORINS

Verteporfin

Other names: benzoporphyrin derivative mono acid ring A, BPD-MA, Visudyne[®]

In spite of its name benzoporphyrin, verteporfin (developed by QLT, Inc.) is a member of chlorin family. It is a derivative obtained semisynthetically from protoporphyrin (Scheme 4). Protoporphyrin dimethyl ester undergoes a Diels-Alder reaction with dimethyl acetylenedicarboxylate. The adduct double bonds are then rearranged by treatment with base to obtain the benzoporphyrin derivative modified on both A and B rings. Chromatographic separation and partial hydrolysis gives desired benzoporphyrin derivative mono acid ring A [93].

Being a chlorin, the photophysical properties of verteporfin are improved – it absorbs at 690 nm with $\epsilon \sim 35000 \text{ M}^{-1} \text{ cm}^{-1}$. Verteporfin is only sparingly water soluble, so it must be administered in the form of liposomal formulations at dose 6 mg/m^2 . It is rapidly cleared from body, its plasma half-life ranges from 5 to 6 hours. The irradiation is performed 15 minutes after start of infusion. The skin photosensitivity is usually developed only for 48 hours.



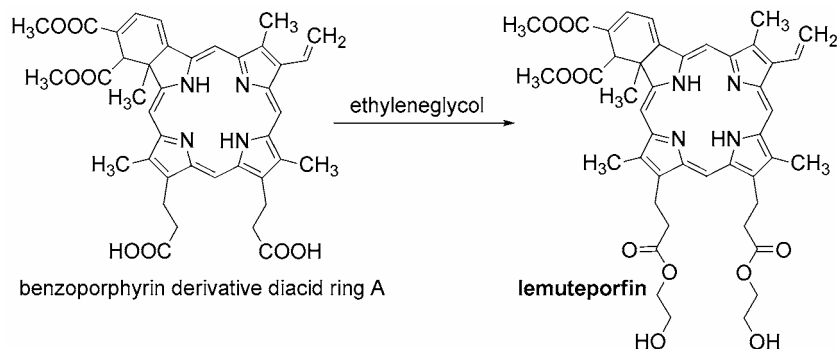
Scheme 4. Synthesis of verteporfin.

Though verteporfin has been tested also for cancer treatment, it received the highest attention in ophthalmic applications for the treatment of age-related macular degeneration (AMD). AMD is the leading cause of severe vision loss among the elderly in western world. It appears in two forms: wet and dry. The wet one is developed from dry one and is characterized by abnormal, leaky blood vessels in the macula, which may create scar tissue, causing permanent blind spots [169]. Verteporfin causes usually vascular shutdown so it is optimal for treatment of neovasculature. It is approved in several countries for treatment of chorioidal neovascularization caused by AMD but also due to other macular disease (pathologic myopia, ocular histoplasmosis). Verteporfin is effective in therapy solely [170], but it is investigated also in combination therapy with other drugs used for treatment of chorioidal neovascularization. It may be administered together with antiangiogenic drugs (ranibizumab, pegaptinib or bevacizumab) or steroids (dexamethasone, triamcinolone acetonide or anecortave acetonide). Although several clinical trials are still running [97] the first results suggest a possible synergistic effect of combination therapy [171, 172]. Verteporfin showed benefit also in dermatology for treatment of non-melanoma skin cancers [173] and port-wine stains [174].

Lemuteporfin

Other names: QLT0074, diethylene glycol benzoporphyrin derivative.

Lemuteporfin, another photosensitizing drug developed by QLT, Inc., can be considered as a derivative of verteporfin. It is prepared by esterification of benzoporphyrin derivative diacid ring A with ethylene glycol (Scheme 5). Its photophysical properties are close to parent molecule of verteporfin (λ_{max} 690 nm) but its pharmacokinetic is much faster. In tests on DBA/2 mice lemuteporfin showed good uptake within first 15-20 minutes, very rapid clearance from whole body and lack of accumulation in skin [175, 176]. It did not show any prolonged photosensitivity.



Scheme 5. Synthesis of lemuteporfin.

In test on cells, lemuteporfin showed possibility of immunomodulatory answer. Sublethal doses may result in the modification of cell surface receptor expression levels and cytokine release and consequently influence cell behavior [177]. It seems to affect mainly activated T-lymphocytes [178]. Several studies, including clinical trials phase I/II [97, 179], have been performed also for treatment of benign prostate hyperplasia [180].

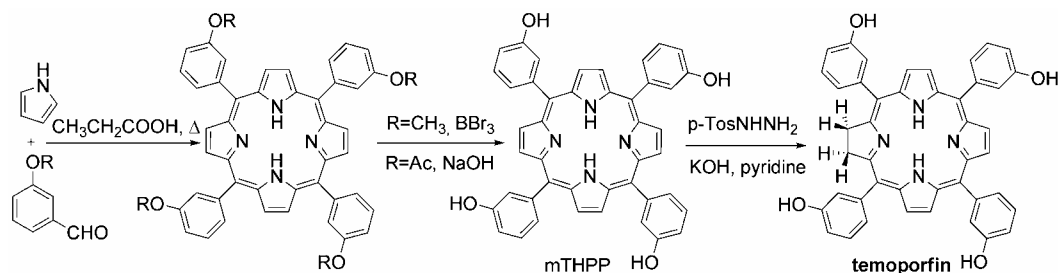
Temoporfin

Other names: *m*-tetrahydroxyphenylchlorin, *m*THPC, Foscan[®].

Temoporfin is a completely synthetic chlorin prepared by diimide reduction of double bond in 5,10,15,20-tetrakis(*m*-hydroxyphenyl)porphyrin (*m*THPP) which is fully built up from pyrrol and protected 3-hydroxybenzaldehyde [93] (Scheme 6). In a series of positional isomers, *ortho* substituted THPP caused skin photosensitization [181] and that is why it was not even introduced to studies with chlorins. Comparing *meta* and *para* substituted hydroxyphenylchlorins, the *meta* isomer showed much better cost/benefit ratio (expressed as damage to normal and tumor tissue, respectively) [182]. That is why 5,10,15,20-tetrakis(*m*-hydroxyphenyl)chlorin was chosen as the most suitable for clinical evaluation.

Temoporfin absorption is shifted to only 652 nm with $\epsilon \sim 30000 \text{ M}^{-1} \text{ cm}^{-1}$. Its solubility in water is not excellent, so it is administered in a mixture of water, ethanol and PEG. The best selectivity to tumor is achieved after 4 days and that is why it takes a long time between administration and irradiation protocol. However, recently a liposomal formulation of temoporfin showed the same efficacy [183] and high tumor/muscle or tumor/skin ratio were observed within few hours after administration [184]. It is very efficient photosensitizer, which enables administration in dose of only 0.15 mg/kg. Temoporfin has a low clearance with terminal plasma half-life 65 hours. Skin photosensitivity lasts for at least 15 days.

Biolitec Pharma has received the first approval for temoporfin in 2001 for treatment of head and neck cancer and it is still the only PDT-drug approved for this kind of cancer [185]. Good cosmetic results were obtained using this drug also for basal cell carcinoma (BCC) in clinical trials [186, 187]. The advantage of temoporfin over ALA-mediated PDT treatment of BCC is deeper penetration of activating light. Several other clinical trials were performed using this photosensitizer with satisfying results, including photodetection of brain tumors [188] and prostate cancer [189, 190].



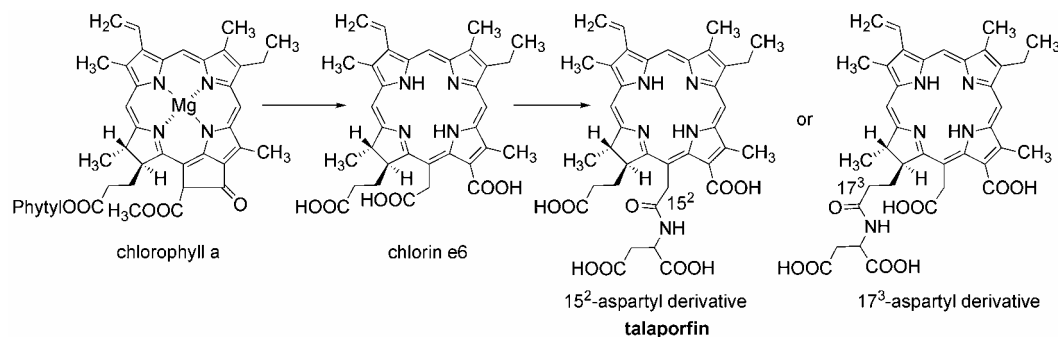
Scheme 6. Synthesis of temoporfin.

Talaporfin

Other names: mono-*L*-aspartyl chlorin e6, Npe6, LS11, MACE or Laserphyrin[®], Litx[™].

Talaporfin is a semisynthetic derivative of chlorin e6. Chlorin e6 is available directly from chlorophyll a (isolated from certain *Spirulina* species) under vigorous basic conditions [93]. Coupling of chlorin e6 with aspartic acid gives rise to mono-*L*-aspartyl chlorin e6 [191] (Scheme 7). However, three possible carboxy groups can be substituted during the reaction. In the beginning, the structure was attributed to 17³-aspartyl derivative mainly based on theoretical predictions of reactivity and sterical hindrance. Later, 2D NMR studies [192] and more recently also single crystal X-ray diffraction [193] confirmed unequivocally that the structure corresponds to 15²-aspartyl derivative. It was also accepted by WHO and INN name for talaporfin is attributed to 15²-regioisomer.

Q-band position of talaporfin occurs at 664 nm with $\epsilon \sim 40000 \text{ M}^{-1} \text{ cm}^{-1}$. Talaporfin in the form of tetra sodium salt is well water-soluble and can be administered at dose 40 mg/m² by *i.v.* injection without the need for any special solubilizing agent. Irradiation of tumors starts in 15-60 minutes after application of the drug because animal models have shown that the response corresponds rather to plasma levels of photosensitizer than to accumulation in tumor tissue [194]. It shows two compartment pharmacokinetic with alpha, beta and terminal half-lives to be 9 h, 106-136 h and 168 h, respectively [195, 196]. It causes only minimal skin photosensitivity, usually within 3-7 days [195, 197] with complete disappearance after 2 weeks [198].



Scheme 7. Synthesis of talaporfin.

Talaporfin sodium, under the name Laserphyrin[®], has been approved in Japan for treatment of early-stage bronchopulmonary cancer and is sold for that indication by Meiji Seika Kaisha, Ltd. It is also investigated by Light Sciences Oncology using Litx[™] technology for the treatment of liver cancer – both hepatoma (primary liver cancer) and liver metastasis of colorectal carcinoma [199]. They perform also clinical trials on treatment of glioma (brain tumor). Other performed clinical trials involve cutaneous diseases of various cancers [200], superficial squamous cell carcinoma of the lung [198] and showed future promise for the use of talaporfin as efficient and safe photosensitizer. Recent *in vitro* tests with HL-60 cells were performed using this drug in combination with ultrasound (sonodynamic therapy). These results suggest that it sonochemically induces apoptosis as well as necrosis in HL-60 cells [201].

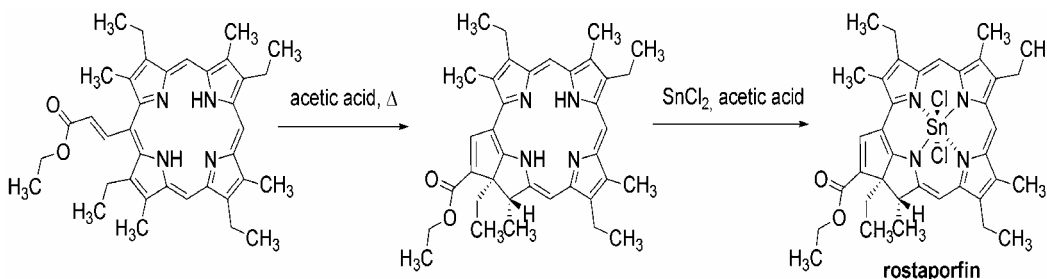
Rostaporfin

Other names: tin etiopurpurin, SnEt₂, Purlytin[™], Photrex[®].

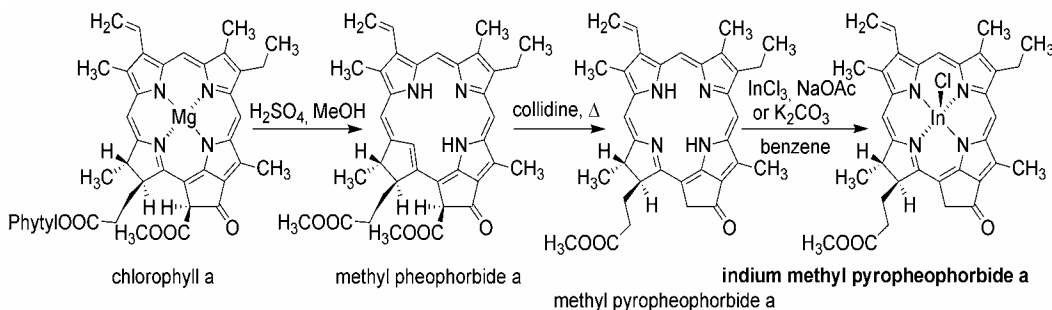
The purpurins are semisynthetic derivatives obtained by intramolecular cyclization of porphyrins *meso*-substituted with derivatives of acrylic acid [93]. Tin etiopurpurin has been prepared in 1988 by insertion of metal into corresponding purpurin derivative using SnCl₂ in acetic acid (Scheme 8) [202]. Although insertion of metal into purpurin macrocycle shifts its absorption hypsochromically for almost 30 nm, their tumoricidal activity was significantly greater [202] and that is why they were more suitable for PDT applications. From Ag, Ni, Sn and Zn, the most suitable metals were found to be Zn and Sn [202] and in following study on mice tin etiopurpurin showed the best results [203].

Rostaporfin absorbs at 659 nm with $\epsilon \sim 30000 \text{ M}^{-1} \text{ cm}^{-1}$. The compound is hydrophobic and has to be administered in emulsifying agent. The dose is usually 1.2 mg/kg, irradiation starts 24 h after administration.

The drug was developed by Miravant for treatment of AMD (wet form). The drug finished the phase III clinical trials and approval to FDA has been submitted. However, FDA required more trials to confirm efficacy and safety. Miravant has started the confirmation studies in late 2005 [97] but no information have been available since that time. Positive results were obtained with rostaporfin also for treatment of cutaneous metastatic cancers of various origin [204, 205] and treatment of canine prostate [206].



Scheme 8. Synthesis of rostaporfin.



Scheme 9. Preparation of indium methyl pyropheophorbide a.

Indium Methyl Pyropheophorbide A

Other names: MV6401, InCh

Indium methyl pyropheophorbide a is another lipophilic photosensitizer developed by Miravant. Methyl pyropheophorbide a is prepared using standard conditions. Chlorophyll a is isolated from *Spirulina* and demetalated using sulfuric acid in methanol. Thus prepared methyl pheophorbide a is thermally decarboxylated in collidine to yield methyl pyropheophorbide a and subsequently converted in benzene under basic conditions (sodium acetate or potassium carbonate) in the presence of InCl_3 to desired indium methyl pyropheophorbide a (Scheme 9) [207]. Due to low solubility in water it must be administered using delivery systems, in this case based on liposomes of egg yolk phosphatidylcholines. It absorbs at 664 nm, usual dosage in animal models is only about 0.1 mg/kg and it has plasma half-life about 20 min [208]. It has been tested for chorioidal neovascularization on animal models with positive results. The best selectivity for this application was achieved when the drug was activated short times after administration (from 10 min to 90 min) [209, 210] indicating importance of vascular targeting. On the other hand, tumor treatment responds better using new approach of fractionated photosensitizer dosing when both tumor tissue and tumor vasculature are affected [208].

2-(1-hexyloxyethyl)-2-devinyl Pyropheophorbide a

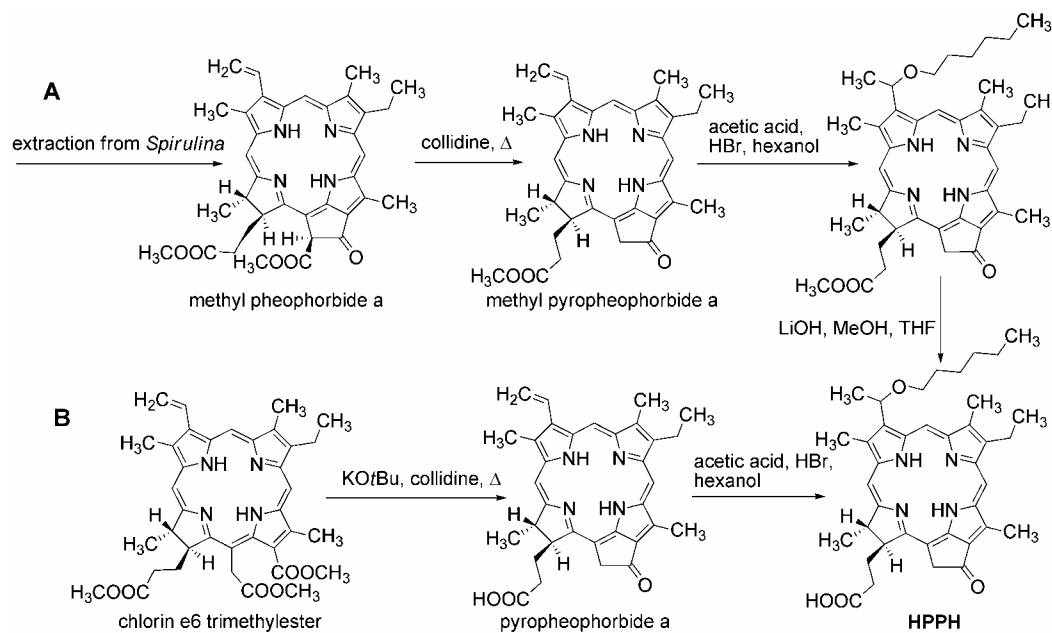
Other names: HPPH, Photochlor.

This photosensitizer is example of semisynthetic improvement of naturally occurring porphyrinoids developed in Roswell Park Cancer Institute [211]. HPPH is an extremely hydrophobic compound that was found, in a quantitative structure-activity relationship study that addressed the general property of lipophilicity, to be the most effective photosensitizer against murine tumors amongst a series of homologues with different numbers of methylene groups on the ether function [212]. The original 5-step method of synthesis starts from precursor methyl pheophorbide a which is isolated from *Spirulina maxima* and converted to methyl pyropheophorbide a by refluxing in collidine. Its vinyl group is hydrobrominated in next step and immediately reacted with hexanol. The methyl ester is then hydrolyzed using LiOH (Scheme 10-A) [213]. The older method was recently replaced using much simpler

and faster procedure (Scheme 10-B) [214]. It involves Dieckmann condensation and subsequent thermal decarboxylation of easily obtainable trimethylester chlorin e6 and allows preparation of this promising photosensitizer in large scale.

This second generation photosensitizer absorbs at 665 nm with $\epsilon \sim 47000 \text{ M}^{-1} \text{ cm}^{-1}$. Low solubility in water requires presence of solubilizers and therefore the drug is formulated in 5% dextrose in sterile water containing 2% ethanol and 1% polyoxyethylene sorbitan monooleate (Tween 80). However, a new nanocrystal suspension of HPPH without the need of any stabilizers was successfully tested recently and its *in vitro* and *in vivo* efficacy was comparable with above mentioned application form [215]. The tests of HPPH on patients are performed usually at doses 2-6 mg/m². Due to its high hydrophobicity, its pharmacokinetic is slow with plasma half-lives 7.7 h and 596 h and the drug can be detected in plasma even several month after single infusion [216]. In spite of such slow excretion, no or only minimal skin photosensitivity appears [217].

HPPH has been entered into phase I trials at Roswell Park Cancer Institute for early and late stage lung cancer [218]. Clinical trials for treatment of esophageal, head and neck and nonmelanomatous skin cancers are also under run [97].



Scheme 10. Methods of preparation of HPPH.

Padoporfin

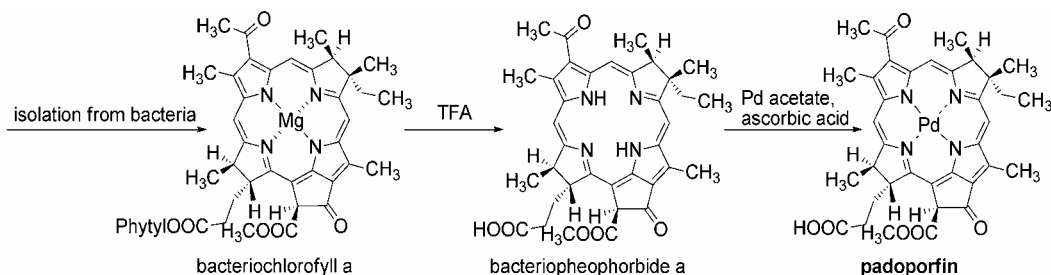
Other names: WST09, palladium bacteriopheophorbide a, Pd-BPheid, Tookad[®].

Padoporfin is example of semisynthetic modification of naturally occurring photosensitizers of bacteriochlorin family. In the first step, bacteriochlorophyll a is isolated from lyophilized bacteria *Rhodovulum sulfidophilum*. Transformation to bacteriopheophorbide a can be done either by direct treatment in trifluoroacetic acid (provides

both hydrolysis of phytol esters and demetallation) or phytols are hydrolyzed using enzyme chlorophyllase with subsequent acidic demetallation. Palladium is usually inserted using palladium acetate in the presence of ascorbic acid (Scheme 11) [219].

As padoporfin is a member of bacteriochlorin family, both double bonds out of the [18]annulene ring are reduced and its absorption is red-shifted to 763 nm and also strengthened ($\epsilon \sim 88000 \text{ M}^{-1} \text{ cm}^{-1}$). Padoporfin is not water soluble, so that it must be administered in a Cremophor-based vehicle, in which a fraction of the drug is aggregated upon administration but disaggregates rapidly *in vivo*. Typical dose in human and animal models is 2 mg/kg. It is rapidly excreted from the body with no important accumulation. Plasma half-life in humans is about 20 minutes. Using mouse models, it was not detected in skin or muscles at all and plasma was cleared from the drug within 3 hours [220]. As a probable consequence of no skin accumulation, no photosensitivity was observed on patients in phase I clinical trials [221]. Due to fast clearance from the body, the irradiation usually starts during administration and the effects are contributed almost exclusively to vascular targeted PDT [84].

Padoporfin is tested as possible PDT-drug for prostate cancer and clinical trials phase II/III are under run [97]. Its efficacy and safety have been already confirmed both on human [84] and dogs [222, 223]. Based on vascular effects, it has also high potential to treat chorioidal neovascularization [224].



Scheme 11. Synthesis of padoporfin.

PHTHALOCYANINES

Phthalocyanines (Pc) are synthetic dyes used in many industrial applications [225]. They are structurally related to tetraazaporphyrins, with the four bridging carbon atoms at the *meso*-positions replaced by nitrogen atoms. Moreover, Pcs have benzene rings fused to the β -positions of each of the four pyrrolic subunits. This benzene ring addition strengthens the absorption of the chromophore in the near infrared region and shifts the maximum more to the red region [226]. Their high extinction coefficients and appearance of the absorption spectra Q-bands in 670–700 nm region suggest them as potentially suitable molecules for PDT [227]. Unlike of the HpD and some other porphyrin-type dyes, the presence of a suitable chelated metal atom (preferentially Zn, Al, Si) is essential for their photodynamic activity [226]. Comparative advantage of the Pcs considering the PDT is their high singlet oxygen quantum yield. However, they have also some unfavorable properties, which limit their

photodynamic applications. Owing to the extended π -electron system, they exhibit a strong tendency to aggregation resulting in dimeric and oligomeric species formation in solutions [228]. It has been shown that such association of the Pc molecules greatly influences their spectroscopic [229], photophysical [230], electrochemical [231], and conducting properties [232], and it decreases solubility in both water and organic solvents. The aggregation makes the purification and characterization of the Pc problematic and shortens their triplet-state lifetime so reducing the singlet oxygen quantum yield.

Apart from the considerable influence of the solvent and concentration of the Pc in solution [233], the aggregation can be suppressed by several structure modifications: chelation of central atoms with more coordinating sites with following central atom substitution [234], introduction of aliphatic bulky substituents to the periphery of the Pc macrocycle [235-237], introduction of eight anionic [238] or eight cationic [239] ionized moieties or eight quarternary ammonium substituents [240] on the periphery, which causes a complete monomerization especially in water environment. The use of less than four cationic [241, 242] or anionic [243] peripheral substituents suppresses the aggregation only partially. There are three Pcs in clinical trials or clinical PDT (Figure 7).

Zinc Phthalocyanine CGP55847

Other names: ZnPc

It is the simplest Pc in clinical trials. Because of its very low solubility a liposomal formulation has been developed by QLT Phototherapeutics (Vancouver, Canada) and it has undergone clinical trials phase I/II in Switzerland (sponsored by Ciba Geigy, Novartis, Basel, Switzerland) for treatment of squamous cell carcinomas of the upper aerodigestive tract [244, 245].

Photosens

Other names: Aluminium tetrasulfophthalocyanine, Al-PcTs, AlPcS4, Aluminium phthalocyanine tetrasulfonate

Considerable attention has been paid to the sulfonated phthalocyanines. This type of peripheral substitution both decreases the aggregation and increases the water solubility of Pc. The sodium salts of a mixture of peripherally di- to tetrasulfonated chloro aluminium phthalocyanines (absorption maximum of Q-band in water at 676 nm) is used in Russia since 2001 for human PDT as Photosens [246]. It is approved and used for treatment of cancer of stomach, skin [247], lips, oral cavity, tongue [248, 249], and multidrug resistant skin and subcutaneous metastases of breast cancer [250]. The drug is administered as a 0.2% solution in the isotonic sodium chloride/water solution, in doses of 0.5-0.8 mg/kg of body weight in the case of a systemic administration. Because of relatively long term photosensitization, the patient should avoid intense day light exposition for a period of 4 to 6 weeks.

Another sulfonated phthalocyanine, zinc phthalocyanine tetrasulfonate, finished in 2007 Phase I clinical trial of the use as a photosensitizer for photodynamic therapy in dogs [251].

Pc4

Other names: SiPc IV.

The third Pc on the way to clinical PDT is a silicon complex Pc4. Its ability to kill HIV viruses in red blood cells concentrates was examined by V.I. Technologies, Melville, NY, USA. Currently, the Pc4 starts two Phase I clinical trials for the topical treatment of malignant and pre-malignant skin conditions [97, 252].

Naphthalocyanines (Ncs) are Pc derivatives with additional benzene rings attached to each isoindole subunit on the periphery of the Pc structure. Thanks to the extended chromophore system, the Ncs exhibit strong absorption maxima at wavelengths of approx. 740-800 nm, which predisposes them as good potential PS with two outstanding advantages: possibility of employment of high wavelength light with deeper tissue penetration and especially application on highly pigmented skin lesions [253-255], since they absorb above the absorption region of the melanins, reaching only slightly over 700 nm. They have been investigated also for effectiveness against other types of cancer [256-260]. However, there are some problems to be resolved at the Nc as photosensitizers: comparatively low both chemical and photochemical stability, even higher tendency to aggregation than Pcs and consequently also even worse solubility [226]. Relatively big molecule can also limit their ability to cross biological membranes.

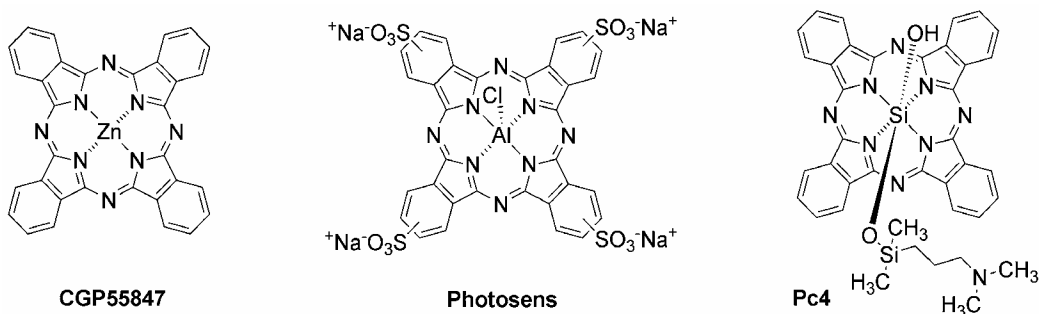


Figure 7. Phthalocyanines that entered clinical trials.

TRICYCLIC DYES

Although vast majority of examined and used photosensitizers is of the porphyrin structure, there are some additional chromophores exhibiting photodynamic activity after irradiation by red light. Among the most important belong the phenothiazinium dyes [261] and xanthenes. Their use as photosensitizers is supported by several reasons, including good water solubility, satisfactory singlet oxygen production at the best of them, main absorption peak in the “phototherapeutic window” and relatively low price and good availability.

The main drawback of the phenothiazinium structure is its metabolic instability. It undergoes relatively quick enzymatic reduction to its leuco-form, which is photodynamically inactive. Therefore, their use in PDT is limited mainly to topical application in dermatology or local treatment after intratumoral injection. The strongly polar character caused by ionic

structure of their molecules also limits ability of the phenothiazinium salts to cross the cell membranes and other lipophilic biological barriers. Considerable dark toxicity of the main commercially available phenothiazinium dyes found at some cell lines could be also a disadvantage for systemic clinical use [262].

Some attempts to improve the phototherapeutic properties of phenothiazinium salts and their analogues were done in effort to obtain compound absorbing at higher wavelengths, compounds with increased singlet oxygen production, or with moderately enhanced lipophilicity [263, 264]. These targets could be achieved by some ring system substitutions, e.g. halogenation, which is known to enhance the singlet oxygen quantum yield [261]. Even better results can be achieved by isosteric replacement of heteroatom in basic structure by an another one with extended electron system (O→S→Se) [261, 265, 266]. On the other hand, the expanded aromatic system of benzo [a]phenothiazinium salts or their benzo [a]phenoxazinium analogues with red-shifted absorption maxima usually resulted in decreased singlet oxygen production [265, 267]. Although some of the newly prepared compound exhibited improved some of the photodynamic properties, until now the well-known dyes stay the only used in human clinical treatment.

As already mentioned above, the phenothiazinium photosensitizers could be successfully used especially in external topical or internal local application. In such cases they can considerably spread the scope of photodynamic therapy to involve antimicrobial [268] and antifungal [269] PDT and melanoma [270]. Methylene blue and toluidine blue O have been the most frequently explored, even if also some other dyes have been tested for their photodynamic activity.

Methylene Blue

Chemical name and synonyma: 3,7-bis(dimethylamino)phenothiazinylium chloride, methylthioninium chloride.

Methylene blue (MB) (Figure 8) is the most common phenothiazinium dye, primarily used in histology for staining. It shows a strong absorption band in range of 550-700 nm with maximum at 664 nm. In high concentrated solutions and in acidic environment, the arising dimers show shift of the absorption maximum to 590 nm.

A comprehensive review of photophysical, photochemical, and biological properties as well as of the experimental clinical use of MB was done by Tardivo *et al.* The authors describe the main human clinical applications including basal cell carcinoma, Kaposi's sarcoma, melanoma, and some non-cancerous skin conditions like onychomycosis, skin HSV infections and warts [271]. MB mediated PDT of melanoma seems to be more effective than in the case of 5-ALA or HpD. The latter compounds shown low efficiency [272], while MB treatment exhibited complete response of the tumor in more than 60% [270, 271]. Important photodynamic application of MB is the photodynamic inactivation of pathogens in blood *ex vivo* [273, 274].

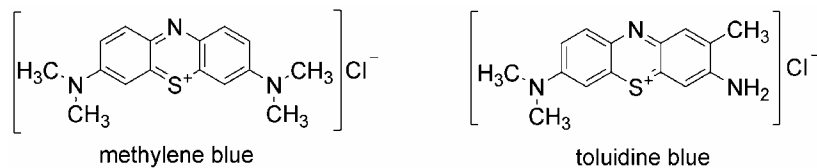


Figure 8. Structures of methylene blue and toluidine blue.

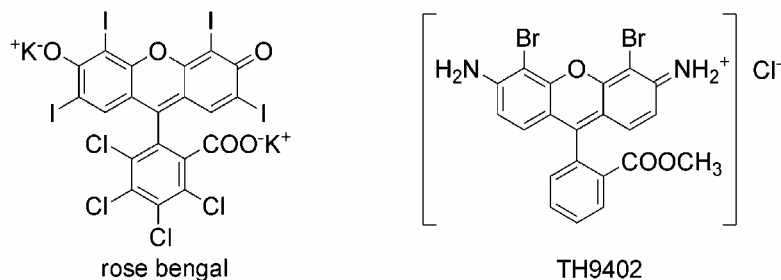


Figure 9. Structures of rose bengal and brominated rhodamin TH9402.

Toluidine Blue

Chemical name and synonyma: 3-amino-7-dimethylamino-2-methylphenothiazinylium chloride, tonium chloride.

Toluidine blue (TB) (Figure 8) is a second important phenothiazinium dye in PDT. Its absorption maximum is only about 625 nm and the singlet oxygen quantum yield is also somewhat lower than in the case of methylene blue [261, 275, 276]. TB has been also tested for various photodynamic application, e.g. for treatment of cystic fibrosis [277] and in a mucoadhesive patch formulation in topical photodynamic treatment of fungal infections of the mouth [278]. However, the best results were achieved in inactivation of human mouth plaque bacteria [279-284] or in animal model of periodontitis [285]. This was the reason for introduction the dye as photosensitizer in photoactivated oral disinfection technique. It is used by the PerioWave™ system [286], which finished phase III clinical study in December 2006 [97] and approached clinical praxis. It is marketed by Ondine Biopharma Corporation (Canada) [287]. Another photoactivated oral disinfection technique system was introduced by Denfotex Ltd (UK) [288].

Rose Bengal

Another tricyclic dyes known to have photodynamic properties are xanthene structure based photosensitizers. While the non-substituted xanthene dye fluoresceine shows excellent fluorescence but negligible singlet oxygen production, the halogenation of the xanthenes structure results in good singlet oxygen quantum yields. The photodynamic potential of rose bengal (RB) (Figure 9) was confirmed in both physico-chemical [289] and cell culture experiments [290, 291] as well as against viruses [292]. Since the relatively selective uptake of the RB by tumor cells unlike of normal cells, the dye was selected by the Provectus

Pharmaceuticals Inc. (USA) as promising candidate for treatment of some cancer and other lesions [293]. Currently it is in the phase I study for treatment of recurrent breast carcinoma, phase II study for treatment of metastatic melanoma and phase II study in form of topical aqueous gel for photodynamic therapy of psoriasis [97].

Rhodamines

Properly substituted iminoxanthene dyes – rhodamines – also exhibited potential for PDT. Rhodamine dyes frequently used in microbiology and molecular biology for staining and as fluorescent tools showed highly selective uptake into neoplastic unlike normal hematopoietic progenitor cells [294]. This phenomenon suggested possibility of selective neoplastic cells photoeradication via *ex-vivo* photodynamic treatment [295].

Since the basic rhodamine derivatives exhibit only low singlet oxygen production, halogenation of their molecule analogously to fluoresceine was performed, because it was described to increase the efficiency of the intersystem crossing to the triplet state and consequently to increase the singlet oxygen quantum yield [39]. The 4,5-dibromorhodamine methyl ester (TH9402, Theratechnologies, Montreal, QC, Canada) (Figure 9) was selected as the most promising, with low dark toxicity and satisfactory stability. Its absorption maximum in water solution is 504 nm. Preparations with this brominated rhodamine are under development by Kiadis Pharma (The Netherlands) [97, 296]. TH9402 under name Reviroc™ starts phase II clinical trial on autologous stem cells transplantation at patients with blood cancer [97]. The same dye has finished phase II clinical trial for prevention (as ATIR™) and treatment (as Rhitol™) of Graft Versus Host Disease (GVHD).

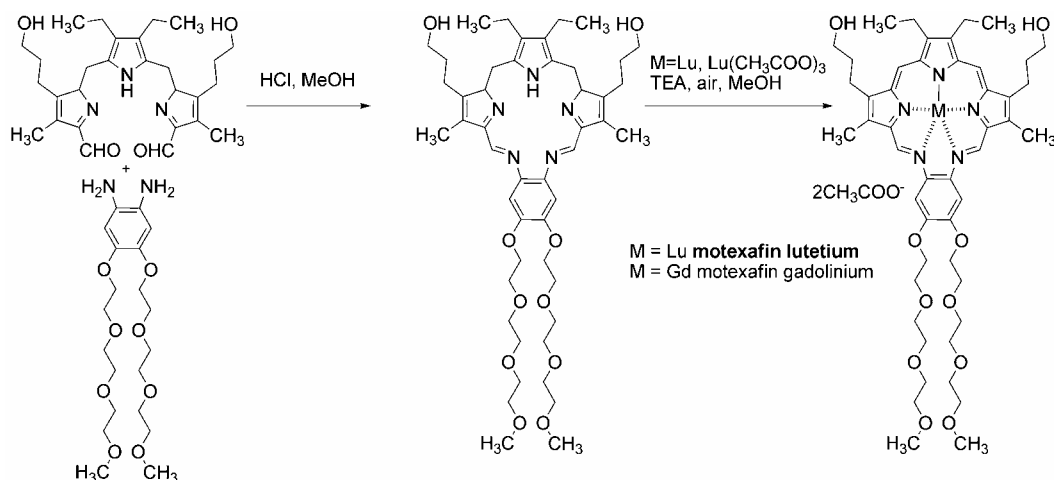
OTHER PHOTSENSITIZERS

Motexafin Lutetium

Other names: Lu-Tex, Optrin, Antrin, Lutrin, PCI-0123.

Motexafin lutetium is a member of texaphyrin group, a Texas shape macrocycles with pentaaza core [297]. Texaphyrins are completely synthetic dyes prepared for the first time in 1987 [298]. The core is built by condensation reaction of substituted *o*-phenyldiamine with diformyltripyrane, which is obtained using condensation of three suitably substituted pyrrol rings. The macrocyclic ligand is then oxidatively metallated using lutetium(III) acetate and triethylamine in air-saturated methanol (Scheme 12) [299].

Thanks to presence of polar peripheral groups, motexafin lutetium is a water soluble photosensitizer. It absorbs at 732 nm with $\epsilon \sim 42000 \text{ M}^{-1} \text{ cm}^{-1}$. Dose is approximately 2-3 mg/kg, however, the optimal times of illumination vary with the treatment target. For example, the prostate cancer is illuminated 3 h postinjection, while coronary artery disease and breast cancer treatment use 18-24 h illumination delay. The drug is retained in neoplastic tissues and neovascularization. It binds well to lipoproteins so it may have activity against atherosclerotic plaques [300]. The drug is rapidly excreted from the body with half-life in tens of hours (13-39 h) [300].



Scheme 12. Synthesis of motexafin lutetium.

Motexafin lutetium is a prospective treatment for human prostate adenocarcinoma. However, the observed variation in PDT dose distribution translates into uncertain therapeutic reproducibility [301] and suggests the use of individualized treatment planning for prostate PDT [302]. Other neoplastic conditions treated with motexafin lutetium include recurrent breast cancer [303] and due to absorption at higher wavelengths it allows also treatment of melanoma [304]. As the drug specifically localizes also within atheromatous plaque, it may be used in a novel therapeutic approach for atherosclerosis – photoangioplasty [300, 305].

The motexafin ligand can bind also other lanthanide metals, the most important being gadolinium. Complexation with gadolinium does not form a photosensitizer for PDT but the drug can be used for cancer treatment based on different mechanism of action. It accumulates selectively in cancer cells due to their increased rates of metabolism. Once inside the cell, it induces apoptosis (programmed cell death) by disrupting redox-dependent pathways. Motexafin gadolinium inhibits the enzyme thioredoxin reductase, which is a tumor growth promoter. This mechanism provides the opportunity to use the drug in a wide range of cancers. Gadolinium is paramagnetic, and therefore is detectable by magnetic resonance imaging (MRI), allowing the visualization of the drug in tumors [306].

Porphycenes are fully synthetic constitutional isomers of porphyrins [307]. Porphycene derivatives show higher absorption than porphyrins in the red spectral region ($\lambda > 600$ nm, $\epsilon > 50000$ M⁻¹ cm⁻¹) owing to the lower molecular symmetry. Photophysical and photobiological properties of porphycenes make them suitable candidates as photosensitizers, showing fast uptake and diverse subcellular localizations (mainly membranous organelles) [308]. The most studied porphycene for PDT application is perhaps acetoxy-2,7,12,17-tetrakis-(β -methoxyethyl)-porphycene (ATMPn) absorbing at 640 nm which has been evaluated for PDT application both *in vitro* [309, 310] and *in vivo* [311].

Hypericin, an aromatic diantraquinone originating from the herb *Hypericum perforatum*, exhibits photodynamic action too [312]. It absorbs at 590 nm with $\epsilon \sim 44000$ M⁻¹ cm⁻¹. Several *in vitro* and *in vivo* tests have evaluated this photosensitizer for treatment of various cancers using PDT [313]. Clinical trials were performed on patients with squamous cell carcinoma and basal cell carcinoma [314].

Also mixtures of different photosensitizers isolated from natural sources are used in therapy. Thus, *Radachlorin*[®] developed in Russia is a *Spirulina* extract containing purpurin 5, chlorin e6 and purpurin 18 as alkali metal salts [315]. On the other hand, its manufacturer states slightly different composition: chlorin e6 (90-95 %), chlorin p6 (5-7%) and the third chlorin which is not preferred to be disclosed (1-5%) [316]. It is administered at dose from 0.2 to 1 mg/kg and irradiated using light of wavelength 662 nm, irradiation starts usually 2-5 hours after administration. Photosensitivity is very short; patient should avoid direct sunlight for about 24 hours.

NEW APPROACHES CONNECTED WITH PDT

PDT is not the only one new approach to treat cancer. Several new techniques took some advantages of PDT to find new mechanisms of better selectivity to tumors, simpler administration, higher efficiency or they are trying to remove some limitations concerned with PDT. They include e.g. catalytic therapy, photothermal therapy, photochemical internalization and sonodynamic therapy.

Catalytic Therapy (CT)

Catalytic therapy (CT) is a cancer treatment modality based on the generation of reactive oxygen species (ROS) using a combination of substrate molecules and a catalyst. Contrary to PDT, it does not require activation by light that limits the PDT treatment only to tissues and areas accessible to light or light-producing devices. The radicals are formed after the oxidation of substrate (most often ascorbic acid) with oxygen catalyzed by phthalocyanine metal (cobalt or iron) complexes (Figure 10). Recently, also porphyrins were found to be effective in CT [317].

The mechanism involves formation of the superoxide anion in the first step which is followed by the production of hydrogen peroxide and hydroxyl radical [318, 319]. The most promising compound for CT is a sodium salt of cobalt(II)-2,3,9,10,16,17,23,24-octacarboxyphthalocyanine, developed under the name Theraphthal[®] (Figure 10).

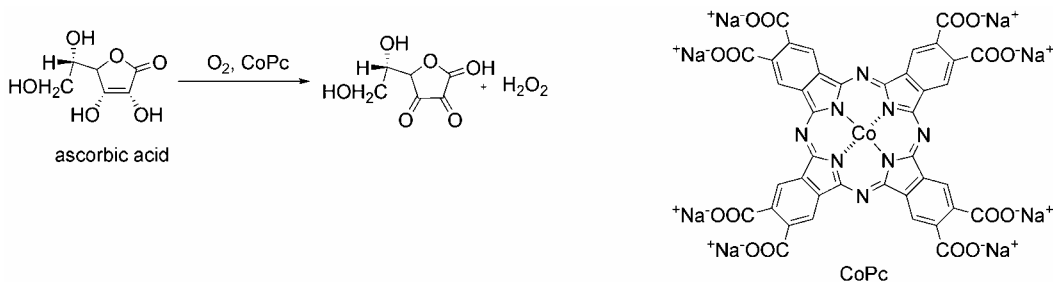


Figure 10. Mechanism of hydrogen peroxide formation in catalytic therapy and structure of the most studied compound Theraphthal[®] (CoPc).

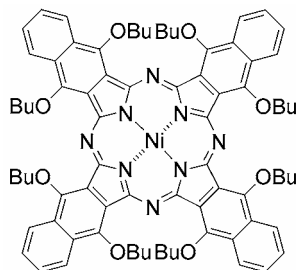


Figure 11. Structure of Ni(II)-5,9,14,18,23,27,32,36-octabutoxy-2,3-naphthalocyanine used in photothermal therapy.

Photothermal Therapy (PTT)

This new approach is based on the promotion of photothermally sensitized processes in tumor cells or tissues. Photothermal processes reflect the tendency of a light-absorbing species to dissipate electronic excitation energy through heating the local environment [320]. The temperature rise can reach 130 °C above the basal value [320]. The consequent sudden expansion of the proximate water shell generates a shock wave which leads to extensive mechanical (*e.g.* ultrasonic shock) and chemical (*e.g.* bond cleavage) damage. This method does not require presence of oxygen and efficiently works in its absence [321]. Similar compounds (phthalocyanines, porphyrins) as in the PDT can be used for therapy and the effect of both methods is considered to be synergistic. The aggregation of sensitizers which is often a problem in PDT, because it strongly decreases singlet oxygen production, is on the other hand an advantage in PTT since the energy is then released preferentially in the form of heat. Therefore, PTT allows the use of sensitizers with enlarged hydrophobic macrocycles (*e.g.* naphthalocyanines) which often tend to strong aggregation in biological media. Also their absorption at wavelength far behind 800 nm cannot be used for efficient production of singlet oxygen due to possible low energy of triplet state. Irradiation of the targets is performed by strong laser pulses.

Several *in vitro* [40] and *in vivo* [320, 322] tests confirmed efficiency of this approach which is oxygen independent and uses wavelength which penetrates deeper through human tissues. The most studied sensitizer in PTT is Ni(II)-5,9,14,18,23,27,32,36-octabutoxy-2,3-naphthalocyanine (Figure 11) absorbing at wavelength 850 nm with $\epsilon \sim 280000 \text{ M}^{-1} \text{ cm}^{-1}$.

Photochemical Internalization (PCI)

Photochemical internalization (PCI) is a technology for light-directed drug delivery and was developed to introduce therapeutic molecules in a biologically active form specifically into diseased cells [323]. In this case, photosensitizers do not serve as therapeutic agents but only as delivery enhancers.

It is widely acknowledged that macromolecules have great potential as therapeutic agents. However, their use is often limited because they do not leave the endosomes within cells after endocytosis. Adjacently substituted photosensitizers (*e.g.* disulfonated phthalocyanines and

meso-phenylporphyrins (Figure 12)) localize primarily into membranes of lysosomes and endosomes of cells. After irradiation, these subcellular structures rupture and release their content. So, the PCI principle is based on common administration of photosensitizer and the macromolecule drug into blood stream. They are both taken up into endosomes of targeted cells and macromolecules are released into cytosol after irradiation [324, 325] (Figure 12). This approach showed *in vitro* increased uptake for several types of molecules, e.g. protein toxins [326], oligonucleotides [327], nanoparticles [328] and many others. It also proved to be efficient *in vivo* in improvement of tumor therapy using protein toxins [329], gene therapy [330] and delivery of bleomycin [331]. The most studied photosensitizers are disulfonated aluminium phthalocyanine and disulfonated tetraphenylporphyrin where sulfonation takes place on adjacent benzene (or phenyl) rings. Clinical trials on patients treated with bleomycine-PCI shall start soon [325].

Sonodynamic Therapy

Sonodynamic therapy (SDT) is a treatment employing combination of ultrasound in doses which are normally non-destructive to tissues and a chemical called sonosensitizer, which is non-toxic without the exposition to the ultrasound. The idea is similar to the one of photodynamic therapy, replacing the light by ultrasound, which brings an advantage of much deeper penetration of the activating agent into the tissues. Often similar types of sensitizers are used. Also in some studies an improved effectiveness was observed using the PDT and SDT *in combination*.

Ultrasound is a mechanical wave realized by vibrations of particles of medium, where the ultrasound is spread, at frequencies equal to or higher than 20 kHz. It is generally considered as safe and used commonly in medical diagnostic methods. However, it can interact with biological media and the interactions can be amplified in presence of the sonosensitizers. Unlike of the photosensitizers, the mechanism of ultrasound enhanced cytotoxicity is probably different at various types of molecules tested as sonosensitizers [332].

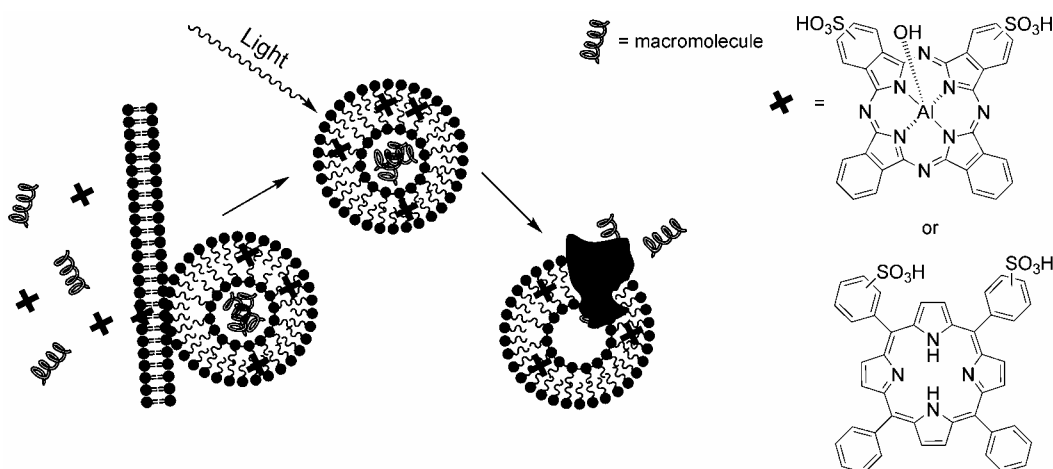


Figure 12. Mechanism of action of photochemical internalization and structures of two most studied photosensitizers in this application.

Among suggested mechanisms of sonodynamic therapy belong:

- (1) hydrodynamic stress caused by fast moving bubbles in the tissue, where sonosensitizers work probably as membrane destabilizing molecules physically reducing the strength of the cell membrane, as described e.g. at extracellular localized porphyrins [333, 334];
- (2) generation of sonosensitizer derived peroxy, alkoxy and/or other free radicals resulting in peroxidation of membrane lipids chains or similar radical damage of cells [335];
- (3) the sonosensitizer attributed physical destabilization of the cell membrane rendering the cell more susceptible to shear forces or ultrasound enhanced drug transport across the cell membrane (sonoporation) [336];
- (4) singlet oxygen formation as a result of sonoluminescence caused by the ultrasound in tissue, which was observed e.g. at hematoporphyrin [337, 338], porfimer [339, 340], gallium-porphyrin complex [341], pheophorbide a [342], rose bengal [343], and some other compounds.

The mechanism of mutual potentiation of PDT and SDT when used in combination can be attributed to a combination of different mechanisms of action and also to the ability of the ultrasound to monomerize aggregated photosensitizers [344].

Until now, various types of compounds have been tested in combination with ultrasound in order to find possible increased toxicity of the combined treatment unlike of the sole components. We would like to concentrate more on the compounds possessing both the photo- and sonosensitizing activities, while the “pure” sonosensitizers we mention only marginally, since their mechanisms of action usually does not include photodynamic components. Among sonosensitizing compounds without photodynamic activity or with potential of singlet oxygen formation, but not absorbing in the “phototherapeutic window” belong some alkylating anticancer drugs [345-347], anthracycline anticancer antibiotics, especially to adriamycin or its derivatives [348-352], oxiam-type non-steroidal anti-inflammatory drugs piroxicam and tenoxicam [353, 354] and some azo-dyes [355, 356].

Unlike the alkylating agents and anthracyclines the *porphyrins* are non-toxic when administered without additional treatment. The combined use of the hematoporphyrin and ultrasound was tested in several studies. In most of the cases, the enhanced cell killing was observed. The results of the studies suggest that the cell damage enhancement is probably mediated *via* singlet oxygen generated by ultrasonically activated hematoporphyrin [357-360].

On the other hand, no significant ultrasound mediated cytotoxicity of hematoporphyrin was observed in the cases when extracellular fraction of the sensitizer was removed or missing [333, 334]. Therefore it seems to be probable that only the extracellular porphyrin sensitizer participates in the ultrasound-induced interactions. Similar findings were described also at some other porphyrins tested for their sonodynamic activity [332]. The sonodynamically induced antitumor effect was also confirmed at porfimer sodium against mammary tumor grow in rats [361], at protoporphyrin IX against sarcoma 180 cells grow [362, 363] and at Photofrin II in several various studies. The effect were dose dependent [339, 364-366]. Another porphyrin derivative tested for its sonodynamic activity is 7,12-bis(1-decyloxyethyl)-Ga(III)-3,8,13,17-tetramethylporphyrin-2,18-dipropionyl-diaspartic acid

(ATX-70). Similarly to Photofrin II, a dose dependent ultrasound mediated cytotoxicity was observed [333, 334, 367-369].

A *chlorin* derivative 4-formyloxymethylidene-3-hydroxy-2-vinyl-deuterioporphynyl (IX)-6,7-diaspartic acid (ATX-S10) was successfully tested on both cells and animal model for its sonodynamic activity, with more than two-fold increase of cytotoxicity after combined application compared to ultrasound alone [370]. Sonodynamically induced apoptosis, caspase-3 activation and nitroxide generation were observed after application of ultrasound in the presence of talaporfin on HL-60 cells [201]. Up to a twice enhanced sonodynamically induced antitumor effect of pheophorbide-a was observed both *in vitro* and *in vivo* on sarcoma 180 cells or tumors [342].

A second-generation photosensitizer, chloroaluminium *phthalocyanine* tetrasulfonate (Photosens) was subjected to activation by ultrasound 24 hr after intravenous application to mice bearing subcutaneously localized colon 26 carcinoma. The combined treatment showed significant effect, although total eradication of the tumor was not achieved [371]. Simple zinc and chloroaluminum phthalocyanines were effective as potential sonosensitizers as well [372].

The xanthene structure based photosensitizing compounds rose bengal and erythrosine B has been successfully tested for its sonosensitizing effectiveness on sarcoma 180 cells. The application of ultrasound increased the dye cytotoxicity up to three times and five times, respectively [343, 373].

CONCLUSION

PDT generally is a very effective treatment, almost without any developed resistance to drugs and perfectly targets the diseased tissues. The great advantage of PDT in targeting the chosen area is, at the same time, the major drawback. PDT is a localized therapy; it means you treat only what you see, the metastases disseminated through the whole body, unfortunately, are not treatable.

Since the times of Raab and von Tappeiner, the photodynamic therapy has come a long way. Scientists have uncovered the mechanisms of this procedure, developed several compounds accepted in clinical practice for treatment of various diseases and still are searching for more suitable photosensitizers. Similarly to development of every new group of drugs, the first accepted compound (porfimer, 1993, Canada) is of course not lacking side effects. However, the newest compounds seem to get very close to the "optimal" photosensitizer for therapy. Their photophysical, photochemical, and sometimes also pharmacokinetic properties were optimized for chosen treatments, although there is still a long way to go before they will be accepted in practice.

ACKNOWLEDGEMENT

The work was supported by Research Project MSM 002160822.

REFERENCES

- [1] Ackroyd, R., Kelty, C., Brown, N. and Reed, M. (2001). The history of photodetection and photodynamic therapy. *Photochem. Photobiol.*, *74*, 656-669.
- [2] Moan, J. and Peng, Q. (2003). An outline of the hundred-year history of PDT. *Anticancer Res.*, *23*, 3591-3600.
- [3] Manniche, L.: Egyptian Luxuries: Fragrance, aromatherapy, and cosmetics in pharaonic times. Cairo: American University in Cairo Press; 1999.
- [4] Shaat, M. and Shaat, N.: Ancient Egyptian cosmetics, toiletries and essentials oils. In: *IFSCC 23rd Congress: 2004*; Orlando, Florida; 2004: paper 7.
- [5] Boulos, L.: Flora of Egypt. vol. 1 and 2: Egypt: Al Hadra Publishing; 2000.
- [6] American Academy of Dermatology (1994). Guidelines of care for phototherapy and photochemotherapy. Practice management information. *J. Am. Acad. Dermatol.*, *31*, 643-648.
- [7] Ledo, E. and Ledo, A. (2000). Phototherapy, photochemotherapy, and photodynamic therapy: Unapproved uses or indications. *Clin. Dermatol.*, *18*, 77-86.
- [8] Fitzpatrick, T. B. and Pathak, M. A. (1959). Historical Aspects of Methoxsalen and Other Furocoumarins. *J. Invest. Dermatol.*, *32*, 229-231.
- [9] Daniell, M. D. and Hill, J. S. (1991). A History of Photodynamic Therapy. *Aust. N. Z. J. Surg.*, *61*, 340-348.
- [10] Parrish, J. A., Fitzpatrick, T. B., Tanenbau., L and Pathak, M. A. (1974). Photochemotherapy of Psoriasis with Oral Methoxsalen and Longwave Ultraviolet-Light. *N. Engl. J. Med.*, *291*, 1207-1211.
- [11] Scherer, H. (1841). Chemisch-physiologische untersuchungen. *Ann. Chem. Pharm.*, *40*, 1.
- [12] Thudichum, J. L. W.: Report on researches intended to promote an improved chemical identification of disease. London: HMSO; 1867; 152-233.
- [13] Hoppe-Seyler, F. (1871). The haematins. *Tubinger Med. Chem. Untersuchungen*, *4*, 523-533.
- [14] Finsen, N.: Phototherapy. London: Arnold; 1901.
- [15] Raab, O. (1900). Über die Wirkung fluoreszierender Stoffe auf Infusorien. *Z. Biol.*, *39*, 524-546.
- [16] Prime, J.: Les accidentes toxiques par l'eosinate de sodium. Paris: Jouve and Boyer; 1900.
- [17] von Tappeiner, H. and Jesionek, A. (1903). Therapeutische Versuche mit fluoreszierenden Stoffen. *Münch. Med. Wochenschr.*, *47*, 2042-2044.
- [18] von Trappeiner, H. and Jodlbauer, A. (1904). Über Wirkung der photodynamischen (fluorieszierenden) Stoffe auf Protozan und Enzyme. *Dtsch. Arch. Klin. Med.*, *80*, 427-487.
- [19] von Tappeiner, H. and Jodlbauer, A.: Die Sensibilisierende Wirkung fluorieszierender Substanzer. Gesamnte Untersuchungen über die photodynamische Erscheinung. Leipzig: F. C. W. Vogel; 1907.
- [20] Hausmann, W. (1908). Über die sensibilisierende Wirkung tierischer Farbstoffe und ihre physiologische Bedeutung. *Biochem. Z.*, *14*, 275-278.

-
- [21] Hausmann, W. (1911). The sensitizing action of haematoporphyrin. *Biochem. Z.*, *30*, 276-316.
- [22] Fisher, H. and Meyer-Betz, F. (1912). Formation of porphyrins. *Z. Physiol. Chem.*, *82*, 96-108.
- [23] Meyer-Betz, F. (1913). Untersuchungen über die Biologische (photodynamische) Wirkung des Haematoporphyrins und anderer Derivative des Blut- und Galenfarbstoffs. *Dtsch. Arch. Klin. Med.* *112*, 476-503.
- [24] Policard, A. (1924). Etudes sur les aspects offerts par des tumeurs experimentales examinee a la lumiere de Woods. *Compt. Rend. Soc. Biol.*, *91*, 1423-1424.
- [25] Figge, F. H. J., Weiland, G. S. and Mangeniello, L. O. J. (1948). Affinity of neoplastic, embryonic and traumatized regenerating tissue for porphyrins and metalloporphyrins. *Proc. Soc. Exp. Biol. Med.*, *68*, 143-146.
- [26] Rasmussen-Taxdal, D.S., Ward, G. E. and Figge, F. H. (1954). Fluorescence of human lymphatic and cancer tissues following high doses of intravenous hematoporphyrin. *Surg. Forum*, *5*, 619-624.
- [27] Lipson, R. L., Baldes, E. J. and Olsen, A. M. (1961). Use of a Derivative of Hematoporphyrin in Tumor Detection. *J. Natl. Cancer Inst.*, *26*, 1-11.
- [28] Lipson, R. L., Baldes, E. J. and Olsen, A. M. (1964). Further Evaluation of the Use of Hematoporphyrin Derivative as a New Aid for the Endoscopic Detection of Malignant Disease. *Dis. Chest*, *46*, 676-679.
- [29] Gray, M. J., Lipson, R., Maeck, J. V., Parker, L. and Romeyn, D. (1967). Use of Hematoporphyrin Derivative in Detection and Management of Cervical Cancer - a Preliminary Report. *Am. J. Obstet. Gynecol.*, *99*, 766-771.
- [30] Weishaupt, K.R., Gomer, C. J. and Dougherty, T. J. (1976). Identification of singlet oxygen as the cytotoxic agent in photoinactivation of a murine tumor *Cancer Res*, *36*, 2326-2329.
- [31] Dougherty, T. J., Kaufman, J. E., Goldfarb, A., Weishaupt, K. R., Boyle, D. and Mittleman, A. (1978). Photoradiation Therapy for Treatment of Malignant-Tumors. *Cancer Res.*, *38*, 2628-2635.
- [32] Hayata, Y., Konaka, C., Takizawa, N. and Kato, H. (1982). Hematoporphyrin Derivative and Laser Photoradiation in the Treatment of Lung-Cancer. *Chest*, *81*, 269-277.
- [33] McCaughan, J. S., Hicks, W., Laufman, L., May, E. and Roach, R. (1984). Palliation of Esophageal Malignancy with Photoradiation Therapy. *Cancer*, *54*, 2905-2910.
- [34] Barr, H., Krasner, N., Boulos, P. B., Chatlani, P. and Bown, S. G. (1990). Photodynamic Therapy for Colorectal-Cancer - a Quantitative Pilot-Study. *Br. J. Surg.*, *77*, 93-96.
- [35] Kaye, A. H., Morstyn, G. and Brownbill, D. (1987). Adjuvant High-Dose Photoradiation Therapy in the Treatment of Cerebral Glioma - a Phase 1-2 Study. *J. Neurosurg.*, *67*, 500-505.
- [36] Laws, E. R., Cortese, D. A., Kinsey, J. H., Eagan, R. T. and Anderson, R. E. (1981). Photoradiation Therapy in the Treatment of Malignant Brain-Tumors - a Phase-I (Feasibility) Study. *Neurosurgery*, *9*, 672-678.
- [37] Fritsch, C., Lang, K., Neuse, W., Ruzicka, T. and Lehmann, P. (1998). Photodynamic diagnosis and therapy in dermatology. *Skin Pharmacol. Appl. Skin Physiol.*, *11*, 358-373.

- [38] Jichlinski, P., Guillou, L., Karlsen, S. J., Malmstrom, P. U., Jocham, D., Brennhovd, B., Johansson, E., Gartner, T., Lange, N., van den Bergh, H. *et al* (2003). Hexyl aminolevulinat fluorescence cystoscopy: A new diagnostic tool for the photodiagnosis of superficial bladder cancer - A multicenter study. *J. Urol.*, *170*, 226-229.
- [39] Pal, P., Zeng, H., Durocher, G., Girard, D., Li, T., Gupta, A. K., Giasson, R., Blanchard, L., Gaboury, L., Balassy, A. *et al* (1996). Phototoxicity of Some Bromine-Substituted Rhodamine Dyes: Synthesis, Photophysical Properties and Application as Photosensitizers. *Photochem. Photobiol.*, *63*, 161-168.
- [40] Soncin, M., Busetti, A., Fusi, F., Jori, G. and Rodgers, M. A. J. (1999). Irradiation of Amelanotic Melanoma Cells with 532 nm High Peak Power Pulsed Laser Radiation in the Presence of the Photothermal Sensitizer Cu(II)-Hematoporphyrin: A New Approach to Cell Photoinactivation. *Photochem. Photobiol.*, *69*, 708-712.
- [41] Lang, K., Mosinger, J. and Wagnerová, D. M. (2004). Photophysical properties of porphyrinoid sensitizers non-covalently bound to host molecules; models for photodynamic therapy. *Coord. Chem. Rev.*, *248*, 321-350.
- [42] MacDonald, I. J. and Dougherty, T. J. (2001). Basic principles of photodynamic therapy. *J. Porphyr. Phthalocyanines*, *5*, 105-129.
- [43] Egorov, S. Y., Kamalov, V. F., Koroteev, N. I., Krasnovsky, A. A., Toleutaev, B. N. and Zinukov, S. V. (1989). Rise and Decay Kinetics of Photosensitized Singlet Oxygen Luminescence in Water - Measurements with Nanosecond Time-Correlated Single Photon-Counting Technique. *Chem. Phys. Lett.*, *163*, 421-424.
- [44] Rodgers, M. A. J. (1983). Solvent-Induced Deactivation of Singlet Oxygen - Additivity Relationships in Non-Aromatic Solvents. *J. Am. Chem. Soc.*, *105*, 6201-6205.
- [45] Baker, A. and Kanofsky, J. R. (1992). Quenching of Singlet Oxygen by Biomolecules from L1210 Leukemia-Cells. *Photochemistry and Photobiology*, *55*, 523-528.
- [46] Hatz, S., Lambert, J. D. C. and Ogilby, P. R. (2007). Measuring the lifetime of singlet oxygen in a single cell: addressing the issue of cell viability. *Photochem. Photobiol. Sci.*, *6*, 1106-1116.
- [47] Henderson, B. W. and Dougherty, T. J. (1992). How Does Photodynamic Therapy Work. *Photochem. Photobiol.*, *55*, 145-157.
- [48] Moan, J. and Boye, E. (1981). Photodynamic Effect on DNA and Cell-Survival of Human-Cells Sensitized by Hematoporphyrin. *Photobiochem. Photobiophys.*, *2*, 301-307.
- [49] Lee, P. C. C. and Rodgers, M. A. J. (1987). Laser Flash Photokinetic Studies of Rose-Bengal Sensitized Photodynamic Interactions of Nucleotides and DNA. *Photochem. Photobiol.*, *45*, 79-86.
- [50] Henderson, B. W. and Fingar, V. H. (1987). Relationship of Tumor Hypoxia and Response to Photodynamic Treatment in an Experimental Mouse-Tumor. *Cancer Res.*, *47*, 3110-3114.
- [51] Sitnik, T. M., Hampton, J. A. and Henderson, B. W. (1998). Reduction of tumour oxygenation during and after photodynamic therapy in vivo: effects of fluence rate. *Br. J. Cancer*, *77*, 1386-1394.
- [52] Berg, K. and Moan, J. (1994). Lysosomes as Photochemical Targets. *International Journal of Cancer*, *59*, 814-822.
- [53] Lo, P. C., Chan, C. M. H., Liu, J. Y., Fong, W. P. and Ng, D. K. P. (2007). Highly photocytotoxic glucosylated silicon(IV) phthalocyanines. Effects of peripheral chloro

- substitution on the photophysical and photodynamic properties. *J. Med. Chem.*, *50*, 2100-2107.
- [54] Sibrian-Vazquez, M., Ortiz, J., Nesterova, I. V., Fernandez-Lazaro, F., Sastre-Santos, A., Soper, S. A. and Vicente, M. G. H. (2007). Synthesis and properties of cell-targeted Zn(II)-phthalocyanine-peptide conjugates. *Bioconjugate Chem.*, *18*, 410-420.
- [55] Dummin, H., Cernay, T. and Zimmermann, H. W. (1997). Selective photosensitization of mitochondria in HeLa cells by cationic Zn(II) phthalocyanines with lipophilic side-chains. *J. Photochem. Photobiol. B-Biol.*, *37*, 219-229.
- [56] Trivedi, N. S., Wang, H. W., Nieminen, A. L., Oleinick, N. L. and Izatt, J. A. (2000). Quantitative analysis of Pc 4 localization in mouse lymphoma (LY-R) cells via double-label confocal fluorescence microscopy. *Photochem. Photobiol.*, *71*, 634-639.
- [57] Kessel, D. and Reiners, J. J. (2007). Apoptosis and autophagy after mitochondrial or endoplasmic reticulum photodamage. *Photochem. Photobiol.*, *83*, 1024-1028.
- [58] Teiten, M. H., Bezdetnaya, L., Morliere, P., Santus, R. and Guillemin, F. (2003). Endoplasmic reticulum and Golgi apparatus are the preferential sites of Foscan(R) localisation in cultured tumour cells. *Br. J. Cancer*, *88*, 146-152.
- [59] Marchal, S., Francois, A., Dumas, D., Guillemin, F. and Bezdetnaya, L. (2007). Relationship between subcellular localisation of Foscan (R) and caspase activation in photosensitized MCF-7 cells. *Br. J. Cancer*, *96*, 944-951.
- [60] Aveline, B. M. and Redmond, R. W. (1999). Can Cellular Phototoxicity be Accurately Predicted on the Basis of Sensitizer Photophysics? *Photochem. Photobiol.*, *69*, 306-316.
- [61] Hsieh, Y. J., Wu, C. C., Chang, C. J. and Yu, J. S. (2003). Subcellular localization of Photofrin (R) determines the death phenotype of human epidermoid carcinoma A431 cells triggered by photodynamic therapy: When plasma membranes are the main targets. *J. Cell. Physiol.*, *194*, 363-375.
- [62] Nilsson, R., Swanbeck, G. and Wennersten, G. (1975). Primary Mechanisms of Erythrocyte Photolysis Induced by Biological Sensitizers and Phototoxic Drugs. *Photochem. Photobiol.*, *22*, 183-186.
- [63] Sun, X. and Leung, W. N. (2002). Photodynamic therapy with pyropheophorbide-a methyl ester in human lung carcinoma cancer cell: Efficacy, localization and apoptosis. *Photochem. Photobiol.*, *75*, 644-651.
- [64] Berg, K., Madslie, K., Bommer, J. C., Oftebro, R., Winkelmann, J. W. and Moan, J. (1991). Light-Induced Relocalization of Sulfonated Meso-Tetraphenylporphines in Nhk 3025 Cells and Effects of Dose Fractionation. *Photochem. Photobiol.*, *53*, 203-210.
- [65] Moan, J., Berg, K., Anholt, H. and Madslie, K. (1994). Sulfonated Aluminum Phthalocyanines as Sensitizers for Photochemotherapy - Effects of Small Light Doses on Localization, Dye Fluorescence and Photosensitivity in V79 Cells. *Int. J. Cancer*, *58*, 865-870.
- [66] Melnikova, V. O., Bezdetnaya, L. N., Bour, C., Festor, E., Gramain, M. P., Merlin, J. L., Potapenko, A. Y. and Guillemin, F. (1999). Subcellular localization of meta-tetra(hydroxyphenyl) chlorin in human tumor cells subjected to photodynamic treatment. *J. Photochem. Photobiol. B-Biol.*, *49*, 96-103.
- [67] Chen, J. Y., Mak, N. K., Wen, J. M., Leung, W. N., Chen, S. C., Fung, M. C. and Cheung, N. H. (1998). A comparison of the photodynamic effects of temoporfin

- (mTHPC) and MC540 on leukemia cells: Efficacy and apoptosis. *Photochem. Photobiol.*, 68, 545-554.
- [68] Castano, A. P., Demidova, T. N. and Hamblin, M. R. (2004). Mechanisms in photodynamic therapy: part one--photosensitizers, photochemistry and cellular localization. *Photodiagn. Photodyn. Ther.*, 1, 279-293.
- [69] Rashid, F. and Horobin, R. W. (1990). Interaction of Molecular Probes with Living Cells and Tissues .2. a Structure-Activity Analysis of Mitochondrial Staining by Cationic Probes, and a Discussion of the Synergistic Nature of Image-Based and Biochemical Approaches. *Histochemistry*, 94, 303-308.
- [70] Woodburn, K. W., Vardaxis, N. J., Hill, J. S., Kaye, A. H. and Phillips, D. R. (1991). Subcellular-Localization of Porphyrins Using Confocal Laser Scanning Microscopy. *Photochem. Photobiol.*, 54, 725-732.
- [71] Hilf, R., Warne, N. W., Smail, D. B. and Gibson, S. L. (1984). Photodynamic inactivation of selected intracellular enzymes by hematoporphyrin derivative and their relationship to tumor cell viability in vitro. *Cancer Lett.*, 24, 165-172.
- [72] Castano, A. P., Demidova, T. N. and Hamblin, M. R. (2005). Mechanisms in photodynamic therapy: part two--cellular signaling, cell metabolism and modes of cell death. *Photodiagn. Photodyn. Ther.*, 2, 1-23.
- [73] Hilf, R. (2007). Mitochondria are targets of photodynamic therapy. *J. Bioenerg. Biomembr.*, 39, 85-89.
- [74] Fingar, V. H., Wieman, T. J., Karavolos, P. S., Doak, K. W., Ouellet, R. and Vanlier, J. E. (1993). The Effects of Photodynamic Therapy Using Differently Substituted Zinc Phthalocyanines on Vessel Constriction, Vessel Leakage and Tumor Response. *Photochem. Photobiol.*, 58, 251-258.
- [75] Fingar, V. H., Wieman, T. J. and Haydon, P. S. (1997). The effects of thrombocytopenia on vessel stasis and macromolecular leakage after photodynamic therapy using photofrin. *Photochem. Photobiol.*, 66, 513-517.
- [76] Fingar, V. H., Wieman, T. J., Wiehle, S. A. and Cerrito, P. B. (1992). The Role of Microvascular Damage in Photodynamic Therapy - the Effect of Treatment on Vessel Constriction, Permeability, and Leukocyte Adhesion. *Cancer Res.*, 52, 4914-4921.
- [77] McMahan, K. S., Wieman, T. J., Moore, P. H. and Fingar, V. H. (1994). Effects of Photodynamic Therapy Using Mono-L-Aspartyl Chlorin E(6) on Vessel Constriction, Vessel Leakage, and Tumor Response. *Cancer Res.*, 54, 5374-5379.
- [78] Fingar, V. H., Wieman, T. J. and Doak, K. W. (1990). Role of Thromboxane and Prostacyclin Release on Photodynamic Therapy-Induced Tumor Destruction. *Cancer Res.*, 50, 2599-2603.
- [79] Dolmans, D., Kadambi, A., Hill, J. S., Waters, C. A., Robinson, B. C., Walker, J. P., Fukumura, D. and Jain, R. K. (2002). Vascular accumulation of a novel photosensitizer, MV6401, causes selective thrombosis in tumor vessels after photodynamic therapy. *Cancer Res.*, 62, 2151-2156.
- [80] Brown, S. B. and Mellish, K. J. (2001). Verteporfin: a milestone in ophthalmology and photodynamic therapy. *Expert Opin. Pharmacother.*, 2, 351-361.
- [81] Chen, B., Pogue, B. W., Hoopes, P. J. and Hasan, T. (2005). Combining vascular and cellular targeting regimens enhances the efficacy of photodynamic therapy. *Int. J. Radiat. Oncol. Biol. Phys.*, 61, 1216-1226.

- [82] Chen, B., Pogue, B. W., Luna, J. M., Hardman, R. L., Hoopes, P. J. and Hasan, T. (2006). Tumor vascular permeabilization by vascular-targeting photosensitization: Effects, mechanism, and therapeutic implications. *Clin. Cancer Res.*, 12, 917-923.
- [83] Webber, J., Leeson, B., Fromm, D. and Kessel, D. (2005). Effects of photodynamic therapy using a fractionated dosing of mono-L-aspartyl chlorin e6 in a murine tumor. *J. Photochem. Photobiol. B-Biol.*, 78, 135-140.
- [84] Trachtenberg, J., Bogaards, A., Weersink, R. A., Haider, M. A., Evans, A., McCluskey, S. A., Scherz, A., Gertner, M. R., Yue, C., Appu, S. *et al* (2007). Vascular targeted photodynamic therapy with palladium-bacteriopheophorbide photosensitizer for recurrent prostate cancer following definitive radiation therapy: Assessment of safety and treatment response. *J. Urol.*, 178, 1974-1979.
- [85] Korbelik, M., Kros, G., Kros, J. and Dougherty, G. J. (1996). The role of host lymphoid populations in the response of mouse EMT6 tumor to photodynamic therapy. *Cancer Res.*, 56, 5647-5652.
- [86] Korbelik, M. (1996). Induction of tumor immunity by photodynamic therapy. *J. Clin. Laser Med. Surg.*, 14, 329-334.
- [87] Castano, A. P., Demidova, T. N. and Hamblin, M. R. (2005). Mechanisms in photodynamic therapy: Part three--Photosensitizer pharmacokinetics, biodistribution, tumor localization and modes of tumor destruction. *Photodiagn. Photodyn. Ther.*, 2, 91-106.
- [88] Kros, G. and Korbelik, M. (1994). Potentiation of photodynamic therapy by immunotherapy: the effect of schizophyllan (SPG). *Cancer Lett.*, 84, 43-49.
- [89] Gollnick, S. O., Vaughan, L. and Henderson, B. W. (2002). Generation of effective antitumor vaccines using photodynamic therapy. *Cancer Res.*, 62, 1604-1608.
- [90] Sasaki, S. and Tamiaki, H. (2006). Synthesis and optical properties of bacteriochlorophyll-a derivatives having various C3 substituents on the bacteriochlorin pi-system. *J. Org. Chem.*, 71, 2648-2654.
- [91] Sternberg, E. D., Dolphin, D. and Bruckner, C. (1998). Porphyrin-based photosensitizers for use in photodynamic therapy. *Tetrahedron*, 54, 4151-4202.
- [92] Labbe, R. F. and Nishida, G. (1957). A new method of hemin isolation. *Biochim. Biophys. Acta*, 26, 437.
- [93] Bonnett, R. (1995). Photosensitizers of the Porphyrin and Phthalocyanine Series for Photodynamic Therapy. *Chem. Soc. Rev.*, 24, 19-33.
- [94] Huang, Z. (2006). Photodynamic therapy in China: Over 25 years of unique clinical experience: Part One--History and domestic photosensitizers. *Photodiagn. Photodyn. Ther.*, 3, 3-10.
- [95] Anti cancer drug: PDT therapy against cancer growth tumor [online]. 2008 [cited 2008-02-18]. Available from: www.photogem.ru.
- [96] Triesscheijn, M., Baas, P., Schellens, J. H. M. and Stewart, F. A. (2006). Photodynamic Therapy in Oncology. *Oncologist*, 11, 1034-1044.
- [97] ClinicalTrials.gov [online]. 2008 [cited 2008-02-07]. Available from: www.clinicaltrials.gov.
- [98] Schweitzer, V. G. (2001). PHOTOFRIN-mediated photodynamic therapy for treatment of early stage oral cavity and laryngeal malignancies. *Lasers Surg. Med.*, 29, 305-313.
- [99] Muller, P. J. and Wilson, B. C. (2006). Photodynamic therapy of brain tumors - A work in progress. *Lasers Surg. Med.*, 38, 384-389.

- [100] Madsen, S. J. and Hirschberg, H. (2006). Photodynamic therapy and detection of high-grade gliomas. *J. Environ. Pathol. Toxicol. Oncol.*, 25, 453-465.
- [101] Wolfsen, H. C. (2005). Uses of photodynamic therapy in premalignant and malignant lesions of the gastrointestinal tract beyond the esophagus. *J. Clin. Gastroenterol.*, 39, 653-664.
- [102] Wiedmann, M., Berr, F., Schiefke, I., Witzigmann, H., Kohlhaw, K., Mossner, J. and Caca, K. (2004). Photodynamic therapy in patients with non-resectable hilar cholangiocarcinoma: 5-year follow-up of a prospective phase II study. *Gastrointest. Endosc.*, 60, 68-75.
- [103] Huang, Z. (2006). Photodynamic therapy in China: Over 25 years of unique clinical experience: Part two-Clinical experience. *Photodiagn. Photodyn. Ther.*, 3, 71-84.
- [104] Martin, D.: Porphyrins. In: Martin D., Mayes, P. and Rodwel, V. editors. *Harper's Review of Biochemistry*. Los Altos, CA: Lange Medical Publications; 1983: pp. 317-333.
- [105] Albert, A. (1958). Chemical Aspects of Selective Toxicity. *Nature*, 182, 421-423.
- [106] Peng, Q., Warloe, T., Berg, K., Moan, J., Kongshaug, M., Giercksky, K. E. and Nesland, J. M. (1997). 5-aminolevulinic acid-based photodynamic therapy - Clinical research and future challenges. *Cancer*, 79, 2282-2308.
- [107] Peng, Q., Berg, K., Moan, J., Kongshaug, M. and Nesland, J. M. (1997). 5-aminolevulinic acid-based photodynamic therapy: Principles and experimental research. *Photochem. Photobiol.*, 65, 235-251.
- [108] Redmond, R. W. and Gamlin, J. N. (1999). A compilation of singlet oxygen yields from biologically relevant molecules. *Photochem. Photobiol.*, 70, 391-475.
- [109] Malik, Z. and Lugaci, H. (1987). Destruction of Erythroleukemic Cells by Photoactivation of Endogenous Porphyrins. *Br. J. Cancer*, 56, 589-595.
- [110] Peng, Q., Evensen, J. F., Rimington, C. and Moan, J. (1987). A Comparison of Different Photosensitizing Dyes with Respect to Uptake C3h-Tumors and Tissues of Mice. *Cancer Lett.*, 36, 1-10.
- [111] Moan, J., Peng, Q., Evensen, J. F., Berg, K., Western, A. and Rimington, C. (1987). Photosensitizing Efficiencies, Tumor-Uptake and Cellular-Uptake of Different Photosensitizing Drugs Relevant for Photodynamic Therapy of Cancer. *Photochem. Photobiol.*, 46, 713-721.
- [112] Sandberg, S. and Romslo, I. (1980). Porphyrin-Sensitized Photodynamic Damage of Isolated Rat-Liver Mitochondria. *Biochim. Biophys. Acta*, 593, 187-195.
- [113] Sandberg, S. and Romslo, I. (1981). Porphyrin-Induced Photodamage at the Cellular and the Subcellular Level as Related to the Solubility of the Porphyrin. *Clin. Chim. Acta*, 109, 193-201.
- [114] Sandberg, S., Romslo, I., Hovding, G. and Bjorndal, T. (1982). Porphyrin-Induced Photodamage as Related to the Sub-Cellular Localization of the Porphyrins. *Acta Derm.-Venereol.*, 75-80.
- [115] Kennedy, J. C., Pottier, R. H. and Pross, D. C. (1990). Photodynamic Therapy with Endogenous Protoporphyrin .9. Basic Principles and Present Clinical-Experience. *J. Photochem. Photobiol. B-Biol.*, 6, 143-148.
- [116] Kennedy, J. C. and Pottier, R. H. (1992). Endogenous Protoporphyrin-Ix, a Clinically Useful Photosensitizer for Photodynamic Therapy. *J. Photochem. Photobiol. B-Biol.*, 14, 275-292.

- [117] Babilas, P., Landthaler, M. and Szeimies, R. M. (2006). Photodynamic therapy in dermatology. *Eur. J. Dermatol.*, 16, 340-348.
- [118] Ettler, K. (2004). Our Clinical Experience with the Use of Photodynamic Therapy in Patients with the Basal Cell Carcinoma and Morbus Bowen (Comparison of Efficacy of Two Photosensitizers). *Cesk. Dermatol.*, 70, 200-204.
- [119] Calzavara-Pinton, P. G., Venturini, M. and Sala, R. (2005). A comprehensive overview of photodynamic therapy in the treatment of superficial fungal infections of the skin. *J. Photochem. Photobiol. B-Biol.*, 78, 1-6.
- [120] Ettler, K. (2006). Photodynamic Therapy Used in Dermatology - Further Method Development. *Cas. Lek. Cesk.*, 145, 184-187.
- [121] Hwang, E. J., Chang, S. H., Kim, B. S. and Cho, M. K. (2008). Treatment of acne vulgaris by photodynamic therapy with aminolevulinic acid: Clinical and histopathologic findings. *J. Am. Acad. Dermatol.*, 58, AB17-AB17.
- [122] Wiegell, S. R. and Wulf, H. C. (2006). Photodynamic therapy of acne vulgaris using 5-aminolevulinic acid versus methyl aminolevulinate. *J. Am. Acad. Dermatol.*, 54, 647-651.
- [123] Niwa, A. B. M., Godoi, L., Torezan, L. and Osorio, N. (2008). Photodynamic therapy for facial acne vulgaris using methyl aminolaevutinate: Six month follow up. *J. Am. Acad. Dermatol.*, 58, Suppl. 2, AB141-AB141.
- [124] Stringer, M. R., Collins, P., Robinson, D. J., Stables, G. I. and SheehanDare, R. A. (1996). The accumulation of protoporphyrin IX in plaque psoriasis after topical application of 5-aminolevulinic acid indicates a potential for superficial photodynamic therapy. *J. Invest. Dermatol.*, 107, 76-81.
- [125] Collins, P., Robinson, D. J., Stringer, M. R., Stables, G. I. and SheehanDare, R. A. (1997). The variable response of plaque psoriasis after a single treatment with topical 5-aminolaevulinic acid photodynamic therapy. *Br. J. Dermatol.*, 137, 743-749.
- [126] Fabbrocini, G., Di Costanzo, M. P., Riccardo, A. M., Quarto, M., Colasanti, A., Roberti, G. and Monfrecola, G. (2001). Photodynamic therapy with topical delta-aminolaevulinic acid for the treatment of plantar warts. *J. Photochem. Photobiol. B-Biol.*, 61, 30-34.
- [127] Smetana, Z., Malik, Z., Orenstein, A., Mendelson, E. and BenHur, E. (1997). Treatment of viral infections with 5-aminolevulinic acid and light. *Lasers Surg. Med.*, 21, 351-358.
- [128] Wainwright, M. (2003). Local treatment of viral disease using photodynamic therapy. *Int. J. Antimicrob. Agents*, 21, 510-520.
- [129] Webber, J., Kessel, D. and Fromm, D. (1997). Plasma levels of protoporphyrin IX in humans after oral administration of 5-aminolevulinic acid. *J. Photochem. Photobiol. B-Biol.*, 37, 151-153.
- [130] Leibovici, L., Schoenfeld, N., Yehoshua, H. A., Mamet, R., Rakowsky, E., Shindel, A. and Atsmon, A. (1988). Activity of Porphobilinogen Deaminase in Peripheral-Blood Mononuclear-Cells of Patients with Metastatic Cancer. *Cancer*, 62, 2297-2300.
- [131] Schoenfeld, N., Epstein, O., Lahav, M., Mamet, R., Shaklai, M. and Atsmon, A. (1988). The Heme Biosynthetic-Pathway in Lymphocytes of Patients with Malignant Lymphoproliferative Disorders. *Cancer Lett.*, 43, 43-48.

- [132] Kondo, M., Hirota, N., Takaoka, T. and Kajiwara, M. (1993). Heme-Biosynthetic Enzyme-Activities and Porphyrin Accumulation in Normal Liver and Hepatoma-Cell Lines of Rat. *Cell Biol. Toxicol.*, 9, 95-105.
- [133] Dailey, H. A. and Smith, A. (1984). Differential Interaction of Porphyrins Used in Photoradiation Therapy with Ferrochelatase. *Biochem. J.*, 223, 441-445.
- [134] Vanhillegersberg, R., Vandenberg, J. W. O., Kort, W. J., Terpstra, O. T. and Wilson, J. H. P. (1992). Selective Accumulation of Endogenously Produced Porphyrins in a Liver Metastasis Model in Rats. *Gastroenterology*, 103, 647-651.
- [135] Fukuda, H., Casas, A. and Battle, A. (2006). Use of ALA and ALA derivatives for optimizing ALA-based photodynamic therapy: A review of our experience. *J. Environ. Pathol. Toxicol. Oncol.*, 25, 127-143.
- [136] Tunstall, R. G., Barnett, A. A., Schofield, J., Griffiths, J., Vernon, D. I., Brown, S. B. and Roberts, D. J. H. (2002). Porphyrin accumulation induced by 5-aminolaevulinic acid esters in tumour cells growing in vitro and in vivo. *Br. J. Cancer*, 87, 246-250.
- [137] Lopez, R. F. V., Lange, N., Guy, R. and Bentley, M. (2004). Photodynamic therapy of skin cancer: controlled drug delivery of 5-ALA and its esters. *Adv. Drug Deliv. Rev.*, 56, 77-94.
- [138] Alasensum [online]. 2008 [cited 10-04-2008]. Available from: <http://www.niopik.ru/products/medicine/alasense/#>.
- [139] Kloek, J. and vanHenegouwen, G. (1996). Prodrugs of 5-aminolevulinic acid for photodynamic therapy. *Photochem. Photobiol.*, 64, 994-1000.
- [140] Kaliszewski, M., Juzeniene, A., Juzenas, P., Kwasny, M., Kaminski, J., Dabrowski, Z., Golinski, J. and Moan, J. (2005). Formation of protoporphyrin IX from carboxylic- and amino-derivatives of 5-aminolevulinic acid. *Photodiagn. Photodyn. Ther.*, 2, 129-134.
- [141] Berger, Y., Greppi, A., Siri, O., Neier, R. and Juillerat-Jeanneret, L. (2000). Ethylene glycol and amino acid derivatives of 5-aminolevulinic acid as new photosensitizing precursors of protoporphyrin IX in cells. *J. Med. Chem.*, 43, 4738-4746.
- [142] Berger, Y., Ingrassia, L., Neier, R. and Juillerat-Jeanneret, L. (2003). Evaluation of dipeptide-derivatives of 5-aminolevulinic acid as precursors for photosensitizers in photodynamic therapy. *Bioorg. Med. Chem.*, 11, 1343-1351.
- [143] Ninomiya, Y., Itoh, Y., Tajima, S. and Ishibashi, A. (2001). In vitro and in vivo expression of protoporphyrin IX induced by lipophilic 5-aminolevulinic acid derivatives. *J. Dermatol. Sci.*, 27, 114-120.
- [144] Zenzen, V. and Zankl, H. (2003). Protoporphyrin IX-accumulation in human tumor cells following topical ALA- and h-ALA-application in vivo. *Cancer Lett.*, 202, 35-42.
- [145] Whitaker, C. J., Battah, S. H., Forsyth, M. J., Edwards, C., Boyle, R. W. and Matthews, E. K. (2000). Photosensitization of pancreatic tumour cells by delta-aminolaevulinic acid esters. *Anticancer Drug Des.*, 15, 161-170.
- [146] Uehlinger, P., Zellweger, M., Wagnieres, G., Juillerat-Jeanneret, L., van den Bergh, H. and Lange, N. (2000). 5-Aminolevulinic acid and its derivatives: physical chemical properties and protoporphyrin IX formation in cultured cells. *J. Photochem. Photobiol. B-Biol.*, 54, 72-80.
- [147] Brunner, H., Hausmann, F. and Knuechel, R. (2003). New 5-aminolevulinic acid esters - Efficient protoporphyrin precursors for photodetection and photodynamic therapy. *Photochem. Photobiol.*, 78, 481-486.

- [148] Di Venosa, G., Batlle, A., Fukuda, H., MacRobert, A. and Casas, A. (2006). Distribution of 5-aminolevulinic acid derivatives and induced porphyrin kinetics in mice tissues. *Cancer Chemother. Pharmacol.*, 58, 478-486.
- [149] Di Venosa, G., Fukuda, H., Batlle, A., MacRobert, A. and Casas, A. (2006). Photodynamic therapy: Regulation of porphyrin synthesis and hydrolysis from ALA esters. *J. Photochem. Photobiol. B-Biol.*, 83, 129-136.
- [150] Fotinos, N., Campo, M. A., Popowycz, F., Gurny, R. and Lange, N. (2006). 5-aminolevulinic acid derivatives in photomedicine: Characteristics, application and perspectives. *Photochem. Photobiol.*, 82, 994-1015.
- [151] Gaullier, J. M., Berg, K., Peng, Q., Anholt, H., Selbo, P. K., Ma, L. W. and Moan, J. (1997). Use of 5-aminolevulinic acid esters to improve photodynamic therapy on cells in culture. *Cancer Res.*, 57, 1481-1486.
- [152] Vena, F. C. B., Turchiello, R. F., Laville, I., Pigaglio, S., Blais, J. and Tedesco, A. C. (2004). 5-Aminolevulinic acid ester-induced protoporphyrin IX in a murine melanoma cell line. *Lasers Med. Sci.*, 19, 119-126.
- [153] Taylor, E. L., Vernon, D. I. and Brown, S. B.: Mechanism of protoporphyrin IX formation from ALA esters. In: *Program and Abstracts of the 9th Congress of European Society for Photobiology*. Aix-les-bains; 2005; 178.
- [154] Di Venosa, G., Fukuda, H., Batlle, A., MacRobert, A. and Casas, A. (2006). Photodynamic therapy: Regulation of porphyrin synthesis and hydrolysis from ALA esters. *J. Photochem. Photobiol. B-Biol.*, 83, 129-136.
- [155] Moan, J., Ma, L. W. and Iani, V. (2001). On the pharmacokinetics of topically applied 5-aminolevulinic acid and two of its esters. *Int. J. Cancer*, 92, 139-143.
- [156] Perotti, C., Casas, A., Fukuda, H., Sacca, P. and Batlle, A. (2003). Topical application of ALA and ALA hexyl ester on a subcutaneous murine mammary adenocarcinoma: tissue distribution. *Br. J. Cancer*, 88, 432-437.
- [157] Casas, A., Perotti, C., Fukuda, H., Rogers, L., Butler, A. R. and Batlle, A. (2001). ALA and ALA hexyl ester-induced porphyrin synthesis in chemically induced skin tumours: the role of different vehicles on improving photosensitization. *Br. J. Cancer*, 85, 1794-1800.
- [158] Fritsch, C., Homey, B., Stahl, W., Lehmann, P., Ruzicka, T. and Sies, H. (1998). Preferential relative porphyrin enrichment in solar keratoses upon topical application of delta-aminolevulinic acid methylester. *Photochem. Photobiol.*, 68, 218-221.
- [159] Donnelly, R. F., McCarron, P. A. and Woolfson, A. D. (2005). Drug delivery of aminolevulinic acid from topical formulations intended for photodynamic therapy. *Photochem. Photobiol.*, 81, 750-767.
- [160] Rud, E., Gederaas, O., Hogset, A. and Berg, K. (2000). 5-aminolevulinic acid, but not 5-aminolevulinic acid esters, is transported into adenocarcinoma cells by system BETA transporters. *Photochem. Photobiol.*, 71, 640-647.
- [161] Doring, F., Walter, J., Will, J., Focking, M., Boll, M., Amasheh, S., Clauss, W. and Daniel, H. (1998). Delta-aminolevulinic acid transport by intestinal and renal peptide transporters and its physiological and clinical implications. *J. Clin. Invest.*, 101, 2761-2767.
- [162] Gederaas, O. A., Holroyd, A., Brown, S. B., Vernon, D., Moan, J. and Berg, K. (2001). 5-aminolaevulinic acid methyl ester transport on amino acid carriers in a human colon adenocarcinoma cell line. *Photochem. Photobiol.*, 73, 164-169.

- [163] I.J., K. and E., S. P. (1947). The pyrazines. *Chem. Rev.*, *40*, 290-358.
- [164] Granick, S. and Mauzerall, D. (1958). Porphyrin Biosynthesis in Erythrocytes .2. Enzymes Converting Delta-Aminolevulinic Acid to Coproporphyrinogen. *J. Biol. Chem.*, *232*, 1119-1140.
- [165] Butler, A. R. and George, S. (1992). The Nonenzymatic Cyclic Dimerization of 5-Aminolevulinic Acid. *Tetrahedron*, *48*, 7879-7886.
- [166] Novo, M., Huttmann, G. and Diddens, H. (1996). Chemical instability of 5-aminolevulinic acid used in the fluorescence diagnosis of bladder tumours. *J. Photochem. Photobiol. B-Biol.*, *34*, 143-148.
- [167] Bunke, A., Zerbe, O., Schmid, H., Burmeister, G., Merkle, H. P. and Gander, B. (2000). Degradation mechanism and stability of 5-aminolevulinic acid. *J. Pharm. Sci.*, *89*, 1335-1341.
- [168] Dalton, J. T., Zhou, D. S., Mukherjee, A., Young, D., Tolley, E. A., Golub, A. L. and Meyer, M. C. (1999). Pharmacokinetics of aminolevulinic acid after intravesical administration to dogs. *Pharm. Res.*, *16*, 288-295.
- [169] Visudyne.com [online]. 2008 [cited 2008-02-11]. Available from: www.visudyne.com.
- [170] Wickens, J. and Blinder, K. J. (2006). A preliminary benefit-risk assessment of verteporfin in age-related macular degeneration. *Drug Saf.*, *29*, 189-199.
- [171] Costa, R. A., Jorge, R., Calucci, D., Melo, L. A. S., Cardillo, J. A. and Scott, I. U. (2007). Intravitreal bevacizumab (Avastin) in combination with verteporfin photodynamic therapy for choroidal neovascularization associated with age-related macular degeneration (IBeVe Study). *Graefes Arch. Clin. Exp. Ophthalmol.*, *245*, 1273-1280.
- [172] Donati, G. (2007). Emerging therapies for Neovascular age-related macular degeneration: State of the art. *Ophthalmologica*, *221*, 366-377.
- [173] Lui, H., Hobbs, L., Tope, W. D., Lee, P. K., Elmets, C., Provost, N., Chan, A., Neyendorff, H., Su, X. Y., Jain, H. *et al* (2004). Photodynamic therapy of multiple nonmelanoma skin cancers with verteporfin and red light-emitting diodes - Two-year results evaluating tumor response and cosmetic outcomes. *Arch. Dermatol.*, *140*, 26-32.
- [174] Mordon, S. (2007). Vascular-Targeted Photodynamic Therapy: a new technique for port wine stain treatment. *Ann. Dermatol. Venereol.*, *134*, 281-286.
- [175] Boch, R., Canaan, A. J., Cho, A., Dolphin, D. D., Hong, L., Jain, A. K., North, J. R., Richter, A. M., Smits, C. and Sternberg, E. D. (2006). Cellular and antitumor activity of a new diethylene glycol benzoporphyrin derivative (lemuteporfin). *Photochem. Photobiol.*, *82*, 219-224.
- [176] Boch, R. E., Sternberg, E., Dolphin, D., Levy, J. G., Richter, A. M., Hunt, D. W. C., Jain, A., Waterfield, E. M. and Tovey, A. N. (2002). Use of ethylene glycol esters of monohydrobenzoporphyrin derivatives as photoactive agents. European Patent EP1177795. Available also from: www.freepatentsonline.com.
- [177] Ratkay, L. G., Waterfield, J. D. and Hunt, D. W. C. (2000). Photodynamic therapy in immune (non-oncological) disorders - Focus on benzoporphyrin derivatives. *Biodrugs*, *14*, 127-135.
- [178] Jiang, H. J., Granville, D. J., North, J. R., Richter, A. M. and Hunt, D. W. C. (2002). Selective action of the photosensitizer QLT0074 on activated human T lymphocytes. *Photochem. Photobiol.*, *76*, 224-231.

- [179] Perez-Marrero, R., Goldenberg, S. L., Shore, N., Benaim, E., Fay, R., Manyak, M. J. and Elhilali, M. (2005). A phase I/II dose-escalation study to assess the safety, tolerability, and preliminary efficacy of transurethral photodynamic therapy with lemuteporfin in men with lower urinary tract symptoms due to benign prostatic hyperplasia. *J. Urol.*, *173*, Suppl. S, 421-422.
- [180] Xiao, Z. W., Dickey, D., Owen, R. J., Tulip, J. and Moore, R. (2007). Interstitial photodynamic therapy of the canine prostate using intra-arterial administration of photosensitizer and computerized pulsed light delivery. *J. Urol.*, *178*, 308-313.
- [181] Berenbaum, M. C., Akande, S. L., Bonnett, R., Kaur, H., Ioannou, S., White, R. D. and Winfield, U. J. (1986). Meso-Tetra(Hydroxyphenyl)Porphyrins, a New Class of Potent Tumor Photosensitizers with Favorable Selectivity. *Br. J. Cancer*, *54*, 717-725.
- [182] Berenbaum, M. C., Bonnett, R., Chevretton, E. B., Akandeadebakin, S. L. and Ruston, M. (1993). Selectivity of Meso-Tetra(Hydroxyphenyl)Porphyrins and Chlorins and of Photofrin-Ii in Causing Photodamage in Tumor, Skin, Muscle and Bladder - the Concept of Cost-Benefit in Analyzing the Results. *Lasers Med. Sci.*, *8*, 235-243.
- [183] Kiesslich, T., Berlanda, J., Plaetzer, K., Krammer, B. and Berr, F. (2007). Comparative characterization of the efficiency and cellular pharmacokinetics of Foscan (R) and Foslip (R)-based photodynamic treatment in human biliary tract cancer cell lines. *Photochem. Photobiol. Sci.*, *6*, 619-627.
- [184] Svensson, J., Johansson, A., Grafe, S., Gitter, B., Trebst, T., Bendsoe, N., Andersson-Engels, S. and Svanberg, K. (2007). Tumor selectivity at short times following systemic administration of a liposomal temoporfin formulation in a murine tumor model. *Photochem. Photobiol.*, *83*, 1211-1219.
- [185] Biel, M. A. (2007). Photodynamic therapy treatment of early oral and laryngeal cancers. *Photochem. Photobiol.*, *83*, 1063-1068.
- [186] Baas, P., Saarnak, A. E., Oppelaar, H., Neering, H. and Stewart, F. A. (2001). Photodynamic therapy with meta-tetrahydroxyphenylchlorin for basal cell carcinoma: a phase I/II study. *Br. J. Dermatol.*, *145*, 75-78.
- [187] Triesscheijn, M., Ruevekamp, M., Antonini, N., Neering, H., Stewart, F. A. and Baas, P. (2006). Optimizing meso-tetra-hydroxyphenyl-chlorin-mediated photodynamic therapy for basal cell carcinoma. *Photochem. Photobiol.*, *82*, 1686-1690.
- [188] Zimmermann, A., Ritsch-Marte, M. and Kostron, H. (2001). mTHPC-mediated photodynamic diagnosis of malignant brain tumors. *Photochem. Photobiol.*, *74*, 611-616.
- [189] Moore, C. M., Nathan, T. R., Lees, W. R., Mosse, C. A., Freeman, A., Emberton, M. and Bown, S. G. (2006). Photodynamic therapy using meso tetra hydroxy phenyl chlorin (mTHPC) in early prostate cancer. *Lasers Surg. Med.*, *38*, 356-363.
- [190] Nathan, T. R., Whitelaw, D. E., Chang, S. C., Lees, W. R., Ripley, P. M., Payne, H., Jones, L., Parkinson, M. C., Emberton, M., Gillams, A. R. *et al* (2002). Photodynamic therapy for prostate cancer recurrence after radiotherapy: a phase I study. *J. Urol.*, *168*, 1427-1432.
- [191] Bommer, J. C. and Burnham, B. F. (1987). Tetrapyrrole therapeutic agents. United States Patent US4693885. Available also from: www.freepatentsonline.com.
- [192] Gomi, S., Nishizuka, T., Ushiroda, O., Uchida, N., Takahashi, H. and Sumi, S. (1998). The structures of mono-L-aspartyl chlorin e6 and its related compounds. *Heterocycles*, *48*, 2231-2243.

- [193] Hargus, J. A., Fronczek, F. R., Vicente, M. G. H. and Smith, K. M. (2007). Mono-(l)-aspartylchlorin-e6. *Photochem. Photobiol.*, *83*, 1006-1015.
- [194] Saito, K., Mikuniya, N. and Aizawa, K. (2000). Effects of photodynamic therapy using mono-L-aspartyl chlorin e6 on vessels and its contribution to the antitumor effect. *Jpn. J. Cancer Res.*, *91*, 560-565.
- [195] Chan, A. L., Juarez, M., Allen, R., Volz, W. and Albertson, T. (2005). Pharmacokinetics and clinical effects of mono-L-aspartyl chlorin e6 (NPe6) photodynamic therapy in adult patients with primary or secondary cancer of the skin and mucosal surfaces. *Photodermatol. Photoimmunol. Photomed.*, *21*, 72-78.
- [196] Kessel, D. (1997). Pharmacokinetics of N-aspartyl chlorin e6 in cancer patients. *J. Photochem. Photobiol. B-Biol.*, *39*, 81-83.
- [197] Kujund, M., zcaron, cacute, Rustemovi, T. J. V. D. S. N., cacute, Kati, R. A. H. M. R. M., ccaron, cacute and Wang, R. C. R. A. L. S. (2007). A Phase II safety and effect on time to tumor progression study of intratumoral light infusion technology using talaporfin sodium in patients with metastatic colorectal cancer. *J. Surg. Oncol.*, *96*, 518-524.
- [198] Kato, H., Furukawa, K., Sato, M., Okunaka, T., Kusunoki, Y., Kawahara, M., Fukuoka, M., Miyazawa, T., Yana, T., Matsui, K. *et al* (2003). Phase II clinical study of photodynamic therapy using mono-L-aspartyl chlorin e6 and diode laser for early superficial squamous cell carcinoma of the lung. *Lung Cancer*, *42*, 103-111.
- [199] Light Science Oncology, Inc. [online]. 2008 [cited 2008-02-13]. Available from: www.lightsciences.com.
- [200] Taber, S. W., Fingar, V. H., Coots, C. T. and Wieman, T. J. (1998). Photodynamic therapy using mono-L-aspartyl chlorin e6 (Npe6) for the treatment of cutaneous disease: a Phase I clinical study. *Clin. Cancer Res.*, *4*, 2741-2746.
- [201] Yumita, N., Han, Q. S., Kitazumi, I. and Umemura, S. (2008). Sonodynamically-induced apoptosis, necrosis, and active oxygen generation by mono-l-aspartyl chlorin e6. *Cancer Sci.*, *99*, 166-172.
- [202] Morgan, A. R., Garbo, G. M., Keck, R. W. and Selman, S. H. (1988). New Photosensitizers for Photodynamic Therapy: Combined Effect of Metalloporpurin Derivatives and Light on Transplantable Bladder Tumors. *Cancer Res.*, *48*, 194-198.
- [203] Morgan, A. R., Garbo, G. M., Keck, R. W., Eriksen, L. D. and Selman, S. H. (1990). Metalloporpurins and light: effect on transplantable rat bladder tumors and murine skin. *Photochem. Photobiol.*, *51*, 589-592.
- [204] Mang, T. S., Allison, R., Hewson, G., Snider, W. and Moskowitz, R. (1998). A phase II/III clinical study of tin ethyl etiopurpurin (Purlytin)-induced photodynamic therapy for the treatment of recurrent cutaneous metastatic breast cancer. *Cancer J.*, *4*, 378-384.
- [205] Kaplan, M. J., Somers, R. G., Greenberg, R. H. and Ackler, J. (1998). Photodynamic therapy in the management of metastatic cutaneous adenocarcinomas: Case reports from phase 1/2 studies using tin ethyl etiopurpurin (SnET2). *J. Surg. Oncol.*, *67*, 121-125.
- [206] Selman, S. H., Albrecht, D., Keck, R. W., Brennan, P. and Kondo, S. (2001). Studies of tin ethyl etiopurpurin photodynamic therapy of the canine prostate. *J. Urol.*, *165*, 1795-1801.
- [207] Chen, Y., Zheng, X., Dobhal, M. P., Gryshuk, A., Morgan, J., Dougherty, T. J., Oseroff, A. and Pandey, R. K. (2005). Methyl Pyropheophorbide-a Analogues:

- Potential Fluorescent Probes for the Peripheral-Type Benzodiazepine Receptor. Effect of Central Metal in Photosensitizing Efficacy. *J. Med. Chem.*, 48, 3692-3695.
- [208] Dolmans, D. E. J. G. J., Kadambi, A., Hill, J. S., Flores, K. R., Gerber, J. N., Walker, J. P., Rinkes, I. H. M. B., Jain, R. K. and Fukumura, D. (2002). Targeting Tumor Vasculature and Cancer Cells in Orthotopic Breast Tumor by Fractionated Photosensitizer Dosing Photodynamic Therapy. *Cancer Res.*, 62, 4289-4294.
- [209] Ciulla, T. A., Criswell, M. H., Danis, R. P., Snyder, W. J. and Small, W. (2004). Evaluation of photopoint photosensitizer MV6401, indium chloride methyl pyropheophorbide, as a photodynamic therapy agent in primate choriocapillaris and laser-induced choroidal neovascularization. *Retin.-J. Retin. Vit. Dis.*, 24, 521-529.
- [210] Ciulla, T. A., Criswell, M. H., Snyder, W. J. and Small, W. (2005). Photodynamic therapy with PhotoPoint photosensitizer MV6401, indium chloride methyl pyropheophorbide, achieves selective closure of rat corneal neovascularisation and rabbit choriocapillaris. *Br. J. Ophthalmol.*, 89, 113-119.
- [211] Pandey, R. K., Bellnier, D. A., Smith, K. M. and Dougherty, T. J. (1991). Chlorin and Porphyrin Derivatives as Potential Photosensitizers in Photodynamic Therapy. *Photochem. Photobiol.*, 53, 65-72.
- [212] Henderson, B. W., Bellnier, D. A., Greco, W. R., Sharma, A., Pandey, R. K., Vaughan, L. A., Weishaupt, K. R. and Dougherty, T. J. (1997). An in Vivo Quantitative Structure-Activity Relationship for a Congeneric Series of Pyropheophorbide Derivatives as Photosensitizers for Photodynamic Therapy. *Cancer Res.*, 57, 4000-4007.
- [213] Pandey, R. K., Shiau, F. Y., Sumlin, A. B., Dougherty, T. J. and Smith, K. M. (1992). Structure-Activity-Relationships among Photosensitizers Related to Pheophorbides and Bacteriopheophorbides. *Bioorg. Med. Chem. Lett.*, 2, 491-496.
- [214] Pallenberg, A. J., Dobhal, M. P. and Pandey, R. K. (2004). Efficient synthesis of pyropheophorbide-a and its derivatives. *Org. Process Res. Dev.*, 8, 287-290.
- [215] Baba, K., Pudavar, H. E., Roy, I., Ohulchansky, T. Y., Chen, Y. H., Pandey, R. K. and Prasad, P. N. (2007). New method for delivering a hydrophobic drug for photodynamic therapy using pure nanocrystal form of the drug. *Mol. Pharm.*, 4, 289-297.
- [216] Bellnier, D. A., Greco, W. R., Loewen, G. M., Nava, H., Oseroff, A. R., Pandey, R. K., Tsuchida, T. and Dougherty, T. J. (2003). Population pharmacokinetics of the photodynamic therapy agent 2- [1-hexyloxyethyl]-2-devinyl pyropheophorbide-a in cancer patients. *Cancer Res.*, 63, 1806-1813.
- [217] Bellnier, D. A., Greco, W. R., Nava, H., Loewen, G. M., Oseroff, A. R. and Dougherty, T. J. (2006). Mild skin photosensitivity in cancer patients following injection of Photochlor (2- [1-hexyloxyethyl]-2-devinyl pyropheophorbide-a; HPPH) for photodynamic therapy. *Cancer Chemother. Pharmacol.*, 57, 40-45.
- [218] Loewen, G. M., Pandey, R., Bellnier, D., Henderson, B. and Dougherty, T. (2006). Endobronchial photodynamic therapy for lung cancer. *Lasers Surg. Med.*, 38, 364-370.
- [219] Scherz, A., Salomon, Y., Brandis, A. and Scheer, H. (2003). Palladium-substituted bacteriochlorophyll derivatives and use thereof. United States Patent US6569846. Available also from: www.freepatentsonline.com.
- [220] Brun, P. H., DeGroot, J. L., Dickson, E. F. G., Farahani, M. and Pottier, R. H. (2004). Determination of the in vivo pharmacokinetics of palladium-bacteriopheophorbide

- (WST09) in EMT6 tumour-bearing Balb/c mice using graphite furnace atomic absorption spectroscopy. *Photochem. Photobiol. Sci.*, *3*, 1006-1010.
- [221] Weersink, R. A., Forbes, J., Bisland, S., Trachtenberg, J., Elhilali, M., Brun, P. H. and Wilson, B. C. (2005). Assessment of cutaneous photosensitivity of TOOKAD (WST09) in preclinical animal models and in patients. *Photochem. Photobiol.*, *81*, 106-113.
- [222] Huang, Z., Chen, Q., Dole, K. C., Barqawi, A. B., Chen, Y. K., Blanc, D. Q., Wilson, B. C. and Hetzel, F. W. (2007). The effect of Tookad-mediated photodynamic ablation of the prostate gland on adjacent tissues - in vivo study in a canine model. *Photochem. Photobiol. Sci.*, *6*, 1318-1324.
- [223] Huang, Z., Chen, Q., Luck, D., Beckers, J., Wilson, B. C., Trncic, N., LaRue, S. M., Blanc, D. and Hetzel, F. W. (2005). Studies of a vascular-acting photosensitizer, Pd-bacteriopheophorbide (Tookad), in normal canine prostate and spontaneous canine prostate cancer. *Lasers Surg. Med.*, *36*, 390-397.
- [224] Framme, C., Sachs, H. G., Flucke, B., Theisen-Kunde, D. and Birngruber, R. (2006). Evaluation of the new photosensitizer tookad (WST09) for photodynamic vessel occlusion of the choroidal tissue in rabbits. *Invest. Ophthalmol. Vis. Sci.*, *47*, 5437-5446.
- [225] Armstrong, N. R. (2000). Phthalocyanines and porphyrins as materials. *J. Porphyr. Phthalocyanines*, *4*, 414-417.
- [226] Ali, H. and van Lier, J. E. (1999). Metal complexes as photo- and radiosensitizers. *Chem. Rev.*, *99*, 2379-2450.
- [227] Allen, C. M., Sharman, W. M. and Van Lier, J. E. (2001). Current status of phthalocyanines in the photodynamic therapy of cancer. *J. Porphyr. Phthalocyanines*, *5*, 161-169.
- [228] Nevin, W. A., Liu, W. and Lever, A. B. P. (1987). Dimerization of Mononuclear and Binuclear Cobalt Phthalocyanines. *Can. J. Chem.*, *65*, 855-858.
- [229] Kobayashi, N., Higashi, R., Ishii, K., Hatsusaka, K. and Ohta, K. (1999). Aggregation, complexation with guest molecules, and mesomorphism of amphiphilic phthalocyanines having four- or eight tri(ethylene oxide) chains. *Bull. Chem. Soc. Jpn.*, *72*, 1263-1271.
- [230] Lang, K., Kubat, P., Mosinger, J. and Wagnerova, D. M. (1998). Photochemical consequences of porphyrin and phthalocyanine aggregation on nucleoprotein histone. *J. Photochem. Photobiol. A-Chem.*, *119*, 47-52.
- [231] Isago, H., Leznoff, C. C., Ryan, M. F., Metcalfe, R. A., Davids, R. and Lever, A. B. P. (1998). Aggregation effects on electrochemical and spectroelectrochemical properties of [2,3,9,10,16,17,23,24-octa(3,3-dimethyl-1-butynyl)phthalocyaninato]cobalt t(II) complex. *Bull. Chem. Soc. Jpn.*, *71*, 1039-1047.
- [232] Deng, H. H., Mao, H. F., Zhang, H., Lu, Z. H. and Xu, H. J. (1998). Photoelectric effect of tetrasulfonated gallium phthalocyanine on a nanostructured TiO₂ electrode. *J. Porphyr. Phthalocyanines*, *2*, 171-175.
- [233] Lagorio, M. G., Dicelio, L. E. and Roman, E. S. (1993). Visible and near-IR Spectroscopic and Photochemical Characterization of Substituted Metallophthalocyanines. *J. Photochem. Photobiol. A-Chem.*, *72*, 153-161.

- [234] Maree, M. D., Nyokong, T., Suhling, K. and Phillips, D. (2002). Effects of axial ligands on the photophysical properties of silicon octaphenoxypthalocyanine. *J. Porphyr. Phthalocyanines*, *6*, 373-376.
- [235] Choi, M. T. M., Li, P. P. S. and Ng, D. K. P. (2000). A direct comparison of the aggregation behavior of phthalocyanines and 2,3-naphthalocyanines. *Tetrahedron*, *56*, 3881-3887.
- [236] Bench, B. A., Beveridge, A., Sharman, W. M., Diebold, G. J., van Lier, J. E. and Gorun, S. M. (2002). Introduction of bulky perfluoroalkyl groups at the periphery of zinc perfluorophthalocyanine: Chemical, structural, electronic, and preliminary photophysical and biological effects. *Angew. Chem.-Int. Edit.*, *41*, 748-+.
- [237] Kostka, M., Zimcik, P., Miletin, M., Klemera, P., Kopecky, K. and Musil, Z. (2006). Comparison of aggregation properties and photodynamic activity of phthalocyanines and azaphthalocyanines. *J. Photochem. Photobiol. A-Chem.*, *178*, 16-25.
- [238] Kudrevich, S. V., Galpern, M. G. and Vanlier, J. E. (1994). Synthesis of Octacarboxytetra(2,3-Pyrazino)Porphyrazine - Novel Water-Soluble Photosensitizers for Photodynamic Therapy. *Synthesis (Stuttg.)*, 779-781.
- [239] De Filippis, M. P., Dei, D., Fantetti, L. and Roncucci, G. (2000). Synthesis of a new water-soluble octa-cationic phthalocyanine derivative for PDT. *Tetrahedron Lett.*, *41*, 9143-9147.
- [240] Zimcik, P., Miletin, M., Musil, Z., Kopecky, K., Kubza, L. and Brault, D. (2006). Cationic azaphthalocyanines bearing aliphatic tertiary amino substituents--Synthesis, singlet oxygen production and spectroscopic studies. *J. Photochem. Photobiol. A-Chem.*, *183*, 59-69.
- [241] Sakamoto, K., Kato, T., Ohno-Okumura, E., Watanabe, M. and Cook, M. J. (2005). Synthesis of novel cationic amphiphilic phthalocyanine derivatives for next generation photosensitizer using photodynamic therapy of cancer. *Dyes Pigment.*, *64*, 63-71.
- [242] Scalise, I. and Durantini, E. N. (2005). Synthesis, properties, and photodynamic inactivation of Escherichia coli using a cationic and a noncharged Zn(II) pyridyloxypthalocyanine derivatives. *Bioorg. Med. Chem.*, *13*, 3037-3045.
- [243] Abramczyk, H., Szymczyk, I., Waliszewska, G. and Lebioda, A. (2004). Photoinduced redox processes in phthalocyanine derivatives by resonance Raman spectroscopy. *J. Phys. Chem. A*, *108*, 264-274.
- [244] Sharman, W. M., Allen, C. M. and van Lier, J. E. (1999). Photodynamic therapeutics: basic principles and clinical applications. *Drug Discov. Today*, *4*, 507-517.
- [245] Nyman, E. S. and Hynninen, P. H. (2004). Research advances in the use of tetrapyrrolic photosensitizers for photodynamic therapy. *J. Photochem. Photobiol. B-Biol.*, *73*, 1-28.
- [246] Photosense [online]. 2008 [cited 2008-04-10]. Available from: <http://www.niopik.ru/products/medicine/photosense/>.
- [247] Vakulovskaya, E. G. and Shental, V. V. (2002). Combination of photodynamic therapy and cryosurgery in treatment of advanced skin cancer. *Int. J. Cancer*, Suppl. 13, 404-404.
- [248] Vakulovskaya, E. G., Shental, V. V. and Kondratjeva, T. T. (2002). Photodynamic therapy and fluorescent diagnostics of head and neck tumors with photosense. *Int. J. Cancer*, Suppl. 13, 262-262.

- [249] Vakulovskaya, E. G., Ungiadze, G. V. and Tabolinovskaya, T. D. (2005). PD10. Photodynamic therapy of oral cancer and cancer of oropharynx with second-generation photosensitizers. *Oral Oncology Supplement, 1*, 68.
- [250] Vakulovskaya, E., Shental, V., Letyagin, V., Oumnova, L., Vorozhscov, V., Philinov, V. and Stranadko, E. (2002). Photodynamic therapy and fluorescent diagnostics of breast cancer with photosense. *Int. J. Cancer, Suppl. 13*, 211-211.
- [251] Borgatti-Jeffreys, A., Hooser, S. B., Miller, M. A. and Lucroy, M. D. (2007). Phase I clinical trial of the use of zinc phthalocyanine tetrasulfonate as a photosensitizer for photodynamic therapy in dogs. *Am. J. Vet. Res., 68*, 399-404.
- [252] Miller, J. D., Nancy, O., Scull, H. M., Hsia, A., Cooper, K. D. and Baron, E. D. (2006). Phase I clinical trial using topical silicon phthalocyanine Pc 4-photodynamic therapy for the treatment of malignant and pre-malignant skin conditions: an update. *J. Invest. Dermatol., 126*, 46-46.
- [253] Shopova, M., Woehrle, D., Mantareva, V. and Mueller, S. (1999). Naphthalocyanine complexes as potential photosensitizers for photodynamic therapy of tumors. *J. Biomed. Opt., 4*, 276-285.
- [254] Soncin, M., Busetti, A., Biolo, R., Jori, G., Kwag, G., Li, Y. S., Kenney, M. E. and Rodgers, M. A. J. (1998). Photoinactivation of amelanotic and melanotic melanoma cells sensitized by axially substituted Si-naphthalocyanines. *J. Photochem. Photobiol. B-Biol., 42*, 202-210.
- [255] Biolo, R., Jori, G., Soncin, M., Pratesi, R., Vanni, U., Rihter, B., Kenney, M. E. and Rodgers, M. A. J. (1994). Photodynamic Therapy of B16 Pigmented Melanoma with Liposome-Delivered Si(IV)-Naphthalocyanine. *Photochem. Photobiol., 59*, 362-365.
- [256] Shopova, M., Wohrle, D., Stoichkova, N., Milev, A., Mantareva, V., Muller, S., Kassabov, K. and Georgiev, K. (1994). Hydrophobic Zn(II)-Naphthalocyanines as Photodynamic Therapy Agents for Lewis Lung-Carcinoma. *J. Photochem. Photobiol. B-Biol., 23*, 35-42.
- [257] Muller, S., Mantareva, V., Stoichkova, N., Kliesch, H., Sobbi, A., Wohrle, D. and Shopova, M. (1996). Tetraamido-substituted 2,3-naphthalocyanine zinc(II) complexes as phototherapeutic agents: Synthesis, comparative photochemical and photobiological studies. *Journal of Photochemistry and Photobiology B-Biology, 35*, 167-174.
- [258] Zuk, M. M., Rihter, B. D., Kenney, M. E., Rodgers, M. A. J. and Kreimer-Birnbaum, M. (1996). Effect of delivery system on the pharmacokinetics and tissue distribution of bis(Di-isobutyl octadecylsiloxy)silicon 2,3-naphthalocyanine (isoBOSINC), a photosensitizer for tumor therapy. *Photochem. Photobiol., 63*, 132-140.
- [259] Mantareva, V., Shopova, M., Spassova, G., Wohrle, D., Muller, S., Jori, G. and Ricchelli, F. (1997). Si(IV)-methoxyethylene-glycol-naphthalocyanine: synthesis and pharmacokinetic and photosensitizing properties in different tumour models. *J. Photochem. Photobiol. B-Biol., 40*, 258-262.
- [260] Brasseur, N., Nguyen, T. L., Langlois, R., Ouellet, R., Marengo, S., Houde, D. and Vanlier, J. E. (1994). Synthesis and Photodynamic Activities of Silicon 2,3-Naphthalocyanine Derivatives. *J. Med. Chem., 37*, 415-420.
- [261] Wainwright, M. and Giddens, R. M. (2003). Phenothiazinium photosensitisers: choices in synthesis and application. *Dyes Pigment., 57*, 245-257.

- [262] Wainwright, M., Phoenix, D. A., Rice, L., Burrow, S. M. and Waring, J. (1997). Increased cytotoxicity and phototoxicity in the methylene blue series via chromophore methylation. *J. Photochem. Photobiol. B-Biol.*, *40*, 233-239.
- [263] Wainwright, M., Grice, N. J. and Pye, L. E. C. (1999). Phenothiazine photosensitizers: part 2. 3,7-Bis(arylamino)phenothiazines. *Dyes Pigment.*, *42*, 45-51.
- [264] Wainwright, M. (2007). Phenothiazinium photosensitizers: V. Photobactericidal activities of chromophore-methylated phenothiazinium salts. *Dyes Pigment.*, *73*, 7-12.
- [265] Cincotta, L., Foley, J. W. and Cincotta, A. H. (1993). Phototoxicity, Redox Behavior, and Pharmacokinetics of Benzophenoxazine Analogs in Emt-6 Murine Sarcoma-Cells. *Cancer Res.*, *53*, 2571-2580.
- [266] Georgakoudi, I. and Foster, T. H. (1998). Effects of the subcellular redistribution of two Nile blue derivatives on photodynamic oxygen consumption. *Photochem. Photobiol.*, *68*, 115-122.
- [267] Cincotta, L., Foley, J. W. and Cincotta, A. H. (1987). Novel Red Absorbing Benzo [a]Phenoxazinium and Benzo [a]Phenothiazinium Photosensitizers - Invitro Evaluation. *Photochem. Photobiol.*, *46*, 751-758.
- [268] Wainwright, M. (2005). The development of phenothiazinium photosensitizers. *Photodiagn. Photodyn. Ther.*, *2*, 263-272.
- [269] Donnelly, R. F., McCarron, P. A. and Tunney, M. M. (2008). Antifungal photodynamic therapy. *Microbiol. Res.*, *163*, 1-12.
- [270] Tardivo, J. P., Del Giglio, A., Paschoal, L. H. C., Ito, A. S. and Baptista, M. S. (2004). Treatment of melanoma lesions using methylene blue and RL50 light source. *Photodiagn. Photodyn. Ther.*, *1*, 345-346.
- [271] Tardivo, J. P., Del Giglio, A., de Oliveira, C. S., Gabrielli, D. S., Junqueira, H. C., Tada, D. B., Severino, D., de Fatima Turchiello, R. and Baptista, M. S. (2005). Methylene blue in photodynamic therapy: From basic mechanisms to clinical applications. *Photodiagn. Photodyn. Ther.*, *2*, 175-191.
- [272] Brown, S. B., Brown, E. A. and Walker, I. (2004). The present and future role of photodynamic therapy in cancer treatment. *Lancet Oncol.*, *5*, 497-508.
- [273] Mohr, H., Lambrecht, B. and Selz, A. (1995). Photodynamic Virus Inactivation of Blood Components. *Immunol. Invest.*, *24*, 73-85.
- [274] Wainwright, M., Mohr, H. and Walker, W. H. (2007). Phenothiazinium derivatives for pathogen inactivation in blood products. *J. Photochem. Photobiol. B-Biol.*, *86*, 45-58.
- [275] Usacheva, M. N., Teichert, M. C. and Biel, M. A. (2001). Comparison of the methylene blue and toluidine blue photobactericidal efficacy against gram-positive and gram-negative microorganisms. *Lasers Surg. Med.*, *29*, 165-173.
- [276] Pottier, R., Bonneau, R. and Joussetdubien, J. (1975). Ph-Dependence of Singlet Oxygen Production in Aqueous-Solutions Using Toluidine Blue as a Photosensitizer. *Photochem. Photobiol.*, *22*, 59-61.
- [277] Donnelly, R. F., McCarron, P. A., Cassidy, C. M., Elborn, J. S. and Tunney, M. M. (2007). Delivery of photosensitizers and light through mucus: Investigations into the potential use of photodynamic therapy for treatment of *Pseudomonas aeruginosa* cystic fibrosis pulmonary infection. *J. Control. Release*, *117*, 217-226.
- [278] Donnelly, R. F., McCarron, P. A., Tunney, M. M. and David Woolfson, A. (2007). Potential of photodynamic therapy in treatment of fungal infections of the mouth.

- Design and characterisation of a mucoadhesive patch containing toluidine blue O. *J. Photochem. Photobiol. B-Biol.*, 86, 59-69.
- [279] Qin, Y. L., Luan, X. L., Bi, L. J., He, G. P., Bai, X. F., Zhou, C. N. and Zhang, Z. G. (2008). Toluidine blue-mediated photoinactivation of periodontal pathogens from supragingival plaques. *Lasers Med. Sci.*, 23, 49-54.
- [280] Wilson, M., Burns, T., Pratten, J. and Pearson, G. J. (1995). Bacteria in Supragingival Plaque Samples Can Be Killed by Low-Power Laser-Light in the Presence of a Photosensitizer. *J. Appl. Bacteriol.*, 78, 569-574.
- [281] Williams, J., Wilson, M., Conway-Wallace, H., Pearson, G. and Colles, J. (2003). Action of tolonium chloride against *S mutans* in a collagen matrix. *J. Dent. Res.*, 82, 498-498.
- [282] Williams, J. A., Pearson, G. J., Colles, M. J. and Wilson, M. (2003). The effect of variable energy input from a novel light source on the photoactivated bactericidal action of toluidine blue O on *Streptococcus mutans*. *Caries Res.*, 37, 190-193.
- [283] Bonsor, S. J., Nichol, R., Reid, T. M. S. and Pearson, G. J. (2006). Microbiological evaluation of photo-activated disinfection in endodontics (An in vivo study). *Br. Dent. J.*, 200, 337-341.
- [284] Bonsor, S. J., Nichol, R., Reid, T. M. S. and Pearson, G. J. (2006). An alternative regimen for root canal disinfection. *Br. Dent. J.*, 201, 101-105.
- [285] Qin, Y. L., Luan, X. L., Bi, L. J., Sheng, Y. Q., Zhou, C. N. and Zhang, Z. G. (2008). Comparison of toluidine blue-mediated photodynamic therapy and conventional scaling treatment for periodontitis in rats. *J. Periodont. Res.*, 43, 162-167.
- [286] PerioWave.com [online]. 2008 [cited 2008-04-02]. Available from: <http://www.periowave.com/>
- [287] OndineBiopharma.com [online]. 2008 [cited 2008-04-02]. Available from: <http://www.ondinebiopharma.com/>
- [288] Denfotex.com [online]. 2008 [cited 2008-04-02]. Available from: <http://www.denfotex.com/>
- [289] Rozanowska, M., Ciszewska, J., Korytowski, W. and Sarna, T. (1995). Rose-bengal-photosensitized formation of hydrogen peroxide and hydroxyl radicals. *J. Photochem. Photobiol. B-Biol.*, 29, 71-77.
- [290] Carballo, M., Alvarez, S. and Boveris, A. (1993). Cellular stress by light and Rose Bengal in human lymphocytes. *Mutat. Res.-Fundam. Mol. Mech. Mutagen.*, 288, 215-222.
- [291] Matthews, E. K. and Cui, Z. J. (1989). Photodynamic action of rose bengal on isolated rat pancreatic acini: stimulation of amylase release. *FEBS Lett.*, 256, 29-32.
- [292] Stevenson, N. R. and Lenard, J. (1993). Antiretroviral activities of hypericin and rose bengal: Photodynamic effects on Friend leukemia virus infection of mice. *Antiviral Res.*, 21, 119-127.
- [293] ProvectusPharmaceuticals.com [online]. 2008 [cited 2008-04-02]. Available from: <http://www.pvct.com/index.html>.
- [294] Udomsakdi, C., Eaves, C. J., Sutherland, H. J. and Lansdorp, P. M. (1991). Separation of Functionally Distinct Subpopulations of Primitive Human Hematopoietic-Cells Using Rhodamine-123. *Exp. Hematol.*, 19, 338-342.
- [295] Brasseur, N., Menard, I., Forget, A., El Jastimi, R., Hamel, R., Molfino, N. A. and van Lier, J. E. (2000). Eradication of multiple myeloma and breast cancer cells by TH9402-

- mediated photodynamic therapy: Implication for clinical ex vivo purging of autologous stem cell transplants. *Photochem. Photobiol.*, 72, 780-787.
- [296] KiadisPharma.com [online]. 2008 [cited 2008-04-02]. Available from: <http://www.kiadis.com/home.html>.
- [297] Sessler, J. L., Hemmi, G., Mody, T. D., Murai, T., Burrell, A. and Young, S. W. (1994). Texaphyrins: Synthesis and Applications. *Acc. Chem. Res.*, 27, 43-50.
- [298] Sessler, J. L., Johnson, M. R. and Lynch, V. (1987). Synthesis and crystal structure of a novel tripyrrane-containing porphyrinogen-like macrocycle. *J. Org. Chem.*, 52, 4394-4397.
- [299] Young, S. W., Woodburn, K. W., Wright, M., Mody, T. D., Fan, Q., Sessler, J. L., Dow, W. C. and Miller, R. A. (1996). Lutetium Texaphyrin (PCI-0123): A Near-Infrared, Water-Soluble Photosensitizer. *Photochem. Photobiol.*, 63, 892-897.
- [300] Kereiakes, D. J., Szyniszewski, A. M., Wahr, D., Herrmann, H. C., Simon, D. I., Rogers, C., Kramer, P., Shear, W., Yeung, A. C., Shunk, K. A. *et al* (2003). Phase I drug and light dose-escalation trial of motexafin lutetium and far red light activation (phototherapy) in subjects with coronary artery disease undergoing percutaneous coronary intervention and stent deployment: procedural and long-term results. *Circulation*, 108, 1310-1315.
- [301] Du, K. L., Mick, R., Busch, T. M., Zhu, T. C., Finlay, J. C., Yu, G., Yodh, A. G., Malkowicz, S. B., Smith, D., Whittington, R. *et al* (2006). Preliminary results of interstitial motexafin lutetium-mediated PDT for prostate cancer. *Lasers Surg. Med.*, 38, 427-434.
- [302] Verigos, K., Stripp, D. C., Mick, R., Zhu, T. C., Whittington, R., Smith, D., Dimofte, A., Finlay, J., Busch, T. M., Tochner, Z. A. *et al* (2006). Updated results of a phase I trial of motexafin lutetium-mediated interstitial photodynamic therapy in patients with locally recurrent prostate cancer. *J. Environ. Pathol. Toxicol. Oncol.*, 25, 373-387.
- [303] Dimofte, A., Zhu, T. C., Hahn, S. M. and Lustig, R. A. (2002). In vivo light dosimetry for motexafin lutetium-mediated PDT of recurrent breast cancer. *Lasers Surg. Med.*, 31, 305-312.
- [304] Woodburn, K. W., Fan, Q., Kessel, D., Luo, Y. and Young, S. W. (1998). Photodynamic Therapy of B16F10 Murine Melanoma with Lutetium Texaphyrin. *J. Invest. Dermatol.*, 110, 746-751.
- [305] Rockson, S. G., Kramer, P., Razavi, M., Szuba, A., Filardo, S., Fitzgerald, P., Cooke, J. P., Yousuf, S., DeVault, A. R., Renschler, M. F. *et al* (2000). Photoangioplasty for Human Peripheral Atherosclerosis : Results of a Phase I Trial of Photodynamic Therapy With Motexafin Lutetium (Antrin). *Circulation*, 102, 2322-2324.
- [306] Pharmacyclics [online]. 2008 [cited 2008-02-18]. Available from: www.pharmacyclics.com.
- [307] Sanchez-Garcia, D. and Sessler, J. L. (2008). Porphycenes: synthesis and derivatives. *Chem. Soc. Rev.*, 37, 215-232.
- [308] Stockert, J. C., Canete, M., Juarranz, A., Villanueva, A., Horobin, R. W., Borrell, J., Teixido, J. and Nonell, S. (2007). Porphycenes: Facts and prospects in photodynamic therapy of cancer. *Curr. Med. Chem.*, 14, 997-1026.
- [309] Szeimies, R.-M., Karrer, S., Abels, C., Steinbach, P., Fickweiler, S., Messmann, H., Baumler, W. and Landthaler, M. (1996). 9-Acetoxy-2,7,12,17-tetrakis([beta]-methoxyethyl)-porphycene (ATMPn), a novel photosensitizer for photodynamic

- therapy: uptake kinetics and intracellular localization. *J. Photochem. Photobiol. B-Biol.*, *34*, 67-72.
- [310] Fickweiler, S., Abels, C., Karrer, S., Baumler, W., Landthaler, M., Hofstadter, F. and Szeimies, R.-M. (1999). Photosensitization of human skin cell lines by ATMPn (9-acetoxy-2,7,12,17-tetrakis-([beta]-methoxyethyl)-porphycene) in vitro: mechanism of action. *J. Photochem. Photobiol. B-Biol.*, *48*, 27-35.
- [311] Segalla, A., Fedeli, F., Reddi, E., Jori, G. and Cross, A. (1997). Effect of chemical structure and hydrophobicity on the pharmacokinetic properties of porphycenes in tumour-bearing mice. *Int. J. Cancer*, *72*, 329-336.
- [312] Duraan, N. and Song, P.-S. (1986). Hypericine and its photodynamic action. *Photochem. Photobiol.*, *43*, 677-680.
- [313] Agostinis, P., Vantieghem, A., Merlevede, W. and de Witte, P. A. M. (2002). Hypericin in cancer treatment: more light on the way. *Int. J. Biochem. Cell Biol.*, *34*, 221-241.
- [314] Alecu, M., Ursaciuc, C., Halalau, F., Coman, G., Merlevede, W., Waelkens, E. and de Witte, P. (1998). Photodynamic treatment of basal cell carcinoma and squamous cell carcinoma with hypericin. *Anticancer Res.*, *18*, 4651-4654.
- [315] SciFinder Scholar 2007 [database online]. 2008 © American Chemical Society [cited 2008-02-22] Available from: www.cas.org/products/sfacad/index.html.
- [316] RadaPharma [online]. 2008 [cited 2008-02-22]. Available from: www.radapharma.ru/radachlorin.
- [317] Rozanova, N., Zhang, J. Z. and Heck, D. E. (2007). Catalytic therapy of cancer with porphyrins and ascorbate. *Cancer Lett.*, *252*, 216-224.
- [318] Girenko, E. G., Borisenkova, S. A. and Kaliya, O. L. (2002). Oxidation of ascorbic acid in the presence of phthalocyanine metal complexes. Chemical aspects of catalytic anticancer therapy. 1. Catalysis of oxidation by cobalt octacarboxyphthalocyanine. *Russ. Chem. Bull.*, *51*, 1231-1236.
- [319] Petrova, E. G., Borisenkova, S. A. and Kaliya, O. L. (2004). Oxidation of ascorbic acid in the presence of phthalocyanine metal complexes. Chemical aspects of catalytic therapy of cancer 2. Catalysis by cobalt octacarboxyphthalocyanine. Reaction products. *Russ. Chem. Bull.*, *53*, 2322-2326.
- [320] Camerin, M., Rello, S., Villanueva, A., Ping, X., Kenney, M. E., Rodgers, M. A. J. and Jori, G. (2005). Photothermal sensitisation as a novel therapeutic approach for tumours: Studies at the cellular and animal level. *Eur. J. Cancer*, *41*, 1203-1212.
- [321] Camerin, M., Rodgers, M. A. J., Kenney, M. E. and Jori, G. (2005). Photothermal sensitisation: evidence for the lack of oxygen effect on the photosensitising activity. *Photochem. Photobiol. Sci.*, *4*, 251-253.
- [322] Buseti, A., Soncin, M., Reddi, E., Rodgers, M. A. J., Kenney, M. E. and Jori, G. (1999). Photothermal sensitization of amelanotic melanoma cells by Ni(II)-octabutoxy-naphthalocyanine. *J. Photochem. Photobiol. B-Biol.*, *53*, 103-109.
- [323] Berg, K., Sandvik, K. and Moan, J. (1996). Transfer of molecules into the cytosol of cells. Wipo Patent WO/1996/007432. Available also from: www.freepatentsonline.com.
- [324] Berg, K., Kristian Selbo, P., Prasmickaite, L., Tjelle, T. E., Sandvig, K., Moan, J., Gaudernack, G., Fodstad, O., Kjolsrud, S., Anholt, H. *et al* (1999). Photochemical

- Internalization: A Novel Technology for Delivery of Macromolecules into Cytosol. *Cancer Res.*, 59, 1180-1183.
- [325] PCI Biotech AS [online]. 2008 [cited 2008-25-02]. Available from: www.pcibiotech.com.
- [326] Selbo, P. K., Sandvig, K., Kirveliene, V. and Berg, K. (2000). Release of gelonin from endosomes and lysosomes to cytosol by photochemical internalization. *Biochim. Biophys. Acta-Gen. Subj.*, 1475, 307-313.
- [327] Shiraishi, T. and Nielsen, P. E. (2006). Photochemically enhanced cellular delivery of cell penetrating peptide-PNA conjugates. *FEBS Lett.*, 580, 1451-1456.
- [328] Fretz, M. M., Hogset, A., Koning, G. A., Jiskoot, W. and Storm, G. (2007). Cytosolic delivery of liposomally targeted proteins induced by photochemical internalization. *Pharm. Res.*, 24, 2040-2047.
- [329] Selbo, P. K., Sivam, G., Fodstad, O., Sandvig, K. and Berg, K. (2001). In vivo documentation of photochemical internalization, a novel approach to site specific cancer therapy. *Int. J. Cancer*, 92, 761-766.
- [330] Ndoye, A., Dolivet, G., Hogset, A., Leroux, A., Fifre, A., Erbacher, P., Berg, K., Behr, J. P., Guillemin, F. and Merlin, J. L. (2006). Eradication of p53-mutated head and neck squamous cell carcinoma xenografts using nonviral p53 gene therapy and photochemical internalization. *Mol. Ther.*, 13, 1156-1162.
- [331] Berg, K., Dietze, A., Kaalhus, O. and Hogset, A. (2005). Site-Specific Drug Delivery by Photochemical Internalization Enhances the Antitumor Effect of Bleomycin. *Clin. Cancer Res.*, 11, 8476-8485.
- [332] Rosenthal, I., Sostaric, J. Z. and Riesz, P. (2004). Sonodynamic therapy - a review of the synergistic effects of drugs and ultrasound. *Ultrason. Sonochem.*, 11, 349-363.
- [333] Kessel, D., Jeffers, R., Fowlkes, J. B. and Cain, C. (1994). Porphyrin-Induced Enhancement of Ultrasound Cytotoxicity. *Int. J. Radiat. Biol.*, 66, 221-228.
- [334] Miyoshi, N., Misik, V. and Riesz, P. (1997). Sonodynamic toxicity of gallium-porphyrin analogue ATX-70 in human leukemia cells. *Radiat. Res.*, 148, 43-47.
- [335] Tata, D. B., Biglow, J., Wu, J. R., Tritton, T. R. and Dunn, F. (1996). Ultrasound-enhanced hydroxyl radical production from two clinically employed anticancer drugs, adriamycin and mitomycin C. *Ultrason. Sonochem.*, 3, 39-45.
- [336] Saad, A. H. and Hahn, G. M. (1992). Ultrasound-Enhanced Effects of Adriamycin against Murine Tumors. *Ultrasound Med. Biol.*, 18, 715-723.
- [337] Yumita, N., Nishigaki, R., Umemura, K., Morse, P. D., Swartz, H. M., Cain, C. A. and Umemura, S. (1994). Sonochemical Activation of Hematoporphyrin - an ESR Study. *Radiat. Res.*, 138, 171-176.
- [338] Yumita, N., Umemura, S., Magario, N., Umemura, K. and Nishigaki, R. (1996). Membrane lipid peroxidation as a mechanism of sonodynamically induced erythrocyte lysis. *Int. J. Radiat. Biol.*, 69, 397-404.
- [339] Yumita, N., Nishigaki, R. and Umemura, S. (2000). Sonodynamically induced antitumor effect of Photofrin II on colon 26 carcinoma. *J. Cancer Res. Clin. Oncol.*, 126, 601-606.
- [340] Yumita, N., Umemura, S. and Nishigaki, R. (2000). Ultrasonically induced cell damage enhanced by photofrin II: Mechanism of sonodynamic activation. *In Vivo*, 14, 425-429.

- [341] Umemura, S. I., Yumita, N. and Nishigaki, R. (1993). Enhancement of Ultrasonically Induced Cell-Damage by a Gallium-Porphyrin Complex, Atx-70. *Jpn. J. Cancer Res.*, 84, 582-588.
- [342] Umemura, K., Yumita, N., Nishigaki, R. and Umemura, S. I. (1996). Sonodynamically induced antitumor effect of pheophorbide a. *Cancer Lett.*, 102, 151-157.
- [343] Umemura, S., Yumita, N., Umemura, K. and Nishigaki, R. (1999). Sonodynamically induced effect of rose bengal on isolated sarcoma 180 cells. *Cancer Chemother. Pharmacol.*, 43, 389-393.
- [344] Miyoshi, N., Takeshita, T., Misik, V. and Riesz, P. (2001). Monomerization of photo sensitizers by ultrasound irradiation in surfactant micellar solutions. *Ultrason. Sonochem.*, 8, 367-371.
- [345] Kremkau, F. W., Kaufmann, J. S., Walker, M. M., Burch, P. G. and Spurr, C. L. (1976). Ultrasonic Enhancement of Nitrogen-Mustard Cytotoxicity in Mouse Leukemia. *Cancer*, 37, 1643-1647.
- [346] Longo, F. W., Tomashefsky, P., Rivin, B. D. and Tannenbaum, M. (1983). Interaction of Ultrasonic Hyperthermia with 2 Alkylating-Agents in a Murine Bladder-Tumor. *Cancer Res.*, 43, 3231-3235.
- [347] Moore, W. E., Lopez, R., Matthews, D. E., Sheets, P. W., Etchison, M. R., Hurwitz, A. S., Chalian, A. A., Fry, F. J., Vane, D. W. and Grosfeld, J. L. (1989). Evaluation of High-Intensity Therapeutic Ultrasound Irradiation in the Treatment of Experimental Hepatoma. *J. Pediatr. Surg.*, 24, 30-33.
- [348] Saad, A. H. and Hahn, G. M. (1989). Ultrasound Enhanced Drug Toxicity on Chinese-Hamster Ovary Cells-Invitro. *Cancer Res.*, 49, 5931-5934.
- [349] Harrison, G. H., Balcerkubiczek, E. K. and Eddy, H. A. (1991). Potentiation of Chemotherapy by Low-Level Ultrasound. *Int. J. Radiat. Biol.*, 59, 1453-1466.
- [350] Harrison, G. H., Balcerkubiczek, E. K. and Gutierrez, P. L. (1996). In vitro action of continuous-wave ultrasound combined with adriamycin, X rays or hyperthermia. *Radiat. Res.*, 145, 98-101.
- [351] Yumita, N., Umemura, S., Kaneuchi, M., Okano, Y., Magario, N., Ishizaki, M., Shimizu, K., Sano, Y., Umemura, K. and Nishigaki, R. (1998). Sonodynamically-induced cell damage with fluorinated anthracycline derivative, FAD104. *Cancer Lett.*, 125, 209-214.
- [352] Yumita, N., Kaneuchi, M., Okano, Y., Nishigaki, R., Umemura, K. and Umemura, S. (1999). Sonodynamically induced cell damage with 4'-O-tetrahydropyranyladriamycin, THP. *Anticancer Res.*, 19, 281-284.
- [353] Sakusabe, N., Okada, K., Sato, K., Kamada, S., Yoshida, Y. and Suzuki, T. (1999). Enhanced sonodynamic antitumor effect of ultrasound in the presence of nonsteroidal anti-inflammatory drugs. *Jpn. J. Cancer Res.*, 90, 1146-1151.
- [354] Okada, K., Itoi, E., Miyakoshi, N., Nakajima, M., Suzuki, T. and Nishida, J. (2002). Enhanced antitumor effect of ultrasound in the presence of piroxicam in a mouse air pouch model. *Jpn. J. Cancer Res.*, 93, 216-222.
- [355] Feril, L. B., Tsuda, Y., Kondo, T., Zhao, Q. L., Ogawa, R., Cui, Z. G., Tsukada, K. and Riesz, P. (2004). Ultrasound-induced killing of monocytic U937 cells enhanced by 2,2'-azobis(2-amidinopropane) dihydrochloride. *Cancer Sci.*, 95, 181-185.

- [356] Misik, V., Miyoshi, N. and Riesz, P. (1996). EPR spin trapping study of the decomposition of azo compounds in aqueous solutions by ultrasound: Potential for use as sonodynamic sensitizers for cell killing. *Free Radic. Res.*, 25, 13-22.
- [357] Yumita, N., Nishigaki, R., Umemura, K. and Umemura, S. (1989). Hematoporphyrin as a Sensitizer of Cell-Damaging Effect of Ultrasound. *Jpn. J. Cancer Res.*, 80, 219-222.
- [358] Yumita, N., Nishigaki, R., Umemura, K. and Umemura, S. (1990). Synergistic Effect of Ultrasound and Hematoporphyrin on Sarcoma-180. *Jpn. J. Cancer Res.*, 81, 304-308.
- [359] Umemura, S., Yumita, N., Nishigaki, R. and Umemura, K. (1990). Mechanism of Cell-Damage by Ultrasound in Combination with Hematoporphyrin. *Jpn. J. Cancer Res.*, 81, 962-966.
- [360] Quan-hong, L., Shi-hui, S., Ya-ping, X., Hao, Q., Jin-xuan, Z., Yao-hui, R., Meng, L. and Pan, W. (2004). Synergistic Anti-Tumor Effect of Ultrasound and Hematoporphyrin on Sarcoma180 Cells with Special Reference to the Changes of Morphology and Cytochrome Oxidase Activity of Tumor Cells. *J. Exp. Clin. Cancer Res.*, 23, 333-341.
- [361] Yumita, N., Okuyama, N., Sasaki, K. and Umemura, S. (2004). Sonodynamic therapy on chemically induced mammary tumor: Pharmacokinetics, tissue distribution and sonodynamically induced antitumor effect of porfimer sodium. *Cancer Sci.*, 95, 765-769.
- [362] Umemura, S., Kawabata, K., Sasaki, K., Yumita, N., Umemura, K. and Nishigaki, R. (1996). Recent advances in sonodynamic approach to cancer therapy. *Ultrason. Sonochem.*, 3, S187-S191.
- [363] Liu, Q. H., Wang, X. B., Wang, P., Xiao, L. N. and Hao, Q. (2007). Comparison between sonodynamic effect with protoporphyrin IX and hematoporphyrin on sarcoma 180. *Cancer Chemother. Pharmacol.*, 60, 671-680.
- [364] Tachibana, K., Kimura, N., Okumura, M., Eguchi, H. and Tachibana, S. (1993). Enhancement of Cell-Killing of HI-60 Cells by Ultrasound in the Presence of the Photosensitizing Drug Photofrin-Ii. *Cancer Lett.*, 72, 195-199.
- [365] Yumita, N. and Umemura, S. (2003). Sonodynamic therapy with photofrin II on AH130 solid tumor - Pharmacokinetics, tissue distribution and sonodynamic antitumoral efficacy of photofrin II. *Cancer Chemother. Pharmacol.*, 51, 174-178.
- [366] Tachibana, K., Sugata, K., Meng, J., Okumura, M. and Tachibana, S. (1994). Liver-Tissue Damage by Ultrasound in Combination with the Photosensitizing Drug, Photofrin-Ii. *Cancer Lett.*, 78, 177-181.
- [367] Yumita, N., Sasaki, K., Umemura, S. and Nishigaki, R. (1996). Sonodynamically induced antitumor effect of a gallium-porphyrin complex, ATX-70. *Jpn. J. Cancer Res.*, 87, 310-316.
- [368] Yumita, N., Sasaki, K., Umemura, S., Yukawa, A. and Nishigaki, R. (1997). Sonodynamically induced antitumor effect of gallium-porphyrin complex by focused ultrasound on experimental kidney tumor. *Cancer Lett.*, 112, 79-86.
- [369] Sasaki, K., Yumita, N., Nishigaki, R. and Umemura, S. (1998). Antitumor effect sonodynamically induced by focused ultrasound in combination with Ga-porphyrin complex. *Jpn. J. Cancer Res.*, 89, 452-456.
- [370] Yumita, N., Nishigaki, R., Sakata, I., Nakajima, S. and Umemura, S. (2000). Sonodynamically induced antitumor effect of 4-formyloximethylidene-3-hydroxy-2-

- vinyl-deuterio-porphynyl(IX)-6,7-diaspartic acid (ATX-S10). *Jpn. J. Cancer Res.*, 91, 255-260.
- [371] Yumita, N. and Umemura, S. (2004). Sonodynamic antitumour effect of chloroaluminum phthalocyanine tetrasulfonate on murine solid tumour. *J. Pharm. Pharmacol.*, 56, 85-90.
- [372] Milowska, K. and Gabryelak, T. (2005). Synergistic effect of ultrasound and phthalocyanines on nucleated erythrocytes in vitro. *Ultrasound Med. Biol.*, 31, 1707-1712.
- [373] Yumita, N., Kawabata, K., Sasaki, K. and Umemura, S. (2002). Sonodynamic effect of erythrosin B on sarcoma 180 cells in vitro. *Ultrason. Sonochem.*, 9, 259-265.

Chapter 2

PTHALOCYANINE TO USE PHOTSENSITIZER FOR PHOTODYNAMIC THERAPY OF CANCER

Keiichi Skamoto^{1,} and Eiko Ohno-Okumura²*

¹Department of Applied Molecular Chemistry, College of Industrial Technology, Nihon University, 1-2-1 Izumi-cho, Narashino-shi, Chiba-ken, 275-8575 Japan

²Research Institute of Chemical Science, Technology and Education, 8-37-1-104 Narashinodai, Funabashi-shi, Chiba-ken 274-0063 Japan

ABSTRACT

Phthalocyanine analogues containing alkyl-substituted benzenoid rings and pyridine rings are interesting compounds, because quaternation of the pyridine nitrogen is expected to form cationic amphiphilic compounds.

Non peripheral long alkyl substituted zinc phthalocyanine derivatives, zinc bis(1,4-didecylbenzo)-bis(3,4-pyrido)porphyrzine and zinc bis(1,4-didecylbenzo)-bis(2,3-pyrido)porphyrzine were reacted with dimethyl sulfate and monochloroacetic acid to give their quaternary products. Also the zinc phthalocyanine derivatives reacted with diethyl sulfate to afford the sufo-substituted products. All reacted compounds showed amphiphilic character.

Regio isomers of zinc bis(1,4-didecylbenzo)-bis(3,4-pyrido)porphyrzine were also quaternized with dimethyl sulfate.

Identical peaks in cyclic voltammograms appeared for these products before and after quaternization.

Zinc bis(1,4-didecylbenzo)-bis(2,3-pyrido)porphyrzine was evaluated the the photodynamic therapy of cancer efficacy by cancer cell culture.

The light exposed dimethyl sulfate quaternized zinc bis(1,4-didecylbenzo)-bis(2,3-pyrido) porphyrzines in IU-002 cells produces cell disruption that can be detected as a decrease as fluorescence.

* Correspondence should be addressed to Keiichi Sakamoto, k5saka@cit.nihon-u.ac.jp

INTRODUCTION

Phthalocyanine was accidentally discovered as a blue colored by-product of the *o*-cyanobenzamide from phthalimide in 1907. The blue colored by-product was named “phthalocynine”. Phthalocynine and metal containing derivatives have established as blue and green dyes, and are an important industrial commodity since 1942 [1].

Phthalocyanine derivatives have a similar structure to porphyrin. In general, porphyrins consist of four pyrrole units, while phthalocyanine derivatives construct four isoindole and nitrogen atoms at *meso* positions. The central cavity of phthalocyanine derivatives can place 63 different elemental ions include hydrogens (metal-free phthalocyanine). One or two metal ions containing phthalocyanine is called metal phthalocyanine.

Over the last decade, phthalocyanine derivatives have attracted attention as functional chromophores for applications [1–3], especially organic charge carriers in photocopiers [2], as laser light absorbers in data storage systems [4, 5], as photoconductors in photovoltaic cells [6], and in electrochromic displays [7].

Moreover, phthalocyanine derivatives known to have the potential as second-generation photosensitizers for the photodynamic therapy of cancer (PDT) [2], because they show strong absorption of far-red region between 600 and 850 nm wavelength, which has a greater penetration of tissue [3], and photo-sensitization of singlet oxygen [4].

It is well known that aluminum and zinc phthalocyanine derivatives expected to be used as the photosensitizer for PDT [8]. In these days, porphyrin derivatives such as hematoporphyrin derivatives and Photofrin™ have been used as photosensitizers for PDT at medical institutions [9, 10].

In general, the sensitizer for PDT requires a high photostability, high selectivity to tumors, no cytotoxicity when no light is irradiated, strong absorption in the region between 600 and 800 nm where penetration of tissue is good, and a long triplet state lifetime [11]. However porphyrin derivatives including hematoporphyrin derivatives and Photofrin™ are known to have a main absorption of around 400 nm where tissue penetration is low and a weak absorption. On the other hand, phthalocyanine derivatives exhibit the maximum absorption in the far-red range between 600 and 850 nm, and have a greater penetration of tissue [12] and a long triplet lifetime, and high singlet oxygen quantum yields [13]. The aggregation properties of phthalocyanine derivatives are a strong influence on the bioavailability, the *in vivo* distribution and the oxygen production efficiency [14].

Unsubstituted phthalocyanine derivatives are known to insoluble or lower soluble in common organic solvents. Insolubility or lower solubility of unsubstituted phthalocyanine derivatives has problems to utilize in many fields including PDT. Insolubility or lower solubility in common organic solvents is improved to introduce substituents such as alkyl groups onto the ring system. Alkyl group substituted phthalocyanine derivatives become soluble in common organic solvents, and have lipophilic property. Lipophilic phthalocyanine derivatives are reported to have a higher tumor affinity [15].

Whereas, introduction of hydrophilic groups into substituted phthalocyanine derivatives were performed in order to soluble in aqueous media. Water solubility of phthalocyanine derivatives has a strong influence on the bioavailability and *in vivo* distribution. Synthesized water-soluble phthalocyanine derivatives possess sulfo-, carboxy- and phosphono-

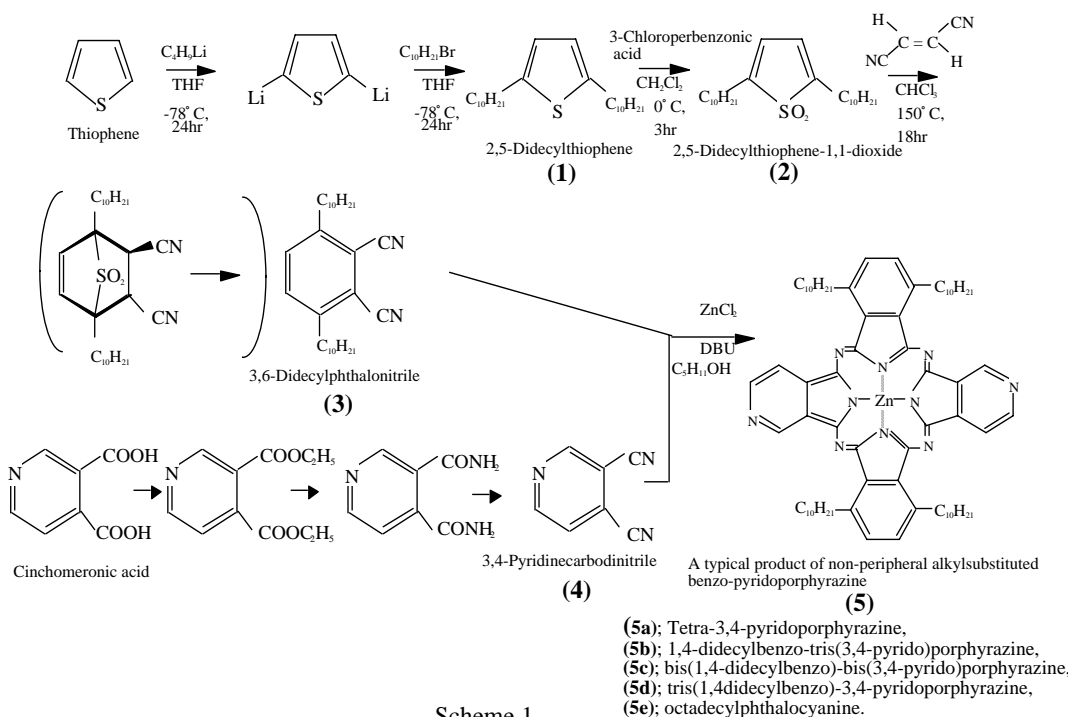
substituents, which used to compound have been synthesized to use tumor treatment [11, 14, 16-22].

Phthalocyanine analogues in which one or more of benzenoid rings are replaced by pyridine rings are interesting compound because quaternation of the pyridine nitrogen is expected to confer solubility in aqueous media [23]. Tetrapyrroldiporphyrazines containing four pyridinoid rings in place of four benzenoid ones were first synthesized by Linstead and his co-workers [24]. Tetramethylated tetrapyrroldiporphyrazines by quaternation were reported to become soluble in water [25, 26], and then these compounds were studied for PDT [27].

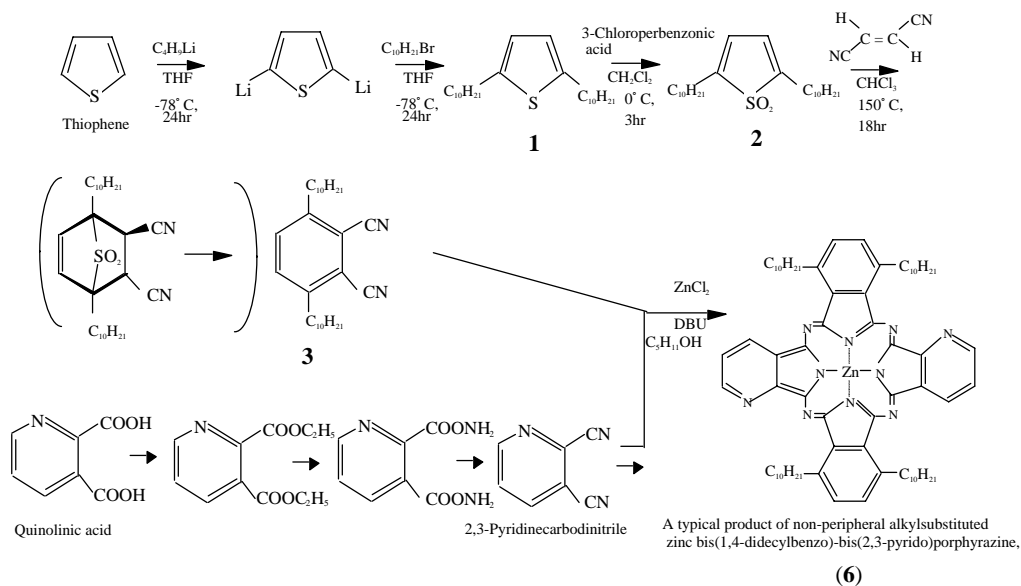
The authors reported a fundamental study on PDT by measuring for the triplet state lifetime of non-peripheral substituted phthalocyanine derivatives [27]. We synthesized to use non-peripheral substituted phthalocyanine derivative, zinc bis(1,4-didecylbenzo)-bis(3,4-pyrido)porphyrazine (**5c**), which possesses two didecylbenzenoid and two pyridinoid moieties in the molecule (Scheme 1) [23].

The compound **5c** exhibits solubility in organic solvents and is expected to have a higher tumor affinity than water soluble phthalocyanines such as tetrasulfophthalocyanines. Then, quaternation of the pyridine nitrogen in **5c** is expected to confer solubility in an aqueous media [25, 26], and to have bioavailability and *in vivo* distribution. The amphiphilic phthalocyanine derivatives are considered the best compound for a new generation of photosensitizers for PDT [13, 14, 15, 23]. Thus, the quaternation of **5c** will provide to be amphiphilic phthalocyanine derivatives.

Another type novel non-peripheral substituted phthalocyanine derivative, zinc bis(1,4-didecylbenzo)-bis(2,3-pyrido)porphyrazine (**6**) was synthesized (Scheme 2).



Scheme 1.



Scheme 2.

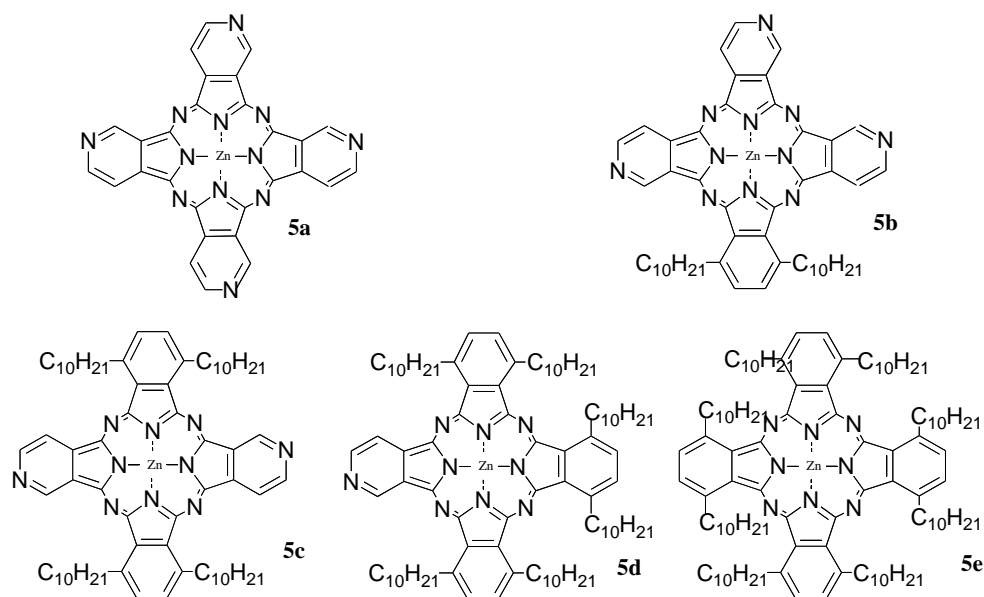


Figure 1. Molecular structures of zinc tetrapyrrodo porphyrazine **5a**, zinc 1,4-didecylbenzo-tris(3,4-pyridino)porphyrazine **5b**, zinc bis(1,4-didecylbenzo)-bis(3,4-pyridino)porphyrazine **5c**, zinc tris(1,4-didecylbenzo)-3,4-pyridino porphyrazine **5d**, and zinc octadecylphthalocyanine **5e**.

In the case of related compounds, 2,3-pyridoporphyrazines are known to have not longer wavelength but stronger absorption intensity than corresponding phthalocyanines and 3,4-pyridoporphyrazines [27]. In accordance with the literature [27], it is expected that **6** and its quaternation compounds have stronger absorption intensities than that of before reported **5c** [28-35]. Therefore, novel compound, **6** and its quaternation compounds are expected

excellent photosensitizer for PDT. Electron transfer ability of **6** is estimated with cyclic voltammetry (CV) technique.

The **6** was evaluated the PDT efficacy by cancer cell culture.

SYNTHESIS

Phthalocyanines can be prepared from cyclization of the appropriate phthalic acid derivatives such as the anhydride, imide or dinitrile.

Zinc non-peripheral substituted phthalocyanine derivatives **5** and **6** were synthesized by cross cyclotetramerization. Synthesized zinc non-peripheral substituted phthalocyanine derivatives **5** have different numbers of pyridine rings in the molecule (Figure 1).

The intermediates **1** - **3** and **4** were analysed by infrared (IR), proton nuclear magnetic resonance ($^1\text{H-NMR}$), mass (MS) spectra and elemental analysis, and the results are shown in Table 1. The analytical data for all compounds were in good agreement with the proposed structures.

The compound **5a** was also obtained by condensation of **4** with zinc chloride in the presence of 1,8-diazabicyclo[5,4,0]undec-7-ene (DBU). As a non-pyridinoide phthalocyanine derivative, non-peripheral substituted **5e** of which the substituents were 1, 4, 8, 11, 15, 18, 22, 25 region was synthesized from **3** and zinc chloride in the presence of DBU in accordance with the literature [29, 30]. The preparation of the alkylbenzopyridoporphyrazines was carried out by statistical condensation of zinc chloride, a catalytic amount of DBU, and mixtures of **3** and **4**, 3:1, 1:1 and 1:3 mol ratio, respectively.

A typical synthetic procedure of **5c** is described as following; a mixture of **3** and **4** for 1 (0.12 g, 0.29 mmol):1 (0.04 g, 0.29 mmol) mol ratio was dissolved in pentanol (7 cm³) and anhydrous zinc (II) chloride (0.05 g) was added. The mixture was heated at 137 °C for 4 h in the presence of DBU as a catalyst. After cooling, the reaction mixture was dissolved in toluene (50 cm³) and the solution filtered. The solvent was removed by evaporation. The products were separated and purified by thin layer chromatography (TLC) (Merk Silica gel 60 F₂₅₄ on aluminium sheet, eluent: toluene). Blue solid (0.18 g; yield 84%). $^1\text{H-NMR}$ (δ 400 MHz, benzene-d₆ (C₆H₆-d₆)/ppm) 0,9 (m, 12H, CH₃), 1.61-2.61 (m, 64H, CH₂), 4.18-4.36 (m, 8H, α -CH₂), 7.45 (m, 4H, arom), 8.26 (m, 6H, Py); IR(v KBr/cm⁻¹) 2970 ($\nu_{\text{C-H}}$), 1600 ($\nu_{\text{C-C}}$), 1500 ($\nu_{\text{C-C}}$), 1470 ($\nu_{\text{C-C}}$), 1450 ($\nu_{\text{C-C}}$), 1210 ($\delta_{\text{C-H}}$), 1090 ($\delta_{\text{C-H}}$), 720 ($\delta_{\text{C-H}}$); UV-Vis [λ_{max} toluene/nm (log ϵ_{max})] 686 (4.814), 636, 617; Anal Calcd. for C₇₀H₉₄N₁₀Zn: C. 73.68: H. 8.30: N.12.28. Found: C.73.67: H. 8.30: N. 12.28.

The compounds **5b** - **5d** and octadecylphthalocyanine **5e** were characterized by IR, ultraviolet-visible (UV-Vis) spectroscopy and elemental analysis.

The compounds **5a** and **5e** are composed of only one constituent. Whereas it is expected that the alkylbenzopyridoporphyrazines synthesized from mixed raw materials are prepared as a mixture of products, which have different numbers of pyridine rings in the molecule [26, 36]. Therefore, the alkylbenzopyridoporphyrazines can be separated into more than three blue-colored constituents. Then, each alkylbenzopyridoporphyrazine synthesized from mixed raw materials has the desired molecular structure for its main constituents [26, 36].

Table 1. Synthetic data of intermediates 1-4 of 5

Compound	Yield (%)	ν_{\max} $\text{KB}^{-1}/\text{cm}^{-1}$	δ (^1H 90MHz)/ppm $\text{CHCl}_3\text{-d}$	Formula	MS[M] ⁺ m/z	Found (calculation)		
						C	H	N
1	71	2960 (ν C-H), 1610 (ν C-C), 1490 (ν C-C), 1460 (ν C-C), 1370 (ν C-C), 1230 (δ C-H), 730 (δ C-H), 680 (ν C-S)	0.88(t,6H), 1.26(m,32H), 2.72(t,4H), 6.52(s,2H)	$\text{C}_{24}\text{H}_{44}\text{S}$	365	79.06 (79.04)	12.06 (12.06)	-
2	39	2970 (ν C-H), 1650 (ν C-C), 1480 (ν C-C), 1440 (ν C-C), 1370 (ν C-C), 1290 (ν S=O), 1220 (δ C-H), 1140 (ν S=O), 730 (δ C-H), 680 (ν C-S)	0.88(t,6H), 1.26(m,32H), 2.47(t,4H), 6.25(s,2H)	$\text{C}_{24}\text{H}_{44}\text{SO}_2$	397	72.66 (72.67)	11.18 (11.18)	-
3	26	2960 (ν C-H), 2240 (ν C-N), 1560 (ν C-C), 1460 (ν C-C), 1410 (ν C-C), 1230 (δ C-H), 730 (δ C-H),	0.88(t,6H), 1.26(m,32H), 2.85(t,4H), 7.46(s,2H)	$\text{C}_{28}\text{H}_{44}\text{N}_2$	409	82.26 (82.29)	10.84 (10.85)	6.84 (6.86)
4	17	3090 (ν C-H), 2240 (ν C-N), 1600 (ν C-C), 1550 (ν C-C), 1470 (ν C-C), 1220 (δ C-H), 750 (δ C-H),	7.26(s,1H), 7.75(s,1H), 9.09(s,1H)	$\text{C}_7\text{H}_3\text{N}_3$	129	65.12 (65.11)	2.34(2.34)	32.56(32.55)

Table 2. Characterization of 5 after purification by TLC

Compound	Yield (%)	Formula	Found (calculation)			Q-band λ_{\max} toluene/nm	ν_{\max} KBr/cm ⁻¹
			C	H	N		
5a	29	C ₂₈ H ₁₂ N ₁₂ Zn	57.81(57.79)	2.11(2.08)	28.90(28.89)	675*, 664*, 603*	2960 (v C-H), 1500(v C-C), 1470(v C-C), 1450 (v C-C), 1210(δ C-H), 1090(δ C-H), 790(δ C-H)
5b	65	C ₄₉ H ₅₃ N ₁₁ Zn	68.31(68.32)	6.22(6.20)	17.90(17.89)	686, 635, 617	2960 (v C-H), 1600(v C-C), 1460(v C-C), 1440 (v C-C), 1210(δ C-H), 1080(δ C-H), 720(δ C-H)
5c	84	C ₇₀ H ₉₄ N ₁₀ Zn	73.67(73.68)	8.30(8.30)	12.28(12.28)	686, 636, 617	2970 (v C-H), 1600(v C-C), 1500(v C-C), 1470 (v C-C), 1450 (v C-C), 1210(δ C-H), 1090(δ C-H), 720(δ C-H)
5d	84	C ₉₁ H ₁₃₅ N ₉ Zn	76.94(76.94)	9.57(9.58)	8.86(8.88)	686, 635, 617	2970 (v C-H), 1600(v C-C), 1500(v C-C), 1470 (v C-C), 1210(δ C-H), 1100(δ C-H), 720(δ C-H)
5e	96	C ₁₁₂ H ₁₇₆ N ₈ Zn	79.12(79.13)	10.41(10.43)	6.61(6.59)	703,	2960 (v C-H), 1600(v C-C), 1500(v C-C), 1460 (v C-C), 1210(δ C-H), 1100(δ C-H), 730(δ C-H)

* In pyridine under line; main peak.

Table 3. The relative number of each types of hydrogen atoms determined on 90MHz ¹H-NMR spectra 5 after purification by TLC

Compound	Number of hydrogen atom (calculation)			
	0.9 ppm	1.3 ppm	2.8 ppm	7.4 ppm
5b	6.7 (6)	33.4 (32)	4.2 (4)	11.0 (11)
5c	12.3 (12)	63.8 (64)	8.4 (8)	10.0 (10)
5d	18.8 (18)	95.9 (96)	12.3 (12)	9.0 (9)
5e	24.1 (24)	128.0 (128)	16.0 (16)	8.0 (8)

The analytical data of 5 are summarized in Table 2. These elemental analyses data agree with the desired molecular structure. It is concluded that compounds 5 synthesized from mixed raw materials are compounds 5*b* - 5*d*, respectively.

The compounds 5*b* - 5*d* and octadecylphthalocyanine 5*e* exhibited solubility in common organic solvents such as benzene (C₆H₆), toluene, dichloromethane (CH₂Cl₂), chloroform (CHCl₃), *N,N*-dimethylformamide (DMF) and dimethylsulfoxide (DMSO), etc.

Each synthesized product was purified by TLC (eluent: toluene). After purification, each product had only one blue-colored constituent together with colorless raw materials. The each constituent of the synthesized compounds was recovered from each TLC plate.

The compounds 5 displayed strong absorption peaks around 680 nm as the Q-band which could be attributed to the allowed $\pi - \pi^*$ transition [25, 29, 30, 34-42]. The Q-band absorption of 5 was shifted by 50 - 80 nm to a longer wavelength in comparison with unsubstituted phthalocyanines.

Table 3 shows the ¹H-NMR spectral data (90 MHz in CHCl₃-d) of 5*b* - 5*d* synthesized from mixed raw materials, and 5*e*. Each constituent of 5*b* - 5*d* obtained after purification by TLC gave satisfactory analytical data by proposed molecular structures.

It was confirmed that each product synthesized from the mixed raw materials of 3 and 4 was not included in the mixture of phthalocyanine analogous having a different pyridine ring number. Then, each product was obtained as the stoichiometric compound in accordance with the mole ratio of mixed raw materials, and contained their regio isomers except for 5*d*.

The target compound 5*c* synthesized from a 1:1 mol ratio raw material of 3 and 4 has five regio isomers (Figure 2).

Compound 5*c* has two non-peripheral substituted benzenoid and pyridinoid rings, which are different locations. In the molecule, the pyridinoid rings are adjacent and opposite to each other. In the case of adjacent to the pyridinoid rings, three types of isomer exist in accordance with the orientation of the ring. Meanwhile, two types of isomers exist in the case of opposite to the pyridinoid rings.

Compound 6 was synthesized as following; 3 (0.12 g, 0.29 mmol) and 2,3-dicyanopyridine (0.04 g, 0.29 mmol) were dissolved in pentanol (7 cm³) and zinc chloride (0.05 g) was added; the ensuing mixture was heated for 4 h in the presence of DBU as

catalyst. After cooling, the reaction mixture was dissolved in toluene (50 cm^3) and filtered; the solvent was removed by evaporation. The product was purified by TLC (eluent : toluene) yielding a blue solid (0.13 g; yield 80%). $^1\text{H-NMR}$ (δ 400 MHz, $\text{C}_6\text{H}_6\text{-d}_6$ /ppm) 0.9 (m, 12H, CH_3), 1.61-2.61 (m, 64H, CH_2), 4.18-4.36 (m, 8H, $\alpha\text{-CH}_2$), 7.45 (m, 4H, arom), 8.26 (m, 6H, Py); IR(v KBr / cm^{-1}) 2960 ($\nu_{\text{C-H}}$), 1600 ($\nu_{\text{C-C}}$), 1500 ($\nu_{\text{C-C}}$), 1420 ($\nu_{\text{C-C}}$), 1200 ($\delta_{\text{C-H}}$), 1100 ($\delta_{\text{C-H}}$), 750 ($\delta_{\text{C-H}}$); UV-Vis [λ_{max} toluene / nm (log ϵ_{max})] 665 (5.494); Anal Calcd. for $\text{C}_{70}\text{H}_{94}\text{N}_{10}\text{Zn}$: C. 73.68: H. 8.30: N.12.28. Found: C.73.67: H. 8.30: N. 12.28.

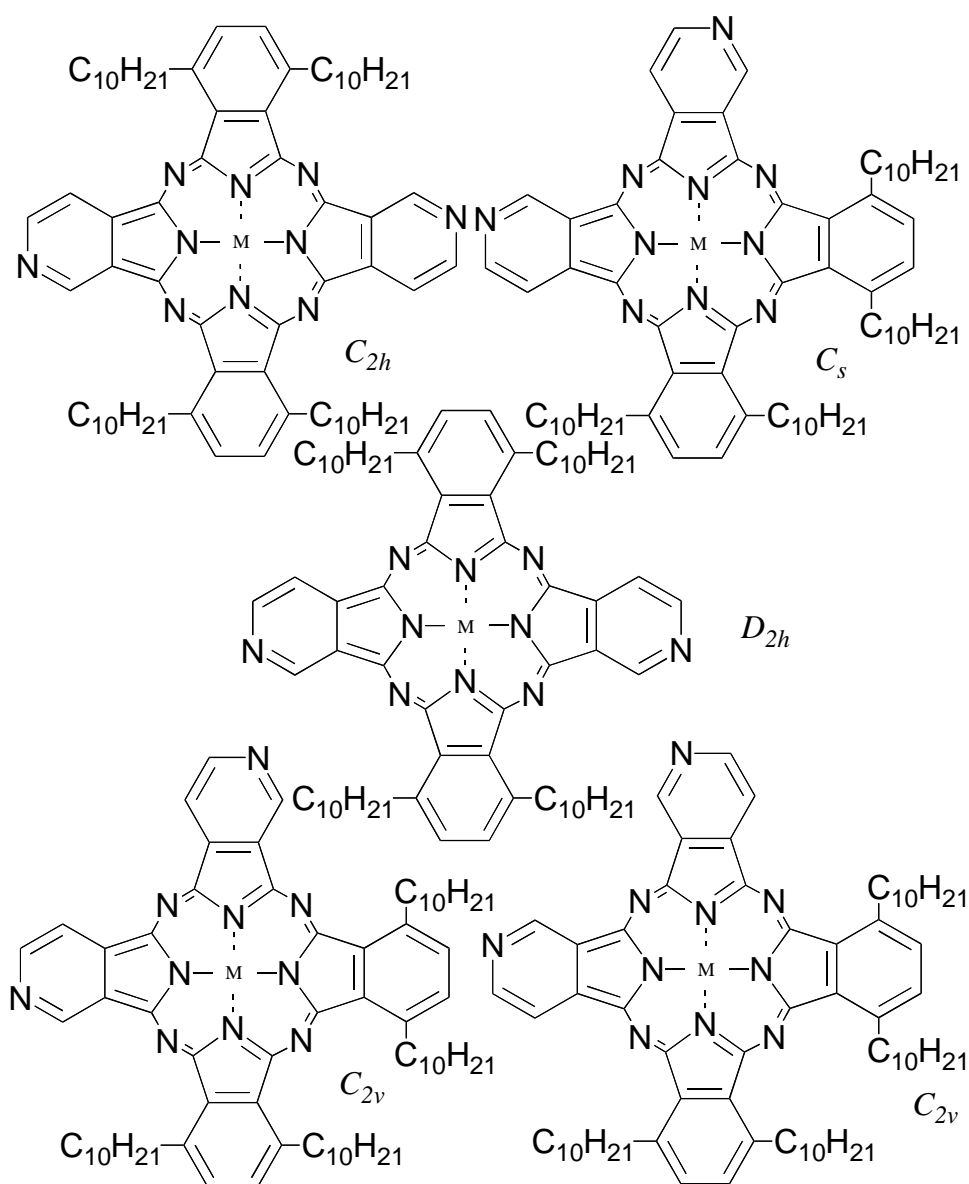


Figure 2. Molecular structures of resio isomers in 5c.

CHARACTERIZATION OF REGIO ISOMERS

We attempted to separate the regio isomers of the compound, *5c* using TLC (eluent: toluene - pyridine, 7:3). The compound *5c* was separated into four green- to blue-colored fractions by TLC. These fractions were numbered from 1, 2, 3 and 4, according to the R_f values, and the R_f values were 0.95, 0.91, 0.75 and 0.65, respectively. Each fraction was recovered by scraping from the TLC plate, dissolved in pyridine, the solution filtered, and the solvent removed. The four fractions have different $^1\text{H-NMR}$, UV-Vis and fluorescent spectra. The four fractions separated by TLC have been attributed to four of five possible regio isomers of the *5c*. The total amounts of fractions 1 - 4 are 26.1, 17.4, 17.4 and 39.1%, respectively.

The $^1\text{H-NMR}$ spectra (400 MHz, in $\text{C}_6\text{H}_6\text{-d}_6$) of the four fractions are shown in Table 4.

In this table, the assignment of hydrogens is the following; around 0.9 ppm is methyl protons; around 1.2 - 1.8 ppm is methylene protons γ or further removed from aromatic rings; 1.8 - 2.7 ppm is methylene protons β to aromatic rings; peaks around 4 and 4.3 ppm are methylene protons α to aromatic rings; peaks at 7.4 - 8.0 ppm are aromatic protons; more than 8.0 ppm are pyridyl protons.

The peaks of fractions in $\text{C}_6\text{H}_6\text{-d}_6$ around 8.3 ppm are separated after the addition of pyridine- d_5 [43-45]. The pyridyl protons of fractions appear as follows; the fraction 1: $\delta = 9.32$ (d, 2H), 9.47 (d, 2H), 11.19 (s, 2H); the fraction 2: $\delta = 9.23$ (d, 2H), 9.47 (d, 2H), 11.10 (s, 2H); the fraction 3: $\delta = 9.11$ (d, 1H), 9.16 (d, 1H), 9.34 (d, 1H), 9.40 (d, 1H), 10.98 (s, 1H), 11.06 (s, 1H); fraction 4: $\delta = 9.04$ (d, 1H), 9.11 (d, 1H), 9.38 (d, 1H), 9.44 (d, 1H), 10.97 (s, 1H), 11.05 (s, 1H).

The UV-Vis spectra of the four fractions are shown in Figure 3.

The UV-Vis spectra of four fractions show the typical pattern for phthalocyanine derivatives and analogous, mainly the $\pi\text{-}\pi^*$ transition with the heteroaromatic 18 π electron system. The Q bands around 700 nm are accompanied by characteristic weak satellite bands. In the UV-Vis spectra, the Q band is split into two bands (Q_1 and Q_2), except fraction 3.

Table 4. Spectral data (400 MHz $^1\text{H-NMR}$ in benzene- d_6) of fractions of *5c*

Compound	Chemical shift / ppm
Fraction 1	0.93 (t, 12H) 1.21-1.88 (m, 48H) 1.88-2.23 (m, 8H) 2.24-2.69 (m, 8H) 4.13 (t, 4H) 4.32 (t, 4H) 7.35 (d, 2H) 7.49 (d, 2H) 8.30 (m, 6H)
Fraction 2	0.92 (t, 12H) 1.24-1.80 (m, 48H) 1.82-2.29 (m, 8H) 2.32-2.62 (m, 8H) 4.12 (t, 4H) 4.30 (t, 4H) 7.36 (d, 2H) 7.49 (d, 2H) 8.31 (m, 6H)
Fraction 3	0.92 (t, 12H) 1.16-1.95 (m, 48H) 1.95-2.20 (m, 4H) 2.20-2.36 (m, 4H) 2.36-2.70 (m, 8H) 3.99 (t, 4H) 4.23 (t, 4H) 7.36 (d, 2H) 7.49 (d, 2H) 8.30 (m, 6H)
Fraction 4	0.92 (t, 12H) 1.27-1.83 (m, 48H) 1.83-2.26 (m, 8H) 2.30-2.68 (m, 8H) 4.07 (t, 4H) 4.29 (t, 4H) 7.35 (d, 2H) 7.48 (d, 2H) 8.31 (m, 6H)

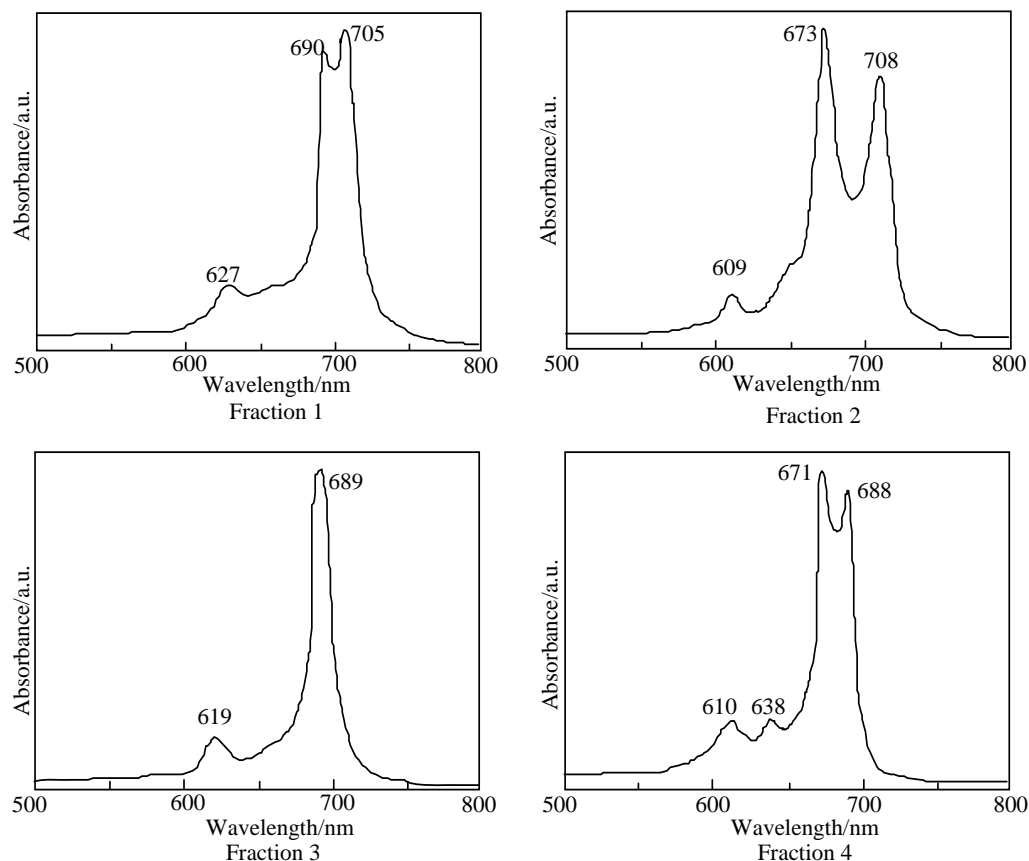


Figure 3.

The fluorescent spectra of the four fractions have different maxima at 703.6, 705.8, 694.8 and 701.0 nm for fraction 1, 2, 3 and 4, respectively (Figure 4). The fluorescence maxima were almost the same values for the four fractions. Similar phenomena were observed in the UV-Vis spectra of the four fractions.

It is known that fluorescence is expected in the molecules, which are aromatic and/or conjugation double bond with a high degree of resonance stability. The difference in the fluorescence maxima of the four fractions means dependence on the π electron environment of molecular structure.

The symmetry of the regio isomers of *5c* was decreased in the orders C_{2h} , D_{2h} , C_{2v} , C_s . The assignment of the spectra obtained from each fraction has been based on the theory of the relationship between symmetry and Q band [37-42], and consideration of the most probable formed isomer. Of the highest isomer symmetry, the Q band splits into two peaks, the splitting Q band is decreased with decreasing symmetry [23]. The Q band appearing at a higher wavelength corresponds to an electron transition from HOMO to LUMO, while the other is based on the one from HOMO to NLUMO.

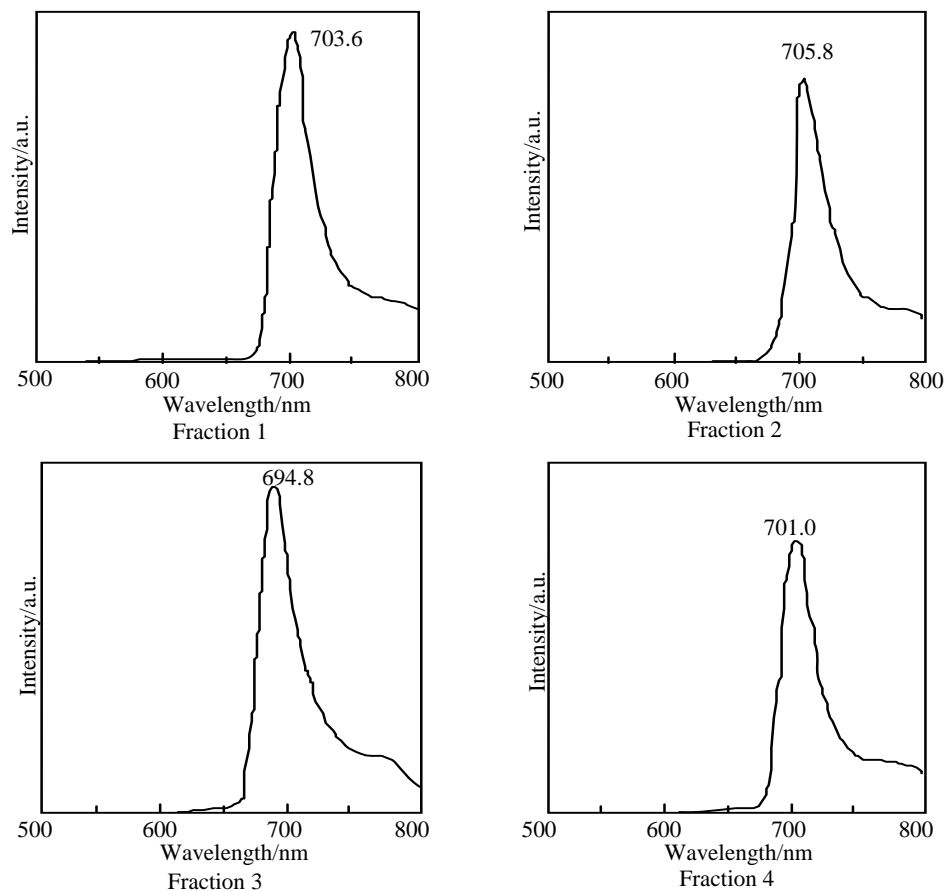


Figure 4.

The Q band absorption for fraction 2 is split into two peaks at λ_{\max} 708 and 673 nm, the observation attributes to the highest symmetry isomer C_{2h} . The lowest symmetrical isomer C_s probably corresponds to the single absorption peak shown in fraction 3. The Q band absorption of fraction 1 is split into two peaks at λ_{\max} 705 and 690 nm, and that of fraction 4 is at λ_{\max} 688 and 671 nm. Fractions 1 and 4 are associated with C_{2v} or D_{2h} isomers. However, the confirmation between C_{2v} or D_{2h} is difficult since the difference of Q band has almost same, and two C_{2v} isomers cannot be isolated and identified.

The molecular orbital calculation of the isomers was achieved in order to obtain their theoretical Q band absorptions with the ZINDO/S semi-empirical CI configurations which were performed using HyperChem 5.1Pro software. The theoretical data of Q band regions and splits are as follows; C_{2h} : λ_{\max} , 717.0 nm, 685.6 nm; δ_{Q1-Q2} , 31.4 nm; D_{2h} : λ_{\max} , 702.6 nm, 684.6 nm; δ_{Q1-Q2} , 18.0 nm; C_{2v} : λ_{\max} , 703.3 nm, 691.7 nm; δ_{Q1-Q2} , 11.6 nm; C_{2v} : λ_{\max} , 702.5 nm, 694.3 nm; δ_{Q1-Q2} , 8.2 nm; C_s : λ_{\max} , 700.4 nm, 697.3 nm; δ_{Q1-Q2} , 3.1 nm. The theoretical Q band splits in the isomers are decreased in the orders C_{2h} , D_{2h} , C_{2v} , C_s , and are in good agreement with the experimental data.

CV can be used to make an estimation of the electrochemical difference for regio isomers. CV was carried out with a BAS CV-50W voltammetric analyzer at room temperature in acetonitrile containing a 0.01 mol dm^{-3} solution of *tert*-butylammonium perchlorate (TBAP). CVs were recorded by scanning the potential at the rate of 50 mV s^{-1} . The working and counter electrodes were platinum wires, and the reference electrode was a silver/silver chloride (Ag/AgCl) saturated sodium chloride electrode. The area of the working electrode was $2.0 \times 10^{-2} \text{ cm}^2$.

The important parameters of a CV are the reduction and oxidation potentials for irreversible peaks, and the mid-point potential for a reversible couple, E_{mid} (Table 5).

Before separation of regio isomers, the reduction and oxidation potentials of *5c* are sorted into six irreversible peaks.

After separation, fractions 1 - 3 have one pair of reversible oxidation potential and four irreversible peaks. Fraction 4 has one pair of reversible oxidation and three irreversible reduction waves. The reduction and oxidation of metal phthalocyanine derivatives are due to the interaction between the phthalocyanine ring and the central metal [43-50].

The porphyrazine ring in the molecules of metal phthalocyanine derivatives or analogous is influenced by the π electrons about the closed system [49-53]. Although the π electron system of *5c* and fractions 1 - 4 consist of one porphyrazine, two pyridinoido and two didecyl substituted phenylene rings, the locations of these rings except for porphyrazine are different from each regio isomer.

Table 5. Reduction and oxidation potential of *5c* and dits position isomers (fractions 1-4)

Materials	Potential (V vs. Ag/AgCl)					
	Reduction			Oxidation		
<i>5c</i> , before separation of position isomers	-0.97*	-0.71*	-0.45*	-0.15*	0.37*	0.93*
Fraction 1	-1.00*	-0.58*	-0.24*		0.44	0.93*
ΔE^{**}					0.17	
Fraction 2	-1.05*	-0.60*	-0.19*		0.37	0.90*
ΔE^{**}					0.10	
Fraction 3	-0.96*	-0.65*	-0.22*		0.37	0.89*
ΔE^{**}					0.13	
Fraction 4	-0.87*	-0.63*	-0.21*		0.34	
ΔE^{**}					0.01	

Potentials of reversible wave are midpoint potential of anodic and cathodic peaks for each couple, E_{mid}

* Irreversible peak.

** The anodic peak to cathodic peak separation for reversible couple.

The irreversible peaks are attributed to the oxidation of the central metal and the reversible couples represent the redox of the phthalocyanine ring [54].

Substituents and pyridinoid rings influenced the π electron environment in the *5c* and fractions 1 - 4. It is thought that the effect of pyridinoid rings gives rise to changes of the electron density of the metal phthalocyanine derivative. The difference of reduction and oxidation peaks between fractions 1 - 4 is attributed to the effect of the variation of the interaction between the central metal and the alkylbenzoporphyrazine. And then, the difference of cyclic voltammogram between the *5c* and fractions 1 - 4 is also the effect of the interaction, since *5c* is a mixture of its regio isomers.

The ΔE values are the anodic peak to cathodic peak separation located in the oxidation potential region. The ΔE values are around 100 mV and the redox processes are the same for regio isomers, except for fraction 4. This means that the electron process of regio isomers between fractions 1 - 3 involve approximately one electron transfer. The ΔE values of fraction 4 show different behaviour in comparison to the others. It is thought that the different behavior for fraction 4 is attributable to the mixture of two types of C_{2v} regio isomers. In other words, the reduction and oxidation potentials of fraction 4 are based on the interaction between two types of C_{2v} regio isomers. No observation on the reversible couple in *5c* resulted in the interaction between the regio isomers.

The potential difference between the reduction and oxidation is expressed in the HOMO - LUMO energy gap [55]. The values of λ_{\max} in the Q band correlated with the potential difference between the reduction and oxidation.

The compound *6* fluoresced on exposure to ultraviolet light. Although fluorescence spectra generally were known to be mirror images of UV-Vis spectra at the longer wavelengths, the Q bands nearly overlapped with the wavelengths at which fluorescence occurs in the case of *6*, thus, the differences between λ_{\max} of UV-Vis and the F_{\max} of fluorescence spectra, called the Storks shift, were very small. These observations are similar to that seen with the *6*.

LASER-FLASH PHOTOLYSIS OF ALKYLBNZOPYRIDOPORPHYRAZINES

The absorption maxima of the compounds appeared around 660 – 710 nm in the solutions. The UV-Vis spectra of *5a*, *5c* and *5e* show the typical shape for phthalocyanine derivatives. The strongest peaks are assigned as the Q band, which could be attributed to the allowed $\pi - \pi^*$ transition of a phthalocyanine ring. The *5c* had the strongest absorption intensity of the products. The λ_{\max} and $\log \epsilon_{\max}$ of products are summarized in the Table 6.

Laser flash photolysis in film was performed using a total reflection sapphire cell (10 x 30 mm, 1 mm thick, and both of the short side were cut at a 45° angle), which was spin-coated with a 1.2 μm thick photopolymer film. An excitation light pulse (20 ms, 355 nm and 10 mJ per pulse) from a YAG laser was expanded and exposed over the entire sample cell. A monitoring light from a xenon lamp passed through the multireflection cell which was connected to the head of an optical fiber attached to a monochromator equipped with a photomultiplier or to a spectral multichannel analyzer system[57-65].

Table 6. UV-Vis spectral data of 5a-5c in toluene at 5.0×10^{-5} M, and 5e in pyridine at 2.6×10^{-5} mol dm⁻³

Compounds	λ_{max} / nm	log ϵ_{max}
5a*	675	4.243
5b	686	4.472
5c	687	4.814
5d	686	4.661
5e	707	4.720

* Pyridine solution.

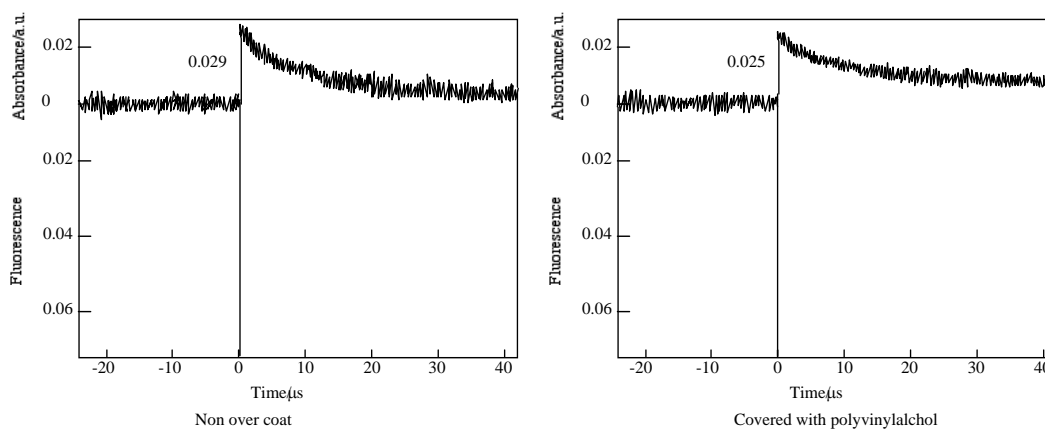


Figure 5. Decay trace of 5c in PMMA film on 560 nm.

Wxcitation wavelength is 355 nm in the presence and absence of PVA coatings.

The films were prepared as follows: A 10 wt% poly(methyl methacrylate) (PMMA) solution was made up in cyclohexanone, alkylbenzopyridoporphyrazines were added to this solution by dissolving to a thickness of 1.2 μm thick by spin-coating a solution onto a sapphire cell. After that the films were covered with a poly(vinyl alcohol) (PVA) solution.

Figure 5 shows the time profiles of the triplet state for one of the alkylbenzopyridoporphyrazines, 5c in PMMA was observed using laser-flash photolysis.

The triplet state lifetime of alkylbenzopyridoporphyrazines, 5b – 5d and 5e were also summarized in Table 7.

In each alkylbenzopyridoporphyrazine 5, it is shown that 5b and 5c have longer triplet lifetimes than 5d and 5e. The length of the triplet lifetime for alkylbenzopyridoporphyrazine depends upon its molecular structure. The triplet lifetime of alkylbenzopyridoporphyrazines increased with increasing pyridine numbers in the molecule. It seems that if

tetrapyrroldiopyrroazine *5a* can be soluble in common solvents and measured for laser-flash photolysis, its triplet lifetime will be shown the longest value.

The photoexcited triplet state lifetimes of *5b* and *5c* in PMMA without a PVA coating were estimation to be 11.4 and 10.1 μs , respectively. While covered with a PVA coating, the photoexcited triplet state lifetimes of *5b* and *5c* were estimated as 51.8 and 46.9 μs , respectively. Compared with each compound, the triplet state lifetime in PMMA covered with PVA was longer than without the PVA coating.

The Q-band absorption of *5* in PMMA films was similar to that in solution, but the profile of Q-band in PMMA film became wider than that in solution and moved to a longer wavelength, except for *5e*.

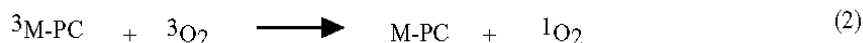
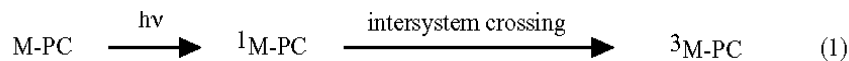
Non-transition metal phthalocyanine derivatives were known to be excellent photosensitizers because of their chemical stability and high absorbance in the 650 – 700 nm region [56]. In the presence of a photosensitizer, photooxidation progresses via singlet state oxygen [57–66]. Phthalocyanine derivatives in the excited triplet state react with ground triplet state dioxygen. The triplet state dioxygen generated singlet excited state oxygen. The singlet excited oxygen reacts with a substrate to produce oxide, Equations. (1) – (3) [23, 35].

Both, covered with a coating and without PVA, the photooxidation proceeded as the same mechanism. However, in the case of being covered with PVA, the photoexcited triplet state lifetimes of alkylbenzopyrroldiopyrroazines, *5b* – *5d* and *5e*, were longer than in the case of non-overcoating with PVA. In the case of non-coated with PVA the shorter decay time was considered due to M-PC quenching by oxygen existing in an air atmosphere. While under the coated state with PVA, they suppressed the oxygen-permeation from the air atmosphere into the photopolymer layer. As a result, ground triplet state dioxygen was not furnished from the surrounding to the system.

Compounds *5* in the case of being covered with PVA behaved as a model for a practical photosensitizer in tumors or cancer cells.

Table 7. Triplet lifetime of 5b-5e

Compound	Q-band/nm in PMMA film	Lifetime/ μs	
		non over coat	over coat
5b	675.2	11.4	51.8
5c	717.6	10.1	46.9
5d	670.0	5.7	18.2
5e	703.9	2.6	17.9



In comparison with *5b* and *5c*, the photoexcited triplet lifetime of *5b* was slightly longer than *5c*, the absorption intensities for *5c* were stronger than *5b*. So that in these aspects, there is little to choose as a sensitizer for PDT between the two. As pyridine rings in the molecule of *5* increased, the water-solubility is expected to increase. In the case of the *N,N',N'',N'''*-tetramethylated quaternized forms of tetrapyrroldiporphyrins, it was reported that the complexes do not form an aggregation in an aqueous solution [35, 67, 69]. Although the long alkyl-chain substituents in *5b* and *5c* will occur in aggregation, *5b* and *5c* are expected to undergo rapidly photodecomposition after the photooxidation process, similar to alkyl phthalocyanine derivatives [15].

Consequently, since *5b* and *5c* have the most intense absorption and a longer triplet state lifetime, we think *5b* and *5c* will become a useful sensitizer for PDT. The photosensitizer should be made in isomerically pure form [15]. Isomers of *5b* have not been reported yet, but *5c* has been separated and identified [23]. Thereupon, isomers of *5c* were examined by laser-flash photolysis, and *5b* will be reported next time.

LASER- FLASH PHOTOLYSIS OF REGIO ISOMERS

The regio isomers of the compound, *5c* were separated into four green- to blue-colored fractions by TLC [24]. The four fractions have a different ^1H NMR, UV-Vis and fluorescent spectra. The four fractions separated by TLC have been attributed to four of the five possible regio isomers of *5c*.

Figure 6 shows the fluorescence and excitation spectra of *5c*. The excitation spectra of *5c* and its fractions have almost the same profile. No significant change on the fluorescence spectra was observed for *5c* and its fractions.

Table 8 shows the Q-band and fluorescent maximum of fractions of *5c*. The assignment of the Q-band from each fraction was carried out on the theory of the relationship between symmetry and the Q-band [37, 38, 40, 41]. The Q-band splits into two peaks of the highest isomer symmetry, the splitting Q-band is decreased with a decreasing symmetry [41]. The symmetry of the position isomer of *5c* was decreased in orders of C_{2h} , D_{2h} , C_{2v} , C_s [21].

The position isomers of *5c* were the symmetry of molecular structures as D_{2h} , C_{2h} , C_s and C_{2v} for fractions 1, 2, 3 and 4, respectively [23]. Two types of C_{2v} isomers were not able to be isolated [23].

Table 9 shows the photoexcited triplet lifetime of fractions separated from *5c*. In spite of the presence or absence of PVA coatings, the triplet lifetime was increased with a decreasing symmetry of position isomers, which were ordered as C_{2h} , D_{2h} , C_{2v} and C_s for fractions 2, 1, 4 and 3, respectively. The photoexcited triplet state lifetimes of fraction 3 in PMMA absence and presence of a PVA coating were estimated to be 14.29 and 25.97 μs , respectively. Of each fraction except for fraction 3, the length of the lifetime was shorter than *5c*, and the sensitivities of triplet-triplet (T-T) absorptions were observed as very low.

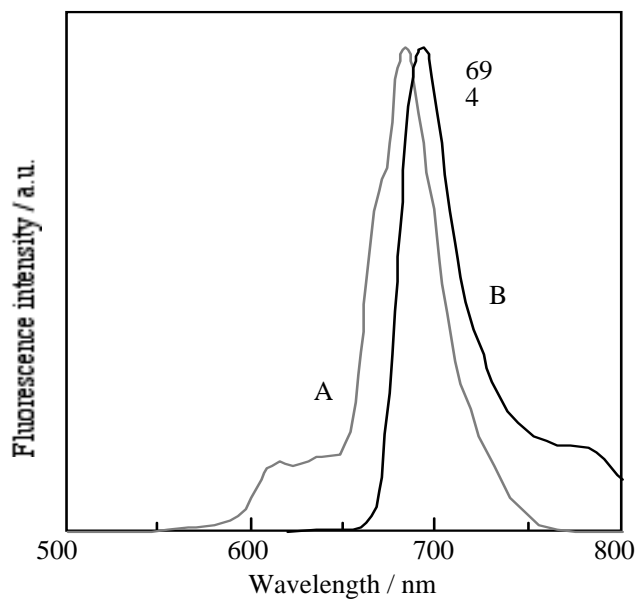


Figure 6. Fluorescence and excitation spectra of **5c** in DMF. A: Excitation spectrum, B: fluorescence spectrum.

Table 8. Absorption and fluorescence maxima for each fraction of **5c in solution**

Compound	Absorption Q band / nm	Fluorescence / nm	Symmetry
Fraction 1	627, 690, 705	704	D_{2h}
Fraction 2	609, 673, 708	706	C_{2h}
Fraction 3	619, 689	695	C_s
Fraction 4	610, 638, 671, 688	701	C_{2v}

==== : Most intense peak

——— : Next intense peak

Although the length of the triplet lifetime of *5c* was observed by approximately 4 times that of the absence of a PVA over coating, the fractions of *5c* were only about 1.5 times as long as triplet lifetimes in comparison with the absence and presence of PVA coatings.

Unfortunately, a precise solution to the cause cannot be obtained. However, it seems to be the followings. Phthalocyanine derivatives were well known to aggregate in water and non-coordinating solvents. Zinc non-peripheral phthalocyanine derivatives having long side chains formed an aggregation at least 10^{-5} mol dm⁻³ in cyclohexane [18, 64]. It is enough thought that the samples in this study for laser-flash photolysis were formed in aggregation in the experimental condition. The aggregation degree for *5c* and its isomers is different from each other. And then, the ability of aggregation for *5c* and each of its isomers is a difference and complication. Since compounds *5b* and *5c* were consisted mixtures of their isomers, the aggregation and relationships of the energy levels between samples and the triplet state of dioxygen became a complication. For this reason, compounds *5b* and *5c* could measure relatively long lifetimes. The molecular structure of fraction 3 is suitable to occur in the T-T absorption in the system.

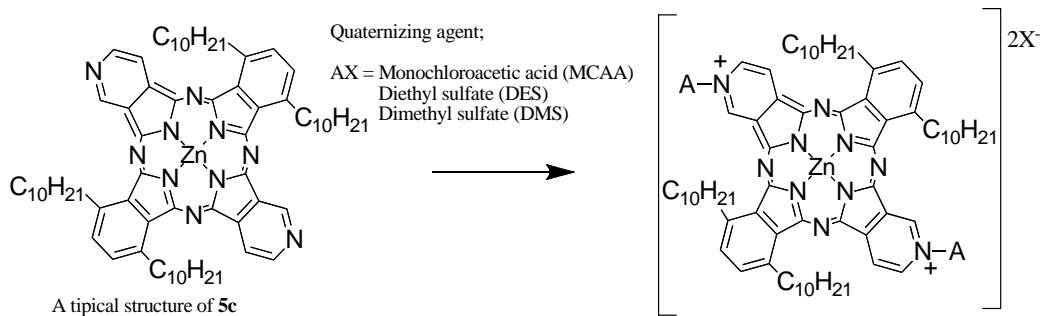
In order to estimate the photoexcitation mechanism, the triplet lifetime of each fraction was measured, containing *N,N'*-tetramethyl-4,4'-diaminobenzophenon (Michler's keton) as an additional quencher. As using Michler's keton, the lifetimes without PVA coatings were estimated as 21.19 and 14.03 μ s for fractions 3 and 4, respectively (Table 10). These values of lifetime were longer than in the absence of Michler's keton. In the case of fractions 1 and 2, no T-T absorption occurred. The results were thought to be that each fraction has different energy levels of ground and excited states. The T-T absorption took place via the interactions between the energy levels of ground or excited states of fractions and the triplet of dioxygen or Michler's keton.

Table 9. Triplet lifetime of each fraction of *5c*

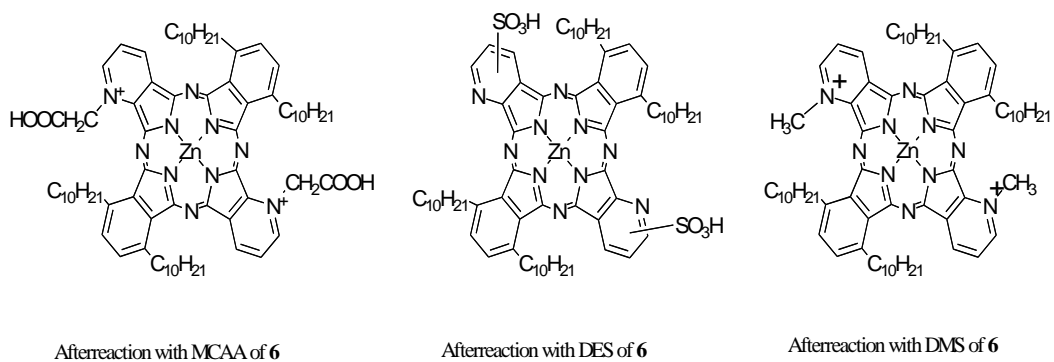
Compound	Q-band/nm in PMMA film	Lifetime/ μ s	
		non over coat	over coat
Fraction 1	728.2, 681.6, 653.5	7.0	11.3
Fraction 2	670.0	0.9	1.6
Fraction 3	696.4	14.29	25.97
Fraction 4	665.5	6.4	9.2

Table 10. Triplet lifetime of each fraction of 5c using Micher's keton as a quencher

Compound	Lifetime μ s	
	non over coat	over coat
Fraction 1	-	-
Fraction 2	-	-
Fraction 3	21.19	72.72
Fraction 4	14.03	47.32



Scheme 3.



Scheme 4.

QUATERNATION OF ALKYL BENZOPYRIDOPORPHYRAZINE

Compound **5c** and **6** were reacted with quaternizing agents such as monochloroacetic acid (MCAA), diethyl sulfate (DES) and dimethyl sulfate (DMS) (Scheme 3 & 4).

Quaternized **5c** is performed as followings: **5c** (0.17 g, 0.15 mmol) was reacted with quaternizing agents such as MCAA (0.57 g, 6 mmol), DES (0.1 g, 0.6 mmol) and DMS (0.2 g, 1.5 mmol), respectively, in DMF as solvent at 140 °C for 2h. The reaction mixture was dissolved in acetone (20 cm³), cooled to room temperature and the solution filtered. The solvent was removed. The products were purified by TLC (eluent: THF-toluene, 8 : 2). Each product was recovered by scraping from the TLC plate, dissolved in pyridine, the solution filtered, and the solvent removed.

Yields of products were 23%, 17% and 28% for MCAA, DES and DMS as quaternizing agents, respectively. After reaction with quaternizing agents, **5c** were identified through spectroscopic techniques such as ¹H-NMR, IR and UV-Vis spectra.

- (a) Product with MCAA: dark blue solid (32 mg; yield 23%). ¹H-NMR (δ 400 MHz, DMSO-d₆/ppm) 0.85 (m, 12H, CH₃), 1.19-1.71 (m, 48H, γ-CH₂), 1.79-2.12 (m, 8H, β-CH₂), 2.27-2.68 (m, 8H, β-CH₂), 4.15 (m, 4H, α-CH₂), 4.39 (m, 4H, α-CH₂), 6.19 (s, 2H, CH₂), 7.37 (m, 4H, arom), 8.32 (m, 6H, Py); IR (ν KBr/cm⁻¹) 3050 (ν_{C-H}), 2980 (ν_{C-H}), 1730 (ν_{C=O}), 1620 (ν_{C-C}), 1400 (ν_{C-C}), 1210 (δ_{C-H}), 1080 (δ_{C-H}), 790 (δ_{C-H}), 690 (δ_{C-H}); UV-Vis (λ_{max} toluene/nm) 686; (λ_{max} pyridine/nm) 690; (λ_{max} water/nm) 681; Anal Calcd. for C₇₄H₁₀₀N₁₀O₄Zn: C. 45.05; H. 2.52; N.17.50. Found: C.45.02; H. 2.49; N. 17.48;
- (b) Product with DES: blue solid (37 mg, yield 17%). ¹H-NMR (δ 400 MHz, DMSO-d₆/ppm) 0.86 (m, 12H, CH₃), 1.02-1.70 (m, 48H, γ-CH₂), 1.88-2.11 (m, 8H, β-CH₂), 2.30-2.68 (m, 8H, β-CH₂), 4.11 (m, 4H, α-CH₂), 4.25 (m, 4H, α-CH₂), 7.38 (m, 4H, arom), 8.18 (m, 4H, Py); IR (ν KBr/cm⁻¹) 3050 (ν_{C-H}), 2960 (ν_{C-H}), 1500 (ν_{C-C}), 1450 (ν_{C-C}), 1400 (ν_{C-C}), 1340 (ν_{S-O}), 1180 (ν_{S-O}), 1250 (δ_{C-H}), 920 (δ_{C-H}), 760 (δ_{C-H}), 590 (δ_{C-S}); UV-Vis (λ_{max} toluene/nm) 687; (λ_{max} pyridine/nm) 731; (λ_{max} water/nm) 679; Anal Calcd. for C₇₀H₉₈N₁₀S₂O₆Zn: C. 37.11; H. 1.78; N.18.54. Found: C.37.10; H. 1.78; N. 18.49;
- (c) Product with DMS: dark blue solid (53 mg, yield 28%). ¹H-NMR (δ 400 MHz, DMSO-d₆/ppm) 0.88 (m, 12H, CH₃), 1.14-1.72 (m, 48H, γ-CH₂), 1.82-2.17 (m, 8H, β-CH₂), 2.29-2.62 (m, 8H, β-CH₂), 4.06 (s, 6H, CH₃), 4.27 (m, 4H, α-CH₂), 4.51 (m, 4H, α-CH₂), 7.34 (m, 4H, arom), 8.23 (m, 6H, Py); IR (ν KBr/cm⁻¹) 3060 (ν_{C-H}), 2980 (ν_{C-H}), 1500 (ν_{C-C}), 1450 (ν_{C-C}), 1400 (ν_{C-C}), 1250 (δ_{C-H}), 1100 (δ_{C-H}), 950 (δ_{C-H}), 830 (δ_{C-H}), 660 (δ_{C-H}); UV-Vis (λ_{max} toluene/nm) 739; (λ_{max} pyridine/nm) 739; (λ_{max} water/nm) 684; Anal Calcd. for C₇₂H₁₀₀N₁₀Zn: C. 49.03; H. 3.09; N.21.43. Found: C.49.03; H. 3.08; N. 21.40.

Compound **6** (0.17 g, 0.15 mmol) was also reacted with MCAA (0.57 g, 6 mmol), DES (0.1 g, 0.6 mmol) and DMS (0.2 g, 1.5 mmol), respectively, in *N,N*-dimethylformamide (DMF) 140 °C for 2h. The reaction mixture was dissolved in acetone (20 cm³), cooled to room temperature and the resulting solution was filtered. The solvent was removed and the product was purified by TLC (eluent: THF-

toluene, 8:2); the product was recovered from the TLC plate, via dissolution in pyridine followed by filtration and solvent removal.

- (d) Product with MCAA: dark blue solid (yield 25%). $^1\text{H-NMR}$ (400 MHz, $\text{C}_6\text{H}_6\text{-d}_6$ /ppm) 0.87(m, 12H, CH_3), 1.13-1.70(m, 56H, $\gamma\text{-CH}_2$), 1.82-2.61(m, 8H, $\beta\text{-CH}_2$), 4.11-4.38(m, 4H, $\alpha\text{-CH}_2$), 6.20(s, 2H, CH_2), 7.14-7.27(m, 4H, Arom), 8.73-.16(m, 6H, Py); IR(KBr / cm^{-1}) 3480($\nu_{\text{O-H}}$), 3050, 2970($\nu_{\text{C-H}}$), 1740($\nu_{\text{C=O}}$), 1600, 1500, 1400($\nu_{\text{C=C}}$), 1210, 1100, 940, 790, 690($\delta_{\text{C-H}}$);
- (e) Product with DES: blue solid (yield 21%). $^1\text{H-NMR}$ (400 MHz, $\text{C}_6\text{H}_6\text{-d}_6$ /ppm) 0.86(m, 12H, CH_3), 1.02-1.63(m, 56H, $\gamma\text{-CH}_2$), 1.88-2.61(m, 8H, $\beta\text{-CH}_2$), 4.26-4.50(m, 4H, $\alpha\text{-CH}_2$), 7.37(m, 4H, Arom), 8.22(m, 4H, Py); IR(v KBr / cm^{-1}) 3480($\nu_{\text{O-H}}$), 3050, 2960($\nu_{\text{C-H}}$), 1600, 1460, 1400($\nu_{\text{C=C}}$), 1350, 1150($\nu_{\text{S=O}}$)1250, 920, 770($\delta_{\text{C-H}}$), 580($\delta_{\text{C-S}}$);
- (f) Product with DMS: dark blue solid (yield 25%). $^1\text{H-NMR}$ (400 MHz, $\text{C}_6\text{H}_6\text{-d}_6$ /ppm) 0.90(m, 12H, CH_3), 0.95-1.45(m, 56H, $\gamma\text{-CH}_2$), 1.60-2.41(m, 8H, $\beta\text{-CH}_2$), 4.05(s, 6H, CH_3), 4.25-4.42(m, 4H, $\alpha\text{-CH}_2$), 7.45(m, 4H, Arom), 8.02(m, 6H, Py); IR(v KBr / cm^{-1}) 3070, 2980($\nu_{\text{C-H}}$), 1500, 1400($\nu_{\text{C=C}}$), 1250, 1100, 950, 810, 660($\delta_{\text{C-H}}$).

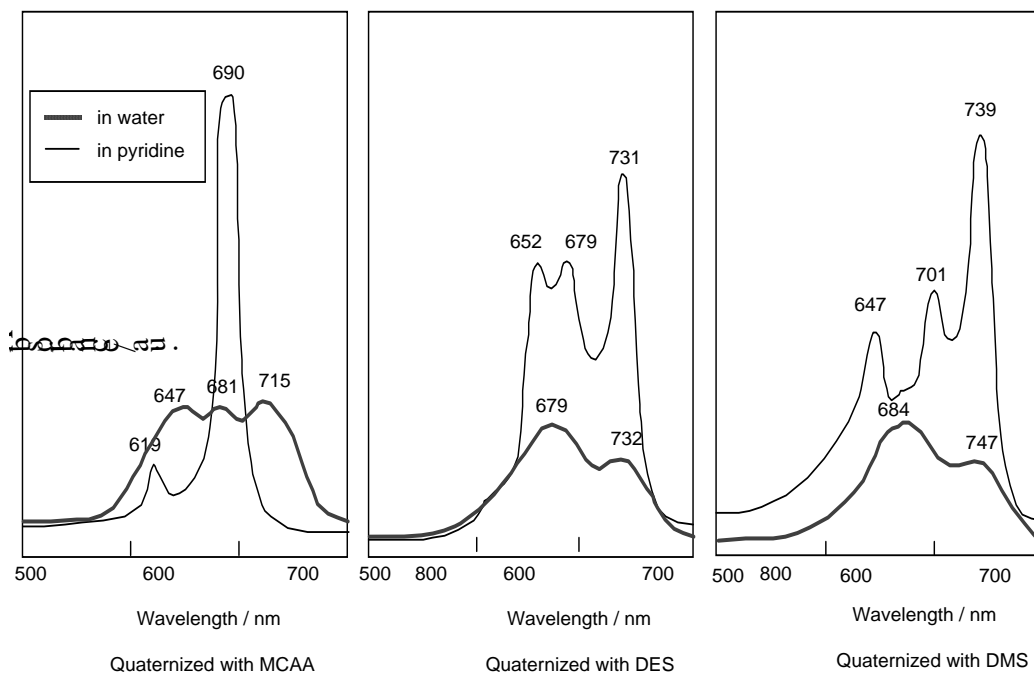
When MCAA or DMS was employed as the quaternizing agent, it is confirmed that $N\text{-CH}_2\text{COOH}$ or $N\text{-CH}_3$ bond was obtained on the pyridinoide rings in **5c** and **6**, while as DES was used, we verified quaternation was not achieved but sulfonation occurred [18]. The shapes of UV-Vis spectra of pyridine solution changed after quaternation. It is thought that interactions between molecules are complicated, when DES and DMS were used as quaternizing agents. Then the quaternized products give rise to easy aggregation in aqueous media.

After reaction with quaternizing agents, all compounds gave the water solubility, and got amphiphilic property (Table 11).

Table 11. Solubilities of 5c, 6 and quaternized compounds with MCAA, DES and DMS in solvents

Compound	Toluene	Chloroform	Pyridine	Water
5c or 6	○	○	○	×
Quaternized with MCAA	○	○	○	○
Quaternized with DES	○	○	○	○
Quaternized with DMS	○	○	○	○

○ : Soluble, × : insoluble



Compounds *5c* and *6* are readily soluble in pyridine with strongest absorption at 687 nm ($\log \epsilon_{\max}$ 4.81). The Q band absorption of the compound quaternized with DMS showed 739 nm and shifted by 56 nm to longer wavelength in comparison with compounds reacted with MCAA and DES. After react with MCAA, DES and DMS, all compounds are very soluble in water, they show strongest absorptions in the Q band at 715, 731 and 747 nm for *5c*, and 676, 687 and 687 nm for *6*, respectively (Figure 7 & Table).

Table 12. Uv-vis and fluorescence spectral data of quaternized *6*.

Quaternizing agent	Q-band		Fluorescence	
	λ_{\max} pyridine/nm	λ_{\max} water/nm	F_{\max} pyridine/nm	F_{\max} water/nm
DMS	746 <u>673</u> , 649, 606 *738;668*641;600	723 <u>676</u> , 646	683	681
DES	693 <u>658</u> , 628, 597 *673*645*605	708 <u>687</u> , 652	698	691
MCAA	679 <u>650</u> *677*620	687 <u>647</u>	692	688

underline; main peak.

^a in toluene.

Table 13. Redox potentials of 5c and its quaternized compound with MCAA, DES and DMS in DMF solution containing with TBAP

Compound	Potential (V vs. Ag/AgCl)		
	Reduction		Oxidation
5c	-0.97 [*]	-0.71 [*] -0.45 [*] -0.15 [*]	0.37 [*] 0.93 [*]
Quaternized with MCAA	-0.95 [*]	-0.45 [*] -0.14 [*]	0.45 [*] 0.97 [*]
Quaternized with DES ΔE^{**}	-0.95 [*]	-0.89 [*] -0.65 [*] -0.19 [*] 0.13	0.50 [*] 1.01 [*]
Quaternized with DMS ΔE^{**}	-0.78 [*]	-0.58 [*] -0.14 [*] 0.10	0.31 [*] 0.50 [*] 1.13 [*]

Potentials of reversible wave are midpoint potential of anodic and cathodic peaks for each couple, E_{mid}

* Irreversible peak.

** The anodic peak to cathodic peak separation for reversible couple.

Table 14. Potentials of quaternized 6 in DMF with TBAP

Compound	Potential (V vsAg/AgCl)		
	Reduction		Oxydation
6	-0.94 [*]	-0.62 [*] -0.29 [*] -0.03 [*]	0.32 [*] 0.48 [*] 0.97 [*]
Quaternized with DMS ΔE^{**}	-1.15 [*]	-0.77 [*] -0.14 [*] -0.05 [*] 0.11	0.50 [*]
Quaternized with DES ΔE^{**}	-0.83 [*]	-0.51 [*] -0.05 [*] 0.14	0.25 [*] 1.05 [*]
Quaternized with MCAA ΔE^{**}	-0.75 [*]	-0.52 [*] -0.12 [*]	0.96 [*] 1.28 [*]

Potentials of reversible wave are midpoint potential of anodic and cathodic peaks for each couple.

* Irreversible peak.

** The anodic peak to cathodic peak separation for reversible couple.

The important parameters of a CV are the reduction and oxidation potentials for irreversible peaks, and the mid-point potential for a reversible couple, E_{mid} (Tables 13 & 14). The reduction and oxidation potentials of 5c are sorted into six irreversible peaks. The irreversible peaks are attributed to the oxidation of the central metal and the reversible couples represent the redox of the phthalocyanine ring.

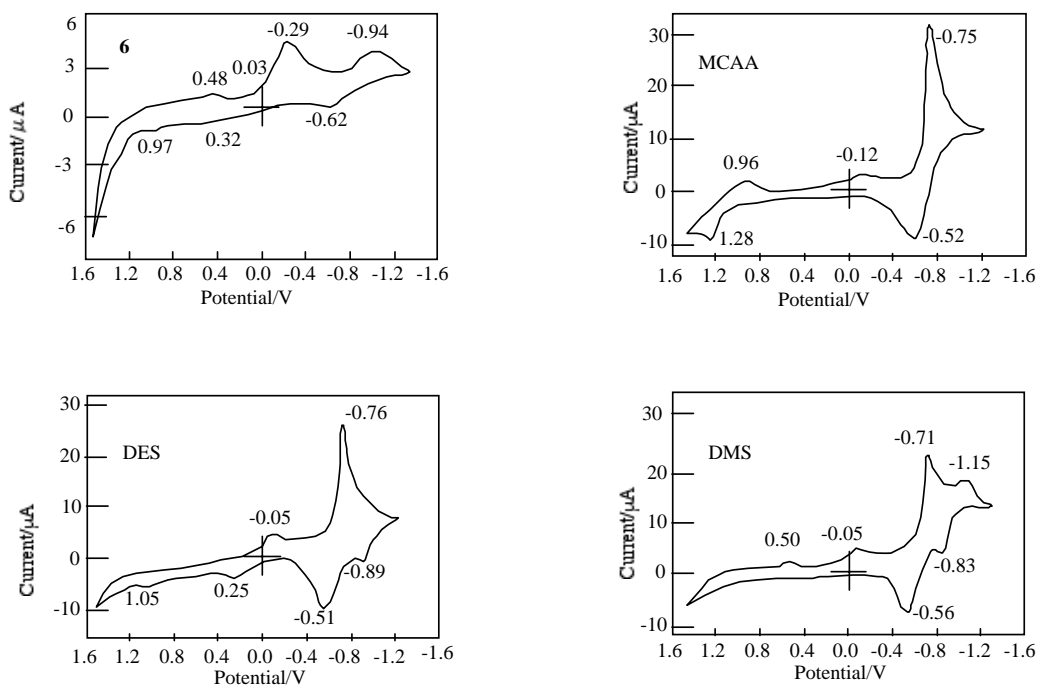


Figure 8. CVs of 6 and its quaternized compounds with MCAA, DES and DMS.

Shapes of CVs were changed between before and after reaction. The redox potential of 5c have six irreversible peaks. The redox potentials of quaternized compound were different from each other. The CVs of compounds quaternized with MCAA, DMS showed three anodic peaks and two cathodic peaks, while DES had four anodic peaks and two cathodic peaks. It is thought that no effect on quaternation takes place for redox properties of phthalocyanine analogous, because redox potentials were not changed.

The reduction and oxidation potentials of 6 comprise seven irreversible peaks which consist of three anodic and four cathodic peaks (Figure 8). The irreversible peaks can be attributed to oxidation of the central metal and the reversible couples represent the reduction and oxidation of the phthalocyanine ring [1-3, 51, 52].

The potential difference in CVs between the reduction and oxidation correspond to the HOMO-LUMO energy gaps of the compound [58]. Just as chemical reactions occur during the electron transfer between HOMO and LUMO energy levels, photochemical reactions are also based on similar phenomena of energy transfer. Before and after the quaternization, the HOMO-LUMO energy gap of 6 was unchanged.

QUATERNATION OF REGIO ISOMERS

The separated regioisomers of 5c were quaternized with DMS.

Quaternized regio isomers 5c: Regio isomers of 5c (0.4 mg, 0.35 μmol) was reacted with quaternizing agent as DMS (0.5 mg, 3.5 μmol) in DMF as solvent at 140 $^{\circ}\text{C}$ for 2h. The products were purified with TLC (eluent: THF-toluene, 8: 2). Each product was recovered by

scraping from the TLC plate, dissolved in pyridine, the solution filtered, and the solvent removed.

Yields of products were 11%, 9%, 15% and 11% for fractions 1, 2, 3 and 4, respectively. Quaternized regio isomers were also identified through spectroscopic techniques such as $^1\text{H-NMR}$, IR, UV-Vis and fluorescence spectra.

(a) Fraction 1 with DMS: dark blue solid (0.053 mg, yield 13 %). $^1\text{H-NMR}$ (δ 400 MHz, DMSO- d_6 /ppm) 0.86 (t, 12H, CH_3), 1.15-1.70 (m, 48H, $\gamma\text{-CH}_2$), 1.82-2.12 (m, 8H, $\beta\text{-CH}_2$), 2.19-2.49 (m, 8H, $\beta\text{-CH}_2$), 3.67 (s, 6H, CH_3), 3.92 (t, 4H, $\alpha\text{-CH}_2$), 4.19 (t, 4H, $\alpha\text{-CH}_2$), 7.37 (m, 4H, arom), 8.20 (m, 6H, Py); IR (ν KBr/cm^{-1}) 3070 ($\nu_{\text{C-H}}$), 2980 ($\nu_{\text{C-H}}$), 1500 ($\nu_{\text{C-C}}$), 1400 ($\nu_{\text{C-C}}$), 1250 ($\delta_{\text{C-H}}$), 1100 ($\delta_{\text{C-H}}$), 950 ($\delta_{\text{C-H}}$), 820 ($\delta_{\text{C-H}}$), 660 ($\delta_{\text{C-H}}$); UV-Vis (λ_{max} toluene/nm) 680: (λ_{max} pyridine/nm) 703: (λ_{max} water/nm) 690; Fluorescence (F_{max} pyridine/nm) 687: (F_{max} water/nm) 695; Anal Calcd. for $\text{C}_{72}\text{H}_{100}\text{N}_{10}\text{Zn}$: C. 49.03: H. 3.09: N.21.43. Found: C.49.00: H. 3.01: N. 21.33;

(b) Fraction 2 with DMS: dark blue solid (0.065 mg, yield 15 %). $^1\text{H-NMR}$ (δ 400 MHz, DMSO- d_6 /ppm) 0.87 (t, 12H, CH_3), 1.16-1.73 (m, 48H, $\gamma\text{-CH}_2$), 1.73-2.10 (m, 8H, $\beta\text{-CH}_2$), 2.10-2.55 (m, 8H, $\beta\text{-CH}_2$), 3.90 (s, 6H, CH_3), 3.99 (t, 4H, $\alpha\text{-CH}_2$), 4.17 (t, 4H, $\alpha\text{-CH}_2$), 7.23 (m, 4H, arom), 8.25 (m, 6H, Py); IR (ν KBr/cm^{-1}) 3070 ($\nu_{\text{C-H}}$), 2980 ($\nu_{\text{C-H}}$), 1500 ($\nu_{\text{C-C}}$), 1400 ($\nu_{\text{C-C}}$), 1250 ($\delta_{\text{C-H}}$), 1100 ($\delta_{\text{C-H}}$), 980 ($\delta_{\text{C-H}}$), 830 ($\delta_{\text{C-H}}$), 660 ($\delta_{\text{C-H}}$); UV-Vis (λ_{max} toluene/nm) 689: (λ_{max} pyridine/nm) 675: (λ_{max} water/nm) 686; Fluorescence (F_{max} pyridine/nm) 684: (F_{max} water/nm) 690; Anal Calcd. for $\text{C}_{72}\text{H}_{100}\text{N}_{10}\text{Zn}$: C. 49.03: H. 3.09: N.21.43. Found: C.48.99: H. 2.98: N. 21.22;

(c) Fraction 3 with DMS: dark blue solid (0.055 mg, yield 11 %). $^1\text{H-NMR}$ (δ 400 MHz, DMSO- d_6 /ppm) 0.85 (m, 12H, CH_3), 1.09-1.63 (m, 48H, $\gamma\text{-CH}_2$), 1.70-2.11 (m, 8H, $\beta\text{-CH}_2$), 2.11-2.42 (m, 8H, $\beta\text{-CH}_2$), 3.86 (s, 6H, CH_3), 3.97 (t, 4H, $\alpha\text{-CH}_2$), 4.21 (t, 4H, $\alpha\text{-CH}_2$), 7.23-7.33 (m, 4H, arom), 8.21 (m, 6H, Py); IR (ν KBr/cm^{-1}) 3080 ($\nu_{\text{C-H}}$), 2970 ($\nu_{\text{C-H}}$), 1500 ($\nu_{\text{C-C}}$), 1400 ($\nu_{\text{C-C}}$), 1250 ($\delta_{\text{C-H}}$), 1100 ($\delta_{\text{C-H}}$), 950 ($\delta_{\text{C-H}}$), 830 ($\delta_{\text{C-H}}$), 660 ($\delta_{\text{C-H}}$); UV-Vis (λ_{max} toluene/nm) 681: (λ_{max} pyridine/nm) 689: (λ_{max} water/nm) 689; Fluorescence (F_{max} pyridine/nm) 690: (F_{max} water/nm) 698; Anal Calcd. for $\text{C}_{72}\text{H}_{100}\text{N}_{10}\text{Zn}$: C. 49.03: H. 3.09: N.21.43. Found: C.49.03: H. 3.03: N. 21.40;

(d) Fraction 4 with DMS: dark blue solid (0.078 mg, yield 19 %). $^1\text{H-NMR}$ (δ 400 MHz, DMSO- d_6 /ppm) 0.87 (t, 12H, CH_3), 1.20-1.63 (m, 48H, $\gamma\text{-CH}_2$), 1.71-2.17 (m, 8H, $\beta\text{-CH}_2$), 2.17-2.47 (m, 8H, $\beta\text{-CH}_2$), 3.85 (s, 6H, CH_3), 4.09 (t, 4H, $\alpha\text{-CH}_2$), 4.27 (t, 4H, $\alpha\text{-CH}_2$), 7.21-7.36 (m, 4H, arom), 8.22 (m, 6H, Py); IR (ν KBr/cm^{-1}) 3070 ($\nu_{\text{C-H}}$), 2980 ($\nu_{\text{C-H}}$), 1500 ($\nu_{\text{C-C}}$), 1400 ($\nu_{\text{C-C}}$), 1250 ($\delta_{\text{C-H}}$), 1100 ($\delta_{\text{C-H}}$), 950 ($\delta_{\text{C-H}}$), 830 ($\delta_{\text{C-H}}$), 660 ($\delta_{\text{C-H}}$); UV-Vis (λ_{max} toluene/nm) 677: (λ_{max} pyridine/nm) 730: (λ_{max} water/nm) 673; Fluorescence (F_{max} pyridine/nm) 686: (F_{max} water/nm) 687; Anal Calcd. for $\text{C}_{72}\text{H}_{100}\text{N}_{10}\text{Zn}$: C. 49.03: H. 3.09: N.21.43. Found: C.49.02: H. 3.08: N. 21.43.

In comparison with UV-Vis spectra of before and after the quaternation of regio isomers with DMS, the Q band absorption of quaternized regio isomer were split into two or more. Then after quaternation, the Q band absorptions were moved to longer wavelength (Figure 9).

In general, fluorescence spectra are measured as mirror image of excitation spectra. Excitation spectra show the same profile of absorption bands. Fluorescence spectra show longer wavelength than absorption and excitation spectra.

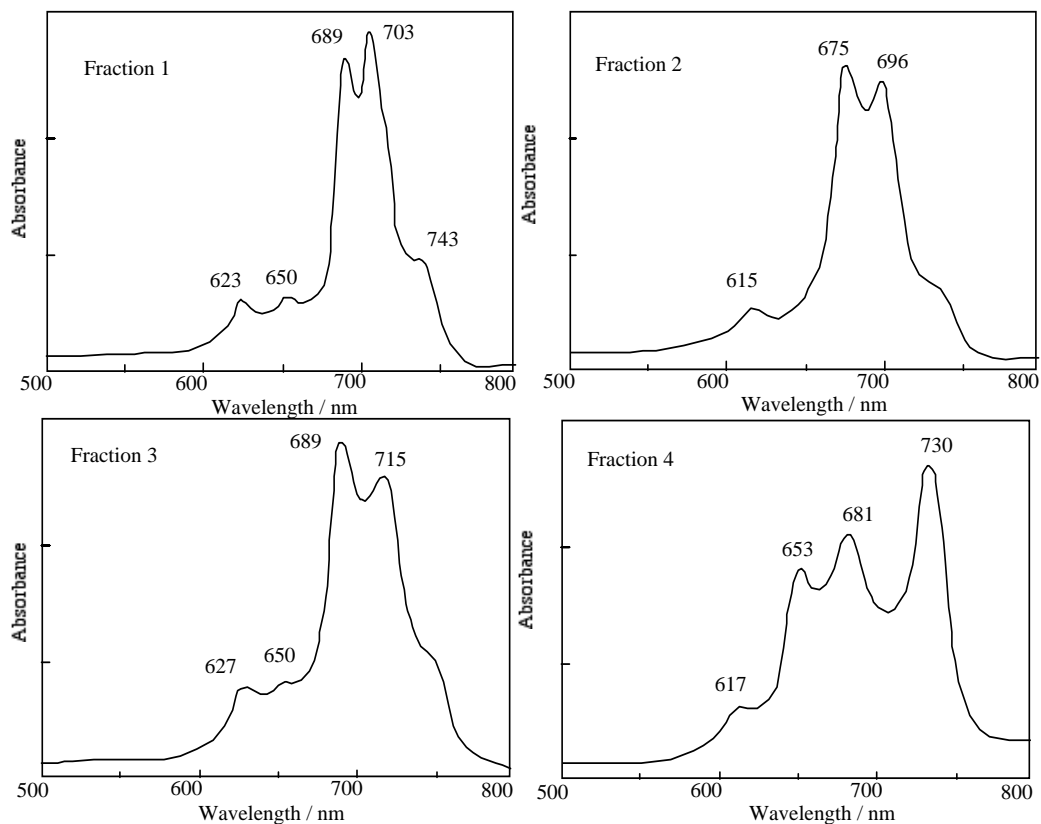


Figure 9. UV-Vis spectra of each regioisomer in 5c quaternized with DMS. The UV-Vis spectra of each quaternized isomer was measured in pyridiene.

For quaternized products except for fractions 1 and 4, fluorescence spectra showed longer wavelength than their own absorption spectra.

In fraction 1 and 4, the degree of overlaps between absorption and fluorescence spectra was determined. These phenomena result from re-absorption or re-emission of fluorescence.

Accordingly, fluorescence spectra of fractions 1 and 4 showed shorter wavelength than the longest wavelength of absorption bands.

The CVs of fractions 1-3 have one pair of reversible oxidation potential and four irreversible peaks. Fraction 4 has one pair of reversible oxidation and three irreversible reduction waves. The reduction and oxidation of metal phthalocyanine derivatives are due to the interaction between the phthalocyanine ring and the central metal.

The porphyrazine ring in the molecules of metal phthalocyanine derivatives or analogous is influenced by the π electrons about the closed system. Although the π electron system of 5c and fractions 1-4 consist of one porphyrazine, two pyridinoido and two didecyl substituted phenylene rings, the locations of these rings except for porphyrazine are different from each regio isomer.

The irreversible peaks are attributed to the oxidation of the central metal and the reversible couples represent the redox of the phthalocyanine ring.

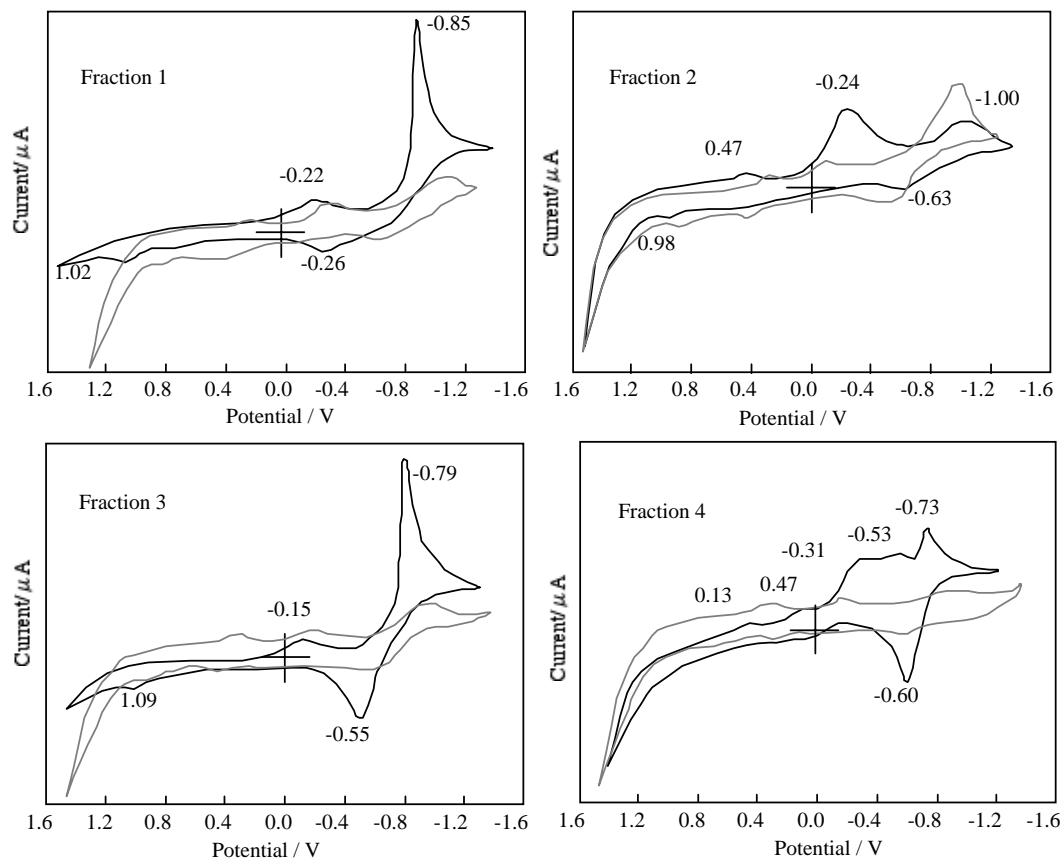


Figure 10. Cyclic voltammograms of each regioisomer in *5c* quaternized with DMS. Black line; After quaternation with DMS, Gray line; before quaternation.

Substituents and pyridinoid rings influenced the π electron environment in the fractions 1–4 of *5c*. It is thought that the effect of pyridinoid rings gives rise to changes of the electron density of the metal phthalocyanine derivative. The difference of reduction and oxidation peaks between fractions 1–4 is attributed to the effect of the variation of the interaction between the central metal and the alkylbenzoporphyrazine. And then, the difference of CV between *5c* and fractions 1–4 is also the effect of the interaction, since *5c* is a mixture of its regio isomers (Figure 10).

The ΔE values are the anodic peak to cathodic peak separation located in the oxidation potential region. The ΔE values are around 100 mV and the redox processes are the same for regio isomers, except for fraction 4. This means that the electron process of regio isomers between fractions 1–3 involve approximately one electron transfer. The ΔE values of fraction 4 show different behaviour in comparison to the others. It is thought that the different behaviour for fraction 4 is attributable to the mixture of two types of C_{2v} isomers. The redox potentials of fraction 4 are based on the interaction between two types of C_{2v} regio isomers. No observation on the reversible couple in *5c* resulted in the interaction between the regio isomers.

The redox potential of quaternized regio isomer were varied. After quaternation of regio isomers, the shapes of CVs appeared clearly. It is thought that electron transfer ability of regio isomers have been increased remarkably by the acquisition of cation groups. The CVs showed two anodic and two cathodic peaks, two anodic and three cathodic peaks, two anodic and two cathodic peaks, and one anodic and five cathodic peaks for fractions 1, 2, 3 and 4, respectively. Fractions 1 and 4 have a reversible couple in a reduction potential region at -0.24 and -0.57 V vs. Ag/AgCl, respectively. For quaternized regio isomers, some of redox potentials are recognized before the reaction.

Consequently, it suggested that the photoelectron transfer ability is kept unchanged regardless of the quaternation.

CELL CULTURE

IU-002 cells were maintained in MEM medium supplemented 5% fetal calf serum.

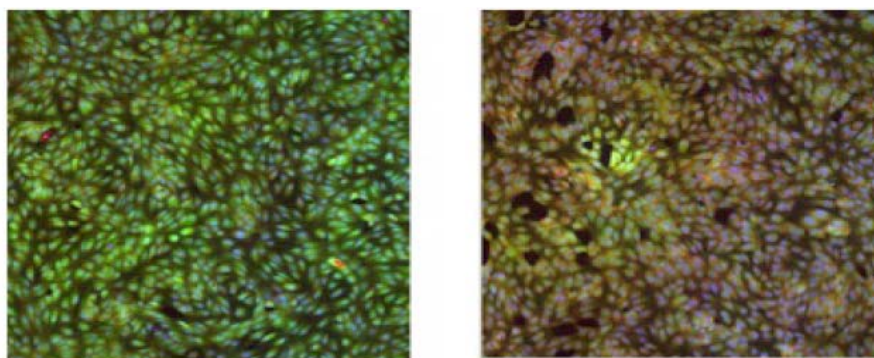
Cells seeded into 96-well tissue culture plates and incubated to allow attachment to the plates. The sensitizer was. Cells were incubated for 3h. The medium was removed, the cells were washed with phosphate-buffered saline (PBS), and fresh medium was added. Cells were exposed halogen light for 10 minutes. Appearance of cells was observed used a fluorescence microscope.

The uptake of DMS quaternized **6** was done in IU-002 cells. IU-002 cells were incubated at 37°C . After incubation for 3h, Cellular quaternized **6** was observed with a fluorescence microscope.

A fluorescent substance was noted when the uptake of DMS quaternized **6** in IU-002 cells was carried out.

Cell rupture can be detected. Intact cells selectively concentrated fluorescence. After exposed halogen light for 10 minutes showed damage and loss of fluorescence, although fluorescence in cells occurred in perinuclear area (Figure 11).

Consequently, the light exposed DMS quaternized **6** in cells produces cell disruption that can be detected as a decrease as fluorescence.



(a)

Figure 11. Fluorescence image of IU-002 cells. (a) Control, (b) Incubated with DMS quaternized **6** and irradiated with halogen light for 10 minutes.

CONCLUSION

The compound *5c* and *6* were synthesized from an equimolar mixture of *3* and *4* or 2,3-pyridine carbonitrile in the presence of basic catalyst as DBU.

The triplet state of *5* was measured using laser-flash photolysis in PMMA film.

The triplet life times of *5* increased with an increasing pyridine number in the molecule. One of the zinc non-peripheral substituted alkylbenzopyridoporphyrazines, *5c* in the PMMA layer showed the most intense absorption and a longer triplet state lifetime. The photoexcited triplet state lifetimes of *5b* and *5c* in PMMA without a PVA coating were estimated to be 11.4 and 10.1 μ s, respectively. While covered with a PVA coating, the photoexcited triplet state lifetimes of *5b* and *5c* were estimated as 51.8 and 46.9 μ s, respectively. The compound *5c* was suitable for use of the sensitizer for PDT, since *5c* has the most intense absorption and a longer triplet state lifetime.

The triplet lifetime for position isomers in *5c* was increased with the decreasing symmetry of position isomers, which were ordered as C_{2h} , D_{2h} , C_{2v} and C_s for fractions 2, 1, 4 and 3, respectively. The photoexcited triplet state lifetime of fraction 3 in PMMA in the absence and presence of PVA coatings were estimated to be 14.29 and 25.97 μ s, respectively.

The compound *5c* and *6* having two pyridine and two alkyl-substituted benzene rings were reacted with DMS, DES and MCAA as quaternizing agents.

When MCAA or DMS was employed as quaternization agents, *5c* and *6* were changed to quaternized compounds, while as DES was used, we verified quaternation was not achieved but sulfonation occurred. All compounds showed amphiphilic property.

After quaternation, the shapes of CVs appeared clearly. It is thought that electron transfer ability has been increased remarkably by the acquisition of cation groups. It suggested that the photoelectron transfer ability is kept unchanged regardless of the quaternation.

The uptake of DMS quaternized *6* was done in IU-002 cells.

The light exposed DMS quaternized *6* in cells produces cell disruption that can be detected as a decrease in fluorescence.

ACKNOWLEDGEMENT

The authors are favored to have the assistance of Mr. Taku KATO and Mr. Masaki WATAMABE who contributed his experimental skill, sustained effort, and grasp of objectives to the accomplishment of experimental program.

The assistance of Miss T. KOMORIYA, Research Associate of Nihon University, in the taking of data for part of cell culture is greatly appreciated. We also thank Professor Dr. KOHONO for his helpful advice given to us regarding our paper.

This research work was supported financially by Advanced Research Center for Life Science and Human Environment, Graduate School of Industrial Technology, Nihon University, which was adopted by a project for the promotion of high technology within The Ministry of Education and Science, Japan's Academic Frontier Project.

REFERENCES

- [1] Lezonoff, CC. & Lever, AB. Phthalocyanines -Properties and Applications- Vol. 1. New York: VCH Publishers; 1989.
- [2] McKeown, NB. Phthalocyanine Materials. Cambridge: Cambridge Univ. Press: 1998.
- [3] Hirohasi, R; Sakamoto, K. & Ohno-Okumura, E. Phthalocyanines as Functional Dyes. Tokyo: IPC; 2004.
- [4] Ao, R; Kummert, L. & Haarer, D., 1995, *Adv. Mater.*, 5, 495.
- [5] Maruta, M. 1999, *J. Jpn. Soc. Colour Mater.*, 72, 397.
- [6] Wohrle, D. & Meissener, D. 1991, *Adv. Mater.*, 3, 129.
- [7] Frampton, CS; O'Connor; Peterson, JMJ. & Silver, J. 1988, *Display*, 1998, 74.
- [8] Fernandez, DA; Awruch, J. & Dicello, LE. 1996, *Photochem. Photobiol.* 63, 784.
- [9] Jori, G. 1990, *Photochem. Photobiol.* 52, 439.
- [10] Kessel, D., 1990, *Spectrum* 3, 13.
- [11] Tabata, K; Fukushima, K; Oda, K; & Okura, I., 2000, *J. Porphyrins Phthalocyanines* 4, 278.
- [12] Moan, J. 1990, *J. Photochem. Photobiol. B: Biol.* 5, 521.
- [13] Cook, MJ; Chambrier, I; Cracknell, SJ; Mayes, DA. & Russell, D.A. 1995, *Photochem. Photobiol.* 62, 542.
- [14] De Filippis, MP., Dei, D., Fantetti, L., and Roncucci, G., 2000, *Tetrahedron Lett.* 41, 9143.
- [15] Jori, G. 1996, *J. Photochem. Photobiol. B: Biol.*, 36, 87.
- [16] Yang, YC; Ward, JR; & Seiders, RP. 1985, *Inorganic Chem.*, 24, 1765.
- [17] Ogawa, K; Kinoshita, S; Yonehara, H; Nakahara, H & Fukuda, K. 1989, *J. Chem. Soc. Chem. Commun.*, 1989, 477.
- [18] Klech, H; Weitemeyer, A; Muller, S; & Wohrle, D. 1995, *Liebigs Ann.*, 1269, 1273.
- [19] Boyle, R. & van Lier JE. 1993, *Synlett.*, 351, 352.
- [20] Shorman, WN., Kudrevich, SV. & van Lier, JE. 1996, *Tetrahedron Lett.*, 37, 5831.
- [21] Chan, WS; Basseur, N; La Madeleine, C; Oullet, R & van Lier, JE. 1997, *Eur. J. Cancer*, 33, 1855.
- [22] Urizzi, P; Allen, CM; Langlois, AR; Oullet, R; La Madeleine, C. & van Lier, JE. 2001, *J. Porphyrins Phthalocyanines*, 5, 154.
- [23] Sakamoto, K; Kato, T. & Cook, M. J. 2001, *J. Porphyrins Phthalocyanines*, 4, 742.
- [24] Yokote, M; Shibamiya, F. & Shoji, S. 1964, *Kogyo Kagaku Zasshi*, 67, 166.
- [25] Sakamoto, K; Kato, T; Kawaguchi, T; Ohno-Okumura, E; Urano, T; Yamaoka, T; Suzuki, S. & Cook MJ. 2002. *J Photochem Photobiol A: Chem.* 153, 245.
- [26] Sakamoto, K; Ohno-Okumura, E; Kato, T; Kawaguchi, T. 2003. *J Porphyrins Phthalocyanine*, 7, 83.
- [27] Sakamoto, K; Kato, T; Ohno-Okumura, E; Watanabe, M. & Cook MJ. 2005, *Dye Pigments*, 64, 63.
- [28] Seotsanya-mokhosi, I; Kuznetsova, N. & Nyokong T. 2001, *J. Photochem Photobiol A: Chem.*, 140, 215.
- [29] Yokote, M; Shibamiya, F & Shoji, S. 1964, *Kogyo Kagaku Zasshi*, 67, 166.
- [30] McKeown, NB., Chambrier, I. & Cook, M.J. 1990, *J. Chem. Soc. Perkin Trans. 1*, 1990, 1167.

- [31] Chambrier, I; Cook, MJ; Cracknell, SJ. & McMurdo, J. 1993, *J. Mater. Chem.*, 3, 841.
- [32] Sakamoto, K. & Shibamiya, F. 1986, *J. Jpn. Soc. Colour Mater.*, 59, 517.
- [33] Hanack, M; Meng, D; Beck, A; Sommerauer, M. & Subramanian, L. R. 1993, *J. Chem. Soc. Chem. Commun.*, 1993, 58.
- [34] Markovitsi, D; Lecuyer, I. & Simon, J. 1991, *J. Phys. Chem.*, 95, 3620.
- [35] Khatib, NEL; Boudjema, B; Maitrot, M; Chermette, H. & Pote, L. 1988, *Can. J. Chem.*, 66, 2313.
- [36] Rollmann, LD. & Iwamoto, RT. 1968, *J. Am. Chem. Soc.*, 90, 1455.
- [37] Fierro, C; Anderson, AB. & Scherson, DA. 1988, *J. Phys. Chem.*, 92, 6902.
- [38] Cook, MJ. & Jafari-Fini, A. 1997, *J. Mater Chem.*, 7, 2327.
- [39] Sommerauer, M; Rager, C. & Hanack, M. 1996, *J. Am. Chem. Soc.*, 118, 10085.
- [40] Gaspard, S. & Maillard, PH. 1987, *Tetrahedron*, 43, 1083.
- [41] Negrimovskii, VM; Bouvet, M; Luk'yanets, EV. & Simon, J. 2000, *J. Porphyrins Phthalocyanines*, 4, 248.
- [42] Kobayashi, N. & Konami, H. 1996, *Phthalocyanines -Properties and Applications- Vol. 4*, (Ed.) Lezonoff, C. C., and Lever, A. B. P. VCH Publishers, New York, 343.
- [43] Kasuga, K. & Tsutsui, M. 1980, *Coordination Chem. Rev.*, 32, 67.
- [44] Lever, ABP; Licoccis, S; Magrell, M. & Ramanamy, B. S. 1982, *Adv. Chem. Ser.*, 210, 237.
- [45] Sakamoto, K. & Ohno, E. 1996, *J. Soc. Dyers and Colorists*, 112, 368.
- [46] Sakamoto, K. & Ohno, E., 1997, *Dyes Pigments*, 35, 375.
- [47] Sakamoto, K. & Ohno, E., 1998, *Dyes Pigments*, 37, 291.
- [48] Sakamoto, K. & Ohno, E., 1997, *Prog. Org. Coat.*, 31, 139.
- [49] Sakamoto, K. & Ohno-Okumura, E., 1999, *J. Porphyrins Phthalocyanines*, 3, 634.
- [50] Sakamoto, K. & Ohno-Okumura, E., 1999, *J. Jpn. Soc. Color Mater.*, 72, 2.
- [51] Kadish, KM; Moninot, G; Hu, Y; Dubois, D; Ibnlfassi, A; Barbe, J-M. & Guillard, R., 1993, *J. Am. Chem. Soc.*, 115, 8153.
- [52] Darwent, JR; Douglas, P; Harriman, A; Porter, G. & Richoux, MC. 1982, *Coord. Chem. Rev.*, 44, 83.
- [53] Ozomen, K., Kuznetsova, N. & Nyokong, T. 2001, *J. Photochem. Photobiol. A: Chem.*, 139, 217.
- [54] Murphy, ST; Konda, K. & Foote, CS. 1999, *J. Am. Chem. Soc.*, 121, 3751.
- [55] Gerdes, R; Wohrle, D; Spiller, W; Schmeider, G. & Schulz-Ekloff, G. 1997, *J. Photochem. Photobiol. A: Chem.*, 111, 65.
- [56] Lang, K; Wagnerova, DM. & Brodilova, J. 1993, *J. Photochem. Photobiol. A: Chem.*, 72, 9.
- [57] Iliiev, V; Alexiev, V. & Bilyarska, L. 1999, *J. Mol. Catal. A: Chem.*, 137, 15.
- [58] Lukyanets, EA. 1999, *J. Porphyrins Phthalocyanines*, 3, 592.
- [59] Kaliya, OL; Lukyanets, EA. & Vorozhtsov, GV. 1999, *J. Porphyrins Phthalocyanines*, 3, 592.
- [60] Edrei, R; Gottfried, V; Van Lier, JE., & Kimel, S. 1998, *J. Porphyrins Phthalocyanines*, 2, 191.
- [61] Dhami, D. & Phillips, D. 1996, *J. Photochem. Photobiol. A: Chem*, 100, 77.
- [62] Spiller, W; Kliesch, H; Wohrle, D; Hackbarth, S; Roder, B. & Schmurpfeil, G. 1998, *J. Porphyrins Phthalocyanines*, 2, 145.
- [63] Tokumar, K. 2001, *J. Porphyrins Phthalocyanines*, 5, 77.

- [64] Wohrle, D; Gitzel, J; Okura, I. & Aono, S. 1985, *J. Chem. Soc., Perkin Trans. II*, 1985, 1171.
- [65] Yhamae, M. & Nyokong, T. 1999, *J. Electroanal. Chem.*, 470, 126.

Chapter 3

DYES, PIGMENTS AND SUPERCRITICAL FLUIDS: SELECTION OF EMERGING APPLICATIONS

M. D. Gordillo¹, C. Pereyra and E. J. Martínez de la Ossa

Department of Chemical Engineering, Food Technology and Environmental
Technologies, Faculty of Sciences, University of Cádiz,
11510 Puerto Real (Cádiz), Spain

ABSTRACT

The textile industry uses large amounts of water in its dyeing processes. Due to environmental problems the supercritical dyeing process has been developed. In this process supercritical carbon dioxide is used as the solvent for dyes.

On the other hand, pigments, used in the formulation of paints, inks, toners and photographic emulsions can be micronized by supercritical antisolvent process. Their production in form of micrometric particles with controlled particle size distribution can largely improve their characteristics.

For these reason, in the last years, supercritical fluids more and more have been proved as environmentally benign media for dyeing processes and as antisolvent to control the formation of micrometric particles.

The physico-chemical properties of supercritical fluids are halfway between those of gases and liquids; more these properties can be easily modified by a simple variation of pressure or/and temperature. Therefore, supercritical fluids can be used to develop solventless or solvent reduced processes and their mass transfer properties are useful to produce micronized particles with controlled size and distribution.

In this field, the publications appeared over the past years could be reviewed under two groupings, one involving the measurements of solubilities of dyes in supercritical carbon dioxide, with and without co-solvent, and supercritical CO₂ dyeing of fibre, and the other involving the micronization of dyes with narrow particle size distribution using a supercritical antisolvent process. In the following, a lot of recent papers will be cited, which should give an overview of actual results on solubility and precipitation of dyes in supercritical carbon dioxide.

¹ Phone: 956016458. Fax: 956016411. E-mail: dolores.gordillo@uca.es.

1. INTRODUCTION

A supercritical fluid can be defined as a substance above its critical temperature and pressure. Under this condition the fluid has unique properties, in that it does not condense or evaporate to form a liquid or gas. Although a number of substances are useful as supercritical fluids, carbon dioxide has been the most widely used supercritical CO₂ gives an option avoiding water discharge; it is low in cost, non-toxic and non-flammable. It has low critical parameters (31 °C, 73.8 bar) and the carbon dioxide can also be recycled (Özcan et al., 1998).

Supercritical fluids have a great potential for wide fields of processes: extraction processes with supercritical fluids, fractionation of products, dyeing of fibres, treatment of contaminated soils, and production of powders in micron and submicron range and reactions in or with supercritical fluids (Marr and Gamse, 2000).

An emerging technology is waterless supercritical fluid textile dyeing using supercritical carbon dioxide as the solvent medium. The large quantity of water used during the dyeing process results in a large volume of wastewater that contains not only all of the auxiliary agents but also great remains of the dye. The use of the supercritical dyeing technique circumvents the needs for water and wastewater treatment in the dyeing process. In addition, the fibres that are dyed in the supercritical fluid are completely dry after reducing the pressure to atmospheric conditions, thus recluding the requirement of drying step associated (Saus et al., 1993).

Supercritical dyeing requires studies of phase equilibrium between dyes and the supercritical solvent. For this reason, we have undertaken a review of solubility of dye in supercritical fluids.

On the other hand, nanometric or submicron pigment particles are essential materials for use in photo resists, which are used for fabricating color filters and for color liquid crystal displays. Instead of traditional mechanical milling, the supercritical anti-solvent process may provide an innovative route to meet this demand ultra-fine particles formation of pigments in different phase regions via a supercritical anti-solvent process (Wu et al., 2007).

This review is the first comprehensive review specifically focused on dyes and supercritical fluids. The review is presented in subsections according to the type of article: solubility of dyes, dyeing process and precipitation of pigments.

2. SOLUBILITY

Over the last few decades, the solubilities of solids and liquids in supercritical fluids (SCF) have been measured extensively. Such information forms an important part of establishing the technical and economic feasibility of any supercritical fluid process. Most of the investigations on solubility have been concerned with binary systems consisting of a single solute in contact with a single SCF.

In the 90s until now, many articles of solubility of dyes were published. For example, Özcan et al. measured the solubilities of eight disperse dyes in supercritical CO₂ (Özcan et al., 1997), the solubility of anthraquinone and azo dyes in supercritical CO₂ was measured by Joung and Yoo. The anthraquinone dyes showed higher solubility than the azo dyes (Joung and Yoo, 1998). Investigations on the solubility of anthraquinone dyes in supercritical carbon

dioxide were carried out by Warner et al. (Warner et al., 1999). Lee et al. measured the solubility of disperse dyes, C.I. Disperse Red 60 and C.I. Disperse Orange 3 in supercritical carbon dioxide (Lee et al., 1999). Again, the solubility of C.I. Disperse Red 60 and C.I. Disperse Blue 60 in supercritical carbon dioxide was measured by Sung and Shim (Sung and Shim, 1999). Guzel and Akgerman measured solubilities of two disperse dyes (C.I. Disperse Yellow 7, C.I. Disperse Oranges 11) and three mordant dyes (C.I. Mordant Brown, C.I. Mordant Yellow 12, and C.I. Mordant Red 11) (Guzel and Akgerman, 1999). Lee et al. published the solubility in supercritical carbon dioxide of two disperse dyes, C.I. Disperse Blue 3 and C.I. Disperse Blue 79 (Lee et al., 2000). Draper et al. measured the solubility of ten disperse dyes in supercritical carbon dioxide, and obtained results were used to develop correlations between disperse dye structures and supercritical CO₂ solubility (Draper et al., 2000). Tuma et al. compared solubility of several anthraquinone disperse dyes in near- and supercritical fluids (Tuma et al., 2001). Solubilities of Blue 79, Red 153, and Yellow 119 in supercritical carbon dioxide were measured by Lin et al. (Lin et al., 2001). In 2002, Mishima et al. measured the solubilities of azo dyes and anthraquinone in supercritical carbon dioxide (Mishima et al., 2002). In 2003, Lee et al. studied cosolvent effects on the solubilities of disperse dyes of blue 79, red 153 and yellow 119 in supercritical carbon dioxide (Lee et al., 2003). The experimental results showed how the solubilities increased by adding ethanol in supercritical carbon dioxide. Shinoda and Tamura measured solubilities of C.I. Disperse Red 1, C.I. Disperse Red 13, C.I. Disperse Orange 25 and C.I. Disperse Blue 354 in Supercritical CO₂ (Shinoda and Tamura, 2003a; Shinoda and Tamura, 2003b).

In 2003, we published the solubility of Disperse Blue 14 in supercritical carbon dioxide (Gordillo et al., 2003). Experimental solubility data as mole fraction for Disperse Blue 14 in supercritical carbon dioxide at 313, 333 and 353 K and 100- 350 bar were measured. The Disperse Blue 14 solubility always increases as the pressure does. The solubility behavior with temperature is more complex. At pressures of 100 and 150 bar, the solubility behavior with temperature is not clear. For pressures above 150 bar, the solubility increases with increasing temperature. This solubility trend is consistent with those observed by different authors for different dyes, for example Joung et al. and Draper et al. (Joung et al., 1998; Draper et al., 2000). Joung et al. measured the solubility of the same dye. The data reported by the aforementioned authors are also shown in the paper.

In 2004, Ferri et al. measured the solubilities of C.I. Disperse Orange 3, Red 324, Blue 79 and quinizarin in supercritical carbon dioxide with a flow method. Experimental data for Disperse Orange 3 were also compared with similar results obtained by the authors using a batch method in a previous work. The comparison of the results showed how the flow method reveals to be the simplest and more efficient technique to evaluate dye solubility in supercritical fluids (Ferri et al., 2004). In 2004, binary and ternary solubilities of C.I. Disperse Blue 134, C.I. Disperse Yellow 16 and their dye mixture in supercritical carbon dioxide were measured by a flow-type apparatus by Tamura and Shidona again (Tamura and Shidona, 2004). Baek et al. published the solubility of C.I. Disperse Orange 30 dye in CO₂ measured by using a batch solid-fluid equilibrium apparatus (Baek et al., 2004). Fasihia et al. investigated on solubilities of some disperse azo dyes in supercritical carbon dioxide. The measurements were performed using a simple static method. As evidenced from the experimental results, the solubilities increase with increasing density of supercritical CO₂ and the higher the melting point, the lower the solubility (Fasihi et al. 2004). Lin et al. measured

solubilities of disperse dyes of Blue 79:1, Red 82 and modified Yellow 119 in supercritical carbon dioxide and nitrous oxide (Lin et al., 2004).

In 2005, Bao and Dai published relationships between the Solubility of C. I. Disperse Red 60 and uptake on poly(ethylene terephthalate) (PET) in Supercritical CO₂. In this work the solubilities of C. I. Disperse Red 60 in supercritical CO₂ at different temperatures and pressures were measured. As all paper, the results showed that the solubilities were increasing with increasing pressure or density at constant temperature. To reveal the relationships between dye solubility and its uptake on the fibre, Bao and Dai carried out dyeing of PET fibre in supercritical CO₂ at corresponding pressures and temperatures. The results showed that very high solubility was not beneficial for high dye uptake because the dyeing of PET in SC-CO₂ also obeyed the partition rule as in water (Bao and Dai, 2005).

For the design of supercritical fluid dyeing process, it is essential to have a sound knowledge of the solubilities of dyes and the accurate solubility representation. This representation can be based on thermodynamic equations or empirical equation.

In 2005, we published solubility estimations for Disperse Blue 14 in supercritical carbon dioxide. In this paper, the solubility values of Disperse Blue 14 in supercritical CO₂ published in our previous work (Gordillo et al., 2003) were correlated with fairly good accuracy using a model based on thermodynamic aspects and the use of equations of state. The results obtained in predicting the solubility show that the choice of group contribution method (GCM) has a greater influence than the choice of one of the three equations of state investigated (Gordillo et al., 2005). Huang et al. employed four semiempirical density-based models to correlate solubilities of 32 dyestuffs in supercritical carbon dioxide. The results show that these models perform very well with three temperature-independent parameters and could be applied for satisfactory solubility predictions (Huang et al., 2005).

Recently, Tabaraki et al. related the solubility of 21 azo dyes in supercritical carbon dioxide with several descriptors over a wide range of pressures and temperatures. The prediction ability of the model was also evaluated for five azo dyes, the molecules and data of which were not in any previous data sets (Tabaraki et al., 2007). Cabral et al proposed a new methodology which correlates the dye solubility in supercritical CO₂. This methodology uses the expanded liquid model, which the solid–fluid equilibrium is modeled using the Margules model. The experimental dye solubility of CI disperse red 60, CI disperse orange 3, CI disperse blue 3, and CI disperse blue 79 in supercritical carbon dioxide were used for evaluating this new methodology. The results obtained using the proposed technique showed good agreement with the experimental data used (Cabral et al., 2007). Numerous articles of estimation of properties and correlation of solubility data of dyes can be found in the bibliography. In this work only the articles of solubility are mentioned not to extend the content of the same one.

With respect to the solubility, it is fully proven that the addition of a small amount of an organic solvent as ethanol can remarkably increase the solubility of a variety of solid solutes in the supercritical fluid (Banchero et al., 2006; Li et al., 2003; Ke et al., 1996; Chafer et al., 2002; Kopcak et al., 2005). The supercritical condition of high temperature and pressure is necessary for supercritical fluid dyeing, at which dye can be much more solved and impregnated into the polymer fibre swelled by supercritical fluid (Bae et al., 2004). It is experimentally known that dyeing of polyester fibre in supercritical carbon dioxide can be carried out over 100 °C and 200 bar (Bae et al., 2004). For more advanced development of the supercritical dyeing process, the dyeing process must be performed possibly at lower

pressure. Many investigators had reported that the solubility of disperse dye with high-molecular weight in supercritical carbon dioxide is remarkably increased by adding a small amount of co-solvent (Bae et al., 2004).

Bae et al. (Bae et al., 2004) estimated the solubility of solute in ternary supercritical fluid + solute + co-solvent mixture by using an expanded liquid model that is considered the supercritical fluid as a liquid phase. The effect of co-solvent concentration on the solubility of solute in a supercritical mixed solvent can be predicted by the model. They reported solubility measurements of disperse Red 60 in a mixture of CO₂ and co-solvents but the comparison between data with and without co-solvents was not carried out. Banchero et al. (Banchero et al., 2006) published the experimental investigation of the solubility of three disperse dyes in a mixture of CO₂ and ethanol as well as a comparison with the corresponding solubilities without co-solvent presented in previous works (Ferri et al., 2004; 2004a).

Recently, the solubility of various dispersed dyes (C. I. Disperse Red 60, Blue 56, and Yellow 54, C. I. Disperse Red 360, Blue 79, and Yellow 114) in supercritical carbon dioxide was measured by Kim et al. (Kim et al., 2006) and, subsequently, based on the solubility data, the dry dyeing was conducted in a temperature range of 363.15-423.15 K and at pressures of 10-30 MPa. Solubility data of the dispersed dyes in CO₂ were correlated in terms of the density of carbon dioxide, using an empirical equation of Bartle et al. The highest color depth of the dyed fibre was obtained when the experiment was performed at 423.15 K and 30 MPa.

Solubility of Acid Red 57 (AR57), which is an anionic dye, in supercritical CO₂ was investigated by Özcan and Özcan (Özcan and Özcan, 2006) using an ion-pairing with dodecyltrimethylammonium (DTMA) bromide. The measurements of AR57 and AR57-DTMA in supercritical CO₂ without/with methanol as a modifier solvent were carried out at temperatures from 45 to 100 °C and pressures from 250 to 325 bar. Although AR57 is insoluble in supercritical CO₂ even with methanol as a modifier solvent, AR57-DTMA can dissolve in methanol modified supercritical CO₂. The hydrophobic ion-pairing provides a possibility for the solubility of hydrophilic dye in supercritical CO₂.

3. DYEING PROCESS

In recent, waterless dyeing that used the supercritical carbon dioxide as an alternate solvent instead of water in conventional dyeing process had been gaining much interest in the textile industry for environmental reasons. Conventional dyeing process of PET fibre discharges much waste water that is contaminated by various kinds of dispersing agents, surfactants and unused dye. It is very difficult that a conventional biological process treats the wastewater including many additives. The dyeing technique with supercritical fluid is an alternative one which has been developed without environmental contamination since early 1990s. Schollmeyer and coworkers did the pioneering works for the process (Park and Bae, 2002). Saus et al. (Saus et al., 1993) reported on dyeing of PET and polypropylene with different dyes.

In 90s, Saus et al. have published numerous papers about supercritical dyeing process: *Dyeing with supercritical carbon dioxide - an alternative to high-temperature dyeing of polyester* (1993), *Dyeing with supercritical carbon dioxide - physico-chemical fundamentals* (1993), *Dyeing with supercritical carbon dioxide* (1993), *Dyeing of textiles in*

supercritical carbon dioxide (1993), *Application of supercritical carbon dioxide in finishing processes* (1993), *Dyeing from supercritical CO₂ - fastnesses of dyeing* (1994), *Dyeing natural fibres with disperse dyes in supercritical carbon dioxide* (1994), *Determination of the dye uptake of cotton with trichromatic dyes. I. Basis of quantitative multicomponent analysis* (1994), *Dyeing with carboxyl-group-containing dyes in supercritical CO₂* (1995), *Water-free dyeing of textile accessories using supercritical carbon dioxide* (1997). (Saus et al., 1993; 1993a; 1993b; 1993c ; 1994) (Knittel et al., 1993; 1994 ;1995 ;1997) (Gebert et al., 1994).

When dyeing polyester fibres from an aqueous medium, reduction clearing of the dyed fibres is carried out to maximise wet fastness properties, thus producing further effluent problems. Reduction clearing is not necessary following disperse dyeing of polyester from supercritical carbon dioxide. Supercritical CO₂ has other advantages. The application of the dye to the fabric can be controlled and a better quality of application achieved. Densities and viscosities in supercritical fluids are less and diffusion more rapid than liquids, thus shortening the process time. The solubility of the dyes can be controlled by changing the pressure and temperature (Özcan et al., 1998).

Supercritical fluids have very low surface tension, which enables easy penetration into the fibrous structure of the textile fibres. In addition, the dissolved dyestuff can easily be separated from the supercritical fluid by simple expansion enabling recycle of the valuable dyestuff and almost completely eliminating the problems related to the wastewater contamination (Guzel and Akgerman, 2000). For these reasons, supercritical CO₂ is attractive as a solvent and transport medium for disperse dyes.

Banchero et al. from Dipartimento di Scienze dei Materiali e Ingegneria Chimica – Politecnico di Torino, Italy (Banchero et al., 2006), authors of several published papers about dye and supercritical fluids, say that since Saus et al. (Saus et al., 1993) described the process for the first time in 1992, many literature works have shown that dyeing of PET fibres using supercritical carbon dioxide could be successfully performed (Özcan and Özcan, 2005; Son et al., 2004; Park and Bae, 2002; De Giorgi et al., 2000; Bach et al., 2002). Nowadays, it is known that the dye uptake as well as the fastness are comparable with those of the traditional watery dyeing (Park and Bae, 2002) and that PET is not subjected to appreciable morphological changes during dyeing (Smole and Zipper, 2002 ; Hou et al., 2004). Studies have also been done on scale-up and a number of pilot plants have been built-up all over the world (Bach et al., 1998). In spite of this, this process seems not to be attractive to the textile industry. The reasons of this lack of interest are, of course, economic: the process is carried out at relatively high pressure, which implies high investment costs for the machinery and the training of skilled staff.

Banchero et al. affirmed that a possibility to reduce the process working pressure consists in adding little quantities of low molecular weight co-solvents to the dyeing medium. The co-solvent has a twofold effect: the enhancement of the dye solubility in the fluid (Bae et al., 2004) and the promotion of the dye uptake into the fibre (West et al., 1998).

The experience achieved by the research group of Banchero, Ferri, Manna, and Sicardi is reported in a paper entitled *Supercritical Dyeing of Textiles – From the Laboratory Apparatus to the Pilot Plant* and published in *Textile Research Journal* (Banchero et al., 2008). This work shows the results obtained for polyester textiles. Laboratory scale experiments were performed to determine the equilibrium partition of each dye between the two phases. In a second part, the pilot plant was set up. The dyeing results were successful: good

reproducibility, together with a good dye uniformity and fastness (comparable with that of the traditional process) were obtained. The maximum productivity of the pilot plant is about 5 kg/h and the total duration of the dyeing process (approximately 1.5 h) is much shorter than that of the traditional method (3–4 h). Now, synthetic and natural fibres are dyed in supercritical carbon dioxide.

Since 1992, several published paper about supercritical dyeing can be cited. Since 2000, regard to the review articles and general papers, in 2001, Golob y Tusek published *The dyeing of textiles in supercritical CO₂* (Golob y Tusek, 2001), *A pragmatic approach to supercritical fluid dyeing of textile fibres with natural dyes* was published by Mukhopadhyay and Bhattacharyya, where they reviews different techniques of supercritical fluid dyeing, solubility behaviour and performance of dyeing and natural and synthetic fibres with disperse natural textile dyes from a supercritical CO₂ medium (Mukhopadhyay and Bhattacharyya, 2001) and Hendrix published *Progress in supercritical CO₂ dyeing* (Hendrix, 2001). In 2002, Bach et al. published a paper entitled *Past, present and future of supercritical fluid dyeing technology - an overview* (Bach et al., 2002). In 2004, *Progress in Supercritical Fluid Dyeing (SFD)* and *Supercritical fluid dyeing (SFD): A green technology* were published by Sayem and Rossbach (Sayem and Rossbach, 2004a y 2004b). In 2005, Malik and Kaur published a paper entitled *Supercritical carbon dioxide-The dyeing technique of future* (Malik and Kaur, 2005). In 2006, Zheng et al. published *Technique of dyeing in supercritical CO₂* (Zheng et al., 2006) and recently an article entitled *Supercritical fluid dyeing technology and application* has been published by Qun (Qun, 2007).

Regard to the type of fibre, initial applications of supercritical fluids in textile dyeing have been on dyeing of hydrophobic fibres with disperse dyes dissolved in supercritical carbon dioxide. Saus et al. (Saus et al., 1993) studied the dyeing of synthetic fibres such as polyesters, polyamides, polystyrene, polyacrylics with disperse dyes dissolved in supercritical CO₂. Gebert et al. (Gebert et al., 1994) investigated of dyeing of natural fibres (wool and cotton) with disperse dyes employing supercritical CO₂ as the solvent; after a special pretreatment with a modifying agent. Özcan et al. (Özcan et al., 1998) applied supercritical dyeing to natural fibres and successful dyeing of cotton were carried out. Guzel and Akgerman (Guzel and Akgerman, 2000) dyed wool fibres with mordant dyes (C.I. Mordant Brown, C.I. Mordant Yellow 12 and C.I. Mordant Red 11) dissolved in supercritical carbon dioxide.

Since 2000, in the bibliography, dyeing of synthetic and natural fibres can be found. Polylactide fibres (Wen and Dai, 2007; Bach et al., 2006), cotton (Fernández et al., 2007; Vankar et al., 2002, Vankar et al., 2001), wool (Zhang et al., 2007, Jun et al., 2005; Cegarra, 2002), acrylic fibres (Jun et al., 2005), nylon (Liao, 2005; Cegarra, 2002; Liao et al., 2000), polyester/cotton blends (Maeda et al., 2004), silk (Sawada et al., 2002), cellulose (Maeda et al., 2002), ramie (which is composed mainly of cellulose and is an age-old graceful textile material from China) (Liu et al., 2008; Liu et al., 2006), polypropylene (Tataba et al., 2001, Liao et al., 2001; Liao, 2000) and polyester fibres (polyethylene terephthalate) (Van der Kraan et al., 2007; Joshi et al., 2006; Li et al., 2006; Santos et al., 2005; Liao, 2005; Hou and Dai, 2005; Hou et al., 2004; Cegarra, 2002; Park and Bae, 2002; Tataba et al., 2001; Kawahara et al., 2001; Wang and Lin, 2001, Tusek et al., 2000; De Giorgi et al., 2000; Giessmann et al., 2000) among others.

4. PRECIPITATION

Nano-metric or submicron pigment particles are essential materials for use in photo resists, which are used for fabricating color filters and for color liquid crystal displays (Wu et al., 2007). The smaller sizes of pigment particles in the dispersion media yield superior color strength, contrast, and transmittance (Wu et al., 2005). Therefore, searching for feasible methods and favourable process parameters to produce nano-metric pigment particles with narrow particle size distribution (PSD) is technically important for the industrial applications. Instead of traditional mechanical milling, the supercritical anti-solvent (SAS) process may provide an innovative route to meet this demand (Wu et al., 2005; Reverchon et al., 1999; Jung and Perrut, 2001).

The supercritical antisolvent process uses both the high power of supercritical fluids to dissolve the organic solvents and the low solubility of the compounds in supercritical fluids (Shekunov and York, 2000) to cause the precipitation of such compounds once they are dissolved in the organic phase. The dissolution of the supercritical fluid into the organic solvent is accompanied by a large volume expansion and, consequently, a reduction of the liquid density, and therefore, of its solvent power, causing a sharp rise in the supersaturation within the liquid mixture. Because of the high and uniform degree of supersaturation, small particles with a narrow particle size distribution are expected (Dukhin et al., 2005).

Wu et al. in their paper entitle *Ultra-fine particles formation of C.I. Pigment Green 36 in different phase regions via a supercritical anti-solvent process* (2007) do a review of previous studies on pigment particle formation using supercritical techniques. They affirmed that these works are rather limited. Gao et al. (Gao et al., 1998) prepared micrometric particles of Pigment Red Lake C, C.I. Pigment Yellow 1, and C.I. Pigment Blue 15 using an SAS method. Micro-metric pigment particles of Bronze Red were produced by Hong et al. (Hong et al., 2000) with a continuous SAS apparatus. Wu et al. (Wu et al., 2005; Wu et al., 2006) extensively investigated the effects of the SAS process parameters on the PSD of C.I. Pigment Red 177 and C.I. Pigment Blue 15:6. Nano-metric or submicron particles were obtained from these studies. The precipitation kinetic parameters of Pigment Blue 15:6 were determined with the aid of the population balance theory (Wu et al., 2006). Reverchon et al. (Reverchon et al., 2005) investigated micronization of C.I. Disperse red 60 using both SAS and supercritical-assisted atomization (SAA) methods. They found that nano-metric particles could be formed using SAS, whereas micro-metric particles were produced using SAA. Wu et al. (Wu et al., 2006) developed a supercritical-assisted dispersion apparatus to C.I. Pigment Red 177 in propylene glycol monomethyl ether acetate with blended dispersants. In addition to Wubbolts et al. (Wubbolts et al., 1999) and Wu et al. (Wu et al., 2006), Reverchon et al. (Reverchon et al., 2003) found that the phase behaviour of mixtures in precipitator, rather than the mass transfer, governed SAS precipitation. As shown from their experimental results, submicron particles were produced when the mixtures of solvent + anti-solvent + solute in the precipitator were manipulated at supercritical homogeneous states during the particle formation stage (Wu et al., 2007).

REFERENCES

- Bach, E., Cleve, E., Schollmeyer, E. Past, present and future of supercritical fluid dyeing technology - an overview, *Review of Progress in Coloration and Related Topics* 32 (2002) 88-102
- Bach, E.; Cleve, E. and Schollmeyer, E. Past, present and future of supercritical fluid dyeing technology - an overview, *Review of Progress in Coloration and Related Topics* 32 (2002) 88-102
- Bach, E.; Cleve, E.; Schollmeyer, E.; Bork, M. and Korner, P. Experience with the Uhde CO₂-dyeing plant on technical scale. I. Optimization steps of the pilot plant and first dyeing results, *Melliand Internacional* 3 (1998) 192-194
- Bach, E.; Knittel, D. and Schollmeyer, E. Dyeing poly(lactic acid) fibres in supercritical carbon dioxide, *Coloration Technology* 122 (5) (2006) 252-258
- Bae, H.W.; Jeon, J.H. and Lee, H. Influence of co-solvent on dye solubility in supercritical carbon dioxide, *Fluid Phase Equilibria* 222-223 (2004) 119-125
- Baek, J.-K.; Kim, S.; Lee, G.-S. and Shim, J.-J. Density Correlation of Solubility of C. I. Disperse Orange 30 Dye in Supercritical Carbon Dioxide, *Korean Journal of Chemical Engineering* 21 (1) (2004) 230-235
- Banchero, M., Sicardi, S.; Ferri, A.; Mann, L., Supercritical dyeing of textiles-From the laboratory apparatus to the pilot plant, *Textile Research Journal* 78(3), 2008, 217-223
- Banchero, M.; Ferri, A.; Manna, L. and Sicardi, S. Solubility of disperse dyes in supercritical carbon dioxide and ethanol, *Fluid Phase Equilibria* 243 (1-2) (2006) 107-114
- Bao, P. and Dai, J. Relationships between the solubility of C. I. disperse red 60 and uptake on PET in supercritical CO₂, *Journal of Chemical and Engineering Data* 50 (3) (2005) 838-842
- Cabral, V. F.; Santos, W. L. F.; Muniza, E. C.; Rubira, A. F. and Cardozo-Filho, L. Correlation of dye solubility in supercritical carbon dioxide, *J. of Supercritical Fluids* 40 (2007) 163-169
- Cegarra, J. Dyeing textile fibres in supercritical carbon dioxide [Tintura de fibras textiles en dióxido de carbono supercrítico], *Revista de la Industria Textil* 398 (2002) 77-84
- Chafer, A.; Berna, A.; Monton, J.B. and Munoz, R. High-pressure solubility data of system ethanol (1) + epicatechin (2) + CO₂ (3), *Journal of Supercritical Fluids* 24 (2002) 103-109
- Chang, K.H.; Bae, H.K. and Shim, J.J. Dyeing of pet textile fibres and films in supercritical carbon dioxide, *Korean J. Chem. Eng.* 13 (1996) 310-316
- De Giorgi, M. R.; Cadoni, E.; Maricca, D. and Piras, A. Dyeing polyester fibres with disperse dyes in supercritical CO₂, *Dyes and Pigments* 45 (2000) 75-79
- Draper, S.L.; Montero, G.A.; Smith, B. and Beck, K. Solubility relationships for disperse dyes in supercritical carbon dioxide, *Dyes and Pigments* 45 (3) (2000) 177-183
- Dukhin, S. S.; Shen, Y.; Dave, R. and Pfeffer, R. Droplet mass transfer, intradroplet nucleation and submicron particle production in two-phase flow of solvent-supercritical antisolvent emulsion, *Colloid Surf. A: Physicochem. Eng. Aspect.* 261 (2005) 163
- Fasihi, J.; Yamini, Y.; Nourmohammadian, F. and Bahramifar, N. Investigations on the solubilities of some disperse azo dyes in supercritical carbon dioxide, *Dyes and Pigments* 63 (2) (2004) 161-168

- Fernandez Cid, M. V.; Buijs, W. and Witkamp, G. J. Application of molecular modeling in the optimization of reactive cotton dyeing in supercritical carbon dioxide, *Industrial and Engineering Chemistry Research* 46 (12) (2007) 3941-3944
- Ferri, A.; Banchemo, M.; Manna, L. and Sicardi, S. A new correlation of solubilities of azoic compounds and anthraquinone derivatives in supercritical carbon dioxide, *Journal of Supercritical Fluids* 32 (2004a) 27-35
- Ferri, A.; Banchemo, M.; Manna, L. and Sicardi, S. An experimental technique for measuring high solubilities of dyes in supercritical carbon dioxide, *Journal of Supercritical Fluids* 30 (1) (2004) 41-49
- Gao Y, Mulenda TK, Shi YF, Yuan WK. Fine particles preparation of red lake C pigment by supercritical fluid, *Journal of Supercritical Fluids* 13 (1998) 369
- Gebert, B.; Saus, W.; Knittel, D.; Buschmann, H.-J. and Schollmeyer, E. Dyeing natural fibres with disperse dyes in supercritical carbon dioxide, *Textile Research Journal* 64 (7) (1994) 371-374
- Giessmann, M.; Schafer, K. and Hocker, H. Dyeing of polyester/wool from supercritical carbon dioxide with disperse and disperse reactive dyes, *DWI Reports* (123) (2000) 465-469
- Golob, V. and Tusek, L. The dyeing of textiles in supercritical CO₂ [Farbenie textilu v superkritickom CO₂], *Vlakna a Textil* 8 (4) (2001) 250-253
- Gordillo, M.D.; Pereyra, C. and Martínez de la Ossa, E.J. Measurement and correlation of solubility of Disperse Blue 14 in supercritical carbon dioxide. *J. of Supercritical Fluids* 27 (2003) 31-37
- Gordillo, M.D.; Pereyra, C. and Martínez de la Ossa, E.J. Solubility estimations for Disperse Blue 14 in supercritical carbon dioxide, *Dyes and Pigments* 67 (3) (2005) 167-173
- Guzel, B. and Akgerman, A. Mordant dyeing of wool by supercritical processing, *Journal of Supercritical Fluids*, 18 (2000) 247-252
- Guzel, B. and Akgerman, A. Solubility of disperse and mordant dyes in supercritical CO₂, *Journal of Chemical and Engineering Data* 44 (1) (1999), 83-85
- Hendrix, W.A. Progress in supercritical CO₂ dyeing, *Journal of Industrial Textiles* 31 (1) (2001) 43-56
- Hong, L.; Guo, J. Z.; Gao, Y. and Yuan, W. K. Precipitation of microparticulate organic powders by a supercritical antisolvent process, *Ind Eng Chem Res* 39 (2000) 4482
- Hou, A. and Dai, J. Kinetics of dyeing of polyester with CI Disperse Blue 79 in supercritical carbon dioxide, *Coloration Technology* 121 (1) (2005) 18-20
- Hou, A.; Xie, K. and Dai, J. Effect of supercritical carbon dioxide dyeing conditions on the chemical and morphological changes of poly(ethylene terephthalate) fibres, *Journal of Applied Polymer Science* 92 (2004) 2008-2012
- Huang, Z.; Guo, Y.-H.; Sun, G.-B.; Chiew, Y.C. and Kawi, S. Representing dyestuff solubility in supercritical carbon dioxide with several density-based correlations, *Fluid Phase Equilibria* 236 (1-2) (2005) 136-145
- Joshi, A.S.; Malik, T. and Parmar, S. Supercritical carbon dioxide dyeing of polyester, *Asian Dyer* 3 (5) (2006) 51-54
- Joung, S. N.; Shin, H. Y.; Park, Y. H. and Yoo, K. Measurement and correlation of solubility of disperse anthraquinone and azo dyes in supercritical carbon dioxide, *Korean J. Chem. Eng.* 15 (1) (1998) 78.

- Joung, S.N. and Yoo, K.-P. Solubility of disperse anthraquinone and azo dyes in supercritical carbon dioxide at 313.15 to 393.15 K and from 10 to 25 MPa, *Journal of Chemical and Engineering Data* 43 (1) (1998) 9-12
- Jun, J. H.; Ueda, M.; Sawada, K.; Sugimoto, M. and Urakawa, H. Supercritical carbon dioxide containing a cationic perfluoropolyether surfactant for dyeing wool, *Coloration Technology* 121 (6) (2005) 315-319
- Jung, J. and Perrut, M. Particle design using supercritical fluids: literature and patent survey, *Journal of Supercritical Fluids* 20 (2001) 179
- Kawahara, Y.; Kikutani, T.; Sugiura, K. and Ogawa, S. Dyeing behaviour of poly(ethylene terephthalate) fibres in supercritical carbon dioxide, *Coloration Technology* 117 (5) (2001) 266-269
- Ke, J.; Mao, C.; Zhong, M.; Han, B. and Yan, H. Solubilities of salicylic acid in supercritical carbon dioxide with ethanol cosolvent, *Journal of Supercritical Fluids* 9 (1996) 82-87
- Kim, T.; Kim, G.; Park, J. Y.; Lim, J. S. and Yoo, K. P. Solubility Measurement and Dyeing Performance Evaluation of Aramid NOMEX Yarn by Dispersed Dyes in Supercritical Carbon Dioxide, *Ind. Eng. Chem. Res.* 45 (2006) 3425-3433
- Knittel, D., Saus, W., Hoger, S., Schollmeyer, E. Dyeing from supercritical CO₂ - fastnesses of dyeing, *Melliand Textilberichte* 75 (5) (1994) 388-394
- Knittel, D., Saus, W., Schollmeyer, E. Application of supercritical carbon dioxide in finishing processes, *Journal of the Textile Institute* 84 (4) (1993) 534-552
- Knittel, D.; Saus, W. and Schollmeyer, E. Water-free dyeing of textile accessories using supercritical carbon dioxide. *Indian Journal of Fibre and Textile Research* 22 (3) (1997) 184-189
- Knittel, D.; Schollmeyer, E. and Saus, W. Dyeing with carboxyl-group-containing dyes in supercritical CO₂, *Melliand Textilberichte* 76 (10) (1995) 854-858
- Kopcak, U. and Mohamed, R.S. Caffeine solubility in supercritical carbon dioxide/co-solvent mixtures, *Journal of Supercritical Fluids* 34 (2005) 209-214
- Lee, J.W.; Min, J.M. and Bae, H.K. Solubility measurement of disperse dyes in supercritical carbon dioxide, *Journal of Chemical and Engineering Data* 44 (4) (1999) 684-687
- Lee, J.W.; Park, M.W. and Bae, H.K. Measurement and correlation of dye solubility in supercritical carbon dioxide, *Fluid Phase Equilibria* 173 (2) (2000) 277-284
- Lee, M.-J.; Cheng, C.-H. and Lin, H.-M. Cosolvent effects on the solubilities of disperse dyes of blue 79, red 153 and yellow 119 in supercritical carbon dioxide, *Journal of the Chinese Institute of Chemical Engineers* 34 (2) (2003) 255-261
- Li, Q.; Zhang, Z.; Zhong, C.; Liu, Y. and Zhou, Q. Solubility of solid solutes in supercritical carbon dioxide with and without cosolvents, *Fluid Phase Equilibria*. 207 (2003) 183-192
- Li, Z. Y.; Meng, T. Y.; Zhang, X. D.; Liu, X. W.; Xia, Y. J.; Hu, D. P. and Jiang, T. Experimental research on dyeing poly(ethylene terephthalate) fibres with disperse blue 60 in supercritical carbon dioxide, *Gao Xiao Hua Xue Gong Cheng Xue Bao/Journal of Chemical Engineering of Chinese Universities* 20 (2) (2006) 203-207
- Liao, S. K. Dyeing of microdenier polyester fabric in supercritical carbon dioxide, *Indian Journal of Fibre and Textile Research* 30 (3) (2005) 324-330
- Liao, S. K.; Chang, P. S. and Lin, Y. C. Dyeing of polypropylene fibres with disperse dyes by supercritical carbon dioxide, *Seni Kikai Gakkai Shi/Journal of the Textile Machinery Society of Japan* 54 (1) (2001) 63

- Liao, S.K. Analysis on the dyeing of polypropylene fibres in supercritical carbon dioxide, *Journal of Polymer Research* 7 (3) (2000) 155-159
- Lin, H.-M.; Ho, C.-C. and Lee, M.-J. Solubilities of disperse dyes of blue 79:1, red 82 and modified yellow 119 in supercritical carbon dioxide and nitrous oxide, *Journal of Supercritical Fluids* 32 (1-3) (2004) 105-114
- Lin, H.-M.; Liu, C.-Y.; Cheng, C.-H.; Chen, Y.-T. and Lee, M.-J. Solubilities of disperse dyes of blue 79, red 153, and yellow 119 in supercritical carbon dioxide, *Journal of Supercritical Fluids* 21 (1) (2001) 1-9
- Liu, Z. T.; Sun, Z.; Liu, Z. W.; Lu, J. and Xiong, H. Benzylated modification and dyeing of ramie fibre in supercritical carbon dioxide, *Journal of Applied Polymer Science* 107 (3) (2008) 1872-1878
- Liu, Z. T.; Zhang, L.; Liu, Z.; Gao, Z.; Dong, W.; Xiong, H.; Peng, Y. and Tang, S. Supercritical CO₂ dyeing of ramie fibre with disperse dye, *Industrial and Engineering Chemistry Research* 45 (26) (2006) 8932-8938
- Maeda, S.; Hongyou, S.; Kunitou, K. and Mishima, K. Dyeing cellulose fibres with reactive disperse dyes in supercritical carbon dioxide, *Textile Research Journal* 72 (3) (2002) 240-244
- Maeda, S.; Kunitou, K.; Hihara, T. and Mishima, K. One-bath dyeing of polyester/cotton blends with reactive disperse dyes in supercritical carbon dioxide, *Textile Research Journal* 74 (11) (2004) 989-999
- Malik, S.K., Kaur, H. Supercritical carbon dioxide - The dyeing technique of future, *Man-Made Textiles in India* 48 (1) (2005) 27-32
- Marr, R. and Gamse, T. Use of supercritical fluids for different processes including new developments-a review. *Chemical Engineering and Processing* 39 (2000) 19-28
- Mishima, K.; Matsuyama, K.; Ishikawa, H.; Hayashi, K.-I. and Maeda, S. Measurement and correlation of solubilities of azo dyes and anthraquinone in supercritical carbon dioxide, *Fluid Phase Equilibria* 194-197 (2002) 895-904
- Özcan, A. and Özcan, A. S. Solubility of an acid dye in supercritical carbon dioxide by ion-pairing with dodecyltrimethylammonium bromide, *Fluid Phase Equilibria* 249 (2006) 1-5
- Özcan, A. S.; Özcan, A. Adsorption behavior of a disperse dye on polyester in supercritical carbon dioxide, *Journal of Supercritical Fluids* 35 (2005) 133-139
- Özcan, A.S.; Clifford, A.A.; Bartle, K.D. and Lewis, D.M. Dyeing of cotton fibres with disperse dyes in supercritical carbon dioxide, *Dyes and Pigments*, 36(2) (1998) 103-110
- Özcan, A.S.; Clifford, A.A.; Bartle, K.D. and Lewis, D.M. Solubility of disperse dyes in supercritical carbon dioxide, *Journal of Chemical and Engineering Data*, 42 (3) (1997), 590-592
- Park, M. W. and Bae, H. K. Dye distribution in supercritical dyeing with carbon dioxide, *Journal of Supercritical Fluids* 22 (2002) 65-73
- Qun, X. Supercritical fluid dyeing technology and application, *China Textile and Apparel* 25 (5) (2007) 76-78
- Reverchon, E. Supercritical antisolvent precipitation of micro- and nanoparticles, *Journal of Supercritical Fluids* 15 (1999) 1
- Reverchon, E.; Adami, R.; De Macro, I.; Laudani, C. G. and Spada, A. Pigment red 60 micronisation using supercritical fluids based techniques, *Journal of Supercritical Fluids* 35 (2005) 76

- Reverchon, E.; Caputo, G.; De Marco, I. Role of phase behavior and atomization in the supercritical antisolvent precipitation, *Ind Eng Chem Res* 42 (2003) 6406
- Santos, W. L. F.; Moura, A. P.; Povh, N. P.; Muniz, E. C. and Rubira, A.F. Anthraquinone and azo dyes in dyeing processes of PET films and PET knitted fabrics using supercritical CO₂ medium, *Macromolecular Symposia* 229 (2005) 150-159
- Saus, W., Hoger, S., Knittel, D., Schollmeyer, E. Dyeing with supercritical carbon dioxide (1993b), *Textilveredlung* 28 (3) 38-40
- Saus, W.; Knittel, D. and Schollmeyer, E. Dyeing of textiles in supercritical carbon dioxide, *Textile Research Journal* 63 (3) (1993c) 135-142
- Saus, W.; Cleve, E.; Denter, U.; Duffner, H. and Schollmeyer, E. Determination of the dye uptake of cotton with trichromatic dyes. I. Basis of quantitative multicomponent analysis, *Textilveredlung* 29 (1-2) (1994) 13-18
- Saus, W.; Knittel, D. and Schollmeyer, E. Dyeing of textiles in supercritical carbon dioxide, *Textile Res. J.* 63 (3) (1993) 135
- Saus, W.; Knittel, D. and Schollmeyer, E. Dyeing with supercritical carbon dioxide - physico-chemical fundamentals, *Textile Praxis* 47 (1993a) 1052-1054
- Sawada, K., Takagi, T., Jun, J.H., Ueda, M., Lewis, D.M. Dyeing natural fibres in supercritical carbon dioxide using a nonionic surfactant reverse micellar system, *Coloration Technology* 118 (5) (2002) 233-237
- Sayem, A.S.M., Roszbach, V. Progress in Supercritical Fluid Dyeing (SFD) Taiwan *Textile Research Journal* 14 (4) (2004) 259-267
- Sayem, A.S.M., Roszbach, V. Supercritical fluid dyeing (SFD): A green technology [La teinture par fluide supercritique (SFD): Une technologie verte] *Textile Journal* 121 (5) (2004) 22-25
- Shekunov, B. Y. and York, P. Crystallization processes in pharmaceutical technology and drug delivery design, *J. Cryst. Growth* 211 (2000) 122
- Shinoda, T. and Tamura, K. Solubilities of C.I. Disperse orange 25 and C.I. Disperse blue 354 in supercritical carbon dioxide, *Journal of Chemical and Engineering Data* 48 (4) (2003) 869-873
- Shinoda, T. and Tamura, K. Solubilities of C.I. Disperse Red 1 and C.I. Disperse Red 13 in supercritical carbon dioxide, *Fluid Phase Equilibria* 213 (1-2) (2003) 115-123
- Smole, M. and Zipper, P. The influence of different treatment media on the structure of PET fibres, *Materials Research Innovations* 6 (2002) 55-64
- Son, Y. A.; Hong, J. P. and Kim, T. K. An approach to the dyeing of polyester fibre using indigo and its extended wash fastness properties, *Dyes and Pigments* 61 (2004) 263-272
- Sung, H.-D. and Shim, J.-J. Solubility of C. I. Disperse Red 60 and C. I. Disperse Blue 60 in supercritical carbon dioxide, *Journal of Chemical and Engineering Data* 44 (5) (1999) 985-989
- Tabaraki, R.; Khayamian, T. and Ensafi, A. A. Solubility prediction of 21 azo dyes in supercritical carbon dioxide using wavelet neural network, *Dyes and Pigments* 73 (2007) 230-238
- Tamura, K. and Shinoda, T. Binary and ternary solubilities of disperse dyes and their blend in supercritical carbon dioxide, *Fluid Phase Equilibria* 219 (1) (2004) 25-32
- Tataba, I.; Miyagawa, S.; Lyu, J. H.; Cho, S. M. and Hori, T. Fluid density dependency of the partition coefficient of disperse dyes between synthetic fibre and supercritical CO₂ in supercritical dyeing, *Kobunshi Ronbunshu* 58 (10) (2001) 521-526

- Tuma, D.; Wagner, B. and Schneider, G.M. Comparative solubility investigations of anthraquinone disperse dyes in near- and supercritical fluids, *Fluid Phase Equilibria* 182 (1-2) (2001) 133-143
- Tušek, L.; Golob, V. and Knez, Ž. Effect of pressure and temperature on supercritical CO₂ dyeing of PET-dyeing with mixtures of dyes, *International Journal of Polymeric Materials* 47 (4) (2000) 657-665
- Van Der Kraan, M.; Cid, M. V. F.; Woerlee, G. F.; Veugelers, W. J. T. and Witkamp, G. J. Equilibrium study on the disperse dyeing of polyester textile in supercritical carbon dioxide, *Textile Research Journal* 77 (8) (2007) 550-558
- Vankar, P.S.; Tiwari, V. and Ghorpade, B. Supercritical fluid extraction: Of natural dye from Eucalyptus bark used for cotton dyeing in microwave and sonicator, *Canadian Textile Journal* 119 (5) (2002) 32-35
- Vankar, P.S.; Tiwari, V. and Ghorpade, B. Supercritical fluid extraction of natural dye from eucalyptus bark used for cotton dyeing in microwave and sonicator, *Asian Textile Journal* 10 (2) (2001) 68-70
- Wagner, B.; Kautz, C.B. and Schneider, G.M.. Investigations on the solubility of anthraquinone dyes in supercritical carbon dioxide by a flow method, *Fluid Phase Equilibria* 158-160 (1999) 707-712
- Wang, C. T. and Lin, W. F. Scouring and dyeing of polyester fibres in supercritical carbon dioxide, *Journal of Chemical Engineering of Japan* 34 (2) (2001) 244-248
- Wen, H., Dai, J. J. Dyeing of polylactide fibres in supercritical carbon dioxide, *Journal of Applied Polymer Science* 105 (4) (2007) 1903-1907
- West, B.L., Kazarian, S.G., Vincent, M.F., Brantley, N.H., Eckert, C.A., Supercritical fluid dyeing of PMMA films with azo-dyes, *Journal of Applied Polymer Science* 69 (5) (1998) 911-919
- Wu, H. T.; Lee, M. J. and Lin H. M. Precipitation kinetics of pigment blue 15:6 sub-micro particles with a supercritical anti-solvent process, *Journal of Supercritical Fluids* 37 (2006) 220
- Wu, H. T.; Lee, M. J.; Lin, H. M. Supercritical fluid-assisted dispersion of ultrafine pigment red 177 particles with blended dispersants, *Journal of Supercritical Fluids* 39 (2006) 127-134
- Wu, H. T.; Lin, H. M. and Lee, M. J. Ultra-fine particles formation of C.I. Pigment Green 36 in different phase regions via a supercritical anti-solvent process, *Dyes and Pigments* 75 (2) (2007) 328-334
- Wu, H. T.; Lee, M. J. and Lin, H. M. Nano-particles formation for pigment red 177 via a continuous supercritical anti-solvent process. *Journal of Supercritical Fluids* 33 (2005) 173
- Wu, H.T.; Lin, H.M. and Lee, M.J. Ultra-fine particles formation of C.I. Pigment Green 36 in different phase regions via a supercritical anti-solvent process, *Dyes and Pigments* 75 (2007), 328-334
- Wubbolts, F. E.; Bruinsma, O. S. L. and van Rosmalen, G. M. Dry-spraying of ascorbic acid or acetaminophen solutions with supercritical carbon dioxide, *J Cryst Growth* 198/199 (1999) 767
- Zhang, L.-G.; Wu, Z.-M. and Zhang, C. Research on dyeing effect of wool fibre with natural pigment in supercritical carbon dioxide, *Wool Textile Journal* (4) (2007) 5-7

Chapter 4

PHOTO-CONTROLLED MOLECULAR SWITCHES BASED ON PHOTOCHROMIC SPIROOXAZINE DYES

Sung-Hoon Kim^a and Sheng Wang^b

^aDepartment of Textile System Engineering, Kyungpook National University,
Daegu, 702-701, Korea

^bSchool of Chemistry Science and Technology,
Zhanjiang Normal University, Zhanjiang, 524048, P.R. China

ABSTRACT

Photochromism refers to a reversible phototransformation of a chemical species between two forms having different absorption spectra. Photochromic compounds reversibly change not only the absorption spectra but also their geometrical and electronic structures. The molecular structure changes induce physical property changes of the molecules, such as fluorescence, refractive index, polarizability, electrical conductivity, and magnetism. When such photochromophores are incorporated into functional molecules, such as polymers, host molecules, conductive molecules, liquid crystals, the properties can be switched by photo irradiation. Among of all kinds of photochromic compounds, the spirooxazine dyes (SPO) are well-known photochromic compounds that show their high fatigue resistance and excellent photostability, which is one of the most promising candidates for applications in molecular electronics such as optical memory, molecular switching devices. In this review, we describe the recent development of spirooxazine dye as photo-controlled molecular switches in molecular materials, especially photochromism of spirooxazine in single crystal phase, spirooxazine dye polymer materials as fluorescence molecular switches, electrical conductivity switches, and viscosity switches, liquid crystal switches, gel switches and so on. In addition, layer by layer self-assemble spirooxazine dye in supermolecular chemistry as a photoswitching unit is described. We mainly present specific examples from our own research, which highlight our research group's contribution.

Key words: photochromism; photoswitching; spirooxazine dye; fluorescence; liquid crystal; viscosity; conductivity;

INTRODUCTION

In recent years, molecular switches have attracted considerable interest because they hold great promises as molecular electronic and photonic devices. In contrast to commonplace switches that turn electric appliances on and off, molecular switches enable the storage of information on a molecular level, which have the potential to significantly influence the development of optical-electronic materials science and information technologies.[1] Usually, molecular switches act as switching units in various optoelectronic devices and functional materials are addressed by stimulating it with light, electricity, or chemical reagents to specifically switch the physical properties between two states. Alternatively, a photoswitch exhibits two stable and selectively addressable states. Especially, photoinduced alteration of chemical and physical properties of photochromic molecules is of great interest because of its potential applications for optoelectronic devices, such as ultrahigh-density optical data storage and photoregulated molecular switches [2].

Among various types of photochromic molecules, the spirooxazine dyes (SPO) are well-known photochromic compounds that show their high fatigue resistance and excellent photostability. The photochromism of spirooxazine dye is attributable to the photochemical cleavage of the spiro C-O bond (Figure 1), which results in the extension of π -conjugation in the colored photomerocyanine conformer and thus shifts the absorption to the visible region. The function is based on the structure changes of single molecules which reversibly change not only the absorption spectra but also their geometrical and electronic structures. The molecular structure changes induce physical property changes of the molecules, such as fluorescence, refractive index, polarizability, electrical conductivity, and magnetism [3-7].

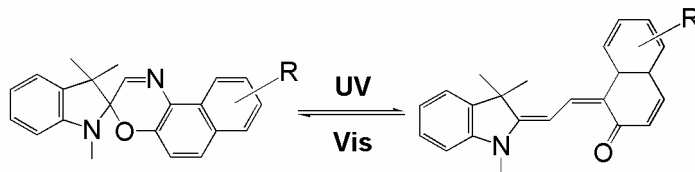


Figure 1. The photoswitching process of spirooxazine dyes

The high fatigue resistance and excellent photostability of the spirooxazine dyes in both the open-ring and closed-ring isomers makes it possible to demonstrate novel photoswitching effects, such as changes in fluorescent intensity and absorption spectra, electrochemical properties, optical rotation, magnetic properties, and electron-transfer interaction, the refractive index, dielectric constant and geometrical structure and so on[8-11]. Photoswitching of these physical properties can be accomplished by appropriate design of the molecules. By feeding back the evaluation of the physical properties to the molecular design, more sophisticated photoresponsive molecular systems can be constructed.

In generally, among the various physical properties which can be photo-switched by using spirooxazine as a photoswitching unit, molecules which change color (photochromism) and fluorescence, electrical conductivity, and viscosity upon photoirradiation, these molecular property changes can be applied to design photoswitching materials including photochromic single crystal switch, fluorescent molecular switch, conductivity switch, liquid crystal switch,

photochromic gel switch and so on. Figure 2 showed the classification of spirooxazines dye as photoswitching unit in photocontrolled molecular switches.

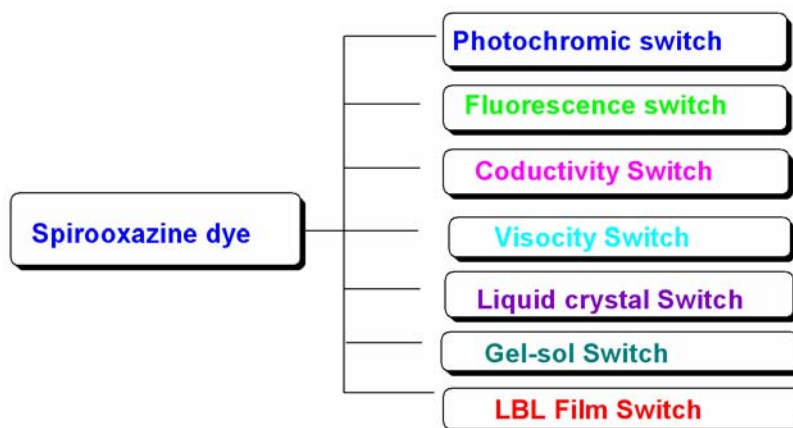


Figure 2. Classification of spirooxazine dyes as photoswitching unit

In this review, we describe recent development of spirooxazine dye as a photoswitching unit in molecular materials, especially spirooxazine single crystal photochromism, spirooxazine dye polymer materials as fluorescence molecular switch, electrical conductivity switch, and viscosity switch. In addition, layer by layer self –assemble film switch in supermolecular chemistry as a photoswitching unit. We mainly present specific examples from our own research, which highlight our research group’s contribution.

PHOTOSWITCHING OF SINGLE CRYSTAL PHOTOCHROMISM

Crystal engineering of photochromic single crystal is attractive and hot topic in recent years. The photochromism of single crystal is photochromic behavior in the solid state. The photochromic crystals switches showing thermally irreversible and fatigue-resistant characters have promising potential for optoelectronic devices such as rewritable optical memory media, optical switches, and color displays and photo-driven nano-scale actuators [12-16]. In generally, the high performance photochromic crystals switches have the following characteristic properties and functions. i) The photogenerated colored crystals exhibit dichroism under polarized light [17-18]. ii) The molecular conformations in the crystals strongly affect photocyclization and photocycloreversion quantum yields[19]. iii) Molecular structural changes following photocyclization/cycloreversion reactions induce reversible nano-scale surface morphological changes[20]. Although many photochromic compounds have been reported thus far, compounds which show photochromic reactivity in the crystalline phase are rare. Spirooxazine dyes (SPO) are known to offer remarkable stability towards photo-fatigue in solution and in various matrices, but there seldom have been reported to be photochromic spirooxazines in the crystalline state. Recently Natia L. Frank’s group synthesized a photochemically reversible, thermally irreversible isomerization of a spirooxazine dye **1** in the single crystalline phase (Figure 3) [21].

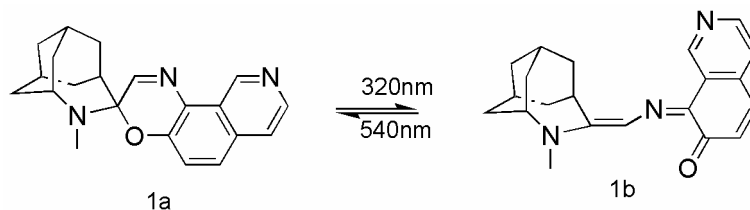


Figure 3. The photoswitching process of the spirooxazine dye **1**

The spirooxazine dye **1** was synthesized according to synthetic routes as shown in Figure 4. The effect of constrained media on the photoswitching behavior of **1** was investigated in both polymer films and the microcrystalline state. The spirooxazine dye **1** showed the excellent photochromic switching behavior in polymer films and in the microcrystalline state.

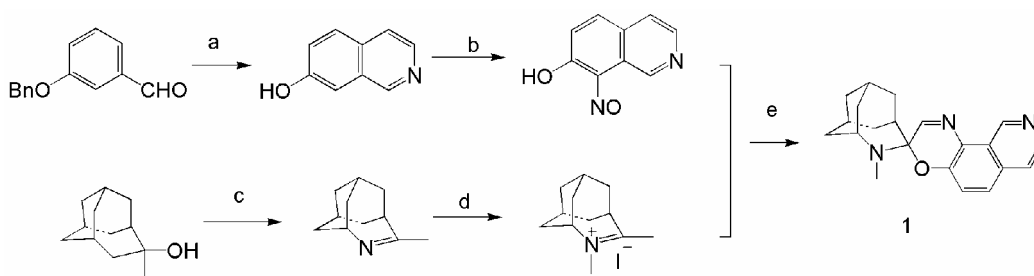


Figure 4. Synthetic routes of the spirooxazine dye **1** (a) aminoacetaldehyde dimethylacetal, trifluoroacetic anhydride, $\text{BF}_3 \cdot \text{OEt}_2$, (b) sodium nitrite, $\text{HCl}/\text{H}_2\text{O}$; (c) sodium azide, methanesulfonic acid, CH_2Cl_2 ; (d) methyl iodide, CH_2Cl_2 ; (e) Et_3N , CH_2Cl_2 .

X-ray quality single crystals of **1a** were obtained by recrystallization from hexane to give colorless monoclinic $\text{P}2_1/c$ prisms (ORTEP diagram of **1a** shown in Figure 5). The closed form (SPO) crystallizes with four molecules in the unit cell in pairs of head-to-tail dimers that sit orthogonal to each other in the crystal lattice (Figure 6).

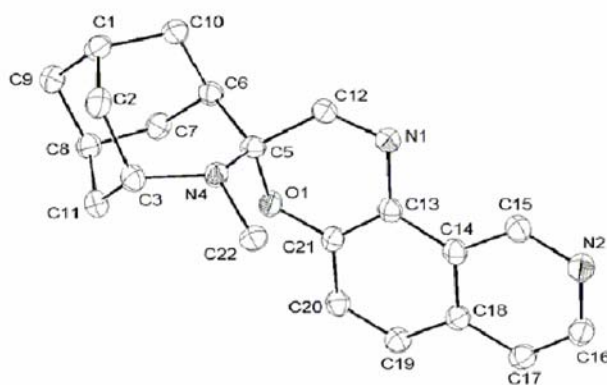


Figure 5. ORTEP diagram of **1a**. Thermal ellipsoids are shown at 50% probability. Hydrogen atoms have been omitted for clarity.

Intermolecular π - π contacts within each dimer are weak, with an intermolecular mean plane distance of 3.818 Å. Analysis of bond lengths and angles reveals little deviation from typical bond lengths and angles of other spirooxazines [22–25]. The cycle of photoisomerization is photochemically reversible, thermally irreversible, and fatigue resistant, as evidenced by numerous cycles of irradiation (>10 cycles).

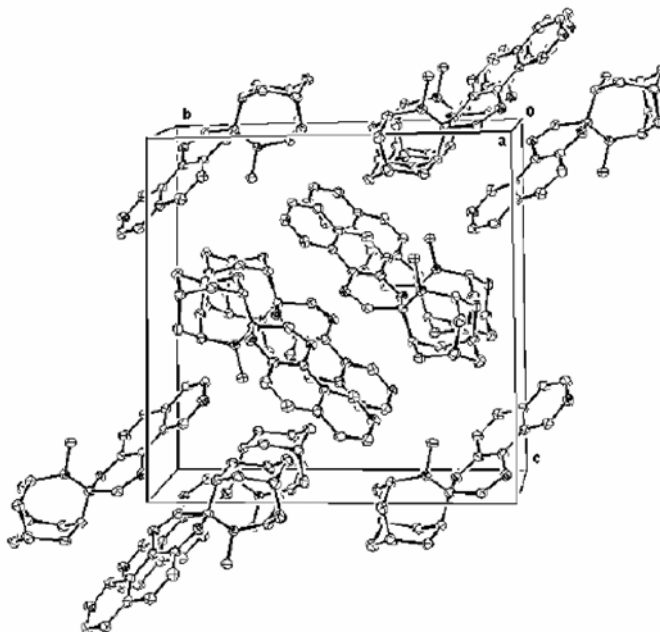


Figure 6. Packing diagram of the unit cell of the closed form of spirooxazine (**1a**). Thermal ellipsoids are shown at 50% probability. Hydrogen atoms have been omitted for clarity.

We also report herein the spirooxazine dye to exhibit photochromism both in solution and in the pure crystalline state [26]. The spirooxazine dye **2** was prepared according to the following synthetic routes (shown in Figure 7). The spirooxazine dye **2** showed the excellent photochromic switching behavior in solution and in the crystalline state.

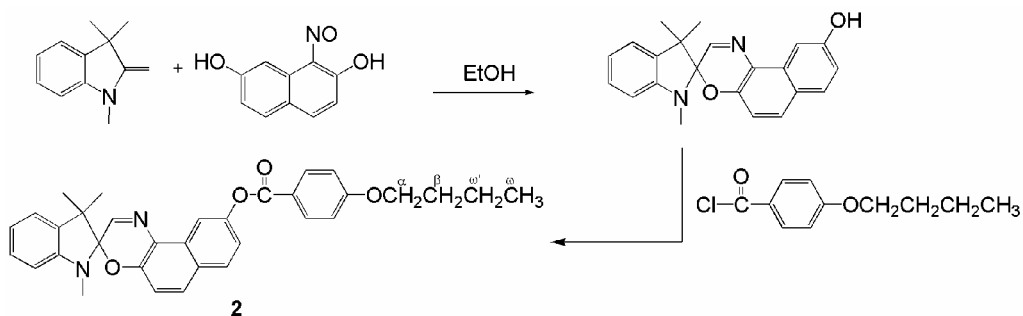


Figure 7. Synthetic routes of the spirooxazine **2**

Analysis of single crystal structure of spirooxazine dye **2**, it is evident that the molecules of the spirooxazine arrange themselves in a monoclinic crystallographic system (C_2), unit cell

of dimensions: $a=25.421$, $b=8.298$, $c=30.567$ Å with $\beta=111.51(3)^\circ$. This closed form transforms to the coloured open form upon UV irradiation. From the ORTEP diagram, it was concluded that the spiro centre was tetrahedral (Figure 8). The crystal packing scheme is shown in Figure 9. Only the phenyl groups overlapped with face-to-face geometry, with an interplanar separation of 3.5 Å, the molecules being held together by π - π stacking interaction. The general hydrogen bond is constituted with a donor X-H and an acceptor A, in the form X-H—A. The bond may be described in terms of d , the distance between H—A, and D , the distance between X—A. The weak C-H—O hydrogen bonds have d and D separations of around 2.0–3.0 Å and 3.0–4.0 Å, respectively [27]. From the results of the intermolecular distance N2—C33=3.9 Å, the molecules are also held together through weak intermolecular hydrogen bonding.

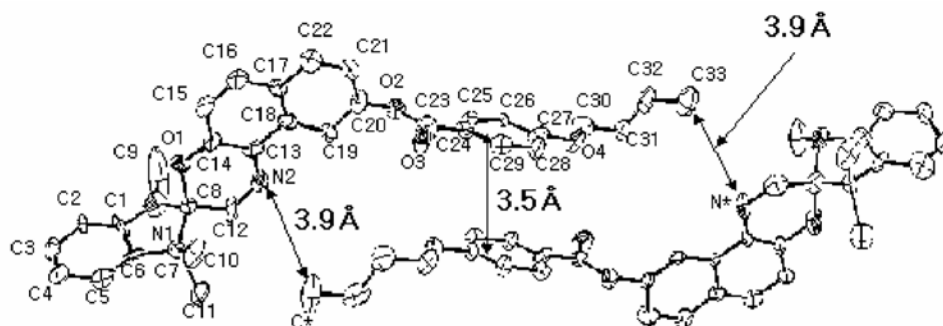


Figure 8. ORTEP view of molecular structure of spirooxazine dye 2

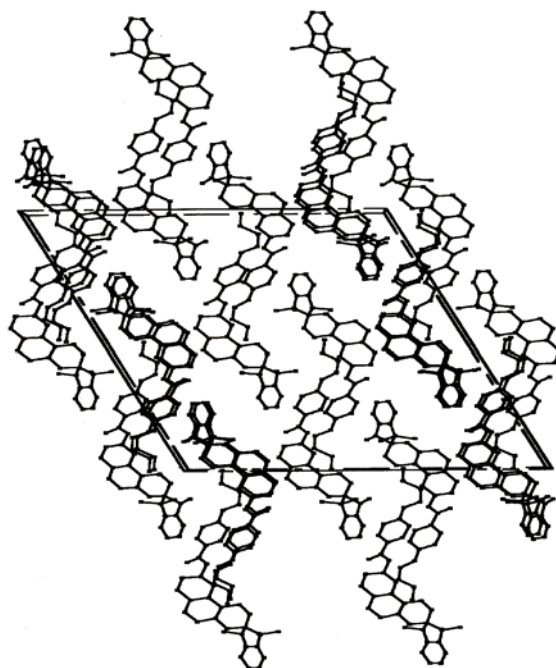


Figure 9. Crystal packing structure of spirooxazine dye 2 in unit cell

PHOTOSWITCHING OF FLUORESCENCE

Fluorescent photochromic switches attract strong interest for their possible application in optical memory as well as in fluorescent probe [28-29]. There have reported a lot of fluorescent photochromic switches including fluorescent diarylethene, spiropyran and so on. However, photocontrollable fluorescent changes of spirooxazine are very scarce [30]. Understanding the fluorescent spirooxazine photochromic reactions at a single-molecule level is very important, which can help ultimate realize the ultrahigh-density single molecule optical memory. Recently, Tian's group [31] reported a novel spironaphthoxazine molecule with a much more stable open-ring photomerocyanine form by incorporating a ferrocene moiety in the parent spirooxazine (abbreviated as SOFC) and successfully demonstrated 2D and 3D optical memory. Figure 10 represents the structure and photochemical isomerization of the novel spironaphthoxazine molecule (abbreviated as SOFC).

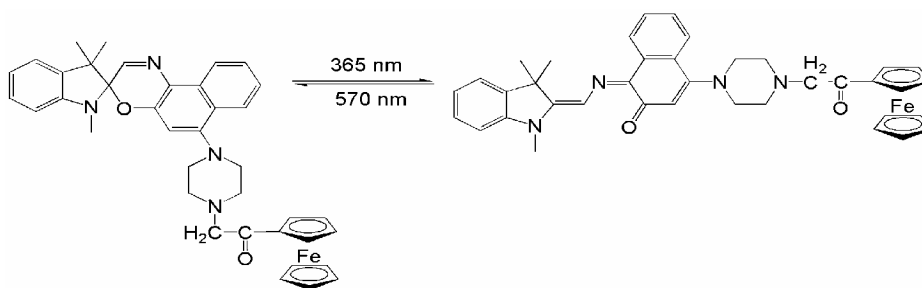


Figure 10. Photoisomerizing behavior of the spironaphthoxazine SOFC. Left: Spirooxazine Right: Photomerocyanine form

Like other spirooxazine molecules, SOFC undergoes reversible photochromic reaction. Corresponding to the difference between the UV-vis absorption before and after photoisomerization, the luminescence response of SOFC is also dictated by the binary status (Figure 11).

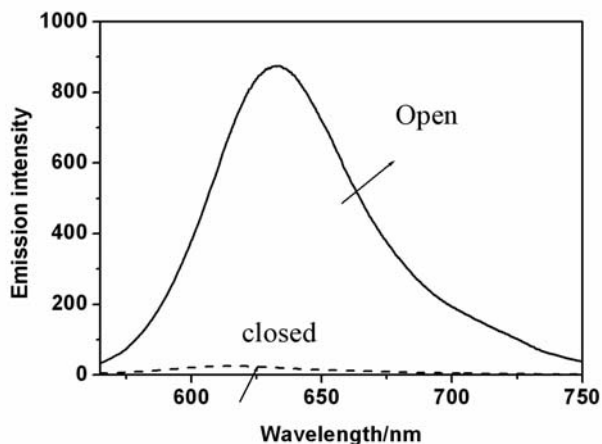


Figure 11. Emission spectra of SOFC before (broken line) and after (solid line) irradiation of the same sample

Excitation (at $\lambda=532\text{nm}$) of the closed-ring form, which has no absorption in the visible region at room temperature, produced no fluorescence emission, but the corresponding opening form luminesced strongly due to the formation of an extended π -conjugation system following the cleavage of the spiro-C-O bond. Thus, the binary data stored in the two isomers can be transduced into the fluorescence signals and read out conveniently.

In addition, The SOFC-PMMA films for imaging micrometer-sized objects in two dimensions utilizing fluorescence as the read-out method. The polymer films were prepared by spin-coating a dichloromethane solution of SOFC-PMMA mixture onto glass substrates, and then exposed to 365nm light irradiation through a mask with features in the micrometer-size regime. Subsequent to irradiation, the mask was removed and the image was successfully transferred to the polymer film as fluorescence patterns with a fine resolution. Figure 12 illustrates one such representative fluorescence image generated. The masked areas are dark and those areas exposed to 365nm light irradiation appear luminescent.

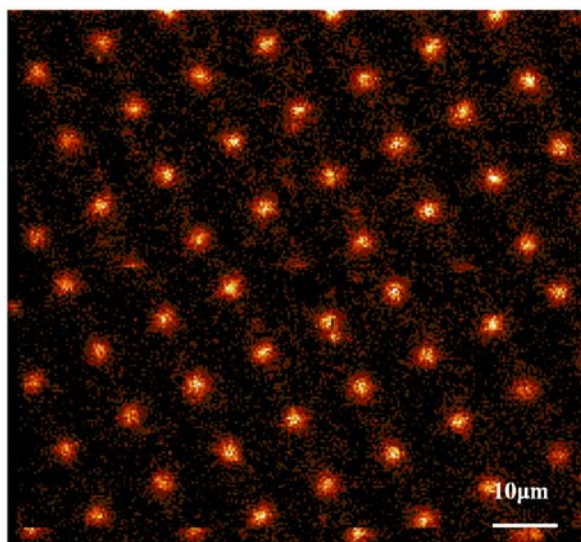


Figure 12. Fluorescence image generated from irradiation (5min) at 365nm of SOFC-PMMA film through a dot-patterned contact mask. The light regions indicate luminescence and the dark regions are non-luminescent ($\lambda_{\text{ex}}=532\text{nm}$). The size of one dot is approximately 4µm.

Dispersing the spirooxazine dye in a polymer matrix is by far the easiest strategy to prepare photochromic films. However, it has some serious limitations. Because the doped system were easily crystallization, phase separation, or the formation of concentration gradients in long-term storage. Undoped photochromic polymers would be advantageous over their dispersed monomeric counterparts because a high concentration of the active photochromic component can be incorporated into a polymer film resulting in the amplification of the desired effect, while maintaining the optical homogeneity of the material. Our group synthesized a fluorescent photochromic spirooxazine polymers switch containing carbazole (Cz) and spironaphthoxazine (SPO) moieties in the pendant groups (PMMA-Cz-SPO) (as shown in Figure 13) [32-33].

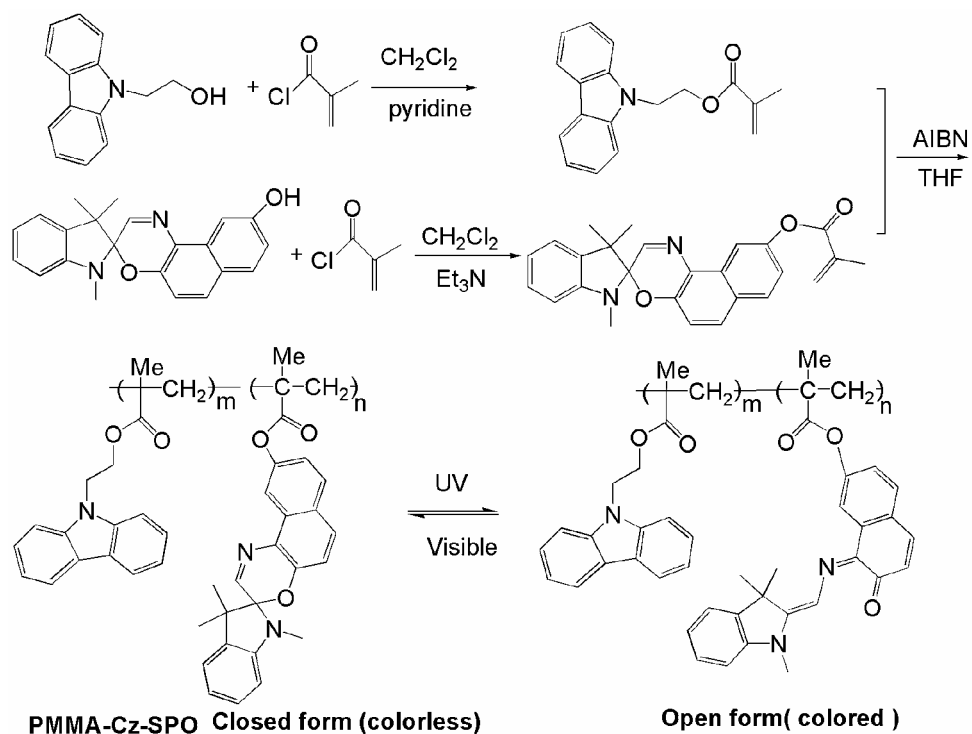


Figure 13. Synthetic routes and photoswitchable process of PMMA-Cz-SPO copolymer

The PMMA-Cz-SPO showed the excellent photochromic switching behavior in solution and in film. The PMMA-Cz-SPO copolymer exhibited photoluminescence at 348 nm and 364nm in THF solution at room temperature when excited at 320 nm. The fluorescence intensity of the copolymer decreased along with the photochromism from the ring-closed form to the ring open form irradiation with UV light (as shown in Figure 14).

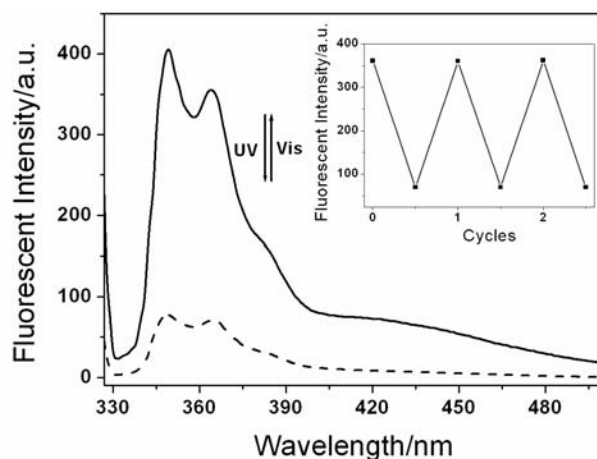


Figure 14. Fluorescence emission spectra change of PMMA-Cz-SPO copolymer in THF solution upon irradiation with UV/Vis light at room temperature. The inset figure shows the fluorescence monitoring of cycles on and off (Excited at 320nm, $\lambda_{em}=348\text{nm}$).

The blue emission was suppressed and almost wholly quenched of the photoluminescence at the photostationary state. The original photoluminescence was also recovered within 5 seconds restored by irradiation with visible light. Figure 14 inset shows a cycling experiment in which the maximum emission of PMMA-Cz-SPO in THF solution is monitored upon alternate irradiation with UV and Visible light.

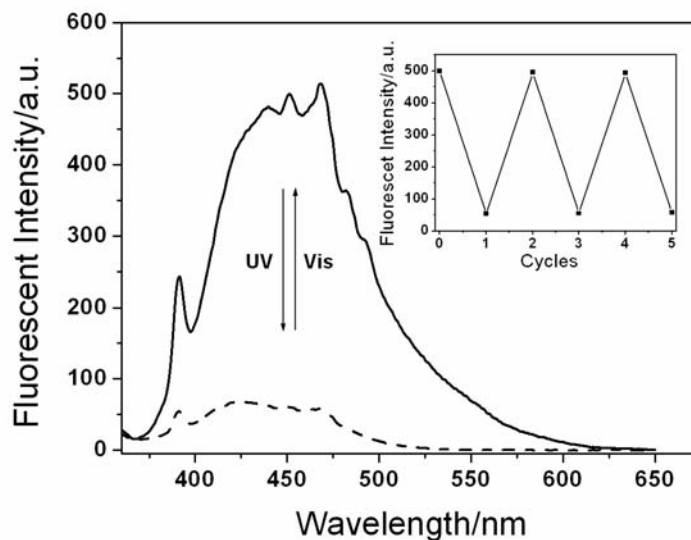


Figure 15. Fluorescence emission spectra changes of PMMA-Cz-SPO copolymer in film upon irradiation with UV/Vis light (excited at 342nm). The inset figure shows fluorescence monitoring of cycles on and off (Excited at 340nm, $\lambda_{em}=450$ nm).

Figure 15 shows the fluorescence spectra change of PMMA-Cz-SPO in film with excitation wavelength at 342 nm. The fluorescence intensity change was regulated by the photochromic reaction. Before irradiation with UV light, it showed a broad emission in the range of 400-550 nm with λ_{em} round 450 nm. Upon irradiation with UV light, the fluorescent intensity of PMMA-Cz-SPO gradually decreased and almost wholly quenched. The possible explanation for the fluorescence quenching is due to an increase in photoinduced electron transfer (PET) between the carbazole units and the spirooxazine isomers in PMMA-Cz-SPO film [34]. After irradiation with visible light, the original emission spectra are regenerated. Irradiation of photo-stationary of PMMA-Cz-SPO film with visible light led to a complete recovery of the initial fluorescence signal. From it can be seen Figure 15 inset, the fluorescence intensity reversibly changed at 450 nm (excitation: 342 nm) by alternate irradiation with UV and Visible light and this cycle could be repeated more than 10 times, which is an excellent photochromic spirooxazine fluorescence switch. The luminescence of carbazole chromophore is effectively regulated by toggling between the two isomers of the spirooxazine subunit in solid film, attributed to the change in PET between the carbazole and each form of the spirooxazine photochrome. It exhibits good photochromic properties, especially high fluorescent quantum efficiency and excellent fatigue resistance, which are promised to application all photon-mode memory media and fluorescent molecular switch.

PHOTOSWITCHING OF VISCOSITY

The photocontrolled molecules incorporated into supramolecular/macromolecular structures comprise a powerful approach towards the development of new materials and devices of nanoscale dimensions [35-36], and the control of these organisational processes by chemical or physical elements is a major challenge. A promising approach towards such responsive or smart materials is the integration of photochromic moieties into the supramolecular building blocks, which would offer the possibility to alter the self-assembly process of the individual molecules or change the properties of the supramolecular arrays by means of light [37].

A polymer having photoisomerizable unsaturated linkage in the backbone is suspected to change its conformation under photoirradiation. The change of intramolecular interactions in polymer systems induces a conformational change in the polymer chain and can be detected by viscosity measurement. Irie et al. [38] reported a viscosity change by photoirradiation of spiropyran system was observed for the first time for poly (methacrylate) with spiropyran pendant groups. A change in dipole moment due to isomerization from photochromic spiroxazine to the merocyanine form would be expected to alter intramolecular interaction of polymer chain when the spiroxazines are incorporated into the polymer pendant groups or backbone groups. We synthesized a photochromic spirooxazine copolymer which shows a photocontrolled viscosity switch (Figure 16) (abbreviated as PDDM-SPO) [39].

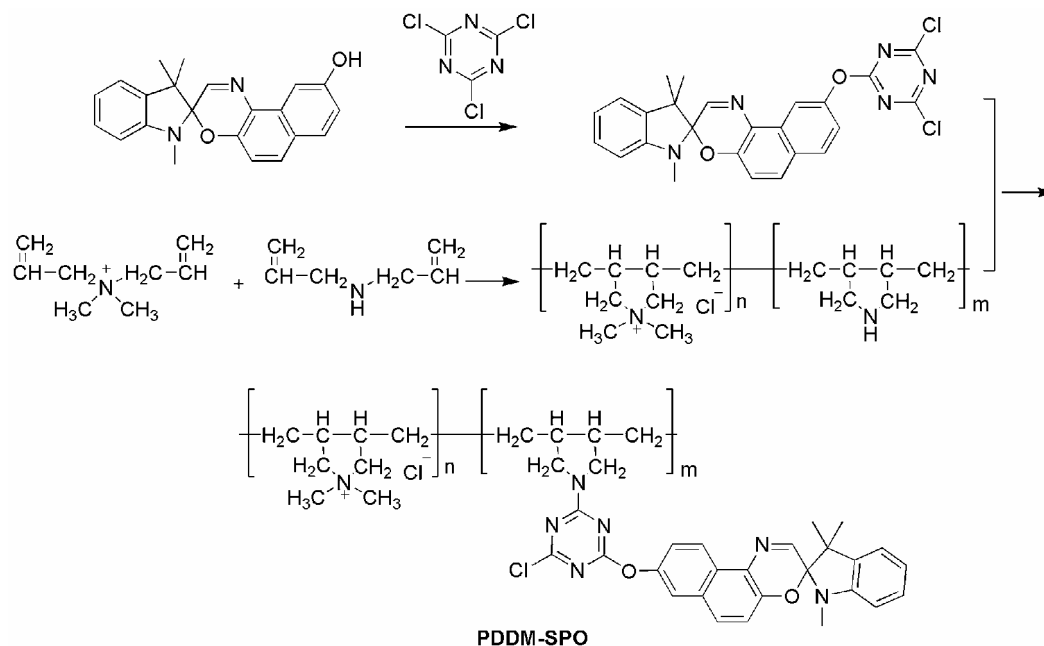


Figure 16. Synthetic routes of the PDDM-SPO polymer

We find the photochromic spirooxazine dye incorporated polymer showed excellent the photoswitching behavior of viscosity. Figure 17 shows the viscosity changes of the polymer having spiroxazine as side group in methanol before and after UV irradiation. The viscosity during UV irradiation returns to the initial value in less than 5 min at -5°C after the light is

removed. In methanol the relative viscosity after UV irradiation is 5% lower than the viscosity in dark. The recovery cycles of the viscosity can be repeated many times without any noticeable fatigue.

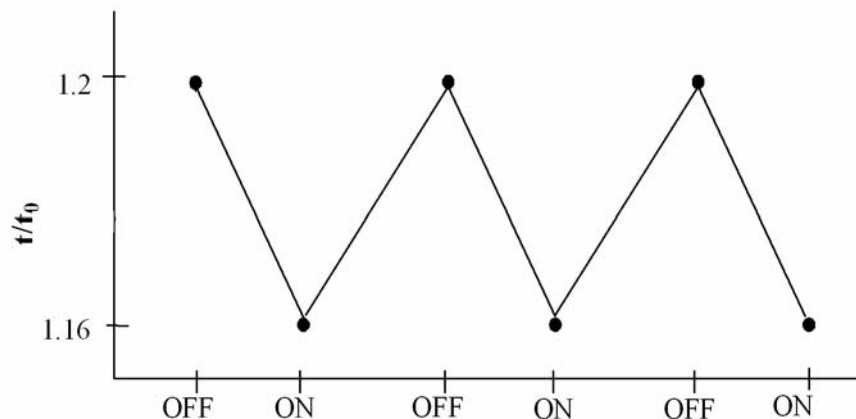


Figure 17. Change of the viscosity of a methanol solution of polymer having spirooxazine pendant group on UV irradiation at $-5\text{ }^{\circ}\text{C}$. Concentration of the polymer is 2% w/v.

These changes can be attributed to different molecular properties like shape and conformational freedom of the open and closed form of spirooxazine dye. Electrostatic attractive forces between the zwitterions and the charges on positive ammonium residues of the polymer chain tend to contract the polymer chain. In dark the attractive force considerably decreases because of the disappearance of the zwitterions structures of spirooxazine (Figure 18).

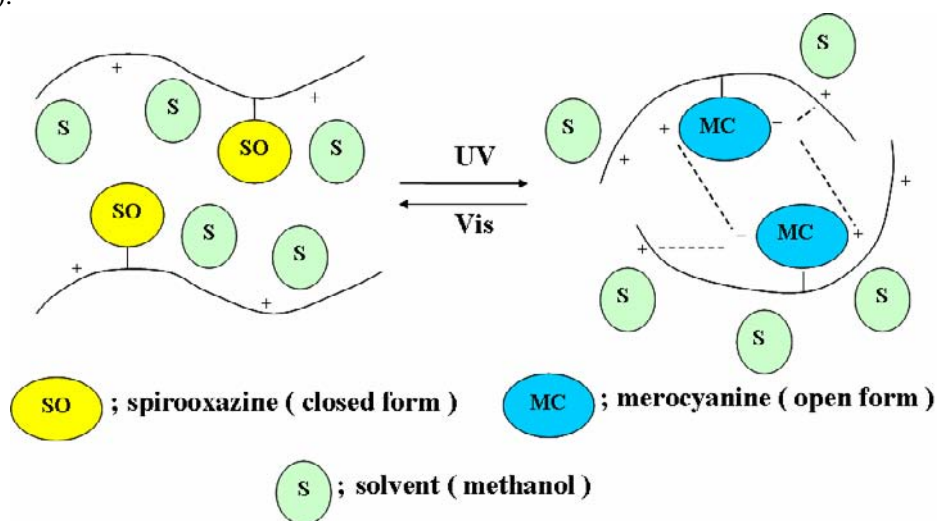


Figure 18. Schematic illustration of photostimulated conformation change of polymer chain on UV irradiation.

In addition, we calculated and simulated the photo-induced structural changes from spiro to merocyanine in order to understand the viscosity changes of the photochromic spirooxazine

polymer. Figure 19 shows the optimized photochromic spirooxazine molecular structure changes from the closed form to open form. All the theoretical calculations were performed by DMol³ program in the Materials Studio 4.2 package [40-41]. The photo-induced structural change from spiro to merocyanine causes the volume decrease, the diameter of photochromic spirooxazine polymer decreased from 32.52 Å to 29.18 Å. From the above result, we easily understand the photoswitching viscosity changes of the photochromic spirooxazine polymer. The theoretical calculations accorded with the experimental result. In addition, we investigated the other photochromic spirooxazine polymers viscosity changes, they show the excellent photoswitching viscosity behavior [33, 42].

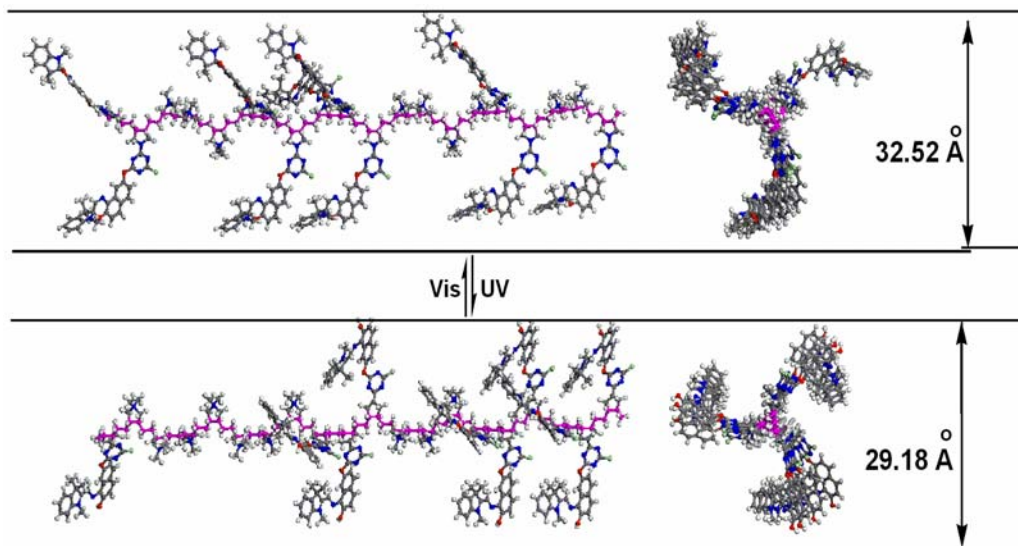


Figure 19. Calculations schematic illustration of photostimulated conformation change of polymer chain on UV/Vis light irradiation.

PHOTOSWITCHING OF CONDUCTIVITY

The design and creation of molecular systems that show chemical and physical changes in response to external stimuli is a topic of current interest because of their potential applications, as sensing and switching devices. In particular, the photo-induced electrical properties of photo-electric active materials, such as photoconductivity, have attracted considerable attention from the viewpoint of fundamental interest as well as from their practical applications. There is an important characteristic feature in the electronic structure changes of spirooxazine from the closed-form to open-form. So we hope to modulate the conductivity of spirooxazine and its derivative by light. We synthesized the a poly[N,N-[(3-dimethylamino)propyl]methacrylamide] having spirooxazine pendant group (Figure 20), which showed the excellent photochromic behavior with UV/Vis light irradiation [42].

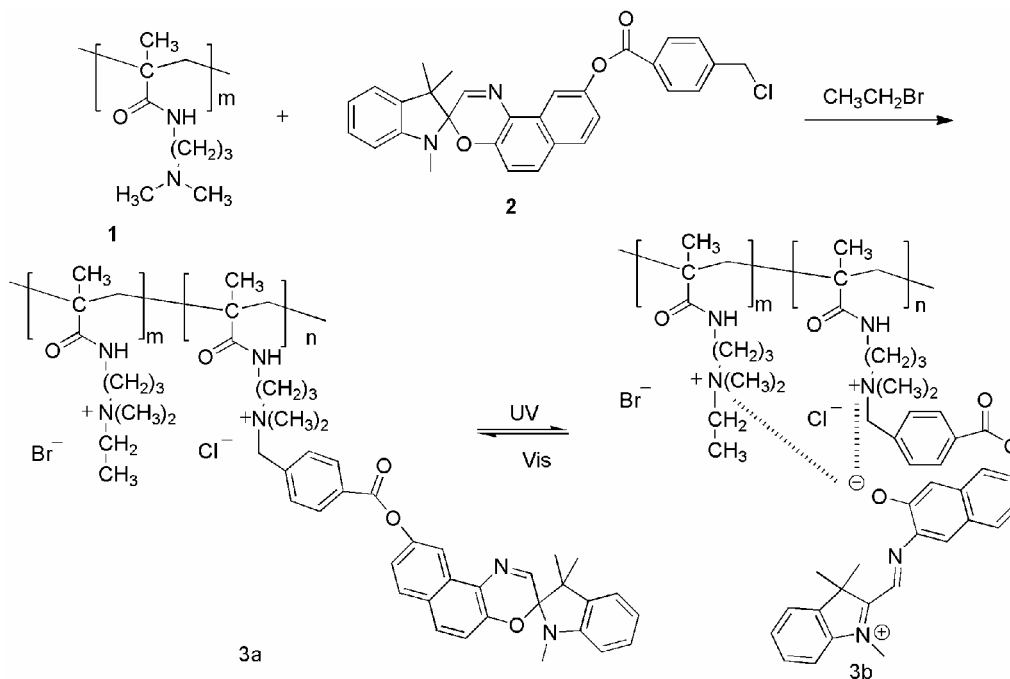


Figure 20. Synthetic routes and photoswitching process of the polymer **3**

This is a typical ionic polymer. In generally, the ionic polymers show the conductance behavior in electric field. When the spirooxazine dyes were incorporated in ionic polymer. We hope it can modulate the conductivity of the ionic polymer by light stimulation. We devised the following device to monitor the conductivity change of the ionic polymer by UV-Vis light (Figure 21).

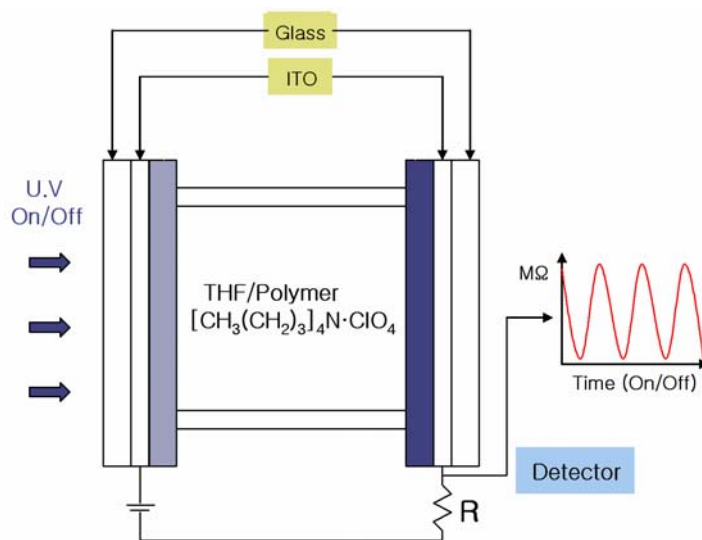


Figure 21. Schematic diagram of the conductivity measurement system

The photoinduced ionic conductivity response was analyzed at 15 °C and is shown in Figure 22. The photoinduced ionic conductivity can be estimated from the expression $(1/R_t)/(1/R_0)$ where R_0 and R_t are the resistance before and after UV irradiation. The ionic conductivity increased upon UV irradiation, which brought about the generation of zwitterions form, and subsequently decreased in dark, which in turn brought about the generation of closed spiro form. Sufficient reversibility was found in this polymer and this response was completely synchronized with that in the absorbance changes.

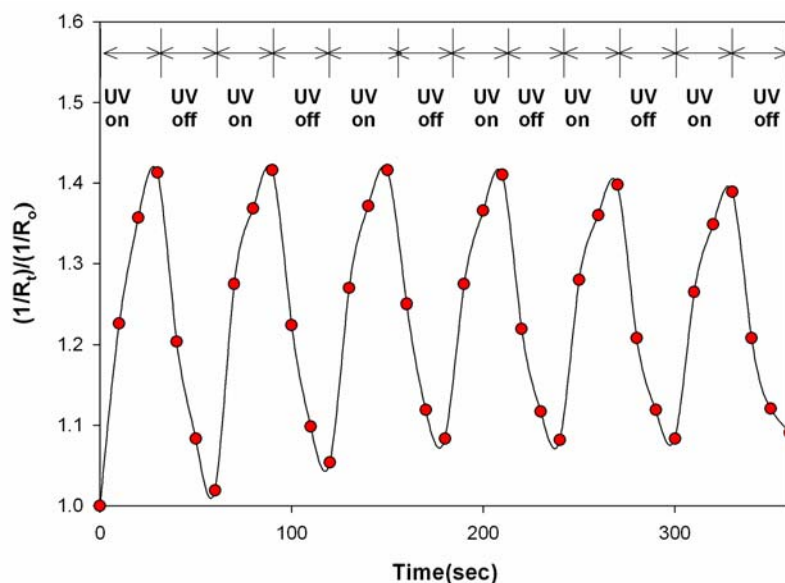


Figure 22. Photoinduced ionic conductivity response for polymer **3** at 15 °C

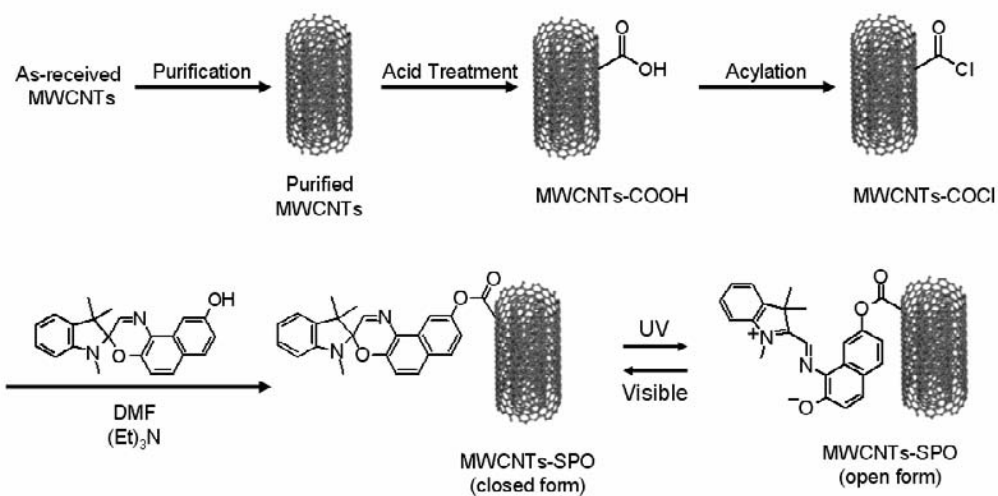


Figure 23. The synthetic routes of SPO-MWNTs.

In addition, we designed and synthesized that the photoinduced conductivity response in SPO dye molecules attached to the multi-walled carbon nanotubes (MWNTs). The preparation of covalently bonded MWNTs-SPO is depicted in Figure 23.

We demonstrate the photoinduced conductivity switch (shown in Figure 24.) The photoinduced conductivity can be also estimated from the expression $(1/R_t)/(1/R_0)$, where R_0 and R_t are the resistances before and after UV irradiation, respectively. The conductivity increased upon UV irradiation, which brought about the generation of merocyanine form. In dark the conductivity of MWNTs-SPO considerably decreased because of the disappearance of the merocyanine structure of SPO. The common feature of most intrinsically conducting organic materials is the presence of alternating single and double bonds along the entire molecule, which enables the delocalization or mobility of charge along the π -system. The conductivity is thus assigned to the delocalization of π -bonded electrons over the molecule. On UV irradiation the C-O bond of the colorless SPO is cleaved and colored merocyanine form is obtained. Thus, the interconversion between spiro form and merocyanine systems has been extensively investigated due to their potential applications in molecular devices and uses in nano- and biotechnology.

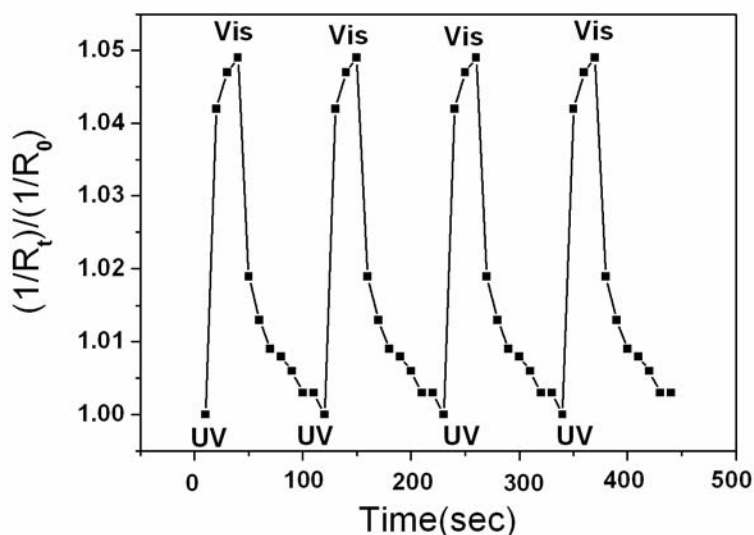


Figure 24. The photoinduced resistance changes for MWNTs-SPO thin film at 20°C.

In the merocyanine form, the electronic distribution should be described by delocalization of the π electrons with a negative charge on the oxygen and with a positive charge on the heterocyclic ring. A change in HOMO-LUMO band gap due to isomerization from spiro form to the merocyanine of SPO would be expected to alter conductivity of MWNT itself. Figure 25 shows the optimized molecular structure of the SPO and the electron distribution of its HOMO and LUMO. All the theoretical calculations were performed by DMol³ program in the MS Modeling 3.2 package which is the quantum mechanical code using density functional theory [43]. Perdew-Burke-Ernzerhof (PBE) functional of generalized gradient approximation (GGA) level [44] with double numeric polarization basis set [40] was used to calculate the

energy level of the frontier molecular orbital. The photo-induced structural change from spiro to merocyanine causes a large decrease in LUMO and a small increase in HOMO, producing a large bathochromic shift of the first band. Comparison of the electron distribution in the frontier orbitals of merocyanine reveals that HOMO-LUMO excitation moved the electron distribution from the indoline moiety to the naphthalene moiety. Excitation of the open form SPO leads to the injection of the excited electrons from the excited state dye to MWNT via naphthalene moiety connected to MWNT by an ester linkage. The recovery cycle of the conductivity before and after UV irradiation could be repeated many times without any noticeable change.

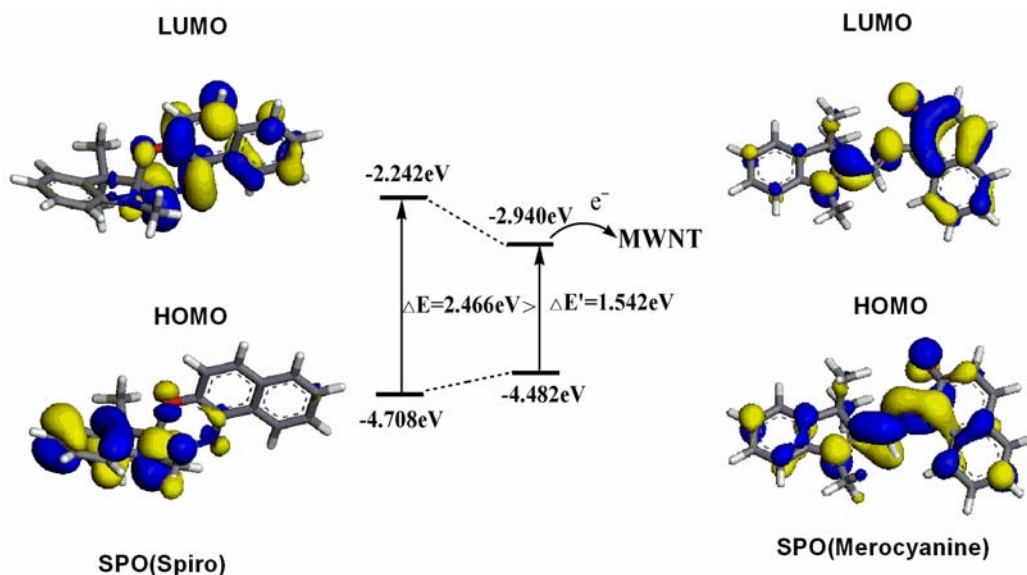


Figure 25. Electron distribution of the HOMO and LUMO energy level of SPO (Spiro) and SPO (Merocyanine).

PHOTOSWITCHING OF LIQUID CRYSTAL

The control of the structure and optical properties of liquid-crystalline (LC) phase by means of light is a major challenge in development of molecular devices and optical data storage system. So far various types of photoresponsive liquid crystals have been reported [45-46]. The combination of liquid-crystallinity and photochromic behavior in molecular systems promises to be very useful in optical technological devices. We have designed and prepared a new spirooxazines photochromic liquid crystal switch (as shown in Figure 26) [47].

We demonstrate that the photoswitching process of spirooxazines dye liquid crystal and optimize the the closed-form and closed form of spirooxazines dye liquid crystal (Figure 27). All the theoretical calculations were performed calculations were performed by DMol³ program in the MS Modeling 3.2 package. From the Figure 27 can be seen that the molecular structure of spirooxazine dye liquid crystal change a large by UV/Vis light irradiation.

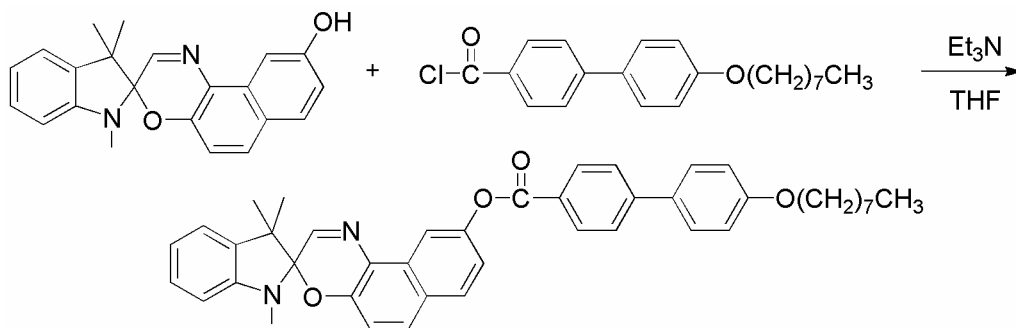


Figure 26. The synthetic route of SPO liquid crystal.

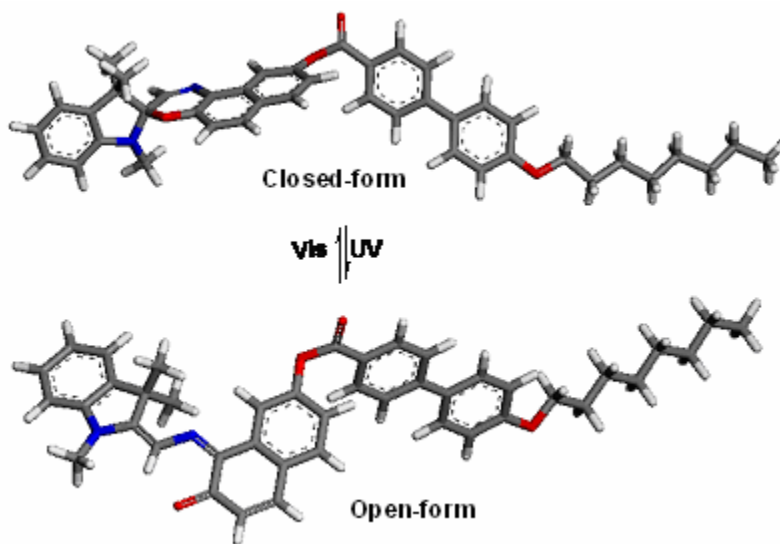


Figure 27. The photoswitching process of spirooxazine dye liquid crystal

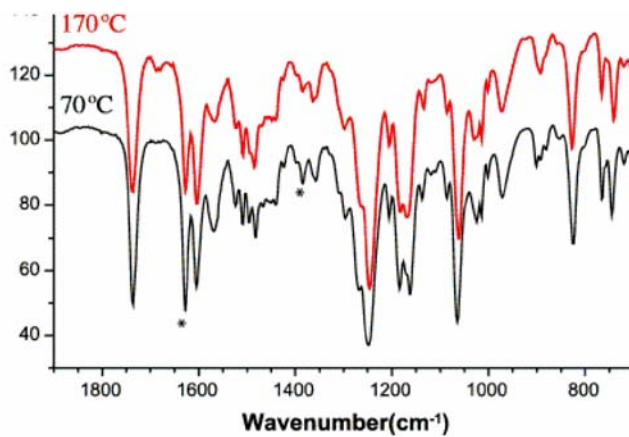


Figure 28. FT-IR spectra of the SPO liquid crystal. during heating

To conform the structural changes of the SPO liquid crystal, the FT-IR spectra of the compound were monitored by as shown in Figure 28. Due to ring opening reaction of the spirooxazine, the chromophoric structure changes to a form of merocyanine. This structural changes reflect in IR spectra; the C=N stretching band at 1628 cm^{-1} and the CH_3 deformational stretching band in O-linkage at 1384 cm^{-1} were markedly decreased at $170\text{ }^\circ\text{C}$.

DSC data also showed that SPO liquid crystal demonstrated a phase transition with a low ΔH (about 4.0 mJ/g) at $\sim 65\text{ }^\circ\text{C}$ during the cooling and heating cycle following the nematic–isotropic phase transition as indicated in Figure 29.

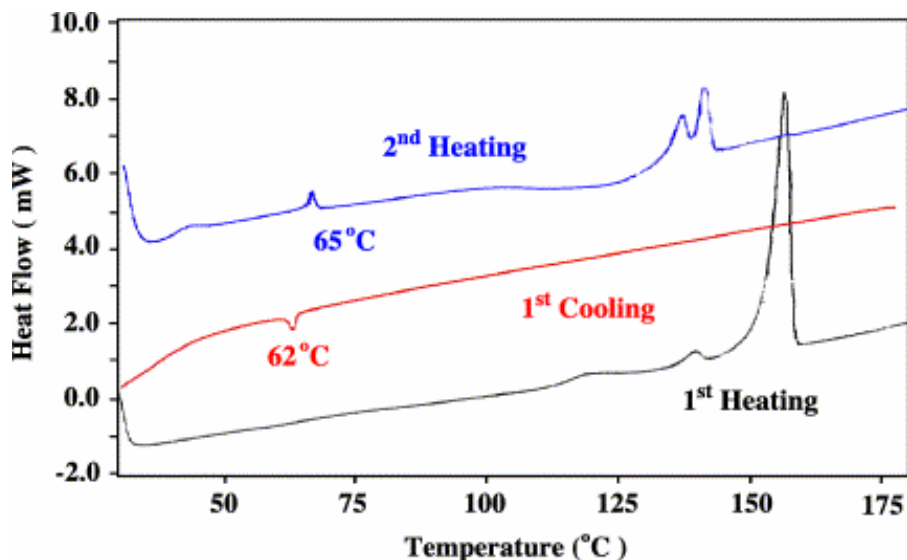


Figure 29. DSC data of SPO liquid crystal.

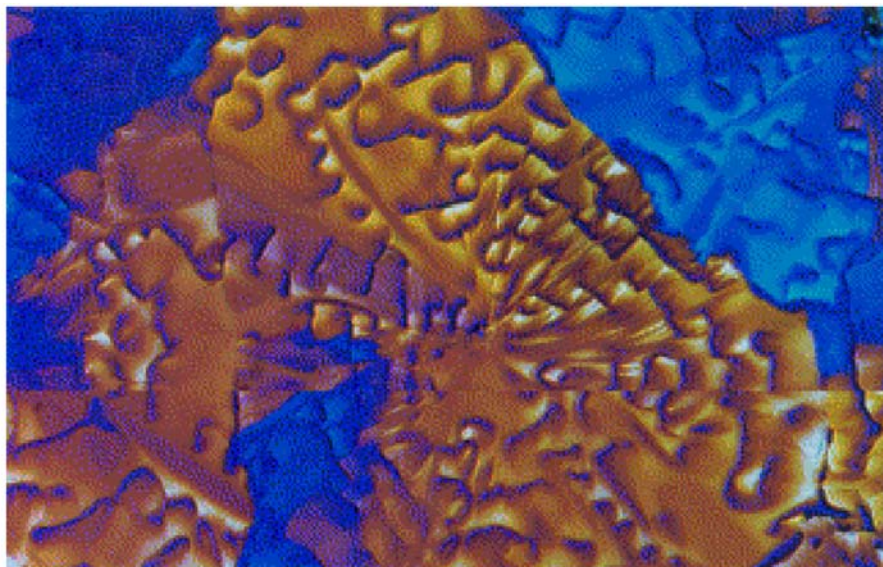


Figure 30. The Schlieren texture of SPO liquid crystal near T_c .

To characterize the liquid crystal behaviors of SPO liquid crystal, we investigated microscopic structural changes by the polarizing microscope and the small-angle XRD spectra during heating and cooling cycle of the film. The SPO liquid crystal showed the Schlieren texture during cooling near T_c (liquid crystalline temperature) as shown in Figure 30.

It also shows the definite distance, 19 Å, between molecules in the wide-angle XRD data in Figure 31. The alignment of molecules in the film near T_c was estimated by an order parameter (S) of the merocyanine dye formed on UV-irradiation of the film. The order parameter of the merocyanine is given by

$$S = (D_{\parallel} - D_{\perp}) / (2 \times D_{\perp} + D_{\parallel})$$

where D_{\parallel} and D_{\perp} are the relative absorption parallel and perpendicular to the molecular orientation, respectively, as shown in Figure 32. The order parameter S was estimated to 0.233, which was similar with the values obtained in previous reports [48-50].

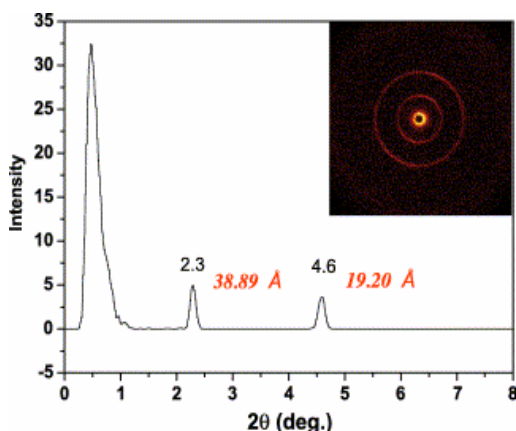


Figure 31. Small-angle spectra of SPO crystal.

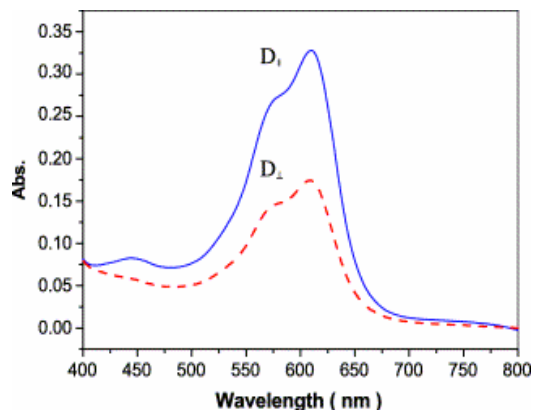


Figure 32. Polarized UV spectra of SPO liquid crystal.

PHOTOSWITCHING OF MULTI-LAYER SELF-ASSEMBLE FILM

Recently, more and more attention has been paid to “layer-by-layer self-assemble” technique in both theoretical and application fields due to its simplicity, versatility, and systematic control of the film structure and thickness. Incorporation of photochromic molecules provides the layer-by-layer self-assembled film with additional interesting properties such as optically induced orientation, linear optical properties, nonlinear optical properties and so on[51-54]. We designed and synthesized a series of spirooxazine dyes and successfully applied them in constructing layer by layer self-assemble ultra thin films switches (Figure 33) [55-57].

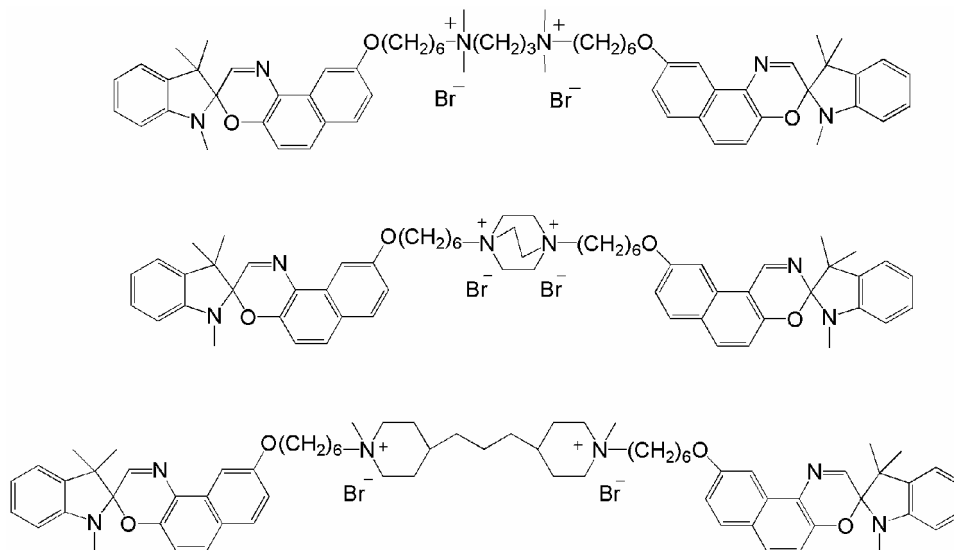


Figure 33. The chemical structure of SPO dyes for layer by layer self-assembly ultra thin films

In generally, one of the most important and universal techniques to construct ultra thin organic films is the alternating assembly of oppositely charged polyelectrolytes, so-called “layer-by-layer self-assemble” method [58-61]. This approach to thin-film deposition involves the assembly of oppositely charged layers of organic materials and can provide a 1-30nm growth step for a bilayer. The layer-by-layer deposition as a simple and versatile method for preparing supported multilayer thin films. The basic process involves dipping a charged substrate into a dilute aqueous solution of an anionic polyelectrolyte and allowing the polymer to absorb and reverse the charge of the substrate surface. The negatively charged substrate is rinsed and dipped into a solution of cationic polyelectrolyte, which absorbs and re-creates a positively charged surface. Sequential absorptions of anionic and cationic polyelectrolytes results in creation of multilayer films. The Figure 34 describes the process of spirooxazine dye layer-by-layer self-assembly deposition. In the first step, a substrate with a negative charged surface is immersed in the solution of the positively charged spirooxazine (SPO). In the second step, the substrate is dipped into the solution containing the negatively charged PSS. By repeating both steps, alternating multilayer are obtained with a precisely repeatable layer thickness.

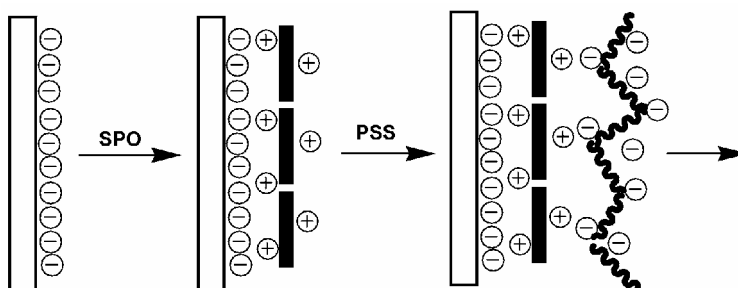


Figure 34. Schematic view of a self alternating multilayer film composed of a cationic spirooxazine and polystyrenesulfonate

A self-assembly multilayer photochromic spirooxazine switch is constructed. Figure 35 showed a self-assembly multilayer photochromic spirooxazine switch on the ITO substrate surface.

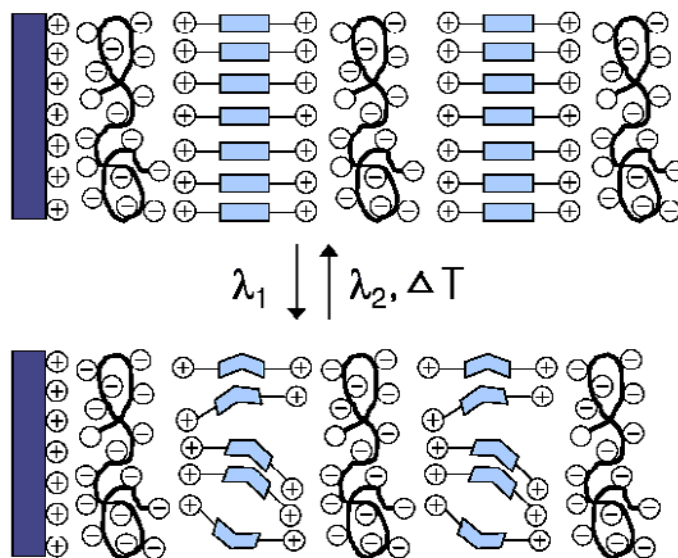


Figure 35. Schematic view of a self alternating multilayer photochromic spirooxazine switch film

The growth of SPO/PSS multilayer films formed by the sequential adsorption of SPO and PSS was examined by using UV-vis spectroscopy. The adsorption spectra upon UV irradiation in self-assembled multilayer containing SPO and PSS are shown in Figure 36. The regularity of the LBL adsorption is demonstrated in the plot of the absorbance of SPO in its maximum at $\lambda_{\max} = 610$ nm versus the number of dipping cycles applied.

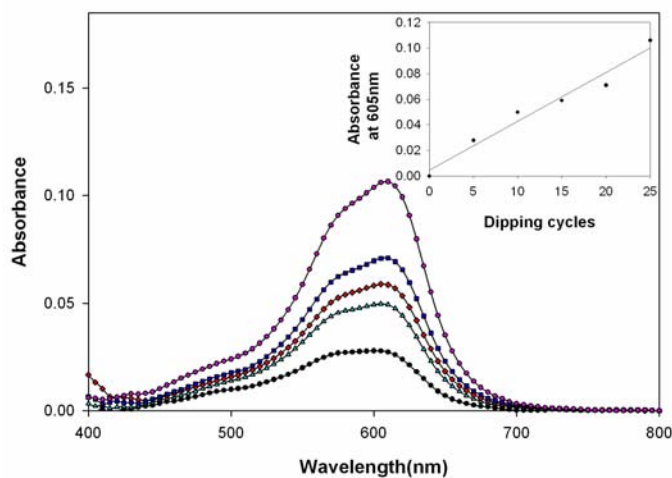


Figure 36. UV-vis absorption spectra of SPO/PSS multilayer films through a consecutive LBL deposition. The insert shows the increase in absorbance at 610 nm as a function of deposition cycles.

More detailed information on the surface structure and the direct image of the self-assembled multilayer on glass surface can also be obtained with AFM. The morphology of 2, 5, 10 pair layer SPO/PSS films was observed by AFM (Figure 37).

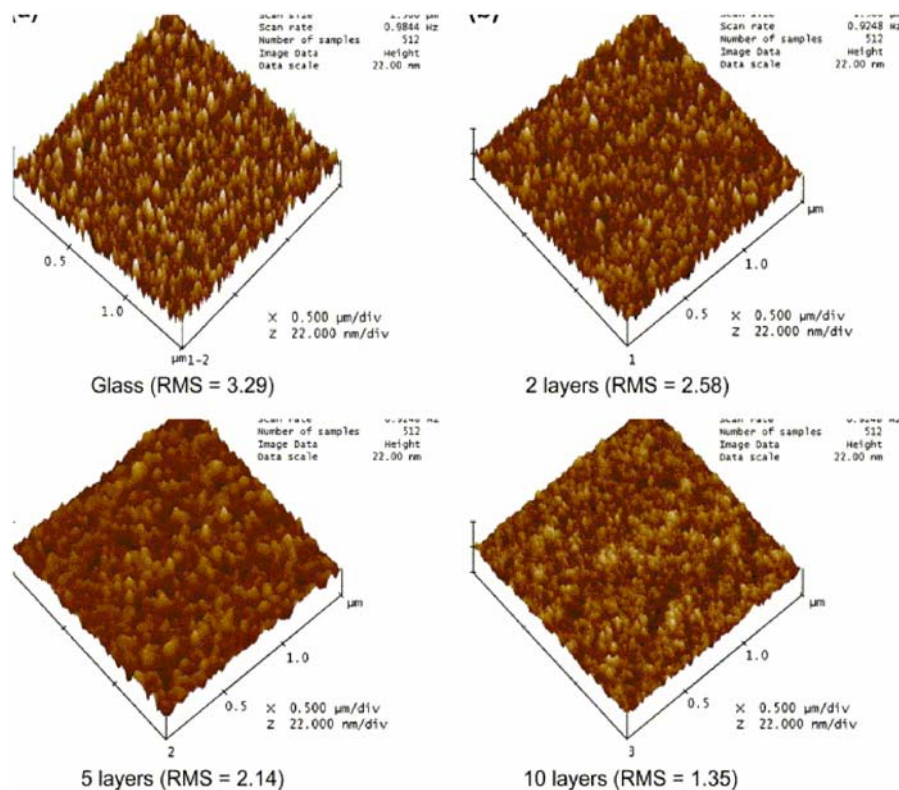


Figure 37. Morphology of the SO/PSS layers: (a) nude glass, (b) 2 layers, (c) 5 layers, and (d) 10 layers.

The mean value of the height from the cross-sectional analysis of raw glass, the surface roughness, RMS, is about 3.29 nm. The roughness of the 2, 5 and 10 pair SPO/PSS multilayer is determined to be 2.58, 2.14 and 1.35 nm, respectively. This decreased surface roughness arises from the stepwise chemical assembly.

PHOTOSWITCHING OF SPIROOXAZINE GEL

Organical gelators have attracted much attention in recent years[62-66]. Hydrogel switch is popular smart materials that can hold large volumes of water, but shrink in volume in the environmental conditions, such as pH, ionic strength, temperature, electric field, and light [67-71]. Such responsive systems are highly desirable in thermo- and mechano-responsive sensor materials or applications like drug delivery or catalysis, or nano- and mesoscopic assemblies with interesting optical and electronic properties and so on[72-74]. We designed and synthesized a bistable photoswitching in poly (N-isopropylacrylamide) with

spironaphthoxazine hydrogel as a new recording media for optical information storage, which have successfully demonstrated erasable and rewritable optical information on the hydrogel [75]. Figure 38 represents the structure and photochemical isomerization of the poly (N-isopropylacrylamide) with spironaphthoxazine hydrogel (abbreviated as PNIPA-SPO-BIS).

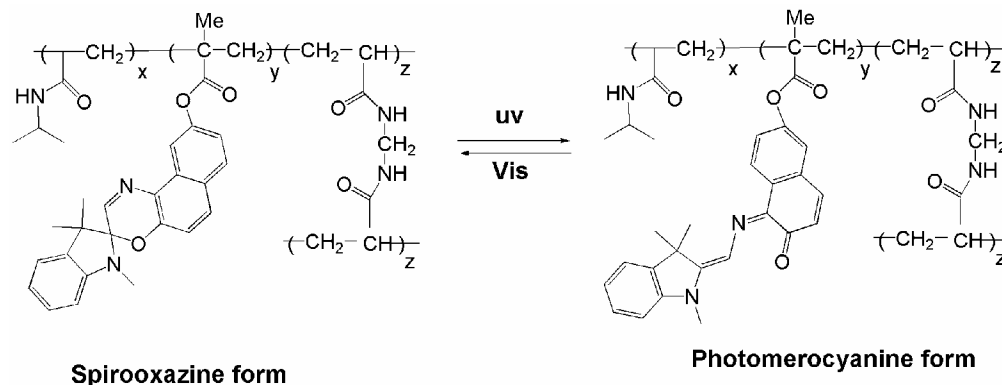


Figure 38. Photoisomerizing behavior of PNIPA-SPO-BIS hydrogel. Left: spirooxazine form; Right: photomerocyanine form

In water, PNIPA-SPO-BIS hydrogel showed excellent photochromic behavior. Figure 39 showed the UV-Vis absorption spectra changes of PNIPA-SPO-BIS copolymer in water solution upon irradiation with UV and Visible light. The inset shows absorption monitoring of cyclical on and off photoconversions of PMMA-SPO-BIS hydrogel in water solution. It can be repeated more than 20 times without any essential loss in color characteristics in repeated on and off process. In addition, we measured the absorption spectral changes of PNIPA-SPO hydrogel to obtain an insight into their photochromic properties in gel phase, which show similarly photochromic performance as in solution (Figure 40). In the same time, the PMMA-SPO-BIS hydrogel showed excellent fatigue resistance.

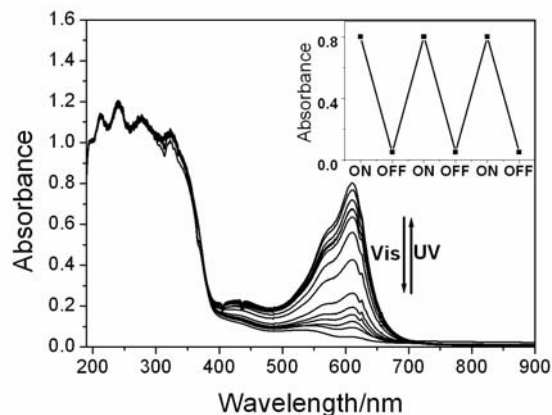


Figure 39. UV-Vis absorption spectra changes of PNIPA-SPO-BIS copolymer in water solution upon irradiation with UV and Visible light. The inset shows absorption monitoring of cyclical on and off photoconversions of copolymer (at $\lambda_{\max}=605\text{nm}$).

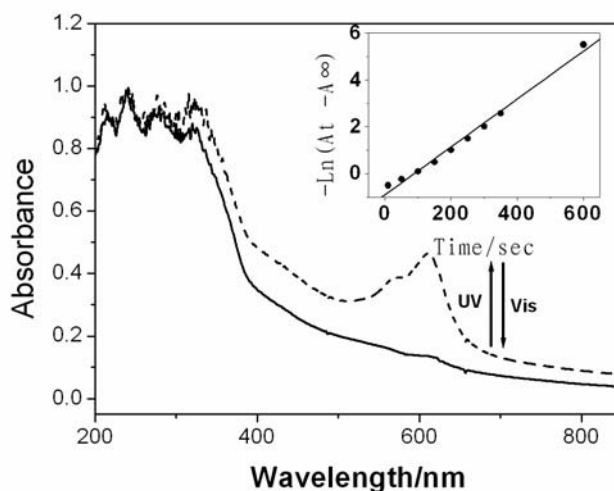


Figure 40. UV-Vis absorption spectra changes of PNIPA-SPO-BIS copolymer in hydrogel state upon irradiation with UV and Visible light at 28°C. The inset shows plot of the decolouration of PNIPA-SPO-BIS hydrogel (at $\lambda_{\text{max}}=615\text{nm}$).

When the PNIPA-SPO-BIS solution is heated above the lower critical solution temperature) value of 30°C (LCST), the transmittance starts to decrease dramatically. The transmittance decreases from 100% at room temperature to 0% at 36°C, and then stabilizes at even higher temperatures. There is no macroscopic phase separation after storage at 40°C for 24 h. when the stabilized PNIPA-SPO-BIS hydrogel is cooled below the LCST value of 31°C from 40°C, the transmittance starts to increase dramatically. When the PNIPA-SPO-BIS hydrogel is cooled at room temperature, it recovers the original PNIPA-SPO-BIS solution. The whole process from **1** state to **2** state is reversible as shown in Figure 41. However, when the PNIPA-SPO-BIS hydrogel was heated from 40 °C to higher temperature, the volume of PNIPA-SPO hdrogel began to shrink and form an agglomerate and separate wholly from the water at 60°C, when the PNIPA-SPO-BIS agglomerate was cooled to at room temperature, which can not recover the original state. This behavior is the typical shrinking change of bulk NIPA copolymer gels in water [76-78]. Interestingly, we use the UV light to irradiate the PNIPA-SPO-BIS agglomerate hdrogel, the red PNIPA-SPO-BIS agglomerate hdrogel turned to blue and kept the color for 2 hour. After visible light irradiation, the blue PNIPA-SPO-BIS agglomerate hdrogel converted back to the initial color. The whole process can repeat more than 15 times and keep the agglomerate from **3** and **4** states (shown in Figure 41).

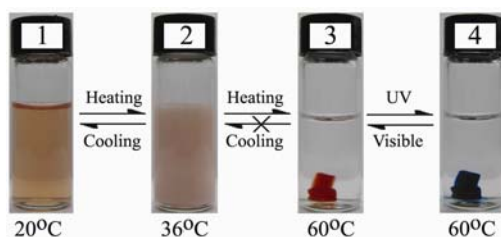


Figure 41. The bistable switching photos of PNIPA-SPO-BIS hydrogel in solution and gel by thermal and light stimuli at different temperature. **1**: Sol (20°C); **2**: Gel (36°C); **3**: Spirooxazine form of Gel (60°C); **4**: Photomerocyanine form of Gel (60°C).

In addition, the morphology of the internal microstructures of the PNIPA-SPO-BIS hydrogels were observed by scanning electron microscopy (SEM). Figure 42 shows the SEM image of the internal microstructure of PNIPA-SPO-BIS hydrogel that the gel has homogeneous porous coral-like microstructure. This morphology indicated that PNIPA-SPO-BIS could form stable hydrogel when the temperature was above the LCST value of PNIPA-SPO-BIS.

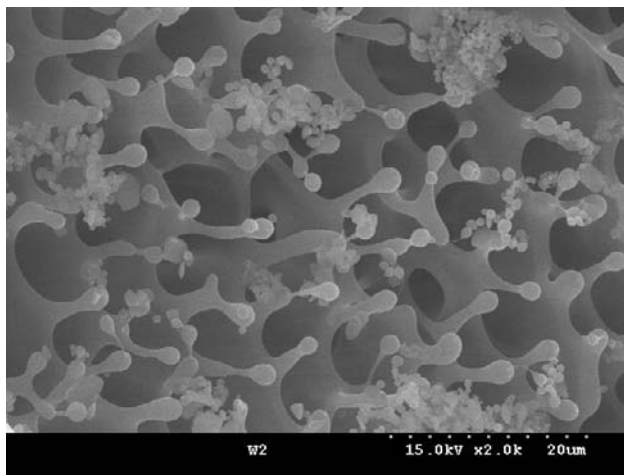


Figure 42. SEM images of PNIPA-SPO-BIS hydrogel. (The gels were prepared from freezing dried in water, PNIPA-SPO-BIS =0.5 wt %).

The inherent characteristics of PNIPA-SPO-BIS hydrogel make it possible to use such materials for data recording. A possible procedure for data recording and erasing is presented in Figure 43 (I). Upon UV light irradiation through the mask, the optical data were recorded on PNIPA-SPO-BIS hydrogel irradiation region. When irradiation with Visible light on irradiation region, the optical data were erased. To obtain visual bistable photoswitching images of PNIPA-SPO-BIS hydrogels, we make the optical storage device that comprised with two slide glasses separated by a 0.1 mm thickness spacer of PET film and placed so as to face each other on the inside of the cell, and the edges of the cell were unsealed. The cell was filled with 0.2% (w/v) PNIPA-SPO-BIS hydrogel water solution. Figure 43 (II) showed the process of the bistable photoswitching in PNIPA-SPO-BIS hydrogel for optical data storage. In gel state, the practical capability of rewritable photoimaging on hydrogel was investigated by patterned illumination through photomasks. The word “KNU”(Kyungpook Nation University abbreviated) was recorded as a first image (Figure 43 C), which was subsequently erased and followed by the recording of a second image, the Korean last name (KIM).The cycles of writing and erasing was repeated more than 20 times. This successful demonstration of rewritable photoimage suggests the potential application of PNIPA-SPO-BIS hydrogel to rewritable optical memory media or imaging processes.

In addition, we have designed and synthesized a multi-switching photochromic poly (N-isopropylacrylamide) with spironaphthoxazine hydrogel copolymer (shown in Figure 44, PNIPA-SPO) [79]. This novel photochromic hydrogel copolymer exhibits excellent reversible photochromic behavior in solution and hydrogel phase undergoes reversible switching process from solution phase to gel phase at a critical temperature (LCST) by thermal

controlling. In addition, this polymer is sensitive to acid and base in water solution, which is promising multiple molecular switches by light, thermal, proton and base stimuli.

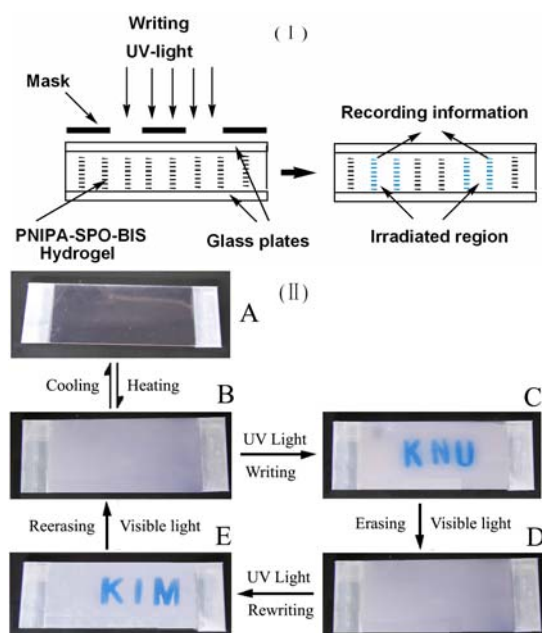


Figure 43. (I) Principle scheme of the optical data recording on PNIPA-SPO-BIS hydrogel. (II) The switching and optical storage images of PNIPA-SPO-BIS hydrogel. A: Sol; B: Gel; C: Writing; D: Erasing; E: Rewriting. Photo-rewritable imaging on the hydrogel by using UV-vis light. The blue regions represent the writing optical data parts irradiated with UV light.

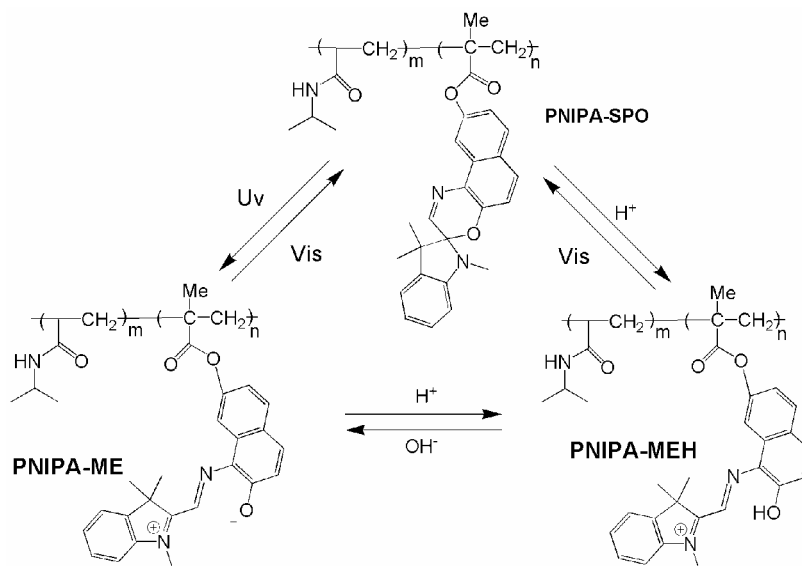


Figure 44. The structure and multiple switching process of photochromic PNIPA-SPO copolymer associated with the three states PNIPA-SPO, PNIPA-ME, and PNIPA-MEH

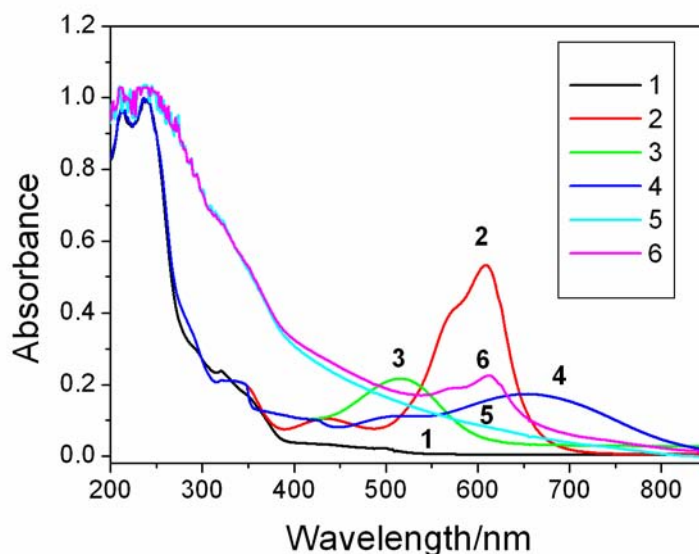


Figure 45. (1) Absorption spectra of multi-switching of PNIPA-SPO copolymer in water solution with the trigger of UV-Vis light, thermal, base, proton.

Figure 45 shows the multi-switching absorption spectral changes of PNIPA-SPO in a water solution and hydrogel by light, proton and base stimuli. Like other spirooxazine molecular, the PNIPA-SPO undergoes reversible photochromic reaction. Irradiation of a water solution of PNIPA-SPO with UV light lead to the appearance of a new absorption band at around 605nm and the colorless solution of PNIPA-SPO turned to blue (shown in Figure 45: line 2). The PNIPA-SPO copolymer showed interesting acidchromic reaction like photochromic compound spiropyran/spirooxazine [80-81]. The interaction of PNIPA-SPO with proton was investigated in water solution through spectrophotometric titration experiment. Upon equivalent proton addition, the colorless solution of PNIPA-SPO became pink red. In Figure 45 line 3 shows the titration spectra of PNIPA-SPO with proton. Upon addition of equivalent H^+ , the band with a peak at round 520nm occurred and produced the protonated merocyanine PNIPA-MEH form. And after visible light irradiation the original absorption spectrum was converted back to the initial state of PNIPA-SPO. Interestingly, upon addition of equivalent OH^- in the solution titrated with proton, the pink solution became blue color. In Figure 45 line 4 showed the absorption spectra of PNIPA-SPO with proton then titration with base. Upon addition of equivalent OH^- , the maximum absorption peak occurred the large red shift and the band with a peak at round 660nm form. And after titrated with proton the original absorption spectrum was converted back to the pink red state of PNIPA-SPO. And after visible light irradiation the original absorption spectrum was converted back to the initial closed-ring isomer of PNIPA-SPO. When a water solution of PNIPA-SPO was heated above the LCST value, the PNIPA-SPO converted from the solution state to hydrogel state. After cooling to at room temperature, the PNIPA-SPO could be recovered the solution state, the whole process was reversible and could be repeated more than 10 times. In addition, we measured the absorption spectra of PNIPA-SPO hydrogel to obtain an insight into their photochromic properties in gel phase, which show resemblely photochromic performance as in solution. The colorless PNIPA-SPO hydrogel turned to blue and a new absorption band

appeared at around 615nm and gradually increased and reached a photostationary state (shown in Figure 45): line 5 gel (closed); line 6 gel (open)). Therefore, the light, thermal proton and base actions may be exploited to modulate the multiple switches between the species PNIPA-SPO, PNIPA-ME and PNIPA-MEH in solution and hydrogel states.

Figure 46 showed the whole multiple switching processes with photographic images of PNIPA-SPO in the trigger of light, thermal, base and proton. Upon irradiation with UV light and visible light, the colorless closed spirooxazine form of PNIPA-SPO can be interconverted with the blue color open-ring PNIPA-ME form in the gel or in solution, i.e. photochromic processes both in hydrogel and in solution. The interconversion between the hydrogel phase and solution could be easily achieved by thermal stimuli at different temperature. In addition, the solution of PNIPA-SPO was both sensitive to proton and base ion, which resulted in obvious changes in the absorption (shown in Figure 45). The reversible chemical switches could be obtained by proton and base stimuli.

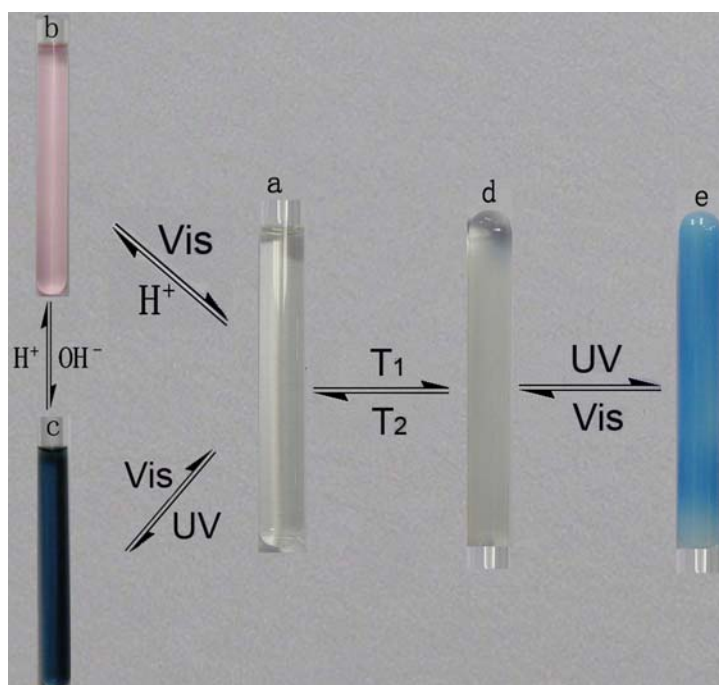


Figure 46. Multiple switching images of PNIPA-SPO copolymer in NMR-tube with the trigger of light, thermal, base, proton. (a) Sol(closed) (b) Sol(closed)+H⁺; (c) Sol(closed)+H⁺+OH⁻; (d) Gel(closed); (e) Gel(open).

CONCLUSION

In this review, we described the recent development of spirooxazine dye as a photoswitching unit in molecular materials, especially spirooxazine single crystal photochromism, spirooxazine dye polymer materials as fluorescence molecular switch, electrical conductivity switch, and viscosity switch. In addition, the layer-by-layer self –

assemble in supermolecular chemistry as a photoswitching unit also is demonstrated. The photochromic spirooxazine dyes show potential applications for ultra-high-density optical information storage, fluorescent molecular probe, and photoregulated molecular switches.

REFERENCES

- [1] B. L. Feringa ed., *Molecular Switches*, Wiley-VCH, Weinheim, 2001.
- [2] V. Balzani, A. Credi, M. Venturi, *Molecular Devices and Machines: A Journey into the Nano World*, Wiley-VCH, Weinheim, 2003.
- [3] H. Dürr, H. Bouas-Laurent In: *Photochromism: Molecules and Systems*, Eds., Elsevier: Amsterdam, 1990.
- [4] J. C. Crano, R. J. Gugliemetti, *Organic Photochromic and Thermochromic Compounds*, New York: Plenum, 1999.
- [5] V. I. Minkin, *Chem. Rev.*, 2004, 104(5), 2751-2776.
- [6] G. Berkovic, V. Krongauz, V. Weiss, *Chem. Rev.*, 2000, 100(5), 1741-1754.
- [7] V. Lokshin, A. Samat, A.V. Metelitsa, *Russ. Chem. Rev.* 2002, 71, 893.
- [8] F. M. Raymo, *Chem. Soc. Rev.* 2005, 34, 327.
- [9] F. M. Raymo and Massimiliano Tomasulo, *Chem. Eur. J.*, 2006, 12, 3186-3193
- [10] H. Tian, S. J. Yang, *Chem. Soc. Rev.*, 2004, 33, 85-.
- [11] H. Tian and S. Wang, *Chem. Commun.*, 2007, 8: 781-792.
- [12] M. Irie, *Photo-Reactive Materials for Ultrahigh-Density Optical Memories*; Elsevier: Amsterdam, 1994.
- [13] A. Toriumi, S. Kawata, M. Gu, *Opt. Lett.*, 1998, 23, 1924-1926.
- [14] S. Kobatake, S. Takami, H. Muto, T. Ishikawa, M. Irie, *Nature*, 2007, 446, 778-781.
- [15] S. L. Gilat, S. H. Kawai, J.-M. Lehn, *Chem. Eur. J.*, 1995, 1, 275-284.
- [16] K. Matsuda, M. Irie, *J. Am. Chem. Soc.*, 2001, 123, 9896-9897.
- [17] S. Kobatake, T. Yamada, K. Uchida, N. Kato, M. Irie, *J. Am. Chem. Soc.*, 1999, 121, 2380-2386.
- [18] S. Kobatake, M. Yamada, T. Yamada, M. Irie, *J. Am. Chem. Soc.*, 1999, 121, 8450-8456.
- [19] M. Morimoto, S. Kobatake, M. Irie, *Chem. Eur. J.*, 2003, 9, 621-627.
- [20] M. Irie, S. Kobatake, M. Horichi, *Science*, 2001, 291, 1769-1772.
- [21] G. P. Dinesh, B.B. Jason, A. K. Roni and L. F. Natia, *Chem. Commun.*, 2005, 2208-2210.
- [22] K. Chamontin, V. Lokshin, A. Samat, R. Gugliemetti, R. Dubest and J. Aubard, *Dyes Pigments*, 1999, 43, 119.
- [23] W. Clegg, N. C. Norman, T. Flood, L. Sallans, W. S. Kwak, P. L. Kwiatkowski and J. G. Lasch, *Acta Crystallogr., Sect. C*, 1991, 47, 817.
- [24] R. Millini, G. del Piero, P. Allegrini, L. Crisci and V. Malatesta, *Acta Crystallogr., Sect. C*, 1991, 47, 2567.
- [25] J.-P. Reboul, A. Samat, P. Lareginie, V. Lokshin and R. Gugliemetti, *Acta Crystallogr., Sect. C*, 1995, 51, 1614.
- [26] H.-J. Suh, W.-T. Lim, J.-Z. Cui, H.-S. Lee, G.-H. Kim, N.-H. Heo and S.-H. Kim *Dyes Pigments*, 2003, 57(2), 149-159

- [27] G. R. Desiraju., T. Steiner, *The weak hydrogen bond*. Oxford University
- [28] M. Irie, T. Fukaminato, T. Sasaki, N. Tamai, T. Kawai, *Nature*, 2002, 420, 759–760.
- [29] L. Zhu, W. Wu, M.-Q. Zhu, J. J. Han, J. K. Hurst, A. D. Q. Li, *J. Am. Chem. Soc.*, 2007, 129(12), 3524-3526.
- [30] X. L. Meng, W. H. Zhu, Z. Q. Guo, J. Q. Wang, and H. Tian, *Tetrahedron*, 2006, 62, 9840.
- [31] W. Yuan, L. Sun, H. Tang, Y. Wen, G. Jiang, W. Huang, L. Jiang, Y. Song, H. Tian, D. Zhu, *Adv. Mater.*, 2005, 17, 156.
- [32] S. Wang, C.Y. Yu, M. S. Choi and S.-H. Kim, *Dyes Pigments*, 2008, 77(1), 245-248.
- [33] S. Wang, C.Y. Yu, M. S. Choi and S.-H. Kim, *J. Photochem. Photobio. A: Chem.*, 2007, 192(1), 17-22.
- [34] A. J. Myles, B. Gorodetsky, N. R. Branda, *Adv. Mater.* 2004, 16, 922.
- [35] Philp and J. F. Stoddart, *Angew. Chem., Int. Ed. Engl.*, 1996, 35, 1154.
- [36] J. W. Steed and J. L. Atwood, *Supramolecular Chemistry*, Wiley, Chichester, 2000.
- [37] M. S. Vollmer, T. D. Clark, C. Steinem and M. R. Ghadiri, *Angew. Chem., Int. Ed.*, 1999, 38, 1598.
- [38] M. Irie, A. Menju, K. Hayashi, *Macromolecules*, 1979, 14, 262.
- [39] S.-H. Kim, S.-Y. Park, N.-S. Yoon., S.-R. Keum, K. Kohc, *Dyes Pigments*, 2005, 66,155-160.
- [40] B. Delley, *J. Chem. Phys.*, 1990, 92, 508-517.
- [41] B. Delley, *J. Chem. Phys.*, 2000, 113, 7756-7764.
- [42] S.-H. Kim, S.-Y. Park, C.-J. Shin and N.-S. Yoon, *Dyes Pigments*, 2007, 72(3), 299-302.
- [43] J. P. Perdew, K. Burke, M. Ernzerhof, *Phys. Rev. Lett.*, 1996, 77, 3865.
- [44] A. D. Boese, N.C. Handy, *J. Chem. Phys.*, 2001, 114, 5497-5503.
- [45] C. Denekamp, B. L. Feringa, *Adv. Mater.*, 1998, 10(14), 1080-1082.
- [46] S. H. Chen, H. M. P. Chen, Y. Geng, S. D. Jacobs, K. L. Marshall, T. N. Blanton, *Adv. Mater.*, 2003, 15(13), 1061-1065.
- [47] J.-H. Park, S.-H. Kim and J.-H. Kim, *Mater. Sci. Engineer. C*, 2004, 24(1-2), 275-279.
- [48] F. P. Shvartsman, V. A. Krongauz, *J. Phys. Chem.* 1984, 88, 6448.
- [49] L. Shragina, F. Buchholtz, S. Yizchaik, V. Krongauz, *Liq. Cryst.* 1990, 7, 643.
- [50] F. P. Shvartsman, V. A. Krongauz, *Nature*, 1984, 309, 608.
- [51] G. Decher, *Science*, 1997, 277, 1232.
- [52] P. Bertrand, A. Jonas, A. Laschewsky. *Macromol. Rapid. Commun.*, 2000, 21, 319.
- [53] P. T. Hammond, *Curr. Opin. Colloid. Interface. Sci.*, 2000, 4, 430.
- [54] X. Zhang, J. C. Shen, *Adv. Mater.*, 1999, 11,1139.
- [55] S.-H. Kim, C.-J. Shin, M.-S. Choi and S. Wang, *Dyes Pigments*, 2008, 77(1) , 70-74.
- [56] S.-H. Kim, C.-J. Shin, S.-R. Keum and K. Koh, *Dyes Pigments*, 2007, 72(3), 378-382.
- [57] S.-H. Kim, C. Yu, C.-J. Shin and M.-S. Choi, *Dyes. Pigments*, 2007, 75(1), 250-252.
- [58] A. Ulman, *From Langmiur-Blodgette to self-assembly*. Boston/New York/Tronto: Academic Press., 1991, p.440.
- [59] G. Decher, J. D. Hong. *Makromol. Chem. Macromol. Symp.*, 1991, 46, 321.
- [60] Y.-A. Son, Y.-M. Park, C.-J. Shin and S.-H. Kim, *Dyes Pigments*, 2007, 72(3), 345-348.
- [61] S.-H. Kim, C.-H. Ahn, S.-Y. Park, C.-J. Shin and H.-J. Suh, *Dyes Pigments*, 2006, 69(1-2), 108-110.

- [62] J. H. van Esch, B. L. Feringa, *Angew. Chem. Int. Ed.*, 2000, 39, 2263.
- [63] D. J. Abdullah, R. G. Weiss, *Adv. Mater.* 2000, 12, 1237;
- [64] Maaïke de Loos, B. L. Feringa, J. H. van Esch, *Eur. J. Org. Chem.* 2005, 3615.
- [65] M. S. Neralagatta, M. Uday, *Chem. Soc. Rev.*, 2005, 34, 821.
- [66] K. Sugiyasu, N. Fujita, S. Shinkai, *Angew. Chem., Int. Ed.* 2004, 43, 1229.
- [67] M. Lei, Y. Gu, A. Baldi, R. A. Siegel, B. Ziaie, *Langmuir*, 2004, 20, 8947.
- [68] G. M. Eichenbaum, P. F. Kiser, S. A. Simon, D. Needham, *Macromolecules*, 1998, 31, 5084.
- [69] M. E. Harmon, M. Tang, C. W. Frank, *Polymer*, 2003, 44, 4547.
- [70] T. Tanaka, I. Nishiq, S. Sun, S. Ueno-Nishio, *Science*, 1982, 218, 467.
- [71] A. Suzuki, T. Tanaka, *Nature*, 1990, 346.
- [72] J. B. Beck, S. J. Rowan, *J. Am. Chem. Soc.*, 2003, 125, 13922.
- [73] N. Fujita, M. Asai, T. Yamashita, S. Shinkai, *J. Mater. Chem.* 2004, 14, 2106.
- [74] M. Numata, K. Sugiyasu, T. Hasegawa, S. Shinkai, *Angew. Chem., Int. Ed.*, 2004, 43, 3279.
- [75] S. Wang, M.-S. Choi and S.-H. Kim, *J. Photochem. Photobio. A: Chemistry*, 2008, in press.
- [76] X. J. Chen, and K. Tsujii, *Macromolecules*, 2006, 39, 8550.
- [77] H. Yan, H. Fujiwara, K. Sasaki, and K. Tsujii, *Angew. Chem. Int. Ed.*, 2005, 44, 1951.
- [78] A. Kacmaz, G. Gurdag, *Macromol. Symp.*, 2006, 239, 138.
- [79] S. Wang, M.-S. Choi and S.-H. Kim, *Dyes Pigments*, 2008, 78(1), 8-14.
- [80] F. M. Raymo, S. Giordani, *J. Am. Chem. Soc.*, 2001, 123(19), 4651-4652
- [81] E. B. Gaeva, V. Pimienta, S. Delbaere, A. V. Metelitsa, N. A. Voloshin, V. I. Minkin, G. Vermeersch and J. C. Micheau, *J. Photochem. Photobio. A: Chemistry*, 2007, 191(2-3), 114-121.

Chapter 5

COMBINED SONOHOMOGENEOUS AND HETEROGENEOUS OXIDATION OF DYES FOR WASTEWATER TREATMENT

Ewere Odaro¹ and Shaobin Wang^{2,}*

¹Department of Chemical Engineering, Loughborough University, Loughborough,
Leicestershire. LE11 3TU, UK

²Department of Chemical Engineering, Curtin University of Technology, GPO Box U1987,
Perth, WA 6845, Australia

ABSTRACT

Dyestuff in water introduces several environmental problems and should be removed for clean water system. Fenton oxidation can be as an effective technique for the water treatment. In this report, homogeneous and heterogeneous catalysis in Fenton oxidation was examined for two dyes with acidic (Naphthol blue-black, NBB) and basic (Methylene Blue, MB) properties. The behaviour of these dyes under different experimental conditions (temperature, pH, peroxide concentration, Fe concentration) was studied using Fenton (Fe^{2+}) and Fenton-like (Fe^{3+}) reactions for the following processes: 1) normal Fenton oxidation, 2) Fenton oxidation combined with sonication effect, 3) Fenton oxidation combined with a solid catalyst (activated carbon). The main Fenton oxidation reactants, Fe^{2+} , Fe^{3+} and H_2O_2 were used in small quantities in order to observe closely the reaction kinetics for decolourisation of these dyes. It was found that both sonication and heterogeneous catalysis offer improvements to the Fenton oxidation under optimised conditions, with Fe^{2+} being faster than Fe^{3+} initially but Fe^{3+} ending up with a higher overall efficiency. 90-95% decolourisation was achieved in some optimised runs after 2 hours; however the general decolourisation was completed for all batch runs after a period of 24 hours, except in conditions where the reaction did not proceed at all. Chemical oxygen demand (COD) removal also occurred during the decolourisation process of both dyes, in maximum efficiencies of about 80% after 48 hours. Methylene blue also showed greater decolourisation efficiency in comparison with Naphthol blue-

* Correspondence author. Email: shaobin.wang@curtin.edu.au, Fax: +61 8 9266 2681

black for most of the experimental runs under the same experimental conditions. The reaction kinetics was mainly pseudo-first order for majority of the homogeneous reaction, as determined by non-linear regression or a combination of first order kinetics for heterogeneous reactions.

1 INTRODUCTION

Wastewater from textile and dyeing industries contains dye stuff, suspended solids, and other soluble substances. Currently several types of dyes such as acid, basic, azo, reactive, dispersive dyes are widely employed in textile and other industries. The textile industry in many countries has to meet with local and national regulations regarding the purification of water from dyeing processes before the treated wastewater can be released into the environment. Dyestuff in waters affects the colour and hence the transparency and light penetration, as well as gas solubility in water, which will cause environmental damage to the biosystem. Also, several commonly used dyes have been reported to be carcinogenic and mutagenic for aquatic life [1].

Many methods of dye removal have been researched, some of which are currently in use. Physical adsorption using activated carbon has been employed as effective method to remove dyes from aqueous solution [2]. However, this method can not destroy the dyestuff. Chemical removal will be an effective alternative technology. The main chemical processes currently used on a large scale are the advanced oxidation processes (AOPs) which involve the generation of the hydroxyl (OH•) radical. Common AOPs involve Fenton (Fe²⁺/H₂O₂, R1) and Fenton-like (Fe³⁺/H₂O₂, R2) processes, ozonation, photochemical and electrochemical oxidation, photolysis with H₂O₂ and O₃, high voltage electrical discharge (corona) process, TiO₂ photocatalysis, radiolysis, wet oxidation, water solutions treatment by electronic beams or γ-beams and various combinations of these methods [3]. Compared with other oxidation processes, processes using the Fenton type reagent are relatively cheap, easily operated and maintained, especially for Fenton-like reaction. However, previous investigations always employed high Fe and H₂O₂ concentrations, which resulted in higher cost and large amount of sludge. Thus, using low dosage of Fenton reagent is highly demanded.



In recent years, considerable interest has been shown on the application of ultrasound (US) as an advanced oxidation process for the treatment of hazardous contaminants in water. Ultrasonic irradiation of aqueous solutions induces acoustic cavitation, which can be defined as the cyclic formation, growth and subsequent collapse of microbubbles or cavities occurring in extremely small intervals of time and releasing large quantities of energy over a small location [4]. During the sonolysis of water and in the presence of oxygen, reactive radicals such as •OH, •O and •OOH are produced through a series of reactions and may participate in the decomposition reactions of target contaminants [5].





where)))) refers to the application of ultrasound.

In the presence of oxygen



The combinations of US and other advanced oxidation processes have also been investigated. The coupling of US with H_2O_2 , ozone, and UV irradiation resulted in higher degradation efficiencies of phenols and chlorinated phenols, as compared to each treatment alone. Humic and fulvic acid mineralisation was enhanced by the combination of sonication with H_2O_2 and with ozone [6]. For dye degradation, some investigations employing US [7-9], US/ozonation [10, 11], UV/US [12] UV/ H_2O_2 /US [13] have been reported. However, few work has been done on US/Fenton combination [14, 15] for dye degradation. Abdelsalam and Birkin [14] investigated sonoelectrochemical degradation of meldola blue employing Fenton's reagent. The effect of adding Fe^{2+} to the rate of dye degradation was measured and demonstrated to be significant. Joseph et al. [15] conducted a sonochemical degradation of azo dyes (methyl orange, o-methyl red, and p-methyl red) at 500 kHz and 50 W, under air, O_2 , or Ar saturation at 15 °C. The acceleration of the sonochemical bleaching and the mineralisation process upon addition of Fe^{2+} was also investigated in Ar-saturated methyl orange solutions. A 3-fold increase in the reaction rate was observed at optimal Fe^{2+} .

In previous investigations, most of reports focus on Fenton oxidation of dyes, few investigations have been reported on the degradation of dyes using Fenton-like oxidations [16-19]. In addition, it is known that different types of dyes will exhibit quite different degradation behaviour. Dutta et al. firstly conducted a systematic investigation on chemical oxidation of methylene blue using Fenton-like reaction [17]. Hsueh et al. [18] investigated Fenton and Fenton-like reactions at low iron concentration ($< 1.78 \times 10^{-4}$ M) to oxidise three commercial azo dyes, namely Red MX-5B, Reactive Black 5 and Orange G. Their results reveal that both of these methods can remove the colour of these dyes completely. Recently, Ntampeglitis et al. reported the decolourisation kinetics of three commercially used Procion H-ex1 dyes using a Fenton-like reagent [19]. But the Fenton reagent concentration is too high.

As stated above, there are other contaminated matters such as ions and solids in textile wastewater and these contaminants will affect the Fenton reaction. However, few investigations have been reported in this aspect. De Laat et al. [20, 21] investigated the effect of chloride, sulfate and nitrate ions on the efficiency of the $\text{Fe}^{2+}/\text{H}_2\text{O}_2$ and $\text{Fe}^{3+}/\text{H}_2\text{O}_2$ systems and reported a negative effect of chloride ion. Ashraf et al. [22] studied the effect of other salts that are normally present in textile waste streams. They used 10 different salt solutions to investigate the effect on Fenton degradation of methyl red and found that some of the ions

tested enhanced the rate and extent of degradation of the dye, whereas some had an inhibitory effect. On the other hand, no investigation has been reported on the effect of solid materials based on our knowledge. Solid materials in wastewater could play a positive or negative role in Fenton oxidation. Activated carbon is an excellent adsorbent showing high adsorption capacity in various metal ions and organics. The presence of activated carbon with Fenton reagent could combine adsorption and catalytic oxidation together. In this paper, we report an investigation of Fenton and sonic promoted Fenton reaction at very low Fe and H₂O₂ concentrations for dye degradation. We employed two types of dyes, azo and basic dyes, and investigated the dye degradation efficiency and kinetics using the combination of sonolysis and Fenton reaction. In addition, we report an investigation of Fenton oxidation with or without activated carbon to study the effect of activated carbon on dye degradation during Fenton oxidation.

2 EXPERIMENTAL

2.1. Chemicals

Naphthol blue-black (C₂₂H₁₄N₆Na₂O₉S₂, NBB) and methylene blue (C₆H₁₈ClN₃S·2H₂O, MB) were selected as corresponding typical type of azo and basic dyes, respectively. Figure 1 shows their chemical structure. These two dyes were obtained from Ajax Chemicals. Other chemicals, sulphuric acid was obtained from BDH Chemicals, sodium hydroxide and hydrogen peroxide (30%) was from Redox Chemicals, and ferrous sulfate and ferric sulphate were obtained from Sigma Chemicals. All chemicals were used as supplied without further treatment. Activated carbon was obtained from BDH Chemicals.

2.2. Reaction Tests

All homogeneous system experiments were carried out in a 1000 ml batch reactor in a controlled temperature environment using a water bath at 30 ± 0.5 °C unless otherwise stated. The solution pH was adjusted using sulphuric acid or sodium hydroxide solutions and measured with a pH meter (PHM 250 Ion analyser). For all tests, only the initial pH was monitored. In some tests, the final pH was also measured. The addition of sulphuric acid or sodium hydroxide had no effect on the dye solution in terms of precipitation or colouration. The dye (MB and NBB) and the ferrous or ferric iron solutions were firstly prepared and pre-mixed in the reactor. The reaction time was recorded when H₂O₂ was added into the mixture. The reacting solution homogeneity was ensured by stirring at a rate of 40 rpm. All iron solutions needed for the experiments were prepared daily and all experiments were carried out at pH 2 ± 0.02 unless otherwise stated. Absorbance measurements were carried out in the visible region using a spectrophotometer (Spectronic 20 Genesys Spectrophotometer, USA) at a λ_{max} of 665 nm for MB and 618 nm for NBB, respectively. The concentration was determined based on calibration curves obtained for both dyes at these λ_{max} values. The experiments were carried out for 120 min continually.

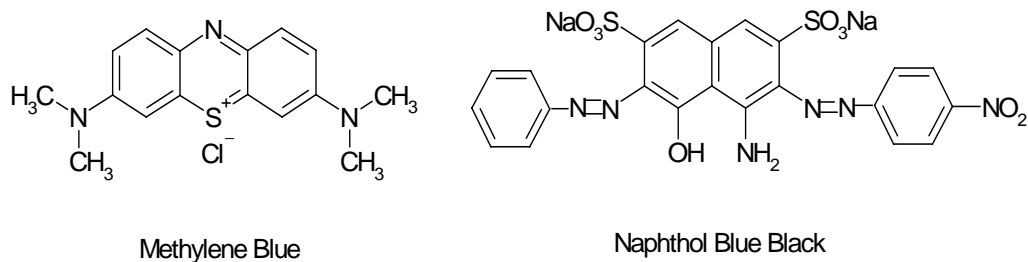


Figure 1. Chemical structure of tested dyes.

The sonication experiments were carried out by an ultrasonic bath (40 Hz, 300W, FXP14M, Unisonics, Australia). Various runs of a 1000 ml dye solution with different combination of varying of H_2O_2 , Fe^{2+} and Fe^{3+} concentrations at pH 2 were conducted. Samples were taken out at varying time for absorbance measurement and the reactions were also carried out for 120 min continually.

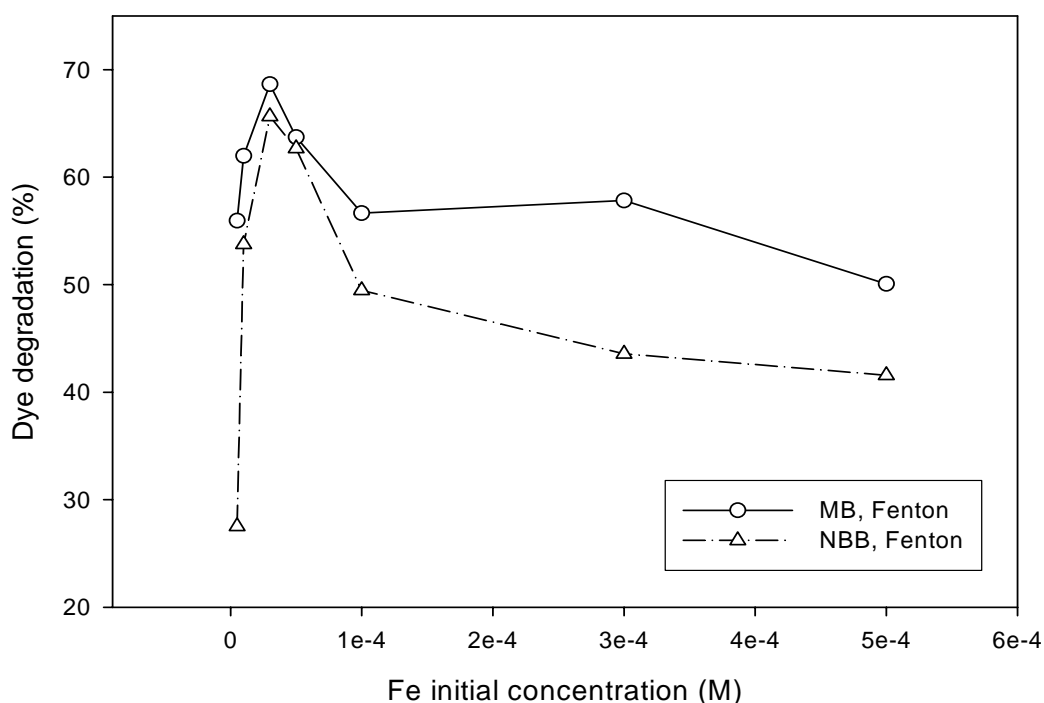


Figure 2. Effect of initial Fe^{2+} concentration on dye degradation.

The adsorption of dye using activated carbon (AC) was performed in an orbital shaker (Thermoline Scientific Orbital shaker incubator). A bottle with 250 ml filled with 200 ml of dye solution and some amount of solids was put in the shaker run at a speed of 100 rpm at 30 °C. At a certain time intervals, the dye solution was drawn from the bottle and measured with a spectrophotometer (Spectronic 20 Genesys Spectrophotometer, USA) at a wavelength (λ_{max}) of 665 nm for MB and 618 nm for NBB. Dye concentration was then determined using a

calibration curve. Fenton oxidation with the presence of activated carbon was carried out similarly to the Fenton oxidation but at 200 ml solution and with varying H₂O₂ concentration, carbon content and initial solution pH.

3 RESULTS AND DISCUSSION

3.1. Dye Degradation in Fenton Reaction

It has been known that several parameters influence the reaction rate. In this investigation, the effects of Fe²⁺ concentration, H₂O₂ concentration, solution pH and temperature were studied.

3.1.1. Effect of Fe²⁺ Concentration

Figure 2 illustrates the overall efficiency of dye degradation at 120 min with the variation of Fe²⁺ initial concentration while keeping H₂O₂ concentration at 5 x 10⁻⁵ M, pH 2 and temperature at 30 °C. For Fenton reactions, no degradation was observed for both dyes in the absence H₂O₂. When a small amount of Fe²⁺ at concentration of 5 x 10⁻⁶ M was added in the solution, dye degradation was remarkably observed. For MB and NBB, the decolourisation efficiencies at 28 and 55% could be achieved. If Fe²⁺ concentration is further increased, the rate of dye decolourisation increases and reaches an optimum of 70% at Fe²⁺ concentration of 3 x 10⁻⁵ M. However, at higher Fe²⁺ concentrations, dye degradation appears to decrease. This might be due to the limited concentration of H₂O₂ in solution. When H₂O₂ is consumed during the reaction, higher Fe²⁺ concentration will not produce further dye degradation. On the contrary, unreacted H₂O₂ will act as a scavenger of [•]OH and produces a less potent perhydroxyl radicals (R10), resulting in less dye degradation. Thus, the optimum Fe²⁺/H₂O₂ ratio will be around 1: 1. For two dyes, it is also seen from the Figure that MB degradation is generally higher than NBB.



Several investigations on dye degradation in Fenton reaction have reported the effect of Fe²⁺. Dutta et al. [17] observed that methylene blue degradation increased with the increasing Fe²⁺ concentration and would be constant at higher Fe²⁺ concentration. Hsueh et al. [18] also found that degradation of several azo dyes would increase with increasing Fe concentration and no improvement would be obtained if more Fe²⁺ is in the solution. The different behaviour of dye degradation observed in this research with others is probably due to the higher H₂O₂ concentration (> 4.4 x 10⁻⁴ M) employed in those investigations.

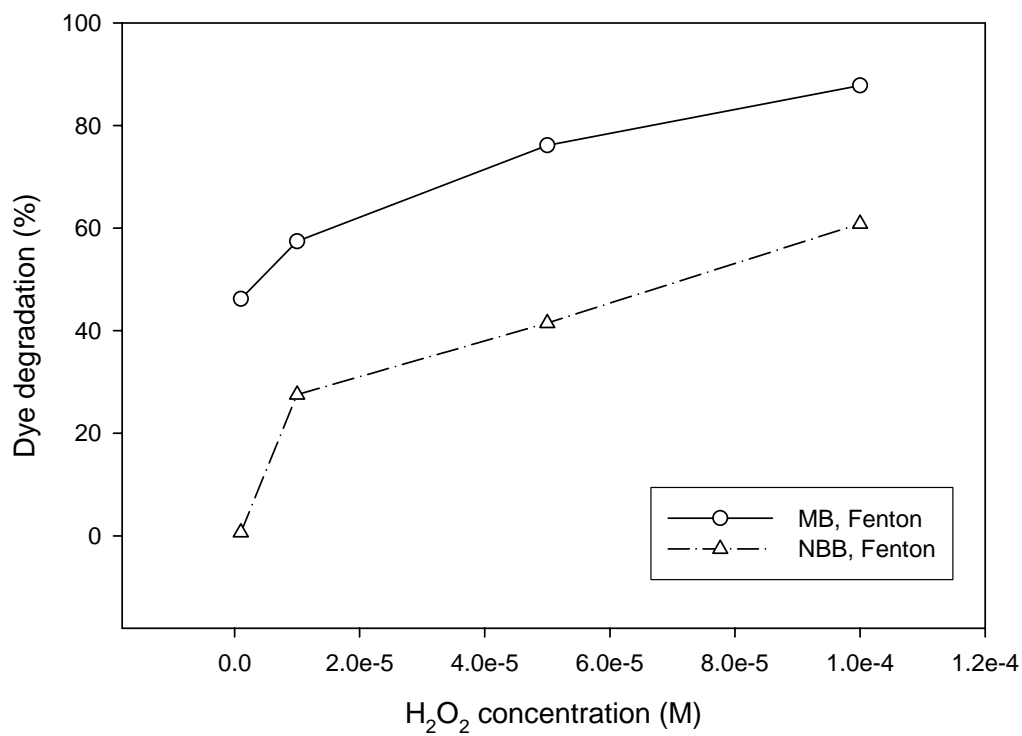


Figure 3. Effect of H_2O_2 initial concentration on dye degradation.

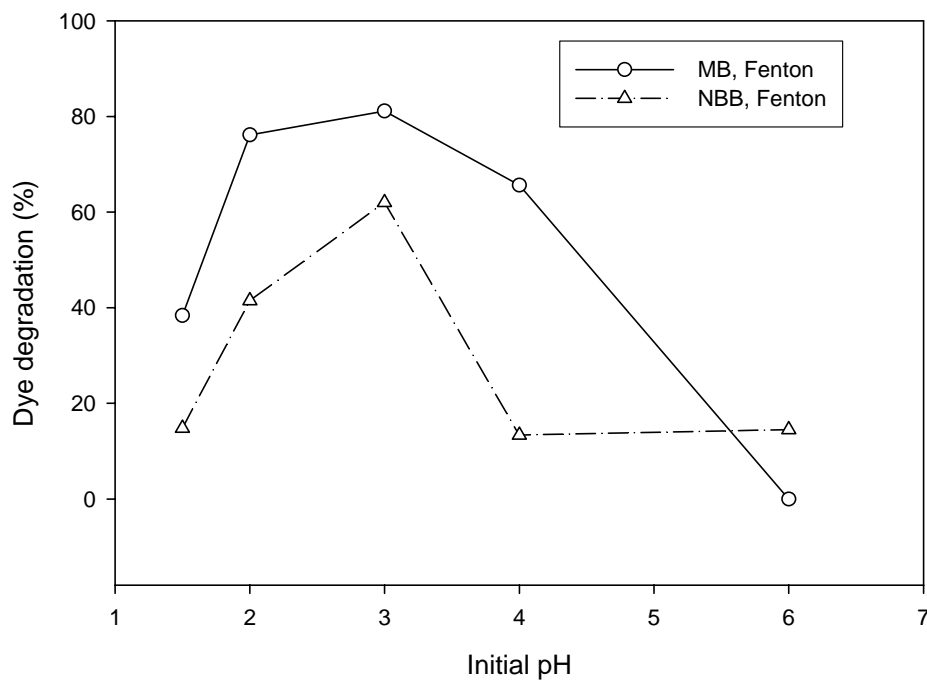


Figure 4. Effect of initial pH on dye degradation.

3.1.2. Effect of H₂O₂ Concentration

The effect of H₂O₂ was studied by increasing the peroxide concentration from 5×10^{-6} M to 1×10^{-4} M while maintaining all other conditions the same. Figure 3 shows the effect of H₂O₂ on dye degradation. The use of peroxide in the absence of Fe²⁺ showed little or no improvement in dye degradation. However, it was observed that the rate of degradation increased with increase in peroxide concentration. At H₂O₂ concentration of 1×10^{-4} M, dye degradation will be 85% and 60% for MB and NBB, respectively.

Some studies [16-18] have reported an optimal peroxide concentration in Fenton oxidation of dyes. Dutta et al. [17] found that at initial [Fe²⁺] = 3.58×10^{-5} M and initial [H₂O₂] < 4.14×10^{-4} M, the rate of decolourisation of methylene blue increased with increasing the initial concentration of hydrogen peroxide. The rate remained almost same for initial H₂O₂ concentration of 4.14×10^{-4} – 2.94×10^{-2} M. Others reported similar results for different dyes [16, 18, 23]. In our investigation, it is seen that dye degradation keeps increasing as H₂O₂ concentration increases, which is somewhat different from previous observations. In fact, the difference is probably due to the different range of H₂O₂ concentration. The maximum H₂O₂ concentration investigated in this work is much lower than that of previous reports.

3.1.3. Effect of Solution pH

It is known that H₂O₂ becomes unstable and loses its oxidising potential in alkaline medium. Thus the pH values in this investigation were varied between 1.5 and 6 and Figure 4 presents the effect of pH on dye degradation. As seen that the highest degradation efficiency was observed at pH 3 for both dyes. For MB, dye decolourisation is little at pH 6 while NBB still shows some decolourisation at pH 6.

Many other studies [16, 18, 24-26] also report similar range between 2.5 and 3.5 for maximum dye degradation; hence this pH range seems suitable for the formation of hydroxyl ions, irrespective of what organic compound is being purified. The low performance at higher and lower pH values is attributed to a number of reasons. For pH < 2, 'scavenging effect' [18] play an important role due to the reaction of ·OH and H⁺ ions and less reactivity of oxonium ion [H₃O₂]⁺ formed at low pH values. In addition, the formation of complex species [Fe(H₂O)₆]²⁺ at low pH which reacts slower with peroxide than [Fe(OH)H₂O]²⁺ also result in the reduced efficiency [26]. Above pH 3, the reduction in degradation efficiency can be attributed to the hydrolysis of Fe³⁺ into Fe(OH)₃ and in this form, iron decomposes H₂O₂ into oxygen and water hence the degradation rate decreases because less hydroxyl radicals are available [14].

3.1.4. Effect of Reaction Temperature

Tests at temperatures varying between 21 and 60 °C for both dyes were conducted and the results show that an increase in temperature leads to an increase in dye decolourisation up to 60 °C (Figure 5). At 21 °C, degradation efficiency was very low, and this increased as the temperature was increased. For two dyes, the effect of temperature on dye degradation seems to be different. For NBB, the increase in temperature led to an increase in degradation efficiency to 94% at 60 °C. For MB, a maximum efficiency was observed at 40 °C. At 50 and 60 °C, no improvement was observed in the overall efficiency; in fact a bit decline was

observed at 60 °C, which can be attributed to the thermal decomposition of H_2O_2 into oxygen and water at high temperatures.

Dutta et al. [17] conducted chemical oxidation of methylene blue using a Fenton reaction. A substantial increase in the extent of degradation of the dye was also observed when the reaction temperature was raised from 8 to 26 °C. A further increase in the reaction temperature from 26 to 40 °C resulted in the decrease in the extent of degradation of the dye. Malik and Saha reported that the extent of degradation of direct dyes, Blue 2B (B54) and Red 12B (R31), increases with increase in temperature from 20 to 40 °C. A further increase in the reaction temperature up to 50 °C results in small increase in the extent of dye degradation [23]. Our results are similar to these investigations.

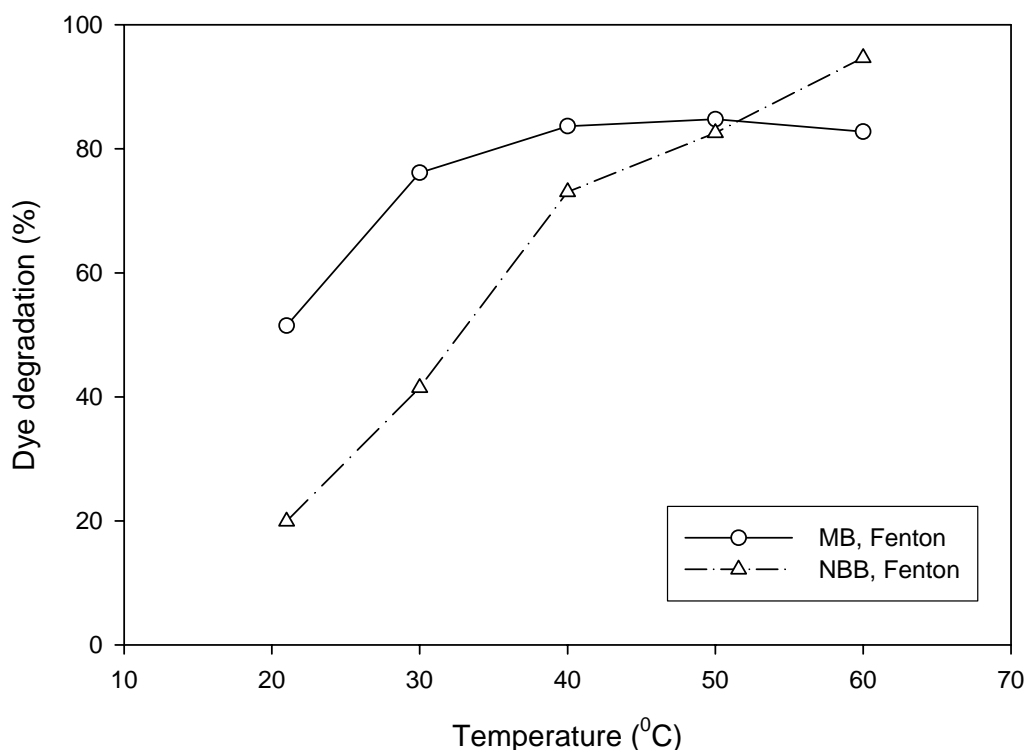


Figure 5. Effect of reaction temperature on dye degradation.

3.2. Comparison of Fenton and Sono-Fenton Reactions for Decolourisation

Figure 6 shows a comparison of decolourisation of MB and NBB under various reactions, sonolysis, Fenton and sono-Fenton reactions. The lowest degradation performances were observed under non-sonic conditions using either H_2O_2 or Fe^{2+} but not with both reactants. Using only H_2O_2 , however, yielded better degradation efficiency than using Fe^{2+} and this was observed for both dyes. Using only sonication without Fenton oxidation yielded better results than the two previous processes. This can be attributed to the presence of hydroxyl ions formed during sonication. Sonication of an aerated aqueous solution can yield $\cdot\text{OH}$ upon the reactions (3) and following reactions [28].

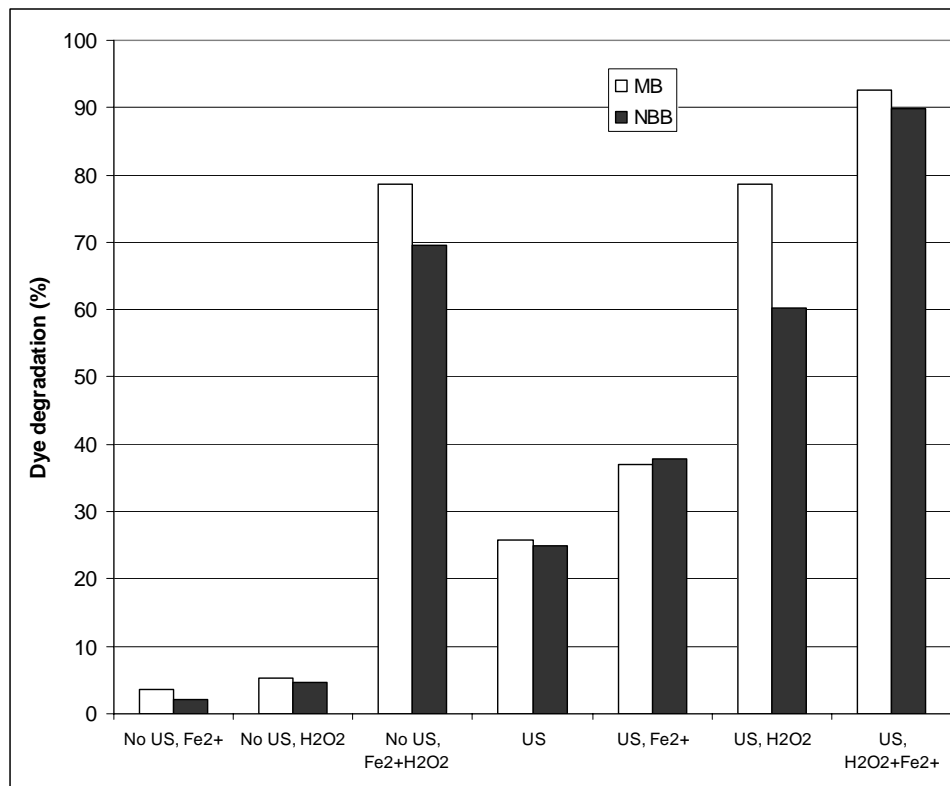


Figure 6. Comparison of dye degradation under different reactions.



Degradation efficiency was further increased by combining sonic effect with the presence of either H_2O_2 or Fe^{2+} in solution. The improvements observed on addition of Fe^{2+} to sonication could be attributed to the occurrence of Fenton's oxidation under sonication. For this to happen, H_2O_2 needs to be made available since both Fe^{2+} and H_2O_2 are needed for Fenton's oxidation. This formation of H_2O_2 is made possible via reaction 5. On the other hand, the combined effects of sonication and H_2O_2 are possibly due to enhanced formation of hydroxyl radicals. Again, sonication with only H_2O_2 proved more efficient compared with sonication with only Fe^{2+} .

For Fenton oxidation without sonication, dye decolourisation is much higher than those with the presence of Fe or H_2O_2 . The removal efficiencies for two dyes are 80% and 70%, respectively. The combined effects of sonication and Fenton oxidation proved to be the most efficient process. The dye degradation can reach 90% for two dyes. The improvements in decolourisation of combined sonication and Fenton's reaction over Fenton oxidation were 15 and 24 % for MB and NBB, respectively.

3.3. Kinetics of Dye Degradation

Figure 7 shows the dynamic variation of dye degradation during Fenton and sono-Fenton reactions. As seen that the sono-Fenton reaction shows faster reaction rates than the Fenton reaction. For two dyes, decolourisation efficiency in Fenton oxidation is only about 70 % and 43 %, while in sono-Fenton oxidation the efficiency will reach 89% and 84% in 60 min for MB and NBB, respectively. After 2 h, the decolourisation efficiency will be 93% and 90%. Further investigations indicate that dye decolourisation will be completely achieved after 6 h for both dyes. Hsueh et al. [18] investigated Fenton and Fenton-like reactions at low iron concentration (10 mg/L) to oxidise azo dyes and found that 96% decolourisation would be achieved in 1 h. Our results indicate that using sonic-Fenton oxidation, similar efficiency could be obtained at even lower Fenton reagent concentration.

The Fenton oxidation of the dye can be represented by the following n^{th} order reaction kinetics

$$\frac{dC}{dt} = -kC^n \quad (13)$$

where C represents the dye concentration, n the order of the reaction, k the reaction rate coefficient and t the time. For a first-order reaction, the above equation after integration becomes

$$C = C_0 \exp(-k_1 t) \quad (14)$$

in which C_0 is the initial dye concentration and k_1 is the first-order reaction rate constant. For a second-order reaction, the integrated equation becomes

$$C = \frac{C_0}{1 + k_2 C_0 t} \quad (15)$$

and k_2 is the second-order rate constant.

The kinetic parameters calculated from the above two models are presented in Table 1. Figure 7 also shows the first-order kinetic curves for the Fenton and sono-Fenton reactions. It is seen that the first-order kinetics will produce better results than that of the second-order kinetics evidenced from the regression coefficients. The reaction rate for sono-Fenton reaction is always higher than the Fenton reaction. Also the reaction rate for MB is generally higher than that of NBB.

Several investigations on dye degradation in Fenton reactions have demonstrated that reaction kinetics of Fenton oxidation follows a pseudo-first order plot [16, 29, 30]. Wang et al. [7] investigated sonochemical degradation kinetics of methyl violet in aqueous solutions and found the reaction to be the first-order and the degradation rate coefficient is $1.35 \times 10^{-2} \text{ min}^{-1}$. Lall et al. [10] also reported a first-order kinetics for decolourisation of reactive blue 19 in ozonation, ultrasound, and ultrasound-enhanced ozonation processes.

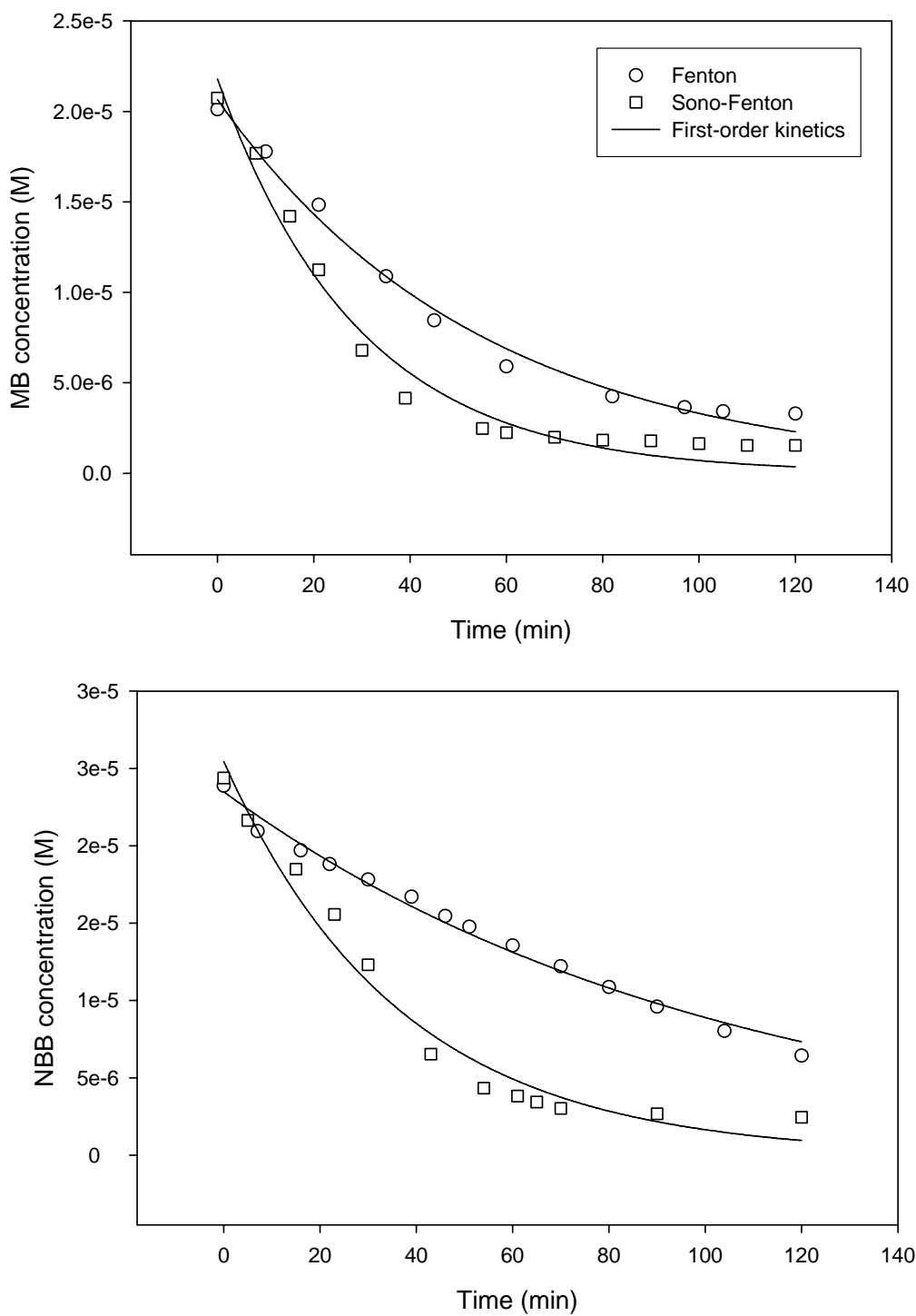


Figure 7. Kinetics of dye degradation in Fenton and sono-Fenton reactions.

Table 1. Kinetic parameters of dye degradation in Fenton and sono-Fenton reactions

System	Dye	First-order kinetics			Second-order kinetics		
		C_0 (M)	k_1 (min ⁻¹)	R^2	C_0 (M)	k_2 (M ⁻¹ min ⁻¹)	R^2
Fenton	MB	2.06×10^{-5}	0.0183	0.989	2.16×10^{-5}	1.59×10^3	0.947
Sonic Fenton	MB	2.18×10^{-5}	0.0343	0.978	2.27×10^{-5}	3.12×10^3	0.911
Fenton	NBB	2.35×10^{-5}	9.70×10^{-3}	0.989	2.44×10^{-5}	6.08×10^2	0.956
Sonic Fenton	NBB	2.54×10^{-5}	0.0274	0.976	2.64×10^{-5}	2.01×10^3	0.906

3.4. Dye Degradation in Fenton-like Reactions

As in the Fenton oxidation several parameters including Fe^{3+} concentration, H_2O_2 concentration, solution pH and temperature influence the reaction rate and decolourisation efficiency and were also investigated.

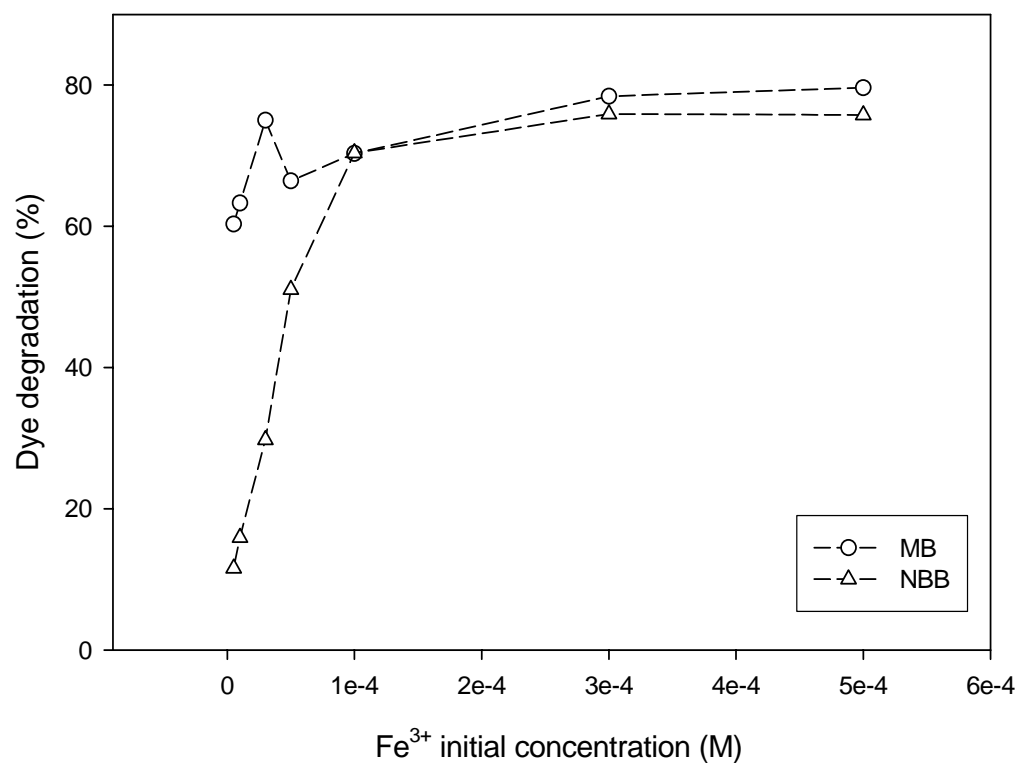


Figure 8. Effect of initial Fe^{3+} concentration on dye degradation.

3.4.1. Effect of Fe^{3+} Concentration

Figure 8 illustrates the overall efficiency of dye degradation at 120 min with the variation of Fe^{3+} initial concentration. For Fenton-like reactions, little degradation was observed for both dyes in the absence of H_2O_2 . When Fe^{3+} is present, dye degradation is significant. From the Figure it is seen that the rate of dye decolourisation increases with the increasing Fe concentration and reaches equilibrium of 75% and 70% for MB and NBB, respectively, at Fe^{3+} concentration of 3×10^{-4} M. At even higher Fe^{3+} concentration, little improvement is achieved in decolourisation efficiency. This is attributed to the limited availability of H_2O_2 . For two dyes, it is also seen that MB degradation is generally higher than NBB.

3.4.2. Effect of H_2O_2 Concentration

The effect of H_2O_2 on decolourisation efficiency was studied by increasing the peroxide concentration between 5×10^{-6} M and 1×10^{-4} M while maintaining all other conditions the same. Figure 9 shows the effect of H_2O_2 on dye degradation. The use of peroxide in the absence of Fe^{3+} showed little or no improvement in dye degradation. However, it was observed that the rate of degradation increased with increase in peroxide concentration. For NBB, the increase in H_2O_2 concentration seems to have less effect on dye degradation. The colourisation efficiency is only 18% at 1×10^{-4} M H_2O_2 concentration while for MB, the decolourisation efficiency is 80%. Some studies [16, 18] reported an optimal peroxide concentration, above which degradation efficiency was reduced due to scavenging effect. In Fenton reaction, H_2O_2 could act as a scavenger of $\cdot OH$ and produce a less potent perhydroxyl radical ($HO_2\cdot$) as shown in R10 [18].

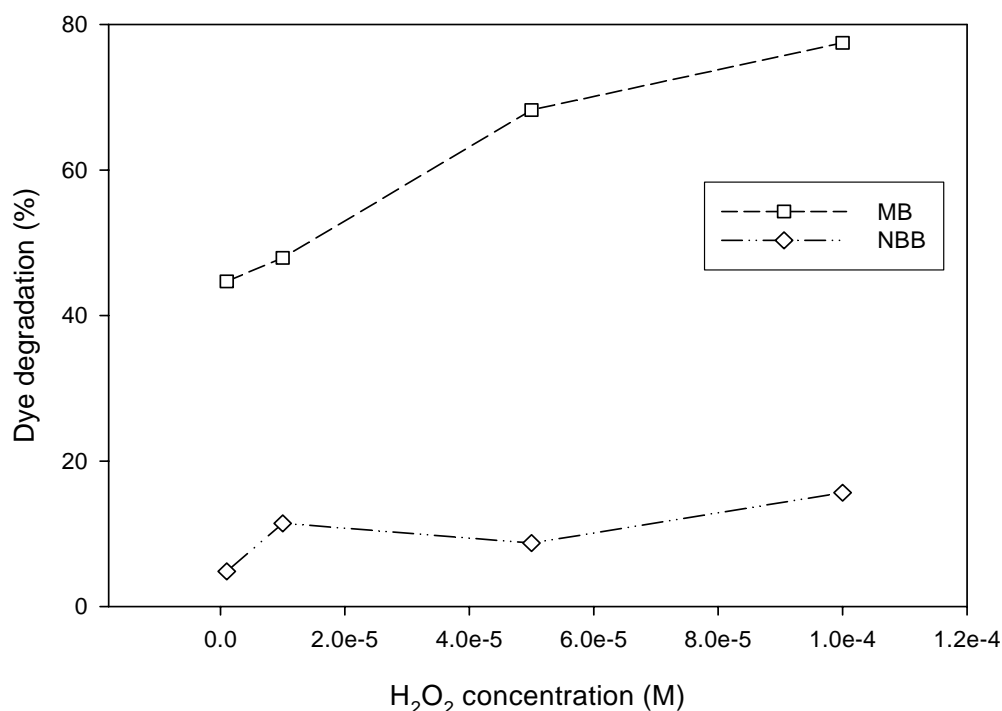


Figure 9. Effect of H_2O_2 concentration on dye degradation.

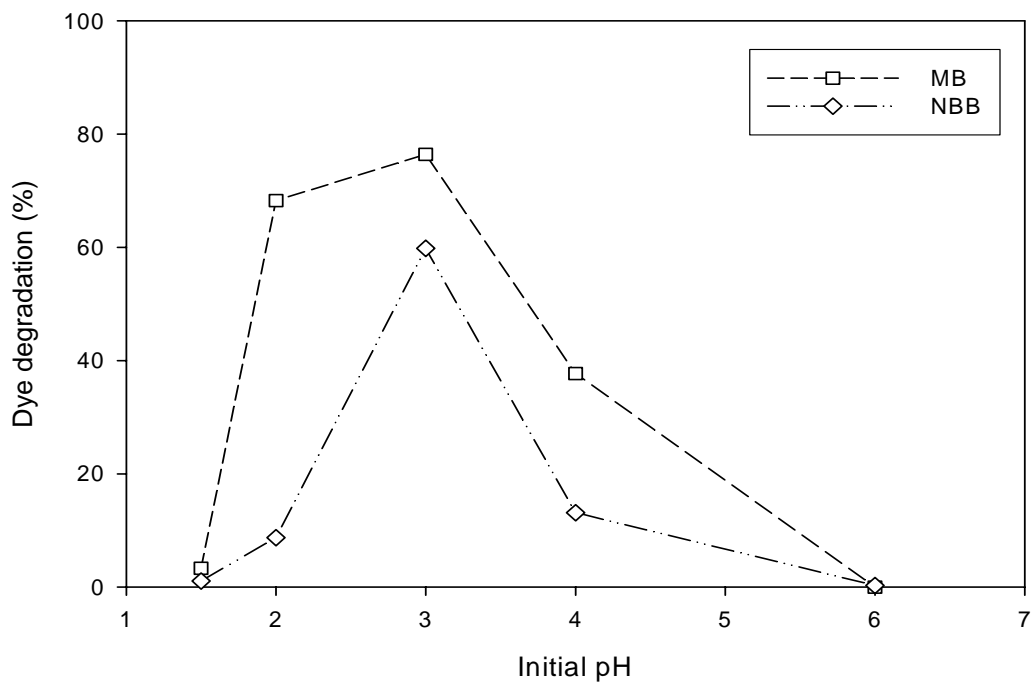


Figure 10. Effect of initial pH on dye degradation.

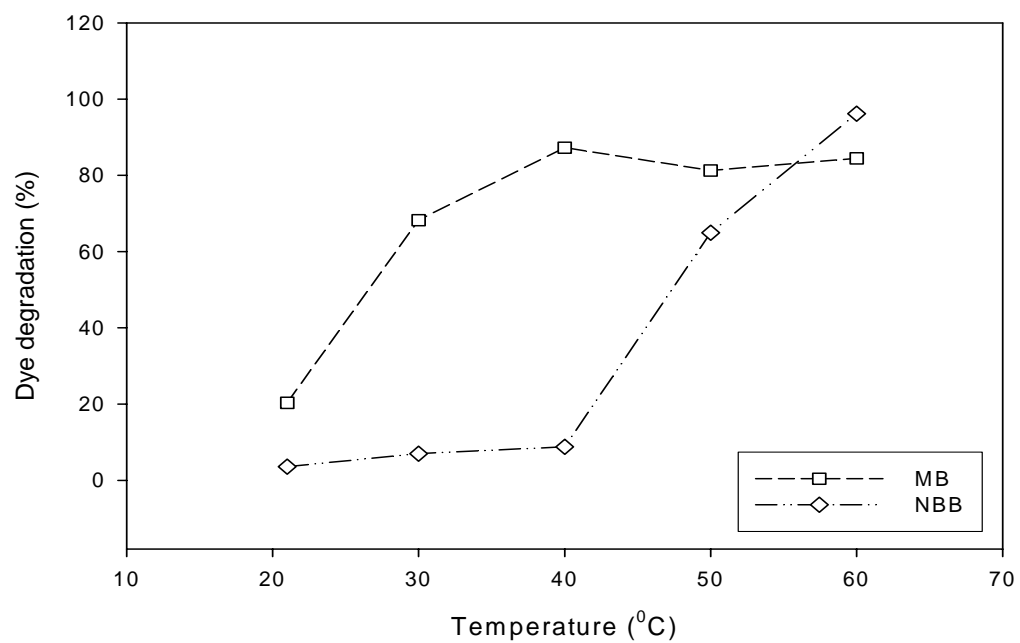


Figure 11. Effect of reaction temperature on dye degradation.

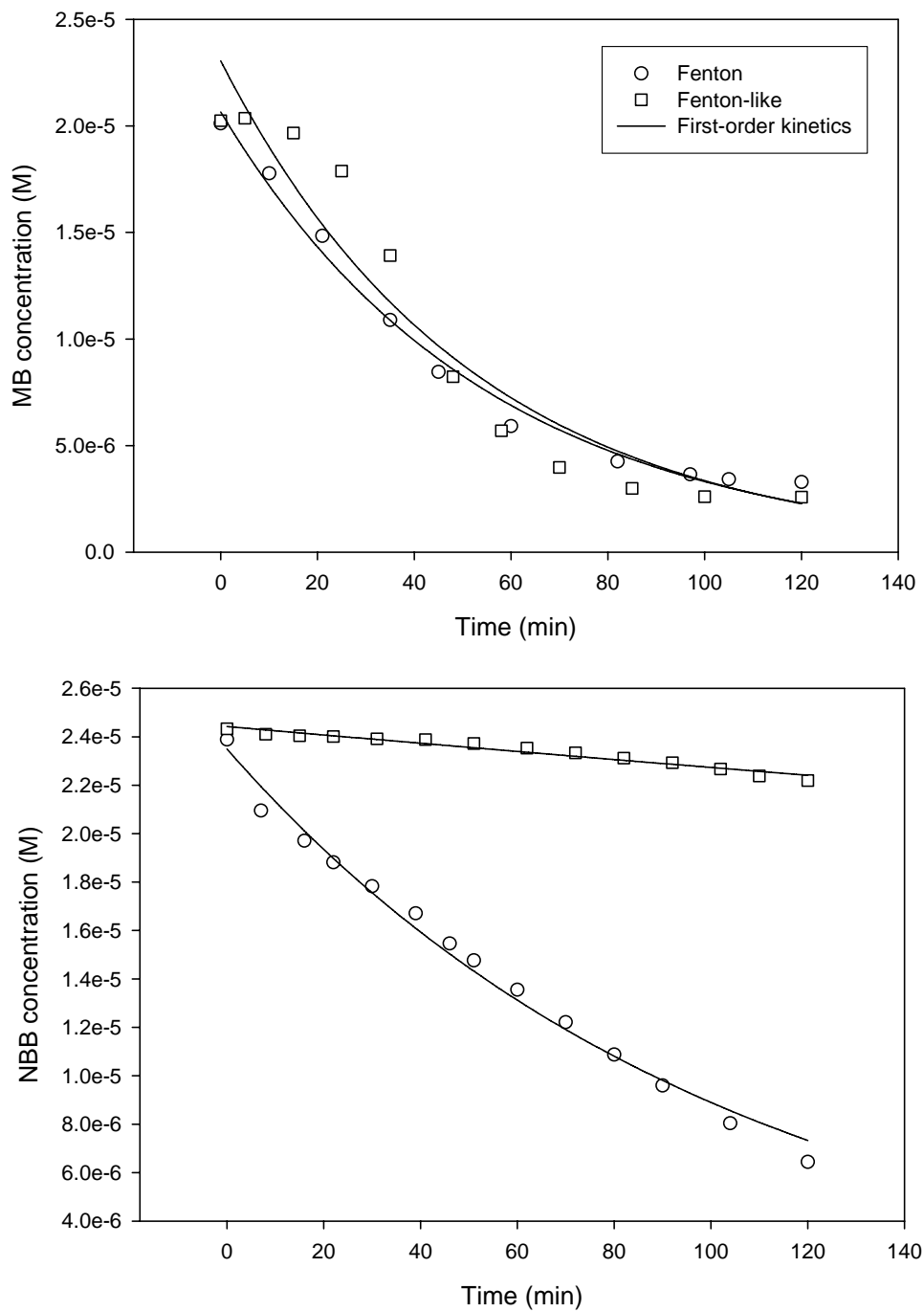


Figure 12. Dynamic dye degradation in Fenton and Fenton-like reactions.

3.4.3. Effect of Solution pH

Figure 10 presents the effect of pH between 1.5 and 6 on dye degradation. As seen that the highest degradation efficiency was observed at pH 3 for both dyes. Lower or higher pH will not favour dye degradation. At pH 6, dye decolourisation is almost zero for two dyes.

Many studies [14-19] also report similar range between 2.5 and 4 for various organic compounds in Fenton and Fenton-like reactions. For $\text{pH} < 2$, $\cdot\text{OH}$ will react with H^+ ions present in acidic conditions, playing the 'scavenging effect' [18], and oxonium ion $[\text{H}_3\text{O}_2]^+$ is also formed at low pH, which shows reduced reactivity. In addition, H_2O_2 is stabilised at low pH and this inhibits the production of the intermediate ion HO_2^- , which reacts with Fe^{3+} to produce Fe-OOH^{2+} . At high pH, decolorisation efficiency is reduced because of the reduction in the solubility of Fe^{2+} and Fe^{3+} and the formation of $\text{Fe}(\text{OH})_3$ and $\text{Fe}_2\text{O}_3 \cdot n\text{H}_2\text{O}$, resulting in the decrease in Fe^{3+} ions in the solution and subsequently in a reduction in the concentration of Fe^{2+} ions, which are more efficient than Fe^{3+} ions because they directly produce $\text{OH}\cdot$ [19]. Also, if the pH is too high, the iron precipitates as $\text{Fe}(\text{OH})_3$ and catalytically decomposes the H_2O_2 to oxygen, which reduces its concentration in the solution, potentially creating a hazardous situation [20].

3.4.4. Effect of Reaction Temperature

Figure 11 shows the dye decolorisation efficiency at varying temperatures between 21 and 60 °C. As shown that temperature is usually presenting a positive effect and an increase in temperature results in an increase in dye decolourisation up to 60 °C. At 21 °C, degradation efficiency is very low at 20% and 3% for MB and NBB, respectively. For two dyes, the effect of temperature on dye degradation seems to be different. For NBB, colourisation efficiency shows lower changes at temperatures below 40 °C but increases significantly at higher temperatures. The degradation efficiency will reach 96% at 60 °C. For MB, a maximum efficiency can be observed at 40 °C. At 50 and 60 °C, no improvement in the overall efficiency is observed; in fact a bit decline is observed at 50 - 60 °C, which can be attributed to the thermal decomposition of H_2O_2 into oxygen and water at high temperatures.

3.5. Comparison of Fenton and Fenton-like Oxidation for Decolourisation

Figure 12 shows the dye degradation as a function of time in Fenton and Fenton-like oxidation. For MB, the initial dye degradation rate in Fenton oxidation is faster than that of Fenton-like oxidation. However, the dye decolourisation efficiency after 2 h is almost the same, reaching 84% and 87% for Fenton and Fenton-like oxidation, respectively. For NBB, dye degradation in two reactions is quite different. Dye degradation rate and efficiency are much higher in Fenton reaction. The efficiencies for two oxidations are 73% and 9%, respectively, all lower than MB.

It has been known that Fenton-like reaction rate is usually lower than that of Fenton reaction, which is also proven in this investigation. However, the dye decolourisation efficiency for MB shows the similar results. Hsueh et al. [18] investigated Fenton and Fenton-like reactions for degradation of azo dyes and reported the similar phenomenon. In the initial stage of reaction (< 30 min), the dye decolorisation rate of Fenton reaction exceeds than that of Fenton-like one. However, when the reactions time over 60 min, there shows almost no difference of the dye decolorisation efficiencies between Fenton and Fenton-like reaction. The reason is that almost all of Fe^{2+} was converted to Fe^{3+} at this time. Ntampeglitis et al. [19] compared the decolorisation kinetics of three commercially used Procion H-ex1 dyes and reported that use of Fenton reagent is more efficient than the use of Fenton-like reagent. Regarding decolorisation efficiency after a 10 min reaction time, the two methods achieve

nearly identical decolorisation efficiencies in the pH range between 3 and 5. The Fenton reagent gives better results at a pH equal to 2 and at a pH higher than 5. At pH 3, decolorisation efficiencies are about 84% for both methods, while at pH 2, decolorisation efficiencies are 94 and 100% for the Fenton-like and Fenton processes, respectively. All these results suggest that decolorisation efficiency would be achieved for Fenton and Fenton-like reactions for some types of dyes.

3.6. Comparison of Fenton-like and Sono-Fenton-like Reactions for Decolourisation

Figure 13 shows a comparison of decolorisation of MB and NBB under various reactions, sonolysis, Fenton-like and sono-Fenton-like reactions. The lowest degradation performances were observed under non-sonic conditions using either H_2O_2 or Fe^{3+} . The degradation efficiencies for two dyes are lower than 5%. Using only H_2O_2 , however, yielded better degradation efficiency than using Fe^{3+} for both dyes. Using only sonication without Fenton oxidation yielded further better results than the two previous processes. The degradation efficiency is above 20% for MB and NBB. This can be attributed to the presence of hydroxyl ions formed during sonication. Sonication of an aerated aqueous solution can yield $\cdot\text{OH}$ upon the reactions (3) and following reactions [21].

It is noted that degradation efficiency was further increased by combining sonic effects with either H_2O_2 or Fe^{3+} in solution. The decolorisation efficiency is significant under sonolysis combined with H_2O_2 and the efficiencies for MB and NBB are 80% and 60%, respectively. The improvements to sonication observed on addition of Fe^{3+} could be attributed to the occurrence of Fenton-like oxidation under sonication. For this to happen, H_2O_2 needs to be made available since both Fe^{3+} and H_2O_2 are needed for Fenton-like oxidation. On the other hand, the combined effects of sonication and H_2O_2 are due to enhanced formation of hydroxyl radicals. Again, sonication with only H_2O_2 proved more efficient compared to sonication with only Fe^{3+} . From the Figure, it is seen that the removal efficiencies for two dyes are 68% and 9%, respectively, in Fenton-like reaction. The combined effect of sonication and Fenton-like oxidation produces the highest efficiency for dye decolorisation. The dye degradation can reach 93% for two dyes. The improvements in decolorisation of combined sonication and Fenton-like reaction over Fenton-like only oxidation is 37% for MB, but 10 times higher for NBB.

3.7. Kinetics of Dye Degradation in Sonolysis and Sono-Fenton-like Reaction

Figure 14 shows the dynamic variation of dye degradation during sonolysis and combined sonolysis with Fenton and Fenton-like reactions. As seen that the combined sonolysis with Fenton reagents, Fe^{2+} or Fe^{3+} , produced similar reaction rate and decolorisation efficiency for two dyes. Sonolysis with H_2O_2 exhibits better reaction rate and efficiency than sono-Fe combination. Sono-Fenton and sono-Fentonlike also present similar reaction rate and decolorisation efficiency. After 1 h, decolorisation with two systems can arrive at 90% for two dyes.

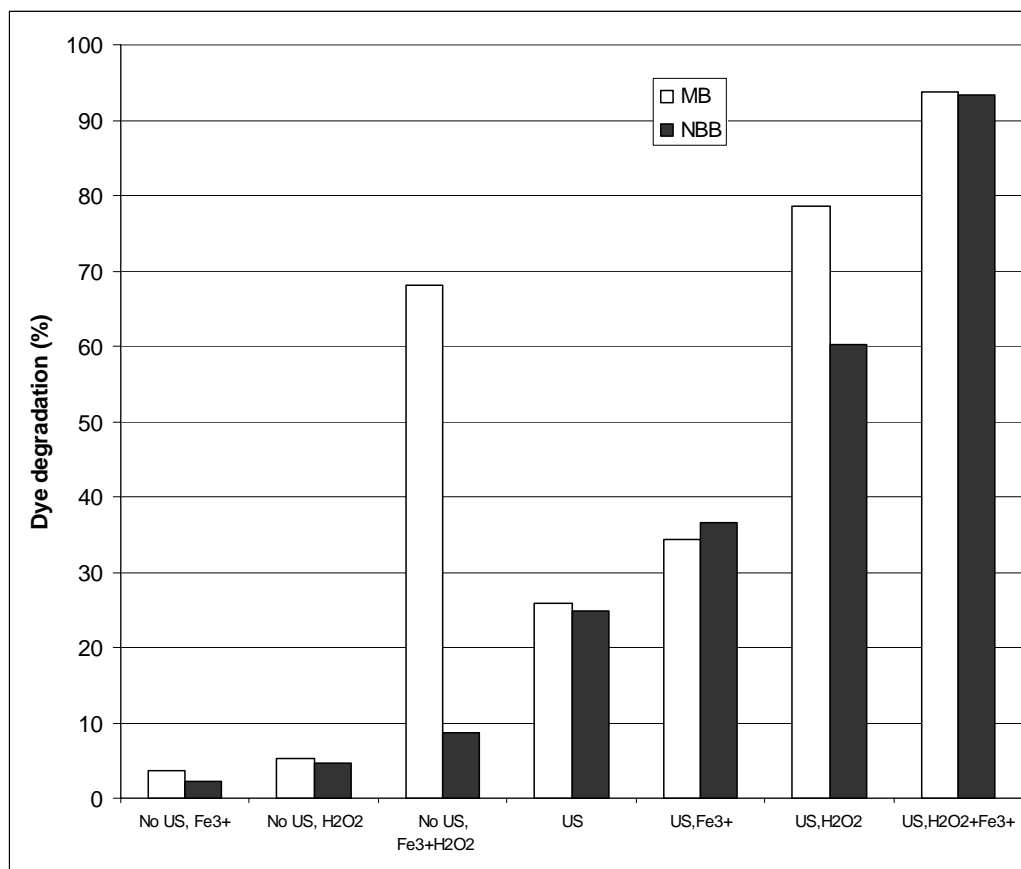


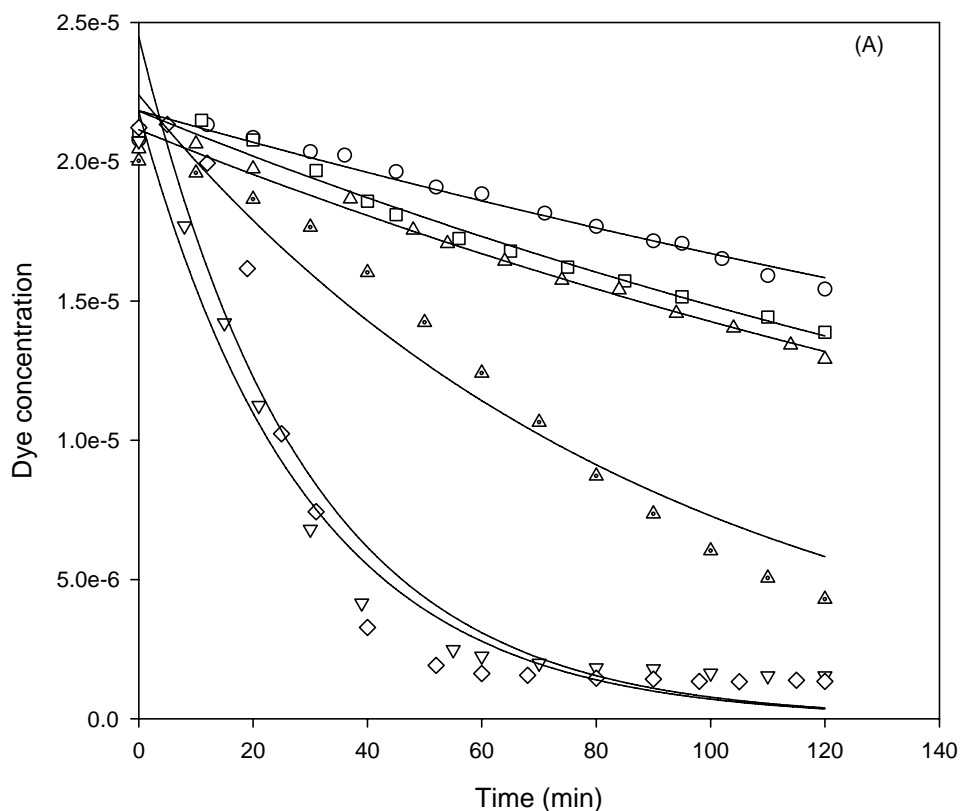
Figure 13. Comparison of dye degradation under none sonic and sonic promoted reactions.

The kinetic parameters calculated from the first-order and second-order kinetic models are presented in Table 2. Figure 14 also shows the first-order kinetic curves for the sono-Fenton and sono-Fentonlike reactions. It is seen that the first-order kinetics will produce better results than that of the second-order kinetics evidenced from the regression coefficients. The reaction rate constants for sono-Fe²⁺ and sono-Fe³⁺ are close each other and the rate constants for sono-Fenton and sono-Fenton-like reaction are also much similar. The order of reaction rate for all sonic based reactions is sonolysis < sono-Fe³⁺ \approx sono-Fe²⁺ < sono-H₂O₂ < sono-Fenton-like \approx sono-Fenton. From the table, one can also see that the reaction rate constant for MB is generally higher than that of NBB.

Several investigations on dye degradation in Fenton reactions have demonstrated that reaction kinetics of Fenton oxidation follows a pseudo-first order plot [16, 22, 23]. Wang et al. [7] investigated sonochemical degradation kinetics of methyl violet in aqueous solutions and reported the first-order kinetics with the degradation rate coefficient of $1.35 \times 10^{-2} \text{ min}^{-1}$. Lall et al. [10] also found a first-order kinetics for decolourisation of reactive blue 19 in ozonation, ultrasound, and ultrasound-enhanced ozonation processes. Thus, our results are similar to the previous investigations.

Table 2. Kinetic parameters of dye degradation in Fenton and sono-Fenton reactions

System	Dye	First-order kinetics			Second-order kinetics		
		C_0 (M)	k_1 (min^{-1})	R^2	C_0 (M)	k_2 ($\text{M}^{-1} \text{min}^{-1}$)	R^2
Sonolysis	MB	2.18×10^{-5}	2.68×10^{-3}	0.964	2.19×10^{-5}	140.5	0.949
Sono- Fe^{2+}	MB	2.11×10^{-5}	3.94×10^{-3}	0.989	2.27×10^{-5}	228.2	0.977
Sono- Fe^{3+}	MB	2.18×10^{-5}	3.85×10^{-3}	0.980	2.21×10^{-5}	215.8	0.976
Sono- H_2O_2	MB	2.24×10^{-5}	0.0112	0.944	2.27×10^{-5}	756.2	0.859
Sono-Fenton	MB	2.18×10^{-5}	0.0343	0.978	2.27×10^{-5}	3.12×10^3	0.911
Sono-Fenton-like	MB	2.45×10^{-5}	0.0345	0.941	2.49×10^{-5}	2.73×10^3	0.840
Sonolysis	NBB	2.24×10^{-5}	2.19×10^{-3}	0.972	2.25×10^{-5}	111.2	0.980
Sono- Fe^{2+}	NBB	2.42×10^{-5}	4.25×10^{-3}	0.970	2.47×10^{-5}	222.3	0.988
Sono- Fe^{3+}	NBB	2.45×10^{-5}	3.95×10^{-3}	0.985	2.48×10^{-5}	200.4	0.994
Sono- H_2O_2	NBB	2.55×10^{-5}	6.51×10^{-3}	0.968	2.59×10^{-5}	341.5	0.934
Sono-Fenton	NBB	2.55×10^{-5}	0.0274	0.976	2.64×10^{-5}	2.01×10^3	0.906
Sono-Fenton-like	NBB	2.70×10^{-5}	0.0252	0.973	2.80×10^{-5}	1.71×10^3	0.885



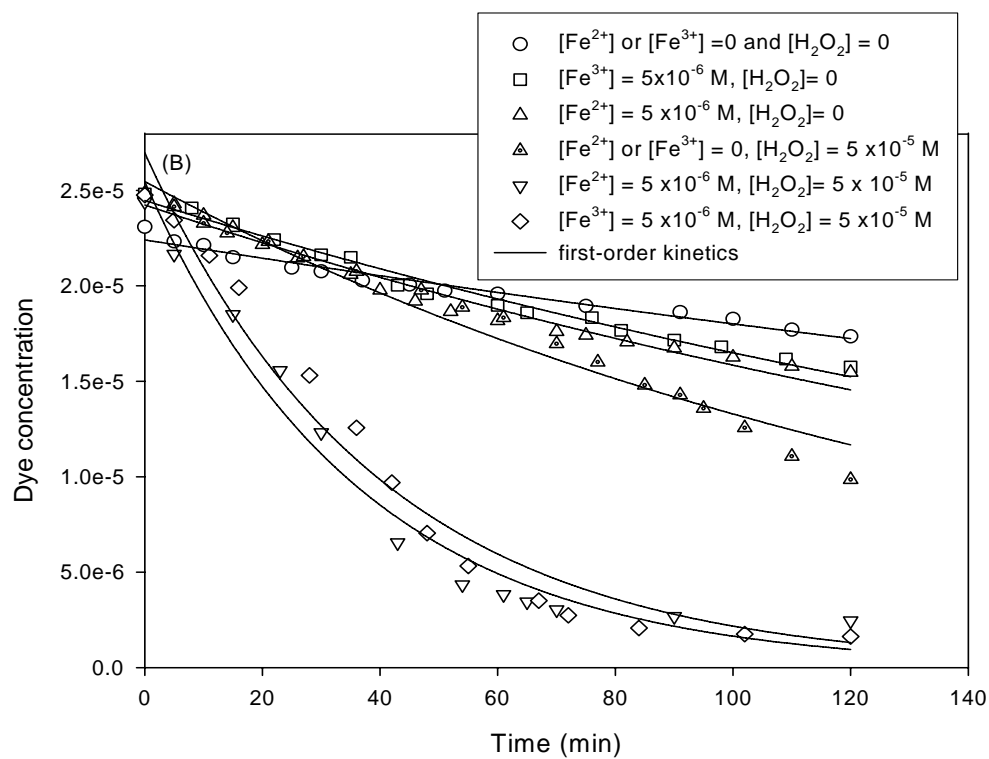


Figure 14. Kinetics of dye degradation in sonolysis, sono-Fenton, and son-Fentonlike reactions.

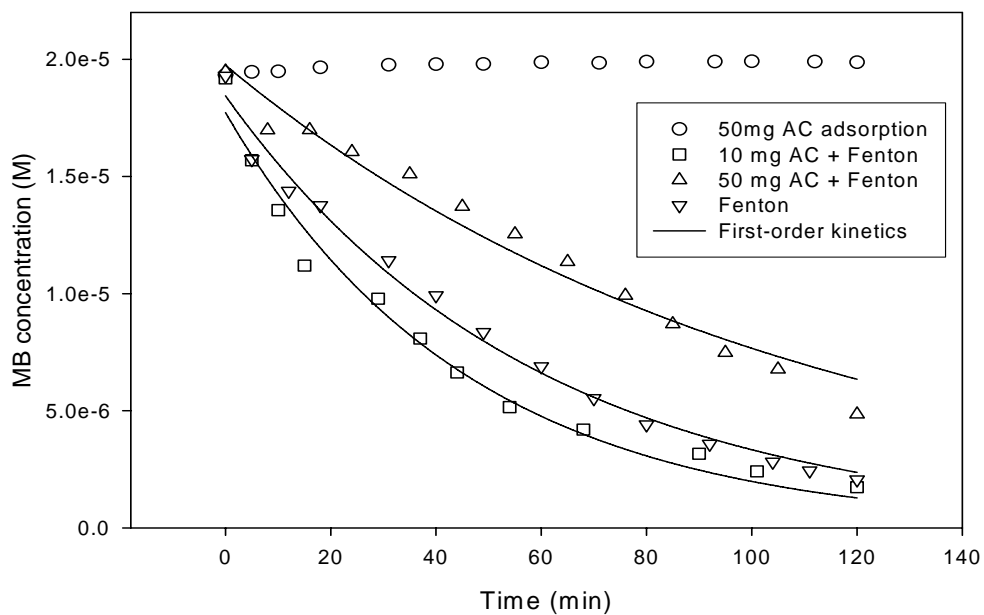


Figure 15. MB decolourisation in adsorption, Fenton oxidation, and combined adsorption with Fenton oxidation.

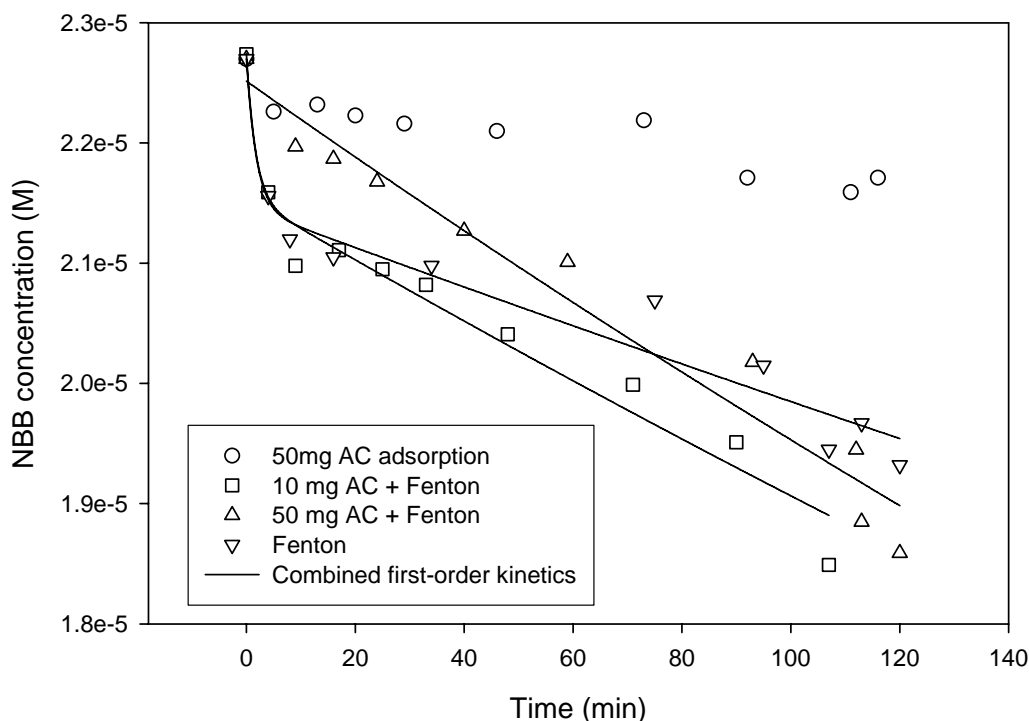


Figure 16. NBB decolourisation in adsorption, Fenton oxidation, and combined adsorption with Fenton oxidation.

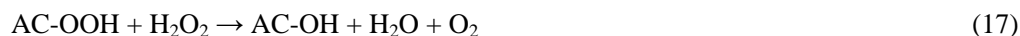
3.8. Effect of Activated Carbon in Fenton Oxidation on Dye Degradation

Figure 15 presents MB decolourisation with time in carbon adsorption, Fenton oxidation, and combined adsorption and Fenton oxidation. As seen that dye concentration does not show any changes during 120 min when only activated carbon is present in the solution. This suggests that no adsorption of MB occurs on activated carbon during the period of time. On the other hands, dye concentration will significantly decrease during Fenton oxidation. After 120 min, dye degradation efficiency will achieve at 89%. If activated carbon is present with Fenton reagents in the solution, dye degradation rate is different depending on the amount of activated carbon. For low amount of activated carbon, dye degradation rate is increased and the efficiency is slight higher at 91% after 120 min. For the higher load of activated carbon, dye degradation is, however, decreased and the degradation efficiency is significantly reduced to 75% at 120 min.

Figure 16 illustrates NBB decolourisation with time in carbon adsorption, Fenton oxidation, and combined adsorption and Fenton oxidation. It is seen that NBB degradation is quite different from MB. Unlike the case of MB, activated carbon shows a faster adsorption at initial stage and continuous adsorption with dye decolourisation of 5% at 120 min. Fenton oxidation can also result in dye degradation and the efficiency is greater than carbon adsorption. But compared with MB, decolourisation rate and efficiency of Fenton oxidation are all lower. At 120 min, dye degradation efficiency is 15%. When activated carbon is

present with Fenton reagents, dye degradation presents similar behaviour to MB. At 10 mg activated carbon, decolourisation rate and efficiency are all enhanced somewhat and the efficiency is 19% at 120 min. At 50 mg activated carbon, decolourisation rate is reduced but efficiency shows an increase at 18% after 120 min.

The presence of activated carbon in Fenton oxidation will produce two effects. One is adsorption of organic compounds and metal ions in the solution on activated carbon and the other is catalytic reaction of carbon with H_2O_2 . It is well known that activated carbon has high adsorption capacity for Fe ions. Also it has been reported that carbon is a catalyst for H_2O_2 decomposition [31-33]. This process can be described in the following equations.



During the process, the surface hydroxyl groups on activated carbon react with a hydrogen peroxide anion to produce carbon surface peroxide, which has an increased oxidation potential, and then is further reacted with another H_2O_2 , causing H_2O_2 decomposition to release oxygen and regeneration of the carbon surface [31]. Thus, this process results in the consumption of H_2O_2 in the solution.

On the other hand, activated carbon and H_2O_2 can react to produce free radicals via the Haber-Weiss mechanism. AC is believed to function as an electron-transfer catalyst with AC and AC^+ as the oxidised and reduced catalyst states[31]:



In this process, the produced free radicals, $\text{OH}\cdot$ and $\text{HO}_2\cdot$, will favour the organic decomposition. Therefore, in Fenton oxidation of dyes, the presence of activated carbon will in one way play adsorption role by adsorbing Fe^{2+} or Fe^{3+} on carbon surface, inhibiting the homogeneous Fenton oxidation of dye. On the other hand, activated carbon can either produce hydroxide free radicals via reactions with H_2O_2 (Eqs. (18) and (19)), which will promote homogeneous Fenton oxidation of dyes, or consume H_2O_2 to produce O_2 (Eqs. (16) and (17)), inhibiting oxidation of dye. These two effects will compensate each other. At the case of low loading of activated carbon in solution, the adsorption rate is slow and thus most of $\text{Fe}^{2+}/\text{Fe}^{3+}$ ions are still presence in the solution, making the homogeneous Fenton oxidation dominates the dye oxidation process. In addition, activated carbon can induce additional formation of hydroxide radicals enhancing the dye decolourisation rate and efficiency. However, when more amount of activated carbon is present in the solution, adsorption of Fe ions on activated carbon will be significant, resulting in lower concentration of Fe ions and thus slower reaction rate of homogeneous Fenton oxidation. Even though the adsorbed Fe ions on activated carbon can induce heterogeneous Fenton oxidation, however, the rate is usually much slow compared with homogeneous Fenton reaction. Meanwhile, the rate of H_2O_2 decomposition to radicals is slow and can not compensate the loss of rate in Fenton oxidation, leading to reduced dye decolourisation rate. Georgi and Kopinke [31] investigated the interaction of adsorption and catalytic reactions in water decontamination processes using

AC and H_2O_2 and reported that sorption on AC has an adverse effect on the oxidation of organic compounds via $\text{OH}\cdot$ radicals, even though the radicals are formed directly on the AC surface, i.e. in close proximity to the sorbed organic compounds.

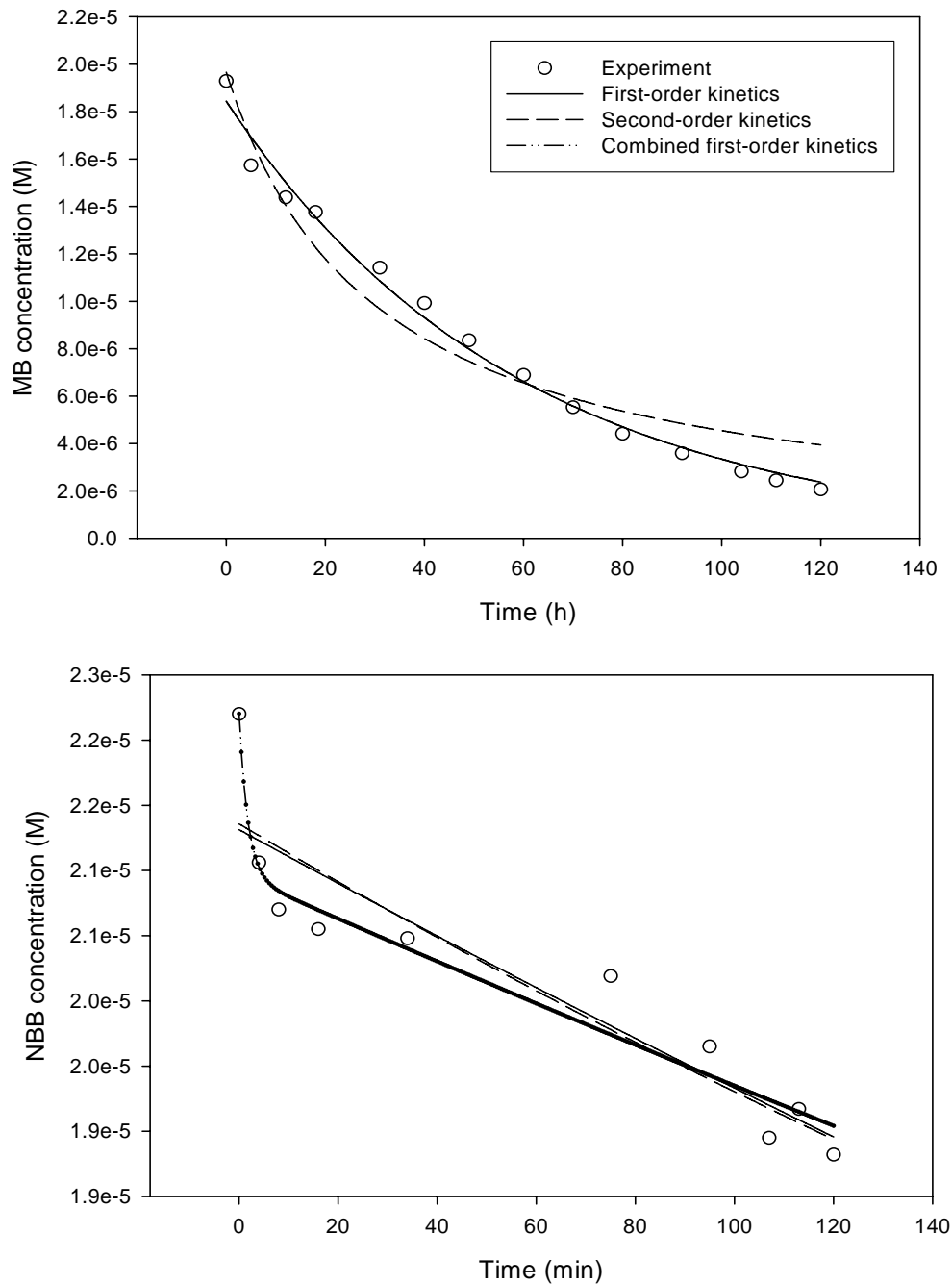


Figure 17. Comparison of kinetics of dye degradation in Fenton oxidation.

3.8.1. Decolourisation Kinetics of Fenton Reaction under Activated Carbon

Two kinetic models, the first-order and second-order kinetics will be evaluated for the dynamic decolourisation of two dyes, which have been discussed before. In addition, a combined first-order reaction can be described as follows

$$C = C_{10} \exp(-k_1 t) + C_{20} \exp(-k_2 t) \quad (20)$$

where, C_{10} and C_{20} are the initial dye concentrations of two independent first-order reactions and k_1 and k_2 are the reaction rate constants, respectively. This model describes parallel reactions occurring at the same time.

Figure 17 shows a comparison of three kinetic models for the experimental results of Fenton oxidation of two dyes. The parameters obtained from the curve fitting are presented in Table 3. For MB, the first-order kinetics will show better fitting results than the second-order kinetics and the combined first-order kinetics is the same as the first-order kinetics. However, for NBB, the first-order and second-order kinetics are much similar and the combined first-order rate model will be the best in simulation of experimental results.

The kinetics of dye degradation in Fenton oxidation has been reported in some investigations. Several investigators have found that the Fenton reaction for dye degradation follows the pseudo first-order kinetics [16, 32, 33]. However, Malik and Saha [26] investigated the oxidation of direct dyes in Fenton reaction and found that the entire degradation reaction could be divided into a two-stage reaction. In the first stage, dyes were decomposed quickly, referred to $\text{Fe}^{2+}/\text{H}_2\text{O}_2$ stage. The second stage of the reaction may be referred to as the $\text{Fe}^{3+}/\text{H}_2\text{O}_2$ stage.

Table 4 compares the kinetic results of dye decolourisation using Fenton oxidation without activated carbon and in the presence of activated carbon in solution. It is seen from the values of kinetic rate constant that MB decolourisation rate constant is 0.0171, 0.0219 and 0.0946 min^{-1} for Fenton oxidation, 10 mgAC+Fenton, and 50 mgAC+Fenton, respectively. For NBB, the decolourisation kinetics for Fenton and 10 mgAC+Fenton can be described by the combined first-order kinetics and the rate constants are also higher in case of 10 mgAC+Fenton. However, the two rate constants for 50 mgAC+Fenton are the same, which suggests that it can be simplified to first-order kinetics.

Table 3. Kinetic parameters for dye degradation in Fenton oxidation

Dye	First-order			Second-order			Combined first-order				
	C_0 (M)	k_1 (min^{-1})	R^2	C_0 (M)	k_2 (M ⁻¹ min ⁻¹)	R^2	C_{01} (M)	k_1 (min^{-1})	C_{02} (M)	k_2 (min^{-1})	R^2
MB	1.84×10^{-5}	0.0171	0.990	1.96×10^{-5}	1.70×10^3	0.947	8.67×10^{-6}	0.0171	9.76×10^{-6}	0.0171	0.990
NBB	2.18×10^{-5}	9.52×10^{-4}	0.850	2.18×10^{-5}	47.5	0.850	1.24×10^{-6}	0.559	2.15×10^{-5}	7.81×10^{-4}	0.957

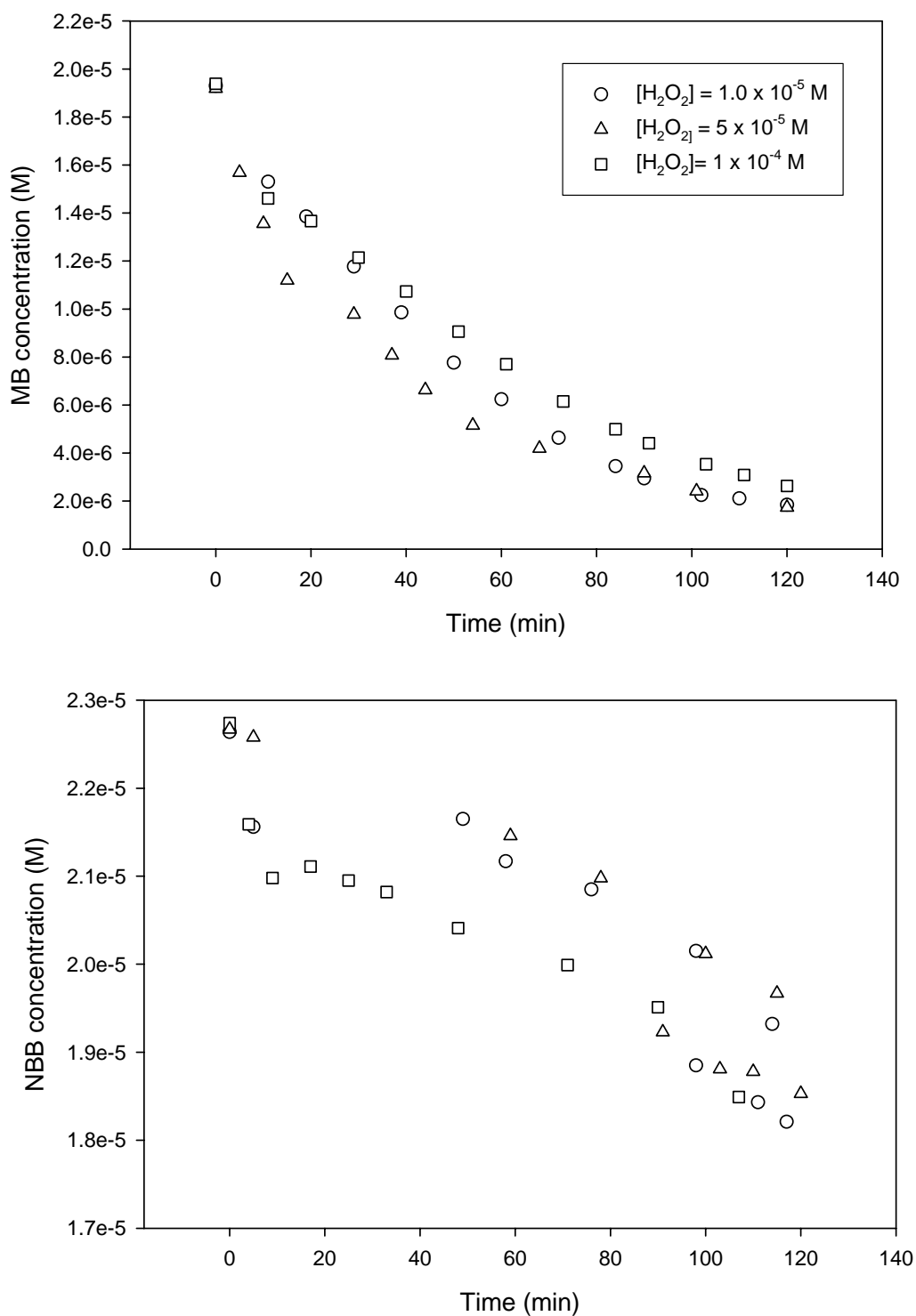
Figure 18. Effect of H_2O_2 concentration on decolourisation.

Table 4. Comparison of kinetic parameters of decolourisation in different activated carbon loading

Dye	AC loading	First-order			Combined first-order				
		C ₀ (M)	k (min ⁻¹)	R ²	C ₀₁ (M)	k ₁ (min ⁻¹)	C ₀₂ (M)	k ₂ (min ⁻¹)	R ²
MB	0	1.84x 10 ⁻⁵	0.0171	0.990					
	10 mg	1.77x10 ⁻⁵	0.0219	0.982					
	50 mg	1.97x10 ⁻⁵	0.00946	0.970					
NBB	0				1.24x10 ⁻⁶	0.559	2.15x10 ⁻⁵	7.81x10 ⁻⁴	0.957
	10 mg				1.19x10 ⁻⁶	0.600	2.16x10 ⁻⁵	1.22x10 ⁻³	0.961
	50 mg				9.85x10 ⁻⁶	1.42x10 ⁻³	1.27x10 ⁻⁵	1.42x10 ⁻³	0.958

3.8.2. Effect of H₂O₂

It has been known that H₂O₂ is an important parameter for Fenton oxidation. Figure 18 presents the effect of H₂O₂ on decolourisation of two dyes at the case of 10 mgAC+Fenton. For the basic dye, decolourisation rate will be increased when H₂O₂ concentration is increased from 1.0 x 10⁻⁵ to 5 x 10⁻⁵ M. However, further increasing H₂O₂ concentration to 1 x 10⁻⁴ M will result in a decrease in decolourisation rate. The decreasing rate of dye decolourisation is attributed to unreacted H₂O₂ acting as a scavenger of [•]OH and producing a less potent perhydroxyl radicals[18] (Eq.10). For azo dye, decolourisation is similar for H₂O₂ concentration at 1.0 x 10⁻⁵ to 5 x 10⁻⁵ M and will increase when H₂O₂ concentration is increased to 1 x 10⁻⁴ M.

Several investigations in wastewater decolourisation using Fenton oxidation have been conducted and reported an optimal peroxide concentration in Fenton oxidation of dyes [16-18]. Dutta et al. [17] found that at initial [Fe²⁺] = 3.58x10⁻⁵ M and initial [H₂O₂] < 4.14x10⁻⁴ M, the rate of decolourisation of methylene blue increased with increasing initial concentration of hydrogen peroxide. The rate remained almost same for initial H₂O₂ concentration of 4.14x10⁻⁴ – 2.94x10⁻² M. Others reported similar results for different dyes [16, 18, 23].

3.8.3. Effect of pH

Solution pH is also important for Fenton oxidation of dyes. Previous investigations show that the optimum pH for Fenton oxidation is 2 – 4 [16, 18]. Low or high pH will reduce the oxidation rate. Figure 19 shows the decolourisation of two dyes at different pH for 10 mgAC+Fenton system. As shown that high pH at 6 will significantly reduce the decolourisation efficiency. For MB, decolourisation efficiency is almost zero while for NBB the decolourisation is only 4% compared with 19% at pH 2. Above pH 4, the reduction in degradation efficiency can be attributed to the hydrolysis of Fe³⁺ into Fe(OH)₃, which helps to

decompose H_2O_2 into oxygen and water. Therefore, the degradation rate will be decreased because less hydroxyl radicals are available [23].

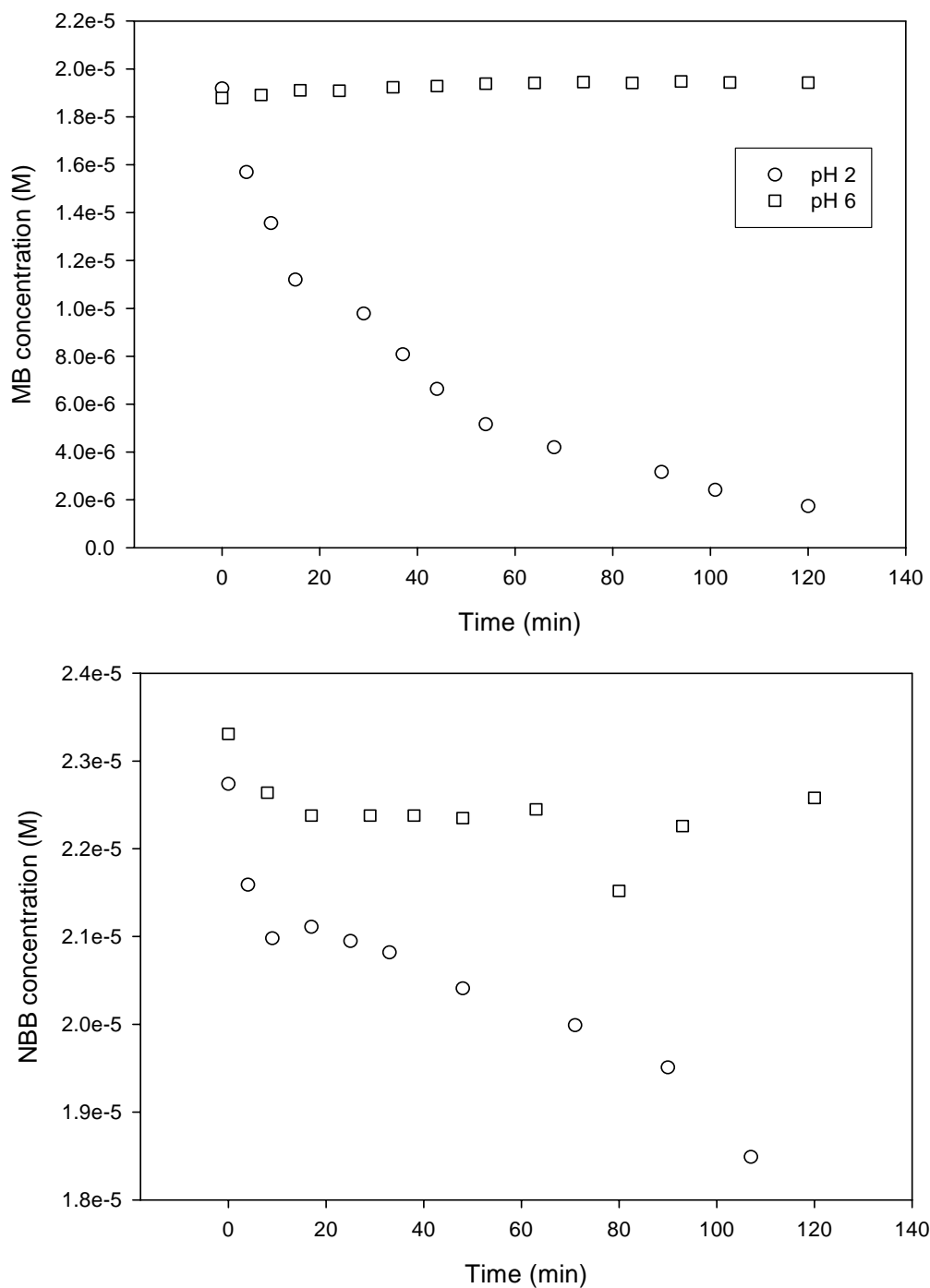


Figure 19. Effect of solution pH on dye degradation.

4. CONCLUSION

Fenton and sono-Fenton oxidations for decolourisation of dye-containing wastewater at very low Fenton reagent concentration (Fe^{2+} and H_2O_2) have been investigated and their efficiencies and kinetics are compared. Fenton oxidation produces high decolourisation efficiency depending on the types of dyes, Fenton reagent concentrations, and reaction conditions, pH and temperature. In general, decolourisation of MB will show higher efficiency than NBB. High H_2O_2 concentration and temperature will promote decolourisation. While maximum efficiency (80%) will be achieved at optimum pH and Fe^{2+} concentration. Sonolysis will promote decolourisation and sono-Fenton oxidation exhibits the highest removal efficiency. Decolourisation efficiency for two types of dyes (> 90% at 2 h) can be realised even at low dosage of Fe and H_2O_2 . Both Fenton and sono-Fenton oxidations show the first-order kinetics.

Fenton-like and sono-Fenton-like oxidations at very low Fenton reagent concentrations for decolourisation of dye-containing wastewater have demonstrated higher efficiencies. Fenton-like oxidation produces high decolourisation efficiency depending on the types of dyes, Fenton reagent concentrations, and reaction conditions, pH and temperature. In general, decolourisation of MB will show higher efficiency than NBB. High H_2O_2 concentration and temperature will promote decolourisation. While maximum efficiency will be achieved at optimum pH and Fe^{3+} concentration. Fenton and Fenton-like oxidation will have much similar decolourisation efficiency. Sonolysis will promote decolourisation and sono-Fenton or sono-Fenton-like oxidation exhibits the highest removal efficiency. Both Fenton, Fenton-like, and sono-Fenton type oxidation show the first-order kinetics.

Activated carbon exhibits some adsorption for NBB but no adsorption of MB. Fenton oxidation is quite effective for dye decolourisation and the efficiency depends on the type of dye. Fenton oxidation presents strong decolourisation of MB but low efficiency for NBB. The presence of activated carbon in Fenton oxidation can promote the decolourisation at low dosage but exhibits inhibiting effect at high loading. H_2O_2 and pH will also affect the decolourisation rate and efficiency. The kinetic studies indicate that decolourisation rate of MB and NBB is different and follows the different kinetics. The decolourisation of MB can be described by simple first-order kinetics while the kinetics of NBB decolourisation is the combined first-order kinetics.

REFERENCES

- [1] Wang, SB and Li, HT, Dye adsorption on unburned carbon: Kinetics and equilibrium. *Journal of Hazardous Materials* 2005; 126: 71-77.
- [2] Wang, S, Zhu, ZH, Coomes, A, Haghseresht, F, and Lu, GQ, The physical and surface chemical characteristics of activated carbons and the adsorption of methylene blue from wastewater. *Journal of Colloid and Interface Science* 2005; 284: 440-446.
- [3] Kusic H, Loncaric Bozic A, Koprivanac N. Fenton type processes for minimization of organic content in coloured wastewaters: Part I: Processes optimization. *Dyes and Pigments*.2007; 74(2):380-387.

-
- [4] Manousaki E, Psillakis E, Kalogerakis N, Mantzavinos D. Degradation of sodium dodecylbenzene sulfonate in water by ultrasonic irradiation. *Water Research*. 2004;38(17):3751-3759.
- [5] Neppolian B, Jung H, Choi H, Lee JH, Kang J-W. Sonolytic degradation of methyl tert-butyl ether: the role of coupled fenton process and persulphate ion. *Water Research*. 2002;36(19):4699-4708.
- [6] Shemer H, Narkis N. Trihalomethanes aqueous solutions sono-oxidation. *Water Research*. 2005;39(12):2704-2710.
- [7] Wang XK, Chen GH, Guo WL. Sonochemical degradation kinetics of methyl violet in aqueous solutions. *Molecules*. 2003;8(1):40-44.
- [8] Vinodgopal K, Peller J, Makogon O, Kamat PV. Ultrasonic mineralization of a reactive textile azo dye, Remazol black B. *Water Research*. 1998;32(12):3646-3650.
- [9] Tezcanli-Guyer G, Ince NH. Degradation and toxicity reduction of textile dyestuff by ultrasound. *Ultrasonics Sonochemistry*. 2003;10(4-5):235-240.
- [10] Lall R, Mutharasan R, Shah YT, Dhurjati P. Decolorization of the dye, reactive blue 19, using ozonation, ultrasound, and ultrasound-enhanced ozonation. *Water Environment Research*. 2003;75(2):171-179.
- [11] Ince NH, Tezcanli G. Reactive dyestuff degradation by combined sonolysis and ozonation. *Dyes and Pigments*. 2001;49(3):145-153.
- [12] Stock NL, Peller J, Vinodgopal K, Kamat PV. Combinative sonolysis and photocatalysis for textile dye degradation. *Environmental Science & Technology*. 2000;34(9):1747-1750.
- [13] Fung PC, Sin KM, Tsui SM. Decolorisation and degradation kinetics of reactive dye wastewater by a UV/ultrasonic/peroxide system. *Journal of the Society of Dyers and Colourists*. 2000;116(5-6):170-173.
- [14] Abdelsalam ME, Birkin PR. A study investigating the sonoelectrochemical degradation of an organic compound employing Fenton's reagent. *Physical Chemistry Chemical Physics*. 2002;4(21):5340-5345.
- [15] Joseph JM, Destailats H, Hung HM, Hoffmann MR. The sonochemical degradation of azobenzene and related azo dyes: Rate enhancements via Fenton's reactions. *Journal of Physical Chemistry A*. 2000;104(2):301-307.
- [16] Dutta K, Bhattacharjee S, Chaudhuri B, Mukhopadhyay S. Chemical oxidation of CI Reactive Red 2 using Fenton-like reactions. *J Environ Monitor*. 2002;4(5):754-760.
- [17] Dutta K, Mukhopadhyay S, Bhattacharjee S, Chaudhuri B. Chemical oxidation of methylene blue using a Fenton-like reaction. *Journal of Hazardous Materials*. 2001;84(1):57-71.
- [18] Hsueh CL, Huang YH, Wang CC, Chen CY. Degradation of azo dyes using low iron concentration of Fenton and Fenton-like system. *Chemosphere*. 2005;58(10):1409-1414.
- [19] Ntampeglitis K, Riga A, Karayannis V, Bontozoglou V, Papapolymerou G. Decolorization kinetics of Procion H-ex1 dyes from textile dyeing using Fenton-like reactions. *Journal of Hazardous Materials*. 2006;136(1):75-84.
- [20] De Laat, J and Le, TG, Effects of chloride ions on the iron(III)-catalyzed decomposition of hydrogen peroxide and on the efficiency of the Fenton-like oxidation process. *Applied Catalysis B: Environmental* 2006; 66: 137-146.

-
- [21] De Laat, J, Truong Le, G, and Legube, B, A comparative study of the effects of chloride, sulfate and nitrate ions on the rates of decomposition of H₂O₂ and organic compounds by Fe(II)/H₂O₂ and Fe(III)/H₂O₂. *Chemosphere* 2004; 55: 715-723.
- [22] Ashraf, SS, Rauf, MA, and Alhadrami, S, Degradation of Methyl Red using Fenton's reagent and the effect of various salts. *Dyes and Pigments* 2006; 69: 74-78.
- [23] Malik, PK and Saha, SK, Oxidation of direct dyes with hydrogen peroxide using ferrous ion as catalyst. *Separation and Purification Technology* 2003; 31: 241-250.
- [24] Meric, S, Kaptan, D, and Tunay, C, Removal of color and COD from a mixture of four reactive azo dyes using Fenton oxidation process. *Journal of Environmental Science and Health Part a-Toxic/Hazardous Substances & Environmental Engineering* 2003; 38: 2241-2250.
- [25] Kavitha, V and Palanivelu, K, Destruction of cresols by Fenton oxidation process. *Water Research* 2005; 39: 3062-3072.
- [26] Ramirez, JH, Costa, CA, and Madeira, LM, Experimental design to optimize the degradation of the synthetic dye Orange II using Fenton's reagent. *Catalysis Today* 2005; 107-08: 68-76.
- [27] Guedes, AMFM, Madeira, LMP, Boaventura, RAR, and Costa, CAV, Fenton oxidation of cork cooking wastewater-overall kinetic analysis. *Water Research* 2003; 37: 3061-3069.
- [28] Minero, C, Lucchiari, M, Vione, D, and Maurino, V, Fe(III)-enhanced sonochemical degradation of methylene blue in aqueous solution. *Environmental Science & Technology* 2005; 39: 8936-8942.
- [29] Ince, NH and Tezcanli, G, Treatability of textile dye-bath effluents by advanced oxidation: Preparation for reuse.. *Water Science and Technology* 1999; 40: 183-190.
- [30] Swaminathan, K, Sandhya, S, Sophia, AC, Pachhade, K, and Subrahmanyam, YV, Decolorization and degradation of H-acid and other dyes using ferrous-hydrogen peroxide system. *Chemosphere* 2003; 50: 619-625.
- [31] Georgi, A and Kopinke, FD, Interaction of adsorption and catalytic reactions in water decontamination processes Part I. Oxidation of organic contaminants with hydrogen peroxide catalyzed by activated carbon. *Applied Catalysis B-Environmental* 2005; 58: 9-18.
- [32] Lucking, F, Koser, H, Jank, M, and Ritter, A, Iron powder, graphite and activated carbon as catalysts for the oxidation of 4-chlorophenol with hydrogen peroxide in aqueous solution. *Water Research* 1998; 32: 2607-2614.
- [33] Huang, H-H, Lu, M-C, Chen, J-N, and Lee, C-T, Catalytic decomposition of hydrogen peroxide and 4-chlorophenol in the presence of modified activated carbons. *Chemosphere* 2003; 51: 935-943.

Chapter 6

DECOLORATION OF TEXTILE WASTEWATERS

Julija Volmajer Valh and Alenka Majcen Le Marechal*

University of Maribor, Faculty of Mechanical Engineering,
Department for Engineering Materials and Design,
Smetanova 17, SI-2000 Maribor, Slovenia

ABSTRACT

Water is an important natural resource for sustainable ecosystems, human life and economical development. The control of water pollution has become of increasing importance in recent years. Dyes make the world more beautiful through colored products, but cause a lot of problems in the environment. For decoloration and degradation of textile wastewater many applicable methods have been developed, but because of the composition complexity of the textile wastewater the use of universal procedures seems to be impossible. So, there is a need to find an efficient and cost-effective wastewater treatment for the decoloration of textile wastewaters. In this chapter a survey of the most widely used and, according to many researches, the most promising textile wastewater decoloration methods are presented.

INTRODUCTION

Industry and agriculture are the two largest water users in Europe. The largest water industry consumer is the textile finishing industry. Processes, where most water is consumed are printing and dyeing, which consume on average 100-150 m³ of water per ton of finished product with peaks above 500 m³/t in multi-stage processes.[1] The annual consumption of fresh water at the European level is 600 million m³. Besides being one of the greatest consumers of water, the textile industry is also one of the highest pollutants because of the large use of numerous organic compounds and different auxiliary substances (1 kg of chemicals and auxiliaries is processed per kg of textile product). On average, 90% of the

* Correspondence author. E-mail: julija.volmajer@uni-mb.si

water input in textile finishing operations needs to be treated end-of-pipe. In Europe, 108 million tons of wastewater is produced on a yearly basis and 36 million tons of chemicals and auxiliaries have to be removed from the textile wastewater. Textile wastewater typically contains a complex mixture of organic and inorganic chemicals, and this is the reason why the processes of cleaning and recycling of wastewater are difficult to perform. Organic contaminants in wastewater present a specific problem due to their toxicity, bioaccumulation and poor biodegradability. The price for waste water treatment varies on average from 0.5-2.5 €/m³ and it is expected that the price in the future will increase (estimation value is from 3-5 €/m³).

There are more than 100 000 commercially available dyes with the production of over 7×10^5 tons.[2] The exact data on the quantity of dyes discharged in the environment are also not available. It is assumed that 2 % of the dyes produced are discharged directly in aqueous effluent, and 10 % are subsequently lost during the textile coloration process.[3] On the other hand, most of the wastewater produced by the textile industry is coloured. Many dyes are difficult to decolourise due to their complex structure and synthetic origin.

Dyes cause a lot of problems in the environment:

1. Depending on exposure time and dye concentration, dyes can have acute and/or chronic effects on exposed organisms.
2. The presence of very small quantities of dyes in water (less than 1 ppm) is highly visible due to their brilliance.
3. The greatest environmental concern with dyes is their absorption and reflection of sunlight entering the water. Light absorption diminishes photosynthetic activity of algae and seriously influence on the food chain.
4. Dyes can remain in the environment for an extended period of time, because of high thermal and photo stability. For instance, the half-life of hydrolysed Reactive Blue 19 is about 46 years at pH 7 and 25 °C.[4]
5. Many dyes and their breakdown products are carcinogenic, mutagenic and/or toxic to life. Dyes are mostly introduced into the environment through industrial effluents. There is ample evidence of their harmful effects. Triple primary cancers involving kidney, urinary bladder and liver of dye workers have been reported. Most of the dyes, used in the textile industry are known only by their trade name, while their chemical nature and biological hazards are not known. Mathur[5] *et. al.* studied the mutagenicity of textile dyes (known only by their trade name, used in Pali, identified as one of the most polluted cities in India) and the effluents containing these dyes, and the influence on the health of textile dyeing workers and the environment. The dyes were used in their crude form and no following purification was attempted, because they wanted to test the potential danger that dyes represent in actual use. The results clearly indicated that most of the used dyes are highly mutagenic. Brown[6] *et. al.*, published an article, to show it is possible to predict the toxicity of new azo dyes. The systematic backtracking of the flows of wastewater from textile-finishing companies led to the identification of textile dyes as a cause of strongly mutagenic effects. The textile dyes used in the textile-finishing companies in the European Union were examined for mutagenicity. According to the obtained results the dyes that proved to be mutagenic have been replaced with less harmful substances.[7],[8]. The degradation product of dyes could be carcinogenic. The formation of

carcinogenic aromatic amine *o*-tolidine from the dye Direct Blue 14 by skin bacteria has been established.[9]

6. Textile dyes can cause allergies such as contact dermatitis[10] and respiratory diseases[11],[12],[13], allergic reaction in eyes, skin irritation, and irritation to mucous membrane and the upper respiratory tract. Reactive dyes form covalent bonds with cellulose, woollen and PA fibres. It is assumed that in the same way reactive dyes can bond with $-NH_2$ and $-SH$ group of proteins in living organisms. A lot of investigations of respiratory diseases in workers dealing with reactive dyes have been made. Certain reactive dyes have caused respiratory sensitisation of workers occupationally exposed to them.[14]

Public perception of water quality is greatly influenced by the colour. So, the removal of colour from wastewater is often more important than the removal of the soluble colourless organic substances. Removal of the dyes from the textile wastewater is often very costly, but a stringent environmental legislation has stimulated the textile sector in developing wastewater treatment plants.

TEXTILE DYES

Organic dyes contain substituted aromatic and heteroaromatic groups. The color of dyes results from conjugated chains or rings that can absorb different regions of wavelength. The chromophores of organic dyes are usually composed of double carbon-carbon bonds, double nitrogen-nitrogen bonds, double carbon-nitrogen bonds, aromatic and heterocyclic rings containing oxygen, nitrogen or sulphur. Reactive dyes are termed chemically as colored compounds with a functional group capable of forming a covalent bond with a suitable substrate. Azo dyes, which contain one or more azo bonds, are the most widely used synthetic dyes. Azo dyes are mostly used for yellow, orange and red colours. Anthraquinone dyes constitute the second most important class of textile dyes. They have a wide range of colours in almost the whole visible spectrum, but they are most commonly used for violet, blue and green colours.

With regard to method and domain of usage the dyes are classified into acid, reactive, direct, basic, disperse, metal complex, vat, mordant and sulphur dyes. Most commonly in use today are reactive and direct dyes for cotton and viscose-rayon dyeing and disperse dyes for polyester dyeing.

Generally, dyes can be classified with regard to their chemical structure, with regard to the method and domain of usage, and with regard to chromogen (Table 1).

Examples of the chemical structure of the azo dye with C.I. Direct Red 254 and reactive dichlorotriazine dye with C.I. Reactive Yellow 4 are presented in Figure 1 and Figure 2.

Table 1. Classification of the dyes

<i>Classification</i>		
	Subclass	Characteristic
With regard to chemical structure (C.I.)	E.g. azo, anthraquinone, triphenylmethane, indigo,...	The classification of a dye by chemical structure into a specific group is determined by the chromophore.
With regard to method and domain of usage (C.I.)	E. g. direct, acid, basic, reactive, reductive, sulphuric, cromatic, metal-complex, disperse, pigments,...	Dyes used in the same technological process of dyeing and with similar fastness are classified into the same group.
With regard to chromogen $n \rightarrow \pi^*$	E. g. absorptive, fluorescent and dyes with energy transfer,...	This classification is based on the type of excitation of electrons, which takes place during light adsorption.
With regard to the nature of donor – acceptor couple	E. g. 1-aminoanthraquinone, p-nitroaniline,...	These chromogenes contain a donor of electrons (unbound electron couple), which directly bonds to the system of conjugated π electrons.
With regard to the nature of polyenes: a) Acyclic and cyclic	E. g. polyolefins, annulenes, carotenoids, rhodopsin,...	Polyene chromogen contains sp^2 (or sp) hybridised atoms. The molecules enclose single and double bonds that form open chains, circles, or a combination of both.
b) Cyanine	E. g. cyanines, amino substituted di- and tri- arylmethane, oxonols, hydroxyarylmethanes,...	Cyanine chromogens have a system of conjugated π electrons, in which the number of electrons matches the number of p orbitals.

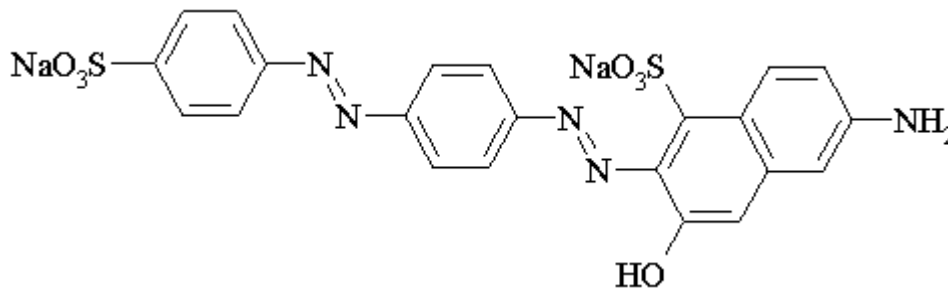


Figure 1. Chemical structure of the azo dye with C.I. Direct Red 254.

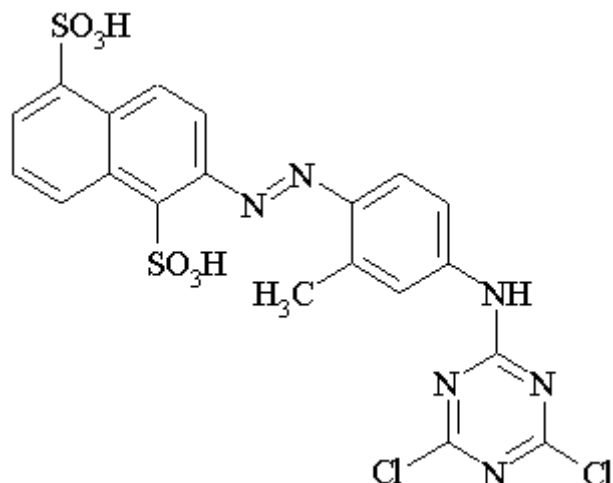


Figure 2. Chemical structure of the reactive dichlorotriazine dye with C.I. Reactive Yellow 4

DECOLORATION

The colour of water, polluted with organic colourants reduces, when the cleavage of the double carbon-carbon bond, double nitrogen-nitrogen bond and heterocyclic and aromatic rings occurs. The absorption of light by the associated molecules shifts from the visible to the ultraviolet or infrared region of the electro magnetic spectrum.

Dyes containing wastewater can be treated in two ways: (i) by chemical or physical methods of dye removal, which refers to the process called decoloration and by means of biodegradation, which tell us more about the fate of dyes in the environment.

In physical treatment methods the applications of physical forces predominate. Physical methods include different precipitation methods (coagulation, flocculation, sedimentation), adsorption (on a wide variety of inorganic and organic supports), filtration, reverse osmosis, ultrafiltration and nanofiltration. Biological treatments differ according to the presence or absence of oxygen to aerobic and anaerobic treatment. Since biological treatments simulate degradation processes that occur in the environment, it is also called biodegradation.

Chemical treatment methods are those, in which the removal or conversion of dyes and other contaminants is brought about by the addition of chemicals or by chemical reactions (reduction, oxidation, compleximetric methods, ion exchange and neutralisation).

The treatment of coloured wastewaters is therefore not restricted to the reduction of ecological parameters only (chemical oxygen demand (COD), biological oxygen demand (BOD), total organic carbon (TOC), adsorbable organic halide (AOX), temperature and pH), but also to reduction of dye concentrations in wastewaters.

PHYSICAL METHODS

Adsorption

Adsorption is the process of collecting soluble substances that are in solution on a suitable interface. Adsorption methods for decoloration are based on the high affinity of many dyes for adsorbent materials. Dye removal by adsorption is influenced by some physical and chemical factors like dye-adsorbent interactions, adsorbent surface area, particle size, temperature, pH and contact time. The main criteria for selection of an adsorbent should be based on characteristics such as high affinity and capacity for target compounds and the possibility of adsorbent regeneration.[15]

Activated carbon is the most commonly used method of dye removal by adsorption and it is very effective in adsorbing cationic, mordant, and acid dyes and to a slightly lesser extent, disperse, direct, vat, pigment and reactive dyes.[16],[17] Performance depends on the type of carbon used and characteristic of the wastewater. It is, like many other dye-removal treatments, well suited for one particular waste system and ineffective for another. Activated carbon is relatively expensive and has to be regenerated offsite with losses of about 10 % in the thermal regeneration process.[18]

Adsorption on sludge is the main abiotic mechanism of removing dyes from the wastewater. The most important factors influencing the adsorption test are sludge quality, water hardness, duration of the test and test substance concentration. Static and dynamic removal studies involving water soluble dyes (acid, reactive) and poorly soluble dyes (disperse) have been described by Pagga[19] et al.

Biomass (dead plant and animal matter) is also a suitable adsorbent for wastewater treatment. The adsorption of organic material onto various types of waste biomass has been studied in detail. This has included sawdust[20], peat[21], chitin[22], bagasse pith[23], carbonised wool waste[24], wood chips[25], maize cob[26], banana pith[27], rice husk, hair, cotton waste and bark[28]. The capacities of these materials have been examined through their adsorption of synthetic dyes. Biomass decoloration is a result of two mechanisms: adsorption and ion exchange, and is influenced by many factors, such as, dye-sorbent interaction, sorbent surface area, particle size, temperature, pH and contact time. Biomass of different origin has been used for decoloration of acid, direct and reactive dyes. Of all the described adsorbents only a few have characteristics necessary for commercial use. Considering the price and binding capacity, quarternized lignocellulose based adsorbents are the most appropriate for treating wastewater containing acid dyes. The disadvantage of adsorption processes is that the adsorbent needs to be regenerated, which adds to the cost of the process, and is sometimes a very time-consuming procedure.

Decoloration with alternative materials such as zeolites, polymeric resins, ion exchangers and granulated ferric hydroxide has also been studied in order to decrease adsorbent losses during regeneration.

Filtration Methods

In the textile industry the filtration methods such as ultrafiltration, nanofiltration and reverse osmosis can be used for both filtering and recycling not only pigment-rich streams, but also mercerising and bleaching wastewaters. The specific temperature and chemical composition of the wastewater determine the type and porosity of the filter to be applied. The main drawbacks of the membrane technology are high investment costs, the potential membrane fouling, and the production of a concentrated dyebath which needs to be treated.[29],[30]

Coagulation-flocculation

Coagulation-flocculation processes are widely used in several wastewater treatments in Germany and France. Coagulation-flocculation methods were successfully applied for colour removal of sulphur and disperse dyes, whereas acid, direct, reactive and vat dyes presented very low coagulation-flocculation capacity. Coagulant agents like aluminium sulphate, ferrous and ferric sulphate, ferric chloride, calcium chloride, copper sulphate, as well as several co-polymers like pentaethylene, hexamine and ethylenediene dichloride are used to form flocs with the dye, which are then separated by filtration or sedimentation. Polyelectrolyte can also be dosed during the flocculation phase to improve the flocs settleability. [31],[32]

The main advantage of these processes is decoloration of the waste steam due to the removal of dye molecules from the dyebath effluents, and not due to a partial decomposition of dyes, which can lead to an even more potentially harmful and toxic aromatic compound. The major disadvantage of coagulation-flocculation processes is the production of sludge.

CHEMICAL METHODS

Oxidative Processes

Oxidation is the most commonly used chemical decoloration process. This is mainly due to its simplicity of application. Modern dyes are resistant to mild oxidation conditions such as those, which exist in biological treatment systems. Conventional oxidation treatments have found it difficult to oxidize dyes (mainly for removing colour) and toxic organic compounds in textile effluents. The chemical limitations of conventional chemical oxidation techniques can be overcome by the development of so-called advanced oxidation processes (AOPs). The goal of AOPs is to generate free hydroxyl radicals (OH^\bullet), which may represent a rate increase of one to several orders of magnitude compared with normal oxidants in the absence of catalysts. Table 2 shows the oxidation potential of common species. Hydroxyl radicals oxidize the dyes and toxic organic compounds that cannot be oxidized by conventional oxidants. In AOPs, oxidizing agents such as ozone and hydrogen peroxide are used with catalysts (Fe, Mn, TiO_2) either in the presence or absence of an irradiation source.

Table 2. Oxidation potential of common oxidizing agents

<i>Oxidizing agents</i>	<i>Oxidation potential/V</i>
Fluorine (F ₂)	3.06
Hydroxyl radical (OH [•])	2.80
Atomic oxygen	2.42
Ozone (O ₃)	2.07
Hydrogen peroxide (H ₂ O ₂)	1.78
Potassium permanganate(KMnO ₄)	1.67
Hypochlorous acid (HClO)	1.49
Chlorine (Cl ₂)	1.36
Bromine (Br ₂)	1.09
Molecular oxygen (O ₂)	1.23

Fenton's Reagent

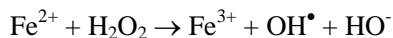
Degradation of hydrogen peroxide into hydrogen radicals is activated by Fe²⁺ (ferrous ions) in an acid solution (pH = 3-4) (Table 3).

In this process it is important to find the optimal concentration of hydrogen peroxide because excess of H₂O₂ acts as a scavenger of radicals, disturbs the COD measurements and is toxic for microorganisms.

Fenton's reagent is very suitable for the oxidation of wastewaters which inhibit biological treatment or are poisonous. This system offers a cost effective source of hydroxyl radicals and it is easy to operate and maintain. Besides offering advantages in COD, colour and toxicity reduction, this process also has disadvantages. The major disadvantage of this method is sludge generation, through the flocculation; impurities are transferred from the wastewater to the sludge, which contains the concentrated impurities and is still ecologically questionable. Conventionally it has been incinerated to produce power, but such disposal is seen by some to be far from being environmentally friendly. To avoid this problem, Gnann[33] et al. suggest the regeneration of Fe²⁺ from iron sludge at pH < 1, with so called the Fenton Sludge Recycling System (FSRS), in which Fe(III)-sludge deposition is eliminated.

A lot of work has been carried out using Fenton's reagent as a decoloration agent. This method is suitable for different dye classes; acid, reactive, direct, metal-complex, disperse and vat dyes as well as pigments. Low decoloration rates were observed when C.I. Vat red (50 %) and C.I. Disperse Blue (0.5 %) were treated. [34]

Studies on the decoloration and mineralization of commercial reactive dyes using solar Fenton and photo-Fenton reaction indicated good colour removal. The use of solar light was proved to be clearly beneficial for the removal of colour, aromatic compounds and TOC.[35],[36]

Table 3. Degradation of hydrogen peroxide into hydrogen radicals activated by Fe²⁺

Ozone

Ozone is a powerful oxidant agent for water and wastewater. Once dissolved in water, ozone reacts with a great number of organic compounds in two different ways, namely direct molecular and indirect free radical-type reactions. The direct reactions are often highly solute selective, slow, and are dominant in acidic solutions. The indirect hydroxyl radical reactions are non-selective, fast, proceed more rapidly with increasing pH and constitute a significant portion of ozonation at basic pH. The direct reactions are very suitable for opening aromatic rings by means of ozone cycloaddition, while indirect attacks are very suitable for mineralization of total organic carbon (TOC).[37]

Although the original purpose of the oxidation with ozone is disinfection of potable water, it can also be used for removing many toxic chemicals from wastewater to facilitate the decomposition of detergents, chlorinated hydrocarbons, phenols, pesticides and aromatic hydrocarbons.[38]

The advantages of ozonation are: (i) decoloration and degradation occur in one step, (ii) danger to humans is minimal, (iii) no sludge remains, (iv) all residual ozone can be decomposed easily into oxygen and water, (v) little space is required and (vi) ozonation is easily performed.[39]

A disadvantage of ozonation is its very short half-life in water – it decomposes in about 20 minutes. The time can be significantly shortened if compounds like dyes are present.[40] Ozone stability is affected by the presence of salts, pH and temperature. If alkaline salts are present, the solubility of ozone is reduced, while neutral salts may increase its solubility.[41] Under alkaline conditions ozone decomposes more rapidly than under acidic conditions. With increasing temperature, ozone solubility decreases.[42]

Results presented by several authors revealed that ozone decolorizes all dyes, except nonsoluble disperse and vat dyes which react slowly and take longer time. [43],[44],[45]. Colour removal strongly depends on dye concentration.

Ozonation alone still has low total organic carbon (TOC) and chemical oxygen demand (COD) removal. Species like oxalic, glyoxalic and acetic acids cannot be completely mineralized by ozone alone at least at neutral or acidic pH.[46] To enhance the efficiency of ozonation various advanced oxidation processes have been developed, such as ozon-H₂O₂, ozon-UV, catalytic ozonation.

Ozone-H₂O₂

The addition of hydrogen peroxide to ozone enhances the production of hydroxyl radicals. The aqueous reaction between ozone and hydrogen peroxide are rather complex. The mechanisms and the kinetics of the production of hydroxyl radicals from ozone and hydrogen peroxide are known. The reactions and reaction rate constants are shown in Table 4. In the initiation sequence, reactive OH[•] radicals are generated. During the promotion reactions, the hydroxyl radicals are converted into the peroxy radical.

At acidic pH, H₂O₂ reacts only very slowly with ozone whereas at pH values above 5 a strong acceleration of ozone decomposition by hydrogen peroxide has been observed.

The ozone decomposition rate will increase with increasing pH.

Table 4. Reactions between O₃-H₂O₂

<i>Initiation:</i>		
$\text{HO}_2^- + \text{O}_3 \rightarrow \text{HO}_2^\bullet + \text{O}_3^{\bullet-}$	$k_r = 2,2 \cdot 10^6 \text{ L}/(\text{mol s})$	
$\text{H}^+ + \text{O}_3^{\bullet-} \rightleftharpoons \text{HO}_3^\bullet \rightarrow \text{OH}^\bullet + \text{O}_2$	$k_r = 1,1 \cdot 10^5 \text{ L}/(\text{mol s})$	
$\text{H}_2\text{O}_2 + \text{O}_3 \rightarrow \text{H}_2\text{O} + 2 \text{O}_2$	$k_r < 10^{-2} \text{ L}/(\text{mol s})$	
<i>Promotion:</i>		
$\text{OH}^\bullet + \text{O}_3 \rightarrow \text{O}_2 + \text{HO}_2^\bullet$	$k_r = 1,1 \cdot 10^8 \text{ L}/(\text{mol s})$	
$\text{OH}^\bullet + \text{H}_2\text{O}_2 \rightarrow \text{H}_2\text{O} + \text{HO}_2^\bullet$	$k_r = 2,7 \cdot 10^7 \text{ L}/(\text{mol s})$	
$\text{OH}^\bullet + \text{HO}_2^\bullet \rightarrow \text{H}_2\text{O} + \text{O}_2^{\bullet-}$	$k_r = 7,5 \cdot 10^9 \text{ L}/(\text{mol s})$	

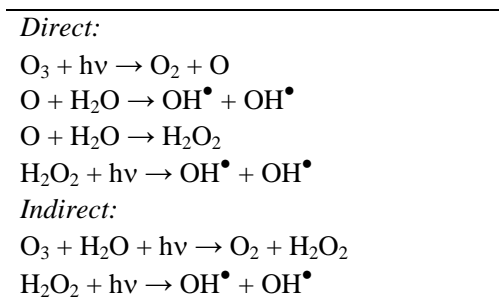
Decoloration with O₃-H₂O₂ combination is applicable for direct, metal-complex or blue disperse dyes. There are some problems with the decoloration of acid and red disperse dyes, though, as well as with mixtures of direct, metal-complex, disperse and reactive dye decoloration. Decoloration of some dyes with O₃-H₂O₂ is presented in Table 5.

Table 5. Decoloration of dyes with O₃-H₂O₂ (adapted from Slokar [34] et.al)

<i>Textile dye</i>	<i>Decoloration/%</i>	<i>Time/min.</i>
Red 219	100	5
Blue 186	85	1
Direct Yellow 44	100	0.5
Direct Yellow 50	100	0.5
Red 23	100	0.5
Red 26	100	0.5
Direct Red 5B	99	45
Direct Blue 1	100	0.5
Direct Blue 25	100	0.5
Direct Blue 71	90	7
Disperse Yellow 3	95	1
Disperse Yellow 64	100	4.5
Red 13	100	0.7
Red 60	100	1
Red 279	99	98
Blue 60	100	0.7
Palanil Blue 3RT	90	31
Sulpho/disperse dye	98	30
Reactive Yellow 37	93	4
Reactive Yellow 125	98	2.5
Reactive Yellow 125	100	7
Remazol Yellow RNL	93	4
Reactive Red 35	99	4.5
Reactive Red 195	100	6
Blue 27	94	0.9
Blue 221	100	9
Green 13	98	4
Reactive dyes	100	1
Vat dyes	80	30
Azoic dyes	87	30

Ozone-UV

UV radiation decomposes ozone in water and generates highly reactive hydroxyl radicals. Hydroxyl radicals oxidize organics more rapidly than ozone itself. Combination of ozone with UV results in a net enhancement of organic matter degradation due to direct and indirect production of hydroxyl radicals upon ozone decomposition and H_2O_2 formation Table 6.

Table 6. Direct and indirect production of hydroxyl radicals in O_3 -UV process

The efficiency of ozone-UV treatment depends on pH (degradation favours neutral or slightly alkaline medium), operating temperature (at higher temperature the ozone solubility is lower) and ozone flow rate.

Degradation of eight commercial azo dyes in water[47] and a model dyehous wastewater[48] has been studied by using ozonation and ozone-UV process. In both studies the ozone-UV process did not significantly enhance the degradation rates, the dye competed with ozone for UV absorbance. But ozone-UV treatment is more effective compared to ozone alone, in terms of COD removal.[49]

 H_2O_2 -UV

In H_2O_2 -UV processes hydroxyl radicals are formed when water-containing H_2O_2 is exposed to UV wavelengths of 200-280 nm. The most commonly used UV source is low-pressure mercury vapor lamps with a 254-nm peak emission.

Problems like sludge formation and regeneration, increased pollution of wastewater caused by ozone can be avoided by oxidation with hydrogen peroxide activated with UV light. The only chemical used in the treatment is H_2O_2 , which, due to its final decomposition into oxygen is not problematic.

The most direct method for generation of hydroxyl radicals is through the cleavage of H_2O_2 . Photolysis of H_2O_2 yields hydroxyl radicals by direct process with a yield of two radicals formed per photon absorbed at 254 nm. Hydroxyl radicals can oxidize organic compounds (RH) producing organic radicals (R^\bullet), which are highly reactive and can be further oxidized (Table 7). [50]

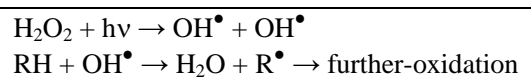
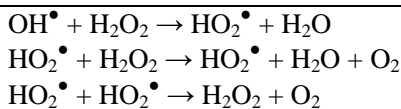
Table 7. The main reactions that occur during the H_2O_2 -UV process

Table 8. Reactions of H₂O₂ as a radical scavenger:

The maximum absorbance of H₂O₂ is needed to generate sufficient hydroxyl radicals because of low-absorption coefficient. However, high concentration of H₂O₂ scavenges the radicals, making the process less effective, while low concentration of hydrogen peroxide doesn't generate enough hydroxyl radicals that are consumed by dye and this leads to a slow rate of oxidation. So, an optimum hydrogen peroxide dose needs to be verified experimentally (Table 8).

The rate of dye removal is influenced by the intensity of UV radiation, pH, dye structure and dyebath composition. In general, decoloration is most effective at neutral pH medium, at higher UV radiation intensity (1600 W rather than 800 W), with an optimal H₂O₂ concentration which is different for different dye classes, and with a dyebath that does not contain oxidising agents having an oxidising potential higher than that of peroxide.

Table 9. Decoloration of dyes with H₂O₂-UV

<i>Textile dye</i>	<i>Decoloration/%</i>	<i>Time/min.</i>	<i>k_dmin⁻¹</i>
Acid Yellow 17 [51]	98.2	40	
Orange 10 [51]	100	60	
Red 1 [51]	99.9	30	
Red 14 [51]	100	60	
Red 18 [51]	99.1	40	
Blue 186 [51]	80	10	
Black 1 [51]	89.9	60	
Direct Yellow 4 [51]	83.2	60	
Direct Blue 71 [59]	98.5	3	
Palanil Blue 3RT [59]	96	10	
Reactive Yellow 37 [59]	85	8	
Reactive Yellow 125 [59]	96	8	
Remazol Yellow RNL [59]	85	8	
Reactive Red 35 [59]	100	8	
Reactive Red 195 [58]	100	60	
Blue 21 [58]	95	150	
Blue 27 [59]	100	5	
Green 13 [59]	93	8	
Vat Blue [59]	15.5	10	
Reactive Black 5 [52]	100	4	0.88
Acid Red 1 [55]			0.063
Acid Red 1 [47]			0.717
Acid Yellow 23 [47]			0.183

According to Shu[53] et.al acid dyes are the easiest to decompose, and with an increasing number of azo groups, the decoloration effectiveness decreases. Yellow and green reactive

dyes need longer decoloration times, while other reactive dyes as well as direct, metal-complex and disperse dyes are decolourised quickly. In the group of blue dyes examined, only blue vat dyes were not decolourised. For pigments, H₂O₂-UV treatment is not suitable, because they form a film-like coating on the UV lamp which is difficult to remove.

Several authors[54],[55],[56],[57] reported complete decoloration of reactive and azo dyes in 30-90 minutes. The results indicated that H₂O₂-UV processes could be successfully used for the decoloration of acid, direct, basic and reactive dyes but it proved to be inadequate for vat and disperse dyes.[58] Decoloration of some dyes with H₂O₂-UV are presented in Table 9.

A comparative study between ozone and H₂O₂-UV was carried out on simulated reactive dye bath effluent containing a mixture of monochlorotriazine type reactive dyes and various auxiliary chemicals. The H₂O₂-UV process presented the decoloration rates close to those rates obtained with ozone but at a lower cost. [59]

H₂O₂-UV systems may be set-up in a batch or continuous column unit.[60]

Ultrasound

Sonolysis is a relatively innovative advanced oxidation process and was found to be a very suitable method for the destruction of textile dyes.

The ultrasonic irradiation of liquids generates cavitation (typically in the range 20-1000 kHz). Cavitation is a phenomenon of micro-bubbles formation. Micro-bubbles grow during the compression/rarefaction cycles until they reach a critical size, and implode generating heat and highly reactive radical species. Inside the cavitation bubbles, the temperature and pressure rise to the order of 5000 K and 100 MPa, respectively. Under such conditions, water molecules degrade releasing hydroxyl radicals (OH[•]) and hydrogen radicals (H[•]) in Table 10.

These radical species can either recombine or react with other gaseous molecules within the cavity or in the surrounding liquid, after their migration. Pyrolytic and radical reactions inside or near the bubble and radical reactions in the solution are two major pathways for sonochemical degradation. Hydrophilic and non-volatile compounds mainly degrade through hydroxyl radical mediated reactions in the solution, while hydrophobic and volatile species degrade thermally inside or in the vicinity of the bubble.

Reactive azo dyes are non-volatile, water soluble compounds and their passage into the gas cavity is unlikely. Hence, oxidative radical reactions in the bulk solution are expected to be the major route for their destruction.

Table 10. Radical formation and depletion during water sonolysis

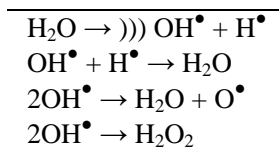


Table 11. Technical Comparison of Oxidative Decoloration

<i>Oxidation process</i>	<i>Advantages</i>	<i>Disadvantages</i>
Fenton	Effective decoloration of both soluble and insoluble dyes. Simple equipment and easy implementation. Reduction of COD (except with reactive dyes). No alternation in volume.	Sludge formation. Long reaction times. Salt formation Hazardous waste. Prohibitively expensive.
FSR (Fenton Sludge Recycling System)	Simple equipment and implementation. Reduction of COD (except with reactive dyes).	Salt formation. Formation of gasses (H ₂ , O ₂ during electrolysis).
Ozone	Applied in gaseous state. no alteration of volume. No sludge production. Effective for azo dye removal.	Short half-life (20 min). Not suitable for disperse dyes. Releases of aromatic amines.
Ozone-H ₂ O ₂	No sludge formation. No salt formation. Short reaction times. Very short reaction times for reactive dyes	Not applicable for all types. Toxicity, hazard, problematic handling. No COD reduction. Additional load of water with ozone.
H ₂ O ₂ -UV	No sludge formation. No salt formation. Short reaction times. Reduction of COD.	Not applicable to all types of dyes. Requires separation of suspended solid particles
Ultrasound	Simplicity in use. Very effective in integrated system.	Relatively new method and awaiting full scale application.

According to several studies, it is difficult to obtain the total mineralization (degradation to carbon dioxide, short-chain organic acid, oxalate, formate and inorganic ions like, sulphate and nitrate) of the complex textile dyes with ultrasound alone. For this reason the combination of ultrasound with other advanced oxidation processes is a more convenient approach in the remediation of such pollutants.

Sonochemical degradation of textile dyes has become quite an interesting research area confirmed by several reports over the last few years.[61]

In Table 11 a comparison of individual AOP is given.

BIOLOGICAL DEGRADATION

Biological degradation or breakdown by living organisms is the most important removal process of organics which are transferred from industry processes into solid and aquatic ecosystems.

The application of microorganisms for the biodegradation of synthetic dyes is an attractive method and offers considerable advantages. The process is relatively inexpensive,

the running costs are low and the end products of complete mineralization are not toxic. An extensive review of large numbers of different species of microorganisms tested for decoloration and mineralization of different dyes has been published by Forgacs[62] et. al.

The efficiency of biological treatment systems is greatly influenced by the operational parameters. To produce the maximum rate of dye reduction the level of aeration, temperature, pH and redox potential of the system must be optimised. The concentration of the electro donor and the redox mediator must be balanced with the amount of biomass in the system and the quantity of the dye present in the wastewater. The compounds present (sulphur compounds, salts) in the wastewater may have an inhibitory effect on the dye reduction process. For these reasons it is important to study the effect of these factors on decoloration before the biological system can be used to treat industrial wastewater.[63]

Biodegradation processes may be anaerobic, aerobic or involve a combination of both.

Aerobic Biodegradation

Aerobic biodegradation is a process that often takes place in the environment, e.g. in natural ecosystems like soil or surface waters, and it is often associated with technical systems such as wastewater treatment plants.

Although for a long time it was thought that azo dyes cannot readily metabolise under aerobic conditions some specific aerobic bacterial cultures were found to be able to reduce the azo linkage via an enzymatic reaction. The aerobic conversions of sulfonated azo dyes were studied by Heiss[64] et. al and Shaul[65] et. al., and sometimes even a complete mineralization of sulfonated azo dyes was found.

In some studies, aerobic color removal of certain azo dyes was achieved, but all these stains required an additional energy and carbon source for growth. Since the supply of this additional substrate could have easily led to the formation of anaerobic niches, the occurrence of anaerobic azo dye reduction certainly cannot be excluded.[66],[67],[68],[69]

The aerobic biodegradation of different aromatic amines (aniline[70], carboxylated aromatic amines[71], chlorinated aromatic amines[72], benzidines[73], sulfonated aromatic amines) has been extensively studied and many of these compounds were found to be degraded. Sulfonated aromatic amines are difficult to degrade.

Anaerobic Biodegradation

Under anaerobic conditions a low redox potential (<-50 mV) can be achieved, which is necessary for the effective decoloration of dyes. Colour removal under anaerobic conditions is also referred as dye reduction. Many bacteria under anaerobic conditions reduce the highly electrophilic azo bond in the dye molecules and produce colourless aromatic amines. The anaerobic decolorization of azo dyes was first investigated using intestinal anaerobic bacteria.[74],[75],[76] Later it was found that azo dyes can also be decolorised with various other anaerobic cultures.[77],[78],[79] The efficacy of various anaerobic treatment applications for the degradation of a wide variety of synthetic dyes has been many times demonstrated. The exact mechanism of azo dye reduction is not clearly understood yet. The different mechanisms may be involved like enzymatic[80],[81], non-enzymatic[82],

mediated[83], intracellular[84],[85], extracellular[86] and various combinations of these mechanisms. A complete anaerobic mineralization of the azo dye azodisalicylate was observed under methanogenic conditions.[87]

The reduction of azo dye under anaerobic condition strongly depends on the presence and disponibility of the cosubstrate. It acts as an electron donor for the azo dye reduction. The decoloration of reactive water soluble azo dyes was achieved under anaerobic conditions using glucose as a cosubstrate.[88] Anaerobic decoloration of reactive dyebath effluents with tapioca as a cosubstrate also enhances the color removal efficiency.[89] The suitable cosubstrates were also hydrolyzed starch, yeast extract, a mixture of acetate, butyrate and propionate.

Much effort has been devoted to the study of the influence of various modern technologies on the decomposition rate of the dyes and the effect of the presence of the other compounds in the media. It has been recently established that the development of high rate systems, in which hydraulic retention times are uncoupled from the solid retention times, facilitate the removal of dyes from textile processing wastewater. [62]

The effect of nitrate and sulfate salts used in textile dyeing on the microbial decoloration of a reactive azo dye has been studied. The results indicated that nitrate delays the onset of decoloration while sulphate did not influence the biodegradation process.[90]

The reduction of azo dyes proceeds better under anaerobic thermophilic conditions than under mesophilic conditions, although the termophilic process seems to be less stable compared to the mesophilic process.[91]

Carliell [92] et. al. studied the biodegradation of reactive dyes and they decolorised 80 % of a range of tested dyes. From a detailed study of a selected dye, it was proposed that this occurred via a reduction mechanism. The results were supported by tentative chemical identification of the dye degradation products.

Hu[93] isolated *Pseudomonas luteola* bacteria, after 6 month adaptation in a coloured wastewater he obtained micro-organisms capable of reductive cleavage of the azo group in the dye. Decoloration with these microorganisms was complete within 4 days.

Zee van der [94] et. al. studied the decoloration of 20 selected azo dyes by granular sludge from an upward-flow anaerobic sludge bed reactor and for all azo dyes tested the complete reduction was achieved.

Aromatic amines, as a result of azo dyes reduction, are not commonly degraded under anaerobic conditions. Many of different aromatic amines were tested, but only a few were degraded. Some aromatic amines, substituted with hydroxyl or carboxyl group were degraded under methanogenic and sulfate reducing conditions.[95],[96],[97]

Combination of Anaerobic/aerobic Biodegradation

Although the anaerobic reduction of azo dyes is generally more satisfactory than aerobic degradation, carcinogenic aromatic amines, as products of anaerobic degradation, have to be degraded by an aerobic process. Diverse technologies for the successive anaerobic/aerobic treatment of textile wastewater have been developed. Anaerobic/aerobic conditions can be implemented by spatial separation of the two sludges using a sequential anaerobic/aerobic reactor system.[98] These conditions can also be imposed in one reactor in the so-called integrated anaerobic/aerobic reactor system.[99]

EXAMPLES OF DECOLORATION STUDIES WITH AOP

Decoloration of Chlorotriazine Reactive Azo Dye with H₂O₂-UV and Optimization of the Process

The decoloration of chlorotriazine reactive azo dye C.I. Reactive Red 120 (Figure 3) with the H₂O₂-UV has been studied. The decoloration with H₂O₂-UV was performed on a pilot plant manufactured by Solvay Interlox. The efficiency of decoloration was examined by time-dependent color intensity reduction, as well as by ecological parameters such as COD, BOD₅ and TC. Decoloration has been performed on a dyebaths containing chlorotriazine reactive azo dye C.I. Reactive Red 120 and chemicals (NaCl, NaOH and oxidizing agent) usually added when dyeing with such dyes. Chemicals used in the dyeing process reduced the efficiency of the decoloration process, especially the oxidizing agent and NaOH. Concerning the reaction conditions, it was further observed that the rate of decoloration was proportional to the output of the UV irradiator. The results show that the decoloration process using UV activated H₂O₂ is very suitable for decoloration of reactive azo dyes of the triazinyl type, since a decrease was noted both in the intensity of the color and in the values of the ecological parameters.[100]

The H₂O₂-UV decoloration process may depend on many different factors. So, the optimization of the decoloration process cannot be solved by simple linear multivariate correlation. Artificial neural networks (ANNs) represent a set of methods that may be useful for optimization of the H₂O₂-UV decoloration process. The decoloration of chlorotriazine reactive azo dye C.I. Reactive Red 120 with the H₂O₂-UV process depends on seven variables, (i) the intensity of UV lamp radiation; (ii) the addition of hydrogen peroxide; (iii) decoloration time; (iv) the concentration of dye; (v) the concentration of salt; (vi) the concentration of an alkali; (vii) the concentration of an oxidizing agent. The experiments needed for determining the significance of the variables' influences were determined by Plackett-Burman's factorial design. In general, the more variables, the more complicated is the model; therefore, the number of variables is tried to be reduced. The purpose of the modelling was, therefore, to optimize the procedure in such a way that it would be possible to "prescribe" the appropriate intensity of UV-light and the addition of peroxide according to the dyebath composition that is actually used in the textile industry. With appropriate decoloration conditions one has in mind the optimum conditions in which the decoloration time would be as short as possible, and also the pertinent ecological parameters. As responses, absorbance and ecological parameters (TIC, TOC and COD) were chosen. For all experiments the reduction of absorbance is larger with more hydrogen peroxide, less alkali and less oxidizing agent present in the bath. TOC values are greater in baths with more dye and more oxidizing agents. The greatest influence on COD is salt. Influence of the variables are greater than the experimental bias, which means that all of them are significant, and need to be taken into consideration for optimization.[101]

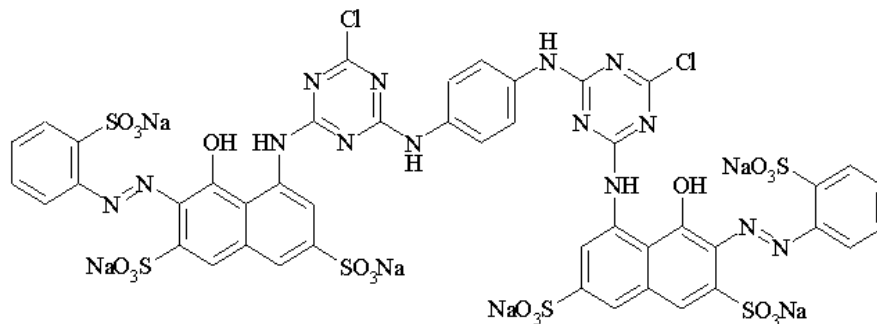


Figure 3. Chemical structure of the chlorotriazine reactive azo dye C.I. Reactive Red 120.

Decoloration of Rective Vinylsulphone Dyes with H_2O_2 -UV, H_2O_2 - O_3 , H_2O_2 - Fe^{2+} and Ultrasound

The influence of chemicals added (concentration of reactive dyes, NaOH, NaCl, urea) and influence of reaction conditions (intensity of UV irradiation, amount of H_2O_2 added, decoloration time) on H_2O_2 -UV decoloration of rective vinylsulphone dye C.I. Reactive Blue 19 (Figure 4) have also been studied.[102]

It was established that with the decoloration of reactive vinylsulphone dye C.I. Reactive Black 5 (Figure 5) treated by H_2O_2 /UV the most important variables are: intensity of UV irradiation, decoloration time, concentration of H_2O_2 , and the dye, NaCl, NaOH and urea concentrations. The values of the ecological parameters are higher than values permitted by the law, since the decolorations were not carried out to complete decoloration, but were stopped at times, specified by Plackett-Burman's experimental design. Experimental design is used to establish which variables influence in the positive or negative sense the efficiency of the decoloration process. The intensity of UV irradiation has mainly a significant influence on measuring the ecological parameters (COD, TOC and absorbance) at maximum level. Decoloration time affects positively absorbance, COD and TOC values. H_2O_2 has positive effect on minimum level. So, better results can be obtained by using lower concentrations of H_2O_2 . The influence of sodium chloride and sodium hydroxide is variable on measuring ecological parameters. In some cases positive and in others negative effects have been observed. Urea has positive effects on absorbance at maximum level, but it has negative influence at minimum level.[103]

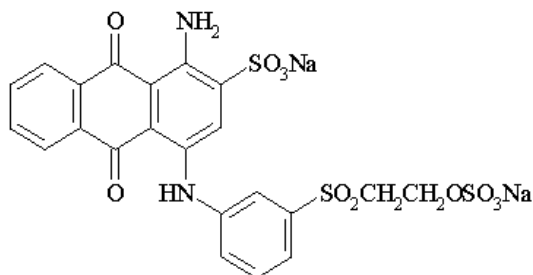


Figure 4. Chemical structure of the reactive vinylsulphone dye with C.I. Reactive Blue 19.

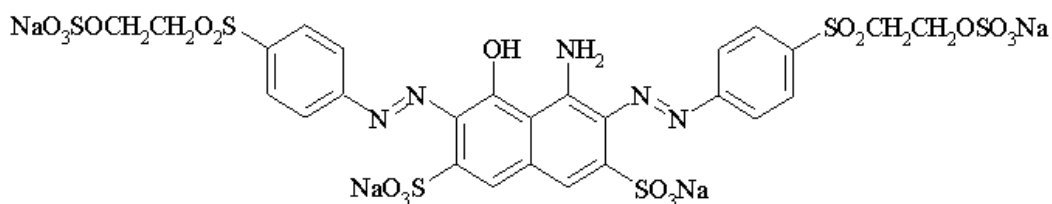


Figure 5. Chemical structure of the reactive vinylsulphone dye with C.I. Reactive Black 5.

The decoloration effectiveness of different advanced oxidation processes like ($\text{H}_2\text{O}_2\text{-UV}$, $\text{H}_2\text{O}_2\text{-O}_3$, $\text{H}_2\text{O}_2\text{-Fe}^{2+}$) in the case of dyebaths of six vinylsulphone reactive dyes (C.I. Reactive Blue 220, C.I. Reactive Black 5 (Figure 5), Remazol Dark Black N, C.I. Reactive Blau 28, C.I. Reactive Red 22 (Figure 6), C.I. Reactive Yellow 15 (Figure 7)) have been studied. The concentration of dyes and chemicals were similar to the concentration in the dyebath after dyeing. The efficiency of decoloration was measured by decoloration time, absorbance, COD and TOC. The decoloration process was stopped at the moment when the solution became visually colorless. The results are on Table 12.

Table 12. Results of comparison studies of $\text{H}_2\text{O}_2\text{-UV}$, $\text{H}_2\text{O}_2\text{-O}_3$, $\text{H}_2\text{O}_2\text{-Fe}^{2+}$

<i>Textile dye</i>	<i>AOP type</i>	<i>COD/ (mg/L)</i>	<i>TOC/ (mg/L)</i>	<i>Time/ min</i>	<i>Decoloration/ %</i>
C.I. Reactive Blue 220	$\text{H}_2\text{O}_2\text{-UV}$	170	1800	120	99.6
C.I. Reactive Black 5	$\text{H}_2\text{O}_2\text{-UV}$	200	1900	50	100
Remazol Dark Black N	$\text{H}_2\text{O}_2\text{-UV}$	200	1900	60	99.5
C.I. Reactive Blau 28	$\text{H}_2\text{O}_2\text{-UV}$	190	2000	40	100
C.I. Reactive Red 22	$\text{H}_2\text{O}_2\text{-UV}$	200	1950	50	100
C.I. Reactive Yellow 15	$\text{H}_2\text{O}_2\text{-UV}$	200	1950	30	100
C.I. Reactive Blue 220	$\text{H}_2\text{O}_2\text{-O}_3$	170	1750	120	99
C.I. Reactive Black 5	$\text{H}_2\text{O}_2\text{-O}_3$	300	1990	80	100
Remazol Dark Black N	$\text{H}_2\text{O}_2\text{-O}_3$	350	2000	90	99.5
C.I. Reactive Blau 28	$\text{H}_2\text{O}_2\text{-O}_3$	190	2000	85	100
C.I. Reactive Red 22	$\text{H}_2\text{O}_2\text{-O}_3$	400	2000	95	100
C.I. Reactive Yellow 15	$\text{H}_2\text{O}_2\text{-O}_3$	300	2000	60	99
C.I. Reactive Blue 220	$\text{H}_2\text{O}_2\text{-Fe}^{2+}$	570	2000	40	100
C.I. Reactive Red 5	$\text{H}_2\text{O}_2\text{-Fe}^{2+}$	620	1900	30	100
Remazol Dark Black N	$\text{H}_2\text{O}_2\text{-Fe}^{2+}$	720	1900	30	99.6
C.I. Reactive Blau 28	$\text{H}_2\text{O}_2\text{-Fe}^{2+}$	605	2000	30	100
C.I. Reactive Red 22	$\text{H}_2\text{O}_2\text{-Fe}^{2+}$	590	1950	30	100
C.I. Reactive Yellow 15	$\text{H}_2\text{O}_2\text{-Fe}^{2+}$	900	2000	20	98

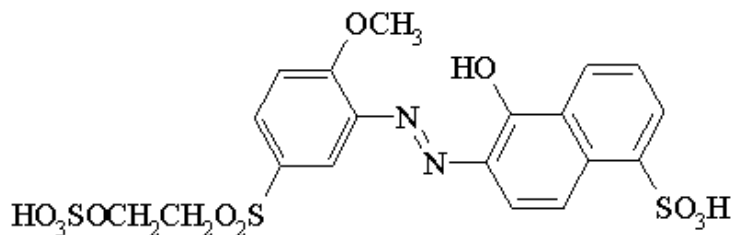


Figure 6. Chemical structure of the reactive vinylsulphone dye with C.I. Reactive Red 22.

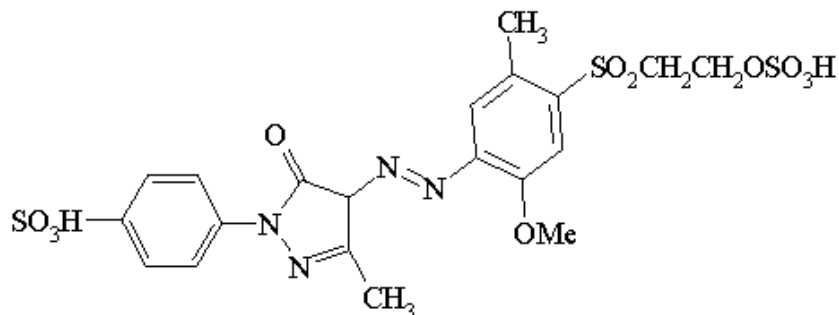


Figure 7. Chemical structure of the reactive vinylsulphone dye with C.I. Reactive Yellow 15.

The decoloration with $\text{H}_2\text{O}_2/\text{Fe}^{2+}$ was the fastest, and the costs of such process are low, but it is not really suitable for environmental reasons (sludge removal).

The decoloration with $\text{H}_2\text{O}_2/\text{O}_3$ yields lower COD values, it causes additional water pollution because of ozone; the disadvantages of this procedure are high investment and operating costs. Decoloration with $\text{H}_2\text{O}_2/\text{UV}$ is an environmentally friendly procedure. It produces no sludge and no additional water pollution, while COD values were low, but investment and operating costs are high.[104]

The decoloration of the same vinylsulphone reactive dyes has also been performed using ultrasound and ultrasound/ H_2O_2 treatment. Decoloration has been performed on an Ultrasound Processor Sonics&Materials VibraCell VCX 600 with a constant frequency of 20 kHz and power of $80 \text{ W}/\text{cm}^2$ and 1 cm^2 titanium horn. It was found that the efficiency of the ultrasound treatment was significantly enhanced when H_2O_2 was added. The rate of color degradation was twice as fast as that accomplished by sonolysis alone (Table 13).[105]

The reactive dye C.I. Reactive Black 5 was also treated by low (20 kHz) and high (279 and 817 kHz) ultrasonic irradiation, without the addition of any oxidant. Experiments were carried out with low frequency probe type, and high frequency plate type transducer at 50, 100 and 150 W of acoustic power. Sonochemical decoloration was increased with rising frequency, acoustic power and irradiation time. The addition of a radical's scavenger (2-methyl-2-propanol) significantly inhibited the sonochemical decoloration, which confirmed radical-induced reactions of decoloration. Acute toxicity to marine bacteria *Vibrio fischeri* have been tested before and after ultrasound irradiation. Under the conditions employed in this study, no toxic compounds were detected. Mineralization of the dye was followed by TOC measurements. Relatively low degradation efficiency (50 % after 6 h of irradiation) indicates that ultrasound is rather inefficient in overall degradation, when used alone. [106]

Table 13. Decoloration of reactive dyes with ultrasound and ultrasound/H₂O₂

<i>Textile dye</i>	<i>AOP type</i>	<i>Time/h</i>	<i>Decoloration/%</i>
C.I. Reactive Blue 220	Ultrasound	7	70.4
C.I. Reactive Black 5	Ultrasound	7	96.2
Remazol Dark Black N	Ultrasound	7	74.9
C.I. Reactive Blau 28	Ultrasound	7	57.4
C.I. Reactive Red 22	Ultrasound	7	81.5
C.I. Reactive Yellow 15	Ultrasound	7	91.0
C.I. Reactive Blue 220	Ultrasound/H ₂ O ₂	4	93.4
C.I. Reactive Black 5	Ultrasound/H ₂ O ₂	4	98.6
Remazol Dark Black N	Ultrasound/H ₂ O ₂	4	92.2
C.I. Reactive Blau 28	Ultrasound/H ₂ O ₂	4	91.0
C.I. Reactive Red 22	Ultrasound/H ₂ O ₂	4	96.7
C.I. Reactive Yellow 15	Ultrasound/H ₂ O ₂	4	96.1

SHORT CONCLUSION

For decoloration and degradation of textile wastewaters many physical, chemical and biological methods have been developed. Every existing technology presents limits; advantages and disadvantages. The composition of textile wastewater is very complex, so the use of a universal wastewater treatment seems to be impossible. Which decoloration process will be used depend on the wastewater characteristic (type, dye concentration and auxiliaries, pH). A single wastewater treatment system is unable to overcome all problems by itself to provide an efficient treatment of effluents and be also cost effective.

REFERENCES

- [1] EPA Report. Best management practices for pollution prevention in the textile industry. EPA Manual 625/R-96-004, 1996.
- [2] Zollinger, H. *Colour Chemistry-Synthesis, Properties of Organic Dyes and Pigments*, VCH Publishers, New York, 1987, pp. 92-100.
- [3] Easton J. The dye marker's view. In: Cooper P, editor. *Colour in dyehouse effluent*. Bradford, UK:Society of Dyers and Colourist; 1995. p.11.
- [4] Hao, O. J., Kim, H., Chiang P. *Crit. Rev. Environ. Sci. Technol.*, 2000, 30, 449-502.
- [5] Mathur, N., Bhatnagar, P., Bakre, P. *Applied ecology and environmental research*, 2005, 4(1), 111-118.
- [6] Brown, M. A., DeVito, S. C. *Crit. Rev. Environ. Sci. Technol.*, 1993, 23(3), 249-324.
- [7] Jäger, I, Hafner, C., Schneider, K. *Mutation Research*, 2004, 561, 35-44.
- [8] Schneider, K., Hafner, C., Jäger, I *J. Appl. Toxicol.*, 2004, 24(2), 83-91.
- [9] Platzek, T, Lang, C., Grohmann, G., Gi, U-S, Baltes, W. *Hum. Exp. Toxicol.*, 1999, 18, 552-559.

- [10] Pratt, M., Taraska, V. *Am. J. Contact Dermatitis*, 2000, 11(1), 30-41.
- [11] Estlander, T. *Contact Dermatitis*, 1988, 18(5), 290-297.
- [12] Wilkinson, S.M., McGechaen, K. *Contact Dermatitis*, 1996, 35(6), 376-378.
- [13] Zuskin, E., Mustajbegovic, J., Schachter, E. N., Doko-Jelinic, J. *Am. J. Ind. Med.*, 1998, 31(3), 344-352.
- [14] Majcen Le Marechal, A., Slokar, Y. M., Lobnik, A. *Tekstilec*, 1996, 39, 4-10.
- [15] Santos, A. B., Cervantes, J. F., Lier, J. B. *Bioresource Technnology*, 2007, 98(12), 2369-2385.
- [16] Nassar, N. M., El-Geundi M. S., *J. Chem. Technol. Biotechnol.*, 1991, 50, 257-264.
- [17] Raghavacharya, C., *Chem. Eng. World*, 1997, 32(7), 53-54.
- [18] Robinson, T., McMullan, G., Marchant, R., Nigman, P. *Bioresource Technology*, 2001, 77, 247-255.
- [19] Pagga, U. and Taeger, K. *Wat. Res.*, 1994, 28(5), 1051-1057.
- [20] Poots, V.J.P., McKay, G., Healy, J.J. *Wat Res.* 1976, 10, 1067-1070.
- [21] Poots, V.J.P., McKay, G., Healy, J.J. *Wat Res.* 1976, 10, 1061-1066.
- [22] McKay, G., Blair, H. S, Gardner, J.R. *J. Appl. Polym. Sci.* 1982, 27, 3043-3057.
- [23] Al-Duri, B., McKay, G., El Geundi, M. S., Abdul Wahab, M.Z. *J. Environ. Eng.* 1990, 116, 487-502.
- [24] Malmay, G., Perineau, F., Molinier, J., Gaset, A. *J. Chem. Tech. Biotechnol.*, 1985, 35A, 431-437.
- [25] Nigam, P., Armou, G., Banat, I.M, Singh, D., Marchant, R. *Biores. Technol.*, 2000, 72, 219-226.
- [26] El Geundi, M. *Wat. Res.*, 1991, 25, 271-273.
- [27] Namasivayam, C., Kanachana, N., Yamuna, R. T. *Waste Manage.*, 1993, 13, 89-95.
- [28] McKay G., Ramprasad G., Mowli, P. *Wat. Res.*, 1987, 21, 375-377.
- [29] Mishra, G., Tripathy, M., *Colourage*, 1993, 40, 35-38.
- [30] Xu, Y., Lebrun, R. E., *Sepa. Sci. Technol.* 1999, 34, 2501-2519.
- [31] Lee, R. *Water Wastewater*, 2000, 141, 29-32.
- [32] Anjaneyulu, Y., Sreedhara Chary, N., Samuel Suman Raj, D. *Reviews in Environmental Science and Bio/Technology*, 2005, 4, 245-273.
- [33] Gnann, A., Gregor, C. H. Schelle, S., Chemical oxidative process for purifying highly contaminated wastewater, WO Patent 93/08/29 (1993), to Peroxide-Chemie GmbH, Germany.
- [34] Slokar, Y. M., Majcen Le Marechal, A. *Dyes Pigm.*, 1997, 37(4), 335-356.
- [35] García-Montaño, J., Torrades F., García-Hortal, J. A., Domènech, X., Peral, J. *Journal of Hazardous Materials*, 2006, 134(1-3), 220-229.
- [36] Torrades, F., García-Montaño, J., García-Hortal, J. A., Núñez, L., Domènech, X., Peral, J. *Coloration Technology*, 2004, 120(4), 188-194.
- [37] Zhao, W., Shi, H., Wang, D. *Chemosphere*, 2004, 57, 1189-1199.
- [38] Science Applications International Corp., *Electrotechnologies for Waste and Water Treatment*. Electric Power Research Institute, Palo Alto, CA, 1987, p. 4.
- [39] Oguz, E., Keskinler, B., Celik, Z. *Dyes Pigm.*, 2005, 64, 101-108.
- [40] Rice, R. G., Bollyky, L.J., Lacy, W. J. *Analytical Aspects of Ozone Treatment of Water and Wastewater*. Lewis, Chelsea, MI, 1986, p. 7.
- [41] Mallevialle, J., *Ozonation Manual for Water and Wastewater treatment*, John wiley and Sons, New York, 1982, p. 53.

- [42] Perkins, W. S. Judkins, J. F., Perry, W. D., *Textile Chemist and Cholorist*, 1980, 12(8),27.
- [43] Namboodri, C. G., Perkins, W. S, Walsh W. K. *American Dystuff Reporerter*, 1994, 83, 17-26.
- [44] Marmagne, O., Coste, C. *American Dystuff Reporter*, 1996, 85(4), 15-21.
- [45] Liakou, S., Pavlou, S., Lyberatos, G. *Water Sci. Technol.*, 1997, 35(4), 279-286.
- [46] Hoigne, J., Bader, H. *Wat. Res.*, 1983, 17(2), 185-194.
- [47] Shu, H. Y and Huang, C. R. *Chemosphere* 1995, 39, 3813-3825.
- [48] Perkowski, J., Kos, L. *Fibres and Textiles in Eastern Europe*, 2003, 11, 67-71.
- [49] Bes-Pia, A., Mendoza-Roca, J.A., Roig-Alcover, L., Iborra-Clar, A., Iborra-Clar, M.I., Alcaina-Miranda, M.I. *Desalination*, 2003, 157, 81-86.
- [50] Tuhkanen, T. A., UV/H₂O₂ processes, In: Parson, S editor *Advanced Oxidation Processes for Water and Wastewater treatment*, 2004, IWA Publishing, London, pp 86-92.
- [51] Pittroff, M, Greorg, K. H. *Melliand English 6*, translation of *Melliand Textilberichte*, 1992, 73, 526.
- [52] Ince, N. H., Görnec, D. T, *Environ. Technol.* 1997, 18, 179-185.
- [53] Shu, H.Y., Huang, C.R., Ultraviolet enhanced oxidation for color removal of azo dye wastewater. *American Dystuff Reporter*, 1995, 84(8), 30-34.
- [54] Georgiou, D., Melidis, P., Aivasidis, A., Gimouhopoulos, K. *Dyes Pigm*, 2002, 52(2), 69-78.
- [55] Neamtu, M., Siminiceanu, I., Yediler, A., Kettrup, A. *Dyes Pigm*, 2002, 53(2), 93-99.
- [56] Galindo C., Kalt A. *Dyes Pigm s*, 1999, 42(3), 199-207.
- [57] Colonna, G.M., Caronna, T, Marcandalli, B. *Dyes Pigm*, 1999, 41(3), 211-220
- [58] Yang, Y. Q., Wyatt, D. T., Bahorsky, M. *Text. Chem. Color*, 1998, 30, 27-35.
- [59] Alaton, I. A., Balcioglu, I. A., Bahnemann, D. W. *Wat. Res.*, 2002, 36, 1143-1154.
- [60] Namboodri, C.G., Walsh, W.K. *American Dystuff Reporter*, 1996, 85(3), 15-25.
- [61] Vajnhandl, S., Majcen Le Marechal, A., *Dyes Pigm*, 2005, 65, 89-101.
- [62] Forgacs, E. Cserhati, T., Oros, G. *Environment International*, 2004, 30, 953-971.
- [63] Pearce, C. I., Lloyd, L. R, Guthrie, J. T. *Dyes Pigm*, 2003, 58, 179-196.
- [64] Heiss G.S., Gowan B. and Dabbs E.R. *FEMS Microbiology Letters*, 1992, 99, 221-226.
- [65] Shaul G.M., Holdsworth T.J., Demmpsey C.R. and Dostal K.A. *Chemosphere*, 1991, 22: 107-119.
- [66] Govindaswami M., Schmidt T.M., White D.C., Loper J.C. *Journal of Bacteriology*, 1993, 175(18), 6062-6066.
- [67] Horitsu H., Takada M., Idaka E., Tomoyeda M., Ogawa T. *European Journal of Applied Microbiologyand Biotechnology*, 1977, 4, 217-224.
- [68] Wong P.K., Yuen P.Y. *Water Research*, 1996, 30(7): 1736-1744.
- [69] Zissi U., Lyberatos G., Pavlou S. *Journal of Industrial Microbiology and Biotechnology*, 1997, 19(1), 49-55.
- [70] Lyons C.D., Katz S., Bartha R. *Applied and Environmental Microbiology*, 1984, 48(3), 491-496.
- [71] Stolz A., Nortemann B., Knackmuss H.J. *Biochemical Journal*, 1992, 282(3), 675-680.

- [72] Loidl M., Hinteregger C., Ditzelmuller G., Ferschl A., Streichsbier F. *Archives of Microbiology*, 1990, 155(1), 56-61.
- [73] Baird R., Camona L., Jenkins R.L. *Journal WPCF*, 1977, july, 1609-1615.
- [74] Allan R. and Roxon J.J. *Xenobiotica*, 1974, 4(10) 637-643.
- [75] Brown J.P. *Applied and Environmental Microbiology*, 1981, 41(5), 1283-1286.
- [76] Chung K.T., Stevens S.E.J., Cerniglia C.E. *Critical Reviews in Microbiology*, 1992, 18(3), 175-190.
- [77] Brown D. and Laboureur P. *Chemosphere*, 1983, 12(3), 397-404.
- [78] Beydilli M.I., Pavlostathis S.G., Tincher W.C. *Water Science and Technology*, 1998, 38(4-5), 225-232.
- [79] Donlon B.A., Razo-Flores E., Luijten M., Swarts H., Lettinga G., Field J.A. *Applied Microbiology and Biotechnology*, 1997, 47(1), 83-90.
- [80] Haug W., Schmidt A., Nortemann B., Hempel D.C., Stolz A., Knackmuss H.J. *Applied and Environmental Microbiology*, 1991, 57(11), 3144-3149.
- [81] Rafii F., Franklin W., Cerniglia C.E. *Applied and Environmental Microbiology*, 1990, 56(7), 2146-2151.
- [82] Gingell R. and Walker R. *Xenobiotica*, 1971, 1(3), 231-239.
- [83] Kudlich M., Keck A., Klein J., Stolz A. *Applied and Environmental Microbiology*, 1997, 63(9), 3691-3694.
- [84] Mechsner K. and Wuhmann K. *European Journal of Applied Microbiology and Biotechnology*, 1982, 15, 123-126.
- [85] Wuhmann K., Menscher K., Kappeler T. *European Journal of Applied Microbiology and Biotechnology*, 1980, 9, 325-338.
- [86] Carliell C.M., Barclay S.J., Naidoo N., Buckley C.A., Mulholland D.A., Senior E. *Water SA*, 1995, 21(1), 61-69.
- [87] Razo-Flores E., Luijten M., Donlon B.A., Lettinga G., Field J.A. *Environmental Science and Technology*, 1997, 31(7), 2098-2103.
- [88] Carliell C.M., Barclay S.J., Buckley C.A. *Water SA*, 1996, 22, 225-233.
- [89] Chinwekitvanich S., Tuntoolvest M., Panswad T. *Water Research*, 2000, 34(8), 2223-2232.
- [90] Carliell C.M., Barclay S.J., Shaw C., Wheatley A.D., Buckley C.A. *Environmental Technology*, 1998, 19(11), 1133-1137.
- [91] Willetts J.R.M., Ashbolt N.J., Moosbrugger R.E., Aslam M.R. *Water Science and Technology*, 2000, 42(5-6), 309-316.
- [92] Carliell, C.M.; Barclay, S.J.; Naidoo, N.; Buckley, C.A.; Mulholland, D.A.; Senior, E. *Water SA*, 1994, 20(4), 341.
- [93] Hu, T.L. *Bioresource Technology*, 1994, 49(1), 47-51.
- [94] Van der Zee, F. P., Lettinga, G., Field, J. A. *Chemosphere*, 2001, 44(5), 1169-1176.
- [95] Kalyuzhnyi S., Sklyar V., Mosoloava T., Kucherenko I., Russkova J.A., Degtyaryova N. *Water Science and Technology*, 2000, 42, 363-370.
- [96] Kuhn E.P. and Suflita J.M. *Hazardous Waste and Hazardous Materials*, 1989, 6(2), 121-134.
- [97] Razo-Flores E., Lettinga G. and Field J.A. *Biotechnology Progress*, 1999, 15(3), 358-365.
- [98] Zitomer D.H., Speece R.H. *Environmental Science and Technology*, 1993, 27(2), 227-244.

-
- [99] Field J.A., Stams A.J.M., Kato M., Schraa G., *Antonie van Leeuwenhoek*, 1995, 67, 47-77.
- [100] Majcen Le Marechal, A., Slokar, Y. M., Taufer, T., *Dyes Pigm.*, 1997, 33(4), 281-298.
- [101] Slokar, Y., M., Zupan, J., Majcen Le Marechal, A., *Dyes Pigm.*, 1999, 42, 123-135.
- [102] Kurbus, T., Slokar, Y., M., Majcen Le Marechal, A., *Dyes Pigm.*, 2002, 54, 67-78.
- [103] Kurbus, T., Slokar, Y., M., Majcen Le Marechal, A., Brodnjak Vončina, D., *Dyes Pigm.*, 2003, 58, 171-178.
- [104] Kurbus, T., Majcen Le Marechal, A., Brodnjak Vončina, D., *Dyes Pigm.*, 2003, 58, 245-252.
- [105] Brodnjak Vončina, D., Majcen Le Marechal, A., *Dyes Pigm.*, 2003, 59, 173-179.
- [106] Vajnhandl, S., Majcen Le Marechal, A., *J. hazard. mater.*, 2007, 41(1), 329-335.

Chapter 7

**NON-CONVENTIONAL SORBENTS FOR THE DYE
REMOVAL FROM WATERS:
MECHANISMS AND SELECTED APPLICATIONS**

Pavel Janoš

Faculty of the Environment, University of J. E. Purkyně, Králova Výchina 7,
400 96 Ústí nad Labem, Czech Republic

ABSTRACT

Synthetic dyes that are extensively used in various industrial branches represent a serious environmental problem when they are emitted into the effluents as they are hardly biodegradable in conventional wastewater treatment plants. Therefore, alternative methods for decolouration of the wastewaters are developed, among them adsorption on solid sorbents is one of the most effective ones. Because the conventional sorbents such as activated carbon are rather expensive for large-scale applications, various low-cost materials have been tested as alternative non-conventional sorbents for the dye removal from waters. Numerous natural materials (zeolites, clays), industrial wastes (fly ash, iron slag), agrowastes or biosorbents exhibit a sufficient ability to retain various kinds of dyes from aqueous solutions and are available (locally and sometimes also globally) in great quantities and at low prices, and thus they can be used potentially for the treatment of the dye-containing effluents. A brief review of the non-conventional sorbents for the dye removal is given in this article together with selected applications. It should be emphasized that the dye sorption onto non-conventional sorbents is a rather complex process in which several mechanisms may be effective simultaneously. Effects of principal operational parameters on the dye sorption are discussed in the article, such as an effect of pH (governing both the dissociation/protonation of the active groups on the sorbent surface as well as side equilibria in solution), the presence of inorganic salts or surfactants. Basic equations describing the sorption equilibria (sorption isotherms) are presented. The results of kinetic measurements that allowed (in some cases) to identify a rate-limiting step of the overall sorption process are also mentioned in this chapter.

Keywords: Synthetic dyes; Adsorption; Non-conventional sorbents; Wastewater treatment

1. INTRODUCTION

Great amounts of synthetic dyestuffs are emitted into wastewaters from various industrial branches, such as from dye manufacturing and textile finishing, causing a serious environmental problem because of their poor biodegradability in conventional wastewater treatment plants. The release of coloured effluents into the environment is undesirable not only from aesthetic reasons, but also because many dyes and their degradation products are toxic or mutagenic to life. Without adequate treatment these dyes are stable and can remain in the environment for tens of years (des Santos et al., 2007).

Synthetic dyes may be classified according to their application and chemical structure. They are composed of groups of atoms responsible for the dye colour, called chromophores, as well as an electron withdrawing or donating substituents that modify or intensify the colour of the chromophores, called auxochromes. The most important chromophores are azo (-N=N-), carbonyl (-C=O), methine (-CH=), nitro (-NO₂) and quinoid groups. The most important auxochromes are amine (-NH₂), carboxyl (-COOH), sulfonate (-SO₃H) and hydroxyl (-OH) (des Santos et al., 2007). It was estimated that the azodyes represent about 70% of the total dye production in the world (Zollinger, 1978). Because of the presence of various ionic or ionisable groups, the dyes exhibit (usually) a very good solubility in water. The ionisable groups bear either positive or negative charges. Thus the dyes behave like large organic cations (basic dyes) or anions (acid dyes) in aqueous solutions.

Traditional wastewater treatment technologies have proven to be markedly ineffective for handling the effluents containing synthetic dyes because of the chemical stability of these pollutants (Forgacs et al., 2004). Up to now, there is no single and economically attractive method for decolourisation of textile wastewaters, although notable achievements were made in the use of biotechnological approaches to this problem in recent years, as reviewed by dos Santos et al. (2007). In addition to the biological treatment, many physical and chemical methods have been employed for the dye removal from wastewaters, including coagulation, flocculation, filtration, oxidation or reduction, complex-formation or neutralization (Slovak and Le Marechal, 1998; Forgacs et al., 2004). Advantages and drawbacks of some non-biological decolourisation processes are summarised briefly in Table 1. Very often, more sophisticated treatment strategies utilizing combined techniques (e.g. membrane microfiltration together with adsorption) are used to remove the dyes from complex industrial effluents (Jirankova et al., 2007). Novel adsorption/oxidation, adsorption/reduction and other combined processes were reviewed recently by Qu (2008), whereas Wojnarovits and Takacs (2008) reviewed the radiation-induced degradation processes for the removal of azodyes from waters.

Adsorption techniques employing solid sorbents are widely used to remove certain classes of chemical pollutants from waters. Currently, the most commonly used adsorption agent in industry is activated carbon that was successfully tested also for the removal of various kinds of synthetic dyes. However, relatively high operating costs and problems with regeneration of the spent activated carbon hamper its large-scale applications. Therefore, a number non-conventional sorbents have been tried for the treatment of wastewaters. Typically, various industrial wastes, agrowastes or natural materials available in great amounts at low prices are classified as alternative sorbents for the removal inorganic (e.g. heavy metals) as well as organic pollutants from wastewaters (Bailey et al., 1999; Babel and

Kurniawan, 2003; Kurniawan et al., 2006; Crini, 2006). Some of these materials will be overviewed briefly in the following chapter.

Table 1. Some non-biological methods for the removal of synthetic dyes from waters (adapted from dos Santos et al., 2007)

Method	Principle	Advantages	Disadvantages
Fenton reaction	Oxidation using mainly H_2O_2 -Fe(II)	Effective decolourisation of soluble and insoluble dyes	Sludge generation
Ozonation	Oxidation with ozone gas	Application in gaseous state – no alteration of volume	Short half-life (20 min.)
Photochemical degradation	Oxidation using mainly H_2O_2 -UV	No sludge production	Formation of by-products
Electrochemical destruction	Oxidation using electricity	Usually non-hazardous products	High cost of electricity
Membrane filtration	Removal of all dye types	Concentrated sludge production	
Ion exchange	Retention on ion exchange resins	Possible regeneration without a loss of efficiency	Not effective for all dyes
Electrokinetic coagulation	Coagulation with FeSO_4 / FeCl_3	Economically feasible	High sludge production

2. OVERVIEW OF NON-CONVENTIONAL SORBENTS

Since its first introduction in the 1940's, *activated carbon* has become the standard adsorbent frequently utilized for the removal of organic and inorganic pollutants in water industry (Pollard et al., 1992), (and as such, it may be hardly called a “non-conventional” sorbent). The term activated carbon is used to include a broad range of carbonaceous materials which exhibit a high degree of porosity and extended interparticulate surface area. Active carbons can be prepared from a huge variety of carbon-containing feedstocks. The production process involves usually carbonisation of the raw material below 800°C in the absence of oxygen typically followed by activation at elevated temperatures in the oxidising atmosphere (steam, carbon dioxide or air). Sometimes, chemical catalysts are used to modify the surface reactivity of the product.

The most common feedstocks for the commercial production of activated carbon are wood, anthracite or bituminous coal (Pollard et al., 1992). However, many alternative raw materials, such as various wastes from industry or agriculture, have been used to prepare activated carbon utilizable as a sorbent in wastewater treatment, as reviewed by Pollard et al.(1992), or more recently by Dias et al. (2007). The non-conventional activated carbons were prepared e.g. from peach stones by the H_3PO_4 treatment at 500°C and used for the removal of Methylene Blue from aqueous solution (Attia et al., 2008), or by the sulphuric

acid treatment method from *Parthenium* biomass and used to remove another basic dye – Rhodamine B (Lata et al., 2008). Activated carbon prepared from oil palm shell was used for an adsorption of Methylene Blue (Tan et al., 2008), whereas jute fiber carbon was used for an adsorption of Eosin Yellow, Malachite Green and Crystal Violet (Porkodi and Kumar, 2007). Effective adsorbents with high adsorption capacity for large molecules including reactive dyes were prepared by the steam-activation method from several solid wastes, namely from waste PET, waste tires, refuse derived fuel and wastes generated during lactic acid fermentation from garbage (Nakagawa et al., 2004).

Among naturally occurring biosorbents, *chitin* is the second abundant biopolymer after cellulose. However, more important than chitin is *chitosan*, which has a molecular structure similar to cellulose and exhibits an excellent sorption ability for the dye retention (Crini, 2006). Chitosan can be prepared by alkaline deacetalation of chitin, which is widely found of the exoskeleton of shellfish and crustaceans. It is available in great amounts as a waste product from fishery industry. It was demonstrated that chitosan is especially suitable for the sorption of reactive and acid dyes – reported sorption capacities ranged from ca. 300 to 2500 mg/g (Crini, 2006). A certain limitation of chitosan as sorbent consists in its solubility in acidic media. To avoid this problem, chemically modified (mostly crosslinked) chitosan-based sorbents were developed and utilised e.g. for the sorption of Methyl Orange (Morais et al., 2007). Crosslinked chitosan prepared by persulfate induced free radical polymerization was used as sorbent for basic dyes (Lazaridis et al., 2007). This modification improved considerably the rates of the dye sorption. An effect of the degree of deacetylation on the sorption ability of chitosan towards acid dyes was studied by Wong et al. (2008). It was shown that the highly deacetylated product exhibited reduced sorption ability, probably due to the changes in the internal structure of chitosan.

Attractive biosorbents with unique sorption properties can be prepared from *beta-cyclodextrin*, a torus-shaped cyclic oligosaccharide with an internal hydrophobic cavity. Thanks to this structure, cyclodextrins are capable to form inclusion complexes and thus retain various pollutants through host-guest interactions. The cyclodextrin-based sorbents are prepared by crosslinking, typically with epichlorhydrin (Crini, 2008). The cyclodextrin polymer exhibited good sorption capacities for basic dyes in the range of ca. 36 to 53 mg/g (Crini, 2008) and can be used also for the sorption of azodyes (Ozmen et al., 2008).

Zeolites are naturally occurring crystalline aluminosilicates consisting of a framework of tetrahedral molecules, linked with each other by shared oxygen atoms. A negative charge on the three dimensional lattice is balanced by cations that are exchangeable with the cations in solution. Zeolites consist of a wide variety of species such as clinoptilolite and chabazite. During 1970's, natural zeolites gained a significant interest among scientists due to their ion-exchange capability that was frequently employed for the removal of metal ions from waters and industrial effluents (Babel and Kurniawan, 2003; Kurniawan et al., 2006). Numerous studies confirmed an ability of zeolites to retain various kinds of dyes from aqueous solutions (Armagan et al., 2004; Benkli et al., 2005; Meshko et al., 2001; Ozdemir et al., 2004; Wang et al., 2006), although the sorption capacities (especially for reactive dyes) were rather low (Armagan et al., 2004; Crini, 2006). More advantageous for the dye removal seem to be *clays* and *clay minerals*. There are several classes clays such as smectites (montmorillonite, saponite), mica (illite) kaolinite, serpentine, pyrophyllite (talc), vermiculite and sepiolite (Shichi and Takagi, 2000). The adsorption capacities result from a net negative charge on the layered structure of minerals. Bentonite and other clay materials were used for the treatment

of coloured wastewaters (Al-Bastaki and Banat, 2004; Al-Ghouti et al., 2003; Alkan et al., 2005; Atun et al., 2003; Ozcan et al., 2004; Li et al., 2007; Yue et al., 2007). The adsorption of ionic dyes onto the clay materials is governed by the ion-exchange mechanism and is strongly pH-dependent. Under common conditions, the sorption capacities for basic (cationic) dyes are higher than those for acid (anionic) ones. The retention of 300 mg/g (monolayer capacity) of Basic Blue 9 onto bentonite was reported by Bagane and Guiza (2000).

Inorganic materials such as zeolites or clays allow a relative simple physical or chemical regeneration. Wang et al. (2006) compared a chemical treatment based on the Fenton oxidation with high temperature combustion as methods for the regeneration of zeolite-based sorbents loaded with basic dye (Methylene Blue). The high-temperature treatment was more effective for the regeneration of synthetic zeolites. For natural zeolites, on the other hand, both regeneration methods gave comparable results, but the original adsorption capacity was not fully recovered – only 60% of the capacity of the fresh sample was achieved.

The surface properties of clays (and less often also other inorganic sorbents) and thus their sorption ability may be altered effectively by modification with surfactants. So called organo-clays are synthesised by exchanging the inorganic cations in the structure of the clay mineral with large organic cations, typically with quaternary ammonium compounds. In this way, Wibulswas (2004) modified the properties of montmorillonite with tetramethylammonium chloride, tetradecyltrimethylammonium bromide, hexadecyltrimethylammonium bromide and benzyldimethylhexadecylammonium chloride, and tested the sorption ability of the prepared sorbents for Methylene Blue. The treatment with surfactants converts the clay surface from organophobic to organophilic in dependence on a number of carbon atoms in the chain of the surfactant molecule. Sepiolite modified with quaternary amines exhibited a high sorption capacity for reactive dyes (Everzol Black B, Everzol Red 3BS, Everzol Yellow 3RS), on contrary to unmodified sepiolite that was almost ineffective (Armagan et al., 2003). A mechanism involving electrostatic attraction of the anionic groups of dye molecules onto the oppositely charged amine-modified sepiolite surface was proposed to be responsible for the uptake of dyes. Cetyltrimethylammonium-bentonite was used for removing an industrial dye Supranol Yellow 4GL from wastewater (Khenifi et al., 2007). The same dye was retained also on pillared clays in the presence of non-ionic surfactants (Bouberka et al., 2005). Several textile dyes were removed successfully from water using hexydecyltrimethylammonium-bentonite as sorbent (Ceyhan and Baybas, 2001). A clay mineral hectorite was modified with cetyltrimethylbenzylammonium chloride and cetylpyridinium chloride and used for an adsorption of an anionic dye Reactive Orange 122 (Baskaralingam et al., 2007). Dodecyltrimethylammonium cation was used to prepare organophilic clays capable to retain Rhodamine 6G (Salleres et al., 2008). A thiol-functionalized clay was prepared by the covalent grafting of 3-mercaptopropyltrimethoxysilane onto the surface of a natural smectite clay mineral. A significant enhancement of the adsorption capacity towards Methylene Blue was observed with the clay bearing thiol groups in comparison with the unmodified one (Tonle et al., 2008). A composite clay-based sorbent was prepared by polymerization of acrylamide with 2-acrylamido-2-methyl-1-propanesulfonic acid and bentonite and tested for the sorption of basic dyes, such as Lauths Violet (Kundakci et al., 2008). An enhanced hydrophobicity of the surface of bentonite was achieved by intercalation of cationic polyelectrolyte polyepichlorhydrin-dimethylamine into the clay structure (Yue et al., 2007), causing better properties for the sorption of Reactive Blue K-GL (Li et al., 2007). Quaternary ammonium cations

(tetraethylammonium-, hexadecyltrimethylammonium-, benzyldimethyltetradecylammonium-) were used also for the modification of the surface properties of fly ashes (Banerjee et al., 2006). The surface modification enhanced considerably the sorption of anionic dyes. Activated carbon modified with cationic surfactant (cetylpyridinium chloride) exhibited a higher sorption capacity for Reactive Black 5 in comparison with the untreated carbon (Choi et al., 2008). Somewhat different strategy was suggested by Eren and Afsin (2008), who employed bentonite pre-treated with divalent metal cations (Ni^{2+} , Co^{2+} , Zn^{2+}) for an adsorption of the basic dye Crystal Violet.

Various *industrial by-products* and *solid wastes* can be advantageously used as alternative sorbents because of their low-cost and local availability. For example, carbon slurry from fertilizer plants and blast furnace slag from steel plants were converted into low-cost sorbents by Gupta et al. (2003) and used for the removal of basic dyes (Basic Red 9) from wastewaters. Ramakrishna and Viraraghavan (1997) tested various low-cost materials available in Canada (peat, steel plant slag, bentonite clay, fly ash) for the removal of acid as well as basic dyes and found the capacities comparable with activated carbon. Waste newspaper was used for the removal of Methylene Blue in a special arrangement utilizing sono-sorption (Entezari and Al-Hoseini, 2007).

Fly ash is a waste material from thermal power plants and numerous other combustion processes that is found in abundance in the world and can be used as a low-cost sorbent for the dye adsorption and destruction from wastewaters (Wang and Wu, 2006), as well as in other technologies for the water pollution control (Viraraghavan and Dronamraju, 1992). The coal fly ash consists typically of silica (SiO_2), alumina (Al_2O_3) and iron oxides, with varying amounts of carbon, calcium, magnesium and sulphur. Two general classes of fly ash are recognised for coal combustion: Class F normally produced from anthracite, bituminous or sub-bituminous coals and containing less than 7 % CaO, and Class C normally produced from lignite coals, containing more lime (5-30%). Fly ash has a hydrophilic surface and porous structure. Unburned carbon plays a significant role in retaining less polar compounds, but also of ionic dyes (Wang and Li, 2007), on the fly ash surface. It was shown that both acid as well as basic dyes can be removed effectively from aqueous solution using coal fly ashes as adsorbents (Janoš et al., 2003). The high lime fly ash was used for an adsorption of Reactive Black 5 (Eren and Acar, 2007). Kumar et al. (2005) have found a relatively low capacity (5.7 mg/g) for the sorption of Methylene Blue onto coal fly ash. Recently, Lin et al. (2008) demonstrated that a treatment of the fly ash with sulphuric acid increased its specific surface area and the sorption capacity for basic dyes. The adsorption capacities in the range of 135-180 mg/g were reported for the reactive dye Remazol Brilliant Blue, but significantly lower values were obtained for Remazol Red or Rifacion Yellow (Dizge et al., 2008). Bottom ash was also used as a sorbent for the removal of dyes, e.g. basic fuchsin (Gupta et al., 2008).

Highly effective sorbents were prepared from *peat* and *low-rank coals* – materials containing *humic substances* as an active constituent. Peat is a complex material containing lignin, cellulose, fulvic acids and humic acids as its major constituents. These compounds carry polar functional groups such as alcohols, aldehydes, carboxylic and phenolic groups, which are responsible for binding chemical pollutants of ionic nature. Because of the presence of non-polar moieties in the structure of humic substances (aliphatic chains, condensed aromatic rings), these compounds are capable to retain also less polar pollutants to some extent. As pointed out by Nandi and Walker (1971), mineral constituents always present in the coal- and peat-based sorbents play a significant role in binding chemical pollutants,

including synthetic dyes. Peat was used for the removal of basic as well as acid dyes from aqueous solutions (Poots et al., 1976a; Allen et al., 1989; Ho and McKay, 1998a; Ho and McKay, 1998b; Ho and McKay, 2003). Poots and McKay (1979) deduced from kinetic measurements that the basic dye adsorption is predominantly a chemisorption process involving exchange sorption reaction with the hydroxylic groups in humic and fulvic acids, lignin and cellulose, whereas the acid dye adsorption is probably a physical process, in which coulombic forces are involved.

Naturally occurring kind of weathered and oxidised young brown coal called oxihumolite was used for an adsorptive removal of basic (Methylene Blue, Malachite Green) as well as acid (Egacid Orange, Midlon Black) dyes from waters. The maximum sorption capacities ranged from 0.070 mmol/g (for Midlon Black) to 0.278 mmol/g (for Malachite Green) and did not differ significantly for basic and acid dyes (Janoš et al., 2005). Karaca et al. (2005) studied the adsorption of Methylene Blue onto lignite–water interface and concluded that the adsorption is governed by physical interactions. Both basic as well as acid dyes were adsorbed also on chemically treated (sulfonated) coal (Mittal and Venkobachar, 1993). More complex composite sorbent in the form of humate/polyacrylamide/clay hydrogel was used for the removal of Methylene Blue from aqueous solutions (Yi and Zhang, 2008).

Sawdust and related waste materials from *timber industry* as relatively abundant, easily available and inexpensive sorbents have been used to remove unwanted chemical substances from waters, including dyes, oils, toxic salts and heavy metals – see a review of Shukla et al. (2002). Several authors tested various kinds of wood-based sorbents, e.g. sawdust from walnut and cherry tree, oak or pitch-pine (Ferrero, 2007), beech sawdust (Batzias and Sidiras, 2007a), cedar sawdust (Hamdaoui, 2006), pine sawdust (Özacar and Sengil, 2005) or spruce wood shavings (Poots et al., 1976b; Poots and McKay, 1979; McKay and Poots, 1980) for the removal of both basic as well as acid dyes from aqueous solutions. A composite sorbent (clay-wood mixture) was also effective in the basic dye retention (Yeddou and Bensmaili, 2005).

Diverse cellulose-based waste materials originate in great amounts from *agroindustry* and many of them can be used as sorbents for synthetic dyes, e.g. banana and orange peels (Annadurai et al., 2002), kohlrabi peel (Gong et al., 2007), olive pomace (Banat et al., 2007), deoiled soya (Gupta et al., 2008), yellow passion fruit waste (Pavan et al., 2008), rice husk (Vadivelan and Kumar, 2005; Kumar and Sivanesan, 2007), palm kernel fibre (Ofomaja, 2007), cotton fibre (Saleem et al., 2007), hazelnut shell (Ferrero, 2007) or silkworm pupa (Noroozi et al., 2008).

To improve a sorption ability of cellulose-based materials towards various kinds of chemical pollutants, some more or less sophisticated pre-treatment procedures have been developed. The sorption of basic dyes onto beech sawdust was enhanced after the sorbent pre-treatment with calcium chloride solution (Batzias and Sidiras, 2004); a similar effect exhibited also other inorganic salts, such as NaCl, MgCl₂ and ZnCl₂ (Batzias and Sidiras, 2007b). Other simple procedures utilized to modify the properties of biosorbents include the treatment with mineral acids and bases or their salts – HCl, NaOH, Na₂CO₃ (Kumar and Bandyopadhyay, 2006), Na₂HPO₄ (Ajmal et al., 1996) or H₂SO₄ (Taty-Costodes et al., 2003). More advanced modification procedures may introduce new active sites on the sorbent surface and enhance in this way its sorption capacity. For example, the ethylenediamine modified rice hull was applied successfully to remove basic and reactive dyes as well as metal cations from waters (Ong et al., 2007).

In recent time, *biosorption* become very popular as a promising technique for the removal and recovery of various chemical species from waters and effluents. It was defined as a property of certain molecules (or types of biomass) to bind and concentrate selected ions or molecules from aqueous solutions. Biosorption is a passive binding process utilizing dead biomass (or some molecules or their active groups) as biosorbent, on contrary to *bioaccumulation* that is a more complex process based on an active metabolic transport in(to) living organisms (Volesky, 2007). Biosorption has been established as an effective method especially for the recovery of metal ions from wastewaters, effluents and industrial solutions (Volesky and Holan, 1995). In numerous works, however, its ability to remove also various problematic organic pollutants (dyes, phenolic compounds, pesticides) was demonstrated, as reviewed by Aksu (2005). Diverse metabolism-independent processes may be effective in the binding of chemical pollutants to biosorbents, such as physical and chemical adsorption, electrostatic interaction, ion-exchange, complexation/chelation and microprecipitation or surface precipitation. As follows from a detailed discussion in the review of Aksu (2005), the biosorption ability depends strongly on the kind of dye and sorbent, as well as on operational conditions (pH, in the first place). Rather high sorption capacities above 100 mg/g were achieved with activated sludge for the removal of basic dyes from wastewaters (Chu and Chen, 2002). Various kinds of the inactivated fungal biomass were used for the removal of different industrial textile dyes (Prigione et al., 2008). Methylene Blue was retained successfully on a marine biomass *Posidonia oceanica* (Ncibi et al., 2007) or on an acid-treated weed *Parthenium hysterophorus* (Lata et al., 2007), whereas another basic dye – Basic Yellow – was retained on a green macroalga *Caulerpa scalpelliformis* (Aravindhan et al., 2007). A green macroalga *Caulerpa lentillifera* was used for the removal of different basic dyes (Astazon Blue, Astazon Red, Methylene Blue) from aqueous solutions and its sorption capacity was higher than the capacity of activated carbon for the same dyes (Marungrueng and Pavasant, 2007). Dried *Penicillium restrictum* biomass exhibited a sufficient sorption capacity close to 100 mg/g (at 20 °C) for the dye Reactive Black 5 (Iscen et al., 2007), which is comparable with the capacity of the NaOH pre-treated fungal biomass *Aspergillus foetidus* for the same dye (Patal and Suresh, 2008). The direct azodye Direct Brown was removed from aqueous solution by sorption onto the algal biosorbent *Spirogyra I02* (Mohan et al., 2008).

Mechanical, chemical and other pre-treatment procedures may improve sorption properties of various natural materials including biosorbents. Different procedures, such as milling and steam, ammonia or alkali steeping, were used to delignify the sorbent, or to increase its surface area (Robinson et al., 2002). The milling was identified as a cost effective procedure improving the dye removal efficiency. The brown seaweed *Laminaria* sp. biomass exhibited a considerably increased sorption capacity for Reactive Black 5 after an acid treatment with 0.1 M HCl (Vijayaraghavan and Yun, 2008). Nevertheless, the acid-treated sorbent (water hyacinth) was effective also in the removal of basic dye, namely Methylene Blue (El-Khaiary, 2007). A cationic sorbent was prepared by esterification of soybean hull by phosphoric acid with urea as catalyst, and used for the sorption of basic dyes Acridine Orange and Malachite Green (Gong et al., 2008). Methods for the preparation of adsorbents by the chemical modification of plant wastes were reviewed recently by Ngah and Hanafiah (2008).

During the past decade, a great attention has been paid to the development of new materials with unusual physical and chemical properties. *Nanosorbents* or *magnetic ion-exchangers* can serve as examples of advanced materials utilizable also in wastewater

treatment for the recovery of both inorganic as well as organic pollutants (Türker, 2007). One of the most important properties on nanomaterials is that a majority of atoms are on the surface of the nanoparticle. The surface atoms are unsaturated, and therefore, they have a high chemical activity and adsorption ability. Magnetic or magnetizable (nano)sorbents allow to develop new and more advantageous separation strategies employing modern magnetic technologies and highly effective permanent magnet systems (Borai et al., 2007). The magnetic nanosorbents are based typically on Fe_3O_4 (magnetite) nanoparticles prepared by co-precipitation of Fe^{2+} and Fe^{3+} ions under controlled conditions (Liao and Chen, 2002). It was also shown that some low-cost waste effluents (e.g. acid mine drainage) can be used as starting materials for the preparation of magnetite nanoparticles (Wei and Viadero, 2007). A magnetic $\text{MnO-Fe}_2\text{O}_3$ composite was used as a novel material for an adsorptive removal of the azodye Acid Red B from water with an adsorption capacity of 105 mg/g (Wu et al., 2005). The iron oxide magnetic nanoparticles are often used in the form of composites – polyacrylic acid-bound magnetic nanoparticles were used for an adsorption of Methylene Blue (Mak and Chen, 2004), similarly to the Fe_3O_4 -activated carbon nanocomposite (Yang et al., 2008). Both basic (Methylene Blue) as well as acid (Methyl Orange) dyes were removed from waters with the aid of magnetic alginate beads; the nanosorbent combined the adsorption properties of activated carbon with magnetic properties of iron oxide nanoparticles (Rocher et al., 2008).

It should be noted that some traditional and naturally occurring materials may be classified as nanosorbents, too, e.g. clay minerals. Adsorption properties of the clay-based nanosorbents (raw clays, activated clays, organoclays) for the adsorption of dyes were reviewed by Liu and Zhang (2007). Chitosan in the form of nanoparticles with particle sizes of 180 nm was used as an adsorbent for the dye Acid Green 27 (Hu et al., 2006), whereas a chitosan/montmorillonite nanocomposite was used for an adsorption of Congo Red (Wang and Wang, 2007).

As can be seen from the above presented overview, there is a great amount of various non-conventional sorbents utilizable potentially for the removal of synthetic dyes from wastewaters. Because of an enormous diversity of the sorbents on one side, and a complex nature of the dye-containing effluents on the other side, it is very difficult to establish generally applicable criteria for the selection of the best sorbent for a given purpose. Naturally, the price of the sorbent will be always one of the main parameters that should be considered. Unfortunately, reliable and mutually comparable prices of the alternative sorbents mentioned in this article are mostly unavailable. Market prices of some non-conventional sorbents can be found in the review of Babel and Kurniawan (2003). In addition to the sorbent purchase costs, many other economical aspects should be considered, such as transportation costs, costs for the sorbent pretreatment, costs for its regeneration or costs for damping/disposal of the spent sorbent, etc. The technical aspects that should be taken into account include, among others: an availability of the sorbent in a sufficient amount and a stable quality, its physico-mechanical properties and homogeneity, chemical stability under desired conditions (working range), durability during the sorption process, possibility to regenerate the spent sorbent, selectivity and/or a resistance against the presence of substances accompanying the dyes, etc.

Table 2. Methylene Blue sorption capacities on various sorbents

Sorbent	Capacity (mg/g)	Experimental conditions	Reference
Steam activated bituminous coal	580		El Quada et al., 2006
Activated carbon from rattan sawdust	294		Hameed et al., 2007
Fly ash	6.4		Wang et al., 2005
Natural zeolite	16		Wang et al., 2005
Diatomaceous silica	127	30 °C	Al-Qodah et al., 2007
Spent activated clay	109	45 °C	Weng and Pan, 2007
Coal fly ash	6.05	22 °C	Janoš et al., 2003
Low-rank coal	21.3	22 °C	Janoš et al., 2005
Fe(III)/Cr(III) hydroxide	22.8		Namasivayam and Sumithra, 2005
Montmorillonite	323		Wibulswas, 2004
Palm kernef fibre	672	24 °C, pH 5	Ofomaja, 2007
Cedar sawdust	142	20 °C	Hamadaoui, 2006
Crushed brick	97	20 °C	Hamadaoui, 2006
Fallen tree's leaves	81	22 °C, pH 4.5-10	Han et al., 2007
Mango seed kernel powder	143	30 °C	Kumar and Kumaran, 2005
Cereal chaff	20.3	25 °C	Han et al., 2006
Paper sludge	35.2		Hojamberdiev et al., 2008
Yellow passion fruit waste	44.7	25 °C	Pavan et al., 2008
Rice husk	44.6	32 °C	Vadivelan and Kumar, 2005
Pomelo peel(<i>Citrus grandis</i>)	345	30 °C	Hameed et al., 2008
Lemon peel	29		Kumar and Porkodi, 2006
Marine seaweed (<i>Caulerpa racemosa</i>)	5.23	18 °C	Cengiz and Cavas, 2008
Guava leaf powder(<i>Psidium guajava</i>)	295		Ponnusami et al., 2008
<i>Pospalum notatum</i>	31		Kumar and Porkodi, 2007
Green macroalga (<i>Caulerpa lentillifera</i>)	417		Marungrueng and Pavasant, 2007
Dead <i>Streptomyces rimosus</i>	34.3	20 °C	Nacera and Aicha, 2006
Immobilized <i>Corynebacterium glutamicum</i>	339	25 °C, pH 8	Vijayaraghavan et al., 2008

Probably the most important operational parameter for the selection of the sorbent is its capacity. Again, a direct comparison of the published values is somewhat questionable, as the measurements were often carried out under laboratory conditions (not always fully specified), and usually with pure (single-component) aqueous solutions of the examined dye. Moreover, only a limited number of data are typically available for any particular dye. Methylene Blue represents one of the exceptions, as it is probably the most frequently examined dye in

adsorption studies and data on its adsorption behaviour on various sorbents are readily available. It may be considered a typical representative of basic dyes. In Table 2, the sorption capacities for the sorption of Methylene Blue on selected sorbents are listed. Acid Orange 7, on the other hand, was selected as representative of acid dyes; the sorption capacities are listed in Table 3.

Table 3. Acid Orange 7 sorption capacities on various sorbents

Sorbent	Capacity (mg/g)	Experimental conditions	Reference
Activated carbon	0.40	25 °C, pH 5.8	Aber et al., 2007
Cross-linked chitosan	1940	30 °C, pH 4	Chiou et al., 2004
Coal fly ash	83	22 °C	Janoš et al., 2003
Low-rank coal	49	22 °C	Janoš et al., 2005
Spent brewery grains	30.5	30 °C	Silva et al., 2004
Macro alga <i>Azolla filiculoides</i>	110	pH 3	Padmesh et al., 2005
Macro alga <i>Azolla rongpong</i>	72.5	30 °C, pH 3	Padmesh et al., 2006

For an effective design of the adsorption unit, data on adsorption kinetics are necessary. It is also desirable to estimate the equilibrium characteristics (parameters of adsorption isotherms) and to take into account the operational parameters that may affect potentially the dye sorption, such as pH, the presence of inorganic salts, surfactants, or other side equilibria in aqueous phase. These items will be discussed in the following paragraphs.

3. MECHANISMS AND KINETICS OF THE DYE REMOVAL

Adsorption of the dye molecules on the surface of non-conventional sorbents, typically highly heterogeneous by its nature, is a rather complicated process, in which various mechanisms may be effective. Because of an ionic nature of the dye species in aqueous solutions, electrostatic forces – attraction or repulsion between the dye species and ionised active groups on the sorbent surface – play an important role. Both chemisorption as well as ion-exchange and other physical phenomena will participate in the dyes sorption process, but their proportions and significance may differ for different dyes and different kinds of sorbents (Poots and McKay, 1979; Mohan et al., 2008). Carboxylic and hydroxylic functional groups are commonly present in the structure of most natural sorbents. These groups undergo dissociation at suitable pH values, forming negatively charged sites on the sorbent surface, which facilitates the retention of cationic (basic) dyes. On the other hand, some popular sorbents, e.g. chitosan, contain aminogroups that may be protonated in acidic medium, which increase their positive charge, and thus their ability to bind anionic (acid) dyes (Morais et al., 2007). A significance of various functional groups in the process of the dye sorption was demonstrated by Gong et al. (2005), who used various chemical treatments (methylation, esterification, acetylation) to modify the sorption ability of biosorbent (peanut hull). Synthetic

dyes, as relatively large organic molecules containing usually several aromatic rings, may also exhibit a certain affinity towards less polar (organophilic) moieties that may be present in the structure of the non-conventional sorbents. Therefore, this kind of non-specific interactions should be also considered.

The dye sorption is usually a quite rapid process, in which most of the dye is retained in a time scale of a few hours or even (tens of) minutes, rather than days (McKay and Poots, 1980; Ho and McKay, 1998a,b; Eren and Acar, 2007; El-Khaiary, 2007; Marungrueng and Pavasant, 2007). To express the sorption kinetics in a mathematic form, two models are applied most often - a pseudo-first order model and a pseudo-second order model. These models are commonly used to describe the sorption of dyes as well as other pollutants (heavy metals) on solid sorbents, although, as pointed out by Ho and McKay (1998a), an application of a single kinetic model to the sorption on solid sorbents may be questionable because of a heterogeneity of the sorbent surfaces and diversity of sorption phenomena (transport, surface reactions). Recently, Azizian (2004) showed that the pseudo-first order kinetic model is more suitable for lower concentrations of solute, whereas the pseudo-second order model is more appropriate at high solute concentrations. A detailed discussion on applicability of these models for adsorption systems can be found in a review of Ho (2006).

The pseudo-first order (Lagergren) kinetic equation may be written in the form of

$$q_t = q_e \left(1 - e^{-k_1 t}\right) \quad (1)$$

whereas the pseudo-second order equation may be expressed as follows:

$$q_t = \frac{k_2 q_e^2 t}{1 + k_2 q_e t} \quad (2)$$

q_e and q_t are amounts of the dye adsorbed per unit mass of the sorbent at equilibrium time and time t , respectively, k_1 and k_2 are the first- and second-order kinetic constants, respectively. Eqs. (1) and (2) are presented usually in their linearized forms (Ho, 2006).

The sorptive removal of dye from aqueous solution involves several mass transfer processes in liquid phase and at the solid-liquid interface. The sorption process consists of four consecutive steps (Vadivelan and Kumar, 2005; Ofomaja, 2007):

- Transport of the solute from the bulk solution.
- Diffusion across the liquid film surrounding the sorbent particle.
- Solute diffusion in the pores of the sorbent.
- Sorption of the solute onto the interior surface of the pores.

The overall rate of sorption is controlled by the slowest step. It is usually assumed that the last step (sorption on the internal surface) is rapid enough and may be neglected. The rate-limiting step will involve diffusion mechanisms – either film diffusion or particle diffusion. In diffusion studies, the rate can be expressed in terms of the square root time. The mathematical dependence of q_t vs. $t^{0.5}$ is obtained if the sorption process is considered to be

influenced by diffusion in the spherical particles and convective diffusion in the solution (Allen et al., 1989; Ho and McKay, 1998). The root time dependence, known also as a Weber-Morris plot (Weber and Morris, 1963), may be expressed by the following equation:

$$q_t = k_{ID} t^{0.5} \quad (3)$$

where k_{ID} is a diffusion rate parameter. Eq. (3) is reported as an intraparticle diffusion model in literature (Vadivelan and Kumar, 2005; Janoš and Smidova, 2005; Ofomaja, 2007; Porkodi and Kumar, 2007) suggesting that the sorption process is considered to be controlled by the internal diffusion with a possible contribution of the external diffusion. The square-root plots for the dye sorption consist typically of two (or even more) separate linear parts with different slopes. This multilinearity is interpreted as a proof that the intraparticle diffusion is not solely the rate-limiting step and that the external mass transfer is also significant for the sorption process (Vadivelan and Kumar, 2005; Ofomaja, 2007). The intercept of the second part of the square-root plot is related to the boundary layer thickness – the contribution of the external surface sorption (Kumar et al., 2005). Marungrueng and Pavasant (2007), for example, deduced from the intraparticle diffusion plot that the sorption of basic dyes on the macroalga biosorbent and activated carbon is initially controlled by both film and pore diffusion, whereas only pore diffusion is the rate-limiting step at the later stage. The external mass transfer was identified as the rate limiting step at the beginning of the adsorption of Methylene Blue on the water hyacinth (El-Khaiary, 2007), and the intraparticle diffusion at the later stage. Both the external mass transfer and the intraparticle diffusion had rate-limiting effects during the sorption of reactive dyes onto fly ash (Dizge et al., 2008).

4. SORPTION EQUILIBRIA AND PARAMETERS AFFECTING THE DYE SORPTION

During the sorption process, solute is transferred from solution to the surface of the solid phase, where its concentration increases until a dynamic equilibrium is reached. At the equilibrium, there is a defined distribution of solute between the liquid and solid phases. The solute distribution function – adsorption isotherm – may be written in various forms. Probably the most commonly used equation is the Langmuir isotherm that can be easily derived from a “law of surface action” (similar to the “law of mass action”) (Langmuir, 1916):

$$q_e = \frac{q_m K c_e}{1 + K c_e} \quad (4)$$

q_e is the adsorbed amount of the dye, c_e is the equilibrium concentration of the dye in the solution, K and q_m are parameters on the Langmuir isotherm. The Langmuir isotherm presupposes a homogeneous nature of the sorbent surface (equivalence of the binding sites) and a non-cooperative behaviour during the sorption (monolayer adsorption). As evident, the dye sorptions on non-conventional sorbents will seldom satisfy these conditions.

The empirical Freundlich isotherm is another popular equation utilized to describe the sorption equilibria:

$$q_e = K_F c_e^n \quad (5)$$

K_F and n are parameters of the Freundlich isotherm.

Although commonly used, the Langmuir and Freundlich isotherms do not express well the sorption behaviour of solutes in real systems, especially when non-conventional sorbents are used, highly heterogeneous by their nature. Many other isotherm equations were introduced – a general classification of the solute adsorption isotherms was given by Giles et al. (1974), a brief overview of the isotherm equations can be found in the paper of Kinniburgh (1986). The Langmuir-Freundlich isotherm is frequently used to describe the sorption processes in environmental chemistry:

$$q_e = \frac{q_m K c_e^m}{1 + K c_e^m} \quad (6)$$

q_m , K and m are parameters of the isotherm, again. q_m is a maximum sorption capacity under given conditions, m is called usually as a “heterogeneity parameter” (Kinniburgh, 1986) reflecting various kinds of a non-ideal behaviour that may occur during the sorption on heterogeneous surfaces (Koopal et al., 1994). The sorption equilibria on the heterogeneous surface can be treated also with the aid of generalized multi-site Langmuir (or Langmuir-Freundlich) isotherms; this approach taking into account several kinds of the active sites on the surface of the sorbent corresponds to the original Langmuir’s concept of “more than one kind of elementary space” (Langmuir, 1918). The multi-site Langmuir isotherm can be written in the form:

$$q_e = \sum_{i=1}^n \frac{q_{m,i} K_i c_e}{1 + K_i c_e} \quad (7)$$

In most cases, the two-site models gave a satisfactory fit to experimental data and no significant improvement was achieved when the three-site or even more complex models were used. It was shown that the two-site Langmuir equation can fit any convex sorption data that tend to a maximum asymptotically (Hinz, 2001).

The concentration of solute (dye) in the sorbent (q_e) depends not only on the solute concentration in solution (as predicted from the simple sorption isotherms presented above), but also on some parameters that may influence potentially the sorption equilibria. pH is probably the most important parameter affecting the sorption of ionic species. In general, both the dye molecules as well as the active sites on the sorbent surface may undergo dissociation/protonation in dependence on the pH value. With increasing pH, the acidic functional groups of the sorbent (e.g. carboxylic or hydroxylic) dissociate and the sorbent

surface becomes negatively charged, which facilitate the sorption of cationic (basic) dyes. See, for example, the pH dependencies for the sorption of Methylene Blue on fly ash (Janoš et al., 2003), on dead macrofungi (Maurya et al., 2006), on palm kernel fibre (Ofomaja, 2007) or on fruit waste (Pavan et al., 2008). The opposite is true for the sorption of anionic (acid) dyes (Maurya et al., 2006; Wang and Li, 2007). A point of zero charge is an important parameter characterizing the surface properties of the sorbent (Ofomaja, 2007; Al-Degs et al., 2008). The dissociation of the dye molecules, on the other hand, plays probably less important role in affecting the sorption equilibria; note that the dye molecules contain often strongly acidic or basic groups (e.g. sulfonic), which degree of dissociation remains virtually unchanged over a wide pH range.

Apart from the dyes, wastewaters from dye-processing or textile finishing industries contain large amounts of dissolved substances, especially of inorganic salts that may potentially affect an effectiveness of the dye removal. An effect of the salt concentration on the dye sorption was studied in several works. Only a very slight decrease of the dye uptake with increasing concentration of NaCl was observed by Maurya et al. (2006) for the biosorption of Methylene Blue onto macro fungus-based sorbent. Possibly, the dye cation compete with inorganic cations for the binding sites on the sorbent surface. The sorption of both basic as well as acid dyes onto fly ash was not affected by the presence of inorganic salts (NaCl, CaCl₂) at concentrations exceeding several times the concentrations of the dyes (Janoš et al., 2003). Ozmen et al. (2008) observed a certain increase in the azodye sorption onto starch-based polymers in the presence of inorganic salts (NaCl) and explained this phenomenon as a result of the charge reduction on the sorbent surface. Similarly, the sorption of reactive (acid) dyes on activated carbon increased (but not dramatically) in the presence of NaCl (0.1 – 0.5 mol/l) (Al-Degs et al., 2008). It could be concluded that inorganic salts do not hamper in the sorption of either basic or acid dyes on the non-conventional sorbents even at high concentrations, which is important for potential practical applications.

Surfactants (especially anionic ones) are typically present in real wastewaters. Therefore, an effect of their presence on the dye sorption was also examined (Janoš et al., 2003; Janoš et al. 2005). It may be generalized that the sorption of ionic dyes is not affected significantly by the presence of the non-ionic surfactants. An increase in the sorption efficiency may occur in the presence of oppositely charged surfactants as a result of the formation of ion pairs or even more complex sub-micellar aggregates that cause an adsolubilization of the dye molecules on the sorbent surface. The surfactants bearing the same charge as the dye ion, on the other hand, exhibit usually a minor effect on the dye sorption, or they decrease the dye sorption to some extent as a result of a competition for the same binding sites on the sorbent. Similar trends were found by Talman and Atun (2006) for the sorption of Toluidine Blue (cationic dye) on fly ash or by Banerjee et al. (2006) for the sorption of anionic dyes in the presence of quaternary ammonium salts. More detailed discussion of the effects of surfactants on the dye sorption can be found in our previous works (Janoš, 2003; Janoš and Šmídová, 2005). It is important to note that surfactants exhibit usually only minor effects on the dye sorption on the non-conventional sorbents and thus do not impede their application in the wastewater treatment.

REFERENCES

- Aber, S., Daneshvar, N., Soroureddin, S.M., Chabok, A., Asadpour-Zeynali, K., 2007. Study of acid orange 7 removal from aqueous solutions by powdered activated carbon and modeling of experimental results by artificial neural network. *Desalination* 211, 87-95.
- Ajmal, M., Rao, R.A.K., Siddiqui, B.A., 1996. Studies on removal and recovery of Cr(VI) from electroplating wastes. *Water Res.* 30, 1478-1482.
- Aksu, Z., 2005. Application of biosorption for the removal of organic pollutants: a review. *Process Biochem.* 40, 997-1026.
- Al-Bastaki, N., Banat, F., 2004. Combining ultrafiltration and adsorption on bentonite in one-step process for the treatment of colored waters. *Resour. Conser. Recycl.* 41, 103-113.
- Al-Degs, Y.S., El-Barghouthi, M.I., El-Sheikh, A.H., Walker, G.M., 2008. Effect of solution pH, ionic strength, and temperature on adsorption behavior of reactive dyes on activated carbon. *Dyes Pigments* 77, 16-25.
- Al-Ghouti, M.A., Khraisheh, M.A.M., Alen, S.J., Ahmad, M.N., 2003. The removal of dyes from textile wastewater: a study of the physical characteristics and adsorption mechanisms of diatomaceous earth. *J. Environ. Manag.* 69, 229-238.
- Alkan, M., Celikcapa, S., Demirbas, O., Dogan M., 2005. Removal of reactive blue 221 and acid blue 62 anionic dyes from aqueous solutions by sepiolite. *Dyes Pigments* 65, 251-259.
- Allen, S.J., McKay, G., Khader, K.Y.H., 1989. Intraparticle diffusion of basic dye during adsorption onto sphagnum peat. *Environ. Pollut.* 56, 39-50.
- Al-Qodah, Z., Lafi, W.K., Al-Anber, Z., Al-Shannag, M., Harahsheh, A., 2007. Adsorption of methylene blue by acid and heat treated diatomaceous silica. *Desalination* 217, 212-224.
- Annadurai, G., Juang, R.S., Lee, D.J., 2002. Use of cellulose-based wastes for adsorption of dyes from aqueous solutions. *J. Hazard. Mater.* 92, 263-274.
- Aravindhan, R., Rao, J.R., Nair, B.U., 2007. Removal of basic yellow dye from aqueous solution by sorption on green alga *Caulerpa scalpelliformis*. *J. Hazard. Mater.* 142, 68-76.
- Armagan, B., Ozdemir, O., Turan, M., Celik, M.S., 2003. Adsorption of negatively charged azo dyes onto surfactant-modified sepiolite. *J. Environ. Eng.* 129, 709-715.
- Armagan, B., Turan, M., Celik, M.S., 2004. Equilibrium studies on the adsorption of reactive azo dyes into zeolite. *Desalination* 170, 33-39.
- Attia, A.A., Girgis, B.S., Fathy, N.A., 2008. Removal of methylene blue by carbons derived from peach stones by H₃PO₄ activation: Batch and column studies. *Dyes Pigments* 76, 282-289.
- Atun, G., Hisarli, G., Sheldrick, W.S., Muhler, M., 2003. Adsorptive removal of methylene blue from colored effluents on Fuller's earth. *J. Colloid Interface Sci.* 261, 32-39.
- Azizian, S., 2004. Kinetic models of sorption: a theoretical analysis. *J. Colloid Interface Sci.* 276, 47-52.
- Babel, S., Kurniawan, T.A., 2003. Low-cost adsorbents for heavy metals uptake from contaminated water: a review. *J. Hazard. Mater.* B 97, 219-243.
- Bagane, M., Guiza, S., 2000. Removal of a dye from textile effluents by adsorption. *Ann. Chim. Sci., Mater.* 25, 615-626.

- Bailey, S.E., Olin, T.J., Bricka, R.M., Adrian, D.D., 1999. A review of potentially low-cost sorbents for heavy metals. *Water Res.* 33, 2469-2479.
- Banat, F., Al-Asheh, S., Al-Ahmad, R., Bni-Khalid, F., 2007. Bench-scale and packed bed sorption of methylene blue using treated olive pomace and chacoal. *Bioresource Technol.* 98, 3017-3025.
- Banerjee, S.S., Joshi, M.V., Jayaram, R.V., 2006. Effect of quaternary ammonium cations on dye sorption to fly ash from aqueous media. *J. Colloid Interface Sci.*, 303, 477-483.
- Baskaralingam, P., Pulikesi, M., Ramamurthi, V., Sivanesan, S., 2007. Modified hectorites and adsorption studies of a reactive dye. *Appl. Clay Sci.*, 37, 207-214.
- Batzias, F.A., Sidiras, D.K., 2004. Dye adsorption by calcium chloride treated beech sawdust in batch and fixed-bed systems. *J. Hazard. Mater. B* 114, 167-174.
- Batzias, F.A., Sidiras, D.K., 2007a. Simulation of dye adsorption by beech sawdust as affected by pH. *J. Hazard. Mater. B* 141, 668-679.
- Batzias, F.A., Sidiras, D.K., 2007b. Simulation of methylene blue adsorption by salts-treated beech sawdust in batch and fixed-bed systems. *J. Hazard. Mater. B* 149, 8-17.
- Benkli, Y.E., Can, M.F., Turan, M., Celik, M.S., 2005. Modification of organo-zeolite surface for the removal of reactive azo dyes in fixed bed reactor. *Water Res.* 39, 487-493.
- Borai, E.H., El-Sofany, E.A., Morcos, T.N., 2007. Development and optimization of magnetic technologies based processes for removal of some toxic heavy metals. *Adsorption* 13, 95-104.
- Bouberka, Z., Kacha, S., Kameche, M., Elmaleh, S., Derriche, Z., 2005. Sorption study of an acid dye from an aqueous solutions using modified clays. *J. Hazard. Mater.* 119, 117-124.
- Cengiz, S., Cavas, L., 2008. Removal of methylene blue by invasive marine seaweed: *Caulerpa racemosa* var. *cylindracea*. *Bioresource Technol.* 99, 2357-2363.
- Ceyhan, O., Baybas, D., 2001. Adsorption of some textile dyes by hexadecyltrimethylammonium bentonite. *Turk. J. Chem.* 25, 193-200.
- Chiou, M.-S., Ho, P.-Y., Li, H.-Y., 2004. Adsorption of anionic dyes in acid solutions using chemically cross-linked chitosan beads. *Dyes Pigments* 60, 69-84.
- Choi, H.-D., Shin, M.-C., Kim, D.-H., Jeon, C.-S., Baek, K., 2008. Removal characteristics of reactive black 5 using surfactant-modified carbon. *Desalination* 223, 290-298.
- Chu, H.C., Chen, K.M., 2002. Reuse of activated sludge biomass: I. Removal of basic dyes from wastewater by biomass. *Process Biochem.* 37, 595-600.
- Crini, G., 2006. Non-conventional low-cost adsorbents for dye removal: A review. *Bioresource Technol.* 97, 1061-1085.
- Crini, G., 2008. Kinetic and equilibrium studies on the removal of cationic dyes from aqueous solution by adsorption onto a cyclodextrin polymer. *Dyes Pigments* 77, 415-426.
- Dias, J.M., Alvim-Ferraz, M.C.M., Almeida, M.F., Rivera-Utrilla, J., Sanchez-Polo, M., 2007. Waste materials for activated carbon preparation and its use in aqueous-phase treatment: A review. *J. Environ. Manag.* 85, 833-846.
- Dizge, N., Aydinler, C., Demirbas, E., Kobya, M., Kara, S., 2008. Adsorption of reactive dyes from aqueous solutions by fly ash. Kinetic and equilibrium studies. *J. Hazard. Mater.* 150, 737-746.
- dos Santos, A.B., Cervantes, F.J., van Lier, J.B., 2007. Review paper on current technologies for decolourisation of textile wastewaters: Perspectives for anaerobic biotechnology. *Bioresource Technol.* 98, 2169-2385.

- El Quada, E.N., Allen, S.J., Walkner, G.M., 2006. Adsorption of Methylene Blue onto activated carbon produced from steam activated bituminous coal: A study of equilibrium adsorption isotherm. *Chem. Eng. J.* 124, 103-110.
- El-Khaiary, M.I., 2007. Kinetics and mechanism of adsorption of methylene blue from aqueous solution by nitric-acid treated water-hyacinth. *J. Hazard. Mater.* 147, 28-36.
- Entezari, M.H., Al-Hoseini, Z.S., 2007. Sono-sorption as a new method for the removal of methylene blue from aqueous solution. *Ultrasonic Sonochem.* 14, 599-604.
- Eren, Z., Acar, F.N., 2007. Equilibrium and kinetic mechanism for Reactive Black 5 sorption onto high lime Soma fly ash. *J. Hazard. Mater.* 143, 226-232.
- Eren, E., Afsin, B., 2008. Investigation of a basic dye adsorption from aqueous solution onto raw and pre-treated bentonite surfaces. *Dyes Pigments* 76, 220-225.
- Ferrero, F., 2007. Dye removal by low cost adsorbents: Hazelnut shell in comparison with wood sawdust. *J. Hazard. Mater. B* 142, 144-152.
- Forgacs, E., Cserhádi, T., Oros, G., 2004. Removal of synthetic dyes from wastewaters: a review. *Environ. Internat.* 30, 953-971.
- Giles, C.H., Smith, D., Huitson, A., 1974. A general treatment and classification of the solute adsorption isotherms. I. Theoretical. *J. Colloid Interface Sci.* 47, 755-765.
- Gong, R., Sun, Y., Chen, J., Liu, H., Yang, C., 2005. Effect of chemical modification on the dye adsorption capacity of peanut hull. *Dyes Pigments* 67, 175-181.
- Gong, R., Zhang, X., Liu, H., Sun, Y., Liu, B., 2007. Uptake of cationic dyes from aqueous solution by biosorption onto granular kohlrabi peel. *Bioresource Technol.* 98, 1319-1323.
- Gong, R., Sun, J., Zhang, D., Zhong, K., Zhu, G., 2008. Kinetics and thermodynamics of basic dye sorption on phosphoric acid esterifying soybean hull with solid phase preparation technique. *Bioresource Technol.* 99, 4510-4514.
- Gupta, V.K., Ali, I., Suhas, Mohan, D., 2003. Equilibrium uptake and sorption dynamics for the removal of a basic dye (basic red) using low-cost adsorbents. *J. Colloid Interface Sci.* 265, 257-264.
- Gupta, V.K., Mittal, A., Gajbe, V., Mittal, J., 2008. Adsorption of basic fuchsin using waste materials – bottom ash and deoiled soya – as adsorbents. *J. Colloid Interface Sci.* 319, 30-39.
- Hamadaoui, O., 2006. Batch study of liquid-phase adsorption of methylene blue using cedar sawdust and crushed brick. *J. Hazard. Mater.* 135, 264-273.
- Hameed, B.H., Ahmad, A.L., Latiff, K.N.A., 2007. Adsorption of basic dye (methylene blue) onto activated carbon prepared from rattan sawdust. *Dyes Pigments* 75, 143-149.
- Hameed, B.H., Mahmoud, D.K., Ahmad, A.L., 2008. Sorption of basic dye from aqueous solution by pomelo (*Citrus grandis*) peel in a batch system. *Colloids Surf. A: Physicochem. Eng. Aspects* 316, 78-84.
- Han, R., Wang, Y., Han, P., Shi, J., Yang, J., Lu, Y., 2006. Removal of methylene blue from aqueous solution by chaff in batch mode. *J. Hazard. Mater.* 137, 550-557.
- Han, R., Zou, W., Yu, W., Cheng, S., Wang, Y., Shi, J., 2007. Biosorption of methylene blue from aqueous solution by fallen phoenix tree's leaves. *J. Hazard. Mater.* 141, 156-162.
- Hinz, C., 2001. Description of sorption data with isotherm equations. *Geoderma* 99, 225-243.
- Ho, Y.S., 2006. Review of second-order models for adsorption systems. *J. Hazard. Mater. B* 136, 681-689.
- Ho, Y.S., McKay, G., 1998a. The kinetics of sorption of basic dyes from aqueous solution by sphagnum moss peat. *Canad. J. Chem. Eng.* 76, 822-827.

- Ho, Y.S., McKay, G., 1998b. Sorption of dye from aqueous solution by peat. *Chem. Eng. J.* 70, 115-124.
- Ho, Y.S., McKay, G., 2003. Sorption of dyes and copper ions onto biosorbents. *Process Biochem.* 38, 1047-1061.
- Hojamberdiev, M., Kameshima, Y., Nakajima, A., Okada, K., Kadirova, Z., 2008. Preparation and sorption properties of materials from paper sludge. *J. Hazard. Mater.* 151, 710-719.
- Hu, Z.G., Zhang, J., Chan, W.L., Szeto, Y.S., The sorption of acid dye onto chitosan nanoparticles. *Polymer* 47, 5838-5842.
- Iscen, C.F., Kiran, I., Ilhan, S., 2007. Biosorption of Reactive Black 5 dye by *Penicillium restrictum*: The kinetic study. *J. Hazard. Mater.* 143, 335-340.
- Janoš, P., 2003. Sorption of basic dyes onto iron humate. *Environ. Sci. Technol.* 37, 5792-5798.
- Janoš, P., Buchtová, H., Rýznarová, M., 2003. Sorption of dyes from aqueous solutions onto fly ash. *Water Res.* 37, 4938-4944.
- Janoš, P., Šedivý, P., Rýznarová, M., Grötschelová, S., 2005. Sorption of basic and acid dyes from aqueous solution onto oxihumolite. *Chemosphere* 59, 881-886.
- Janoš, P., Šmídová, V., 2005. Effect of surfactants on the adsorptive removal of basic dyes from water using an organomineral sorbent – iron humate. *J. Colloid Interface Sci.* 291, 19-27.
- Jirankova, H., Cakl, J., Markvartova, O., Dolecek, P., 2007. Combined membrane process at wastewater treatment. *Separ. Purif. Technol.* 58, 299-303.
- Karaca, S., Gürses, A., Bayrak, R., 2005. Investigation of applicability of the various adsorption models of methylene blue adsorption onto lignite/water interface. *Energy Convers. Manag.* 46, 33-46.
- Khenifi, A., Boubberka Z., Sekrane, F., Kameche, M., Derriche, Z., 2007. Adsorption study of an industrial dye by an organic clay. *Adsorption* 13, 149-158.
- Kinniburgh, D.G., 1986. General purpose adsorption isotherms. *Environ. Sci. Technol.* 20, 895-904.
- Koopal, L.K., van Riemsdijk, W.H., de Wit, J.C.M., Benedetti, M.F., 1994. Analytical isotherm equations for multicomponent adsorption to heterogeneous surfaces. *J. Colloid Interface Sci.* 166, 51-60.
- Kumar, K.V., Kumaran, A., 2005. Removal of methylene blue by mango seed kernel powder. *Biochem. Eng. J.* 27, 83-93.
- Kumar, K.V., Ramamurthi, V., Sivanesan, S., 2005. Modeling the mechanism involved during the sorption of methylene blue onto fly ash. *J. Colloid Interface Sci.* 284, 14-21.
- Kumar, U., Bandyopadhyay, M., 2006. Sorption of cadmium from aqueous solution using pretreated rice husk. *Bioresour. Technol.* 97, 104-109.
- Kumar, K.V., Porkodi, K., 2006. Relation between some two- and three-parameter isotherm models for the sorption of methylene blue onto lemon peel. *J. Hazard. Mater.* 138, 633-635.
- Kumar, K.V., Porkodi, K., 2007. Mass transfer, kinetics and equilibrium studies for the biosorption of methylene blue using *Paspalum notatum*. *J. Hazard. Mater.* 146, 214-226.
- Kumar, K.V., Sivanesan, S., 2007. Sorption isotherm for safranin onto rice husk: Comparison of linear and non-linear methods. *Dyes Pigments* 72, 130-133.

- Kundakci, S., Üzümlü, O.B., Kadarag, E., 2008. Swelling and dye sorption studies of acrylamide/2-acrylamido-2-methyl-1-propanesulfonic acid/bentonite highly swollen composite hydrogels. *React. Funct. Polymers* 68, 458-473.
- Kurniawan, T.A., Chan, G.Y.S., Lo, W., Babel, S., 2006. Comparisons of low-cost adsorbents for treating wastewaters laden with heavy metals. *Sci. Total. Environ.* 366, 409-426.
- Langmuir, I., 1916. The constitution and fundamental properties of solids and liquids. *J. Am. Chem. Soc.* 38, 2221-2295.
- Langmuir, I., 1918. The adsorption of gases on plane surfaces of glass, mica and platinum. *J. Am. Chem. Soc.* 40, 1361-1403.
- Lata, H., Garg, V.K., Gupta, R.K., 2007. Removal of a basic dye from aqueous solution by adsorption using *Parthenium hysterophorus*: An agricultural waste. *Dyes Pigments* 74, 653-658.
- Lata, H., Garg, V.K., Gupta, R.K., 2008. Adsorptive removal of basic dye by chemically activated *Parthenium* biomass: equilibrium and kinetic modelling. *Desalination* 219, 250-261.
- Lazaridis, N.K., Kyzas, G.Z., Vassiliou, A.A., Bikiaris, D.N., 2007. Chitosan derivatives as biosorbents for basic dyes. *Langmuir* 23, 7634-7643.
- Li, Q., Yue, Q.-Y., Su, Y., Gao, B.-Y., Fu, L., 2007. Cationic polyelectrolyte/bentonite prepared by ultrasonic technique and its use as adsorbent for Reactive Blue K-GL dye. *J. Hazard. Mater.* 147, 370-380.
- Liao, M.-H., Chen, D.-H., 2002. Preparation and characterization of a novel magnetic nano-adsorbent. *J. Mater. Chem.* 12, 3654-3659.
- Lin, J.X., Zhan, S.L., Fang, M.H., Qian, X.Q., Yang, H., 2008. Adsorption of basic dye from aqueous solution onto fly ash. *J. Environ. Manag.* 87, 193-200.
- Liu, P., Zhang, L., 2007. Adsorption of dyes from aqueous solutions or suspensions with clay nano-adsorbents. *Separ. Purif. Technol.* 58, 32-39.
- Mak, S.-Y., Chen, D.-H., 2004. Fast adsorption of methylene blue on polyacrylic acid-bonded iron oxide magnetic nanoparticles. *Dyes Pigments* 61, 93-98.
- Marungrueng, K., Pavasant, P., 2007. High performance biosorbent (*Caulerpa lentillifera*) for basic dye removal. *Bioresource Technol.* 98, 1567-1572.
- Maurya, N.S., Mittal, A.K., Cornel, P., Rother, E., 2006. Biosorption of dyes using dead macro fungi: Effect of dye structure, ionic strength and pH. *Bioresource Technol.* 97, 512-521.
- McKay, G., Poots, V.J.P., 1980. Kinetics and diffusion processes in colour removal from effluents using wood as an adsorbent. *J. Chem. Technol. Biotechnol.* 30, 279-292.
- Meshko, V., Markovska, L., Mincheva, M., Rodrigues, A.E., 2001. Adsorption of basic dyes on granular activated carbon and natural zeolite. *Water Res.* 35, 3357-3366.
- Mittal, A.K., Venkobachar, C., 1993. Sorption and desorption of dyes by sulfonated coal. *J. Environ. Eng.* 119, 366-368.
- Mohan, S.V., Ramaniah, S.V., Sarma, P.N., 2008. Biosorption of direct azo dye from aqueous phase onto *Spirogyra* sp. I02. Evaluation of kinetics and mechanistic aspects. *Biochem. Eng. J.* 38, 61-69.
- Morais, W.A., Fernandes, A.L.P., Dantas, T.N.C., Pereira, M.R., Fonseca, J.L.C., 2007. Sorption studies of a model anionic dye on crosslinked chitosan. *Colloids Surf. A: Physicochem. Eng. Aspects* 310, 20-31.

- Nacera, Y., Aicha, B., 2006. Equilibrium and kinetic modelling of methylene blue biosorption by pretreated dead *streptomyces rimosus*: Effect of temperature. *Chem. Eng. J.*, 119, 121-125.
- Nakagawa, K., Namba, A., Mukai, S.R., Tamon, H., Ariyadejwanich, P., Tanthapanichakoon, W., 2004. Adsorption of phenol and reactive dye from aqueous solution on activated carbons derived from solid wastes. *Water Res.* 38, 1791-1798.
- Namasivayam, C., Sumithra, S., 2005. Removal of direct red 12B and methylene blue from water by adsorption onto Fe (III)/Cr (III) hydroxide, an industrial solid waste. *J. Environ. Manag.* 74, 207-215.
- Nandi, S.P., Walker, P.L., 1971. Adsorption of dyes from aqueous solution by coals, chars, and active carbons. *Fuel* 50, 345-366.
- Ncibi, M.C., Mahjoub, B., Seffe, M., 2007. Kinetic and equilibrium studies of methylene blue biosorption by *Posidonia oceanica* (L.) fibres. *J. Hazard. Mater.* 139, 280-285.
- Ngah, W.S.W., Hanafiah, M.A.K.M., 2008. Removal of heavy metal ions from wastewater by chemically modified plant wastes as adsorbents: A review. *Bioresource Technol.* 99, 3935-3948.
- Noroozi, B., Sorial, G.A., Bahrami, H., Arami, M., 2008. Adsorption of binary mixtures of cationic dyes. *Dyes Pigments* 76, 784-791.
- Ofomaja, A.E., 2007. Kinetics and mechanism of methylene blue sorption onto palm kernel fibre. *Process Biochem.* 42, 16-24.
- Ong, S.T., Lee, C.K., Zainal, Z., 2007. Removal of basic and reactive dyes using ethylenediamine modified rice husk. *Bioresour. Technol.* 98, 2792-2799.
- Ozcan, A.S., Erdem, B., Ozcan, A., 2004. Adsorption of acid blue 193 from aqueous solution onto Na-bentonite and DTMA-bentonite. *J. Colloid Interface Sci.* 280, 44-54.
- Ozdemir, O., Armagan, B., Turan, M., Celik, M.S., 2004. Comparison of the adsorption characteristics of azo-reactive dyes on mesoporous minerals. *Dyes Pigments* 62, 49-60.
- Ozmen, E.Y., Sezgin, M., Yilmaz, Y., Yilmaz, M., 2008. Synthesis of β -cyclodextrin and starch based polymers for sorption of azo dyes from aqueous solutions. *Bioresource Technol.* 99, 526-531.
- Padmesh, T.V.N., Vijayaraghavan, K., Sekeran, G., Velan, M., 2005. Batch and column studies on biosorption of acid dyes on fresh water macro alga *Azolla filiculoides*. *J. Hazard. Mater.* 125, 121-129.
- Padmesh, T.V.N., Vijayaraghavan, K., Sekeran, G., Velan, M., 2006. Application of *Azolla rongpong* on biosorption of acid red 88, acid green 3, acid orange 7 and acid blue 15 from synthetic solutions. *Chem. Eng. J.* 122, 55-63.
- Patel, R., Suresh, S., 2008. Kinetic and equilibrium studies on the biosorption of reactive black 5 dye by *Aspergillus foetidus*. *Bioresource Technol.* 99, 51-58.
- Pavan, F.A., Lima, E.C., Dias, S.L.P., Mazzocato, A.C., 2008. Methylene blue biosorption from aqueous solutions by yellow passion fruit waste. *J. Hazard. Mater.* 150, 703-712.
- Pollard, S.J.T., Fowler, G.D., Sollars, C.J., Perry, R., 1992. Low-cost adsorbents for waste and wastewater treatment: a review. *Sci. Total Environ.* 116, 31-52.
- Ponnusami, V., Vikram, S., Srivastava, S.N., 2008. Guava (*Psidium guajava*) leaf powder: Novel adsorbent for removal of methylene blue from aqueous solutions. *J. Hazard. Mater.* 152, 276-286.
- Poots, V.J.P., McKay, G., Healy, J.J., 1976a. The removal of acid dye from effluent using natural adsorbents – I. Peat. *Water Res.* 10, 1061-1066.

- Poots, V.J.P., McKay, G., Healy, J.J., 1976b. The removal of acid dye from effluent using natural adsorbents-II. Wood. *Water Res.* 10, 1067-1070.
- Poots, V.J.P., McKay, G., 1979. The specific surfaces of peat and wood. *J. Appl. Polymer Sci.* 23, 1117-1129.
- Porkodi, K., Kumar, K.V., 2007. Equilibrium, kinetics and mechanism modelling and simulation of basic and acid dyes sorption onto fiber carbon: Eosin yellow, malachite green and crystal violet single component system. *J. Hazard. Mater.* 143, 311-327.
- Prigione, V., Varese, G.C., Casieri, L., Marchisio, V.F., 2008. Biosorption of simulated dyed effluents by inactivated fungal biomasses. *Bioresource Technol.* 99, 3359-3567.
- Qu, J., 2008. Research progress of novel adsorption processes in water purification: A review. *J. Environ. Sci.* 20, 1-13.
- Ramakrishna, K.R., Viraraghavan, T., 1997. Dye removal using low cost adsorbents. *Water Sci. Technol.* 36, 189-196.
- Robinson, T., Chandran, B., Nigam, P., 2002. Effect of pretreatments of three waste residues, wheat straw, corncobs and barley husks on dye adsorption. *Bioresource Technol.* 85, 119-124.
- Rocher, V., Siaugue, J.-M., Cabuil, V., Bee, A., 2008. Removal of organic dyes by magnetic alginate beads. *Water Res.* 42, 1290-1298.
- Saleem, M., Pizada, T., Qadeer, R., 2007. Sorption of acid violet 17 and direct red 80 dyes on cotton fiber from aqueous solutions. *Colloids Surf. A: Physicochem. Eng. Aspects* 292, 246-250.
- Salleres, S., Arbeola, F.L., Martinez, V., Arbeola, T., Arbeola, I.L., 2008. Adsorption of fluorescent R6G dye into organophilic C12TMA laponite films. *J. Colloid Interface Sci.* 321, 212-219.
- Shichi, T., Takagi, K., 2000. Clay minerals as photochemical reaction fields. *J. Photochem. Photobiol. C: Photochem. Rev.* 1, 113-130.
- Shukla, A., Zhang, Y.-H., Dubey, P., Margrave, J.L., Shukla, S.S., 2002. The role of sawdust in the removal of unwanted materials from water. *J. Hazard. Mater.* B 95, 137-152.
- Silva, J.P., Sousa, S., Rodrigues, J., Antunes, H., Porter, J.J., Goncalves, I., Ferreira-Dias, S., 2004. Adsorption of acid orange 7 dye in aqueous solutions by spent brewery grains. *Separ. Purif. Technol.* 40, 309-315.
- Slokar, Y.M., Le Marechal, A.M., 1998. Methods of decoloration of textile wastewaters. *Dyes Pigments* 37, 335-356.
- Talman, R.Y., Atun, G., 2006. Effects of cationic and anionic surfactants on the adsorption of toluidine blue onto fly ash. *Colloids Surf. A: Physicochem. Eng. Aspects* 281, 15-22.
- Tan, I.A.W., Ahmad, A.L., Hameed, B.H., 2008. Adsorption of basic dye using activated carbon prepared from oil palm shell: batch and fixed bed studies. *Desalination* 225, 13-28.
- Taty-Costodes, V.C., Fauduet, H., Porte, C., Delacroix, A., 2003. Removal of Cd(II) and Pb(II) ions, from aqueous solutions, by adsorption onto sawdust of *Pinus sylvestris*. *J. Hazard. Mater.* B 105, 121-142.
- Tonle, I.K., Ngameni, E., Tcheumi, H.L., Tchieda, V., Carteret, C., Walcarius, A., 2008. Sorption of methylene blue on an organoclay bearing thiol groups and application to electrochemical sensing of the dye. *Talanta* 74, 489-497.
- Türker, A.R., 2007. New sorbents for solid-phase extraction for metal enrichment. *Clean* 35, 548-557.

- Vadivelan, V., Kumar, K.V., 2005. Equilibrium, kinetics, mechanism, and process design for the sorption of methylene blue onto rice husk. *J. Colloid Interface Sci.* 286, 90-100.
- Vijayaraghavan, K., Yun, Y.-S., 2008. Biosorption of C.I. Reactive Black 5 from aqueous solution using acid-treated biomass of brown seaweed *Laminaria* sp. *Dyes Pigments* 76, 726-732.
- Vijayaraghavan, K., Mao, J., Yun, Y.-S., 2008. Biosorption of methylene blue from aqueous solution using free and polysulfone-immobilized *Corynebacterium glutamicum*: Batch and column studies. *Bioresource Technol.* 99, 2864-2871.
- Viraraghavan, T., Dronamraju, M.M., 1992. Utilization of coal ash in water pollution control. *Internat. J. Environ. Stud.* 40, 79-85.
- Volesky, B., 2007. Biosorption and me. *Water Res.* 41, 4017-4025.
- Volesky, B., Holan, Z.R., 1995. Biosorption of heavy metals. *Biotechnol. Progress* 11, 235-250.
- Wang, S., Li, L., Wu, H., Zhu, Z.H., 2005. Unburned carbon as a low-cost adsorbent for treatment of methylene blue-containing wastewater. *J. Colloid Interface Sci.* 292, 336-343.
- Wang, S., Li, H., Xie, S., Liu, S., Xu, L., 2006. Physical and chemical regeneration of zeolitic adsorbents for dye removal in wastewater treatment. *Chemosphere* 65, 82-87.
- Wang, S., Li, H., 2007. Kinetic modelling and mechanism of dye adsorption on unburned carbon. *Dyes Pigments* 72, 308-314.
- Wang, L., Wang, A., 2007. Adsorption characteristics of Congo Red onto the chitosan/montmorillonite nanocomposite. *J. Hazard. Mater.* 147, 979-985.
- Wang, S., Wu, H., 2006. Environmental-benign utilization of fly ash as low-cost adsorbents. *J. Hazard. Mater. B* 136, 482-501.
- Weber, W.J., Morris, J.C., 1963. Kinetics of adsorption on carbon from solution. *J. Sanit. Eng. Div.* 89, (SA2), 31-39.
- Wei, X., Viadero, R.C., 2007. Synthesis of magnetite nanoparticles with ferric iron recovered from acid mine drainage: Implications for environmental engineering. *Colloids Surf. A: Physicochem. Eng. Aspects* 294, 280-286.
- Weng, C.-H., Pan, Y.-F., 2007. Adsorption of cationic dye (methylene blue) onto spent activated clay. *J. Hazard. Mater.* 144, 355-362.
- Wibulswas, R., 2004. Batch and fixed bed sorption of methylene blue on precursor and QACs modified montmorillonite. *Separ. Purif. Technol.* 39, 3-12.
- Wojnarovits, L., Takacs, E., 2008. Irradiation treatment of azo dye containing wastewater: An overview. *Radiation Phys. Chem.* 77, 225-244.
- Wong, Y.C., Szeto, Y.S., Cheung, W.H., McKay, G., 2008. Effect of temperature, particle size and percentage deacetylation on the adsorption of acid dyes on chitosan. *Adsorption* 14, 11-20.
- Wu, R., Qu, J., Chen, Y., 2005. Magnetic powder MnO-Fe₂O₃ composite – a novel material for the removal of azo-dye from water. *Water Res.* 39, 630-638.
- Yang, N., Zhu, S., Zhang, D., Xu, S., 2008. Synthesis and properties of magnetic Fe₃O₄-activated carbon nanocomposite particles for dye removal. *Mater. Lett.* 62, 645-647.
- Yi, J.-Z., Zhang, L.-M., 2008. Removal of methylene blue dye from aqueous solution by adsorption onto sodium humate/polyacrylamide/clay hybrid hydrogels. *Bioresource Technol.* 99, 2182-2186.

- Yue, Q.-Y., Li, Q., Gao, B.-Y., Yuan, A.-J., Wang, Y., 2007. Formation and characteristics of cationic-polymer/bentonite complexes as adsorbents for dyes. *Appl. Clay Sci.* 35, 268-275.
- Zollinger, H., 1987. Color Chemistry – Syntheses, *Properties and Applications of Organic Dyes and Pigments*. VCH, New York.

Chapter 8

IRRADIATION TREATMENT OF AZO DYES IN AQUEOUS SOLUTION

László Wojnárovits and Erzsébet Takács

Institute of Isotopes, Hungarian Academy of Sciences,
H-1525 Budapest, P.O.Box 77, Hungary

ABSTRACT

Laboratory investigations, pilot-plant experiments and an industrially established technology illustrated that electron beam (EB) treatment can efficiently destroy textile dyes in aqueous solutions. This treatment belongs to the class of Advanced Oxidation Processes (AOP): here also, as in most of AOP principally $\cdot\text{OH}$ radicals induce the chemical transformations. The final result of the treatment depends on the absorbed radiation energy (dose); with sufficient dose mineralization can be achieved. Major benefits of EB treatment with respect to the conventional methods are: no usage of chemical additives, room temperature operation, penetration in the bulk of water even in case of turbidity, production of high concentrations of oxidizing radicals in a fraction of a second and simultaneous disinfection.

The book chapter summarizes the radiation sources and the experimental techniques used for studying the reactions of dyes in irradiated systems (e.g. pulse radiolysis, gamma radiolysis, UV-VIS spectroscopy), describes the decomposition of water under the effect of ionizing radiation, characterizes the reactive intermediates formed (hydroxyl radical, hydrogen atom, hydrated electron), and discusses their reactions with dye molecules. An essential part of the chapter is the description of the kinetics and mechanism of azo dye decomposition. At the beginning of the treatment the water radicals reacting with the dye cause destruction of the highly conjugated electronic system resulting in decoloration. The decoloration is followed by a step-by-step degradation, destruction of the aromatic rings, ring-opening, fragmentation to smaller molecular mass aldehydes, ketones, carboxylic acids, etc. When oxygen is present compounds with progressively higher oxygen-to-carbon ratio are involved in the conversion of an organic molecule to CO_2 and H_2O . The individual reactions are detailed on the examples of several dye molecules.

Pilot plant experiments on dye containing industrial wastewater have proven that combining conventional treatments with the EB based technology results in a considerable improvement of the treatment efficiency. Considerable reduction of

chemical additive consumption, and also reduction in retention time were observed, with an increase in removal efficiencies as indicated by reduction in Total Organic Carbon content, TOC, Chemical Oxygen Demand, COD and Biological Oxygen Demand, BOD. Based on the pilot-plant experiments a full-scale plant for recycling EB-treated textile wastewater went into operation just at the end of 2005 in Daegu, Republic of Korea.

Keywords: azo dyes, decoloration, mineralization, wastewater, EB irradiation treatment, dose requirement, decomposition, mechanism, pulse radiolysis, kinetics

1. INTRODUCTION

Advances to molecular design of azo dyes have improved their photostability and stability toward aerobic degradation or common oxidants, for these reasons the removal of azo dyes from wastewaters is extremely difficult. Effluents of textile dyeing and finishing industries are known to have considerable color, suspended solids, chlorinated organic molecules, surfactants, some heavy metals and to have variable pH, temperature and Chemical Oxygen Demand (COD). Especially reactive azo dyes cause special environmental concern: their precursors and their degradation products, such as aromatic amines, are considered highly carcinogenic. Consequently, dyes have to be removed from industrial wastewater before discharging. However, even with carefully selected microorganism and under favorable conditions their biodegradation is limited and takes long time. Moreover, conventional chemical methods are not efficient enough for the degradation of azo dyes. Due to these difficulties, the dye containing effluents coming from textile factories are treated by absorption onto activated carbon or by chemical coagulation. These conventional techniques mainly transfer the contaminants from wastewater to solid wastes. Therefore one of the major areas of interest in dye chemistry is to look for new efficient ways for disposal and treatment of azo dye containing wastewater by new oxidation/reduction processes [1-4]. Such processes can be initiated by highly oxidizing radicals (Advanced Oxidation Processes, AOP) that are produced for instance in photo Fenton reaction (UV light induced decomposition of H_2O_2 to produce $\cdot\text{OH}$ radicals), photocatalytic reaction with suspended semiconductor such as TiO_2 (yielding also $\cdot\text{OH}$ radicals) or in ionizing radiation induced decomposition of water. In the latter, in addition to the highly oxidizing $\cdot\text{OH}$ radicals, highly reducing radicals, hydrated electrons (e_{aq}^-) and hydrogen atoms ($\text{H}\cdot$) may also play role in dye degradation.

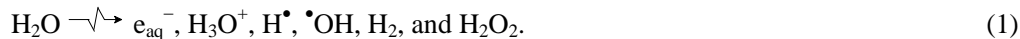
Radiation processing is often used in industry to produce a wide range of products [5-7]. Use of radiolysis in the environmental remediation of wastewater, contaminated soil and sediment is a promising treatment technology; the chemistry behind these technologies is under extensive investigation. Together with the removal of target chemical contaminant, one should also concern the elimination of a series of intermediates of progressively higher oxygen-to-carbon ratios that are involved in the conversion of an organic molecule to CO_2 . Therefore, it is essential to improve substantially our basic understanding of the radiation chemistry of dye molecules (reactions, pathways, and rates) in various systems. The radiolytic reactions with respect to dye decomposition have been intensively studied during the last 10 years [8,9] and the research has led to pilot-plant experiments, and finally also to full-scale realization.

In the present book chapter we summarize the results of scientific investigations, show the industrial realization and the advantages of the technique. Although we mainly refer to radiolysis results, the undergoing processes, the reaction mechanisms are also relevant to other AOP.

2. RADIOLYSIS OF WATER AND AQUEOUS SOLUTIONS

2.1. Primary Intermediate Formation in Oxygen-free System

In the radiolysis of water the transients and products are e_{aq}^- , H_3O^+ , H^\bullet , $\bullet OH$, H_2 , and H_2O_2 (Reaction (1)). Since all the transients and products originate from water molecules, at any time the total number of H atoms in the transients and products should be twice the number of O atoms, and also, the total charge of the transients and products considered should be zero [5-7,10].



The yields of species formed are as follows: 2.7, 2.7, 0.6, 2.7, 0.45, and 0.75 species/100 eV absorbed radiation energy (*G*-value). The traditional (so-called atomic) species/100 eV units can be transformed to SI units of $\mu\text{mol J}^{-1}$ by multiplying with factor of 0.1036.

The so-called water radicals, hydrated electron (synonymous with aqueous electron), hydrogen atom, and hydroxyl radical formed in water radiolysis are extremely reactive and in the absence of other reaction partners, in ultra pure water they disappear in very fast self-termination reactions. In the presence of proper solutes in the solution, e.g. dye molecules, they readily react with these compounds.

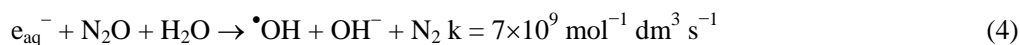
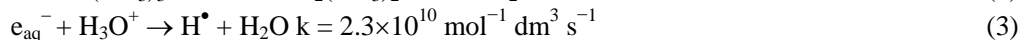
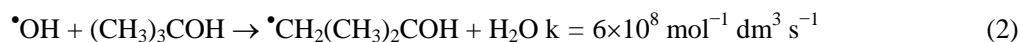
All the water radicals form simultaneously complicating the investigation of their individual reaction steps. By combining appropriately selected experimental conditions there are possibilities to reduce the kinds of primary reacting radicals, and therefore to obtain some information about the mechanism of undergoing reactions, or at least about the main possible reaction pathways [5-7,10].

The reactions of e_{aq}^- are generally studied in deoxygenated (N_2 or Ar bubbled) solutions above pH 3 and in the presence of $0.2 - 1 \text{ mol dm}^{-3}$ *tert*-butanol. *Tert*-butanol converts the highly reactive $\bullet OH$ radicals to less reactive $\bullet CH_2(CH_3)_2COH$ radicals in Reaction (2). In such systems there is a small contribution from the H^\bullet atom reactions.

Reactions of H^\bullet atoms are usually investigated in N_2 or Ar saturated solutions containing $0.2 - 1 \text{ mol dm}^{-3}$ *tert*-butanol below pH 2. In such solutions e_{aq}^- is converted to H^\bullet atom in Reaction (3). The reaction between H^\bullet and *tert*-butanol is slow: $H^\bullet + (CH_3)_3COH \rightarrow \bullet CH_2(CH_3)_2COH + H_2$ ($k = 1 \times 10^6 \text{ mol}^{-1} \text{ dm}^3 \text{ s}^{-1}$) [12]. In the systems used for studying e_{aq}^- and H^\bullet reactions the relatively unreactive radicals formed from *tert*-butanol are also present, these radicals do not react with dye molecules.

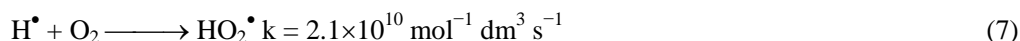
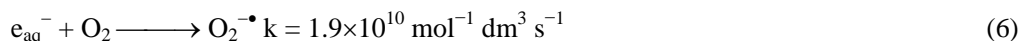
Reactions of $\bullet OH$ radicals are investigated in N_2O saturated solution in the 3 – 11 pH range. In such solution e_{aq}^- is converted to $\bullet OH$ in Reaction (4). (At saturation the N_2O concentration is $0.025 \text{ mol dm}^{-3}$ at room temperature.) There is a small (~10%) contribution

from the H^\bullet atom reactions. In highly alkaline solutions OH^\bullet transforms to O^- with an acid dissociation constant of 11.9 (Reaction (5)). O^- is generally less reactive than OH^\bullet .

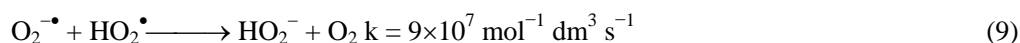


2.2. Solutions with Dissolved Oxygen

In practical systems oxygen is always present with a molar concentration of $0.25 \text{ mmol dm}^{-3}$ at room temperature. It reacts with e_{aq}^- and H^\bullet rapidly to form superoxide radical anion ($\text{O}_2^{\bullet-}$) or perhydroxyl radical (HO_2^\bullet) in reactions (6) and (7):



There is an acid/base equilibrium (8) between the two species with a $\text{p}K_{\text{a}}$ of 4.8. The $\text{O}_2^{\bullet-}/\text{HO}_2^\bullet$ pair has rather low reactivity and in the absence of proper reaction partners the species decay in self-termination reactions [6,11]:



The reaction between two $\text{O}_2^{\bullet-}$ radicals is extremely slow, $k < 3 \times 10^{-1} \text{ mol}^{-1} \text{ dm}^3 \text{ s}^{-1}$.

The hydrogen peroxide formed in water decomposition (Reaction (1)) and also in the reaction of two superoxide radical anion/perhydroxyl radicals, as we will show later, under certain conditions may play an important role in the degradation of dye molecules.

2.3. Scavenging Capacity

The reactive intermediates formed in water radiolysis may react with several different molecules in the solution. E.g. OH^\bullet radical reacts with intact dye molecules, with transformed dye molecules, or with other molecules in the solutions, such as cellulose fragments, carbonate, transition metal ions. The ratios of the different reactions are determined by the

scavenging capacities of the individual molecule types: scavenging capacity is defined as the product of the rate coefficient and the concentration for a given molecule type [11]. Proportion (P) of the reaction of a given water radical with the intact dye molecules is calculated as follows:

$$P = \frac{k_{\text{Dye}} [\text{Dye}]}{k_{\text{Dye}} [\text{Dye}] + \sum_i k_i [X_i]}. \quad (12)$$

In the equation the i summation goes for all types of molecules being in the solution, k_{Dye} [Dye] is the scavenging capacity of the dye, and $\sum_i k_i [X_i]$ is the scavenging capacity of the other molecules together.

2.4. Methods for the Investigation of the Reaction Mechanisms

The degradation of high molecular mass dye compounds is rather complicated and for understanding the details of the processes highly sophisticated techniques are needed. By the application of fast intermediate observation techniques and new final product separation and identification techniques there was a great progress in understanding the degradation mechanism during the last decade [3].

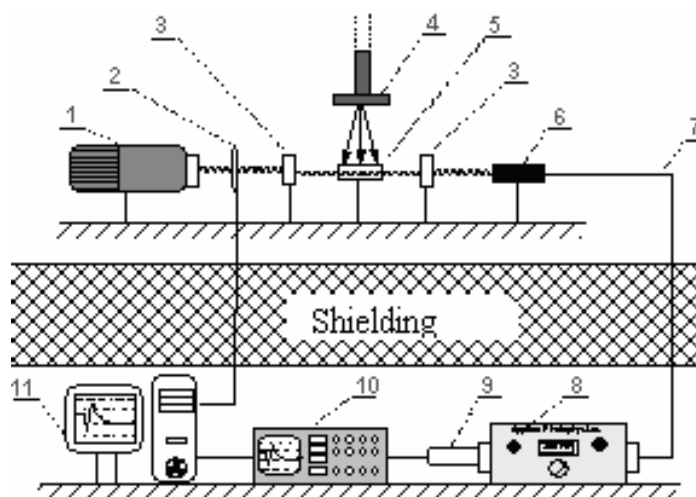
2.4.1. Pulse Radiolysis

The *intermediates* of chemical changes in radiation chemistry are usually highly reactive and therefore their lifetimes are short: for their detection fast techniques are needed. In pulse radiolysis (Figure 1) an electron accelerator produces short pulses of electrons, accelerated to several MeV energy. The accelerated electrons are directed into a cell, which contains the sample to be irradiated. The chemical changes are induced by the energy absorbed when the short electron pulse hits the cell. In pulse radiolysis the time dependence of build-up and decay of intermediates and stable products are followed by their light absorption as illustrated by Figure 2, inset [13-15]. The method, also called kinetic spectrophotometry, or time resolved spectrophotometry, differs from the conventional spectrophotometric technique since it uses a single light path: the reference level is obtained as the light level passing the sample prior to irradiation. This is the basis for the high sensitivity of kinetic spectrophotometry: changes less than 1% in the transmitted light intensity are measured accurately. Averaging of a large number of traces is possible when using computerized data acquisition system. The second important difference as compared to the conventional spectrophotometry is the fast response time.

A schematic illustration of a pulse radiolysis setup is shown on Figure 1. In usual arrangements the measuring system is divided in two parts. The first part, including the light source for sample illumination, the lens system, the shutter preventing the heating and photolysis of the sample, light filters, and the measuring cell itself, is housed in the irradiation room. The measuring cell should be positioned in the beam so as to achieve an approximately homogeneous irradiation. The other parts of the setup are outside the radiation shielding

concrete wall and the Faraday cage protecting against electromagnetic interference. These include monochromator, photodetector, oscilloscope/digitizer and computer system for data acquisition and processing. Light is usually transmitted from the irradiation room to the measuring room through a hole in the shielding by means of mirrors and lenses. Less frequently light guide cable is used.

By kinetic spectrophotometers the time-dependent absorbance (A) of the observed species is measured. According to the Lambert–Beer law:



- 1 – analyzing light source
- 2 – shutter
- 3 – lens
- 4 – electron beam
- 5 – cell
- 6 – light condenser
- 7 – light guide cable
- 8 – monochromator
- 9 – photodetector
- 10 – oscilloscope
- 11 – computer

Figure 1. Schematic representation of pulse radiolysis with kinetic spectroscopic detection.

$$A = \log \frac{I_0}{I} = \log \frac{100\%}{T} = \varepsilon_\lambda cd. \quad (13)$$

Where I_0 and I are the intensities of the incident and the transmitted light, respectively, T is the transmission in %, ε_λ is the linear molar absorption coefficient at wavelength λ , c is the concentration, and d is the optical path-length in the cell.

In dilute aqueous dye solutions basically the water absorbs most part of the energy and the intermediates formed in water radiolysis (e_{aq}^- , $\bullet\text{OH}$ and $\text{H}\bullet$) induce the chemical reactions. The reaction of these primary intermediates with dye molecules results in formation of

secondary (dye) intermediates. The concentration of the intermediates is followed by detecting their light absorption. Kinetic curves taken at several wavelengths are used to compute the spectra of intermediates (Figure 2). The spectra are characteristic to the intermediates formed and any change either in the shape of the spectrum or in the wavelength of the maximum indicates modification in the chemical structure.

From the kinetic curves, usually taken at the maximum of the absorption spectrum on a short time scale (nanosecond or some microseconds), the rate coefficients of addition of the radiolysis intermediates of the solvent to solute molecules are obtained (decay of primary intermediates and formation of secondary (dye) intermediates). Based on long time scale measurements in the millisecond range, the rate coefficients of the disappearance of dye intermediates are calculated.

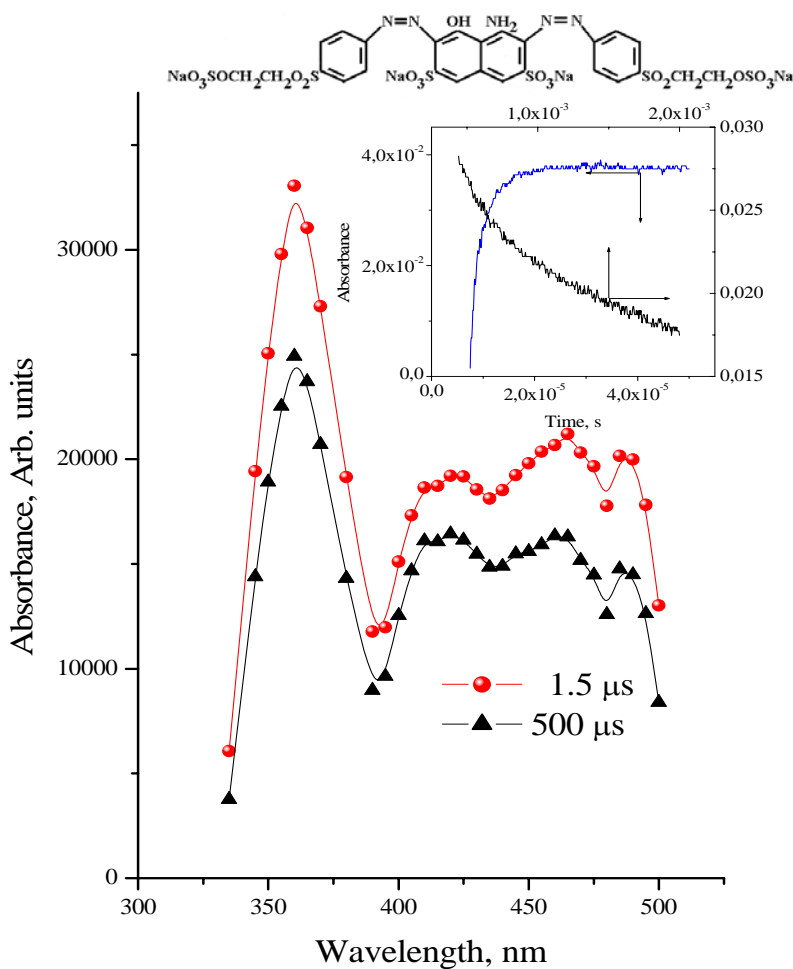


Figure 2. Typical absorption spectra of intermediates obtained in Reactive Black 5 (RB5) solution and typical absorbance build-up and decay profile (inset). (Both measured in the authors' laboratory.)

2.4.2. Steady State Techniques

In the field of environmental applications as irradiation sources mostly electron accelerators are used. These electron accelerators usually deliver 0.5-2 MeV electrons and

have energy outputs up to several hundred kW. However, experiments for research purposes are often carried out by gamma radiolysis, applying ^{60}Co radioactive sources emitting 1.19 and 1.33 MeV gamma photons.

The simplest method to follow the dye degradation caused by irradiation is UV-VIS spectroscopy (see e.g. Figure 3). In this case the degradation products are not separated from the starting compound [16-20]. When UV-VIS spectroscopy is used; the absorption spectrum of the starting dye and those of the products strongly overlap. Usually parallel several products form and their absorption spectra are not characteristic enough to allow identification.

For product separation gas chromatography (GC) or high performance liquid chromatography (HPLC) are used. The products are usually detected by standard techniques as flame ionization or absorbance [21-26]. Fourier-Transformed-Infrared spectroscopy (FTIR), Mass-Spectrometry (MS), and Nuclear-Magnetic-Resonance spectroscopy (NMR) are often useful in the identification of products.

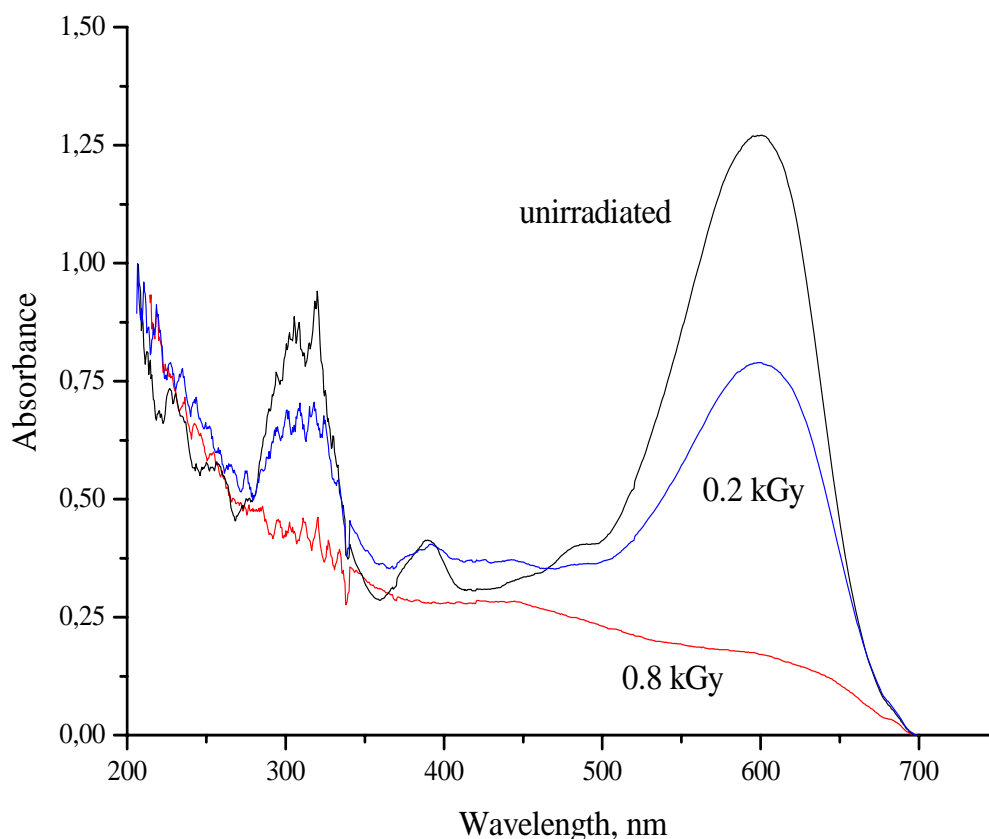


Figure 3. UV-VIS absorption spectrum of $5 \times 10^{-5} \text{ mol dm}^{-3}$ RB5 solution: unirradiated and irradiated with 0.2 and 0.8 kGy dose, air saturated. (Measured in the author's laboratory.)

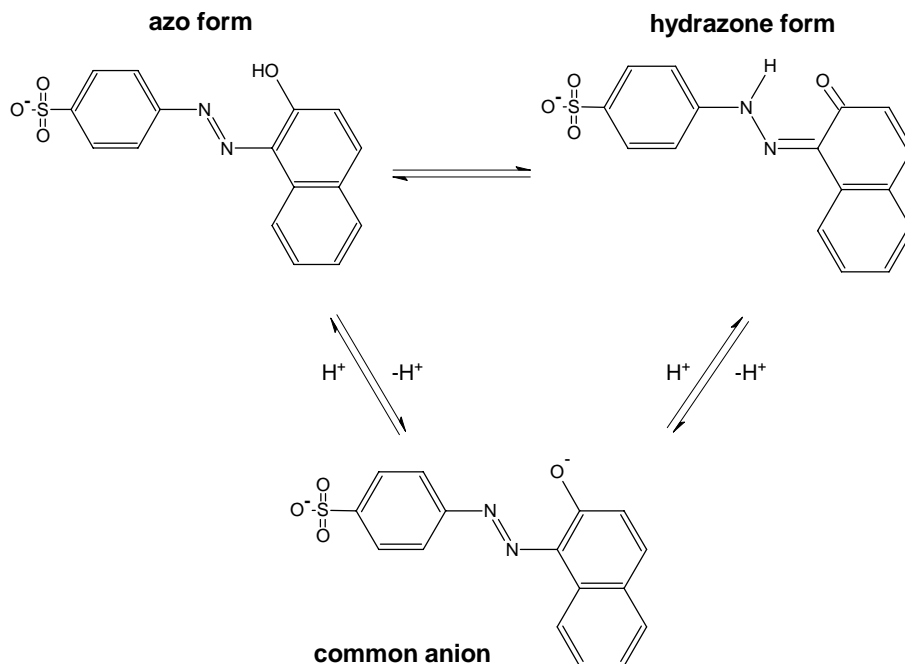


Figure 4. Azo-hydrazone tautomerism of AO7.

3. PREFERRED SITES OF RADICAL ATTACK

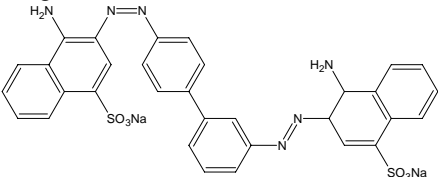
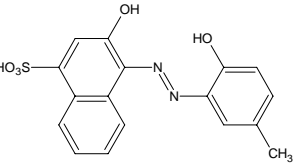
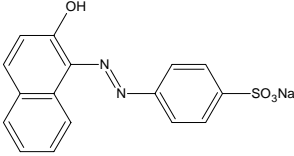
Since most of the azo dyes are high molecular mass structured molecules with several functional groups, it is usually difficult to determine the primary place of radical attack and the reaction mechanism. In this respect experiments with smaller molecular mass model compounds, like phenols, anilines, azobenzenes, H-acid or simpler dye molecules are of great help. Many experiments were carried out in order to identify the intermediates by pulse radiolysis technique. In order to observe the final products chemical separations were applied with simpler model compounds or simpler dye molecules. The authors of these works based on the transient absorption spectra and the final products formed tried to identify the preferential sites of radical attack. Theoretical calculations were also of great help during the identification [3].

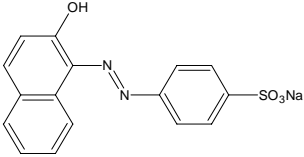
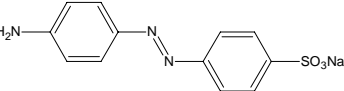
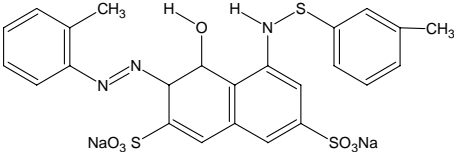
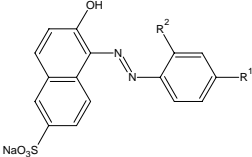
According to the frontier orbital theory, chemical reactions preferentially occur at the position of the molecule where their frontier orbital strongly overlap. Nucleophilic reactions (e_{aq}^- , H^\bullet) may occur at the atom where the electron density of the lowest unoccupied molecular orbital (LUMO) is the largest, whereas electrophilic reactions ($^{\bullet}OH$) may occur at the position where the density of the highest occupied molecular orbital (HOMO) is the largest [2].

3.1. Hydroxyl Radical

Hydroxyl radical ($\cdot\text{OH}$) is a powerful oxidant that adds to unsaturated bonds with practically diffusion-controlled rate coefficient ($k \approx 10^{10} \text{ mol}^{-1} \text{ dm}^3 \text{ s}^{-1}$, Table 1) and abstracts H atom from C-H bonds. The latter reaction is generally 1-3 orders of magnitude slower than the addition reaction; therefore abstraction reaction is unimportant from the point of view of primary radical attack. (However, abstraction reactions are more important in the mineralization process, when all of the aromatic rings have already degraded.) It is considered to be a strong electrophilic radical, therefore, it reacts preferably with molecule sites with higher electron density. Due to the high reactivity, the hydroxyl radical exhibits relatively little selectivity in radical addition reactions.

Table 1. Rate coefficients of $\cdot\text{OH}$ radical reactions with selected organic molecules and dyes

Molecule	Rate coefficient, $k \text{ mol}^{-1} \text{ dm}^3 \text{ s}^{-1}$
Benzene [10]	7.9×10^9
Toluene [10]	5.1×10^9
Phenol [28]	1.4×10^{10}
Aniline, pH basic [10]	8.6×10^9
<i>N,N'</i> -Dimethylaniline [10]	1.4×10^{10}
Azobenzene [10]	2.0×10^{10}
Naphthalene [10]	9.4×10^9
1-Aminonaphthalene-4-sulphonate ion [10]	7.9×10^9
<i>p</i> -phenylazoaniline (<i>p</i> -PPA) [30]	1.1×10^{10}
Congo Red (C.I. Direct Red 28) [31]	1.2×10^{10}
	
Calgamite [32] 	1.1×10^{10}
Orange I [1] 	pH 4, 7×10^9 pH 6.6, 9×10^9 pH 10.5 1.1×10^{10}
Acid Orange 7 (AO7) [33]	4.08×10^9

	
Methyl Orange [32] 	$(2 \pm 0.3) \times 10^{10}$
Acid Red 265 [34] 	$(9.3 \pm 1.4) \times 10^9$
Arylazo-2-naphthol [35] $R^1 = R^2 = H$ $R^1 = H, R^2 = OCH_3$ $R^1 = OCH_3, R^2 = H$ $R^1 = Cl, R^2 = H$ $R^1 = CH_3, R^2 = H$	 1.1×10^{10} 1.0×10^{10} 1.1×10^{10} 1.0×10^{10} 1.2×10^{10}

As probable site of $\bullet OH$ radical attack on dye molecules the following possibilities are considered: attack on the azo bridge or on the azo-linkage bearing carbon atom, attack on the rings, and in case of dyes with amino group, direct oxidation here.

Azobenzene reacts with a rate coefficient of $k = 2.0 \times 10^{10} \text{ dm}^3 \text{ mol}^{-1} \text{ s}^{-1}$ with $\bullet OH$ radicals. About 40% of $\bullet OH$ add to the benzene ring producing a transient with absorption maximum at 330 nm (cyclohexadienyl type radical), and ~60% add to $-N=N-$ double bond forming transient with maximum absorbance at 420 nm (hydrazyl type radical) [27].

Acid Orange 7 (AO7, synonymous with Orange) may be considered a simple, but typical dye in textile wastewaters. It is a phenylazonaphthol with azo and hydrazone forms. In aqueous solution the hydrazone form predominates (Figure 4). Being one of the simplest azo dyes, the radiolytic reactions of Acid Orange 7 were very often studied in dilute solutions by pulse and gamma radiolysis, spectrophotometry and HPLC separation techniques, and also by theoretical calculations. So there is ample possibility to compare analytical results with the results of theoretical calculations.

According to the electron densities of HOMO and LUMO calculated by Hihara et al. [36], the electrophilic attack by $\bullet OH$ radical should occur at the N atom bound to the benzene ring and at the C atom where the naphthalene ring and the azo group of AO7 link up. The electron densities of HOMO at the two positions are similar. The quantum chemical molecular orbital calculations of Özen et al. [37] using density functional theory are more or less in agreement with that of Hihara et al. [36,38]. The oxidative degradation is proposed to occur through cleavage of $N=N$ bond, following the $\bullet OH$ radical addition to the chromophore. The presence of hydrazone tautomers might be responsible for the involvement of C–N cleavage in the degradation of azo dyes.

Spadaro and co-workers [39] used Fenton's $\cdot\text{OH}$ radicals to investigate the decomposition of simple azo dye model compounds. They presented evidence for the generation of benzene and substituted benzenes from $\cdot\text{OH}$ radicals induced decomposition of azo dyes with phenylazo substitution. They suggested a mechanism in which $\cdot\text{OH}$ adds to the azo linkage-bearing carbon atom (C-4) of hydroxyl or amine substituted ring (Figure 5). The resulting $\cdot\text{OH}$ adduct breaks down to produce phenyldiazene (Ph-N=NH) or substituted phenyldiazene and phenoxy radical ($\text{PhO}\cdot$). Phenyldiazene is extremely unstable, $\cdot\text{OH}$, or O_2 can readily transform it by one electron oxidation to yield phenyldiazene radical. The latter intermediate is also unstable and cleaves homolytically to generate phenyl radical and N_2 . Phenyl radical transform to benzene by H atom abstraction, e.g. from $\text{HO}_2\cdot$. The phenoxy radical may stabilize in bimolecular self-termination reactions (Figure 5).

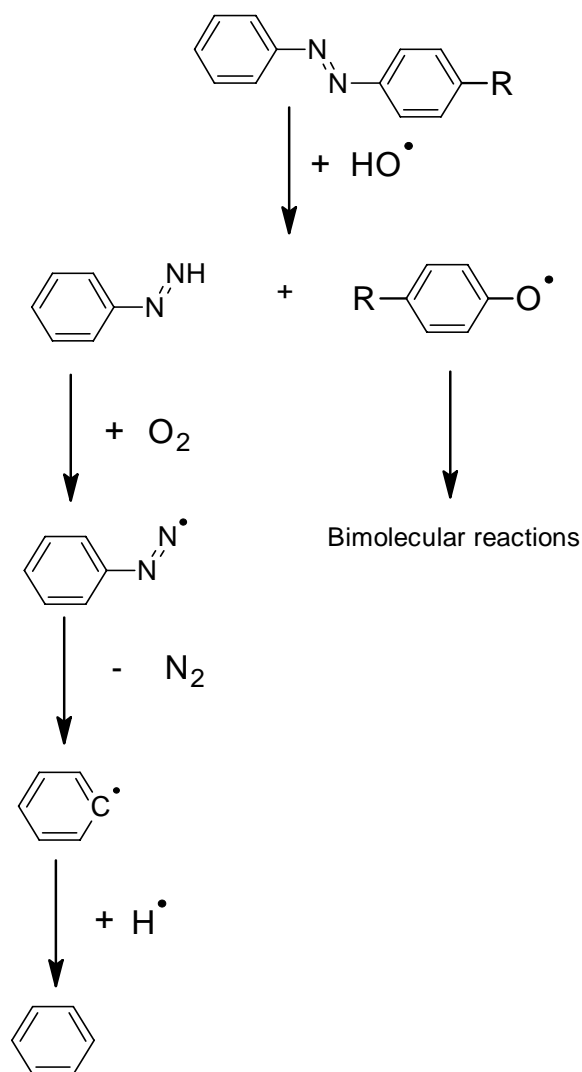


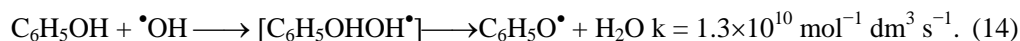
Figure 5. Mechanism of benzene formation in dye decomposition: R = NH_2 , or OH.

No Ph-N=NH formation is reported in experiments using sonochemical initiation [40,41]. In this case the extreme conditions (high pressure, gas-liquid interface) may facilitate immediate decomposition of labile products. By oxidizing azobenzenes and related azo dyes with combined sonochemical and Fenton reactions Joseph et al. [40] reported the oxidation of nitrogen to NO_x yielding nitroaromatic compounds. A portion of these products is able to partition within the gas phase inside the bubbles of cavitations and undergo fast decomposition forming NO₂.

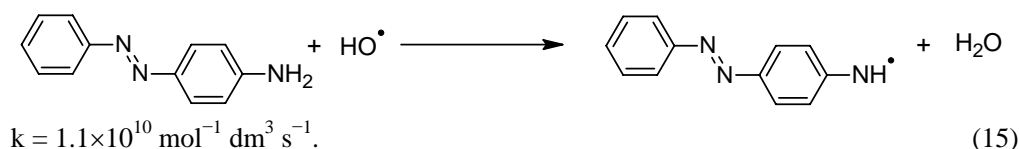
Concerning phenyldiazene product Coen and co-workers suggested a formation route through phenoxy type radical and then carbenium ion intermediate (Figure 6) [42].

We know very little about the preferred site of electrophilic radical attack on the aromatic ring (except the azo bridge bearing carbon atom). Some experimental findings suggest [•]OH radical addition on the carbon atom bearing the sulfonate group, this reaction may be followed by subsequent elimination of SO₃ [29]. The electron withdrawing character of the sulfonate group and steric hindrances do not support this reaction. However, the reaction was observed during the degradation of several dyes e.g. AO7 and AO52.

The H-acid based azo dyes and several other dye molecules contain OH groups on aromatic ring. When [•]OH radical addition takes place on the OH substituent bearing aromatic ring the cyclohexadienyl type radical thus formed may stabilize in an acid-base catalyzed water elimination reaction. This reaction is slow in neutral solutions. Phenoxy type radical forms in the elimination. We show the addition/elimination mechanism on the example of phenol [28,43]:



As we mentioned before hydroxyl radicals as electrophilic oxidants may react with the electron-rich site on the amino group [29,30]. Krapfenbauer et al. [30] for the reaction with *p*-phenylazoaniline suggested a simple H atom abstraction:



Galindo for the [•]OH radical reaction with AO52 which contains dimethylamino group (aminoazobenzene derivative) suggested a more complicated mechanism (Figure 7) [29]. The reaction can be initiated by one-electron extraction from the amino substituent by hydroxyl radical. The resulting radical cation undergoes oxidation to give iminium ion, from which secondary amine can be formed by solvolysis. The eliminated methyl groups are expected to convert to formaldehyde and consequently to formic acid.

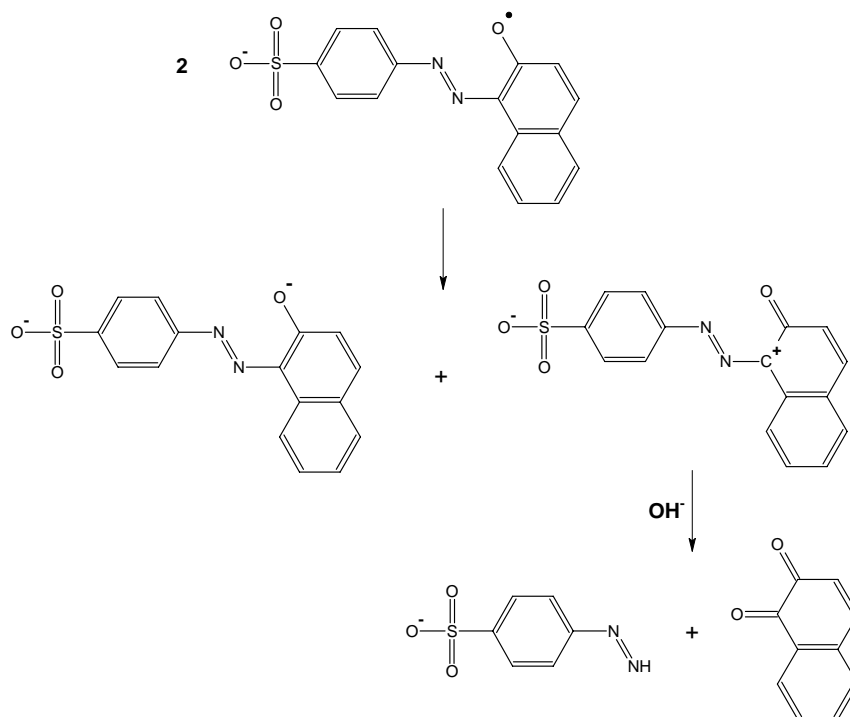


Figure 6. *p*-Sulfonate phenyldiazene formation through disproportionation of two phenoxy radicals.

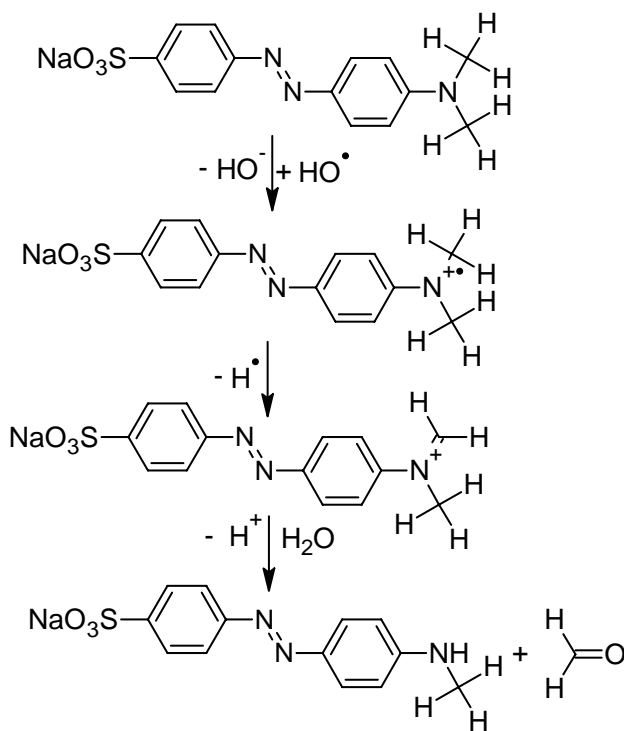
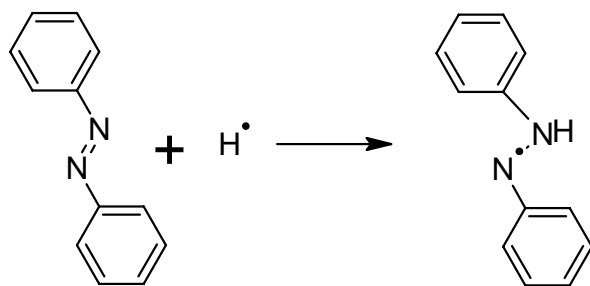


Figure 7. HO^\bullet radical attack on the amino group of AO52.

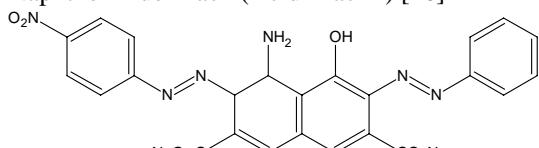
3.2. Hydrogen Atom

Hydrogen atom (H^\bullet), similarly to hydroxyl radical, reacts with double bonded compounds in radical addition reactions, however the rate coefficients of radical additions are often smaller by an order of magnitude than the diffusion controlled limit ($k_{\text{diff}} \approx 3 \times 10^{10} \text{ mol}^{-1} \text{ dm}^3 \text{ s}^{-1}$, Table 2) [44]. Therefore the reactions show higher selectivity. As the experiments of Flamigni and Monti with azobenzene have shown [45] H^\bullet adds to the azo bond:



(16)

Table 2. Rate coefficients of H^\bullet atom reactions with selected organic molecules [10]

Molecule	Rate coefficient, k $\text{mol}^{-1} \text{ dm}^3 \text{ s}^{-1}$
Benzene	1.1×10^9
Phenol	1.7×10^9
Aniline, pH basic	2×10^9
Azobenzene	3.3×10^{10}
Naphthalene	3.4×10^9
2-Naphthol	1×10^9
Naphthol Blue Black (Acid Black I) [46] 	1.04×10^9

3.3. Hydrated Electron

The hydrated electron (e_{aq}^-) in its chemical reactions shows very strong nucleophilic character. According to the frontier orbital theory, nucleophilic reactions (e_{aq}^- , H^\bullet) may occur at the atom where the electron density of the lowest unoccupied molecular orbital (LUMO) is the largest. Hydrated electron reacts with azo compounds usually with very high rate coefficients of $\sim 10^{10} \text{ dm}^3 \text{ mol}^{-1} \text{ s}^{-1}$ (Table 3). As Flamigni and Monti have shown [45] on the example of *trans*-azobenzene e_{aq}^- attacks the $-\text{N}=\text{N}-$ double bond: hydrazyl radicals (the same as produced in H^\bullet reaction (16)) are the primary species resulting from the rapid protonation of the corresponding anions (Reaction (17)). Hydrazyl radicals react with the

parent compound to give dimer radicals in competition with other second order processes. Subsequently the dimer radicals undergo disproportionation with a low rate coefficient (10^6 – $10^7 \text{ mol}^{-1} \text{ dm}^3 \text{ s}^{-1}$).

According to the electron densities of HOMO and LUMO calculated by Hihara et al. [36], the nucleophilic reaction of AO7 may occur primarily at the N atom bound to the naphthalene ring. End-product measurements are in agreement with this suggestion: hydrated electrons (and also H^\bullet atoms) induce decoloration with close to 100% efficiency, which is expected if e_{aq}^- has low reactivity with other parts of the molecules and if Reaction (17) finally leads to destruction of the extensive conjugation through the $-\text{N}=\text{N}-$ double bond.

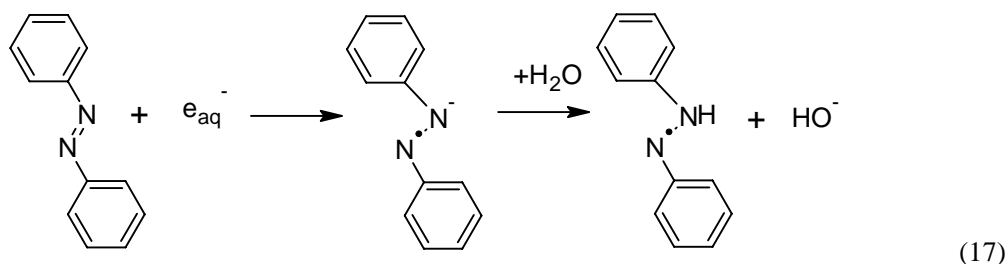


Table 3. Rate coefficients of e_{aq}^- reactions with selected organic molecules and dyes [10]

Molecule	Rate coefficient, k $\text{mol}^{-1} \text{ dm}^3 \text{ s}^{-1}$
Benzene	9.0×10^6
Phenol	3.0×10^7
Aniline, pH basic	3.0×10^7
Azobenzene	3.3×10^{10}
Naphthalene	5.0×10^9
1-Aminonaphthalene-4-sulphonate ion	6.7×10^9
<i>p</i> -phenylazoaniline (<i>p</i> -PPA) [30]	3.5×10^{10}
Congo Red (C.I. Direct Red 28) [31]	1.6×10^9 3.6×10^9
Arylazo-2-naphthol [35]	
$\text{R}^1=\text{R}^2=\text{H}$	2.5×10^{10}
$\text{R}^1=\text{H}, \text{R}^2=\text{OCH}_3$ $\text{R}^1=\text{OCH}_3,$ $\text{R}^2=\text{H}$	1.5×10^{10}
$\text{R}^1=\text{Cl}, \text{R}^2=\text{H}$	8×10^9
$\text{R}^1=\text{CH}_3, \text{R}^2=\text{H}$	1.9×10^{10}
	1.6×10^{10}

The reductive attack of AO7 leads to the formation of amino substituted compounds as it is shown on Figure 8. The e_{aq}^- adds to the sp^2 - hybridized N atom attached to the naphthol moiety of the dye forming dye radical anion, which is protonated in very fast reaction by water leading to the formation of hydrazyl radical [2,35]. Further second order reactions lead to the formation of 1-aminonaphthalene-2-ol and 4-aminobenzenesulfonate stable products.

3.4. Superoxide Radical Anion/perhydroxyl Radical Pair ($O_2^{\bullet-}/HO_2^{\bullet}$)

As the rate coefficient of e_{aq}^- and H^{\bullet} with O_2 are around $2 \times 10^{10} \text{ mol}^{-1} \text{ dm}^3 \text{ s}^{-1}$ (Reactions (6) and (7)) and the concentration of dissolved oxygen in water at room temperature is c.a. $0.25 \text{ mmol dm}^{-3}$, the scavenging capacities for both species are around $5 \times 10^6 \text{ s}^{-1}$. The rate coefficients of e_{aq}^- reactions with dye molecules are in the range of $10^{10} \text{ mol}^{-1} \text{ dm}^3 \text{ s}^{-1}$. In the absence of other competing reactions practically the concentrations determine whether e_{aq}^- predominantly reacts with the dye inducing reduction or e_{aq}^- is captured by the oxygen molecule transforming to the $O_2^{\bullet-}/HO_2^{\bullet}$ pair. In the case of H^{\bullet} , due to its lower reactivity with double bonded molecules, high dye concentrations are needed for effective scavenging.

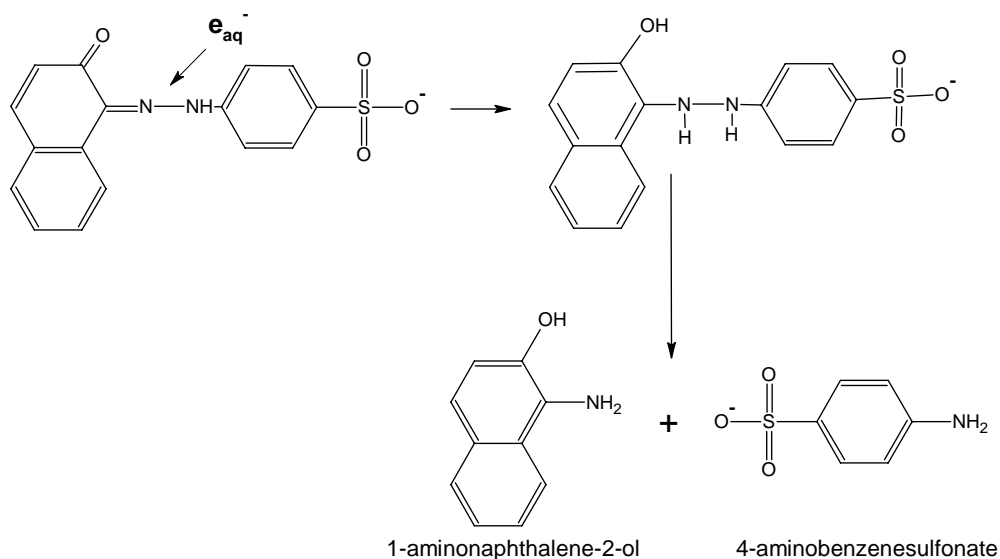


Figure 8. Reductive degradation of AO7.

In connection with the degradation of pesticides and chlorinated aromatic compounds there is an intensive research in order to apply combined irradiation and ozone technique. Ozone addition was found to increase the efficiency of organic molecule decomposition in combined treatment. $O_2^{\bullet-}/HO_2^{\bullet}$ pair also forms in ozone decomposition in alkaline media:





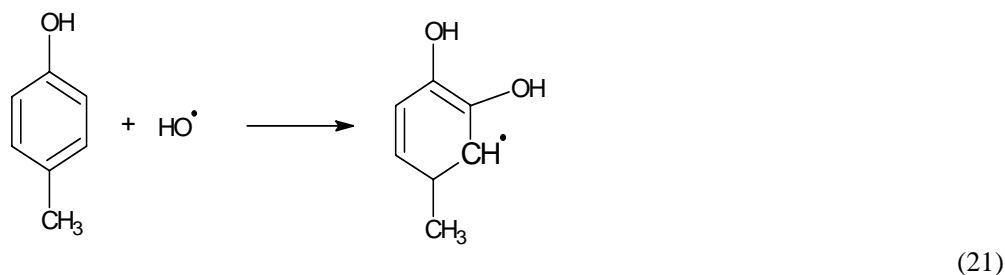
Since the $\text{O}_2^\bullet/\text{HO}_2^\bullet$ pair can easily be produced in radiolysis of aqueous oxygen containing solutions, pulse radiolysis is a convenient method to study their reactions. According to the general experiences HO_2^\bullet and O_2^\bullet are rather unreactive with the intact dye molecules (in general with aromatic molecules) [23,24,30,47].

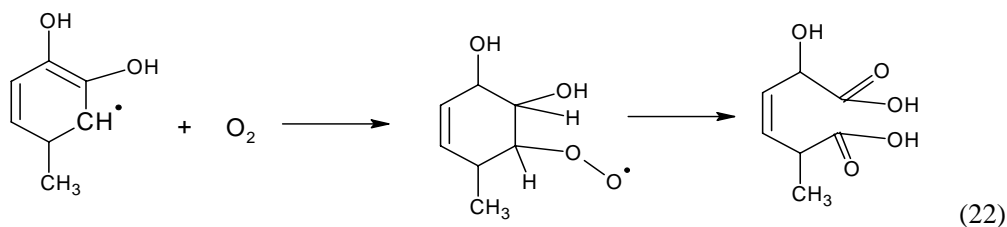
Due to the low pK_a of $\text{O}_2^\bullet/\text{HO}_2^\bullet$ pair (4.8) in neutral and basic solutions the O_2^\bullet form is present. O_2^\bullet is a reducing species with a standard reduction potential of $E(\text{O}_2/\text{O}_2^\bullet) = -0.33 \text{ V}$ versus Normal Hydrogen Electrode (NHE) [7]. Hydrated electron (a strongly reducing species ($E(\text{aq}/e_{\text{aq}}^-) = -2.9 \text{ V}$ vs. NHE), as it was discussed before, reduces the dye molecules (see Figure 8 and Equ. (17)). Similar reduction is also observed with the 2-hydroxy-2-propyl radical ($E(\text{CH}_3\text{COCH}_2\text{H}^\bullet/\text{CH}_3\text{C}(\text{OH})\text{CH}_3) = -1.9 \text{ V}$ vs. NHE). Hydrogen atom which is also strongly reducing species ($E(\text{H}_{\text{aq}}^\bullet/\text{H}^\bullet) = -2.4 \text{ V}$ vs. NHE) causes reduction in radical addition reaction. It seems that the reduction potential of O_2^\bullet is not negative enough to carry out reduction. The reduction potential of methyl orange dye was determined to be $E(\text{Dye}/\text{Dye}^\bullet) = -0.66 \pm 0.02 \text{ V}$, after correction for the ionic strength of the solution [1].

The $\text{O}_2^\bullet/\text{HO}_2^\bullet$ pair is known to react with quinone type molecules [48]. Therefore they may react with some of the intermediate products in the mineralization process [49].

3.5. Reaction of Dye Radical with Dissolved Oxygen

Molecular oxygen reacts with most of the carbon centered radicals with rate coefficients close to the diffusion controlled limit. So when dissolved O_2 is present in the liquid there is a competition between the reactions of dye radicals with each-other (self-termination), with other molecules present, and with oxygen molecules. The peroxy radicals formed in O_2 radical scavenging reaction are involved in a large number of relatively slow bimolecular and unimolecular processes. As Getoff and co-workers have shown [30,47,50] such processes may lead to opening of the aromatic rings forming aliphatic carboxylic or dicarboxylic acids. There is a step-by-step fragmentation to smaller molecular mass aldehydes, ketones, carboxylic acids, etc. In the presence of oxygen compounds with progressively higher oxygen-to carbon ratio are involved in the conversion of an organic molecule to CO_2 and H_2O . We show the ring-opening reaction on the example of *p*-cresol:





4. DYE DEGRADATION

4.1. Decoloration

In most of the works on radiation induced dye degradation decoloration experiments were carried out utilizing UV-VIS spectrophotometry. This is usually done by preparing appropriate solutions, treating them by stepwise increasing doses and after each treatment taking the absorption spectra. In radiolysis investigations this treatment is often done in a glass container, which has attached quartz cuvette for taking the absorption spectra in a spectrophotometer. The cuvette should be made of good quality Suprasil quartz, which does not change its transparency during irradiation.

Azo dyes have wide absorption bands in the visible region [51]. In the absorption spectrum of AO7 (Figure 9) there is a strong peak at 484 nm and a shoulder at 430 nm. The peaks in the UV region at 228, 254 and 310 nm originate from the aromatic rings, the peak in the visible range at 484 nm with a shoulder at the lower wavelength side reflect the conjugated structure. The 484 nm peak suggests the presence of hydrazone form (Figure 4), whereas the shoulder may belong to the azo form [2,52].

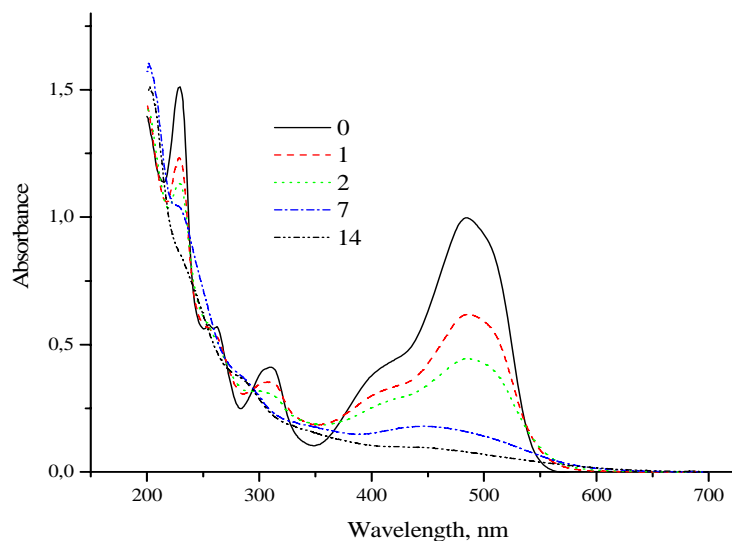


Figure 9. Absorption spectra of aerated AO7 solution prior to irradiation and irradiated with absorbed doses indicated (in kGy). Initial concentration 0.5 mmol dm^{-3} , all solutions were 10 times diluted before spectrophotometric measurements taken in the authors' laboratory.

In Figure 10 we show the absorption spectrum of Apollofix-Red (AR-28, also called as CI. Reactive Red or CI. 18215). AR-28 is a triazine and H-acid containing azo dye with intensive red color, $\lambda_{\max} = 514, 532 \text{ nm}$, $\epsilon_{\max} = 31400 \text{ mol}^{-1} \text{ dm}^3 \text{ cm}^{-1}$. The dye undergoes an acid dissociation at the OH group with $\text{pK}_a = 11.74$. It also exists in azo-hydrazone tautomer pair. (Below the pK_a value of H-acid containing azo dyes either of the two isomers may dominate, depending on the chemical structure of the dyestuff. In the case of *p*-substituted dyes the azo configuration very strongly prevails. When a phenyl group is attached to the $-\text{N}=\text{N}-$ azo group with a substituent in *o*-position, like for AR-28 the hydrazone tautomer dominates.) In the case of H-acid containing dyes with secondary amino group (i.e. there is an H atom attached to the amino N atom), for instance AR-28, the H atom on N may also be involved in the tautomerism.

When a dye containing solution is irradiated, the visible absorbance generally strongly decreases, and the intensity of some of the peaks in the UV region increases, however no clear isobestic point is detected (Figs. 3, 9, 10). This suggests that there is no direct conversion of the dye into a specific product: the degradation occurs through a number of parallel reactions and through a number of stages [2,23,24,29,31,34,53-59].

It follows from the identification of the absorption peaks discussed before, that decoloration simply means destruction of the extended conjugation through the azo bond. The peaks in the UV region (mostly substituted aromatic molecules) show much less alterations due to irradiation than the visible absorbances.

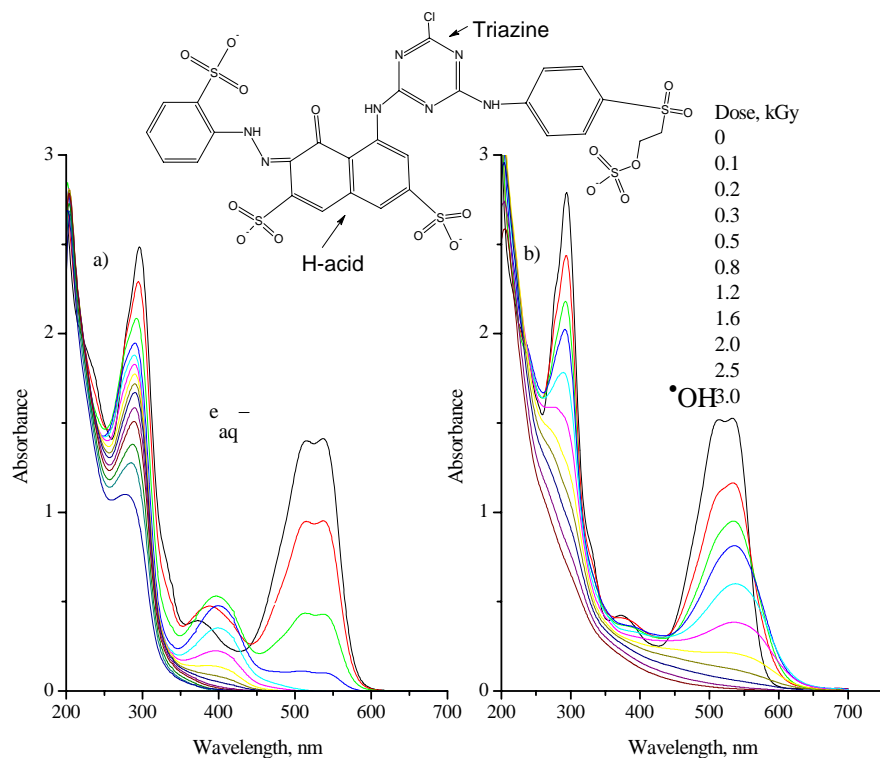


Figure 10. Decoloration of $8.5 \times 10^{-5} \text{ mol dm}^{-3}$ concentration aqueous AR-28 solutions in the reaction of hydrated electron (b) and in the reaction of hydroxyl radical (a) taken in the authors' laboratory.

The degree of decoloration is usually calculated from the decrease of absorbance at a selected wavelength, most conveniently at the maximum absorbance by using the equation:

$$\text{Decoloration(\%)} = \frac{A_0 - A}{A_0} \times 100\%. \quad (23)$$

where A_0 and A_i are the absorbances before and after the treatment, respectively.

When irradiating dye containing solutions the absorbance in the 400 – 600 nm region decreases. In some of the cases together with this decrease the shape of the spectrum also changes [3,23,24,53,54].

In those cases when the absorption spectrum in the visible range *does not change during the treatment* it is also observed that the absorbance at the wavelength of maximum decreases nearly linearly with the absorbed dose (or – at constant dose rate – with the time of treatment). A detailed kinetic analysis was carried out on this system and published in [3,54,60]. Here we show only the developed equation describing the change in dye concentration (proportional to absorbance) with time:

$$[A_1] = [A_1]_{t=0} - rt = [A_1]_{t=0} \left(1 - \frac{r}{[A_1]_{t=0}} t \right) = [A_1]_{t=0} (1 - k_{\text{obs}} t). \quad (24)$$

In the equation $[A_1]_{t=0}$ and $[A_1]$ are the concentration of intact dye molecules (in mol dm⁻³) at the beginning and at time t , r is the formation rate of attacking radicals (in mol dm⁻³ s⁻¹), and $k_{\text{obs}} = r/[A_1]_{t=0}$ is the observed first-order rate coefficient.

At longer irradiation times (higher doses) the depletion of the starting dye molecules can be so high that the intermediate reacts to considerable extent with the transformed molecules [3,30], for that reason the kinetics deviates considerably from linearity (Figure 11).

In the case of linear dose dependence it was also observed that the effectiveness of decoloration is close to unity: $G(\text{decoloration}) \approx G(\text{primary intermediate})$. Such behavior is observed when the intermediate reacts with the color giving chromoforic part (e.g. –C=N=N–C– bridge connecting the aromatic groups) of the dye molecule resulting in irreversible reaction here. This reaction leads to the destruction of extensive electron conjugation giving the color. The products formed do not have considerable light absorption in the visible range (and may have low reactivity with reducing species). The linearity of the dose dependence persists until the main reaction of the given primary intermediate is the reaction that induces the chromophore decomposition. Formerly we mentioned that the H^\bullet atoms and e_{aq}^- react with the azo part of the molecules leading to saturation of the –N=N– bridge or to its complete destruction.

We have to mention also, that although H^\bullet atoms and e_{aq}^- are very effective in the decoloration, these intermediates are much less effective in the mineralization following decoloration: for complete destruction of the organic subparts of molecules (fragments) oxidizing radicals and oxidizing conditions are needed to transfer organic carbon atoms to CO_2 and hydrogen atoms to H_2O .

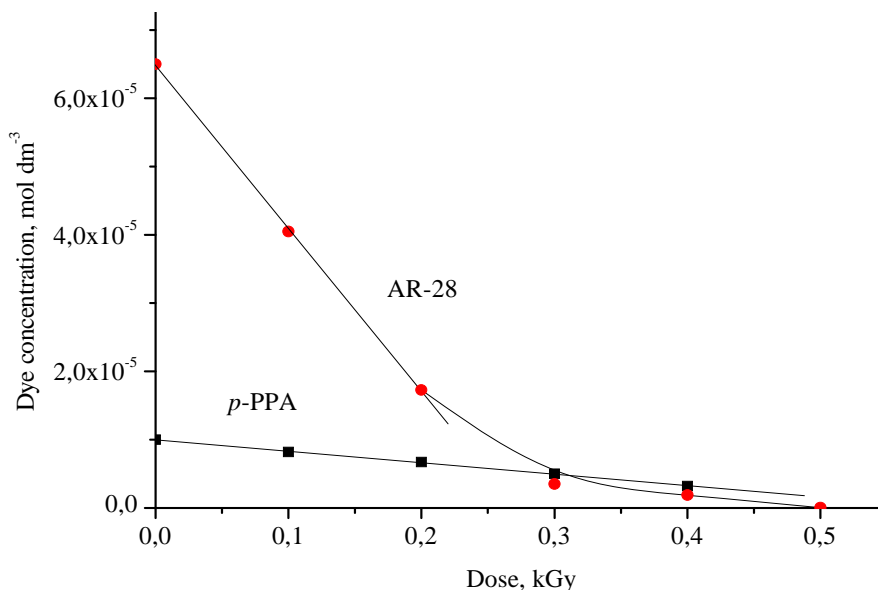


Figure 11. Linear decrease of dye concentration as a function of absorbed dose when Ar-28 or *p*-PPA reacted with e_{aq}^- in N_2 or Ar saturated solutions.

When the decoloration is due to the reaction of $\bullet OH$ radicals with the dye molecules *the absorption spectrum changes in the visible range during the treatment* [34,49,56-59]: the visible band gradually shifts to longer wavelengths as it is shown for AO7 and AR-28 on Figs 9 and 10b. When the visible spectrum changes during the treatment the kinetics of dye disappearance follows logarithmic time (dose) dependence. This dependence is described by the equation [3,54,60]:

$$[A_1] = [A_1]_{t=0} \exp\left(-\frac{r}{[A_1]_{t=0}}\right) = [A_1]_{t=0} \exp(-k_{obs} t). \quad (25)$$

In the equation $[A_1]_{t=0}$, $[A_1]$, t , r and k_{obs} have the same meaning as in the case of Equ. (24).

It should be mentioned that due to the changing absorption spectrum the spectrophotometric measurement does not supply the correct intact dye molecule concentration. For correct concentration measurement GC or HPLC separation and quantitative determination is needed [54].

The non-linear dye concentration-time (dose) dependence and also the changing absorption spectrum are due to the very high reactivity of $\bullet OH$ radicals with double bonds. After the color giving extensive conjugation is destroyed the transformed molecules (products) have still several double bonds to react with $\bullet OH$ radicals. Therefore the reactivity of $\bullet OH$ radicals with the primary products, and also with the secondary, tertiary etc. products is practically the same as with the intact molecules. As we described it in [3,54,60], such behavior leads to logarithmic time dependence. Logarithmic dependencies are shown in Figure 12.

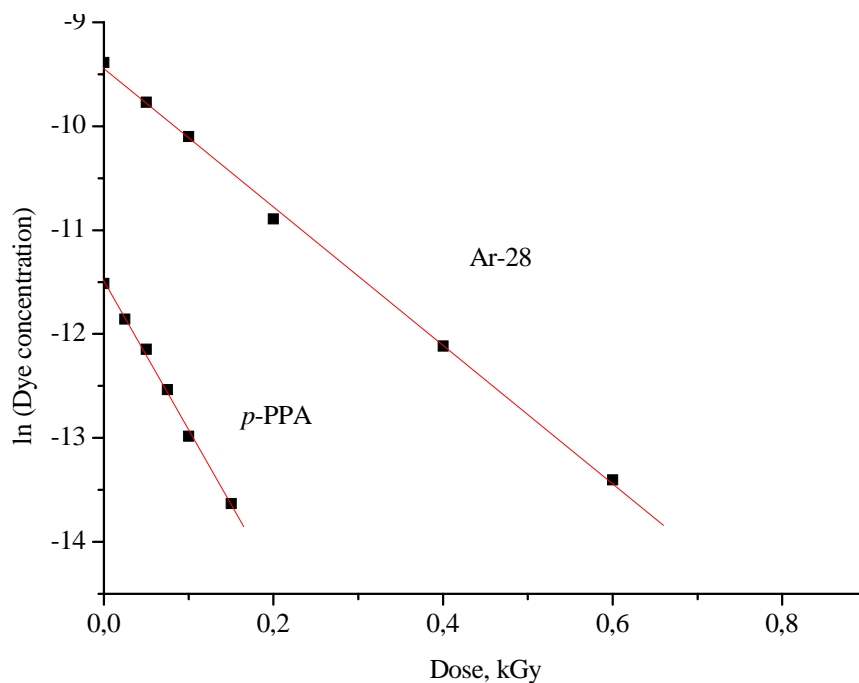
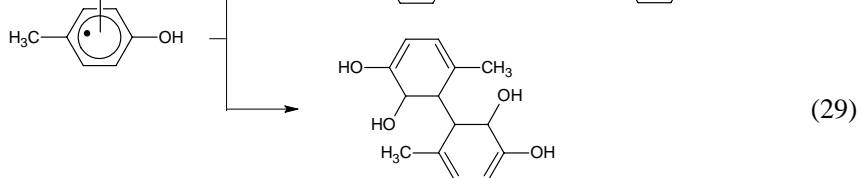
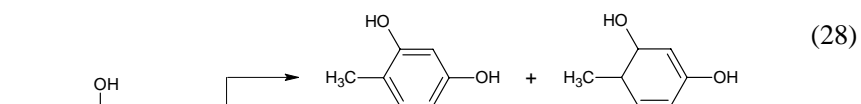
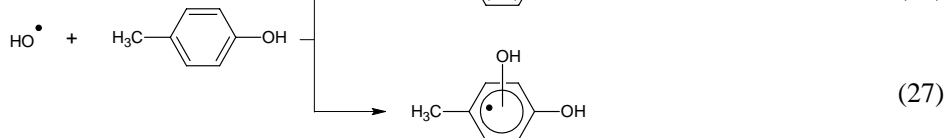
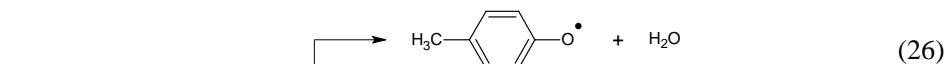


Figure 12. Logarithmic decrease of dye concentration as a function of absorbed dose when Ar-28 or *p*-PPA reacts with $\cdot\text{OH}$ radicals in N_2O saturated solutions.

The change of the absorption spectra and also the relatively small efficiency of decoloration also observed are due to $\cdot\text{OH}$ radical addition to the aromatic rings. As a result of radical addition to any of the aromatic rings cyclohexadienyl type radicals form. In order to illustrate the probable reactions when $\cdot\text{OH}$ radical adds to an aromatic ring (not to the azo bearing carbon atom) we show the example of *p*-cresol:



The cyclohexadienyl type radicals may transform to stable end-products in self-termination (disproportionation or combination) reactions. The combination leads to dimerized molecules in which the connecting rings lost the aromatic character. In disproportionation in one of the reacting molecules one ring loses the aromaticity, in the other molecule the aromatic character and by that the extensive conjugation is regenerated. However, the regenerated dye molecules have extra OH group attached to one of the aromatic rings. If this extra OH-group is on the part of the dye molecule that is involved in the extensive conjugation, the spectrum in the visible range shifts to the red.

When the dye molecules react with $\bullet\text{OH}$ radical with the progress of reaction the number of color giving intact and transformed molecules decreases and those of the transformed decolorated molecules increases. The competition between the $\bullet\text{OH}$ radical reaction with the decolorated and colored molecules can explain the logarithmic-like decoloration curves described by Equ. (25) (Figure 12) often observed under circumstances when $\bullet\text{OH}$ radical is the main reacting species.

4.2. Products of Chemical Transformations

In the previous sections of this chapter we have already touched the question of product formation. In general one can say that due to the attack of $\text{H}\bullet$ atoms and e_{aq}^- transformed molecules with destroyed $-\text{N}=\text{N}-$ bond form: saturation of this bond may occur, N_2 elimination or scission forming $\text{C}-\text{NH}_2$ groups in complex processes may take place. In $\bullet\text{OH}$ radical reactions destruction of the conjugation through the $-\text{N}=\text{N}-$ bond happens when the radical attack occurs on the azo bond, or on the carbon atom bearing the azo group. When the addition occurs on the other parts of aromatic rings OH substituted products form with or without color giving extensive conjugation.

The chemical identification of the individual products formed is extremely complicated because large number of compounds forms parallel and also because some of the products are labile and easily decompose during separation (e.g. in gas-chromatography). For these reasons the products of the primary transformations are known only in very few cases. The secondary, tertiary, etc. transformation products are even less known. In the case of smaller "model" compounds, like AO7 GC or GC coupled with MS can be applied for separation and identification. In case of larger molecular mass "real" dyes HPLC, eventually HPLC-MS is the proper tool [25,26].

Due to the large number of products (large number of parallel reactions) the process of mineralization is generally followed by such standardized methods as the determination of chemical oxygen demand (COD), biological oxygen demand (BOD), and total organic carbon content (TOC) [61,62]. As the degradation products can be toxic, toxicity measurements are also of essential importance [55].

The values of chemical oxygen demand, COD(Cr), biological oxygen demand BOD, and content of suspended solids (SS) are measured in accordance with standard methods, utilizing dichromate method at closed reflux (for COD(Cr)), Wincler's azide modification method (for BOD), and weighting the total filterable residue dried at 105°C (for SS). Permanganate method in acid medium via standard procedure is utilized for measuring COD(Mn). Total organic carbon content (TOC) values are determined as the difference between total carbon

and inorganic carbon contents, both measured by registering CO₂ evolved due to catalytic incineration of dry residue and due to acidifying the solution by phosphoric acid, respectively [63].

When TOC measurement is used to follow the destruction of organic molecules, the degree of mineralization is calculated by the relation [3]:

$$\text{Mineralization \%} = \frac{\text{TOC}_{\text{initial}} - \text{TOC}}{\text{TOC}_{\text{initial}}} \times 100\% . \quad (30)$$

The mineralization curves substantially differ from the decoloration curves (Figure 13) [59,64,65]. Although generally TOC reduction (i.e. mineralization) starts in the early stages of the treatment, during the decoloration period the TOC or COD reduction is very small. The TOC- and COD-values decrease substantially after the color disappeared. Generally COD and TOC measurements indicate a nearly linear decrease of the organic content with the time of treatment. At very high conversions the trends change and COD and TOC removals slow down. This is suggested to be due to formation of some aliphatic by-products which have low reactivity with the oxidizing $\cdot\text{OH}$ radicals [29]:

In mineralization the dissolved oxygen concentration plays a very important role. Experiments carried out with air saturation, oxygen saturation and also with pressurized oxygen applied, have shown that under identical irradiation conditions the degree of TOC reduction increases with the oxygen concentration and the highest values were measured with pressurized O₂ applied [49,56,66-69].

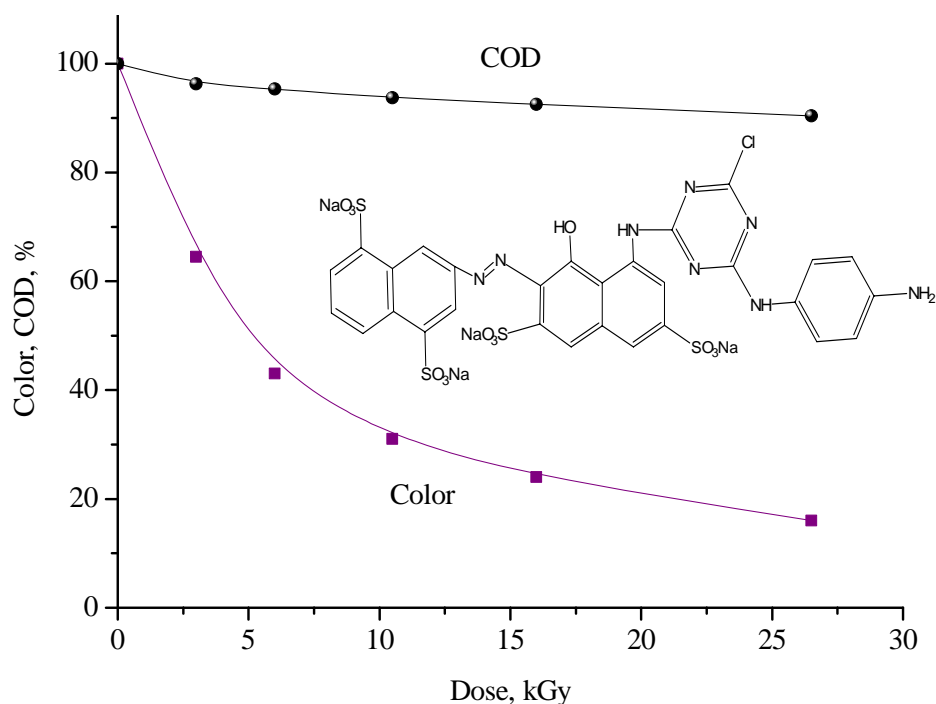
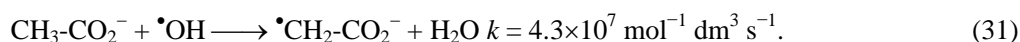
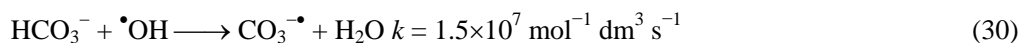


Figure 13. Color and COD removal during EB irradiation of reactive red (KA-3B) in air. Initial concentration $9 \times 10^{-4} \text{ mol dm}^{-3}$.

During dye degradation there is also a change in the pH of the solution, the pH gets more and more acidic with the degradation. In laboratory experiments in neutral solutions with initial dye concentration of 10^{-4} - 10^{-3} mol dm⁻³ the pH decreases by about 2 pH units during the degradation [17,59]. Due to the decreasing pH value it is assumed that the solution contains the oxidized organic fragments in anion forms of their corresponding acids. Among the transformation products of several dye molecules terephthalic-, oxalic- and formic acids and in small quantities malonic-, acetic- and succinic acids were determined together with traces of phenol [62].

4.3. Influence of Contaminants other than Dye Molecules in Wastewater

Dye-bath effluents generally contain a complex mixture of dyes, dispersing, leveling and wetting agents, fragments of the dyed textile (cellulose, polyester, etc.) and trace metals, especially copper and chromium salts. These additives modify the dye degradation rate by competing for the reactive radicals produced in water radiolysis [34]. The effects of such common anions as HCO₃⁻, CH₃CO₂⁻ and SO₄²⁻ at concentrations frequently present in industrial wastewaters was investigated in •OH radical induced decomposition of AO52 [29] (HCO₃⁻ and SO₄²⁻ form also during dye degradation). It was shown that sulfate ion practically does not influence the dye degradation rate since this ion is rather inactive in the reaction with •OH radicals. On the contrary, bicarbonates or acetates inhibited the dye degradation [29,32]. The decomposition rate decreased by 20-50% as compared to the reactions in distilled water, and longer irradiation times were necessary to obtain complete decoloration. The radical ions that form in •OH radical reactions with HCO₃⁻ and CH₃CO₂⁻ have much smaller oxidation potential as hydroxyl radical:



Dissolved transition metals may influence the dye degradation by complexation of organic molecules involving nitrogen atoms of the azo linkage or the amino groups. However, it should be mentioned that adding copper or chromium cations to AO52 solutions did not alter the UV-VIS absorption spectra of the dye reflecting the absence of complexation.

The iron ions present in aqueous solutions during irradiation may induce Fenton reactions since in the direct decomposition of water (Equ. (1)) and in the presence of dissolved oxygen in the self-termination reactions of the O₂^{-•}/HO₂[•] radicals (Reactions (9)-(11)) hydrogen peroxide constantly forms in the system. Fe²⁺/Fe³⁺ ions react with H₂O₂ and HO₂[•]; in catalytic process •OH radicals also form. •OH radicals accelerate the decomposition.

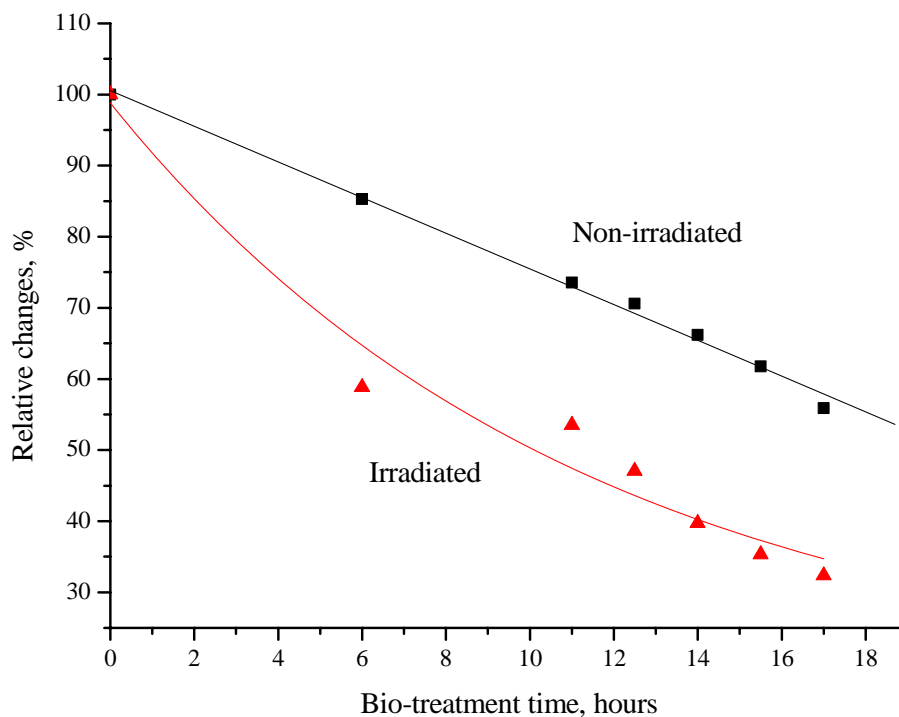
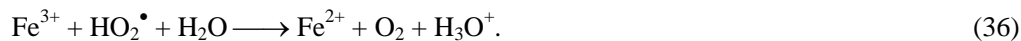
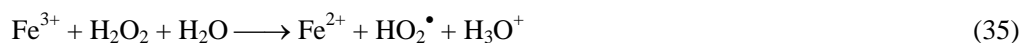
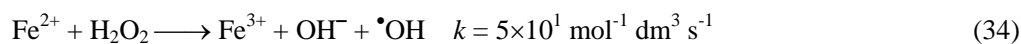
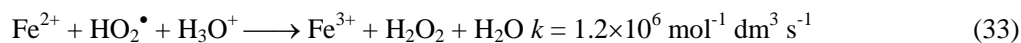


Figure 14. Effect of bio-treatment time on the COD value in electron beam irradiated (2 kGy) and non-irradiated dyeing complex wastewater in the area of Taegu Industrial Complex, Taegu, Republic of Korea. (Courtesy of Bumsoo Han [77])



Many other transition metal ions, e.g. Cu^{2+} or Cr^{3+} can take part in similar, so-called Fenton-like reaction [29]. These ions, similarly to the iron ions are not able to induce the dye decomposition, but through H_2O_2 decomposition may enhance the degradation.

The Fenton-like reactions induced by copper ions are listed as follows:



In the UV/H₂O₂ photocatalytic process copper ions were found to be much more effective in enhancing dye decomposition than chromium ions.



Figure 15. Irradiation of industrial dyeing complex wastewater in the area of Taegu Industrial Complex, Taegu, Republic of Korea (Courtesy of Bumssoo Han [77]).

5. PRACTICAL APPLICATIONS OF EB FOR DYEING WASTEWATER TREATMENT

Pilot plant and industrial scale experiments demonstrated the effectiveness of high-energy irradiation pre-treatment of wastewater when combined with conventional (mechanical screening, biological and chemical) methods [70]. In most cases these plants were constructed to treat municipal wastewater [71], or industrial wastewater containing some organic pollutants [8,70-76]. E.g. a synthetic rubber plant in Voronezh (Russia) had applied electron accelerator to convert the non-biodegradable emulsifier Nekal (isobutyl naftonate) in plant waste to biodegradable form. The dose requirement at 10^{-3} mol dm⁻³ concentration was 300 kGy. The plant had two production lines and could treat up to 2000 m³ effluent per day.

In order to treat industrial wastewater of dyeing factories first a pilot plant (output 1000 m³ day⁻¹) was established in the area of Taegu Industrial Complex, Taegu, Republic of Korea. The Complex includes about 100 factories with some 13,000 employees. The pilot plant is operating since 1998 with ELV electron accelerator (energy 1 MeV, beam power 40 kW) for large-scale test of combined electron-beam and biological treatment of industrial textile dyeing wastewater [62,76]. This plant has shown considerable reduction of chemical additive consumption, and also reduction in retention time, with an increase in removal efficiencies of

COD and BOD (Figure 14). According to the pilot-plant investigations of the dyeing complex wastewater equal purification degree corresponds to 17 h of bio-treatment without preliminary irradiation and about 8 h of bio-treatment with preliminary electron-beam treatment at absorbed dose 1-2 kGy [62].

On the basis of data obtained from pilot plant operation, in the area of the Complex construction of an industrial scale plant was started in 2004, and finished in December 2005 [77,78]. The industrial plant is located on the area of an existing wastewater treatment facility and its capacity is 10,000 m³ of wastewater per day. The facility is operating with 1 MeV, 400 kW accelerator and the radiation pre-treatment is combined with the existing bio-treatment facility. The continuous operation of this facility will provide additional data on reliability and for a detailed economic evaluation (Figure 15). With 10 000 m³/day capacity the price for treating dyeing wastewater for recycling by 2 kGy dose is about 1 \$/m³ [77].

CONCLUSION

1. The reactive intermediates formed in water radiolysis (e_{aq}^- , H^\bullet and $\bullet OH$) react with the dye molecules with high rate coefficient forming dye radicals. Radiation chemical techniques, especially pulse radiolysis with the time resolved observation of intermediates can help to clarify the undergoing chemical reactions. Although in the book chapter the radiolysis results were reviewed, the undergoing processes, the reaction mechanisms are also relevant to other AOP.
2. The water radiolysis intermediates effectively destroy toxic dye molecules causing first decoloration, but with sufficiently high doses mineralization to CO_2 , H_2O , N_2 , NO_x , SO_4^{2-} and to other inorganic ions can be achieved.
3. At the beginning of decoloration the dye concentration decreases linearly with time (dose) when H^\bullet or e_{aq}^- are the main attacking species. In such cases the absorption spectrum in the visible range dose not changes during the treatment.
4. Logarithmic time dependence is observed in the reaction of $\bullet OH$ radicals. There is also a gradual shift in the visible absorption maxima to longer wavelengths. This shift is attributed to formation of hydroxylated dye molecules.
5. $O_2^{\bullet -}/HO_2^\bullet$ species formed in e_{aq}^- and H^\bullet reaction with O_2 molecules have very low effectiveness in decoloration and their contribution to the mineralization process is probably also small. However, there are suggestions that some inorganic ions, e.g. Fe(II)/Fe(III) or Cu(I)/Cu(II) in catalytic reactions transforming the peroxides (formed during radiolysis) to $\bullet OH$ radicals, enhance the efficiency of $O_2^{\bullet -}/HO_2^\bullet$ contribution in dye destruction.
6. Large number of parallel and consecutive reactions are involved in decoloration and mineralization. The products were individually identified in very few cases. As intermediate products compounds with destroyed $-N=N-$ bond, hydroxylated dye molecules, dimers, molecules with opened rings, aldehydes, ketones, carboxylic acids form. The process of mineralization is usually followed by such techniques as chemical or biological oxygen demand, total carbon content measurement, etc.

7. Oxygen is not necessary for the decoloration, but it is essential for the destruction of the skeleton of the dye molecule and for mineralization. As the degradation products can be toxic, toxicity measurements are also of essential importance.
8. The biodegradation of the slightly irradiated solutions needs shorter time than that of the starting wastewater. The efficiency of dye destruction is enhanced when irradiation/ozone or irradiation/hydrogen peroxide combined treatments are applied.
9. Pilot-plant experiments and an industrially established technology show that irradiation treatment is a cost-effective technology that can compete with other dye containing wastewater purification technologies.

ACKNOWLEDGEMENTS

We express our thanks to Hungarian Science Foundation (OTKA K 60 096, and IN72122). Support of the International Atomic Energy Agency (Contract No. 302-F2-HUN-12015) is also acknowledged.

REFERENCES

- [1] Sharma, K. K.; O'Neill, P.; Oakes, J.; Batchelor, S. N.; Rao, B. S. M. *J. Phys. Chem. A* 2003, 107, 7619-7628.
- [2] Zhang, S.-J.; Yu, H.-Q.; Li, Q.-R. *Chemosphere* 2005, 61, 1003-1011.
- [3] Wojnárovits, L.; Takács, E. *Radiat. Phys. Chem.* 2008, 77, 225-244.
- [4] Slokar, Y. M.; Majcen Le Marechal, A. *Dyes Pigm.* 1998, 37, 335-356.
- [5] *CRC Handbook of Radiation Chemistry*; Editor: Tabata, Y., CRC Press, Boca Raton, 1991.
- [6] Spinks, J. W. T.; Woods, R. J. *An Introduction to Radiation Chemistry*. Third Edition, Wiley-Interscience, New York, 1990.
- [7] Woods, R. J.; Pikaev, A. K. *Applied Radiation Chemistry. Radiation Processing*. Wiley and Sons, New York, 1994.
- [8] *Environmental Applications of Ionizing Radiation*; Editors: Cooper, W. J.; Curry, R. D.; O'Shea, K. E.; John Wiley, New York, 1998.
- [9] *Status of industrial scale radiation treatment of wastewater and its future. IAEA-TECDOC-1407*. International Atomic Energy Agency, Vienna, 2004.
- [10] Buxton, G. V.; Greenstock, C. L.; Helman, W. P.; Ross, A. B. *J. Phys. Chem. Ref. Data* 1988, 17, 518-886. Updated version: <http://www.rcdc.nd.edu>.
- [11] von Sonntag, C. *The Chemical Basis of Radiation Biology*. Taylor and Francis, London, 1987.
- [12] Wojnárovits, L.; Takács, E.; Dajka, K.; Emmi, S. S.; Russo, M.; D'Angelantonio, M. *Radiat. Phys. Chem.* 2004, 69, 217-219.
- [13] *The Study of Fast Processes and Transient Species by Electron Pulse Radiolysis. Proceedings of NATO Advanced Study Institute, Capri, 1981*; Editors: Baxendale, J. H.; Busi, F., Reidel, Dordrecht, 1982.
- [14] *Pulse Radiolysis*; Editor: Tabata, Y., CRC Press, Boca Raton, 1991.

- [15] Pálfi, T.; Takács, E.; Wojnárovits, L. *Water Res.* 2007, *41*, 2533-2540.
- [16] Solpan, D.; Güven, O.; Takács, E.; Wojnárovits, L.; Dajka, K. *Radiat. Phys. Chem.* 2003, *67*, 531-534.
- [17] Neamtu, M.; Siminiceanu, I.; Yediler, A.; Kettrup, A. *Dyes Pigm.* 2002, *53*, 93-99.
- [18] Khabarov, V. N.; Kozlov, L. L. *High Energy Chem.* 1987, *21*, 165-169.
- [19] Haag, W. R.; Mill, T. *Environm. Toxikol. Chem.* 1987, *6*, 359-369.
- [20] Takács, E.; Wojnárovits, L.; Pálfi, T. *Nukleonika* 2007, *52*, 69-75.
- [21] Solpan, D.; Güven, O. *Radiat. Phys. Chem.* 2002, *65*, 549-558.
- [22] Huang, M.; Russo, R.; Fookes, B. G.; Sigman, M. E. *J. Forensic Sci.* 2005, *50*, 526-534.
- [23] Wojnárovits, L.; Takács, E.; Pálfi, T. *Res. Chem. Intermed.* 2005, *31*, 679-690.
- [24] Wojnárovits, L.; Pálfi, T.; Takács, E.; Emmi, S. S. *Radiat. Phys. Chem.* 2005, *74*, 239-246.
- [25] Holcapek, M.; Jandera, P.; Zderadicka, P. *J. Chrom. A* 2001, *926*, 175-186.
- [26] Jandera, P.; Fischer, J.; Stanek, V.; Kucerova, M.; Zvonicek, P. *J. Chrom. A*, 1996, *738*, 201-213.
- [27] Panajkar, M. S.; Mohan, H. *Indian J. Chem.* 1993, *32A*, 25-27.
- [28] Roder, M.; Wojnárovits, L.; Földiák, G.; Emmi, S. S.; Beggiato, G.; D'Angelantonio, M. *Radiat. Phys. Chem.* 1999, *54*, 475-479.
- [29] Galindo, C.; Jacques, P.; Kalt., A. *J. Photochem. Photobiol. A: Chemistry* 2000, *130*, 35-47.
- [30] Krapfenbauer, K.; Wolfger, H.; Getoff, N.; Hamblett, I.; Navaratnam, S. *Radiat. Phys. Chem.* 2000, *58*, 21-27.
- [31] Ma, H.; Wang, M.; Yang, R.; Wang, W.; Zhao, J.; Shen, Z.; Yao, S. *Chemosphere* 2007, *68*, 1098-1104.
- [32] Padmaja, S.; Madison, S. A. *J. Phys. Org. Chem.* 1999, *12*, 221-226.
- [33] Vinogdopal, K.; Peller, J.; Makogon, O.; Kamat, P. *Water Res.* 1998, *32*, 3646-3650.
- [34] Suzuki, N.; Nagai, T.; Hotta, H.; Washino, M. *Bull. Chem. Soc. Jpn.* 1975, *48*, 2158-2163.
- [35] Sharma, K. K.; Rao, B. S. M.; Mohan, H.; Mittal, J. P.; Oakes, J.; O'Neill, P. *J. Phys. Chem. A* 2002, *106*, 2915-2923.
- [36] Hihara, T.; Okada, Y.; Morita, Z. *Dyes Pigm.* 2003, *59*, 201-222.
- [37] Özen, A. S.; Aviyente, V.; Klein, R. A. *J. Phys. Chem. A* 2003, *107*, 4898-4907.
- [38] Hihara, T.; Okada, Y.; Morita, Z. *Dyes Pigm.* 2006, *69*, 151-176.
- [39] Spadaro, J. T.; Isabelle, L.; Renganathan, V. *Environ. Sci. Technol.* 1994, *28*, 1389-1393.
- [40] Joseph, J. M.; Destailats, H.; Hung, H.-M.; Hoffmann, M. R. *J. Phys. Chem. A* 2000, *104*, 301-307.
- [41] Vinogdopal, K.; Kamat, V. P. Hydroxyl-radical-mediated oxidation: A common pathway in the photocatalytic, radiolytic, and sonolytic degradation of textile dyes. In *Environmental Applications of Ionizing Radiation*; Editors: Cooper, W. J.; Curry, R. D.; O'Shea, K. E., John Wiley, New York, 1998; pp. 587-599.
- [42] Coen, J. J. F.; Smith, A. T.; Candeias, L. P.; Oakes, J. *J. Chem. Soc., Perkin Trans. 2* 2001, 2125-2129.
- [43] Wojnárovits, L.; Földiák, G.; D'Angelantonio, M.; Emmi, S. S. *Res. Chem. Intermed.* 2002, *28*, 373-386.

- [44] Wojnárovits, L.; Takács, E.; Dajka, K.; Emmi, S. S.; Russo, M.; D'Angelantonio, M. *Tetrahedron* 2003, 59, 8353-8358.
- [45] Flamigni, L.; Monti, S. *J. Phys. Chem.* 1985, 89, 3702-3707.
- [46] Nasr, C.; Vinogdopal, K.; Hotchandani, S.; Chattopadhyay, A. K.; Kamat, P. V. *Radiat. Phys. Chem.* 1997, 49, 159-166.
- [47] Getoff, N. *Radiat. Phys. Chem.* 2002, 65, 437-446.
- [48] Simic, M.; Hayon, E. *Biochem. Biophys. Res. Commun.* 1973, 50, 364-369.
- [49] Földváry, Cs. M.; Wojnárovits, L. *Radiat. Phys. Chem.*, in press
- [50] Getoff, N. The role of peroxy radicals and related species in the radiation-induced degradation of water pollutants. In *Environmental Applications of Ionizing Radiation*. Editors: Cooper, W. J.; Curry, R. D.; O'Shea, K. E; John Wiley, New York, 1998; pp 231-246.
- [51] Bredereck, K.; Schumacher, C. *Dyes Pigm.* 1993, 21, 23-43.
- [52] Bauer, C.; Jacques, P.; Kalt, A. *J. Photochem. Photobiol. A: Chemistry* 2001, 140, 87-92.
- [53] Földváry, Cs. M.; Wojnárovits, L. *Radiat. Phys. Chem.* 2007, 76, 1845-1488.
- [54] Wojnárovits, L.; Pálfi, T.; Takács, E. *Radiat. Phys. Chem.* 2007, 76, 1497-1501.
- [55] Tezcanli-Guyer, G.; Ince, N. H. *Ultrason. Sonochem.* 2003, 10, 235-240.
- [56] Suzuki, N.; Miyata, T.; Sakumoto, A.; Hashimoto, S.; Kawakami, W. *Int. J. Appl. Radiat. Isot.* 1978, 29, 103-108.
- [57] El-Assy, N. B.; Abdel-Rehim, F.; Abdel-Gawad, A. S.; Abdel-Fattah, A. A. *J. Radioanal. Nucl. Chem., Articles* 1992, 157, 133-141.
- [58] Zhang, S.-J.; Yu, H.-Q.; Zhao, Y. *Water Res.* 2005, 39, 839-846.
- [59] Wang, M.; Yang, R.; Wang, W.; Shen, Z.; Bian, S.; Zhu, Z. *Radiat. Phys. Chem.* 2006, 75, 286-291.
- [60] Wojnárovits, L.; Takács, E. *Dyes Pigm.* 2007, 75, 505-506.
- [61] Majcen-Le Marechal, A.; Slokar, Y. M.; Taufer, T. *Dyes Pigm.* 1997, 33, 281-298.
- [62] Han, B.; Ko, J.; Kim, J.; Kim, Y.; Chung, W.; Makarov, I. E.; Ponomarev, A. V.; Pikaev, A. K. *Radiat. Phys. Chem.* 2002, 64, 53-59.
- [63] *Standard Methods for the Examination of Water and Wastewater*; Editors: Eaton, A. D.; Clesceri, L. S.; Greenberg, A. E. 19th Edition. American Public Health Association, American Water Works Association and Water Pollution Control Federation, Washington, DC., 1995.
- [64] Kusic, H.; Koprivanac, N.; Srsan, L. *J. Photochem. Photobiol. A: Chem.* 2006, 181, 195-202.
- [65] Li, G.; Qu, J.; Zhang, X.; Liu, H.; Liu, H. *J. Mol. Catal. A: Chem.* 2006, 259, 238-244.
- [66] Kawakami, W.; Hashimoto, S.; Nishimura, K.; Miyata, T.; Suzuki, N. *Environ. Sci. Technol.* 1978, 12, 189-194.
- [67] Hashimoto, S.; Miyata, T.; Suzuki, T.; Kawakami, W. *Radiat. Phys. Chem.* 1979, 13, 107-113.
- [68] Hashimoto, S.; Miyata, T.; Kawakami, W. *Radiat. Phys. Chem.* 1980, 16, 59-65.
- [69] Hosono, M.; Arai, H.; Aizawa, M.; Yamamoto, I.; Shimizu, K.; Sugiyama, M. *Appl. Radiat. Isot.* 1993, 44, 1199-1203.
- [70] Emmi S. S., Takács, E. Water remediation by electron-beam treatment. In *Radiation Chemistry, From Basics to Applications in Material and Life Sciences*; Editors:

- Spotheim-Maurizot, M.; Mostafavi, M.; Douki, T.; Belloni, J. EDP Sciences, Paris, 2008; pp 87-103.
- [71] Pikaev, A. K., Electron-beam purification of water and wastewater. In *Environmental Applications of Ionizing Radiation*. Editors: Cooper, W. J.; Curry, R.D.; O'Shea, K. E. John Wiley, New York, 1998; pp 495-506.
- [72] Sampa, M. H. O.; Borrely, S. I.; Vieira, J. M.; Rela, P. R.; Calvo, W. A. P.; Duarte, C. L.; Perez, H. E. B.; Lugao, A. B. *Radiat. Phys. Chem.* 1995, 46, 1143-1146.
- [73] Sampa, M. H. O.; Duarte, C. L.; Rela, P. R.; Somessari, E. S. R.; Silveira, C. G.; Azevedo, A. L. *Radiat. Phys. Chem.* 1998, 52, 365-369.
- [74] Cooper, W. J.; Dougal, R. A.; Nickelsen, M. G.; Waite, T. D.; Kurucz, C. N.; Lin, K.; Bibler, J. P. *Radiat. Phys. Chem.* 1996, 48, 81-87.
- [75] Buslaeva, S. P.; Vanyushkin, B. M.; Gogolev, A. V.; Kabakchi, S. A.; Panin, Yu. A.; Putilov, A. V.; Upadyshev, L. B. *Khim. Prom.* 1991, 6, 47-50.
- [76] Han, B.; Kim, D. K.; Pikaev, A. K. Research activities of Samsung Heavy Industries in the conservation of the environment. In *Radiation Technology for the Conservation of the Environment, Proceedings of the Symposium held in Zakopane, Poland, 8-12 September 1997*, IAEA, Vienna, 1998; pp 339-347.
- [77] Han, B. 2006. Personal communication. (Bumsoo Han, EB-TECH CO., LTD. Republic of Korea, E-mail: bshan@eb-tech.com)
- [78] *Radiation Processing: Environmental Applications*, International Atomic Energy Agency: Vienna, 2007.

Chapter 9

APPLICATION OF ADVANCED OXIDATION PROCESSES (AOP) TO DYE DEGRADATION - AN OVERVIEW

M. A. Rauf and S. Salman Ashraf

Department of Chemistry, UAE University,
PO Box 17551, Al-Ain, United Arab Emirates

ABSTRACT

Advanced oxidation Processes (AOP's) are novel methods for water treatment and are extremely useful in the case of substances resistant to conventional technologies. Organic dyes are a group of those chemicals of special interest which have drawn considerable attention in many industrial processes. However due to their high toxicity and low biodegradability, various approaches have been forwarded concerning the degradation of these dyes by means of AOP's. In this work, an overview of such work is presented and the following approaches are presented: processes based on hydrogen peroxide ($H_2O_2 + UV$, Fenton, photo-Fenton and Fenton-like processes), photolysis, photocatalysis and processes based on ozone (O_3 , $O_3 + UV$ and $O_3 + catalyst$). Degradation is reviewed and the different mechanistic degradation pathways are taken into account.

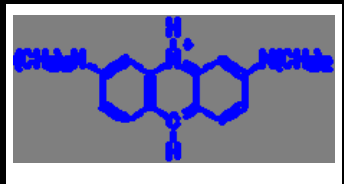
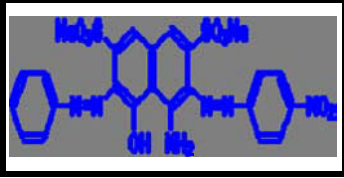
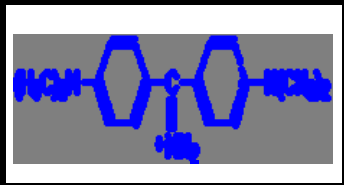
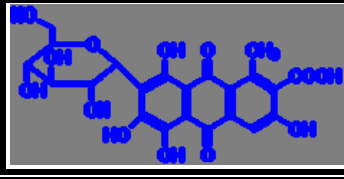
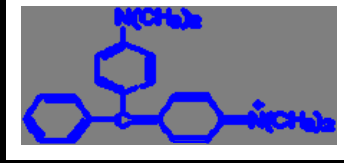
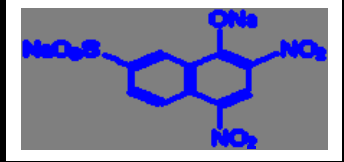
Keywords: Dyes, AOP, Photolysis, Fenton, Photo-Fenton, Ozone, Photocatalysis, Degradation

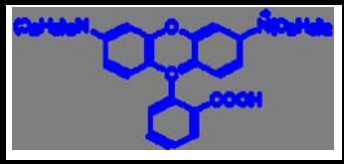
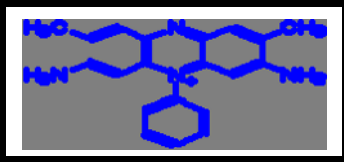
1. INTRODUCTION

With increasing social and political concern on environmental issues, the research activity in the area of water purification has drawn a great deal of attention and has attracted the focus of attention to many workers. Water bodies comprising both polluted wastewaters and groundwater from seas, rivers and lakes are of special concern to people working in water purification and the environment in general. In this regard water quality control standards and regulations against hazardous pollutants have become stricter in many countries.

With increasing revolution in science and technology, there is a bigger demand on opting for newer chemicals which could be used in various industrial processes. Organic dyes come up as one of the many new chemicals which could be used in many industrial activities. Most of these dyes are synthetic in nature and are classified based on their chemical structures into six different classes as azo, anthraquinone, sulfur, indigoid, triphenylmethane and phthalocyanine derivatives. Their general nomenclature along with representative examples is given in Table 1.

Table 1. Different classes of dyes and their structures

Dye	Structure	Class	max
Acridine O		Acridine	497 nm
Amido Black		Azo	618 nm
Auramine O		Diarylmethane	432 nm
Carmine		Anthraquinone	500 nm
Malachite green		Triarylmethane	618 nm
Naphthol Y		Nitro	428 nm

Rhodamine B		Xanthene	555 nm
Safranin O		Quinone-imine	530 nm

Due to the extensive use of these dyes in industries, they have become an integral part of industrial effluent. In fact, of the 450,000 tons of organic dyes annually produced worldwide, more than 11% is lost in effluents during manufacture and application processes [1]. Most of these dyes are toxic and potentially carcinogenic in nature and their removal from the industrial effluents is a major environmental problem [2].

Various methods have been suggested to handle the dye removal from water; these include the biodegradation, coagulation, adsorption, advanced oxidation (AOP) and the membrane process [3-8]. All these processes have some advantages or disadvantages over the other methods. A balanced approach is therefore needed to look into the worthiness on choosing an appropriate method which can be used to degrade the dye in question. Among these techniques, the advanced oxidation processes (AOP's) [9] appear to be a promising field of study, which have been reported to be effective for the near ambient degradation of soluble organic contaminants from waters and soils, because they can provide an almost total degradation [10-20]. Among the various AOP's the main ones taken into account in this work are the following:

- (1) Photolysis (UV or VUV)
- (2) Hydrogen peroxide (H_2O_2)
 - $\text{H}_2\text{O}_2 + \text{UV}$
 - Fenton: $\text{H}_2\text{O}_2 + \text{Fe}^{2+}/\text{Fe}^{3+}$
 - Fenton-like reagents: $\text{H}_2\text{O}_2 + \text{Fe}^{2+}\text{-solid}/\text{Fe}^{3+}\text{-solid}$
 - photo-Fenton: $\text{H}_2\text{O}_2 + \text{Fe}^{2+}/\text{Fe}^{3+} + \text{UV}$
- (3) Ozone (O_3)
 - ozonation: O_3
 - photo-ozonation: $\text{O}_3 + \text{UV}$
 - ozonation + catalysis: $\text{O}_3 + \text{H}_2\text{O}_2$ and $\text{O}_3 + \text{Fe}^{2+}/\text{Fe}^{3+}$
- (4) Photocatalysis
 - Heterogeneous catalysis and photocatalysis
 - $\text{TiO}_2 + \text{CdS} + \text{combinations}$

All the above techniques are versatile in nature and can provide the conversion of contaminants to less harmful compounds such as oxygenated organic products and low molecular weight acids [21]. A common denominator in all these techniques is that they produce highly reactive hydroxyl radicals ($\bullet\text{OH}$) at a certain stage which are supposedly the

active species responsible for the destruction of pollutants [22]. Due to their high standard reduction potential of 2.8 V, these radicals are able to oxidize almost all organic compounds to carbon dioxide and water. Other simple organic compounds, such as acetic, acid, acetone or simple chloride derivatives are also generated [23]. These smaller molecules can be further degraded by various chemical or photochemical reactions.

2. EXPERIMENTAL METHODOLOGY

Different experimental techniques have been proposed for both qualitative and quantitative analysis of various dyes concerning their degradation. These methods usually involve analysis by instrumental methods such as UV/Vis spectrophotometry [24, 25], GC/MS [26], HPLC [27], Ion chromatography [28], Capillary Electrophoresis [29], Radiometry [30] etc. In this regard, prior procedures of extraction of the aqueous sample with an organic solvent or filtration in case a heterogeneous catalyst or solid reactant is also employed. Since most of the dyes would ultimately breakdown into smaller molecules, an important aspect of this study is also to evaluate the Total organic carbon of the system under investigation [31-33].

3. REACTORS AND LAMPS

3a. Reactors Used for Direct Photolysis and AOPs Based on Hydrogen Peroxide

Most of the papers reviewed [34-36] on this topic have shown that the investigators have generally used the completely mixed batch cylindrical glass vessels for direct photolysis studies. Other methods involve using cylindrical glass flasks [29], glass bottles or glass tubes [37, 38] for direct photolysis, photo-Fenton processes, and processes based on H₂O₂/UV reagent. This is done in order to achieve a good interaction between dyes and radiation.

3b. Reactors Used for AOP's Based on Ozone

Literature review has revealed that semi-batch stirred reactors such as glass bottles or cylindrical vessels are the most commonly used reactor types for ozonation processes [39-42]. Besides this, other configurations used are the bubble columns, and wetted-sphere adsorbers [43,44]. These improve the contact between the gaseous ozone stream and the liquid and polluted stream. An ozone generator is generally located close to the reactor to ensure a continuous supply of ozone gas for the reaction. Ozone is generally generated by either an electric discharge or by irradiating oxygen with UV light. The former technique has been used frequently [45-47].

3c. Reactors Used for AOPs Based on Photocatalysis

The most typical laboratory-scale experimental set up includes a vigorously stirred batch photochemical cell, cylindrical flasks or vessels and glass dishes [48-51]. On the other hand, upflow type, membrane based and coated surfaces have also been reported as photo-catalytic reactors for dye studies [52-55].

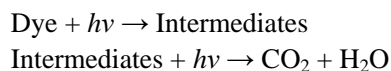
3d. General Information for Lamps Used in AOP's

Different types of lamps are used for irradiation purposes in dye degradation studies. The choice depends on the mode of AOP being used, such as UV/H₂O₂, UV/O₃, photo-Fenton's reagents and photocatalysis. A variety of commercial radiation sources are available for this work which includes the high, medium and low-pressure mercury vapor lamp for the generation of UV radiation [56-58] or xenon lamps [59]. The lamps are generally placed in an axial position with respect to the solution container, or in the center of a photolytic reactor in a vertical position.

4. PHOTOLYSIS BY UV LIGHT

UV photolysis is the process by which chemical bonds of the contaminants are broken under the influence of UV light. Products of photo-degradation vary according to the matrix in which the process occurs, but the complete conversion of an organic contaminant to CO₂, H₂O, etc. is not probable, as stronger and more reactive oxidants are normally needed for complete mineralization of bigger organic compounds.

The duration of operation and maintenance of UV oxidation depends on influent water turbidity, contaminant and metal concentrations, existence of free radical scavengers, and the required maintenance intervals on UV reactors and quartz sleeves. A commonly acceptable mechanistic pathway is suggested as follows [60]



Direct UV-photolysis have resulted in degradation of pollutants, such as dyes, in dilute aqueous solutions [61- 65]. Limitations of UV/oxidation include:

- The aqueous stream being treated must provide good transmission of UV light (high turbidity causes interference). This factor can be more critical for UV/H₂O₂ than UV/O₃ (Turbidity does not affect direct chemical oxidation of the contaminant by H₂O₂ or O₃).
- Free radical scavengers can inhibit contaminant destruction efficiency. Excessive dosages of chemical oxidizers may act as scavengers.

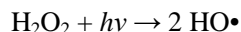
- The aqueous stream to be treated by UV/oxidation should be relatively free of heavy metal ions (less than 10 mg/L) and insoluble oil or grease to minimize the potential for fouling of the quartz sleeves.
- When UV/O₃ is used on volatile organics, the contaminants may be vaporized (e.g., "stripped") rather than destroyed. They would then have to be removed from the off-gas by activated carbon adsorption or catalytic oxidation.
- Costs may be higher than competing technologies because of energy requirements.
- Pretreatment of the aqueous stream may be required to minimize ongoing cleaning and maintenance of UV reactor and quartz sleeves.
- Handling and storage of oxidizers require special safety precautions.

5. HYDROGEN PEROXIDE BASED AOPS

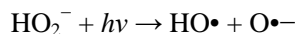
Hydrogen peroxide has been known as an effective oxidant; however it alone is not useful for many organic pollutants such as dyes. It is generally combined with UV light, salts of particular metals or ozone to produce the desired degradation results.

5a. H₂O₂/UV Reagent

This widely applicable AOP is based on the production of •OH radicals in solution on the photolysis of hydrogen peroxide followed by propagation reactions:

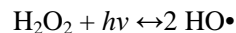


The molar absorptivity of hydrogen peroxide at 253.7 nm is very low (about 20M⁻¹ cm⁻¹) and HO• radicals are formed per incident photon absorbed [99]. Since at this wavelength, the rate of photolysis of aqueous hydrogen peroxide is much slower than ozone, the technique demands a higher dose of H₂O₂ or longer irradiation time. On the other hand, the rate of photolysis of hydrogen peroxide has been found to be pH dependent and increases when more alkaline conditions are used, because, at 253.7 nm, peroxide anions HO₂⁻ may be formed, which have a higher molar absorptivity than hydrogen peroxide [99].

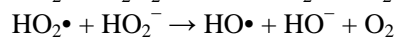
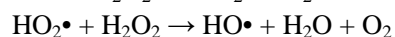
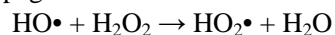


The absorptivity of hydrogen peroxide may be increased by using shorter wavelengths. The reaction scheme in this case is proposed as follows [67].

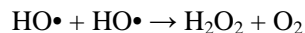
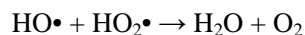
Initiation:



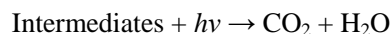
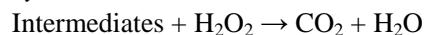
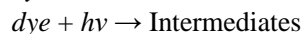
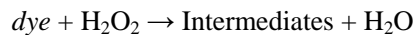
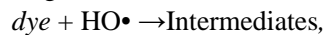
Propagation:



Termination:



Dye degradation:



In the presence of UV absorbers, the effect will be the same as if there is less radiation intensity available for the photolysis of hydrogen peroxide; also that the amount of radiation transformed into $\text{HO}\cdot$ radicals will be lower in the presence of such absorbents.

5a.1. Effect of pH

The pH of the dye solution can have a dramatic effect on the rate of dye decoloration by the $\text{UV}/\text{H}_2\text{O}_2$ photolytic approach. Our experience with an extensive study of different dyes has shown that some a “pH-profile” must be established for each dye and the effect of acidic or alkaline conditions on dye degradation can not be known a priori. For example, dyes like Auramine O shows 81% decoloration at pH 7, but that cuts into half (47% decoloration) at pH 2 and falls even lower to 13% at pH 11 (Figure 1). Surprisingly, the % decoloration for Malachite Green doubled from 50% (at pH 7) to 91% or 99% at pH values of 12 and 1, respectively, as shown below (Figure 1). Other dyes such as Safamin O showed only a marginal effect of pH on dye degradation [60].

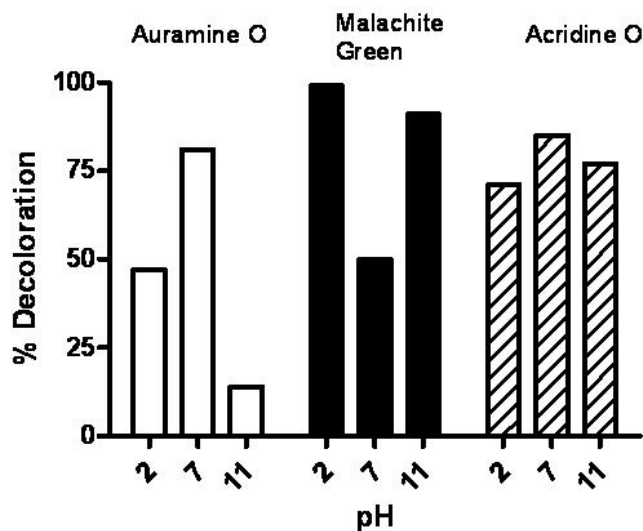


Figure 1. Effect of pH on dye degradation by $\text{UV}/\text{H}_2\text{O}_2$ photolysis.

[Auramine O] = 20 μM , $[\text{H}_2\text{O}_2]$ = 1.67 mM; [Malachite Green] = 20 μM , $[\text{H}_2\text{O}_2]$ = 1.67 ; [Acridine O] = 2 μM , $[\text{H}_2\text{O}_2]$ = 3.33 mM (unpublished data).

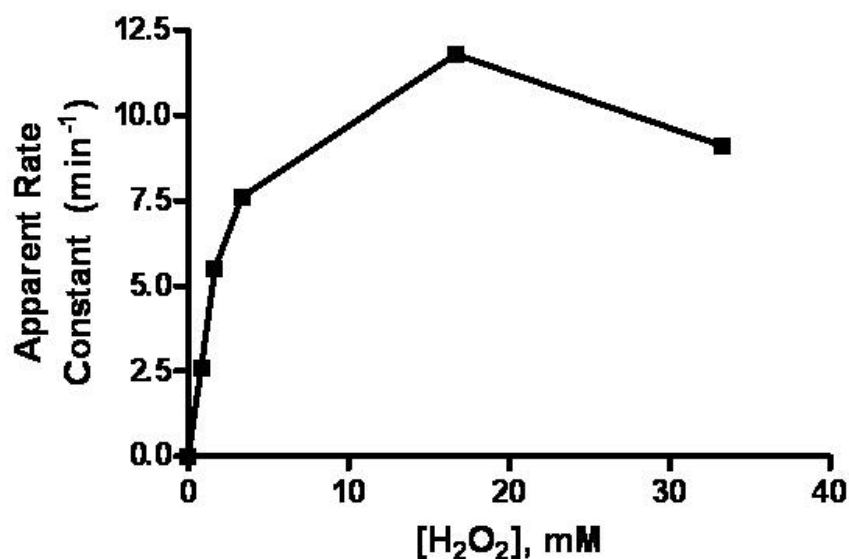
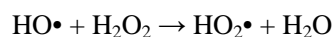


Figure 2. Effect of hydrogen peroxide concentration on dye degradation by UV/H₂O₂ photolysis. Auramine O (20 μM) was exposed to different concentrations of H₂O₂ in the presence of UV light and the apparent rate of dye decoloration was calculated (unpublished data).

5a.2. Effect of Hydrogen Peroxide Concentration [H₂O₂]

As expected, the concentration of hydrogen peroxide plays an important role in dye degradation. Since, hydroxyl radical production depends on the concentration of H₂O₂, it is therefore expected that the higher the hydrogen peroxide concentration, the higher the amount of hydroxyl radicals, and faster the dye degradation. However, it is been reported by various groups (Figure 2) that excessively high concentrations of hydrogen peroxide is in fact, deleterious for efficient dye degradation, as hydrogen peroxide itself reacts with and quenches hydroxyl radicals, as shown below:



5a.3. Effect of Initial Dye Concentration

Dye concentration is another parameter that is very important for efficient degradation using UV/H₂O₂. It is well established that AOPs, specifically the ones that rely on UV or other source of radiation, generally work well at dilute dye concentrations, since highly colored dye solutions block the penetration of UV light and prevent the production of hydroxyl radicals. In fact, a directly inverse relationship between dye concentration and dye degradation is reported by numerous groups. Figure 3 shows the decrease in the apparent rate of Safranin O decoloration as a function of increasing dye concentration [60].

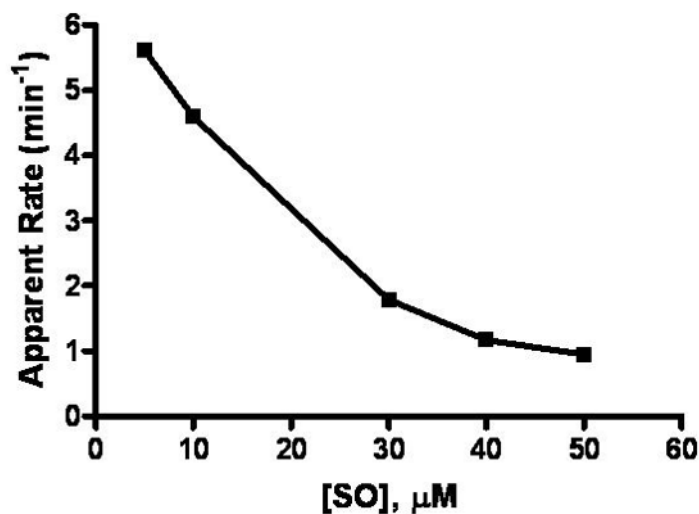
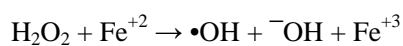


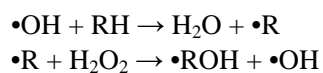
Figure 3. Effect of Safranin O concentration on the apparent rate of degradation by UV/H₂O₂ photolysis. Different concentrations of Safranin O was exposed to 1.67 mM H₂O₂ and the decoloration rate measured as described elsewhere [60].

5b. Fenton's Reagent (H₂O₂/Fe²⁺)

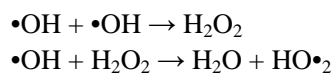
The Fenton system generates ferrous ions to react with hydrogen peroxide, producing hydroxyl radicals, which are strong oxidizing reagents, and can react with the organic pollutant or dye solution and degrade it [66-69].



The hydroxyl radical propagates the reaction by reacting with the organic pollutant/dye (RH) to produce further radicals, which can then react in many different steps.



Additionally many other reactions are also possible, which include the radical-radical reaction or the reaction of the OH radical with H₂O₂



The peroxide radicals (HO•₂) produced in the above case can further oxidize other species present in the solution.

Fenton's reagent has been successfully used to treat a variety of industrial wastes containing a range of organic compounds like phenols, formaldehyde, pesticides, wood

preservatives, plastic additives, and rubber chemicals [70-75]. The process has also been applied to wastewaters, sludge, and contaminated soils [76-80].

5b.1. Effect of pH

Change in pH of dye solution has a pronounced effect on dye degradation as shown in many studies [81-83]. The dye decomposition significantly decreases as the pH increases which is attributed to a decreased dissolved fraction of iron species and also formation of colloidal ferric species [84]. On the other hand, at low pH values (around 2 - 4), more $\text{Fe}(\text{OH})^+$ is formed and the activity of this species is more than Fe^{+2} in Fenton's oxidation. At low pH values, oxygen concentration remains stable because hydrogen peroxide solvates protons to form oxonium ions (H_3O_2^+), which in turn enhances the stability of hydrogen peroxide and reduces its reactivity with ferrous ions [85].

5b.2. Effect of Hydrogen Peroxide Concentration [H_2O_2]

The concentration of hydrogen peroxide plays a vital role in dye degradation as shown in many studies [86-90]. The stoichiometric coefficient for the Fenton reaction has been found to be approximately 0.5 mol organic compound/mol H_2O_2 [13]. As concentration of hydrogen peroxide increases, the degradation of dyes also increases, because the amount of oxidant present in the reaction system is higher for the same initial concentration of dye and catalytic ferrous ions. The linear dependence is only achieved when hydrogen peroxide is in excess compared to dye concentration. Like the UV/ H_2O_2 photolytic AOP, too much hydrogen peroxide can lead to self-quenching and lead to decrease in dye degradation, as shown in Figure 4 [24].

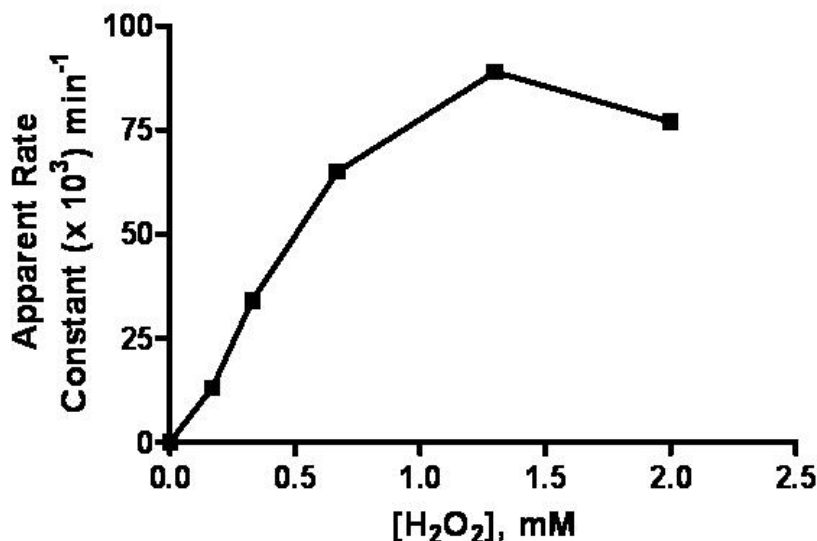
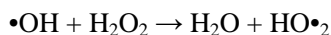


Figure 4. Effect of hydrogen peroxide concentration on Neutral Red degradation by Fenton based AOP. $[\text{Neutral Red}] = 65 \mu\text{M}$, $[\text{Fe}^{2+}] = 0.34 \text{ mM}$. Apparent rate of dye degradation was measured as described elsewhere [24].

Furthermore, since a number of intermediates are produced in dye degradation, sufficient hydrogen peroxide must be added in order to propagate the reaction. This in fact is seen when pre-treating a complex organic wastewater for toxicity reduction. With increasing amounts of H_2O_2 in solution, chemical oxygen demand (COD) value becomes less and results in little or no change in toxicity until a threshold is attained; further increase of hydrogen peroxide results in a rapid decrease in wastewater toxicity [91].

5b.3. Effect of Ferrous Ion Concentration [Fe^{2+}]

The absence of iron causes no considerable production of any intermediates or active species in solution even in the presence of hydrogen peroxide. With an increase in the concentration of iron, dye degradation increases to a point where further addition of iron becomes inefficient. The optimum amount of iron catalyst is characteristic of Fenton's reagent, although its exact amount varies from dye to dye solution. A typical range of such a solution is 1 part iron per 5–25 parts of hydrogen peroxide (w/w) [13]. A given reaction may be initiated in the presence of either ferrous (Fe^{2+}) or ferric (Fe^{3+}) ions, however when low doses of Fenton's reagent are used (e.g. $<10\text{--}25\text{ mg/L-1 H}_2\text{O}_2$), ferrous ions are preferred [13].

The influence of ferrous ions in dye degradation is similar to the one for hydrogen peroxide. When Fenton concentration increases, the degradation of dye also increases, because the amount of catalyst present in the reaction system is higher for the same initial concentration of dye and hydrogen peroxide, as shown below in Figure 5 [66].

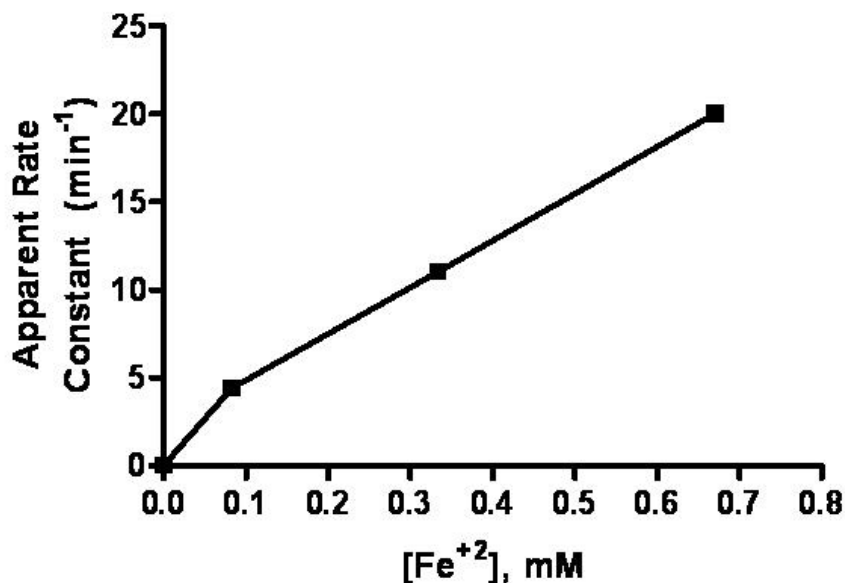


Figure 5. Effect of Fe^{2+} concentration on degradation of Crystal Violet by Fenton based AOP. [Crystal Violet] = $22\ \mu\text{M}$, $[\text{H}_2\text{O}_2] = 0.34\ \text{mM}$. Apparent rate of dye degradation was measured as described elsewhere [66].

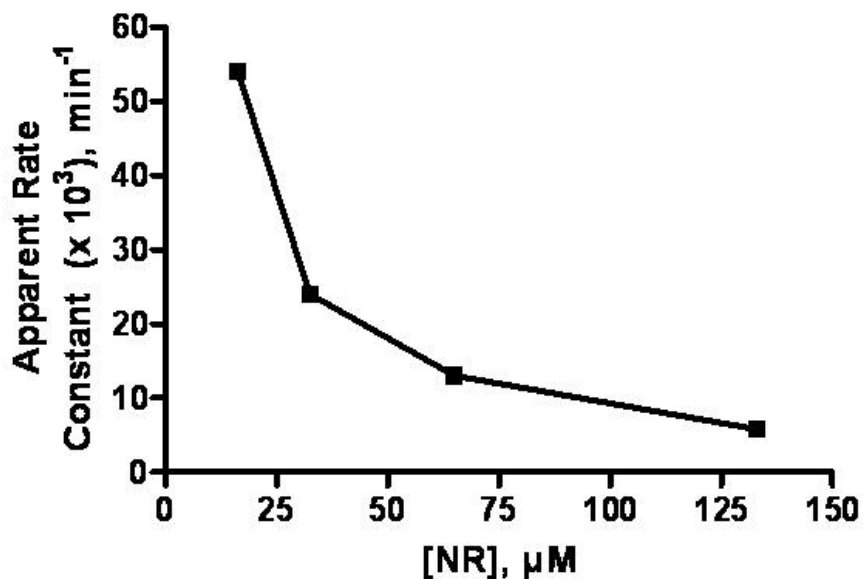


Figure 6. Effect of hydrogen peroxide concentration on Neutral Red degradation by Fenton based AOP. $[\text{H}_2\text{O}_2] = 0.17 \text{ mM}$, $[\text{Fe}^{2+}] = 0.34 \text{ mM}$. Apparent rate of dye degradation was measured as described elsewhere [24].

5b.4. Effect of Initial Dye Concentration

Increasing amounts of dye in solution also is an important factor in dye degradation. When the other factors of the solution are kept constant and the dye concentration is increased, the degradation of solution becomes less, as shown in Figure 7 [24]. Therefore, at higher dye concentrations, the degradation of the dye will not follow the pseudo-first order kinetics.

5b.5. Effect of Temperature

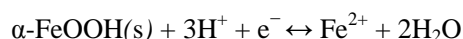
The studies concerning the effect of temperature have shown that the extent of dye degradation increases with an increase in temperature [67]. However at higher temperatures (around 50°C), very less increase in the extent of dye degradation is

observed. This has been attributed to the fact that at these temperatures, the efficiency of H_2O_2 utilisation declines because of the rapid decomposition of H_2O_2 into oxygen and water at high temperatures.

5c. Fenton-like Reagent's ($\text{H}_2\text{O}_2/\text{Fe}^{2+}$ -solid)

Although Fenton reaction has shown promising results in dye degradation, its biggest disadvantage still remains the unavailability of homogeneous catalyst in solution. In many cases the disadvantage has been countered by introducing heterogeneous supported metals [50, 92-95]. In this case the hydroxyl ions are activated by iron ions which are released from the support material. Some common materials used in this regard are *goethite*, *Nafion membranes*, and *iron powder*. Geothite ($\alpha\text{-FeOOH}$) is considered to be a suitable alternative for Fenton-like degradation of dyes and has been used by various investigators to remove

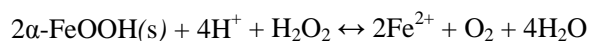
hazardous pollutants [96]. The reaction mechanism involves the production of ferrous ions from the reductive dissolution of the compound [97].



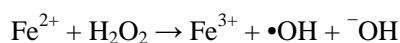
whereas the electrons are produced via the following reaction



On combination of the above two equation gives the following



The Fe^{2+} ions produced in the reaction then react with H_2O_2 to produce the $\bullet\text{OH}$ radicals which can subsequently take part in a series of reactions to degrade the organic species.



Geothite is also known to interact chemically with H^+ , OH^- , cations, and anions, followed by a series of dissolution reactions. The reaction is more feasible under reducing conditions [97,98].

5d. Photo-Fenton's Reagent ($\text{H}_2\text{O}_2/\text{Fe}^{2+}/\text{UV}$)

Photo-Fenton reaction scheme is well known in the literature and has been employed for wastewater and soil treatment [100-105]. The method has shown better results as compared to Fenton or Fenton-like reagents, as it involves interaction of radiation (UV/Vis) with Fenton's reagent [100]. The technique has shown promising results in removing pollutants from natural and industrial waste water and increasing the biodegradability of dyes. It is being used as a pre-treatment method to decrease the toxicity of waste water [106-107]. The dye degradation using this technique in general depends on the initial dye concentration, hydrogen peroxide and ferrous ion and the intensity of radiation. Generally speaking, the pseudo-first kinetic constants obtained in a photofenton reaction are higher than those obtained in the single photolytic process [108]. This can be attributed to the additional contribution of the hydroxyl radicals produced as a result of the photolytic reaction of the overall solution which contains hydrogen peroxide.

In a photofenton reaction, the overall dye degradation is more when compared to Fenton's reaction or $\text{H}_2\text{O}_2/\text{UV}$ technique because of the production of OH radicals by multiple pathways. All initial, propagation, termination and dye degradation steps are the same as the ones for reactions with Fenton's and $\text{UV}/\text{H}_2\text{O}_2$ reagents. However, another step for initial reactions must be added [100,108,109], which does not take place in Fenton reaction, because there is no radiation.

6. AOPs BASED ON OZONATION

6a. Ozone (O₃)

Ozonation has been widely used for drinking water disinfection—bacterial sterilization, odor, algae, and organic compound degradation [89,110-113]. It is more efficient in pollutant degradation and is not harmful for most organisms, because no new compounds are added to treated waters. Ozonation of dissolved compounds in water can constitute an AOP by itself, as hydroxyl radicals can be generated from the decomposition of ozone, which might be catalyzed by hydroxyl ions or initiated by the presence of traces of other substances [114]. The ozone decomposition increases at high pH values. Literature review has shown the use of ozonolysis could be applied to many different compounds. [110,115-117]. The specific application of ozonation to degrade dyes has been reported by many investigators [118-120]. The dye degradation in this case also follows the pseudo-first order kinetics [121]. The degradation of dyes via ozonolysis is reported to be higher at higher pH values and is due to the production of more HO• radicals in alkaline media and the dissociation of dyes to ionic form that can react with ozone easily than the non-dissociated species [121,122]. At low pH values, ozone exclusively reacts with compounds with specific functional groups through selective reactions such as electrophilic, nucleophilic or dipolar addition reactions [123].

6a1. Mechanism of Ozonation

This is divided into two main types, Direct and Indirect:

6a2. Direct Ozonation

In acidic media (pH ≈ 2) the decomposition of ozone is initiated by the action of HO⁻ ions is too low and consequently the concentration of hydroxyl radicals is small in solution [122]. This results in smaller rate constant values in the range of 1–1000M⁻¹ s⁻¹. At higher pH values, HO[•] concentration increases, thereby increasing the dye degradation [121]

6a3. Indirect Ozonation

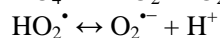
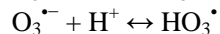
In this reaction, ozone is first decomposed and the resulting species then react in the system with HO⁻ ions to form HO• radicals, which can then enter in several reactions to degrade the dye molecule.

The mechanism can be divided in three different parts [124];

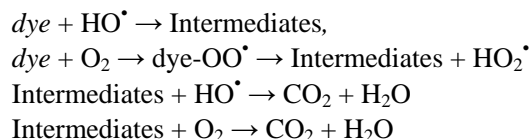
Initiation reactions:



Propagation:



Dye degradation:

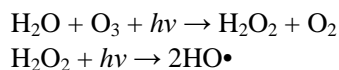


6b. O₃/UV Reagent

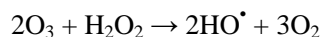
Photolytic ozonation (O₃/UV process) is another of AOP and is an effective mode for the destruction of toxic organics present in water [120,125-127]. The method has a significant potential as a wastewater treatment method. The final products of degradation in this case are merely CO₂, H₂O and low molecular weight organic compound if complete mineralization is achieved [128]. The aqueous systems is saturated with ozone and then irradiated with UV light at 253.7 nm. Since the extinction coefficient of ozone at this wavelength is 3300M⁻¹ cm⁻¹, its decay rate is higher than that of hydrogen peroxide [129].

6b1. Reaction Mechanism

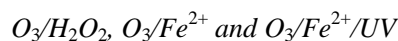
The degradation of organic molecules by O₃/UV reagent follows a similar mechanism to the one described for simple ozonation. However some additional steps are involved in the overall reaction scheme. These are outlined below [125].



The decomposition of H₂O₂ is enhanced in the presence of O₃

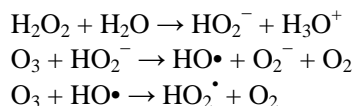


6b2. Ozonation + Homogeneous/heterogeneous Catalysis

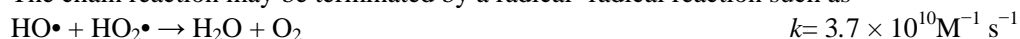


The photodegradation of some organic compounds by ozone and UV radiation, alone or combined with hydrogen peroxide or ferrous and ferric ions, has also been reported by several authors [89,110,130]. A combination of AOP's has shown considerable increase in dye degradation than the single processes. In the case of ozone + H₂O₂, in addition to the general pathway for ozonation, ozone reacts with H₂O₂ when it is present as HO₂⁻.

Other propagation reactions include the following



The chain reaction may be terminated by a radical- radical reaction such as



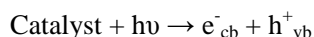
On the other hand, experiments which involve the Fenton reagent and are subjected to ozonolysis have shown improved mineralization of organic compounds. Besides an increase in the rate of degradation, total oxygen content (TOC) have also shown to increase from 21 to 43% by using this method instead of single ozonation.

7. PHOTOCATALYSIS

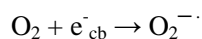
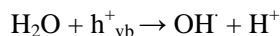
Photocatalytic degradation has proven to be a promising technology for degrading organic compounds [50,54,131-140]. The technique is more effective as compared to other techniques because semiconductors are inexpensive and can easily mineralize various organic compounds [141].

7a. Mechanistic Pathways

The photocatalytic decolouration of a dye is believed to take place according to the following mechanism. When a catalyst is exposed to UV radiation, electrons are promoted from the valence band to the conduction band. As a result of this, an electron-hole pair is produced [50]

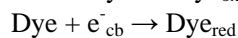
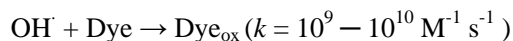
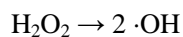
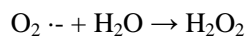


where, e^-_{cb} and h^+_{vb} are the electrons in the conduction band and the electron vacancy in the valence band respectively. Both these entities can migrate to the catalyst surface, where they can enter in a redox reaction with other species present on the surface. In most cases h^+_{vb} can react easily with surface bound H_2O to produce OH^\cdot radicals, whereas, e^-_{cb} can react with O_2 to produce superoxide radical anion of oxygen [55]



This reaction prevents the combination of the electron and the hole which are produced in the first step.

The OH^\cdot and $\text{O}_2^{\cdot-}$ produced in the above manner can then react with the dye to form other species and is thus responsible for the decolouration of the dye



Direct and Indirect photocatalytic pathways are the two suggested mechanisms for a given photocatalytic reaction. These are discussed below

7a1. Direct photocatalytic Pathway

Two different approaches have been suggested for this type of mechanism

(i) Heterogeneous Photocatalysis - The Langmuir–Hinshelwood Process

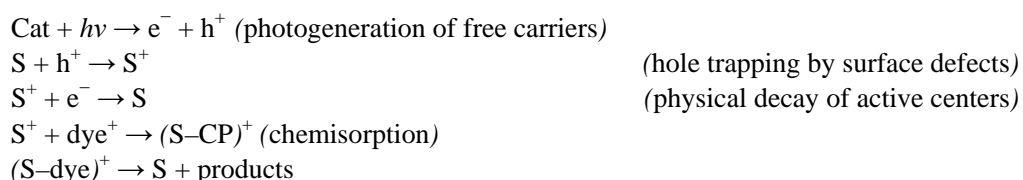
The Langmuir–Hinshelwood process is applied to heterogeneous photocatalysis and can be explained on the basis of production of electrons and holes by the photoexcitation of the catalyst. The hole is then trapped by the adsorbed dye molecule on the catalyst surface to form a reactive radical state which can decay as a result of recombination with an electron. The catalyst is regenerated as a result. Langmuir-Hinshelwood (L-H) expression in its simpler form is given by [142]

$$1/r = 1/k_r + 1/(k_r k_a C)$$

where, r is the reaction rate for the oxidation of reactant (mg /l.min), k_r is the specific reaction rate constant for the oxidation of the reactant (mg /l.min), k_a is the equilibrium constant of the reactant (l / mg) and C is the dye concentration. Numerous examples of dye degradation adhering to such a process are reported in the literature [50,141-143].

(ii) The Eley–Rideal Process

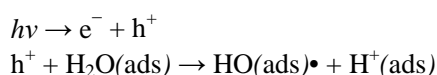
In this process, the free carriers are initially photo-fragmented followed by subsequent trapping of the holes by surface defects. The surface active centers(S) can then react with the dye (chemisorption) to form an adduct species such $(S\text{-dye})^+$ which can further decompose to produce products or can recombine with electrons. The reaction scheme is outlined below [144].

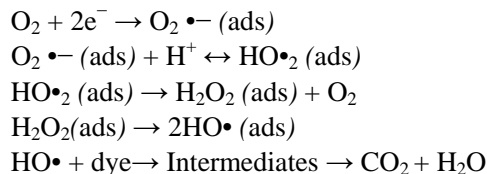


7a2. Indirect Photocatalytic Mechanism

In this process, electron–hole pairs are photogenerated on the surface of the catalyst. The hole is then trapped by the water molecules leading the formation of $\text{HO}\cdot$ radicals and H^+ and the electrons allow the formation of H_2O_2 which further decomposes in more OH^- radicals by means of its reaction with the oxygen supplied in the medium. Finally, the radicals formed during this mechanism are responsible for the oxidation of the organic molecule producing intermediate and end products [48]

The stepwise mechanism is illustrated below





7b. Degradation Studies of dyes

With the advancement of AOP techniques, various semiconductors have been tested for their efficiencies towards dye degradation. Some of these include TiO_2 , V_2O_5 , ZnO , WO_3 , CdS , ZrO_2 and their impregnated forms [50,100,145-149]. Generally, any semiconductor doped with a secondary dopant would increase its activity. Several metals have been used for doping; these include Pt , Li^+ , Zn^{+2} , Cd^{+2} , Co^{+3} , Cr^{+3} , Fe^{+3} , Al^{+3} etc.[150-152]. The presence of transition metals increase the photocatalytic activity either by scavenging electrons that reduce the recombination of charges and therefore favors the HO^{\bullet} formation, or by modifying the surface properties of the material regarding the active sites, presence of defects etc., which could increase the adsorption and favour the interfacial reactions. Titanium dioxide mediated photocatalytic oxidation has been applied more extensively for dye studies [153-156]. This is mainly because of its low cost, stable nature and its optical absorption in the UV region. The use of TiO_2 has also guaranteed good results in detoxification of water samples loaded with molecules like anilines, alcohols, and organochlorides [157-160]. A quick comparison between TiO_2 and other semiconductors such as ZrO_2 reveals that the photocatalytic efficiencies are quite different. Although the bandgap energies for both TiO_2 and ZrO_2 are the same (3.1 eV), the higher activity of TiO_2 could be attributed to a higher efficiency in the separation of the photogenerated charges (less e^-/h^+ recombination rate) due to the structure of the material. On the other hand ZrO_2 presents a low absorbance in the UV range due to intra-band gap surface states, thereby causing its low activity.

7.b.1. Effect of pH

The pH has a great effect on the photodegradation efficiency of dyes. The variation in solution pH changes the surface charge of TiO_2 particles and shifts the potentials of catalytic reactions. As a result, the adsorption of dye on the surface changes thereby causing a change in the reaction rate. Acid yellow 17 (an anionic dye) has shown to be more degraded at pH 3 [161], whereas, Orange II and Amido Black 10B showed maximum degradation at pH 9 [162]. Similar results have been reported for TiO_2 mediated photolytic reactions for the removal of chlorophenols in [163].

7.b.2. Effect of the Dose of Semiconductor

Dye degradation is also influenced by the amount of the photocatalyst. The dye degradation increases with increasing catalyst concentration, which is characteristic of heterogeneous photocatalysis. The increase in catalyst amount increases the number of active sites on the photocatalyst surface thus causing an increase in the number of HO^{\bullet} radicals which can take part in actual decoloration of dye solution. Beyond a certain limit of catalyst

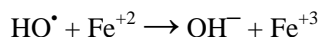
amount, the solution becomes turbid and thus blocks UV radiation for the reaction to proceed and therefore percentage of the degradation starts decreasing [50, 164,165].

7.b.3. Effect of the Initial Concentration of Dye

The initial concentration of dye in a given photocatalytic reaction is also another factor which needs to be taken into account. In this case it was found that percentage degradation decreased with increasing amount of dye concentration, while keeping a fixed amount of catalyst in these studies [50,165]. This can be rationalized on the basis that as dye concentration increases, more organic substances are adsorbed on the surface of TiO_2 , whereas less number of photons are available to reach the catalyst surface and therefore less HO^\bullet are formed, thus causing an inhibition in degradation percentage.

7.b.4. Effect of Additives

The photocatalytic degradation of dyes is also effected by the presence of additives in solution matrix [50,161,162,166-168]. These additives are generally present as ions which are initially added to the dye solution as ionic compounds to improve the industrial process. However on release of wastewater, the ions become an integral part of the effluent. Many common ions present in dye wastewater are Fe^{+2} , Zn^{+2} , Ag^+ , Na^+ , Cl^- , PO_4^{-3} , SO_4^{-2} , BrO_3^- , CO_3^{-2} , HCO_3^- and persulphate ions. Each of these added ions causes a certain decrease in percentage degradation of the dye solution, as shown in Table 2. The change in dye degradation in the presence of some selective ions is explained below on the basis of their chemical reactions in solution. For example, Fe^{+2} ions most likely undergoes the following chemical reaction in solution with HO^\bullet radicals already produced in solution

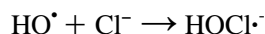
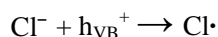


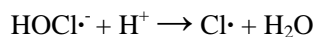
The above reaction has an appreciably high rate constant value of $3.5 \times 10^8 \text{ M}^{-1} \text{ sec}^{-1}$ [169]. Thus in the presence of Fe^{+2} , HO^\bullet radicals are easily converted into OH^- , thereby decreasing their concentration and thus less degradation of dye solution is observed.

Likewise, the presence of CO_3^{-2} and HCO_3^- ions are usually added to the dye bath to adjust the pH of the dye solution. In the presence of these ions, dye degradation also decreases. This can be explained on the basis that the presence of these ions scavenge the HO^\bullet radicals according to the following reactions thus causing a decrease in percentage degradation.

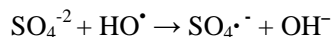


Similarly, a decrease in degradation value in the presence of Cl^- is due to its hole and hydroxyl radical scavenging effect, which occurs as follows [50]

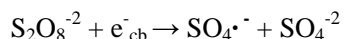




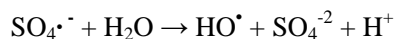
The presence of sulphate ions in solution also causes a decrease in percentage degradation because these ions can react with HO^\cdot radicals in solution and result in their depletion as follows [170]



Addition of a strong oxidizing agent such as persulphate ions ($\text{S}_2\text{O}_8^{-2}$) also decreases the degradation percentage because it can produce sulphate ions in solution;



The sulphate ions can then react with HO^\cdot radicals as shown above. The sulphate radicals can further react with water molecules to produce more sulphate ions as follows:

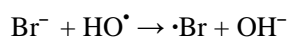


Since SO_4^\cdot is less reactive than HO^\cdot radicals, therefore SO_4^{-2} concentration increases in solution which leads to less dye degradation.

The addition of bromate ion (BrO_3^-) can also decrease percentage degradation. This can be explained on the basis that this species is an efficient electron scavenger and can react in the solution as follows [50]



The bromide ions produced in the reaction can react with HO^\cdot radicals in solution (rate constant value = $1.1 \times 10^9 \text{ M}^{-1} \text{sec}^{-1}$) thus decreasing their concentration which result in less degradation



Likewise the addition of ethanol can inhibit the photodegradation of a dye solution. This is because of the reason that ethanol can quench hydroxyl radicals which are the main source of dye degradation chemistry [161].

Photocatalytic degradation is also influenced by the presence of oxygen or air [171 -176]. The degradation becomes less in the absence of oxygen and this has been attributed to the recombination of photogenerated hole–electron pairs. Oxygen adsorbed on the surface of a semiconductor prevents the recombination process by trapping electrons according to the reaction [177, 178]:

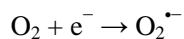


Table 2. Change in percent decoloration of three different dyes in the presence of various ions (ion concentration = 50 mg/L, irradiation time = 20 min)^a

[Ions]	% decoloration		
	<i>TB</i>	<i>SO</i>	<i>CV</i>
–	40	21	17
Fe ²⁺	6	3.5	8.5
Zn ²⁺	11	–	7.5
Ag ⁺	23	7.5	10
CO ₃ ²⁻	23	7	10
HCO ₃ ⁻	23	12.5	10
Cl ⁻	11	9	15
BrO ₃ ⁻	29	–	9.5
S ₂ O ₈ ²⁻	12	11	12
SO ₄ ²⁻	38	9	12.5
PO ₄ ³⁻	33	17	9
NO ₃ ⁻	24	10	13

^a TB = Toluidine Blue, SO = Safranin Orange, CV = Crystal Violet. The studies correspond to [TB] = 80 μM, V₂O₅/TiO₂ = 20 mg/20 mL; [SO] = 80 μM, V₂O₅/TiO₂ = 25 mg/20 mL; [CV] = 40 μM, V₂O₅/TiO₂ = 30 mg/20 mL. (This table taken from our work, ref [50])

It is known that the reaction rate is a function of the fraction of adsorption sites occupied by dissolved oxygen which makes it a limiting factor towards the photooxidative process [177].

CONCLUSION

All the AOP's based on H₂O₂ (Fenton, photo-Fenton and H₂O₂-UV) have been reported to achieve the degradation of dyes. These techniques are of interest because they are less expensive than ozonation. A combination of AOP techniques such as O₃/UV and photo-Fenton techniques has been reported to achieve higher degradation of dyes. The photocatalytic processes have shown higher degradation of dyes than the rest of the AOP's for the treatment of most of the dyes. Photocatalysis is advantageous with respect to the other AOP's as the catalyst is not consumed during the reaction.

ACKNOWLEDGEMENT

The authors would like to acknowledge and thank Dr. Ihsan Shehadi (Chemistry Dept., UAEU University) for reviewing the manuscript and providing helpful feedback.

REFERENCES

- [1] Forgas, E; Cserhati, T and Oros,G. Removal of synthetic dyes from wastewater, *a review. Env.Int.*, 2004,30, 953-971.
- [2] Parsons, S. *Advanced oxidation processes for water and wastewater*. IWA Publishing, 2004.
- [3] Derudi, M; Venturini, G; Lombardi, G; Nano, G and Rota, R. Biodegradation combined with ozone for the remediation of contaminated soils. *European Journal of Soil Biology*, 2007, 43, 297-303.
- [4] Martin, MJ; Artola, A; Balaguer, MD; and Rigola, M. Activated carbons developed from surplus sewage sludge for the removal of dyes from dilute aqueous solutions. *Chemical Engineering Journal*, 2003, 94, 231-239.
- [5] Ahmad, AL and Puasa, SW. Reactive dyes decolourization from an aqueous solution by combined coagulation/micellar-enhanced ultrafiltration process, *Chemical Engineering. Journal*, 2007, 132, 257-265.
- [6] Arslan, I; Balcioglu, IA and Bahnemann, DW. Advanced chemical oxidation of reactive dyes in simulated dyehouse effluents by ferrioxalate-Fenton /UV-A and TiO₂/UV-A processes., *Dyes and Pigments*, 2000, 47, 207-18.
- [8] Rauf ,MA; Ashraf ,SS and Alhadrami,SN. Photolytic oxidation of Coomassie Brilliant Blue with H₂O₂, *Dyes and Pigments*, 2005, 66, 197–200.
- [9] Pérez, MH; Peñuela,G; Maldonado, MI; Malato, O; Ibáñez, PF; Oller, I; Gernjak, W and Malato, S. Degradation of pesticides in water using solar advanced oxidation processes, *Applied Catalysis B. Environmental*, 2006, 64, 272-281.
- [10] Petala, M; Tsiridis, V; Samaras, P; Zouboulis, A and Sakellaropoulos, GP. Waste water reclamation by advanced treatment of secondary effluents *Desalination*, 2006, 195, 109-118.
- [11] Chen, C; Zhang, X; He, W; Lu, W and Han, H. Comparison of seven kinds of drinking water treatment processes to enhance organic material removal, A pilot test. *Science of The Total Environment*, 2007, 382, 93-102.
- [12] Masarwa, A; Calis, SR; Meyerstein, N and Meyerstein, D. Oxidation of organic substrates in aerated aqueous solutions by the Fenton reagent, *Coordination Chemistry Reviews*, 2005, 249, 1937-1943.
- [13] Chamarro, E; Marco, A and Esplugas, S. Use of Fenton reagent to improve organic chemical biodegradability. *Water Research*, 2001, 35, 1047–1051.
- [14] Mounir, B; Pons, MN; Yaacoubi, OA and Benhammou, A. Discoloration of a red cationic dye by supported TiO₂ photocatalysis. *Journal of Hazardous Materials*, 2007, 148, 513-520.
- [15] Torres, RA; Abdelmalek, F; Combet, E; Pétrier, C and Pulgarin, CA. comparative study of ultrasonic cavitation and Fenton's reagent for bisphenol A degradation in deionised and natural waters. *Journal of Hazardous Materials*, 2007, 146, 546-551.
- [16] Will, IBS; Moraes, JEF; Teixeira, ACSC; Guardani, R and Nascimento, CAO. Photo-Fenton degradation of wastewater containing organic compounds in solar reactors. *Separation and Purification Technology*, 2004, 34, 51-57.

- [17] Habibi, MH and Vosooghian, H. Photocatalytic degradation of some organic sulfides as environmental pollutants using titanium dioxide suspension. *Journal of Photochemistry and Photobiology A, Chemistry*, 2005, 174, 45-52.
- [18] Rauf, MA; Ansari, FL and Abassi, G. Photocatalytic degradation of some azo dyes, *J. Fac. Sci.(UAEU)*, 2004, 13, 41-45.
- [19] Malik, PK and Saha, SK. Oxidation of direct dyes with hydrogen peroxide using ferrous ion as catalyst, *Sep. Purif. Tech.*, 2003, 31, 241-250.
- [20] Liu, CC; Hsieh, YH; Lai, PF; Li, CH and Kao, CL. Photodegradation treatment of azo dye waste water by UV/TiO₂ process. *Dyes and Pigments*, 2006, 68, 191-195.
- [21] Li, L; Zhang, C; He, H and Liu, J. An integrated system of biological and catalytic oxidation for the removal of o-xylene from exhaust. *Catalysis Today*, 2007, 126, 338-344.
- [22] Georgiou, D; Melidis, P; Aivasidis, A and Gimouhopoulos, K. Degradation of azo reactive dyes by UV radiation in the presence of hydrogen peroxide. *Dyes and Pigments*, 2002, 52, 69-78. .
- [23] Mater, L; Rosa, EVC; Berto, J; Corrêa, AXR; Schwingel, PR and Radetski, CM. A simple methodology to evaluate influence of H₂O₂ and Fe²⁺ concentrations on the mineralization and biodegradability of organic compounds in water and soil contaminated with crude petroleum. *Journal of Hazardous Materials*, 2007, 149, 379-386.
- [24] Alnuaimi, MM; Rauf, MA and Ashraf, SS. Comparative decoloration study of Neutral Red by different oxidative processes. *Dyes and Pigments*, 2007, 72, 367-371. .
- [25] Sabhi, S; Kiwi, J. Degradation of 2,4-dichlorophenol by immobilized iron catalysts. *Water Research*, 2001, 35, 1994–2002.
- [26] Lunar, L; Sicilia, D; Rubio, S; Bendito, DP and Nickel, U. Degradation of photographic developers by Fenton's reagent: condition optimization and kinetics for metal oxidation. *Water Research*, 2000, 34, 791-1802.
- [27] Abdullah, F; Rauf, MA and Ashraf, SS. Kinetics and optimization of photolytic decoloration of Carmine by UV/H₂O₂. *Dyes and Pigments*, 2007, 75, 194-198. .
- [28] Herrmann, JM; Guillard, Ch; Disdier, J; Lehaut, C; Malato, S and Blanco, J. New industrial titania photocatalysts for the solar detoxification of water containing various pollutants, *Applied Catalysis B*, 2002, 35, 281–294.
- [29] Huling, SCG; Arnold, RG; Sierka, RA; Jones, PK and Fine, DD. Contaminant adsorption and oxidation via Fenton reaction. *Journal of Environmental Engineering*, 2000, 126, 595–600.
- [30] Dionysiou, DD; Khodadoust, A; Kern, AM; Suidan, MT; Baudin, I and Laîné, JM. Continuous-mode photocatalytic degradation of chlorinated phenols and pesticides in water, using a bench-scale TiO₂ rotating disk reactor, *Applied Catalysis B*, 2000, 24, 139–155.
- [31] Tanaka, K; Padermpole, K and Hisanaga, T. Photocatalytic degradation of commercial azo dyes. *Water Research*, 2000, 34, 327-333.
- [32] Wong, Y; Solar photocatalytic degradation of eight commercial dyes in TiO₂ suspension. *Water Research*, 2000, 34, 990-994.
- [33] Arslan, I; Balcioglu, AI and Beahnmann, DW. Photochemical treatment of simulated dye house effluents by novel TiO₂ photocatalysis: Experience with thin film fixed

- bed(TFFB) and double skin sheet(DSS) reactor. *Water Science and Technology*, 2001, 44, 171-178.
- [34] Benitez, FJ; Heredia, JB; Acero, JL and Rubio, FJ. Oxidation of several chlorophenolic derivatives by UV irradiation and hydroxyl radicals. *Journal of Chemical Technology and Biotechnology*, 2001, 76, 312–320.
- [35] Xu, M; Wang, Q and Hao, Y. Removal of organic carbon from wastepaper pulp effluent by lab-scale solar photo-Fenton process. *Journal of Hazardous Materials*, 2007, 148, 103-109.
- [36] Yoon, J; Kim, S; Lee, DS and Huh, J Characteristics of *p*-chlorophenol degradation by photo-Fenton oxidation. *Water Science and Technology*, 2000, 42, 219–224.
- [37] Lücking, F; Köser, H; Jank, M and Ritter, A; Iron powder, graphite and activated carbon as catalysts for the oxidation of 4-chlorophenol with hydrogen peroxide in aqueous solution. *Water Research*, 1998, 32, 2607–2614.
- [38] Ateeq, H; Rauf, MA. and Ashraf, SS. Efficient microbial degradation of Toluidine Blue dye by *Brevibacillus* sp. *Dyes and Pigments*, 2007, 75, 395-400.
- [39] Li, X; Yao, JH and Qi, JY. Degradation of Organic Pollutants in Water by Catalytic Ozonation. *Chemical Research in Chinese Universities*, 2007, 23, 273-275.
- [40] Wu, J and Wang, T. Ozonation of aqueous azo dye in a semi-batch reactor. *Water Research*, 2001, 35, 1093-1099.
- [41] Keskinler, EOB and Çelik, Z. Ozonation of aqueous Bomaplex Red CR-L dye in a semi-batch reactor. *Dyes and Pigments*, 2005, 64, 101-108.
- [42] Shu, HY and Chang, MC. Decolorization effects of six azo dyes by O₃, UV/O₃ and UV/H₂O₂ processes. *Dyes and Pigments*, 2005, 65, 25-31.
- [43] Bijan, L and Mohseni, M. Integrated ozone and biotreatment of pulp mill effluent and changes in biodegradability and molecular weight distribution of organic compounds. *Water Research*, 2005, 39, 3763-3772.
- [44] Wang, X; Gu, X; Lin, D; Dong, F and Wan, X. Treatment of acid rose dye containing waste water by ozonizing – biological aerated filter. *Dyes and Pigments*, 2007, 74, 736-740.
- [45] Muthukumar, M; Sargunamani, D; Senthilkumar, M and Selvakumar, N. Studies on decolouration: toxicity and the possibility for recycling of acid dye effluents using ozone treatment. *Dyes and Pigments*, 2005, 64, 39-44.
- [46] Ni, CH and Chen, JN. Heterogeneous catalytic ozonation of 2-chlorophenol in aqueous solution with alumina as a catalyst. *Water Science and Technology*, 2001, 43, 213–220.
- [47] Selcuk, H. Decolorization and detoxification of textile wastewater by ozonation and coagulation processes, *Dyes and Pigments*, 2005, 64, 217-222.
- [48] Yue, B; Zhou, Y; Xu, J; Wu, Z; Zhang, X; Zou, Y and Jin, S. Photocatalytic degradation of aqueous 4-chlorophenol by silica-immobilized polyoxometalates. *Environmental Science and Technology*, 2002, 36, 1325–1329.
- [49] Habibi, MH and Talebian, N. Photocatalytic degradation of an azo dye X6G in water, A comparative study using nanostructured indium tin oxide and titanium oxide thin films. *Dyes and Pigments*, 2007, 73, 186-194.
- [50] Rauf, MA; Bukallah, SB; Hammadi, A; Soliman, A and Hammadi, F. The effect of operational parameters on the photoinduced decoloration of dyes using a hybrid catalyst V₂O₅/TiO₂. *Chemical Engineering Journal*, 2007, 129, 167-172.

- [51] Wu, CH; Chang, HW and Chern, JM. Basic dye decomposition kinetics in a photocatalytic slurry reactor. *Journal of Hazardous Materials*, 2006, 137, 336-343.
- [52] Saien, J and Soleymani, AR. Degradation and mineralization of Direct Blue 71 in a circulating upflow reactor by UV/TiO₂ process and employing a new method in kinetic study. *J.Hazardous Materials*, 2007, 144, 506-512.
- [53] Mozia, S; Tomaszewska, M and Morawski, AW. Photocatalytic membrane reactor (PMR) coupling photocatalysis and membrane distillation—Effectiveness of removal of three azo dyes from water. *Catalysis Today*, 2007, 129, 3-8.
- [54] Danion, A; Disdier, J; Guillard, C and Renault, NJ. Malic acid photocatalytic degradation using a TiO₂-coated optical fiber reactor. *Journal of Photochemistry and Photobiology A, Chemistry*, 2007, 190, 135-140.
- [55] Mahmoodi, NM; Arami, M; Limaee, NY and Tabrizi, NS. Kinetics of heterogeneous photocatalytic degradation of reactive dyes in an immobilized TiO₂ photocatalytic reactor. *Journal of Colloid and Interface Science*, 2006, 295, 159-164.
- [56] Alnaizy, R and Akgerman, A. Advanced oxidation of phenolic compounds *Advances in Environmental Research*, 2000, 4, 233-244.
- [57] Aleboyeh, A; Moussa, Y and Aleboyeh, H. The effect of operational parameters on UV/H₂O₂ decolourisation of Acid Blue 74. *Dyes and Pigments*, 2005, 66, 129-134.
- [58] Aleboyeh, A; Aleboyeh, H and Moussa, Y. Critical effect of hydrogen peroxide in photochemical oxidative decolorization of dyes, Acid Orange 8, Acid Blue 74 and Methyl Orange. *Dyes and Pigments*, 2003, 57, 67-75.
- [59] Zang, Y and Farnood, R. Photocatalytic decomposition of methyl tert-butyl ether in aqueous slurry of titanium dioxide, *Applied Catalysis B. Environmental*, 2005, 57, 275-282.
- [60] Abdullah, FH; Rauf, MA and Ashraf, SS. Photolytic oxidation of Safranin-O with H₂O₂. *Dyes and Pigments*, 2007, 72, 349-352.
- [61] Modirshahla, N and Behnajady, MA. Photooxidative degradation of Malachite Green (MG) by UV/H₂O₂, Influence of operational parameters and kinetic modeling. *Dyes and Pigments*, 2006, 70, 54-59.
- [62] Zhu, L and Cronin, TJ. Photodissociation of benzaldehyde in the 280–308 nm region. *Chemical Physics Letters*, 2000, 317, 227-231.
- [63] Feng, W; Nansheng, D and Yuegang, Z. Discoloration of dye solutions induced by solar photolysis of ferrioxalate in aqueous solutions. *Chemosphere*, 1999, 39, 2079-2085.
- [64] He, J; Ma, W; He, J; Zhao, J and Yu, JC. Photooxidation of azo dye in aqueous dispersions of H₂O₂/α-FeOOH, *Applied Catalysis B. Environmental*, 2002, 39, 211-220.
- [65] Schrank, SG; dos Santos, JNR; Souza, DS and Souza, EES. Decolourisation effects of Vat Green 01 textile dye and textile wastewater using H₂O₂/UV process, *J. Photochemistry and Photobiology A, Chemistry*, 2007, 186, 125-129.
- [66] Alshamsi, FA; Albadwawi, AS; Alnuaimi, MM; Rauf, MA and Ashraf, SS. Comparative efficiencies of the degradation of Crystal Violet using UV/hydrogen peroxide and Fenton's reagent. *Dyes and Pigments*, 2007, 74, 283-287.
- [67] Wang, S. A Comparative study of Fenton and Fenton-like reaction kinetics in decolourisation of wastewater. *Dyes and Pigments*, 2008, 76, 714-720.

- [68] Ntampeglitis, K; Riga, A; Karayannis, V; Bontozoglou, V and Papapolymerou, G. Decolorization kinetics of Procion H-ex1 dyes from textile dyeing using Fenton-like reactions. *Journal of Hazardous Materials*, 2006, 136,75-84.
- [69] Lucas, MS and Peres, JA. Degradation of Reactive Black 5 by Fenton/UV-C and ferrioxalate/H₂O₂/solar light processes. *Dyes and Pigments*, 2007, 74, 622-629.
- [70] Majcherczyk, CMA; Schormann, W and Hüttermann, A. Degradation of acrylic copolymers by Fenton's reagent, *Polymer Degradation and Stability*, 2002, 75, 107-112.
- [71] Farahnaky, A; Gray, DA; Mitchell, JR and Hill, SE. Ascorbic acid and hydrogen peroxide (Fenton's reagent) induced changes in gelatin systems, *Food Hydrocolloids*, 2003, 17, 321-326.
- [72] Chan, KH and Chu, W. Modeling the reaction kinetics of Fenton's process on the removal of atrazine. *Chemosphere*, 2003, 51, 305-311.
- [73] Rivas, FJ; Beltrán, FJ; Garcia, JF; Navarrete, V and Gimeno, O; Co-oxidation of p-hydroxybenzoic acid and atrazine by the Fenton's like system Fe(III)/H₂O₂. *Journal of Hazardous Materials*, 2002, 91, 143-157.
- [74] Benitez, FJ; Real, FJ; Acero, JL; Leal, AI and Garcia, C. Gallic acid degradation in aqueous solutions by UV/H₂O₂ treatment, Fenton's reagent and the photo-Fenton, system. *Journal of Hazardous Materials*, 2005, 126, 31-39.
- [75] Rivas, FJ; Beltrán, FJ; Frades, J and Buxeda, P. Oxidation of p-hydroxybenzoic acid by Fenton's reagent. *Water Research*, 2001, 35, 387-396.
- [76] Flotron, V; Delteil, C; Padellec, Y and Camel, V. Removal of sorbed polycyclic aromatic hydrocarbons from soil, sludge and sediment samples using the Fenton's reagent process. *Chemosphere*, 2005, 59, 1427-1437.
- [77] Watts, RJ; Haller, DR; Jones, AP and Teel, AL. A foundation for the risk-based treatment of gasoline-contaminated soils using modified Fenton's reactions. *Journal of Hazardous Materials*, 2000, 76, 73-89.
- [78] Di Palma, L; Ferrantelli, P and Petrucci, E. Experimental study of the remediation of atrazine contaminated soils through soil extraction and subsequent peroxidation. *Journal of Hazardous Materials*, 2003, 99, 265-276.
- [79] Dewil, R; Baeyens, J and Neyens, E. Fenton peroxidation improves the drying performance of waste activated sludge. *Journal of Hazardous Materials*, 2005, 117, 161-170.
- [80] Trujillo, D; Font, X and Sánchez, A. Use of Fenton reaction for the treatment of leachate from composting of different wastes. *Journal of Hazardous Materials*, 2006, 138, 201-204.
- [81] Riga, A; Soutsas, K; Ntampeglitis, K; Karayannis, V and Papapolymerou, G. Effect of system parameters and of inorganic salts on the decolorization and degradation of Procion H-ex1 dyes. Comparison of H₂O₂/UV, Fenton, UV/Fenton, TiO₂/UV and TiO₂/UV/H₂O₂ processes, *Desalination*, 2007, 211, 72-86.
- [82] Habibi, MH; Hassanzadeh, A and Mahdavi, S. The effect of operational parameters on the photocatalytic degradation of three textile azo dyes in aqueous TiO₂ suspensions. *Journal of Photochemistry and Photobiology A, Chemistry*, 2005, 172, 89-96.
- [83] Ramirez, JH; Costa, CA and Madeira, LM. Experimental design to optimize the degradation of the synthetic dye Orange II using Fenton's reagent. *Catalysis Today*, 2005, 107-108, 68-76.

- [84] Meriç, S; Selcuk, H; Gallo, M and Belgiorno, V. Decolourisation and detoxifying of Remazol Red dye and its mixture using Fenton's reagent, *Desalination*, 2005, 173, 239-248.
- [85] Sun, JH; Sun, SP; Wang, GL and Qiao, LP. Degradation of azo dye Amido black 10B in aqueous solution by Fenton oxidation process. *Dyes and Pigments*, 2007, 74, 647-652.
- [86] Ghaly, MY; Farah, JY and Fathy, AM. Enhancement of decolorization rate and COD removal from dyes containing wastewater by the addition of hydrogen peroxide under solar photocatalytic oxidation, *Desalination*, 2007, 217, 74-84.
- [87] Dong, Y; He, L and Yang, M. Solar degradation of two azo dyes by photocatalysis using Fe(III)-oxalate complexes/H₂O₂ under different weather conditions. *Dyes and Pigments*, 2008, 77, 343-350.
- [88] Chen, J and Zhu, L. UV-Fenton discoloration and mineralization of Orange II over hydroxyl-Fe-pillared bentonite. *Journal of Photochemistry and Photobiology A, Chemistry*, 2007, 188, 56-64.
- [89] Józwiak, WK; Mitros, M; Czaplńska, JK and Tosik, R. Oxidative decomposition of Acid Brown 159 dye in aqueous solution by H₂O₂/Fe²⁺ and ozone with GC/MS analysis. *Dyes and Pigments*, 2007, 74, 9-16.
- [90] Xu, XR; Li, HB; Wang, WH and Gu, JD. Degradation of dyes in aqueous solutions by the Fenton process. *Chemosphere*, 2004, 57, 595-600.
- [91] Eremektar, G; Selcuk, H and Meric, S. Investigation of the relation between COD fractions and the toxicity in a textile finishing industry waste water, Effect of preozonation, *Desalination*, 2007, 211, 314-320.
- [92] Jin, H; Wu, Q and Pang, W. Photocatalytic degradation of textile dye X-3B using polyoxometalate-TiO₂ hybrid materials. *Journal of Hazardous Materials*, 2007, 141, 123-127.
- [93] Molinari, R; Borgese, M; Drioli, E; Palmisano, L and Schiavello, M. Hybrid processes coupling photocatalysis and membranes for degradation of organic pollutants in water. *Catalysis Today*, 2002, 75, 77-85.
- [94] Wang, CC; Lee, CK; Lyu, MD and Juang, LC. Photocatalytic degradation of C.I. Basic Violet 10 using TiO₂ catalysts supported by Y zeolite, An investigation of the effects of operational parameters. *Dyes and Pigments*, 2008, 76, 817-824.
- [95] Yang, Y; Wu, Q; Guo, Y; Hu, C. and Wang, E. Efficient degradation of dye pollutants on nanoporous polyoxotungstate-anatase composite under visible-light irradiation. *Journal of Molecular Catalysis A, Chemical*, 2005, 225, 203-212.
- [96] Choo, KH and Kang, SK. Removal of residual organic matter from secondary effluent by iron oxides adsorption, *Desalination*, 2003, 154, 139-146.
- [97] Zinder, B; Furrer, G and Stumm, W. The coordination chemistry of weathering II. Dissociation of Fe (III) oxides, *Geochim. Cosmochim. Acta*, 1986, 50, 1861-1869.
- [98] Stone, AT and Morgan, JJ. Reductive and dissolution of manganese (III) and manganese (IV) oxides by organics. I. Reaction with hydroquinone, *Environmental Science and Technology*, 1987, 18, 450-456.
- [99] Glaze, WH; King, JW and Chapin, DH. The chemistry of water treatment processes involving ozone, hydrogen peroxide and UV radiation. *Ozone Science and Engineering*, 1987, 9, 335-352.

- [100] Alnuaimi, MM; Rauf, MA and Ashraf, SS. A comparative study of Neutral Red decoloration by photo-Fenton and photocatalytic processes. *Dyes and Pigments*, 2008, 76, 332-337.
- [101] Peternel, IT; Koprivanac, N; Božić, AML and Kušić, HM. Comparative study of UV/TiO₂, UV/ZnO and photo-Fenton processes for the organic reactive dye degradation in aqueous solution. *Journal of Hazardous Materials*, 2007, 148, 477-484.
- [102] Chen, J and Zhu, L. UV-Fenton discoloration and mineralization of Orange II over hydroxyl-Fe-pillared bentonite. *Journal of Photochemistry and Photobiology A, Chemistry*, 2007, 188, 56-64.
- [103] Liu, R; Chiu, HM; Shiau, CS; Yeh, RYL and Hung, Y.T. Degradation and sludge production of textile dyes by Fenton and photo-Fenton processes. *Dyes and Pigments*, 2007, 73, 1-6.
- [104] Montañó, JG; Torrades, F; Hortal, JAG; Domènech, X and Peral, J. Degradation of Procion Red H-E7B reactive dye by coupling a photo-Fenton system with a sequencing batch reactor. *Journal of Hazardous Materials*, 2006, 134, 220-229.
- [105] Torrades, F; Montañó, JG; Hortal, JAG; Domènech, X and Peral, J. Decolorization and mineralization of commercial reactive dyes under solar light assisted photo-Fenton conditions, *Solar Energy*, 2004, 77, 573-581.
- [106] Zheng, H; Pan, Y and Xiang, X. Oxidation of acidic dye Eosin Y by the solar photo-Fenton processes. *Journal of Hazardous Materials*, 2007, 141, 457-464.
- [107] Bali, U; Çatalkaya, E and Şengül, F. Photodegradation of Reactive Black 5, Direct Red 28 and Direct Yellow 12 using UV, UV/H₂O₂ and UV/H₂O₂/Fe²⁺, a comparative study. *Journal of Hazardous Materials*, 2004, 114, 159-166.
- [108] Benítez, FJ; Heredia, JB; Acero, JL; Rubio, FJ. Rate constants for the reactions of ozone with chlorophenols in aqueous, solutions. *Journal of Hazardous Materials B* 79, 2000, 271-285.
- [109] Modirshahla, N; Behnajady, MA and Ghanbary, F. Decolorization and mineralization of C.I. Acid Yellow 23 by Fenton and photo-Fenton processes. *Dyes and Pigments*, 2007, 73, 305-310.
- [110] Gutowska, A; Czaplińska, JK and Józwiak, WK. Degradation mechanism of Reactive Orange 113 dye by H₂O₂/Fe²⁺ and ozone in aqueous solution. *Dyes and Pigments*, 2007, 74, 41-46.
- [111] Heng, S; Yeung, KL; Djafer, M and Schrotter, JC. A novel membrane reactor for ozone water treatment. *Journal of Membrane Science*, 2007, 289, 67-75.
- [112] Cataldo, F. DNA degradation with ozone International. *Journal of Biological Macromolecules*, 2006, 38, 248-254.
- [113] Ritola, O; Livingstone, DR; Peters, LD and Seppä, PL. Antioxidant processes are affected in juvenile rainbow trout (*Oncorhynchus mykiss*) exposed to ozone and oxygen-supersaturated water, *Aquaculture*, 2002, 210, 1-19.
- [114] Popov, P and Getoff, N. Ozonolysis and combination of ozonolysis and radiolysis of aqueous fluorine, *Radiation Physics and Chemistry*, 2004, 69, 311-315.
- [115] Cataldo, F and Angelini, G. *Some aspects of the ozone degradation of poly(vinyl alcohol) Polymer Degradation and Stability*, 2006, 91, 2793-2800.
- [116] Frezza, M; Soulère, L; Queneau, Y and Doutheau, A. A Baylis-Hillman/ozonolysis route towards (±) 4,5-dihydroxy-2,3-pentanedione (DPD) and analogues *Tetrahedron Letters*, 2005, 46, 6495-6498.

- [117] Lloyd, JA; Spraggins, JM; Johnston, MV and Laskin, J. Peptide Ozonolysis, Product Structures and Relative Reactivities for Oxidation of Tyrosine and Histidine Residues. *Journal of the American Society for Mass Spectrometry*, 2006, 17, 1289-1298.
- [118] Liu, J; Luo, HJ and Wei, CH. Degradation of anthraquinone dyes by ozone *Transactions of Nonferrous Metals Society of China*, 2007, 17, 880-886.
- [119] Zhao, W; Wu, Z and Wang, D. Ozone direct oxidation kinetics of Cationic Red X-GRL in aqueous solution. *Journal of Hazardous Materials*, 2006, 137, 1859-1865.
- [120] Güyer, GT and Ince, NH. Individual and combined effects of ultrasound, ozone and UV irradiation, a case study with textile dyes *Ultrasonics*, 2004, 42, 603-609.
- [121] Muthukumar, M; Sargunamani, D; Selvakumar, N. Statistical analysis of the effect of aromatic, azo and sulphonic acid groups on decolouration of acid dye effluents using advanced oxidation processes. *Dyes Pigments*, 2005, 65, 151-158.
- [122] He, Z; Song, S; Xia, M; Qiu, J; Ying, H; Lü, B; Jiang, Y and Chen, J. Mineralization of C.I. Reactive Yellow 84 in aqueous solution by sonolytic ozonation *Chemosphere*, 2007, 69, 191-199.
- [123] Ma, J; Sui, M; Zhang, T and Guan, C. Effect of pH on MnO_x/GAC catalyzed ozonation for degradation of nitrobenzene. *Water Research*, 2005, 39, 779-786.
- [124] Zhao, W; Shi, H and Wang, D. Ozonation of Cationic Red X-GRL in aqueous solution, degradation and mechanism. *Chemosphere*, 2004, 57, 1189-1199.
- [125] Alaton, IA. Degradation of a commercial textile biocide with advanced oxidation processes and ozone. *Journal of Environmental Management*, 2007, 82, 145-154.
- [126] Winarno, EK and Getoff, N. Comparative studies on the degradation of aqueous 2-chloroaniline by O₃ as well as by UV-light and γ -rays in the presence of ozone *Radiation Physics and Chemistry*, 2002, 65: 387-395.
- [127] Wu, JJ; Muruganandham, M and Chen, SH. Degradation of DMSO by ozone-based advanced oxidation processes. *Journal of Hazardous Materials*, 2007, 149, 218-225.
- [128] Kusic, H; Koprivanac, N and Bozic, AL. Minimization of organic pollutant content in aqueous solution by means of AOPs, UV- and ozone-based technologies. *Chemical Engineering Journal*, 2006, 123, 127-137.
- [129] Lim, HN; Choi, H; Hwang, TM and Kang, JW. Characterization of ozone decomposition in a soil slurry, kinetics and mechanism. *Water Research*, 2002, 36, 219-229.
- [130] Benitez, FJ; Acero, JL and Real, FJ. Degradation of carbofuran by using ozone, UV radiation and advanced oxidation processes. *Journal of Hazardous Materials*, 2002, 89, 51-65.
- [131] Skorb, EV; Ustinovich, EA; Kulak, AI and Sviridov, DV. Photocatalytic activity of TiO₂, In₂O₃ nanocomposite films towards the degradation of arylmethane and azo dyes. *Journal of Photochemistry and Photobiology A, Chemistry*, 2008, 193, 97-102.
- [132] Tariq, MA; Faisal, M; Saquib, M and Muneer, M. Heterogeneous photocatalytic degradation of an anthraquinone and a triphenylmethane dye derivative in aqueous suspensions of semiconductor. *Dyes and Pigments*, 2008, 76, 358-365.
- [133] Mounir, B; Pons, MN; Zahraa, O; Yaacoubi, A and Benhammou, A. Discoloration of a red cationic dye by supported TiO₂ photocatalysis. *Journal of Hazardous Materials*, 2007, 148, 513-520.
- [134] Wang, CT. Photocatalytic activity of nanoparticle gold/iron oxide aerogels for azo dye degradation. *Journal of Non-Crystalline Solids*, 2007, 353, 1126-1133.

- [135] Badr, Y and Mahmoud, MA. Photocatalytic degradation of methyl orange by gold silver nano-core/silica nano-shell. *Journal of Physics and Chemistry of Solids*, 2007, 68, 413-419.
- [136] Bakaullah, SB; Rauf, MA and Ashraf, SS. Photocatalytic decoloration of Coomassie Brilliant Blue with titanium oxide. *Dyes and Pigments*, 2007, 72, 353-356 .
- [137] Tovar, LLG; Martínez, LMT; Rodríguez, DB; Gómez, R and del Angel, G. Photocatalytic degradation of methylene blue on $\text{Bi}_2\text{MnNbO}_7$ (M = Al, Fe, In, Sm) sol-gel catalysts. *Journal of Molecular Catalysis A, Chemical*, 2006, 247, 283-290.
- [138] Asiltürk, M; Sayilkan, F; Erdemoğlu, S; Akarsu, M; Sayilkan, H; Erdemoğlu, M and Arpaç, E. Characterization of the hydrothermally synthesized nano- TiO_2 crystallite and the photocatalytic degradation of Rhodamine B. *Journal of Hazardous Materials*, 2006, 129, 164-170.
- [139] Tariq, MA; Faisal, M and Muneer, M. Semiconductor-mediated photocatalysed degradation of two selected azo dye derivatives, amaranth and bismarck brown in aqueous suspension. *Journal of Hazardous Materials*, 2005, 127, 172-179.
- [140] Arabatzis, IM; Stergiopoulos, T; Andreeva, D; Kitova, S; Neophytides, SG and Falaras, P. Characterization and photocatalytic activity of Au/TiO_2 thin films for azo-dye degradation. *Journal of Catalysis*, 2003, 220, 127-135.
- [141] Sahel, K; Perol, N; Chermette, H; Bordes, C; Derriche, Z and Guillard, C. Photocatalytic decolorization of Remazol Black 5 (RB5) and Procion Red MX-5B— Isotherm of adsorption, kinetic of decolorization and mineralization *Applied Catalysis B. Environmental*, 2007, 77, 100-109.
- [142] Machado, AEH; de Miranda, JA; de Freitas, RF; Duarte, ETFM; Ferreira, LF; Albuquerque, YDT; Ruggiero, R; Sattler, C and de Oliveira, L. Destruction of the organic matter present in effluent from a cellulose and paper industry using photocatalysis. *Journal of Photochemistry and Photobiology A, Chemistry*, 2003, 155, 231-241.
- [143] da Silva, CG and Faria, JL. Photochemical and photocatalytic degradation of an azo dye in aqueous solution by UV irradiation. *Journal of Photochemistry and Photobiology A, Chemistry*, 2003, 155, 133-143.
- [144] Serpone, S; Emelie, V. Suggested terms and definitions in photocatalysis and radiocatalysis. *International Journal of Photoenergy*, 2002, 4, 91-131.
- [145] Ramirez, JH; Maldonado, FJH; Pérez, AF; Moreno, CC; Costa, CA and Madeira, LM. Azo-dye Orange II degradation by heterogeneous Fenton-like reaction using carbon-Fe catalysts, *Applied Catalysis B. Environmental*, 2007, 75, 312-323.
- [146] Hasnat, MA; Uddin, MM; Samed, AJF; Alam, SS and Hossain, S, Adsorption and photocatalytic decolorization of a synthetic dye erythrosine on anatase TiO_2 and ZnO surfaces. *Journal of Hazardous Materials*, 2007, 147, 471-477.
- [147] Andronic, L and Duta, A. TiO_2 thin films for dyes photodegradation, *Thin Solid Films*, 2007, 515, 6294-6297.
- [148] Wang, CT. Photocatalytic activity of nanoparticle gold/iron oxide aerogels for azo dye degradation. *Journal of Non-Crystalline Solids*, 2007, 353, 1126-1133.
- [149] Bizani, E; Fytianos, K; Poullos, I and Tsiridis, V. Photocatalytic decolorization and degradation of dye solutions and wastewaters in the presence of titanium dioxide. *Journal of Hazardous Materials*, 2006, 136, 85-94.

- [150] Sayilkan, F; Asiltürk M; Tatar, P; Kiraz, N; Şener, Ş; Arpaç, E and Sayilkan, H. Photocatalytic performance of Sn-doped TiO₂ nanostructured thin films for photocatalytic degradation of malachite green dye under UV and VIS-lights. *Materials Research Bulletin*, 2008, 43, 127-134.
- [151] Rupa, AV; Manikandan, D; Divakar, D and Sivakumar, T. Effect of deposition of Ag on TiO₂ nanoparticles on the photodegradation of Reactive Yellow-17, *Journal of Hazardous Materials*, 2007, 147, 906-913.
- [152] Sahoo, C; Gupta, AK and Pal, A. Photocatalytic degradation of Methyl Red dye in aqueous solutions under UV irradiation using Ag⁺ doped TiO₂ *Desalination*, 2005, 181, 91-100.
- [153] Skorb, EV; Ustinovich, EA; Kulak, AI and Sviridov, DV. Photocatalytic activity of TiO₂/In₂O₃ nanocomposite films towards the degradation of arylmethane and azo dyes. *Journal of Photochemistry and Photobiology A, Chemistry*, 2008, 193, 97-102.
- [154] Bettinelli, M; Dallacasa, V; Falcomer, D; Fornasiero, P; Gombac, V; Montini, T.; Romanò, L and Speghini, A. Photocatalytic activity of TiO₂ doped with boron and vanadium. *Journal of Hazardous Materials*, 2007, 146, 529-534.
- [155] Caliman, AF; Cojocaru, C; Antoniadis, A and Poullos, I. Optimized photocatalytic degradation of Alcian Blue 8 GX in the presence of TiO₂ suspensions. *Journal of Hazardous Materials*, 2007, 144, 265-273.
- [156] Mahmoodi, NM; Arami, M; Limaee, NY; Gharanjig, K and Ardejani, FD. Decolorization and mineralization of textile dyes at solution bulk by heterogeneous nanophotocatalysis using immobilized nanoparticles of titanium dioxide, *Colloids and Surfaces A. Physicochemical and Engineering Aspects*, 2006, 290, 125-131.
- [157] Xu, XR; Li, HB and Gu, JD. Simultaneous decontamination of hexavalent chromium and methyl tert-butyl ether by UV/TiO₂ process. *Chemosphere*, 2006, 63, 254-260.
- [158] Carpio, E; Zúñiga, P; Ponce, S; Solis, J; Rodriguez, J and Estrada W. Photocatalytic degradation of phenol using TiO₂ nanocrystals supported on activated carbon, *Journal of Molecular Catalysis A, Chemical*, 2005, 228, 293-298.
- [159] Canle, LM; Santaballa, JA and Vulliet, E. On the mechanism of TiO₂-photocatalyzed degradation of aniline derivatives. *Journal of Photochemistry and Photobiology A, Chemistry*, 2005, 175, 192-200.
- [160] Lhomme, L; Brosillon, S; Wolbert, D and Dussaud, J. Photocatalytic degradation of a phenylurea, chlortoluron, in water using an industrial titanium dioxide coated media, *Applied Catalysis B. Environmental*, 2005, 61, 227-235.
- [161] Behnajady, MA; Modirshahla, N and Shokri, M. Photodestruction of acid orange 7(AO7) in aqueous solutions by UV/H₂O₂, influence of operational parameters. *Chemosphere*, 2005, 55, 129-134.
- [162] Qamar, M; Saquib, M and Muneer, M. Photocatalytic degradation of two selected dye derivatives, chromotrope 2B and amido black 10B in aqueous suspensions of titanium dioxide. *Dyes and Pigments*, 2005, 65, 1-9.
- [163] Fabbri, D; Prevot, AB and Pramauro, E. Effect of surfactant microstructures on photocatalytic degradation of phenol and chlorophenols, *Applied Catalysis B. Environmental*, 2006, 62, 21-27.
- [164] Wang, CC; Lee, CK; Lyu, MD and Juang, LC. Photocatalytic degradation of C.I. Basic Violet 10 using TiO₂ catalysts supported by Y zeolite, An investigation of the effects of operational parameters. *Dyes and Pigments*, 2008, 76, 817-824.

- [165] Macedo, LC; Zaia DAM; Moore, GJ and de Santana, H. Degradation of leather dye on TiO₂, A study of applied experimental parameters on photoelectrocatalysis. *Journal of Photochemistry and Photobiology A, Chemistry*, 2007, 185, 86-93.
- [166] Zhang, F; Yediler, A; Liang, X and Kettrup, A. Effects of dye additives on the ozonation process and oxidation by-products, a comparative study using hydrolyzed C.I. Reactive Red 120. *Dyes and Pigments*, 2004, 60, 1-7.
- [167] Ashraf, SS; Rauf, MA and Alhadrami, S. Degradation of Methyl Red using Fenton's reagent and the effect of various salts. *Dyes and Pigments*, 2006, 69, 74-78.
- [168] Muruganandham, M and Swaminathan, M. Photochemical oxidation of reactive azo dye with UV-H₂O₂ process. *Dyes and Pigments*, 2004, 62, 271-277.
- [169] Yoon, J; Lee, Y; Kim, S. Investigation of the reaction pathway of OH radicals produced by Fenton oxidation in the conditions of wastewater treatment. *Water Science and Technology*, 2001, 44, 15-21.
- [170] Muruganandham, M and Swaminathan, M. Photocatalytic decoloration and degradation of Reactive Orange 4 by TiO₂-UV process. *Dyes and Pigments*, 2006, 68, 133-142.
- [171] Chai, F; Wang, L; Xu, L; Wang, X and Huang, J. Degradation of dye on polyoxotungstate nanotube under molecular oxygen. *Dyes and Pigments*, 2008, 76, 113-117.
- [172] Zhou, M and He, J. Degradation of azo dye by three clean advanced oxidation processes, Wet oxidation, electrochemical oxidation and wet electrochemical oxidation—A comparative study, *Electrochimica Acta*, 2007, 53, 1902-1910.
- [173] Rajkumar, D and Kim, JG. Oxidation of various reactive dyes with in situ electro-generated active chlorine for textile dyeing industry wastewater treatment. *Journal of Hazardous Materials*, 2006, 136, 203-212.
- [174] Isik, M and Sponza, DT. Effect of oxygen on decolorization of azo dyes by *Escherichia coli* and *Pseudomonas* sp. and fate of aromatic amines, *Process Biochemistry*, 2003, 38, 1183-1192.
- [175] Thomas, JL and Allen, NS. The degradation of dyed cotton fabrics by the sensitised production of singlet oxygen via an aqueous soluble phthalocyanine dye. *Dyes and Pigments*, 2002, 53, 195-217.
- [176] Li, J; Ma, W; Huang, Y; Tao, X; Zhao, J and Xu, Y. Oxidative degradation of organic pollutants utilizing molecular oxygen and visible light over a supported catalyst of Fe(bpy)₃²⁺ in water, *Applied Catalysis B. Environmental*. 2004, 48, 17-24.
- [177] Filippone, F; Mattioli, G and Bonapasta, AA. Reaction intermediates and pathways in the photoreduction of oxygen molecules at the (1 0 1) TiO₂ (anatase) surface. *Catalysis Today*, 2007, 129, 169-176.
- [178] Qamar, M; Saquib, M and Muneer, M. Titanium dioxide mediated photocatalytic degradation of two selected azo dye derivatives, chrysoidine R and acid red 29 (chromotrope 2R), in aqueous suspensions, *Desalination*, 2005, 186, 255-271.

Chapter 10

**FIRST STEPS TO A DEDUCTIVE CLASSIFICATION
SYSTEM OF COLORANTS FROM THE POINT
OF VIEW OF STRUCTURAL CHEMISTRY***

G. Lincke

Niederrhein University of Applied Sciences, Dept. of Chemistry,
Adlerstrasse 32, D-47798 Krefeld, Germany

Dedicated to my wife

ABSTRACT

Beginning with well known building blocks and putting them together by using noncovalent bonds of the type 1) intermolecular H-bonds and 2) intramolecular $\pi\cdots\pi$ -bonds and 3) inorganic metal-complexes, the deductive classification system of colorants is derived. The building blocks are called 1) 'chromogens' and 2) 'tetrahedral' respectively 'octahedral' metal-complexes.

There are three 'classes' of colorants: 1) 0.4 nm structures, 2) sheets structures, 3) 3-dimensional networks.

The dichotomy soluble-insoluble is due to quality and number of bonds between the building blocks, forming the crystal lattices of colorants. A view on their entirety and characteristics is opened.

This paper makes use of the stack principle of organic molecules of dyestuffs in order to create the deductive classification system of colorants. Important but nevertheless in the second position in the order of rank are solubility/insolubility, stability, counteractions of light with colorants (absorption/reflexion). The author hopes for intriguing queries by colour chemists.

a) * Revised and extended version of a lecture "Organic crystals with $\pi\cdots\pi$ -intrastack forces ("0,4 nm structures". Part 2, "A new Classification System of Colorants", held on 16th of January 2004 in Optiva Inc., Musskaya pl. 1, Moscow (Russia).

The author is of the opinion that the deductive classification of colorants points to an axiomatic wording. Perhaps therefore colorants become more understandable and interesting for students of chemistry?

Keywords: Colorants; classification system; building blocks; one-,two- and threedimensional networks

‘With this you have started a novel classification system on pigments. Sorry, I can’t take your paper into consideration for my monograph ‘Color Chemistry’.¹

*The longest way starts with a first step.
Konfuzius (551-479 v. Chr.)*

1. PREFACE

Always classification comes after experimental results and therefore it is the fundament of scientific endeavours. Many times colorants (colorant materials) have been arranged.

To set the scene studying good textbooks of the last decades referring to inorganic and organic chemistry onto specialist terms as “dyestuff” and “pigment” is charming.

Textbooks are *interlocutors*, because they codify the knowledge of their time and therefore they are very informative. The author has studied nine textbooks of organic chemistry, written between 1950 and 2003. The result:

Fieser 1950 [1,I]; Karrer 1963 [1,II]; Klages 1967 [1,III]; Christen + Vögtle (1989) [1,IV]; Beyer + Walter (1991) [1, V]. The textbooks [I-V] are old fashioned and deal with dyestuffs at some length. However, from 1980 on textbooks take up new features and do not pay much attention to dyestuffs [VI -X].

The state-of-the-art and best book comes from H. Zollinger [2] . In every respect it is worth reading and a future pointing monograph. Professional chemists look for monographs like [2] or [3]. They arrange to different aspects of colorants. Usually dyes and pigments are treated well in textbooks and/or monographs [2], [3] with introducing syntheses. That is undoubtedly necessary and correct.

Schulze’s “Farbentabellen” [4] are predecessors of the most authoritative leading and voluminous work in the field of colorant classification, the ‘Colour Index’ [5]. It is earmarked only for specialists but is the comprehensive compendium of all colorants.

The index forms to 1) hues; 2) chemical constitution, 3) generic names; 4) solubility; 5) syntheses; 6) organic or inorganic origin; 7) application and dyeing techniques; 8) trade names; 9) patents and others. Already this enumeration catches a glimpse on this collection [5].

b) ¹ Answer to the author’s off-print [D&P, 59 (2003), p. 1-24] written by H. Zollinger, prof. emer. ETH Zürich (08.09.03). Original Swiss German: “Vielen Dank für Ihren Sonderdruck. Sie haben damit ein neuartiges Klassifizierungssystem auf Pigmente begonnen. Leider kann ich Ihre Arbeit für mein neues Buch “Color Chemistry” nicht mehr berücksichtigen. Es ist jetzt in den Händen der Druckerei und ich werde es erst nach Druck und Buchbinderei wieder sehen“.

Up till now the entirety of inorganic pigments never had been a subject in inorganic textbooks. Therefore the inorganic counterpart to Herbst/Hunger [3] is written by Buxbaum [6].

The author of this work makes a strong plea for reading J. Shore's "Classification and general properties of colorants", chapter 1 in [7]. Shore outlines many items of colorants classification systems. [2], [3], [6] and [7] compile the knowledge of our time.

Might be correlated organic and inorganic pigments?

- A simple and practical answer give standards like DIN 55944 [8]. This standard gives a *short* survey of colorants. Together with DIN 55943 it introduces immediately into the technical world of colorants. The author draws the reader's attention to the recent editions DIN 55943, 2001-10 and DIN 55944, edition 2003-11, [8]. DIN 55944 classifies colorants *according to coloristic and chemical aspects*. Standards are dedicated right straight for the use of industrial personnel and introduces immediately into the technical world of colorants. They are used for definition of terms, are enumerating, describing and amazingly complete. Without a doubt standards of DIN are important, however, sometimes rather general. DIN 55944 (european norm) specifies 'colorants' as general term with respect to colouring materials. This standard defines dyes as 'soluble' and pigments as 'insoluble' in the application medium.
- Another answer gives Erk: "Although there are some fundamental differences between organic and inorganic pigments which originate from the different bonding situations in the solids, many of the principles outlined here for organic pigments may be applied to inorganic pigments as well" [9].
- A further answer gives the author of this paper, which is interested in the precise meaning of the dichotomy soluble/insoluble in context with colorants. He destines the target by studying their transitions and trying to find correlations with structural chemistry. By introducing the term "building block" [~ building unit] the author of this paper evades tedious discussions between *different bonding situations in the solids*, Erk [9]. The author's 'building blocks' are closely connected with the colorants according to chemical aspects (DIN 55944).

The author classifies the entirety of colorants by introduction of building units (molecules/ions) and the

- *intermolecular (non-covalent) bonds*
- dichotomy soluble/insoluble
- the connections of building units to one-, two- and three-dimensional entities
- size of colorant
- thermal stability.

Every chemist knows the connection of monomers to plastics and man-made fibres as a general principle and about the correlation of cross-linking and solubility. Kind and density of the networking at the same time is the crucial point and is a valid one for inorganic pigments

too. Networking of chemical building blocks (units) is the basic topic of the structural chemistry and their connection reveals bonding rules of solid states.

Some experts will ask for the application and importance of Kitaigorodskii's epoch-making theory (bump-in-hollow-principle) of organic molecules within this classification [10]. Kitaigorodskii's theory however, is complemented by the chloro-rule of G.M.J.Schmidt, see the summary in Desiraju's monograph: [11, p.179-194] "The chloro group may therefore easily identified as a good *steering group* in crystal engineering", [11 p.192] and soon after Desiraju enlarges on to all hetero atoms: "These effects are not specific to sulfur and suggests that all hetero atoms are important in determining 4-Ang. structures of planar aromatics" [11, p. 216]. The early papers of Desiraju (1984-1986) [12, p. 99], [13, p. 160] and [14, p. 222] applicate the chloro-rule of G.M.J.Schmidt.

The publication presented here begins very consciously with finished molecules/complexes, the above mentioned building blocks (units). They crystallise to lager molecule associations [15] or infinite complexes [16], [17]. The author draws the attention to one- two- or three dimensional network architecture with building blocks, an usual procedure with crystal engineering. From this point of view common characteristics and boundaries of colorants emerge. They are the topic of this publication. The common grounds contain also inorganic pigments whose building blocks are introduced as metal-complexes. The studies of the stability of inorganic crystals formed by coordination polyhedrons, s. Pauling [16] and [17] are exemplary.

The herewith submitted publication is restricted to organic $\pi\cdots\pi$ - intrastack bonds, intermolecular H-bonds and ionic-covalent bonds (metal complexes). Up to now the entirety of "colorants" (dyes, pigments) has not been arranged with regard to networking. Indeed the chemist knows inorganic pigments (carbon black, iron oxide, chromium oxide, titanium oxide and other ones). However, for colouring paints, plastics and building materials they lead an individual existence in the field of the inorganic chemistry. Evaluating organic pigments under the view of crystalline character is a field for specialists still today, almost unknown, however. But also the opposite, seeing dyes as a borderline case of crystalline colorants, seems to be absurd.

This is due to the unusually broadly scattered application fields of colorants. Finally it has to be reminded of that pigments are in some respect an unknown technical field (printing inks, enamels, paints, pickles, plastic, fibres). They exist in a technological niche. So phthalocyanine blue is an important example of a pigment, which is an "insoluble" dye. The author designated this as 'road signs blue'. The unsolubility of phthalocyanine blue and the kind of its application are known only to specialists, although chemists nevertheless are working continuously at the change of soluble to insoluble and vice versa. That is valid from the lab up to application technique and production.

The relation soluble-insoluble is the breath of chemistry.

The several application techniques of dyestuffs and pigments (fibres, paint printing ink etc.) are using the basic difference of insoluble pigment to soluble dye. From the viewpoint of university chemists they have the odour of crafts, trade, small industry, technique and shift into low wage countries.

2. INTRODUCTION

In this contribution the author attempts to present a deductive survey of all "colorants" from the viewpoint of *structure chemistry*. Chemists will recognize fast formal similarities to plastics. However, with plastics dominates the covalent bonds between the molecular building blocks. For their deductive arrangement colorants require the principle of bonds between building blocks of ionic, metal-complex like or non-covalent kind. Those ones are in the first place intermolecular H-bridges and intramolecular $\pi\dots\pi$ - stacks. Furthermore the essential groups "dyes", "organic pigments" and "inorganic pigments" must remain recognizable and their common basis becomes understandable.

Anyway, it is a deductive representation anyway possible? Fortunately "dye-chromonics" [18] have become known since 2000 as state-of-the-art "dyes" [19]. They are important as liquid crystals(!) in the field of modern π -functional dyes. According to the opinion of the author they fill exactly the gap between dyes and pigments.

3. DYES

One is astonished again and again as the molecular thinking dominates strongly at chemists. Beyond doubt the success of the textile dyes, which stood at the evolution of the chemical industry, is responsible for that. The dye industry synthesized new molecules (chromogens) continuously and successful, see Zollinger [2] and Herbst/Unger [3]. That led to an abundance of various dyestuffs, having a muddling effect on external chemists (and students).

Among technical knowledge the chemistry of *soluble* molecules suffices for dyeing.

For the author's point of view that seems to be an essential cause for understanding the 3-dimensional arrangement of organic molecules in the field of pigments as a special subject. The chemistry of dyes has developed advanced colouring procedures and has come to reliable findings since 150 years.

Every colour chemist knows about dye aggregate in the dyeing bath [2, p. 379, 386, 406] and [20]. Also herringbone structures [18, 19] or T-structures may be formed in this moment [11]. Both are allied and point at liquid crystals.

The following items indicate the start of crystallization of vat dyestuffs in the fibre:

- Even around 1970 Kratky had been able experimentally by X-ray small angle scattering to prove the agglomeration as "stacks" of up to four dye molecules in the firm cellulose fibre [21, 22].
- Zollinger [2, p. 417] argues in a similar way: "dyes are usually present as single molecules or small clusters". Zollinger also evaluates the relation vat dyestuff to pigment [2, p. 313]: "because of their low solubility in organic solvents and in water, vat dyes are natural candidates for pigments".
- Zollinger writes about vat dyestuffs: "Vat dyes, for instance, even become pigments after their application" [2, p. 2]. One can turn round the last two sentences: The ability of the molecules of vat dyestuffs for the formation of $\pi\dots\pi$ -intramolecular

stacks is not only an essential condition for the formation of crystals of carbonyl pigments, but also for the formation of molecule piles in the fibre.

In the scientific literature many items to this subject are found, e.g. [23-32]. The author recommends the review [20] with excellent references to dye structure and aggregation of textile dyestuffs. The results were obtained by using microscopy, x-rays and spectra. Especially many vat dyes crystallize after absorption onto the fibre as a result of post-treatment [25-28].

Furthermore papers point to the direction of crystallization [26-28]. Sumner et al. [26, p. 186, fig. 3 B] wrote "the molecules are then free to migrate and combine with one another to form crystals. Vat dye crystals are usually needle-shaped, and (...) the molecules are arranged across the length of the needles". Wegmann [28] points out changes in hue in the case of vat dyes in fabric caused by soaping. This results in clearer hues and often in improvements in fastness.

But also advices for the textile industry are helpful, for example the BASF brochure [30]. It is written from the chemical aspect and uses the term "aggregation", that is the polydisperse state, up to the re-oxidation of leuco vat dyes. Only in connection with soaping the terms 'crystals' and 'crystallizing' are introduced. Crystallization is presented as a result of soaping and therefore taken as a cause of the improved fastnesses (wet fastness, chlorine fastness, light fastness). Stack formation is not mentioned anywhere.

Associations of dyes forming crystals are mentioned in [31, p.148]: "Dimers are probably formed first and these grow by addition of further molecules to give lamellar micelles in which the dye molecules are stacked up like cards in a pack".

And "The changes which take place during soaping are essentially those of crystallisation of the vat dye into a more stable crystal habit" [31, p.514]. Already the pioneering monograph of Vickerstaff is to be mentioned [32]. From a contemporary point of view (2002) the mechanism to explain what happens during soaping, see [7, vol. 2, p. 909].

The author is of the opinion that stack formation of vat dyestuffs has to be accepted as the final state of soaping because this is the common feature of *all* pigments (pile rule) [33]: In the cellulose, fibres are arranged as tiny stacks of vat dyestuff molecules, due to the energetically promoting step of *intramolecular* $\pi \dots \pi$ forces.

Which function do those carbonyl groups now have jutting out from the piles at the side? Two diffusion models for dyes in fibres, the pore model and the free-volume model, both developed by dye chemists, give the answer. If we follow the summary explanations of Zollinger [2], p. 403, p. 404, fig.11.8], best suitable will be the "pore model" for cellulose and the "free-volume model" for polyesters.

Obviously the carbonyl group works at cellulose fibres (pores) about intermolecular H-bridges of the type dye-unit-C=O ... HO-Cellulose. In the pores piles take over the function of struts then, which means, pores filled with water are penetrated with piles of vat dyestuffs. Instead of the intermolecular H-bridges of the type

dye-unit-C=O ... HO-cellulose then such of the type
dye-unit-C=O ... H₂O ... HO-cellulose

have to be assumed.

The dyeing process with vat dyestuffs about all steps of operation is absolutely understood. With respect to chemical-physics stack formation (crystallization) could make understandable the fourth operation step "soaping". Too strong soaping leads to a lack of rub resistance [30, p. 30]. The interpretation by stack formation is: When too large "stacks" arise, they are not anymore optimally adjusted to the pore diameter of the fibres (intermolecular H-bonds). Using tissues demands not only flexible fibres, but also flexible stacks, for example in the area of knees, at pressure points, seams. Covalent bonds are rather inflexible (with regard to distance and angle), non-covalent bonds ($\pi \dots \pi$ - intrastack- and H-bonds) are by far more mobile (with regard to distance and angle).

Might small stacks be nuclei of "liquid crystals"?

Berndt mentions the difficulty of re-vatting after soaping [30, p. 30]. In the course of the publication presented one can say: Soaping of vat dyestuffs forms molecule stacks, positions them in the fibre and leads to a lower energy state.

Soaping as a crystallization process and stabilization of vat dyestuffs at cellulose surface becomes understandable as a synergistic effect (cooperation) of two non-covalent bonds.

Clusters may be also T-structures [11], [18], [19]. Everyone chemically trained can recognize post-treatment with soap and water at 100°C between 30 s and 60 min as a suspicious operation for dyes. The dye molecules could transform from the T- over herringbone- to the most stable stack-structure while soaping. Dye manufacturer and dye consumer depend on each other by industrial type-precise dyeing. For that the statements [34] are important.

It is essential to the author to point out at the stable *final state* of dye molecules (fastnesses) in the fabric.

The next step on the way to stacks is the expanded crystallization of dye molecules to large piles. In the first place the molecules aggregate with themselves to "supramolecules". These are called lyotropic liquid crystals (LLC). Already Edwards et al. include some remarks on key physical steps associated with textile dyeing [18, p. 103 – 104]. They have opened completely new industrial perspectives, see chapter 5 "Dye-chromonics". Because already dyes of the type of pseudoisocyanines belong to the "dye-chromonics" (see there), also aggregation of other dyes (s. azoic dyes, [2, p. 200-202] is probable.

Further and important are 'solvent dyes' and 'disperse dyes', the first ones are insoluble in water, but soluble in organic solvents [34], the second ones are almost but not completely insoluble in water, [2, p. 195]. Both are 'non-ionic dyestuffs' and solvent dyes are often classified under pigments as well as dyes.

What think chemists about the formation of stacks in the course of their application? Experiments and evaluations should be seen with respect to this view point, especially the free-volume model [2], p. 403]. Do adopt dyeings of polyester fibres with disperse dyes, 'molecular stacks' and are these the start (begin) of 'recrystallisation' ? What is about the comment of Zollinger: "in recent years, it was found, that combinations of two or more disperse dyes gives rise to higher dyeing rates on polyester as compared to individual dyeings. In the best of our knowledge, this phenomenon has not been investigated scientifically" [2, p. 403]. Are stack formed by molecules of two or more distinct disperse dyes?

Both, anionic and cationic (basic) dyestuffs forms stacks, [35, 36, 37-40].

4. CLASSICAL ORGANIC PIGMENTS, (COP'S)

In the course of the deductive classification of colorants the non-covalent bonds must be emphasized.

In the shadow of previous dye research Pararot (in 1885) was synthesized as the oldest organic pigments, just like CI pigment Red 49:1, (1899), mentioned above. Then Hansa Yellow (in 1909) and Toluidine Red followed, see [4]. All these molecules form 'stacks' with the aromatic (flat) part (pile rule) [33]. At the same time they form the typical distance of ~ 0.35 - 0.42 nm, named also '0.4 nm-structures' by Desiraju [2, p. 160-162, 212-222].

Therefore the " $\pi \dots \pi$ - intramolecular stack"-principle of structure is clear and responsible also for the *technological* properties. $\pi \dots \pi$ - intrastack forces are decisive for stability, however obviously limited by classical organic pigments. At times of the syntheses of Hansa Yellow and Toluidine Red only few application technicians knew the industrial use of the pigments, i.e. unsolubility, recognized it as important. Questions about the cause of the unsolubility, crystallization and 3-dimensional structure were without technical importance and therefore uninteresting. Soluble dyes dominated thinking and action, for example with A. v. Baeyer's indigo synthesis. After that resonance questions of *single dye molecules* came to the fore on the part of basic research.

The fact that two qualified crystallographic researchers during the discussion of crystal structures of important pigments disregarded the existence of $\pi \dots \pi$ - intrastack forces is until today designating for the small interest in the causes to unsolubility of organic pigments.

In this contribution the relationship between structure and unsolubility is placed in the foreground and is the arranging principle of the classification system. A new chromogen (unit, building block) has similarity with a new material permitting to build novel houses. In fig. 2 of the publication [33, p.6] pigment properties are compared with distinct masonries. An addition explanation could give the comparison between houses with pigment crystals: Modern technical evolutions make higher demands on both.

In order to meet these demands, unsolubility had to be increased for example already in the time from 1910. Larger molecules of the BON type (*betaoxynaphthoic acid-anilide*) and disazocondensation pigments (in 1955) were synthesized, see [33, fig.1, p.5]. Also Zollinger mentions in his monograph, that "azoic colorants and pigments can be regarded as a borderline case of dyes and pigments" [2, p.201]. Thus vat dyestuffs became an interesting source for carbonyl pigments [4, p. 313]. The preceding quotations show the narrow gearing of dyes and pigments.

The chromogens mentioned are construction principle for characteristic groups of pigment classes. *Pigment chemistry in the origin sense is architecture with molecules*, and the destination is a 'building', is the (pigment)-crystal.

5. DYE-CHROMONICS, (LLC'S)

A modern survey for the term "chromonics" is given in [19]. Accordingly "chromonics" are known also as medicines (drugs) and are not only limited to dyes. However, only these are of interest in this chapter, which is called therefore dye-chromonics. Speaking in modern terms they are called lyotropic liquid crystals, LLC's.

The earliest experimental investigation goes back to Scheibe [37]. In [37] also indications of preceding literature are contained. Hoppe's publications [38], [39] are of interest likewise. Early as Scheibe Jelley recognized the pseudisocyanine dyes as 'polymers' [40]. Modern speaking $\pi\cdots\pi$ - *intrastack* forces between the flat dye molecules and with it self-aggregation to supramolecular piles (stacks) are the uniform building principle for "dye-chromonics". This increases the *viscosity* of aggregated dyes and causes the name "polymer". However, the "dye-chromonics" have nothing common with polymeric plastics. Scheibe-polymers were the first "chromonics" in modern sense. Their technical importance for sensitization of silver chloride emulsions of photographic films was recognized fast.

Chemically speaking "dye-chromonics" are polyaromatics, which are related to carbonyl dyes and with them to vat dyestuffs. They are attaining industrial importance in coating of glass or plastics by nanofilm crystallisation. These coated substrates (glass or plastic) are suitable for the production of "polarizers", "retarders" and liquid crystal display cells. The first commercial application of this new material technology is creating optical films for the flat panel display market. Today "dye-chromonics" are investigated intensively [41-44]. Probably there are even further technical applications [44].

The chemical constitution of the single molecules (chromogens ~ building blocks) used successfully for polarizers and retarders are essential. Those ones are

- indanthroneblue (!) substituted with sulfonic acid, a sulfonation product of a dibenzimidazoles derivative of
 - a) perylenetetracarboxylic acid (cis and trans) and
 - b) naphthalinetetracarboxylic acid,
- 2,9-disulfonic trans-quinacridone [45].

The combination of hydrophilic and hydrophobic properties is characteristic for this type of the "dye-chromonics": *'With certain modification of hydrophilic-hydrophobic balance', are capable of self-assembly to large supramolecules that act as the major structural element'* [41, p.5]. Self-aggregation is observed also in thinned aqueous solution.

"Dye-chromonics" show a remarkable ability to $\pi\cdots\pi$ - *intrastack* forces, which form supramolecules. For other dyes $\pi\cdots\pi$ - *intrastack* forces may be subordinate perhaps, but they are the supporting scaffold for "dye-chromonics". Polarizers are produced by shearing an aqueous solution of the "dye-chromonics" (supramolecules) using a metal stick (Mayer wire-wound rod) being moved electronically over a glass or plastic substrate in a small distance in parallel. Now the "molecular stacks" (~ rods) have minimal shear-resistance by orientating parallel and in coating direction. The long rod structures align along the shear force direction in a wet layer. After water has evaporated, the layer of parallel supramolecules must be converted to a water insoluble form. Due to sulphonic acid groups, which protrude laterally from the side (edges) of every molecule in the "stack", this is done by immersion in a BaCl₂-solution, 15%, acting for 1-2 seconds. In this treatment Ba²⁺ -ions displace NH₄⁺-counter ions and cross-link sulfonic acid groups of parallel stacks. Therefore many Ba²⁺ -ions tighten mechanically the film [44, p.319]. The "dye-chromonics" are precipitated, (made insoluble) by Ba²⁺ -ions and remain in unchanged positions on the glass substrate. *That is 2-dimensional chemistry.* 1-dimensional $\pi\cdots\pi$ - "stacks" are vertically cross-linked by inorganic O ---Ba²⁺---

O-groups. The endless (infinite) 2-dimensional (flat) network is a chemically bonded by aromatic π -electrons and Barium²⁺-ions.

This chemical procedure reminds of the syntheses of toners. In order to make them insoluble dyes substituted with sulphonic acid groups are precipitated by Me²⁺-ions. Every chemist knows, that for this purpose particularly Ba²⁺-, Sr²⁺-, Ca²⁺-, Mn²⁺-ions are used [33, p.5]. This precipitation is designated also as a partial fitting of (or with) barium sulphate. Zollinger [2, p. 413] designates the Ba²⁺-ions in this connection as “counterions”. The procedure led to the production of an early azopigment. It was synthesized first by Julius: Lithol Red 1899, CI pigment Red R, 49:1, BASF/Ludwigshafen (Germany). See also chapter 4, ‘classical organic pigments’.

Syntheses of 2-dimensional molecular lattices with industrial-physical importance are left to the High Technology (nanotechnology) of our time. The Ba²⁺-crosslinked dye-chromonics can be understood easily as ‘pigments’ having expanded 2-dimensionally on a glass substrate. In the ideal case these are slices of single crystals, crystallographically seen. Since *two* chemical bonds (*periodic bond chain vectors*, that is PBC-vectors) are effective in the crystal plane, F-faces are possible and according to Hartman and Perdok these are morphologically most stable in the respective crystal [46]. The publication uses the expression “building blocks”.

“Dye-chromonics” molecules have large similarity to those of vat dyestuffs. “Dye-chromonics” aggregate (via $\pi\dots\pi$ - intrastack forces) with consequences for the technical use, and like this the same aggregation influences vat dyestuffs during dyeing (diffusion, soaping), see Zollinger [2, p. 288-302] or Berndt [30, p. 8-9].

However “dye-chromonics” do not have colour strength (tinctorial strength) in comparison with dyes and pigments. However, they show properties of π -functional dyes, see 10 (*conclusion*).

6. HIGH PERFORMANCE PIGMENTS (HPP'S)

The author has compiled all published organic crystal lattices of pigments up to the year 2000 in [33]. In this enumeration high performance pigments play an essential role.

The principle of stack-formation is a major aspect again. At the same time every pile from molecule to molecule (intermolecular) is occupied by lateral NH- and CO-groups a million times. These get in touch with neighbouring piles about intermolecular H-bridges in the sense of the formation of –NH...OC- groups. Many millions of piles, parallel to each other, form sheets from molecules through cross-linking. The building principle resembles that of Ba²⁺-crosslinked “dye-chromonics”. Quinacridones [47], Diketopyrrolopyrroles (DPP's) [48b], Benzimidazolones [48a] and Thiazines [48c] have a reputation for these sheet structures.

With reference to Quinacridones, Lincke proposed a 2-dimensional mesomeric structure within crystal lattice in order to interpret their extremely increased stability [49].

Phthalocyanine pigments are characterized by $\pi\dots\pi$ - intrastack bonds, the Cu-containing grades additionally by {CuN₆}-octahedrons. They are $\pi\dots\pi$ - intrastack/ metal-complexes [33, p. 13].

7. CARBON BLACKS

Carbon blacks are typical HPP-pigments, assembled in “*stacks of sheets*”. Speaking in the terms of this paper, the cores of benzene are the “building blocks” of the sheets. However, as each chemist knows, they are of excellent stability by ‘*intrasheet*’ (covalent) $\pi\cdots\pi$ -conjugation. They are precursors of today’s supramolecules. The position of carbon blacks in tab.1 is exactly the borderline of HPP’s and CICP’s. Carbon blacks are children of graphite and this is a typical F-face substance. Strictly speaking, carbon blacks are half organic and half inorganic pigments, i.e. they are transitions from organic to inorganic pigments. The “scope of 0.4 nm – structures” includes carbon blacks [50].

8. EFFECT PIGMENTS

Bronzes are an old group of inorganic pigments, produced of aluminum and/or copper metal, s. Pfaff [48e]. By crushing and sizing of above metals bronzes become the desired thin metal flakes, i.e. pigments. One can understand bronzes as ‘2-dimensional’ metals’. “Building blocks” are metallic Al and/or Cu/Zn. The metal atoms (spheres) are closely packed in layers (111). Bronzes are essential raw material for metallic coatings.

Modern effect pigments (pearlescent or interference pigments) interfere with visible light. For this purpose flat platelets or sheets of aluminium oxide (Al_2O_3) or mica or titanium dioxide (TiO_2) or silica (SiO_2) are selected or synthesized by inorganic preparative chemistry and covered with one or several thin layers of other inorganic oxides (inorganic complexes).

Building blocks are inorganic coordination polyhedrons of the types $\{\text{SiO}_4\}$, $\{\text{TiO}_6\}$, $\{\text{FeO}_6\}$ and $\{\text{AlO}_6\}$. After all, effect pigments use the flat-face principle [46]. These are examples of 2-dimensional preparative inorganic chemistry in industrial scale. The author takes the production of 2-dimensional crystals (pigments) as HighChem Syntheses. The here mentioned coordination polyhedrons are used too in [48e].

For effect pigments and “sheets” weak cohesion (easy cleavability) between the flakes is necessary.

9. COMPLEX INORGANIC COLOUR PIGMENTS (CICP)²

In the field the colorants, 2-dimensional connections of coordination polyhedrons to ‘effect pigments’ (s. chapter 8) are exceptions. 3-dimensional connection is the rule and pronounced subject of inorganic structural chemistry. CICPs consist of close densely packed spheres of oxygen and the more electropositive ions, which are nearly all smaller than oxygen, are found in the interstices between the close-packed oxygen ions, see for example [48d]. Due to the electronic charges of coordination polyhedrons, their bonds are shared 3-dimensionally. Especially, if strong $\text{O}\cdots\text{Me}\cdots\text{O}$ bonds are acting between the sequence of close-packed layers, these result in very stable crystals. However, the layers of close densely

c) ² The abbreviation ‘CICP’ is not in accord to DIN. However, the interested reader is referred to the term ‘CIC’ in DIN 55943:2001-10, p. 6

packed oxygen- and metal ions are not “sheets”. *Every CICP consists of sequences of such layers of atoms, ions or complex ions.* This is the basis of the crystallography. [48d, p. 43] shows two illustrations of TiO₂-rutile and [48d, p. 44] of spinel. One can see clearly the layers of the closed packed ions.

Connecting metal complexes of the type {MeO₆}, {MeO₄} or {MeS₄} 3-dimensionally, so particularly oxide complex bonds {MeO₆}/{MeO₄} achieve highest stability.

Additionally, some sulphide complexes have to be mentioned. Characteristic S...Me...S-bonds are the cause of maximum stability. Besides some of them are brought to a given particle size and -form by burning in presence of salts. Frequently spherical shape is approximated. That's why the particle diameter of TiO₂-pigments is synchronized with the exact wavelength of the visible light and their frequency distribution corresponds to the global solar radiation [51]

CONCLUSION

Table 1 summarizes the colorants in 7 rows:

- 1) From tiny dye stacks (row 1, chapter 3),
- 2) over $\pi\cdots\pi$ - stacks, comprising millions of molecules, however still weak (row 2, chapter 4),
- 3) over strong $\pi\cdots\pi$ - stacks comprising millions, Ba²⁺- cross-linked (row 3, chapter 5),
- 4) to strong $\pi\cdots\pi$ - stacks comprising millions, with lateral networking through intermolecular H-bridges (sheet structures) (row 4, chapter 6),
- 5) to carbon blacks, known to every chemist, (sheet structures) (row 5, chapter 7),
- 6) to effect pigments (inorganic sheet structures) (row 6, chapter 8).
- 7) Finally the 3-dimensional networking to oxide pigments is a qualitative jump and necessary for understanding highest stability (row 7, chapter 9).

Line 'class' arranges the colorants according to the aspects “stack” (1-dimensional), “sheet” (~ F-face; 2-dimensional) and/or “sphere” (3-dimensional). Summing up, one is able to remark an overlap of the groups (1) to (7).

All other lines are self-explanatory.

The characteristics of fabrics are the confusing amounts of dyes, fibres and dyeing techniques. These led to the development of a very special, technical language. The same refers in an adapted manner to porcelain, ceramics, enamels as well as lacquers and printing inks. Coloration of varied objects (substrates) with different basic (primary) materials seem to be insuperable barriers between differing technical fields. The employees of producers and suppliers have their own technical languages. The "high performance final products" demand for skilled people, which have developed a skilled language in the course of time, fitting exactly to their products.

Additionally, the differences between colorants in the fields (1) to (7) are controlled by the substrates 'clothes' and other ones like 'paper', 'car bodies', 'cans', 'furniture', 'tableware' or mass pigmented pieces of 'plastics' or 'man-made fibres'. However, the author supposes, that

substrates like glass/plastic for 'dye-chromonics', at least, create a functional unit with 'dye-chromonics', a sandwich-structure. Keyword: adhesion/cohesion.

The author wants to draw the reader's attention to typical drawbacks of dyes and pigments, see tab.1. Strictly speaking they are characteristics of non-covalent bonds of all colorants:

- Dyestuffs tend to agglomerate in the dyeing bath.
- Dispersing of organic and inorganic pigments is always difficult. However, the most stable organic pigments like phthalocyanines, quinacridones, peryleneimides etc. are *bad* with respect to their dispersibility.
- Organic pigments/inorganic pigments tend to absorb many additives and solvents from the liquidly medium (in preparations).
- After some weeks or months pigments in many liquid lacquers tend to settle down or to form sediments at the bottom of the can. In order to avoid these drawbacks, technicians are engaged in it and therefore working steadily.
- Perhaps, there is a further drawback with non-covalent bonds and "dye-chromonics". Seed growth defects in crystalline structure tend to destroy the crystal long range order.

Readers searching for threedimensional figures, which demonstrate connectivities between colorants, shall have a special look at the papers [33, 47, 49].

11. SUMMARY

Strictly speaking "dye-chromonics" do not appertain to "colorants", since they do not have any coloring strength, but they perform their function as coloring substances under influence of electric current on substrates (glass/plastic) of flat panel displays. Furthermore inorganic oxides within the coated interior of monitors are not colorants either.

Already the monograph of Zollinger [4] exceeds the field of dyes,

- the boundaries between dyes and pigments are emphasized as leaky and
- in several chapters " π -functional systems" [2, p. 3, 13, 429ff] are stressed,
- for example dichroitic dyes for liquid-crystal displays [2, p. 522- 526].

Therefore, at the end of this classification system the previous definition of colorants by Zollinger [2, p.1] is:

"An even more important criterion is the following: colorants are either *dyes* or *pigments*", which might be expanded by: "Up to 1990 colorants had been either dyes or pigments. Soon after 1990 liquid crystals (thermotropic or lyotropic) became bridges between dyes and pigments and they point also to biologically important colorants like hemin, chlorophyll and others.

Modern colorants include functional π -electron systems".

"Dye-chromonics" are bridges - also for understanding - between dyes and organic pigments. They appertain already more to the π -functional systems.

Desiraju writes with respect to “Chemistry – The middle kingdom” [52]: “ Much of this chemistry was built with concepts and models like electronegativity/electropositivity, oxidation/reduction, hardness/softness, enthalpy/entropy, kinetics/thermodynamics, reactivity/selectivity, electrophilicity/nucleophilicity and chirality/achirality”. And some sentences below: ” Chemistry is oceanic with respect to factual information, but it has always been contained with respect to the number of concepts and models that were required to understand all these facts”.

The author of this paper concludes:

All the colorants are small in comparison with the whole of material sciences. Therefore *technological* dichotomies like ‘soluble/insoluble’, ‘stability/instability’, ‘cheap/expensive’, ‘toxic/ nontoxic’ are of decisive practical importance and at the very core of our life.

CONCLUDING REMARKS

Only few datas across the whole of colorants are compiled (summarized) in table 1. Apparently there are *intermolecular* contacts with influences the crystal structure of organic molecules, i.e. ‘steering groups’ or pi...pi-charge-transfer forces. The range ‘soluble-insoluble’ corresponds with the wealth of dyeing techniques and mass colorations (mutual correspondence).

In our life there are many dichotomies ,soluble’ and ,insoluble’, however, application of colorants is the most aesthetical one. This will be confirmed by famous great painters like Hokusai:

Someone interested in the the life of the Japanese illustrator and printmaker Hokusai may study Francois Places’ tale “The old man mad about drawing”. The tale ends with:

“From the age of six I started drawing all sorts of things. At fifty I had already drawn a great deal, but nothing that I did before my seventieth year was worth any great note. It was at seventy-three that I began to understand the true shape of animals, insects, and fishes, and the nature of plants and trees.

Therefore, at eighty-six I will have made more and more progress, and at ninety I shall have penetrated even further into the essence of art. At a hundred I will certainly have reached a marvelous stage, and at a hundred and ten each dot and each of my drawings will have a life of its own. I would like to ask those who survive me to ascertain whether I have not spoken without reason”.

Table 1. Classification of Colorants from the view of structural chemistry (building blocks)

Chemical starting products selectively and variably synthesised to intermediate products and these to chromogens or to selected metal oxides/sulfides								
only a few become a member of					C Graphite	Al, Cu, Fe	{SiO ₄ }, {TiO ₆ }, {FeO ₆ }	{MeO ₆ }, {MeO ₄ }, {MeS ₄ }
	(1)	(2)	(3)	(4)	(5)	(6)		(7)
Colorant	Dyestuff	classical organic pigment (COP)	dyestuff-chromonic (LLC)	High performance pigment (HPP)	Carbon black	bronze, flakes, metallic pigments	pearlescent pigments	Complex inorganic color pigment (CICP)
Bond type	π...π- intrastack + laterally connected bonds by				Intrasheet covalent π-bonds	metallic bonds	silicate and metaloxide complexes	Metal oxide/sulfide complexes
	dyebath + pores of tissue	furthermore van der Waals bonds	Ba ²⁺ - ions	Interstack H-bonds				
Size of colorant	single mol. or tiny stacks	stacks of hundreds of molecules			sheets one on the other	~ 1000 layers (sheets, platelets) of atoms or inorganic complexes		exact adjustment of particle size
Correlation colorant/substrate	dyestuffs in pores of tissue	COP in resins	selfaggregation on substrate + Ba ²⁺ - ions	HPP + plastic, resin, fibres	carbon black in resin	metal oxides, coated sheets of mica, titanium dioxide, hematite		CICP + resin, plastic, plaster, mortar, ceramic
Class	← scope of (1-dimens.) 0.4 nm structures →					× × × × × ×		3-dim. Networks (spheres)
	× × × × ×			← scope of (2-dimens.) F-faces →				
Thermal stability (°C)	~ 120	~ 150	~ 240	~ 400	~ 800	different		~ 1300

REFERENCES

- [1] I) L. Fieser + M. Fieser, D.C. Heath and Company Boston (1950), Organic Chemistry; II) P. Karrer, Lehrbuch der organischen Chemie, G.Thieme, Stuttgart (1963), 14th edition; III) F. Klages, Walther de Gruyter Berlin (1967), Lehrbuch der Organischen Chemie, Bd. III (Sondergebiete); IV) H.R. Christen + F. Vögtle, Salle + Sauerländer, Aarau und Frankfurt/M (1990), Organische Chemie, Bd. II V) H. Beyer + W. Walter, Lehrbuch der Organischen Chemie, S. Hirzel Stuttgart 1991 VI) N.L. Allinger et al., Walther de Gruyter Berlin (1980), Organic Chemistry; VII) R. T. Morrison and R. N. Boyd, Textbook of Organic Chemistry, VCh-Weinheim (1986); VIII) A. Streitwieser + C.H. Heathcook, Organic Chemistry VCH-Weinheim (1986); IX) M.A. Fox + J.K. Whitesell Organische Chemie, Spektrum Akademischer Verlag Heidelberg (1995) X) K.P.C. Vollhardt + N.E. Schore, Organic Chemistry, W.H.Freeman and Co, New York (2003), 4th edition
- [2] H. Zollinger, *Color Chemistry*, Wiley-VCh, Zürich-Weinheim, 3rd edition 2003.
- [3] W. Herbst, K. Hunger, *Industrial Organic Pigments*, Wiley-VCh, Weinheim, (1999).
- [4] G. Schultz, Farbentabellen, *Akademische Verlagsges.*, Leipzig, 7th edition (1934).
- [5] Color Index, 3rd edn., vols. 1-4, Society of Dyers and Colorists, Bradford, and American Association of Textile Chemists and Colorists, *Research Triangle Park*, NC, 1971-1997.
- [6] G. Buxbaum (ed.), *Industrial Inorganic Pigments*, Wiley-VCh, Weinheim, Germany, 2nd edition 1998.
- [7] J. Shore (ed.), *Colorants and Auxiliaries*, Vol. 1 and Vol. 2, Society of Dyers and Colourists, Bradford (England), 2nd edition 2002.
- [8] Beuth-Verlag, *Berlin-Wien-Zürich, DIN 55943*, edition 2001-10 and DIN 55944, edition 2003-11. DIN-paperback 157, „Farbmittel 2“, p. 11-21 (199).
- [9] P. Erk, in “High Performance Pigments”, chapter 8, “*Crystal Design of High Performance Pigments*”, p. 104; ed.H.M. Smith, Wiley-VCh, Weinheim, Germany 2002.
- [10] AI Kitaigorodskii, *Molecular Crystals and Molecules*, Academic Press, New York (1973).
- [11] G.R. Desiraju, *Crystal Engineering: The Design of Organic Solids*. Elsevier (1989).
- [12] N.W. Thomas and G.R. Desiraju, *Chem. Phys. Lett.*, 110, (1984), p. 99.
- [13] J.A.R.P. Sarma and G.R.Desiraju, *Chem.Phys.Lett.*, 117 (1985), p. 160.
- [14] J.A.R.P. Sarma and G.R. Desiraju, *Acc.Chem.Res.* 19 (1986), p.222.
- [15] G.R. Desiraju, *Angew. Chem. Int.Ed. Engl.* 34 (1995), p.2311.
- [16] L. Pauling, *The Nature of the Chemical Bond*. Cornell University Press, 3rd ed. (1963).
- [17] A.F. Wells, *Structural Inorganic Chemistry*. Clarendon Press, Oxford (1975).
- [18] DJ Edwards, AP Ormerod, GJT Tiddy, AA Jaber, *A Mahendrasingham Advances in Color Chemistry Series*, Vol. 4, chapter 3, p.83, Eds. A.T. Peters and H.S. Freeman; Blackie Academics & Professional 1996.
- [19] J. Lydon, Chromonics, pp. 981, *Handbook of Liquid Crystals*, Vol. 2 B., Edt. Goodby, Freeman, Peters, Demus Wiley-VCH 1998.
- [20] J. Oakes, S. Dixon, *Rev.Prog.Col.* 34 (2004), p. 110-128.
- [21] Kratky, H Ledwinka, I Pilz, *Ber. Bunsenges. Phys. Chem.* 70 (1970) 12.

- [22] Kratky, *Röntgenkleinwinkelstreuung zur Erforschung von Faserfeinstrukturen: Austria: Universität Graz*, author's ed., (1972).
- [23] PB Bean, FM Rowe, *J.S.D.C.* 45 (1929) 67-77.
- [24] WT Astbury, JT Dawson, *J.S.D.C.* 54 (1938) 14-15.
- [25] EI Valko, *Am. Chem. Soc.* 63 (1941)1433.
- [26] HH Sumner, T Vickerstaff, E Waters, *J.S.D.C.* 69 (1953) 181-194.
- [27] JO Warwicker, *Jour. Textile Inst.* 49 (1958) T148-169.
- [28] J Wegmann, *J.S.D.C.* 76 (1960) 282.
- [29] H Bach, E Pfeil, W Philipp, W Reich, *Angew. Chem.* 75 (1963) 407.
- [30] J Berndt, *Grundlegende Erkenntnisse und praktische Erfahrungen beim Färben mit Küpenfarbstoffen: BASF/Ludwigshafen*, author's ed., (1960).
- [31] C H. Giles in A. Johnson (Ed.). *The theory of coloration of textiles, Society of Dyers and Colourists*, 2nd ed. Bradford (1989). Further references in [30] are pertinent.
- [32] T Vickerstaff. *The Physical Chemistry of Dyeing*, 2nd edn. Oliver and Boyd, London 1954, p. 68 and 291.
- [33] G Lincke, *Dyes and Pigments*, 59 (2003) 1.
- [34] P. Bamfield, *Chromic Phenomena* (2001) RSC, chapter 2.
- [35] Kobayashi M, Maeda Y, Okubo J, Tanizaki Y, *Jour. Soc. Dyers and Colour.* 1989, 105, 362.
- [36] Valdes-Aquilera, O. Neckers DC, *Acc. Chem. Res.* (1989), 22, p. 171-177.
- [37] G Scheibe, *Zeitschr. Elektrochem.*, 56, 723 (1952).
- [38] W Hoppe *Kolloid-Zeitschrift* 101 (1952) 300.
- [39] W Hoppe *Kolloid-Zeitschrift* 109 (1944) 21.
- [40] EE Jelley *Nature* 1937: 139 (1937) 631.
- [41] I Ignatov, P. Lazarev, V. Nazarov, N Ovchinnikova, M Paukshto, *SPIE's 47th Annual Meeting Seattle WA 2000: July 7-11*.
- [42] A Dembo, A Ionov, P Lazarev, A Manko, *Molecular Materials* 14 (2001) 225.
- [43] P Lazarev, K Lokshin, V Nazarov, *Molecular Materials* 14 (2001) 303.
- [44] Y Bobrov, L Fennel, P Lazarev, M Paukshto, S Remizov, *Journal of the SID*, 10/4, p. 317.
- [45] <http://www.cryscade.com/>
- [46] H Hartman, WG Perdok, *Acta Cryst.* 8 (1955) 49.
- [47] G Lincke, *Dyes and Pigments* 44 (2000) 101.
- [48] HM Smith, Ed. *High Performance Pigments*. Wiley-VCh 2002 Weinheim (Germany): a) HJ Metz, J Morgenroth, *Benzimidazolone Pigments and Related Structures*, p. 135; b) O Wallquist, *Diketopyrrolopyrrole Pigments*, p. 159, c) K Kaul, *Thiazines, Oxazines and other High-Performance Pigments*, p. 317 d) J White, *Complex Inorganic Color Pigments: An Overview*, p. 41, e) G Pfaff, *Special Effect Pigments*, p. 77.
- [49] G Lincke, *Dyes and Pigments*, 52 (2002) 169.
- [50] H Ferch, *PigmentrusseVincentz Verlag*, Hannover 1995, p. 22, 82.
- [51] HG Voelz, *Industrial Color Testing*, Wiley-VCH, Weinheim, 1994 p. 157.
- [52] G.R. Desiraju, *Current Science*, Vol. 88, (2005), p. 374 – 380.

Chapter 11

REMOVAL OF DYES FROM SOLUTION ON CLAY SURFACES - AN OVERVIEW

*M. A. Rauf**

Chemistry Department, PO Box 17551, UAE University, Al-Ain, UAE

ABSTRACT

Organic dyes are a group of those chemicals of special interest which have drawn considerable attention in many industrial processes. However due to their high toxicity and low biodegradability, various approaches such as adsorption, coagulation, sedimentation, membrane-filtration processes (nano-filtration), reverse osmosis, electrodialysis, advanced oxidation processes etc. have been forwarded concerning the removal of these dyes from solution. Adsorption is a well known equilibrium separation process and is an effective method for water decontamination applications. It is well-known that natural materials, waste materials from industry and agriculture and biosorbents can be obtained and employed as inexpensive sorbents. Some of the reported sorbents include commercially activated carbon, clay materials (bentonite, kaolinite), zeolites, siliceous material (silica beads, alunite, perlite) and polymeric materials as low cost adsorbents for dye removal. This overview focuses on using adsorption method to remove dyes from solution and the literature findings of such studies on various types of clays are presented.

Keywords: Clays, Dyes, Adsorption

1. INTRODUCTION

With increasing revolution in science and technology, there was a bigger demand on opting for newer chemicals which could be used in various industrial processes. Amongst the

* Email: raufmapk@yahoo.com

many chemicals used are the organic dyes. Due to the extensive use of these chemicals in industries, they have also become an integral part of industrial effluent. Most of these dyes are of diverse nature and are also potentially toxic and carcinogenic in nature and are classified as pollutants. Their removal from the industrial effluents is therefore a major environmental challenge [1, 2].

Various approaches have been forwarded to handle the removal of dyes from water. These include biodegradation, coagulation, adsorption, advanced oxidation (AOP) and the membrane process [3-8]. Table 1 outlines the various methods which are used for removing pollutants from the environment. Among these techniques, the adsorption process appears to be a promising field of study, and have been reported to be an effective tool for the removal of soluble organic contaminants from water and soil, because they can provide an almost total removal [9-20]. Adsorption is a well known equilibrium separation process. It is an effective means for water decontamination applications [21-25]. The method is cost effective, flexible in usage and simple to handle for handling the removal of different types of pollutants from the environment. Furthermore, adsorption method also does not result in the formation of harmful substances. The chemical composition and the surface properties of the adsorbents largely determine its suitability for pollutant removal. Adsorption techniques employing different solid sorbents are widely used to remove certain classes of chemical pollutants from waters, especially those that are practically unaffected by conventional biological wastewater treatments. Amongst the many solid substances used for such work are activated carbon [26-30], peat [31], resins [32, 33], polymeric substances [34-37], sand [16, 40] and clays [41-44]. This paper presents the literature findings of various researchers on the removal of dyes from solution by using different types of clays. Although the pollutant removal on clays is a vast area, the focus of attention in this work ranges within 2000- 2007 for the removal of dyes on clays.

2. EXPERIMENTAL METHODOLOGY

Different experimental techniques have been proposed for both qualitative and quantitative analysis of various types of pollutants concerning their adsorption behavior. These methods usually involve analysis by instrumental methods such as UV/Vis spectroscopy [10, 16, 45], IR [46], HPLC [47], GC/MS [48], Ion chromatography [49], Capillary Electrophoresis [50], Radiometry [51] etc. However, for adsorption studies of organic dye molecules, researches have mostly opted for spectrophotometric technique as this is easy to use for monitoring the changes in solution color before and after the experimental procedure is finished.

Table 1. Principal existing and emerging processes for dyes removal

	Methods	Advantages	Disadvantages
Conventional treatment processes	Coagulation Flocculation	Simple, economically feasible	High sludge production, handling and disposal problems.
	Biodegradation	Economically attractive, publicly acceptable treatment	Slow process, necessary to create an optimal favorable environment, maintenance and nutrition requirements
	Adsorption on activated carbons, clays etc	The most effective adsorbents, great capacity, produces a high-quality treated effluent	Ineffective against disperse and vat dyes, the regeneration is expensive and results in loss of the adsorbent, non-destructive process
Established recovery processes	Membrane separations	Removes all dye types, produce a high-quality treated effluent	High pressures, expensive, incapable of treating large volumes
	Ion-exchange	No loss of sorbent on regeneration	Not effective for disperse dyes
	Oxidation	Rapid and efficient process	High energy cost, chemicals required
Emerging removal processes	Advanced oxidation process	No sludge production, little or no consumption of chemicals	Economically unfeasible, formation of by-products, technical constraints
	Selective bioadsorbents	Economically attractive, regeneration is not necessary, high selectivity	Requires chemical modification, non-destructive process
	Biomass	Low operating cost, good efficiency and selectivity, no toxic effect on microorganisms	Slow process, performance depends on some external factors (pH, salts)

Ref: G. Crini, Non-conventional low-cost adsorbents for dye removal: A review, *Bioresource Technology* 97 (2006) 1061–1085.

3. DISCUSSION

Clays are naturally occurring substances which are well known and have been used extensively for various purposes by human beings since the early days of history. Because of their low cost, abundance in nature, and high sorption properties, clay materials have drawn a great deal of attention to be employed as adsorbents for removing pollutants from contaminated water. Additionally, clays are used in many industrial units for decontamination and color removal from various products.

The adsorption capability of a given type of clay arises from the net negative charge of the mineral. This negative charge gives clay the capability to adsorb positively charged species. The adsorption capacity depends also on the accessibility of the pollutants to the inner surface of the adsorbent, which in turn depends on their size. The high sorption properties of clays also come from their high surface area and high porosity. The large surface area of clays (upto 800 m²/g) also contributes to their high adsorption capacity. This capacity is mainly due to their structural characteristics and their porous texture which gives them a large surface area. Besides this, the chemical nature of clays can be easily modified by chemical treatment in order to increase their properties.

3.1. Characteristics of Clays [52-57]

Clay mineral is a layer silicate mineral (also called a phyllosilicate) or other mineral which imparts plasticity and which hardens upon drying or firing. The basic structure of the phyllosilicates is based on interconnected six member rings of SiO₄⁻⁴ tetrahedra that extend outward in infinite sheets. Three out of the 4 oxygens from each tetrahedra are shared with other tetrahedra. This leads to a basic structural unit of Si₂O₅⁻². Figure 1 shows the structure of phyllosilicate. Clay materials are classified by the differences in their layered structures. There are several classes of clays such as smectites (montmorillonite, saponite), mica (illite), kaolinite, serpentine, pyrophyllite (talc), vermiculite and sepiolite. This section briefly describes the essential characteristics of those clays which are generally used for adsorption purposes.

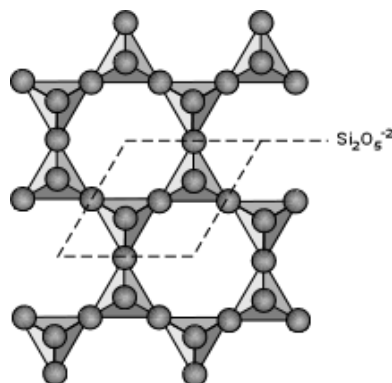


Figure 1. The basic structure of phyllosilicates.

a) *Smectites*

These are a family of clays that swell when immersed in water or some organic liquids (those which, like water, have polar molecules). Formerly they were known as the montmorillonite group; that name is now only used for one mineral in the smectite group. All smectites have very high cation exchange capacity (of the order of 1000 meq/kg = 1 mmole of positive charge per gram). Smectites are 2:1 phyllosilicates with total layer charge between 0.2 to 0.6 negative charges per half unit cell layer. This group was formerly called the Montmorillonite group, but the name was changed in the 1970s to avoid confusion because the name montmorillonite also refers to an individual species of smectite. Their structure is very similar to that of the other 2:1 phyllosilicates except that the total layer charge is 0.2 - 0.6 negative charges per half unit cell layer and they are typically hydrated. Because of this permanent charge, smectite interlayers always contain cations to provide electro neutrality. These cations are generally available to participate in cation exchange reactions unless they are large polyanions of aluminum or iron.

In hydrated smectites, the superposition of one layer over another is not controlled by the presence of K in the ditrigonal holes, as in micas, nor by the hydrogen bonding of one layer to another, as in the kandites. This lack of layer-to-layer rotational limitation produces a condition called as turbostratic stacking, wherein any one layer may assume any degree of rotational orientation with respect to the layers above and below it. Lateral movement of one layer with respect to another is also not limited. Because of this lack of orientation, one cannot describe all the stacking symmetry of smectite layers in any idealized unit cell. Thus, smectites are not true minerals, but rather para-minerals or paracrystalline minerals.

b) *Montmorillonite*

Montmorillonite is a very soft phyllosilicate mineral that typically forms in microscopic crystals, forming clay. Montmorillonite, a member of the smectite family, is 2:1 clay, meaning that it has 2 tetrahedral sheets sandwiching a central octahedral sheet. A representative structure of this clay is shown in figure 2. The particles are plate-shaped with an average diameter of approximately 1 micrometre. It is the main constituent of the volcanic ash weathering product, bentonite. Montmorillonite's water content is variable and it increases greatly in volume when it absorbs water. Chemically it is hydrated sodium calcium aluminium magnesium silicate hydroxide $(\text{Na,Ca})_{0.33}(\text{Al,Mg})_2(\text{Si}_4\text{O}_{10})(\text{OH})_2 \cdot n\text{H}_2\text{O}$. Potassium, iron, and other cations are common substitutes, the exact ratio of cations varies with source. It often occurs intermixed with chlorite, muscovite, illite, cookeite and kaolinite.

c) *Bentonite*

Bentonite is an absorbent aluminium phyllosilicate, generally an impure clay consisting mostly of montmorillonite. When bentonite absorbs water and swells, it is stretched open like a highly porous sponge; the toxins are drawn into these spaces by electrical attraction and bound fast. In fact bentonite can absorb pathogenic viruses, aflatoxin (a mold), and pesticides and herbicides. There are a few types of bentonites and their names depend on the dominant elements, such as K, Na, Ca, and Al. As noted in several places in the geologic literature, there are some nomenclatorial problems with the classification of bentonite clays. Bentonite usually forms from weathering of volcanic ash, most often in the presence of water. However, the term bentonite, as well as a similar clay called tonstein, has been used as clay beds of

uncertain origin. For industrial purposes, two main classes of bentonite exist: sodium and calcium bentonite. In stratigraphy and tephrochronology, completely devitrified (weathered volcanic glass) ash-fall beds are commonly referred to as K-bentonites when the dominant clay species is illite.

d) Kaolinite

Kaolinite is a 1:1 aluminosilicate consisting of stacked pairs of tetrahedral silica sheets and octahedral alumina sheets. Each pair of sheets is bound together through common oxygen atoms, and successive pairs are held together by hydrogen bonding between Si-O and Al-OH groups. The resulting crystal has a silica face of SiO₂ tetrahedra, an alumina face carrying AlOH groups, and edges which carry both SiOH and AlOH sites. The general formula of Kaolinite is $Al_2[(OH)_2|Si_2O_5]$ and its crystal structure is shown in figure 3. Under normal conditions kaolinite does not swell because of the strong hydrogen bonding between the 1:1 pairs. Isomorphous substitution in the silica layer leaves that face with a small permanent negative charge, while the charge on the alumina face and on the edges is pH-dependent. The point of zero charge (pzc) of kaolinite is approximately 4–4.7.

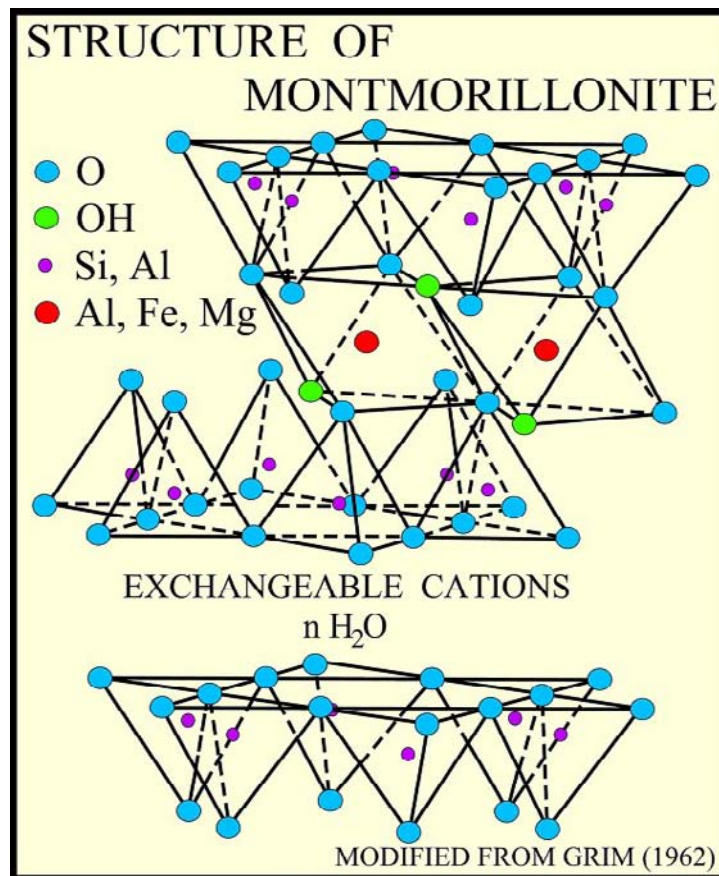


Figure 2. Structure of Montmorillonite.

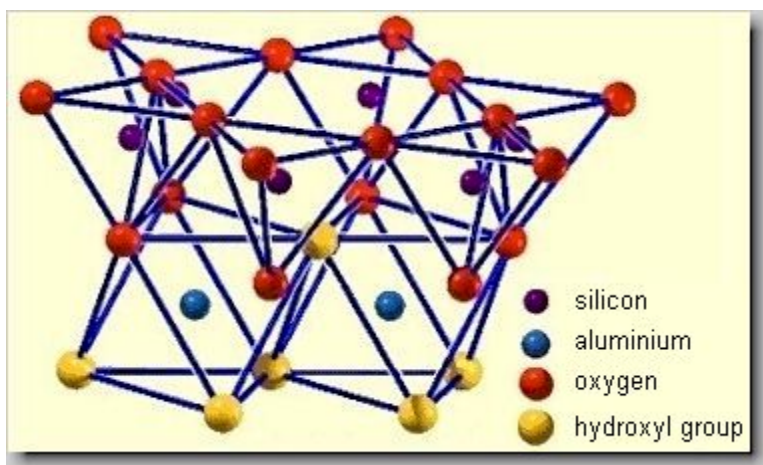


Figure 3. Crystal lattice of kaolinite. Kaolinite consists of an octahedron layer (coordinates around Al) and a tetrahedron layer (coordinates around Si).

The strongest preference for kaolinite is shown by polyaromatic molecules carrying amino groups. Such solutes can associate by pi-stacking, and could also interact with the permanent negative charges on the flat silica faces of the kaolinite crystals. The extent of adsorption of the solutes to the edges of kaolinite crystals is probably much the same as that to the oxides, because the kaolinite edges are structurally similar to the oxide surfaces.

e) Diatomite

Diatomite is a powdery, non-metallic mineral composed of the fossilised skeletal remains of microscopic single-celled aquatic plants called diatoms. Over 10,000 species of these microscopic algae have been recognized, each with its own distinct shape, ranging in size

from under 5 microns to over 100 microns. Diatomite deposits are usually categorized based upon their fresh water or salt water origin. Both the chemical composition and the physical structure of diatomite make it of great commercial value for a wide spectrum of uses, including filter aids, functional fillers, carriers for active ingredients and diluents, and aggregates. Diatoms have the unique ability to absorb water-soluble silica present in their natural environment to form a highly porous, yet rigid, skeletal framework of amorphous silica.

f) Fuller's Earth

It is composed mainly of alumina, silica, iron oxides, lime, magnesia, and water, in extremely variable proportions, and is generally classified as sedimentary clay. The mineral generally contains montmorillonite or palygorskite (attapulgite) or a mixture of the two; some of the other minerals that may be present in fuller's earth deposits are calcite, dolomite, and quartz. Fuller's earth is any nonplastic clay or claylike earthy material that can be used to decolorize, filter, and purify animal, mineral, and vegetable oils and greases. It is characterized by its property of absorbing basic colors and removing them from oils.

g) Sepiolite

Sepiolite is a clay mineral with a typical formula of $\text{Mg}_4\text{Si}_6\text{O}_{15}(\text{OH})_2 \cdot 6\text{H}_2\text{O}$. Removal of the structural water causes the sepiolite crystals to fold by rotation of the fibers on axes through the inverted Si-O-Si edge bonds, thus, allowing the terminal Mg^{2+} to complete their coordination with the oxide surface of the neighboring silica layer.

The thermal behavior of sepiolite has shown that the structural changes of the material with increasing temperature affect the specific surface area and its adsorption capacity. Sepiolite has structurally four water molecules coordinated to magnesium. The loss of these water molecules with increasing temperature will affect the specific surface area and adsorption capacity of sepiolite. It has been known that water molecules coordinated to magnesium lose until 500°C . After losing four water molecules which are coordinated to magnesium, the structure folds. Structural folding is associated with a decrease in the adsorption properties since the channels become narrower and the superficial slots sinter. A further increase in temperature produces the dehydroxylation of the structure and leads to the formation of clinoenstatite [57].

h) Zeolites

Compositionally, zeolites are similar to clay minerals. More specifically, both are aluminosilicates. They differ, however, in their crystalline structure. Clays have a layered crystalline structure (similar to a deck of cards) and are subject to shrinking and swelling as water is absorbed and removed between the layers. In contrast, zeolites have a rigid, 3-dimensional crystalline structure (similar to a honeycomb) consisting of a network of interconnected tunnels and cages. Water moves freely in and out of these pores but the zeolite framework remains rigid. The zeolites are framework silicates consisting of interlocking tetrahedrons of SiO_4 and AlO_4 . In order to be a zeolite the ratio $(\text{Si} + \text{Al})/\text{O}$ must equal $1/2$. The aluminosilicate structure is negatively charged and attracts the positive cations that reside within. Zeolites have an open structure that can accommodate a wide variety of cations, such as Na^+ , K^+ , Ca^{2+} , Mg^{2+} and others. These positive ions are rather loosely held and can readily be exchanged for others in a contact solution. Zeolites have high cation exchange capacity (CEC) which arises during the formation of the zeolite from the substitution of an aluminum ion for a silicon ion in a portion of the silicate framework (tetrahedral units that make up the zeolite crystal). More than 150 zeolite types have been synthesized and 48 naturally occurring zeolites are known. Some of the more common mineral zeolites are: analcime, chabazite, heulandite, natrolite, phillipsite, and stilbite. An example mineral formula is: $\text{Na}_2\text{Al}_2\text{Si}_3\text{O}_{10} \cdot 2\text{H}_2\text{O}$, the formula for natrolite.

3.2. Adsorption of Dyes

Suitable clay should possess not only a porous texture, but also high surface area. The adsorption does not always increase with surface area. Besides the physical structure, the adsorption capacity of given clay is strongly influenced by the chemical nature of the surface. The acid and base character of clay influences the nature of the dye isotherms. The adsorption capacity depends also on the accessibility of the pollutants to the inner surface of the adsorbent, which depends on their size. The specific sorption mechanisms by which the

adsorption of dyes takes place on these adsorbents are still not clear. This is because adsorption is a complicated process depending on several interactions such as electrostatic and non-electrostatic (hydrophobic) interactions. Clays show strong adsorption behavior for both heteroatomic cationic and anionic dyes. Figure 4 shows the chemical structures of some dyes. The clays usually have high sorption capacity for dyes; this property is well known for both acidic and basic dyes [58-61]. However, the sorption capacity for basic dye is much higher than for acid dye because of the ionic charges on the dyes and characteristic properties of the clay. Since the sorption capacity also depends on the surface area of the adsorbent, the higher the surface area the more adsorption will take place.

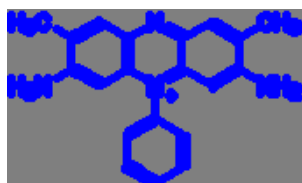
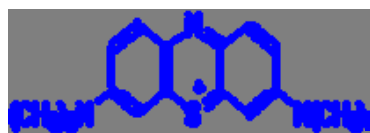
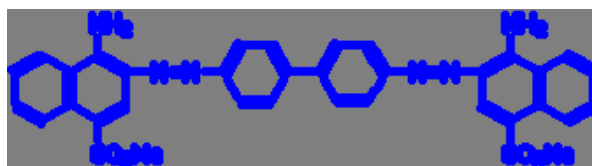
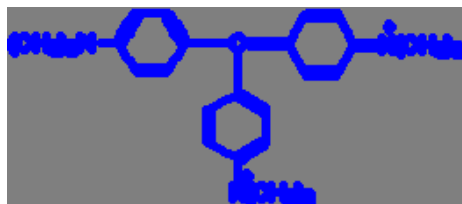
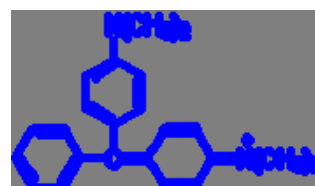
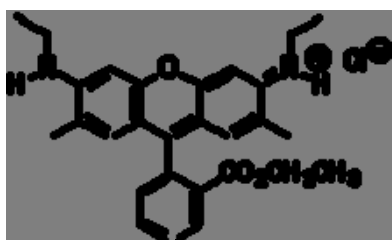
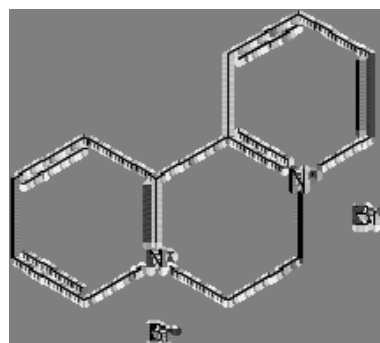
**Basic Red 2 (Safranin O)****Basic Blue 9 (Methylene Blue)****Congo Red****Methyl Green****Malachite Green****Rhodamine 6G****Diquat**

Figure 4. (Continued)

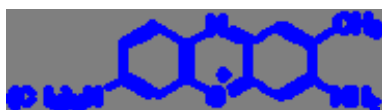
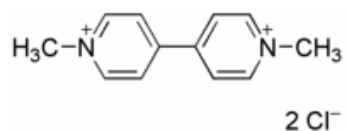
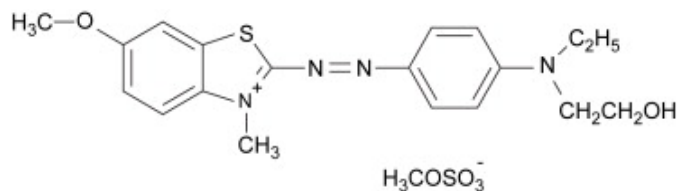
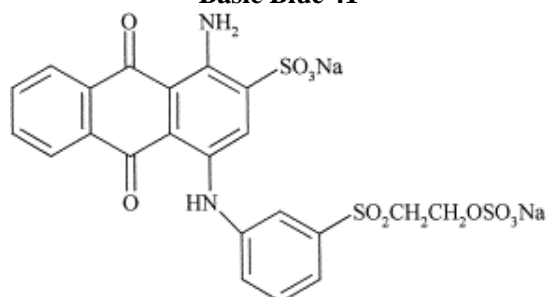
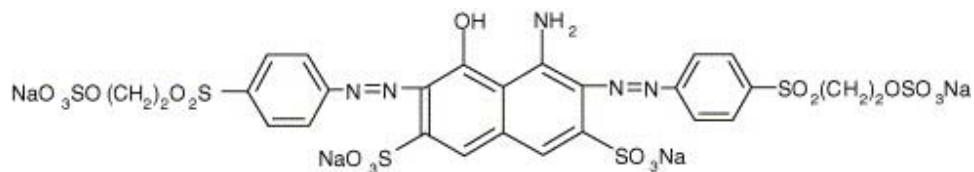
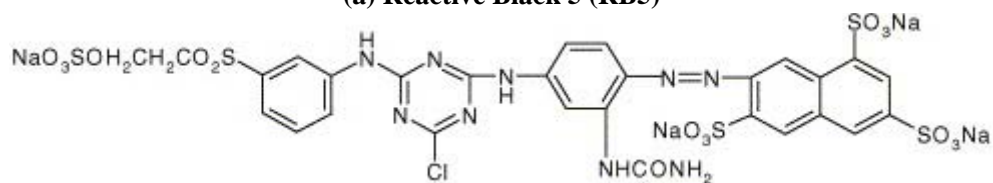
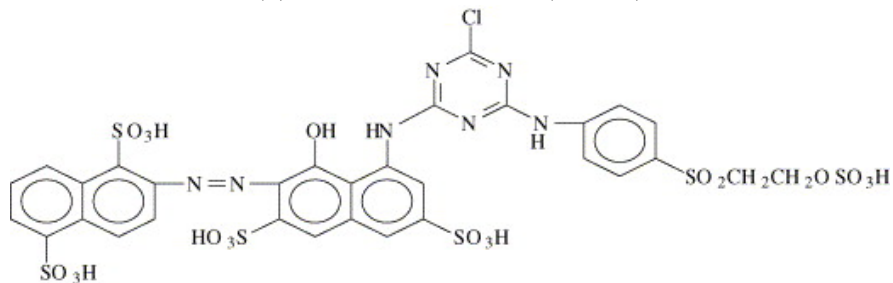
**Toluidine Blue O****Paraquat****Basic Blue 41****Reactive Blue 19****(a) Reactive Black 5 (RB5)****(b) Reactive Yellow 145 (RY145)****Reactive Red 239**

Figure 4. Chemical Structures of some dyes.

Due to the high surface area of bentonite, it has been suggested to be a good adsorbent for (basic) dye removal. An adsorption capacity of 300-360.5 mg of dye/g bentonite has been reported in the literature [62,63]. The adsorption kinetic studies of the adsorption of a commercial dye, Basic Red 2 (BR2) on bentonite from an aqueous solution showed that the removal of BR2 was a rapid process and the adsorption process obeyed the pseudo-second-order model, indicating cationic dye had a very strong affinity on the bentonite surface and had a very high BR2 adsorption capacity of approximately 274 mg/g at 30°C [64]. Modification of bentonite surface has shown improvement in its sorption capacity. The acid-treated bentonite showed a higher adsorption capacity than non-modified bentonite [63]. Bentonite surface modified by a surfactant has shown a sorption capacity of 206.6 mg/g of the Reactive Blue 19 [65]. Enhanced sorption capacity of bentonite has also been reported by other researchers upon modification of the adsorbent surface [66, 67]. Increasing the ionic strength increased the adsorption of Crystal violet (a basic dye) onto bentonite samples. The adsorption capacities of the cation-saturated bentonites were higher than that of the raw and acid activated bentonite. Likewise the adsorption capacity of Acid Red 151 has been found to be 357.14 and 416.66 mg/g for the cetyldimethylbenzylammonium chloride-bentonite (CDBA-bent) and cetylpyridinium chloride-bentonite (CP-bent), respectively [68].

The adsorption of dyes on kaolinite has not been studied widely. There are only a few reports on its use as an adsorbent for dyes [55,69]. In the case of methylene blue adsorption studies on kaolinite, it was shown that the dye adsorbed more to the surface under basic conditions [69]. The increased adsorption in basic conditions was related to preferential affinity of the dye cations for basic sites. In aqueous medium, the exchangeable alkali and other metal cations on the surface and in the interlayer region of the clay undergo hydration creating a hydrophilic environment. Increasing the pH of the adsorbing medium modifies the clay mineral surface thus increasing the adsorption of methylene blue.

Montmorillonite clays have the smallest crystals, the largest surface area and the highest cation exchange capacity. Thus montmorillonite clays would be expected to have the highest sorptive capacity. Due to its salient characteristics the clay has been used for removing dyes from solution as shown in many studies [70-77]. The behavior of adsorption of the cationic dye C.I. Basic Blue 41 onto montmorillonite, bentonite, raw perlite, and expanded perlite has been reported in the literature [78] and it was found that the dye molecules interact with each other as well as with the acidic sites of the silicate surface for all nano-adsorbents used. The H aggregates was found to be formed at the nano-adsorbents surfaces and transferred to dye monomers, dimers, and J-aggregates. This is then followed by migration into the interlamellar space resulting in intercalation of the clay even at low dye loadings. The dye molecules between the silicate sheets may adopt different orientations and, eventually become layered depending on the dye loading and the temperature.

The removal of xanthene basic dye, Rhodamine 6G [79], disazo acid dye, Amido black 10B (C.I. 20470) [80], and disazo acid dye, Methyl Orange 52 (C.I. 13025) [81], by HCl-activated montmorillonite in fixed beds, is also reported in the literature. It was found that the adsorption capacity of acid dye onto raw clay could be largely improved when the clay was activated by HCl. The increase of adsorption capacity was attributed to the replacement of Al^{3+} or Fe^{2+} ions of montmorillonite by H^+ ion after HCl acidification. The nano-clay, montmorillonite, and some modified nanoclays have also been used as sorbents for nonionic, anionic and cationic dyes [81]. The nanoclay showed a sorption of 90% at an initial dye

concentration of 6 g/L, or 60% based on the weight of the sorbent, indicating an extremely high dye affinity.

Polymer/layered silicate nanocomposites frequently exhibit remarkably improved mechanical and materials properties and are attracting considerable interest in polymer science field [44]. The adsorption of tannic acid, humic acid, and some dyes (methylene blue, reactive dye RR222) from water using the composite of CTS and activated clay has also been reported in the literature [82]. Likewise adsorption of Congo Red dye on chitosan/montmorillonite nanocomposite (CTS/MMT) is also reported [44]. The adsorption kinetics obeyed the pseudo-second order model, and the isotherm followed the Langmuir monolayer model. Compared with chitosan(CTS), the CTS/MMT nanocomposite has a good flocculation ability in aqueous solution, comparative low cost and relative high adsorption capacity. Therefore, this nanocomposite was found to be an effective adsorbent for the removal of dyes from wastewaters.

Fuller's earth (FE) has also been reported as a potential adsorbent for the removal of dyes

The adsorption studies of methylene blue on FE has shown that the adsorption process is very fast compared to that on activated carbon and also that FE samples have higher adsorption capacity in the range of 3×10^{-4} to 6.0×10^{-4} mol/g at 298 K [83]. Adsorption characteristics of Toluidine Blue (TB) on nontreated clay were compared with those obtained for acid and alkaline-treated samples [84]. It was found that the adsorption capacity of alkali treated Fuller's earth is higher as compared to untreated clay or acid treated clay. This probably arises from its higher negative charge and the aggregation of the dye molecules on the surface.

The natural abundance and low cost of diatomite has drawn the attention of some researchers as a substitute for activated carbon. For example, the adsorption of basic blue 9 onto diatomaceous earth (diatomite) has been reported in the literature [85]. The adsorption equilibrium revealed that diatomite can uptake 42 mmol dye/100 g in relatively low concentration in aqueous medium. The kinetics of adsorption of methylene blue onto the surface of diatomite at different operating condition was best described by the pseudo first order model. Diatomite has also been used for the removal of Sif Blau BRF (SB), Everzol Brill Red 3BS (EBR), and Int Yellow 5GF (IY) [86]. Values of the removal efficiency of the dyes ranged from 28.60 to 99.23%. The adsorption isotherms of SB, EBR, and IY were found to obey the Langmuir behavior, which indicates monolayer adsorption. It was suggested that the adsorbed dye anions form a monolayer with sulfonate groups as close as possible to the adsorbent surface [63]. In another study, the adsorption of three different dyes namely methylene blue(MB), reactive black (RB), and reactive yellow (RY) from aqueous solution by calcined and raw diatomite was reported [87,88]. It was noted that the percentage MB removal by calcined diatomite dropped from 33% to 2% with decreasing pH of dye solution from 12.0 to 2.0. The maximum removal occurred at basic pH (10–12). Furthermore, the removal rate decreased with the decrease in pH which may be due to excess H^+ ions competing with the dye cation for the adsorption sites. Also that, as the positive surface charge density decreases with an increase in the pH of the solution, the electrostatic repulsion between positively charged dye (MB^+) and the surface of the calcined diatomite was reduced resulting in more adsorption. The percentage removal of Reactive Yellow(RY) by calcined diatomite decreased with further increase in pH above pH 4 and the maximum percentage of removal was in acidic media (pH 2–3), while the percentage of Reactive Black (RB) removal was nearly constant over the pH range. In general, the percentage RB and RY removal was

decreased from 24% to 14% and 22% to 1%, respectively with increasing pH of dye solution from 2.0 to 11.0 when calcined diatomite was used as the adsorption media. The percentage of MB, RB, and RY removal from solution remained constant by raw and calcined diatomite in the pH range from 4 to 10 with better removal by diatomite.

Sepiolite is a good adsorbent for organic species because it exhibits a variety of attractive properties such as high specific surface area, high porosity and surface activity. Because of their structural morphology, sepiolites have received considerable attention with regard to the adsorption of organics on the clay surfaces and to their use as support for catalysts [89]. The adsorption of Acid Red 57 on sepiolite has been reported in the literature [57]. In this case a practical limiting adsorption capacity was found to vary with pH and ionic strength of the solution. Maximum value of adsorbed dye was found to be 13.5 $\mu\text{mol/g}$ of the adsorbent. This value is comparable with other studies on dye adsorption using low cost adsorbents [90,91]. The adsorption of diquat (DQ), paraquat (PQ) and methyl green (MG) on sepiolite has also been reported in the literature [92,93]. The largest amounts of DQ, PQ and MG adsorbed were between 100% and 140% of the cation exchange capacity (CEC) of sepiolite which translates to 0.75 moles of MG per Kg of the clay. There are also few reports in the literature regarding the use of modified sepiolite for adsorption of dyes. In one such report it was found that the adsorption of dye under investigation, namely Crystal Violet (CV) is highly affected by the sepiolite surface features[94]. The observed results showed that the amount of adsorbed CV cations on the base activated sepiolite is 2.6 fold higher than raw sepiolite. This was attributed to the fact that the basic activation leads to the replacement of part of Mg^{2+} ions located at the edges of the channels by Na^+ , the reactivity of basal and edge surface groups is enhanced and consequently the adsorption capacity of base activated adsorbent is increased. On the other hand the low adsorption capacity on the Al-saturated samples of sepiolite arises from the aluminium cation exchange process which leads to pore blocking and the reactivity of basal or edge oxygen atoms of the silicate.

Natural zeolite is an abundant resource of aluminosilicate and has been explored as an effective adsorbent for pollutant removal. It has been shown that this material can be used to remove dyes from solution as well, for example the removal of Malachite Green(MG) was carried out on zeolite and the adsorption capacity was reported to be 5×10^{-5} mol/g [95]. This capacity was found to decrease in the presence of Pb^{2+} ions indicating the selective behavior of zeolite for smaller species. The adsorption behavior for Methylene Blue(MB) and Rhodamine B(RB) is also reported in the literature[96]. For methylene blue, the adsorption capacities were found to be 6.8×10^{-5} and 7.9×10^{-5} mol/g at 30 and 50 °C, respectively. In contrast, the adsorption capacities of rhodamine B were found to be 2.1×10^{-5} and 2.8×10^{-5} mol/g at 30 and 50 °C, respectively. Thermodynamic and kinetic calculations indicate that the adsorption was endothermic reaction with two-step diffusion process.

The adsorption of three reactive azo dyes (Reactive Black 5, Red 239 and Yellow 176) by two natural mesoporous minerals has also been examined in order to identify the ability of these minerals to remove coloured textile dyes from wastewaters [97]. For this purpose natural and modified sepiolites and zeolites were chosen. The adsorption results indicated that both natural sepiolite and zeolite have limited adsorption capacities of the reactive dyes but are substantially improved upon modifying their surfaces with quaternary amines. The maximum adsorption capacities for the three dyes namely Black, Red and Yellow on modified zeolite were found to be 111.1 g/kg, 88.5 g/kg and 60.5 g/kg respectively. The adsorption capacity decreased in the order of hydrophilicity of the dye molecule as: Red >

Yellow > Black. The adsorption of basic dyes (MG-400 and MS-300) from aqueous solutions onto natural zeolite is also reported in the literature and it was found that the adsorption capacities of MG-400 and MS-300 were 15 and 55 mg/g, respectively [98]. Natural zeolite and synthetic zeolite, MCM-22, have also been employed as effective adsorbents for a basic dye, methylene blue, removal from wastewater. It was found that MCM-22 exhibits equilibrium adsorption at 1.7×10^{-4} mol/ g as compared to the equilibrium adsorption value of 5×10^{-5} mol/ g obtained in the case of natural zeolite [99]. ZSM-5 and Beta zeolites, both in NH_4 -form, were found to be the most efficient in enhancing total organic carbon (TOC) for printing ink removal from simulated wastewater water [100]. At concentrations of 5 g/L, the zeolites decreased TOC value by more than 50% from pretreated water by flocculation. In comparison with activated carbon of the same concentration, the zeolites were found to be 20% more effective.

Besides these common clays, there are numerous other examples available in the literature on the use of many other clay types such as halloysite, saponite, spent activated clay, palygorskite, hectorite, activated bleaching earth etc for the adsorption of dyes [101-106]. In some cases a mixture of clays has also been used by some researchers as potential adsorbents for dyes [107-110]. The results presented in all the studies above show that clay materials may be promising adsorbents for environmental and purification purposes.

CONCLUSION

The presence of organic pollutants in our environment has taken a serious turn in modern times. Their removal from soils and water bodies has drawn a great deal of attention from all quarters of scientific community. Various approaches have been put forwarded to remove these pollutants from aqueous media. The adsorption process because of its low cost and easy to handle approach has topped the list of all the methods employed in such work. The use of many adsorbents for such purpose requires that they should be easy to handle, readily available or cheap to produce, environmentally compatible and give good results at the end. Clays of various types have drawn a great deal of attention in this regard and a substantial number of studies in the literature have revealed their usefulness as a potential means of removing pollutants especially dyes from aqueous media. However there is yet little information available in the literature containing a full study of comparison between types of adsorbent clays.

ACKNOWLEDGEMENTS

Reviewed by Prof. Dr.M.Javed Iqbal, Chemistry Department, Quaid-e-Azam University, Islamabad, Pakistan

REFERENCES

- [1] Shichi, T ; Takagi,K. Clay minerals as photochemical reaction fields. *Journal of Photochemistry and Photobiology C: Photochemistry Reviews*, 2000,1, 113-130.
- [2] Forgas, E; Cserhati,T; Oros, G. Removal of synthetic dyes from wastewater: a review, *Environmental International*, 2004,30, 953-971.
- [3] Derudi, M; Venturini,G; Lombardi,G; Nano,G; Rota,R. Biodegradation combined with ozone for the remediation of contaminated soils, *European Journal of Soil Biology*, 2007,43, 297-303 .
- [4] Martin, MJ; Artola, A; Balaguer,MD; Rigola, M. Activated carbons developed from surplus sewage sludge for the removal of dyes from dilute aqueous solutions, *Chemical Engineering Journal*, 2003,94, 231-239.
- [5] Ahmad, AL; Puasa, SW. Reactive dyes decolourization from an aqueous solution by combined coagulation/micellar-enhanced ultrafiltration process. *Chemical Engineering Journal*, 2007,132,257-265 .
- [6] Arslan,I; Balcioglu,IA; Bahnemann,DW. Advanced chemical oxidation of reactive dyes in simulated dyehouse effluents by ferrioxalate-Fenton /UV-A and TiO₂/UV-A processes. *Dyes and Pigments*, 2000, 47, 207-18.
- [8] Rauf,MA; Ashraf,SS; Alhadrami,SN. Photolytic oxidation of Coomassie Brilliant Blue with H₂O₂, *Dyes and Pigments*, 2005,66, 197–200.
- [9] Kula,I; Ugurlu,M; Karaoglu,H; Celik,A. Adsorption of Cd(II) ions from aqueous solutions using activated carbon prepared from olive stone by ZnCl₂ activation, *Bioresource Technology*, 2008,99, 492-501 .
- [10] Hameed,BH; Ahmad,AA; Aziz,N. Isotherms, kinetics and thermodynamics of acid dye adsorption on activated palm ash, *Chemical Engineering Journal*, 2007, 133,195-203 .
- [11] El-Qada, EN; Allen,SJ; Walker,GM. Adsorption of basic dyes from aqueous solution onto activated carbons, *Chemical Engineering Journal*, 2008,135, 174-184 .
- [12] Ozmen,EY; Sezgin,M; Yilmaz,A; Yilmaz,M. Synthesis of β -cyclodextrin and starch based polymers for sorption of azo dyes from aqueous solutions. *Bioresource Technology*, 2008,99,526-531 .
- [13] Eberhardt,TL; Min,SH. Biosorbents prepared from wood particles treated with anionic polymer and iron salt: Effect of particle size on phosphate adsorption. *Bioresource Technology*, 2008,99, 626-630 .
- [14] Fernandes, AN; Almeida,CAP; Menezes,CTP; Debacher,NA; Sierra,MMD. Removal of methylene blue from aqueous solution by peat, *Journal of Hazardous Materials*, 2007,144,412-419 .
- [15] Aroguz,AZ. Kinetics and thermodynamics of adsorption of azinphosmethyl from aqueous solution onto pyrolyzed (at 600 °C) ocean peat moss (*Sphagnum* sp.) *Journal of Hazardous Materials*, 2006,135, 100-105 .
- [16] Rauf,MA; Shehadi,IA; Hassan,WW. Studies on the removal of Neutral Red on sand from aqueous solution and its kinetic behavior, *Dyes and Pigments*, 2007,75, 723-726 .
- [17] Taqvi, SIH; Hasany,SM; Bhangar,MI. Zn(II) ions removal from aqueous solution by Karachi beach sand, a mixed crystal systems, *Separation and Purification Technology*, 2007,61,153–160.

- [18] Haque,N; Morrison,G; Aguilera,IC; Torresdey,JLG. Iron-modified light expanded clay aggregates for the removal of arsenic(V) from groundwater. *Microchemical Journal*, 2008,88, 7-13 .
- [19] Hameed,BH. Equilibrium and kinetics studies of 2,4,6-trichlorophenol adsorption onto activated clay, *Colloids and Surfaces A: Physicochemical and Engineering Aspects*, 2007,307,45-52 .
- [20] Iqbal,MJ; Ashiq,MN. Adsorption of dyes from aqueous solutions on activated charcoal, *Journal of Hazardous Materials*, 2007,139,57-66.
- [21] Adebajo, MO; Frost,RL; Kloprogge,JT; Carmody,O; Kokot,S. Porous materials for oil spill cleanup: a review of synthesis and adsorbing properties. *Journal of Porous Materials*, 2003, 10, 159–170.
- [22] Widiastuti,N; Wu,H; Ang,M; Zhang,DK. The potential application of natural zeolite for greywater treatment, *Desalination*, 2008,218, 271-280 .
- [23] Lu,C; Su,F. Adsorption of natural organic matter by carbon nanotubes, *Separation and Purification Technology*, 2007,58,113-121 .
- [24] Zaspalis,V; Pagana,A; Sklari,S. Arsenic removal from contaminated water by iron oxide sorbents and porous ceramic membranes, *Desalination*, 2007,217,167-180 .
- [25] Ayrançi,E; Duman,O. Adsorption of aromatic organic acids onto high area activated carbon cloth in relation to wastewater purification, *Journal of Hazardous Materials*, 2006,136, 542-552 .
- [26] Chan,LS; Cheung,WH; McKay,G. Adsorption of acid dyes by bamboo derived activated carbon, *Desalination*, 2008,218,304-312 .
- [27] Onal,Y. Kinetics of adsorption of dyes from aqueous solution using activated carbon prepared from waste apricot, *Journal of Hazardous Materials*, 2006,137, 1719-1728 .
- [28] Karagozoglu, B; Tasdemir,M; Demirbas,E; Kobya,M. The adsorption of basic dye (Astrazon Blue FGRL) from aqueous solutions onto sepiolite, fly ash and apricot shell activated carbon: Kinetic and equilibrium studies, *Journal of Hazardous Materials*, 2007,147, 297-306 .
- [29] Onal,Y; Basar,CA; Ozdemir,CS. Investigation kinetics mechanisms of adsorption malachite green onto activated carbon, *Journal of Hazardous Materials*, 2007,146,194-203 .
- [30] Hameed, BH; Din,ATM; Ahmad,AL. Adsorption of methylene blue onto bamboo-based activated carbon: Kinetics and equilibrium studies, *Journal of Hazardous Materials*, 2007,141,819-825 .
- [31] Allen,SJ; Mckay,G; Porter,JF. Adsorption isotherm models for basic dye adsorption by peat in single and binary component systems, *Journal of Colloid and Interface Science*, 2004, 280,322-333 .
- [32] Fan,J; Li,A; Yang,W; Yang,L; Zhang,Q. Adsorption of water-soluble dye X-BR onto styrene and acrylic ester resins, *Separation and Purification Technology*, 2006,51,338-344.
- [33] Zhang, AL; Jiang,Z; Zhang,Q. Adsorption of dyes and phenol from water on resin adsorbents: Effect of adsorbate size and pore size distribution. *Journal of Hazardous Materials*, 2006,137, 1115-1122 .
- [34] Deepatana,A; Valix,M. Comparative adsorption isotherms and modeling of nickel and cobalt citrate complexes onto chelating resins, *Desalination*, 2008,218, 334-342 .

- [35] Eberhardt,TL; Min,SH. Biosorbents prepared from wood particles treated with anionic polymer and iron salt: Effect of particle size on phosphate adsorption. *Bioresource Technology*, 2008,99, 626-630 .
- [36] Lee,YH; Jeong,JY; Jegal,J; Mo,JH. Preparation and characterization of polymer-carbon composite membranes for the removal of the dissolved salts from dye wastewater, *Dyes and Pigments*, 2008,76, 372-378 .
- [37] Delval,F; Crini,G; Morin,N; Vebrel,J; Bertini,S; Torri,G. The sorption of several types of dye on crosslinked polysaccharides derivatives, *Dyes and Pigments*, 2002,53,79-92.
- [38] Sharma,YC; Weng,CH. Removal of chromium (VI) from water and wastewater by using riverbed sand: Kinetic and equilibrium studies, *Journal of Hazardous Materials*, 2007,142, 449-454 .
- [39] Rauf, MA; Bukallah,SB; Hamour,FA; Nasir,AS. Adsorption of dyes from aqueous solutions onto sand and their kinetic behavior, *Chemical Engineering Journal*, Available online 27 April 2007 .
- [40] Khan,MN; Zareen,U. Sand sorption process for the removal of sodium dodecyl sulfate (anionic surfactant) from water, *Journal of Hazardous Materials*, 2006,133,269-275 .
- [41] Salman,M; El-Eswed,B; Khalili,F. Adsorption of humic acid on bentonite. *Applied Clay Science*, 2007,38,51-56 .
- [42] Veli,S; Alyuz,B. Adsorption of copper and zinc from aqueous solutions by using natural clay, *Journal of Hazardous Materials*, 2007,149, 226-233 .
- [43] Ferreira,EA; de Bussetti,SG. Thermodynamic parameters of adsorption of 1,10-phenanthroline and 2,2'-bipyridyl on hematite, kaolinite and montmorillonites, *Colloids and Surfaces A: Physicochemical and Engineering Aspects*, 2007, 301,117-128 .
- [44] Wang,L; Wang,A. Adsorption characteristics of Congo Red onto the chitosan / montmorillonite nanocomposite, *Journal of Hazardous Materials*, 2007,147, 979-985.
- [45] Noroozi,B; Sorial,GA; Bahrami,H; Arami,M. Adsorption of binary mixtures of cationic dyes, *Dyes and Pigments*, 2008,76,784-791 .
- [46] Parida,SK; Dash,S; Patel,S; Mishra,SB. Adsorption of organic molecules on silica surface, *Advances in Colloid and Interface Science*, 2006,121,77-110 .
- [47] Timkovich,R. Analysis of regulatory dye in diesel petroleum, *Dyes and Pigments*, 2000,46, 69-79.
- [48] Gaca,J; Wejnerowska,G. Determination of epichlorohydrin in water and sewage samples, *Talanta*, 2006,70,1044-1050 .
- [49] Senel,S; Say,R; Arica,Y; Denizli,A. Zinc ion-promoted adsorption of lysozyme to Cibacron Blue F3GA-attached microporous polyamide hollow-fiber membranes, *Colloids and Surfaces A: Physicochemical and Engineering Aspects*, 2001,182,161-173.
- [50] Masukawa,Y. Separation and determination of basic dyes formulated in hair care products by capillary electrophoresis, *Journal of Chromatography A*, 2006,1108,140-144.
- [51] Steinhauser,G; Bichler,M. Adsorption of ions onto high silica volcanic glass, *Applied Radiation and Isotopes*, 2008,66, 1-8 .
- [52] Murray,HH. Applied Clay Mineralogy, Volume 2: Occurrences, Processing and Applications of Kaolins, Bentonites, Palygorskitesepiolite, and Common Clays (*Developments in Clay Science*), Elsevier Science, 2007.

- [53] Bergaya,F; Theng,BKG; Lagaly,G.(Editors),Handbook of Clay Science, Volume 1 (*Developments in Clay Science*) (Hardcover), Elsevier Science; 2006.
- [54] Borchardt,G; In: Dixon,JB; Weed,SB (ed.), Smectites. Ch. 14, Minerals in Soil Environments, 2nd Edition, SSSAJ *Special Publication No. 1*, 1989.
- [55] Harris,RG; Wells,RJ; Johnson,BB. Selective adsorption of dyes and other organic molecules to kaolinite and oxide surfaces, *Colloids and Surfaces A: Physicochemical and Engineering Aspects*, 2001,180, 131–140.
- [56] Kavaz, T; Sabah,E; Celik,MS. Structural properties of sepiolite-reinforced cement composite, *Cement and Concrete Research*, 2004,34, 2135-2139.
- [57] Alkan,M; Demirbas,O; Celikcapa,S; Dogan,M. Sorption of acid red 57 from aqueous solution onto sepiolite, *Journal of Hazardous Materials B*,2004,116,135–145.
- [58] Hu,QH; Qiao, SZ; Haghseresht,F; Wilson,MA; Lu,GQ. Adsorption. study for removal of basic red dye using bentonite, *Industrial Engineering and Chemical Research*,2006,45, 733–738.
- [59] Tahir,SS; Rauf,N. Removal of a cationic dye from aqueous solutions by adsorption onto bentonite clay, *Chemosphere*, 2006,63,1842-1848 .
- [60] Martinez,VM; Arbeloa,FL; Prieto,JB; Arbeloa,JT; Arbeloa,IL. Characterization of Rhodamine 6G aggregates, intercalated in solid thin films of laponite clay. 2. Fluorescence spectroscopy, *Journal of Physical Chemistry, B* 2005,109, 7443–7450.
- [61] Gurses,A; Dogar,C; Yalcın,M; Acıkyıldız,M; Bayrak,R; Karaca,S. The adsorption kinetics of the cationic dye, methylene blue, onto clay, *Journal of Hazardous Materials*, 2006,131,217-228 .
- [62] Bagane,M; Guiza,S. Elimination d'un colorant des effluents de l'industrie textile par adsorption, *Annales de Chimie Science des Matériaux*, 2000, 25, 615-625 .
- [63] Espantaleon,AG; Nieto,JA; Fernandez,M; Marsal,A. Use of activated clays in the removal of dyes and surfactants from tannery waste waters, *Applied Clay Science*, 2003,24,105-110 .
- [64] Liu,P; Zhang,L. Adsorption of dyes from aqueous solutions or suspensions with clay nano-adsorbents, *Separation and Purification Technology*, 2007,58,32-39 .
- [65] Ozcan,A; Omeroglu, C; Erdogan,Y; Ozcan,AS. Modification of bentonite with a cationic surfactant: An adsorption study of textile dye Reactive Blue 19, *Journal of Hazardous Materials*, 2007, 140, 173–179.
- [66] Eren,E; Afsin,B. Investigation of a basic dye adsorption from aqueous solution onto raw and pre-treated bentonite surfaces, *Dyes and Pigments*, 2008,76, 220-225 .
- [67] Ozcan,AS; Erdem,B; Ozcan,A. Adsorption of Acid Blue 193 from aqueous. solutions onto BTMA–bentonite, *Colloids Surf. A: Physicochemical Engineering Aspects*, 2005, 266, 73–81.
- [68] Baskaralingam,P; Pulikesi,M; Elango,D; Ramamurthi,V; Sivanesan,S. Adsorption of acid dye onto organobentonite, *Journal of Hazardous Materials*, 2006,28,138-144 .
- [69] Ghosh,D; Bhattacharyya,KG. Adsorption of methylene blue on kaolinite, *Applied Clay Science*, 2002,20,295-300 .
- [70] Wang,L; Wang,A. Adsorption characteristics of Congo Red onto the chitosan/montmorillonite nanocomposite, *Journal of Hazardous Materials*, 2007,147,979-985 .
- [71] Teng,MY; Lin,SH. Removal of methyl orange dye from water onto raw and acidactivated montmorillonite in fixed beds, *Desalination*, 2006,201,71-81 .

- [72] Gemeay,AH. Adsorption Characteristics and the Kinetics of the Cation Exchange of Rhodamine-6G with Na^+ -Montmorillonite, *Journal of Colloid and Interface Science*,2002,251,235-241 .
- [73] Arbeloa,FL; Chaudhuri, R; Lopez,TA; Arbeloa,IL. Aggregation of Rhodamine 3B Adsorbed in Wyoming Montmorillonite Aqueous Suspensions, *Journal of Colloid and Interface Science*, 2002,246,281-287 .
- [74] Wang,CC; Juang,LC; Hsu,TC; Lee,CK; Lee,CF; Huang,FC.Adsorption of basic dyes onto montmorillonite, *Journal of Colloid Interfacial Science*, 2004,273, 80–86.
- [75] Polubesova,T; Epstein,M; Yariv,S; Lapidis,I; Nir,S. Adsorption of alizarinate-micelle complexes on Na-montmorillonite, *Applied Clay Science*, 2004, 24, 177-183.
- [76] Saib,NB; Khouli,K; Mohammedi,O. Preparation and characterization of pillared montmorillonite: application in adsorption of cadmium, *Desalination*, 2007,217,282-290 .
- [77] Gemeay, AH.Adsorption Characteristics and the Kinetics of the Cation Exchange of Rhodamine-6G with Na^+ -Montmorillonite, *Journal of Colloid and Interface Science*, 2002,251, 235-241 .
- [78] Roulia,M; Vassiliadis,AA. Interactions between C.I. basic blue 41 and aluminosilicate sorbents, *Journal of Colloid and Interface Science*,2005, 291, 37-44.
- [79] Yang,YQ; Han,SY; Fan,QQ; Uqbolue,SC. Nanoclay and modified nanoclay as sorbents for anionic, cationic and nonionic dyes, *Textile Research Journal*, 2005,75, 622-627.
- [80] Lin, SH; Juang,RS; Wang,YH. Adsorption of acid dye from water onto pristine and acid-activated clays in fixed beds, *Journal of Hazardous Materials*, 2004,113, 195-200.
- [81] Teng,MY; Lin,SH. Removal of methylene orange dye from water onto raw and acid-activated montmorillonite in fixed beds, *Desalination*,2006, 201, 71-81.
- [82] Chang,MY; Juang,RS. Adsorption of tannic acid, humic acid, and dyes from water using the composite of chitosan and activated clay, *Journal of Colloid Interfacial Science*, 2004,278, 18-25.
- [83] Atun,G; Hisarli,G; Sheldrick,WS; Muhler,M. Adsorptive removal of methylene blue from colored effluents on fuller's earth, *Journal of Colloid and Interface Science*, 2003,261, 32-39 .
- [84] Hisarli,G. The effects of acid and alkali modification on the adsorption performance of fuller's earth for basic dye, *Journal of Colloid and Interface Science*, 2005,281, 18-26 .
- [85] Shawabkeh,RA; Tutunji,MF. Experimental study and modeling of basic dye sorption by diatomaceous clay, *Applied Clay Science*, 2003,24, 111-120.
- [86] Erdem,E; Colgecen,G; Donat,R. The removal of textile dyes by diatomite earth, *Journal of Colloid and Interface Science*, 2005, 282, 314-319.
- [87] Khraisheh,MAM; Al-Ghouti,MA; Allen,SJ; Ahmad,MN. Effect of OH and silanol groups in the removal of dyes from aqueous solution using diatomite, *Water Research*, 2005, 39, 922-932.
- [88] Al-Ghouti,MA; Khraisheh,MAM; Allen,SJ; Ahmad,MN. The removal of dyes from textile wastewater: a study of the physical characteristics and adsorption mechanisms of diatomaceous earth, *Journal of Environmental Management*, 2003,69,229-238.
- [89] Frost,RL; Ding,Z. Controlled rate thermal analysis and differential scanning calorimetry of sepiolites and palygorskites, *Thermochimica Acta* , 2003,397, 119-128.

- [90] Dogan,M; Alkan,M; Onganer,Y. Adsorption of methylene blue from aqueous solution onto perlite, *Water Air Soil Pollution*, 2000,120, 229-248.
- [91] Mohan, D; Singh,KP; Singh,G; Kumar,K. Removal of dyes from wastewater using fly ash, a low cost adsorbent, *Industrial Engineering and Chemical Research*, 2002,42, 1965-1976.
- [92] Rytwo,G; Tropp,D; Serban,C. Adsorption of diquat, paraquat and methyl green on sepiolite:experimental results and model calculations, *Applied Clay Science*, 2002,20, 273-282 .
- [93] Rytwo,G; Nir, S; Crespin,M; Margulies,L. Adsorption and Interactions of Methyl Green with Montmorillonite and Sepiolite, *Journal of Colloid and Interface Science*, 2000,222, 12-19.
- [94] Eren,E; Afsin,B. Investigation of a basic dye adsorption from aqueous solution onto raw and pre-treated sepiolite surfaces, *Dyes and Pigments*, 2007,73,162-167.
- [95] Wang,S; Ariyanto,E. Competitive adsorption of malachite green and Pb ions on natural zeolite, *Journal of Colloid and Interface Science*,2007, 314, 25-31.
- [96] Wang,S; Zhu,ZH. Characterisation and environmental application of an Australian natural zeolite for basic dye removal from aqueous solution, *Journal of Hazardous Materials B*, 2006,136, 946-952.
- [97] Ozdemir,O; Armagan,B; Turan,M; Celik,MS. Comparison of the adsorption characteristics of azo-reactive dyes on mezoporous minerals, *Dyes and Pigments* 2004,62, 49-60.
- [98] Meshko,V; Markovska,L; Mincheva,M; Rodrigues,AE. Adsorption of basic dyes on granular activated carbon and natural zeolite, *Water Research*, 2001,35,3357-3366.
- [99] Wang,S; Li,H; Xie,S; Liu,S; Xu,L. Physical and chemical regeneration of zeolitic adsorbents for dye removal in wastewater treatment, *Chemosphere*, 2006,65, 82-87.
- [100] Metes, A; Kovacevic,D; Vujevic,D; Papic,S. The role of zeolites in wastewater treatment of printing inks, *Water Research*,2004, 38, 3373-3381.
- [101] Chen,H; Zhao,Y; Wang,A. Removal of Cu(II) from aqueous solution by adsorption onto acid-activated palygorskite, *Journal of Hazardous Materials*, 2007,149,346-354 .
- [102] Tsai,WT; Chang,CY; Ing,CH; Chang,CF. Adsorption of acid dyes from aqueous solution on activated bleaching earth, *Journal of Colloid and Interface Science*, 2004,275,72-78 .
- [103] Weng,CH; Pan,YF. Adsorption of a cationic dye (methylene blue) onto spent activated clay, *Journal of Hazardous Materials*, 2007,144, 355-362 .
- [104] Al-Futaisi,A; Jamrah,A; Al-Hanai,R. Aspects of cationic dye molecule adsorption to palygorskite, *Desalination*, 2007,214, 327-342 .
- [105] Orthman,J; Zhu,HY; Lu,GQ. Use of anion clay hydrotalcite to remove coloured organics from aqueous solutions Separation and Purification *Technology*, 2003, 31,53-59 .
- [106] Holzheu,S; Hoffmann, H.Adsorption Study of Cationic Dyes Having a Trimethylammonium Anchor Group on Hectorite Using Electrooptic and Spectroscopic Methods, *Journal of Colloid and Interface Science*, 2002,245,16-23 .
- [107] Yue, QY; Li,Q; Gao,BY; Yuan,AJ; Wang,Y. Formation and characteristics of cationic-polymer/bentonite complexes as adsorbents for dyes, *Applied Clay Science*, 2007, 35, 268-275 .

-
- [108] Liu,P; Guo,J. Polyacrylamide grafted attapulgite (PAM-ATP) via surface-initiated atom transfer radical polymerization (SI-ATRP) for removal of Hg(II) ion and dyes, *Colloids and Surfaces A: Physicochemical and Engineering Aspects*, 2006,282/283, 498-503 .
- [109] de-Lisi,R; Lazzara,G; Milioto,S; Muratore,N. Adsorption of a dye on clay and sand: Use of cyclodextrins as solubility-enhancement agents, *Chemosphere*, 2007,69,1703-1712.
- [110] Corobea,MC; Uricanu,V; Donescu,D; Radovici,C; Serban,S; Garea,S; Iovu,H. Poly(vinyl acetate)-clay hybrids prepared via emulsion polymerization, assisted by a nonionic surfactant, *Materials Chemistry and Physics*, 2007,103, 118-126.

Chapter 12

**THE BEAUTY OF COLORS: THE YELLOW
FLAVONOLS IN SCIENCE AND ART**

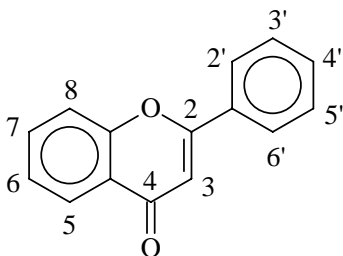
Aldo Romani

University of Perugia, Perugia, Italy

ABSTRACT

Dyes extracted from plants have been used for centuries for coloring materials. In this paper, typical behaviors of some naturally occurring colorants belonging to the class of flavonoids are presented. Their structures derive from that of flavone (2-phenylbenzopyrone), which is colorless, whereas hydroxy derivatives absorb UV and blue light, so appearing yellow colored. Current interest in flavonoids is mainly due to their varied biological activity in medicine, but also to their use as colored components in works of art (tapestries, carpets, miniatures).

The color of hydroxy-substituted flavonoids (flavonols) can be markedly modified by changing the pH or bonding with different metal ions, therefore, it critically depends on the acidity and the presence of metals in the environment. The absorption and emission spectra generally shift to the red by increasing the pH, due to stabilization of anionic forms. The number and sequence of acid-base dissociation steps depend on the number and position of the hydroxy-substituents. These aspects will be illustrated here with some significant examples concerning two naturally occurring colorants, old fustic and weld, and their main chemical components (morin, apigenin and luteolin). Absorption and fluorescence spectra recorded in solution provide the base for developing scientific investigations on the colorants spread on paper as watercolors or used in mordant dyeing of textiles.



Scheme 1.

INTRODUCTION

Since from prehistoric times, human kind have been fascinated by the beauty of colors and used in their artefacts those offered by nature, isolating colorants from minerals, plants and animals. It was only during the nineteenth century that synthetic colorants became available and today synthetic dyes and pigments are industrially produced and make more pleasant our everyday lives in coloring textiles, vehicles, toys and even foods. The sensitivity of the human eye to colors increases from red to yellow and then declines from yellow to violet. So yellow is highly visible and is perceived as the brightest color. Used in the past for signaling sickness on board ship and currently to highlight toxic or radioactive hazards, yellow has been sometimes considered as an unpleasant color, but looking at an expanse of sunflowers or even its representation by outstanding painters, we perceive it as a beautiful color in nature and art.

In this article, our interest is focused on naturally occurring colorants used in works of artistic or historical importance and in particular on some yellow colorants belonging to the class of flavonoids. In nature, these compounds, which are responsible for white, yellow and orange colors of a wide variety of flowers and fruits, occur mainly as glycosides (sugar derivatives). Their structures derive from that of flavone, the 2-phenylbenzopyrone (Scheme 1), which is colorless, whereas its poly-hydroxy derivatives (flavonols) absorb UV and blue light, so appearing yellow colored. An overview on naturally occurring flavones and flavonols has been recently published. [1]

Due to very strong absorption of UV-B light, they may play a role in preventing damage to leaves by ultraviolet radiation as also have insecticidal or insect-repellent properties. [2] This means that plants use flavonoids as defense and signaling compounds. Their beneficial effects are also felt by human kind: characterized as antioxidants, they offer protection against a number of degenerative diseases. Current interest in flavonoids is therefore mainly due to varied biological activity because of their antioxidant, antiradical and anti-inflammatory properties. [3-5] Moreover, they are also stimulating scientific interest in the field of the knowledge, restoration and conservation of works of art where they have been mainly used, such as tapestries, carpets, miniatures, or only used for glazing or final touches, as in paintings with different techniques. When used in painting, dyes are transformed into lakes, [6] which have constituted artists' palette and have been widely used from the Middle Age until the early nineteenth century. Lakes, to be applied on dry surfaces, are previously mixed with a binder (gum Arabic, egg, casein, oil) which allows the pigment to adhere to the

support. When these colorants are used for dyeing textiles, a mordant is generally needed. The mordant plays multiple functions: ensures brightness and fastness of the dye and also has influence on the final color obtained. Because of the chromatic changes they undergo interplaying with various metal ions, [7,8] flavonoids behave like ionochromic compounds. Chelating the transition metals also causes their potentiality to inhibit hydroxy radicals. [9]

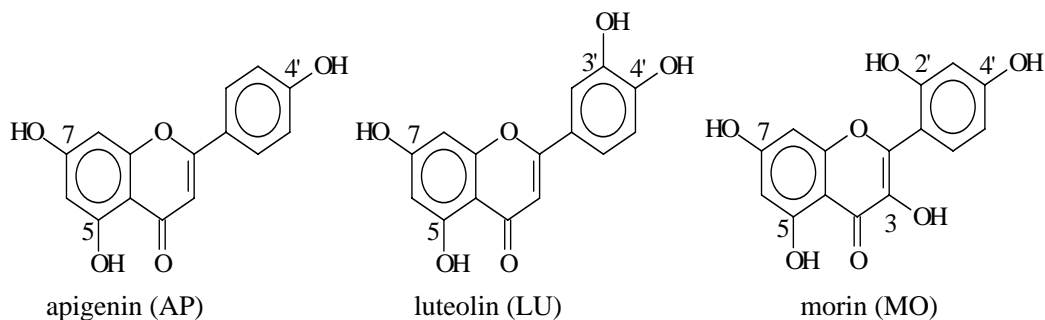
The color of flavonoids can also be markedly modified by changing the pH, [7,10] therefore, critically depends on the acidity of the environment. Thus, they are also acidichromic compounds. The effect of increasing the pH generally results in shifting the absorption and emission spectra of flavonoids to the red. Since artifacts are subject to atmospheric pollutants, they can undergo significant chromatic changes when the environment changes. During the last decades, acidic rains have been one of the most important causes of pollution and may have attacked painted artifacts. One of the reasons to study the effect of pH on the absorption and fluorescence spectra of colorants is to obtain information about the degradation processes in artistic works and to understand which was their original appearance. A further cause of degradation of organic dyes is exposure to light (photoageing) which generally results in bleaching and/or changes of color. [11]

These aspects will be illustrated here through some significant examples concerning the main chemical components of the naturally occurring colorants, fustic and weld. The most common yellow dyes were extracted from weld (*Reseda luteola* L.), young fustic (*Cotinus coggyria* Scop.), old fustic (*Chlorophora tinctoria* L. Gaud.), which came from the West Indies, and berries from *Rhamnus*. [12-14]

The chemical components here investigated are apigenin (5,7,4'-trihydroxyflavone, AP) and luteolin (5,7,3',4'-tetrahydroxyflavone, LU), both from weld, and morin (3,5,7,2',4'-penta hydroxyflavone, MO), from old fustic (Scheme 2):

It will be shown, starting from the less substituted molecule (AP), how the presence of additional hydroxyl groups and their position can alter the photophysical behavior in the flavone structure.

AP, which is present in small percentages in weld, is contained in many fruits and vegetables (parsley, onions, orange, tea, wheat sprouts, chamomile, etc). Being non-toxic and non-mutagenic, it is considered an important component in food and also a drug with high therapeutic potentials. [15]



Scheme 2.

LU is the main component of weld, which has been used since Roman times as an orange pigment, and until recently for dyeing silk. The mordant most frequently adopted to fix and stabilize the color on the fibre, has been alum, but other salts are also used to obtain different shades. With alum mordant, weld produces a yellow-orange color on wool and silk, with copper it generates a greenish yellow color, with iron it becomes olive. [12,16]

MO is the coloring principle of old fustic, [17] the wood of *Morus tinctoria*, a tree of Central America which is used principally for dyeing wool. Changing mordant, the color changes: with chromium it gives an olive green, with aluminum and tin, it is yellow, and with iron, morin becomes a deep olive brown.

METHODOLOGIES AND TECHNIQUES

To investigate organic coloring materials in works of art, several analytical techniques have been applied that were mainly aimed at identifying colorants, understanding their degradation processes and preventing further damages. The main difficulties in this study arise because coloring materials are often present in small quantities, mixed with other compounds and altered by ageing which results in molecular degradation and fading of the original colors. In addition, most techniques require samples to be removed for analysis. Generally, samples are very small in size, usually prepared as thin or cross-sections to be investigated by microscopic techniques, or to be transformed into solutions to be analyzed by some micro-destructive technique. So, there is a great need for analytical means that could perform molecular identification of very small amounts of dyes, present in complex mixtures of aged materials. Moreover, a non-destructive approach is highly desirable, especially for investigating significant operas of historical or artistic importance, and in particular when sampling is absolutely forbidden, as it happens for miniatures. Recent technological developments have made available improved diagnostic techniques and especially easily portable instrumentation for *in situ* non-destructive investigations on original artifacts.

So far, the most widely used techniques have been chromatography and spectroscopy.

For several years, chromatography has been widely applied for the identification of dyes on works of art, [18] mostly using UV– Vis spectrophotometry and mass spectrometry for detection. For example, very recently, high pressure liquid chromatography with mass spectrometric detection (HPLC-MS) has allowed the different components, which are present in the extracts from textiles, to be analyzed [19-23] as well as to investigate color fading on textiles [24] and recognize natural dyes and their degradation products in archeological objects. [25]

At the same time, considerable attention has been paid and efforts have been invested in extending the applications of spectroscopic techniques as methods for identifying materials used in paint. Absorption spectrophotometry has been proposed for identifying organic colorants [26] and fluorimetric techniques have been experienced to characterize both pigments and binders. [27-31]

Information that can be obtained from spectroscopic studies concerns several molecular properties that can be useful in diagnostic of colorants as well as to understand the complex mechanisms of their interactions with supporting materials and of ageing processes. From steady state UV-Visible absorption and fluorescence spectroscopy, wavelength range and

intensity measurements provide information about the electronic excitation energy and the nature of the excited state. From time-resolved techniques, additional information is obtained concerning the different and competing relaxation pathways of the electronically excited state.

Up to date, steady state spectroscopic techniques have been developed in portable version and applied to in situ measurements. [32] Only very recently, an instrument for time resolved fluorescence measurements was realized and tested in portable format. [33]

In situ character of spectroscopic techniques vs immovability of chromatographic techniques makes the former more easily handled in the study of artifacts. Nevertheless, due to the complementary information that they give, application of both is desirable and fruitful, as shown from recent works where these techniques were both applied in the same context. [34,35] Furthermore, modern conservative protocols strongly suggest to perform preliminary non-destructive measurements in order to minimize and guide the sampling procedures for micro-destructive analysis.

EFFECT OF pH ON UV-VISIBLE ABSORPTION AND FLUORESCENCE SPECTRA

The electronic absorption spectrum of flavonols is characterized by two principal bands, that can be related to the moieties constituting their skeleton. Theoretical calculations on the electronic transitions of 2- phenylchromones have been carried out considering that the absorption spectrum is formed by transitions localized on ortho-hydroxybenzaldehyde, chromone and the phenyl fragment. [36] The long-wave transition is mainly localized on the benzaldehyde fragment. The shorter wavelength transitions involve phenyl chromone and benzaldehyde moieties and have a pronounced charge transfer character (Figure 1). [36]

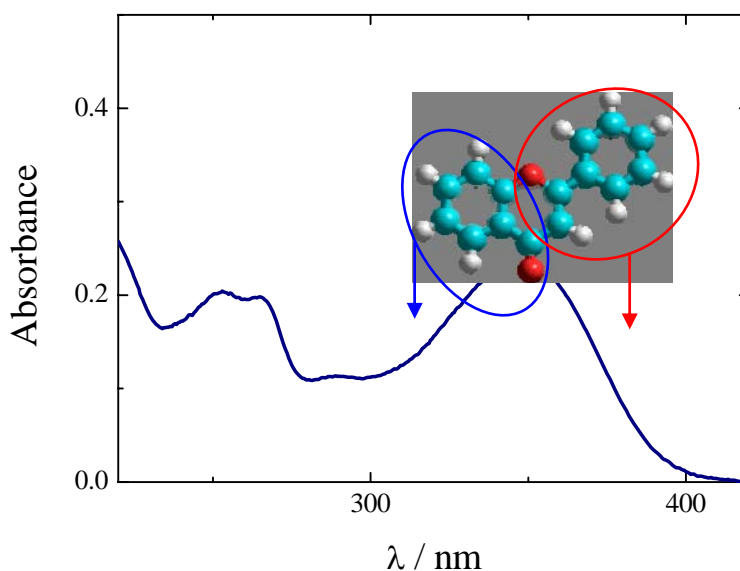


Figure 1. Typical absorption spectrum of flavones and band assignments.

The unsubstituted flavone (Scheme 1) is colorless since both absorption bands are located in the UV spectral region ($\lambda_{\text{max}} = 250$ and 294 nm).

When hydroxyl groups are introduced into the chromone fragment of flavone, they cause changes mainly in the transitions localized on that fragment, affecting the energy of benzaldehyde- and chromone-type transitions. For 5-hydroxy-, 7-hydroxy- and 5,7-dihydroxy-phenylchromones, the lower energy transition is expected to shift towards longer wavelengths, [36] thereby producing color.

When hydroxyl groups are introduced into the phenyl fragment an energy decrease and an increase in the oscillator strength should occur for the phenyl-localized transitions.

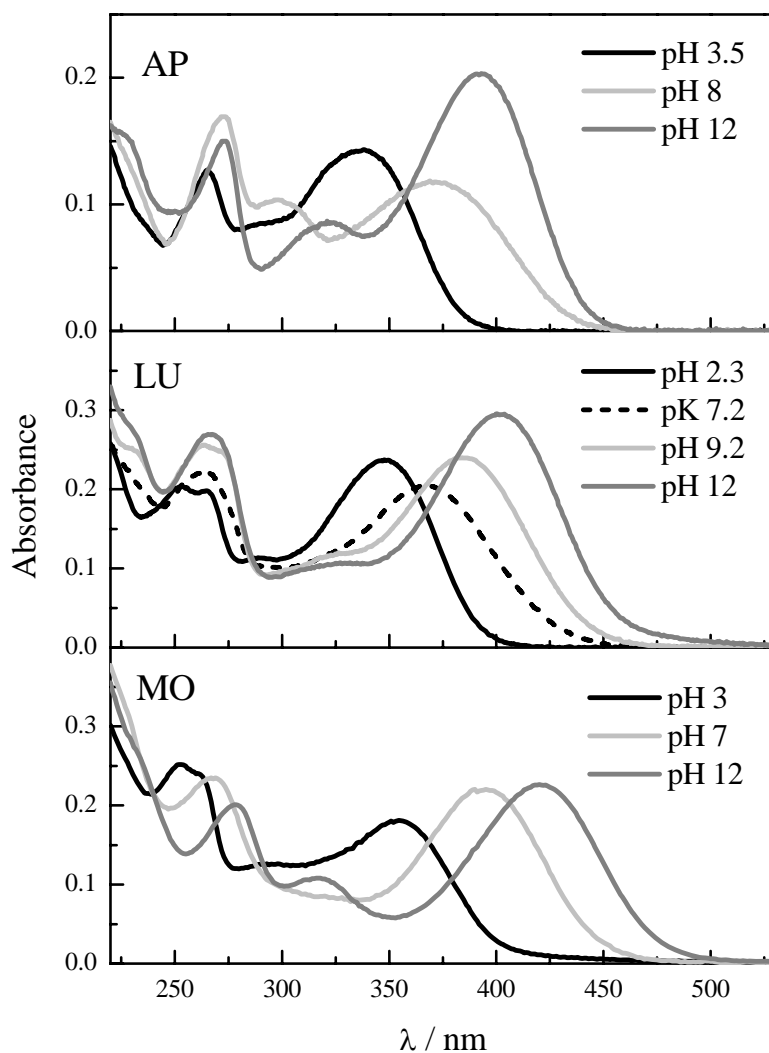


Figure 2. Absorption spectra of the three flavonols in water/methanol 2:1 (v/v) solution at different pH values.

Table 1. pK values and maximum absorption wavelengths (λ_{\max}) of flavonols in water/methanol 2/1 v/v

	AP	LU	MO
λ_{\max} / nm (neutral form)	265, 337	253, 348	253, 355
pK ₁	6.6	6.9	4.6
λ_{\max} / nm (monoanion)	372	366	395
pK ₂	9.31	8.6	10.3
λ_{\max} / nm (dianion)	392	384	421
pK ₃		10.3	
λ_{\max} / nm (trianion)		401	

The spectral behavior of the compounds here presented is in substantial agreement with expectation. When hydroxyl groups are introduced in the 2-phenylbenzopyrone skeleton to yield the flavonol structures (Scheme 2), the higher energy band is scarcely influenced, whereas the lower energy absorption shifts to the red and the solutions become pale yellow. The bathochromic shift increases with the number of hydroxyl groups, as can be seen in Table 1 (λ_{\max} values, first line) on going from AP to LU and to MO.

The spectrum also changes by changing the pH: a pH increase causes the color of the solutions to turn from pale yellow to intense yellow-orange, due to a further bathochromic shift of the absorption spectrum. The absorption spectra of AP, LU and MO at different pH values in water/methanol 2:1 (v/v) solution are shown in Figure 2.

The study of the pH effect on the absorption spectra of AP, LU and MO allows the pKs of these molecules to be determined and the absorption spectra of the neutral, mono-anionic and di-anionic ground state species to be assigned (Table 1 and Figure 2).

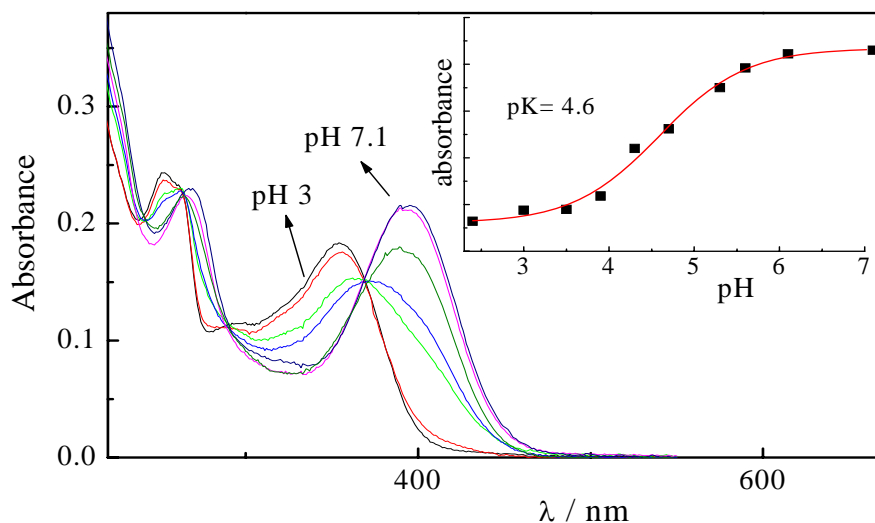


Figure 3. Evolution of the absorption spectrum of MO observed upon increasing the pH. Inset: spectrophotometric titration ($\lambda_{\text{anal}} = 395$ nm).

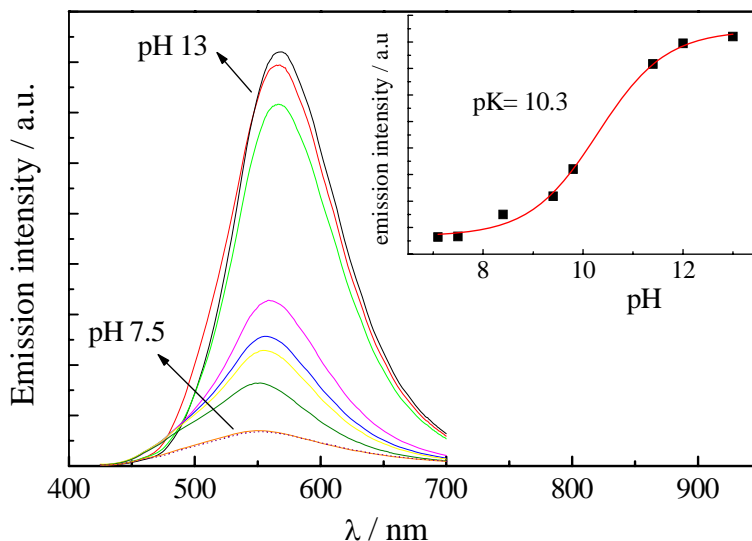


Figure 4. Evolution of the fluorescence spectrum of MO observed upon increasing the pH. Inset: fluorimetric titration ($\lambda_{\text{exc}} = 397 \text{ nm}$, $\lambda_{\text{anal}} = 560 \text{ nm}$).

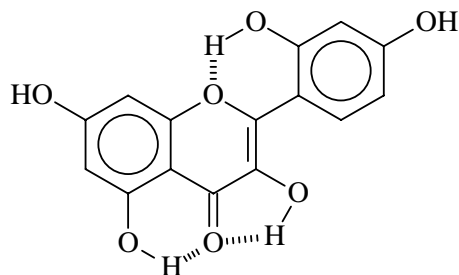
The pKs can be determined by both spectrophotometric and fluorometric titrations; when the values obtained match, as for the compounds under investigation, the excited state relaxes before acid-base equilibration is established in the excited state. The number and sequence of acid-base dissociation steps depend on the number and position of the hydroxyl groups. Examples of spectral evolution upon increasing the pH and of both kinds of titration are shown in Figures 3 and 4 for absorption and fluorescence, respectively.

In the case of LU, three deprotonation steps are detected ($\text{pK} = 6.9; 8.6; 10.3$), [7] only two for AP ($\text{pK} = 6.6; 9.3$) [7] and MO ($\text{pK} = 4.6; 10.3$), see Table 1. Other literature results for LU [37] are substantially in agreement with those here presented, whereas for MO, an intermediate value (8.37) has been also reported. [38] Since pK_1 values are substantially the same for LU and AP, we believe [7] that in both these molecules the first ionization involves the OH group in 7 position, which is the most acidic one due to the inductive electron-attracting effect of the 5-OH, stabilized by H-bonding to the carbonyl. In the mono-anions, the negative charge (O^- in 7 position) decreases the intrinsic acidity of the other OH groups in the molecule. Since the spatial distance between the two negative charges should be as large as possible to stabilize the di-anionic species, the second deprotonation probably occurs at the 4'-OH group in the 2-phenyl moiety. Its acidity is higher for LU than for AP (pK_2 lower for LU than for AP) because the inductive electron-attracting effect of the 3'-OH group on the nearby 4'-OH group increases its acidity.

The situation changes with MO, for which the neutral form results to be notably more acidic than those of AP and LU. The most relevant differences with respect to the other molecules are hydroxy-substitutions in the 3 and 2' positions. The 4-carbonyl can give intramolecular hydrogen bond with both the 5 and 3 hydroxyls. However, the bond with the 3-OH, yielding a pentatomic ring, is weaker than the one with the 5-OH that forms a six membered ring, which is sterically and energetically more favored. [39]. Moreover, the 2'-OH can be hydrogen-bonded to the ring oxygen, leading to a quasi-planar structure (Scheme 3), thus increasing the conjugation and therefore also the acidity.

This is what is experimentally observed. In accordance with others, [40] the first proton dissociation should occur at the 3-hydroxy group, whose greater acidity than any other hydroxyl group of MO is due to its close proximity to the electronegative 4-keto oxygen.

The fluorescence emission of flavonols (Table 2) is more or less intense depending on the structure and the degree of deprotonation. For LU, the emission cannot be detected for the neutral form whereas it is observed in the anionic forms. For AP, the fluorescence intensity, which is very weak in neutral solution (emission quantum yield, $\Phi_F \sim 4 \times 10^{-4}$), increases with increasing the pH and the emission maximum shifts to the red.



Scheme 3.

Table 2. pH effect on the fluorescence properties of the flavonols investigated and their anions in water/methanol 2/1 v/v

	AP	LU	MO
λ_{\max} / nm (neutral form)	440	not observed	524
λ_{\max} / nm (mono-anion)	470	518	545
λ_{\max} / nm (di-anion)	470/570	522	565
λ_{\max} / nm (tri-anion)		518	

Table 3. Photophysical parameters of MO in ethanol and ethanol/water solution (1/2 v/v): maximum wavelength (λ_{\max}), Stoke-shift ($\Delta\nu$), fluorescence quantum yield (Φ_F), fluorescence lifetime (τ_F), relative amplitudes of the two fluorescence components (A %), radiative (k_F) and non-radiative (k_{NR}) relaxation kinetic constants

Solvent (prevalent species)	λ_{\max} (nm)	$\Delta\nu$ (cm^{-1})	Φ_F	τ_F ($\times 10^{-9}$ s)	A %	k_F ($\times 10^8 \text{ s}^{-1}$)	k_{NR} ($\times 10^9$ s^{-1})
methanol	554	7330	0.046	2.63 0.41	9% 91%	1.1	2.3
pH 2.6 (neutral)	524	9085	0.014	2.33 0.07	12% 88%	2.0	14
pH 7.5 (mono-anionic)	545	7032	0.039	2.57 0.20	59% 41%	0.15	0.4
pH 13 (di-anionic)	565	6110	0.097	1.59 0.57	21% 79%	1.7	1.6

The most intense fluorescence is exhibited by MO ($\Phi_F = 1.4 \times 10^{-2}$, in neutral form), for which the results of a detailed photophysical study as a function of the pH are reported in Table 3.

It can be observed that two decay components are present with different contributions. The radiative (k_F) and non-radiative (k_{NR}) relaxation kinetic constants are calculated from the relationships:

$$k_F = \frac{\Phi_F}{\tau_F}$$

and

$$k_{NR} = \frac{1}{\tau_F} - k_F$$

taking into account only the principal component, thus the data obtained have to be considered merely indicative. The relative positions of the absorption and fluorescence spectra of MO at different pH are illustrated in Figure 5, from where the large Stoke-shifts are evident (see Table 3).

In order to interpret the peculiar behavior of MO - that is, the marked spectral Stoke-shift and the acidity higher than for the other two dyes - a comparison with the simpler parent molecule, the 3-hydroxyflavone, 3-HF (Scheme 4), can be useful.

The 3-HF has been object of notable interest as a model molecule suitable for studying intramolecular proton transfer in the excited state (ESPT). [41-44] Interaction of the 3-OH with the adjacent 4-carbonyl brings to a resonance stabilized tautomer (Scheme 5).

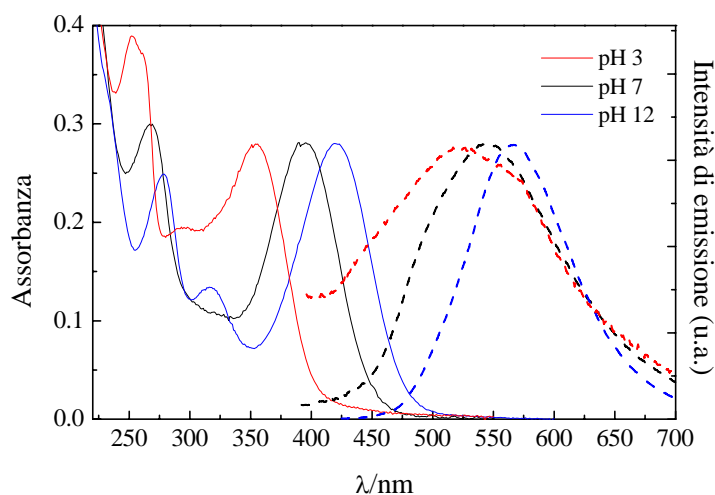
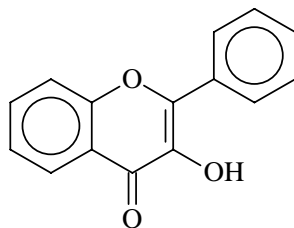
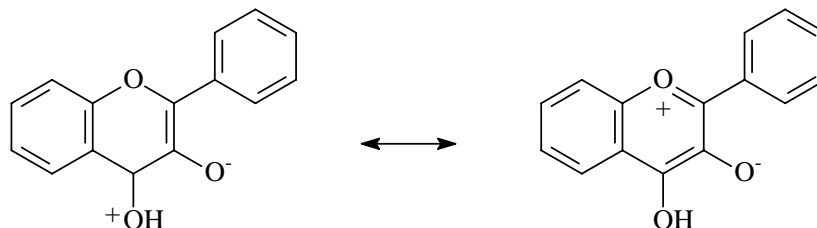


Figure 5. Normalized absorption and emission spectra of MO in MeOH-water (1/2 v/v) solution at different pH values.



Scheme 4.



Scheme 5.

In the ground state, the 4-keto form (Scheme 4) represents the molecular structure at the best, whereas proton transfer leading to the tautomer is favored in the excited state. For this compound emission bands were found at 406 and 531 nm in methanol. [45] The system has been represented by double-minimum potential energy surfaces. [46] In the ground state, the lowest minimum corresponds to the 3-hydroxy-4-keto form, whilst, in the excited state, the lowest energy corresponds to the tautomer. Therefore, the molecule absorbs in the 3-hydroxy-4-keto form but can fluoresce from the tautomeric form, being the tautomerization barrier very low in the excited state (Figure 6).

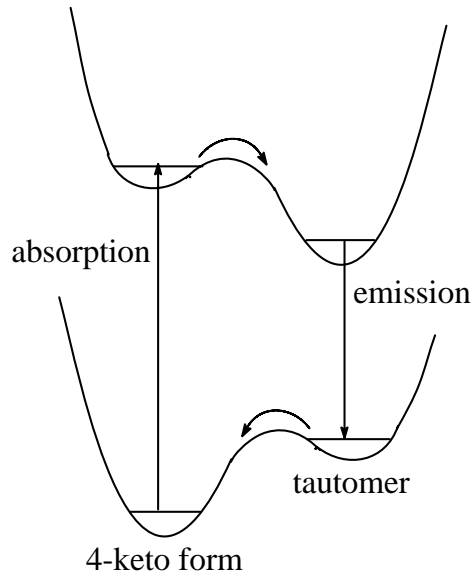


Figure 6. Model for ESPT.

This model explains the unexpected finding that a compound absorbing in the blue-violet, such as MO, exhibits a yellow-green emission, which arises from the tautomer.

EFFECT OF METAL IONS ON UV-VISIBLE ABSORPTION AND FLUORESCENCE SPECTRA

Flavonols exhibit a great propensity towards complex formation with metal ions. Metal ions are used in dyeing textiles as mordants to fix and stabilize the color on the fibre. Thereby, the interactions with metal ions significantly influence the color and fastness of the dye. [9] The ionochromism of flavonols will be here illustrated with some meaningful examples by analyzing the changes in spectral properties due to increasing additions of Al^{3+} and Ca^{2+} ions to their methanol solutions. Multi-step interactions are generally observed.

The occurrence of two consecutive reaction steps following additions of Al^{3+} to an AP methanol solution is illustrated in Figure 7.

In the first step (Figure 7 a), a new band grows at 382 nm, with maintenance of isosbestic points up to $[\text{Al}^{3+}] \sim 8 \times 10^{-5} \text{ mol dm}^{-3}$, which indicates a clean reaction. Further additions of Al^{3+} (from 10^{-4} to $10^{-3} \text{ mol dm}^{-3}$) induce spectral changes in the UV region, without significantly affecting the color band (Figure 7 b), which suggests that a subsequent interaction with the metal ion occurs. The spectral position of the bathochromic absorption is close to that reported for the complex of 5-hydroxyflavone (397 nm). [47,48] The association with Al^{3+} significantly enhances the fluorescence intensity of the dye, originating an emission band at 525 nm, with a large Stokes' shift ($\sim 7100 \text{ cm}^{-1}$). The fluorescence excitation spectrum is quite similar to the absorption one. The emission quantum yield, $\Phi_{\text{F}} = 1.2 \times 10^{-2}$ (with $[\text{Al}^{3+}] = 10^{-3} \text{ mol dm}^{-3}$), is almost two orders of magnitude larger than that of pure AP ($\Phi_{\text{F}} = 4 \times 10^{-4}$).

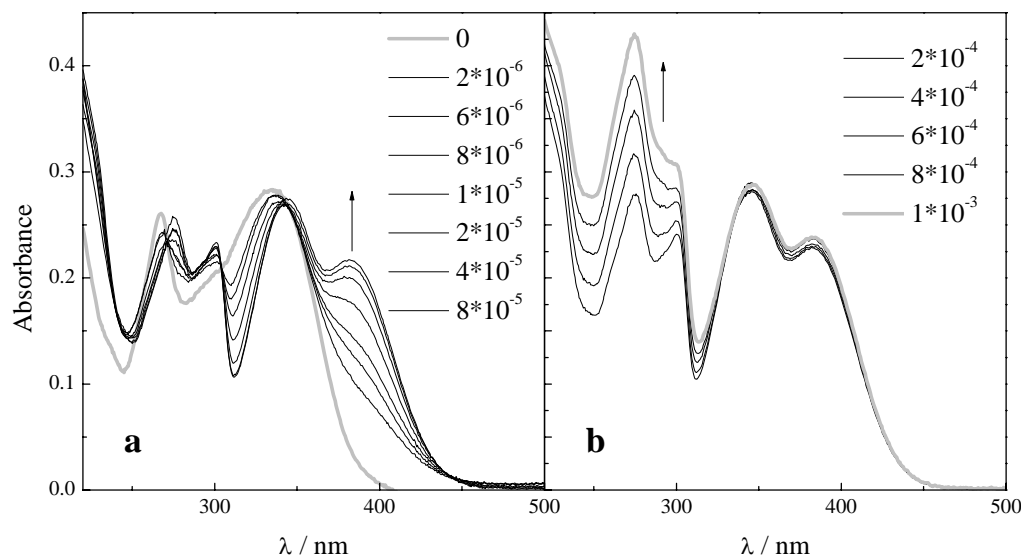


Figure 7. Effect on the absorption spectrum of the addition of Al^{3+} ions to a methanol solution of AP ($1.14 \times 10^{-5} \text{ mol dm}^{-3}$). a: $[\text{Al}^{3+}]$ 0 - $8 \times 10^{-5} \text{ mol dm}^{-3}$; b: $[\text{Al}^{3+}]$ 2×10^{-4} - $1 \times 10^{-3} \text{ mol dm}^{-3}$.

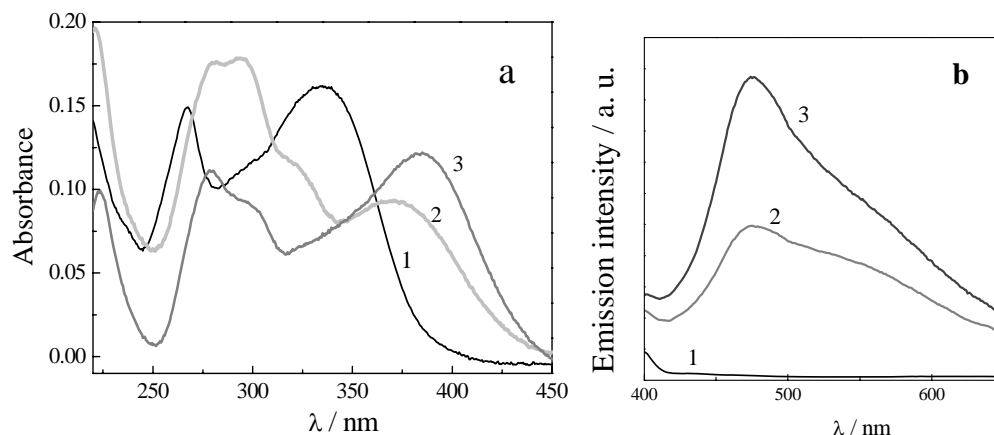


Figure 8. Absorption (a) and emission (b) spectra of a $8 \times 10^{-6} \text{ mol dm}^{-3}$ AP methanol solution. 1: $[\text{Ca}^{2+}] = 0$; 2: $[\text{Ca}^{2+}] = 0.2$ and 3: $[\text{Ca}^{2+}] = 0.5 \text{ mol dm}^{-3}$.

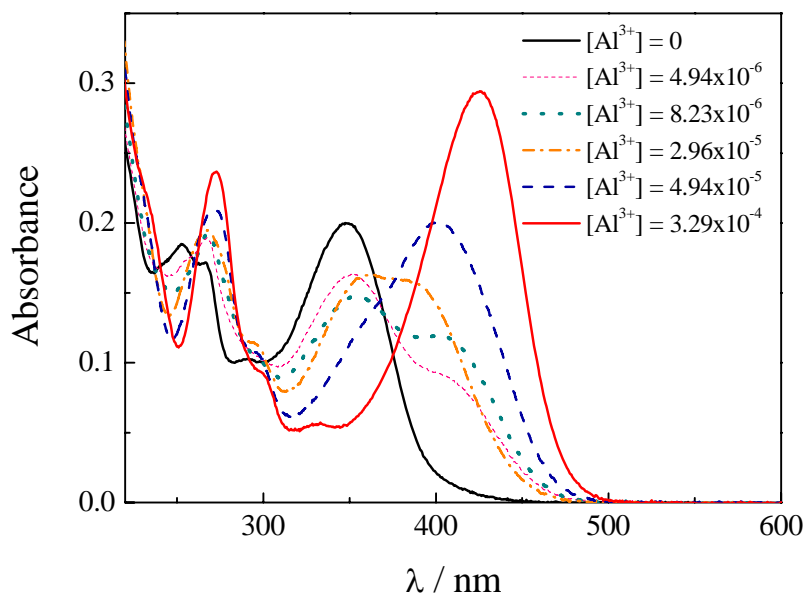


Figure 9. Effect of the addition of Al^{3+} ions ($[\text{Al}^{3+}] : 0 - 3 \times 10^{-4} \text{ mol dm}^{-3}$) on the absorption spectrum of a methanol solution of LU ($2.7 \times 10^{-5} \text{ mol dm}^{-3}$).

This dye is less prone to give complexes with calcium than with aluminium, since the spectrum starts to change only when the concentration of Ca^{2+} is approximately 10^3 times larger than that of AP. This could explain the fact that weld lakes containing calcium salts are less stable than those on hydrated alumina [49]. The absorption spectra of AP/ Ca^{2+} methanol solutions at different Ca^{2+} concentrations (spectra 2 and 3) are compared in Figure 8a with those of free AP (spectrum 1).

Isosbestic points are not maintained, even for restricted concentration ranges of Ca^{2+} additions. This denotes that complex formation occurs in overlapped steps. Here again, the fluorescence of the complex (Figure 8b) is markedly enhanced ($\Phi_{\text{F}} = 1.4 \times 10^{-2}$, at $[\text{Ca}^{2+}] = 0.5$

mol dm⁻³), compared with that of the free dye, and shows a maximum at 474 nm and a broad shoulder around 540 nm. The fluorescence maxima and intensities vary with the amount of added ions, further supporting the hypothesis that different molecular complexes are formed. Some similarities are observed between the spectra of the complexes and those of the deprotonated species.

Also LU exhibits a great affinity with metal ions. The overall spectral changes observed by adding Al³⁺ ions to a methanol solution of LU are shown in Figure 9. As can be argued from the spectra, multiple interactions occur, leading to an overall bathochromic shift of the color band; even in the UV region marked variations are observed.

The individual steps are tentatively separated in Figure 10 a and b. The first interaction occurs in the 10⁻⁶ – 10⁻⁵ mol dm⁻³ Al³⁺ concentration range; new bands appear at 267 and 402 nm and isosbestic points are maintained (Figure 10a).

In the 8 × 10⁻⁶ – 3 × 10⁻⁵ mol dm⁻³ [Al³⁺] range (Figure 10b), where the dye and the ion are present in comparable amounts, no isosbestic point is maintained and the global spectral pattern slightly shifts back to the blue. A regular spectral variation towards the red starts again when [Al³⁺] ~ 5 × 10⁻⁴ mol dm⁻³. The final limit spectrum ([Al³⁺] ≥ 10⁻⁴ mol dm⁻³) shows a bathochromically shifted, very intense band at 425 nm. Absorbances at selected wavelengths, corresponding to the most significant spectral variations, that are plotted as a function of the total Al³⁺ added (logarithmic scale) in Figure 11, illustrate the multiple-step complexations.

Additions of Al³⁺ ions induce fluorescence emission in the non-fluorescent methanol solutions of LU, with a maximum initially located at 570 nm (from [Al³⁺] = 10⁻⁶ to 10⁻⁵ mol dm⁻³), which shifts to the blue (540 nm at [Al³⁺] ~ 3 × 10⁻⁵ mol dm⁻³) and newly to the red (553 nm) upon further Al³⁺ additions (Figure 12). This trend parallels that of the absorption. The emission quantum yield is exceptionally high ($\Phi_F \sim 1$). Therefore, fluorescence is the unique relaxation path of the excited state and this explains the high lightfastness of the chelate [8].

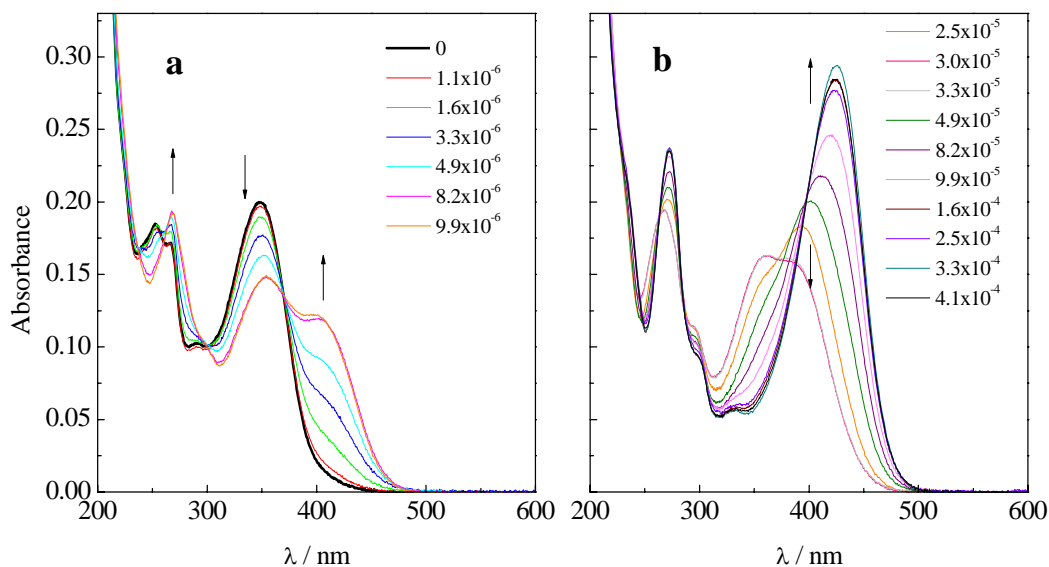


Figure 10. Evolution of the absorption spectrum of LU (2.7×10^{-5} mol dm⁻³) upon addition of Al³⁺ ions. *a*: [Al³⁺] = 0 – 10⁻⁵ mol dm⁻³; *b*: [Al³⁺] = 2.5×10^{-5} – 4.1×10^{-4} mol dm⁻³.

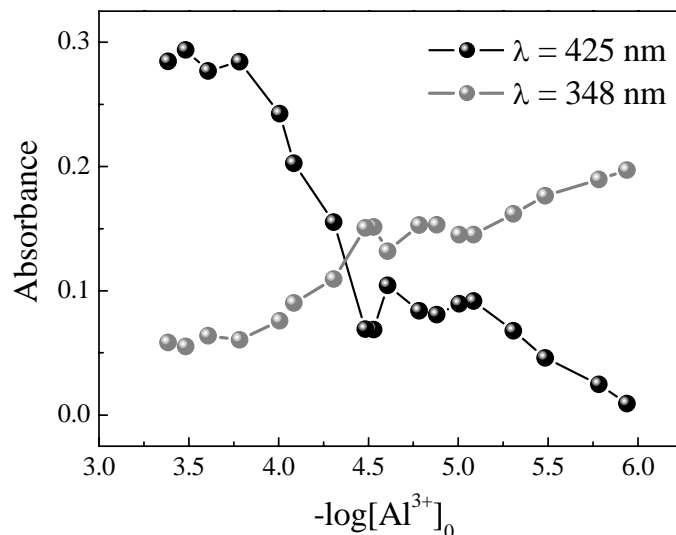


Figure 11. Absorbances of LU solutions (2.7×10^{-5} mol dm $^{-3}$) at two selected wavelengths as a function of $-\log[Al^{3+}]$.

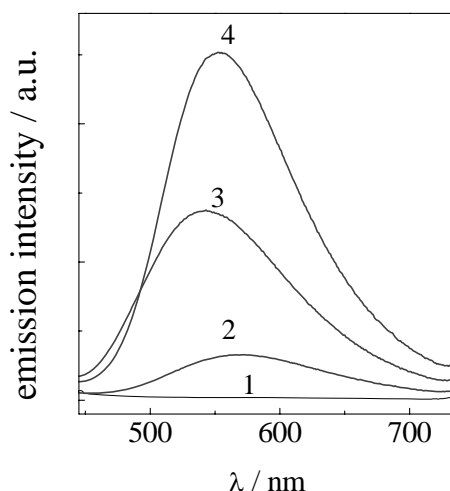


Figure 12. Emission spectra of the LU- Al^{3+} adducts at increasing concentrations of Al^{3+} ions. 1: $[Al^{3+}] = 0$; 2: $[Al^{3+}] = 5 \times 10^{-6}$; 3: $[Al^{3+}] = 2.5 \times 10^{-5}$ and 4: $[Al^{3+}] = 4 \times 10^{-4}$ mol dm $^{-3}$.

Similarly, also MO interplays with various metal ions. With Al^{3+} , the absorption color band has been reported to shift to 420 nm and the corresponding fluorescence peak at 500 nm [50], a spectral evolution that parallels that due to deprotonation. Later, other authors [40] found that Aluminum and morin form complexes of 1:1 and 1:2 and/or 1:3 (Al/MO) stoichiometry, but at low total MO concentrations only 1:1 species were prevalent, exhibiting an absorption maximum at 420 nm and an intense fluorescence emission (not observed by the authors in the absence of metal [40]) at 510 nm. Even for MO, the affinity towards Al^{3+} ions is larger than that towards Ca^{2+} ions. [40]

In the case of MO, where three different stoichiometry were foreseen for the chelates, [40] we can refer to the behavior of the model molecule 3-HF. For this compound a 1:2 (Al^{3+}/MO) stoichiometry complex is formed in methanol. [54] In the complex the normal fluorescence shifts to the red from 406 to 450 nm whereas that of the tautomer disappears, accompanied by an increase of quantum yield of almost two orders of magnitude [45]. It can be thought that for MO the 3-hydroxy-4-keto is the most easily attackable binding site, in accord with its weaker intramolecular hydrogen bond. The spectral findings support this hypothesis.

CONCLUSION

Despite the small structural differences among the three molecules here considered, their spectral properties are well distinguished, even in the absence of additives, as shown by the absorption and fluorescence spectra that shift to the red with increasing the number of the hydroxyl groups.

They behave as acidichromic and ionochromic molecules since in aqueous solution their color changes as the pH changes and in methanol solution their color changes upon metal ion additions.

The absorption and emission maxima move to the red and the fluorescence intensity increases on increasing the pH. Deprotonation increases conjugation, thus producing the bathochromic effect, and enhances the emission, probably because of the greater compactness of the ion where the contribution to deactivation of the excited state through OH vibrations is lost.

Chelation has an effect parallel to deprotonation. It shifts the absorption spectrum to the red, induces fairly intense fluorescence emission in LU ($\Phi_F \sim 1$) and significantly enhances the intensity of AP and MO fluorescence (by almost 100 times). The appearance (or enhancement) of emission when chelation occurs can be attributed to the lack of excited state vibrational relaxation through hydrogen bonding with the solvent, similarly to what happens for the deprotonated forms. The intense fluorescence induced by metal ions can be used as a diagnostic probe for these flavonols. Viceversa, flavonol fluorescence provides a very sensitive signal for the presence of metal ions. It also explains the light-fastness of the colorant on textiles dyed using a mordant, since the absorbed light is given up as emission, thus reducing possible photochemical degradation processes.

In conclusion, an alkaline environment, and much more the presence of chelating agents, transform molecules which are not (or poorly) fluorescent and weakly yellow colored into efficient fluorophores and intensely yellow colored materials.

The results here reported can be generalized to the whole wide class of naturally occurring yellow flavonols.

REFERENCES

- [1] Brahmachari, G.; Gorai, D. *Current Organic Chemistry* 2006, 10, 873-898.
- [2] Mayer, F.; Cook, A. H. *The Chemistry of Natural Coloring Matters*; Reinhold Publishing Corp.: New York, 1943.
- [3] Burda, S.; Oleszek W. *J. Agric. Food Chem.*, 2001, 49, 2774–2779.
- [4] Dangles, O.; Dufour, C.; Bret, S. *J.C.S. Perkin 2* 1999, 737-744.
- [5] Galati, G.; Moridani, M. Y.; Chan, T. S.; O'Brien, P. *J. Free Radic. Biol. Med.* 2001, 30, 370–382.
- [6] Kirby, J. *Dyes in History and Archaeology* 1987, 6, 12-18.
- [7] Favaro, G.; Clementi, C.; Romani, A.; Vickackaite, V. *J. Fluorescence* 2007, 17, 707-714.
- [8] Smith, G. J.; Thomsen, S. J.; Markham, K. R.; Andary, C.; Cardon D. *J. Photochem. Photobiol. A* 2000, 136, 87-91.
- [9] Fiorani, M.; De Sancitis, R.; De Bellis, R.; Dacha, M. *Free. Radic. Biol. Med.* 2002, 32, 64-72.
- [10] Schipfer, R.; Wolfbeis, O. S.; Kniezinger A. *J. Chem. Soc. Perkin Trans. 2* 1981, 1443–1448.
- [11] Giles, C. H. *Applied Chemistry* 1965, 15, 541-550.
- [12] Hofenk de Graaff, J. H. The colorful past, Origins, chemistry and identification of natural dyestuffs; Abegg-Stiftung: Riggisberg, (CH), *Archetype Publications Ltd.*: London (UK), 2004.
- [13] Ferreira, E. S. B.; Quye, A.; McNab, H.; Hulme A. N. *Chem. Soc. Rev.* 2004, 33, 329–336.
- [14] Schweppe, H. *Handbuch der Naturfarbstoffe*; Vorkommen, Verwendung, Nachweis: Hamburg (DE), 1992.
- [15] Havsteen, B.H. *Pharmacol. Ther.* 2002, 96, 67-202.
- [16] Cerrato, A; De Santis, D; Moresi, M. *J. Sci. Food Agric.* 2002, 82, 1189-1199.
- [17] Herzig, J. *Monatshefte fuer Chemie* 1897, 18, 700-713.
- [18] Wouters, J. *Nouvelles de la Science et des Technologies* 1995, 13, 453-455.
- [19] Szostek, J.; Orska-Gawrys, I.; Surowiec, M.; Trojanowicz, J. *J. Chromatogr. A* 2003, 1012, 179–192.
- [20] Ferreira, E. S .B.; Quye, A.; McNab, H.; Hulme, A. N. *Dyes in History and Archaeology* 2003, 19, 13-18; *ibid.* 19-23.
- [21] Puchalska, P.; Poleć-Pawlak, K.; Zadrozna, I.; Hryszko, H.; Jarosz, M. *J.Mass Spectrom.* 2004, 39, 1441–1449.
- [22] Surowiec, I.; Quye, A.; Trojanowicz, M. *J. Chromatography A* 2006, 1112, 209-217.
- [23] Nowik, W. Dyes. *Liquid chromatography in Encyclopaedia of Separation Science*: Wilson, I.D., Adlard, T. R.; Cooke, M.; Poole C. F. Academic Press, London, (UK) 2000, 2602.
- [24] Colombini, M. P.; Andreotti, A.; Baraldi, C.; Degano, I.; Łucejko, J. *J. Microchemical Journal* 2007, 85, 174–182.
- [25] Surowiec, I.; Szostek, B.; Trojanowicz, M. *J. Sep. Sci.* 2007, 30, 2070 – 2079.
- [26] Billmeyer Jr., F. W.; Kumar, R.; Saltzman, M. *J. Chem. Ed.*, 1981, 58, 307.

- [27] Renè de la Rie, E. *Stud. Conserv.* 1982, 27, 1; *Stud. Conserv.* 1982, 27, 65; *Stud. Conserv.* 1982, 227.
- [28] Shimoyama, S.; Noda, Y. *Dyes in History and Archaeology* 1994, 13, 14-26.
- [29] Miliani, C.; Romani, A.; Favaro, G. *Spectrochim. Acta Part A* 1998, 54, 581-588.
- [30] Miliani, C.; Romani, A.; Favaro, G. *J. Phys. Org. Chem.*, 2000, 13, 141-150.
- [31] Clementi, C.; Miliani, C.; Romani, A.; Favaro G. *Spectrochim. Acta Part A* 2006, 64, 906-912
- [32] Clementi, C.; Miliani, C.; Romani, A.; Favaro G. Proceedings Conferenza Nazionale sulle prove non distruttive: Monitoraggio e Diagnostica. 10° Congresso Nazionale AIPnD, 2003, 110.
- [33] Romani, A.; Favaro, G. Italian patent request nr. RM2008A000002 registered January 4th 2008; Romani, A.; Clementi, C.; Miliani, C.; Brunetti, B. G.; Sgamellotti, A.; Favaro, G. *Appl. Spectr.* submitted.
- [34] Clementi, C.; Nowik, W.; Romani, A.; Cibir, F.; Favaro G. *Anal. Chim. Acta* 2007, 596, 46.
- [35] Van Bommel, M. R.; Vanden Berghe, I.; Wallert, A. M.; Boitelle, R.; Wouters, J. *J. Chromatography A*, 2007, 1157, 260-272.
- [36] Roshal, A. D.; Mitina, V. G.; Orlov, V. D.; Ponomarev, O. A.; Sukhorukov, A. A.; Fialkova S. V. *Functional Materials*, 1997, 4, 121-127.
- [37] Wolfbeiss, O. S.; Begun, M.; Geiger, H. *Monatshefte fuer Chemie* 1987, 118, 1403-1411.
- [38] Herrero-Martinez, J. M.; Sanmartin, M.; Rosés, M.; Bosch, E.; Ràfols, C. *Electrophoresis* 2005, 26, 1886-1895.
- [39] Cornard, J. P.; Vrielynck, L.; Merlin, J. C.; Wallet, J.C. *Spectrochim. Acta Part A* 1995, 51, 913-923.
- [40] Browne, B. A.; McColl, J. G.; Driscoll, C. T. *J. Environ. Qual.* 1990, 19, 65-72.
- [41] Strandjord, A. J. G.; Barbara, P. F. *J. Phys. Chem.* 1985, 89, 2355-2361.
- [42] Strandjord, A. J. G.; Smith, D. E.; Barbara, P. F. *J. Phys. Chem.* 1985, 89, 2362-2366.
- [43] Woolfe, G. J.; Thistlethwaite, P. J. *J. Am. Chem. Soc.* 1981, 103, 6916-692.
- [44] Itoh, M.; Tokumura, K.; Tanimoto, Y.; Okada, Y.; Takeuchi, H.; Obi, K.; Tanaka, I. *J. Am. Chem. Soc.* 1982, 104, 4146-4150.
- [45] Protti, S.; Mezzetti, A.; Lapouge, C.; Cornard, J. P. *Photochem. Photobiol. Sci.* 2008, 7, 109-119.
- [46] Sengupta, P. K.; *Kasha M. Chem. Phys. Lett.* 1979, 68, 382-385.
- [47] Cornard, J. P.; Merlin, J. C. *J Mol. Struct.* 2001, 569, 129-138.
- [48] Cornard, J. P.; Merlin, J. C. *J Mol. Struct.* 2003, 651-653, 381-387.
- [49] Saunders, D.; Kirby, J. *National Gallery Technical Bulletin* 1994, 15, 79-97.
- [50] White, C. E.; Hoffman, D. E.; Magee, J. S. jr. *Spectrochim. Acta*, 1957, 9, 105-112.
- [51] Deng, H.; Van Berkel, G. J. *J. Mass Spectr.* 1998, 33, 1080-1087.
- [52] Dušan M.; Vesna K. *J. Serb. Chem. Soc.* 2007, 72, 921-939.
- [53] Cornard, J. P.; Boudet, A. C.; Merlin, J. C. *Spectrochim. Acta Part A* 2001, 57, 591-602.
- [54] Boudet, A. C.; Cornard, J. P.; Merlin, J. C. *Spectrochim. Acta Part A* 2000, 56, 829-839.

Chapter 13

**INORGANIC PIGMENTS TO COLOUR
CERAMIC MATERIALS:
STATE OF THE ART AND FUTURE TRENDS**

Federica Bondioli

Università di Modena e Reggio Emilia
Dipartimento di Ingegneria dei Materiali e dell'Ambiente
Via Vignolese 905, 41100 Modena (I)

ABSTRACT

Inorganic natural and synthetic pigments produced and marketed as fine powders are an integral part of many decorative and protective coatings and are used for the mass coloration of many ceramic materials, including glazes, ceramic bodies, and porcelain enamels. In all these applications, pigments are dispersed (they do not dissolve) in the media, forming a heterogeneous mixture. In conclusion, powders used for colouring ceramics must show thermal and chemical stability at high temperature and must be inert to the action of molten glass (frits or sintering aids). These requirements limit ceramic pigments to a very small number of refractory systems which are fully reacted and relatively inert to the matrix in which they are dispersed. This need for great chemical and thermal stability has dominated research and development in recent years. In this chapter the state of the art will be reported focusing in particular on the specific systems used in this industrial field. The advantages and the limitations of different colours will be underlined with particular emphasis on the current problems and on the possible way to solve them.

INTRODUCTION

Ceramic manufactures have spent the last several years trying to automate repetitive steps, rationalize the production flow and decrease costs without decreasing productivity and production quality. Considerable progress has been made in the development of automated

systems, marking the factory operative 24 hours a day with reduced staff. Studies on how to obtain a better flexibility for the process have resulted in corresponding new developments in kilns, which guarantee faster firing (by 35 to 50 minutes), low energy consumption and optimal quality due to precise vitrification process control and the realization of technology for a continuous production line [1-4]. Conditions for fast firing include the ability to place the products in one layer; a good heat distribution and transfer; the ability to experimentally determine the critical heating rate by carefully monitoring the temperatures of the surface, center and other locations of an actual ceramic product for which the initial firing curve has been designed; the formulation of new, more reactive bodies; the increase of the firing temperatures and the reduction of the particle size to improve the kinetic of the reactions that determine firing; the ability to use more stable glazes based on eutectic compositions; and, finally, the necessity to use more stable coloring solutions. Among all the possible methods of colouring (precipitation, melting of transition metal ions, scattering, etc) the most efficient way, both for technical and economical reasons, to give a ceramic product a stable colouration is still by using pigments introduced inside glazes or bodies before their firing and sintering.

Inorganic natural and synthetic pigments produced and marketed as fine powders are an integral part of many decorative and protective coatings and are used for the mass coloration of many materials, including glazes, ceramic bodies and porcelain enamels.

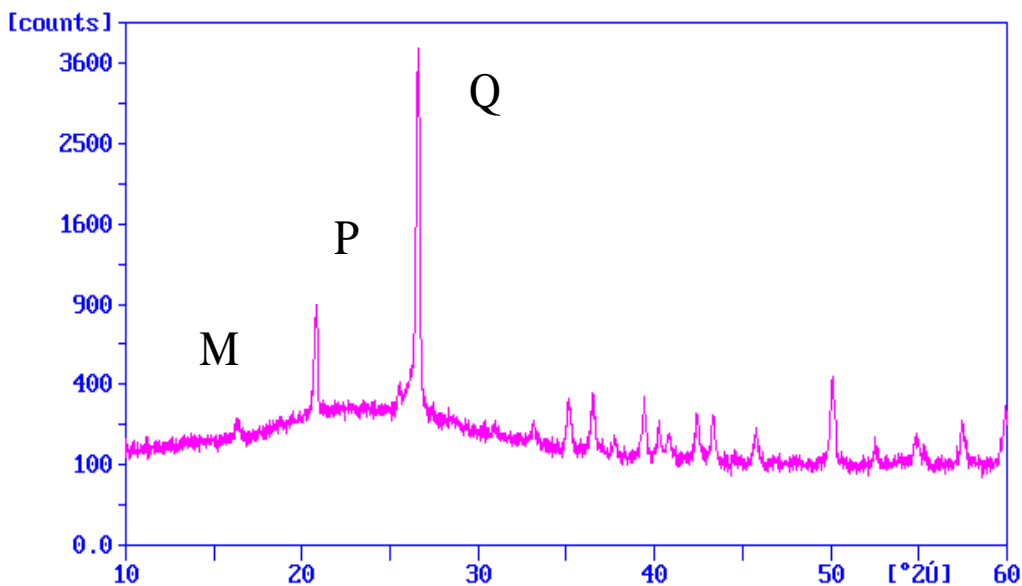


Figure 1. XRD analysis of porcelainized gres coloured with pink $(\text{Cr,Al})_2\text{O}_3$ pigment: characteristic peaks related to pigment structure are visible after firing (Q=quartz; M=mullite; P=pigment)

In all these applications, the pigments are dispersed in the matrix which is to be coloured, forming an heterogeneous mixture. Since they do not have to dissolve in the matrix, one of the most important characteristics of pigments for ceramic materials is their thermal stability at the sinterisation temperature and their chemical stability in respect to the phases, also often

of a fluid nature, that during firing are formed by the action of sinterisation promoters or vitreous frits (Figure 1).

Selecting the right pigments for ceramic decorating requires a basic understanding of pigment characteristics and their reactions with other parts of the production process. Moreover it is rare to be able to find a single pigment that exactly matches the desired color for a given application. Therefore, it is important to understand how to combine colors to give the desired results.

DEFINITION

In general, a pigment is defined as being any solid, organic/inorganic, white, black, coloured or fluorescent that is insoluble in the matrix into which it is incorporated and which does not react chemically or physically with it [5]. By dwelling on pigments in the strict sense of the above definition, only inorganic pigments, containing metallic chromophores as elements of the first transition and rare hearths can be used for the coloration of ceramic materials, both on a large scale as well as being used as an integral part of decorative and protective coatings (glazes).

A classification of ceramic pigment can be done in various way but if we consider how chromophores are incorporated in the base crystalline structure, then it is possible to reach a classification that leads to the distinction of three classes:

- (I) *structural or idiochromatic pigments*: the chromophore is incorporated into the crystalline structure. In this case, therefore, the coloured element is an integral part of the structure as in spinel type pigments, for example CoAl_2O_4 (Figure 2) [6];
- (II) *solid solutions or allochromatic pigments*: the chromophore enters the crystalline structure replacing one of the structural ions; the quantity can vary according to the amount of tonality desired, but, however, it is not stoichiometric. The structure, by itself, is uncoloured but becomes coloured by the introduction, in interstitial or substitutional sites, of chromophoric elements. This is the case of ions V(IV) or Pr(IV) in the ZrSiO_4 crystal that gives, respectively, a blue and a yellow coloration to the white matrix of ZrSiO_4 (Figure 3) [7];
- (III) *inclusion pigments*: coloured oxides that have usually a high instability upon contact with glass, supports or glazes, are made usable through their encapsulation via sinterisation in a vitreous or crystalline matrix, that is extremely stable from a chemical or thermal point of view. Pigments that belong to this class are therefore formed by two, or more, insoluble, phases, that, however, from a colour point of view, act as a single, chromatic unit. The colour does not develop, therefore, by introducing an ion into a crystalline network or by the formation of a solid solution, but rather the crystal which is responsible for colour is occluded in a stable matrix during the process of sinterisation. Examples of this class of pigment are the chromophore molecule $\text{Cd}(\text{S}_x\text{Se}_{1-x})$ and Fe_2O_3 included in a matrix of silicate of zirconium [8-9] or Fe_2O_3 in SiO_2 (Figure 4) [10].

The classification widely used for synthetic inorganic pigments on an international scale is still, however, the American *DCMA (Dry Colour Manufacturers Association)*, that subdivides all crystalline inorganic pigments according to colour, crystallographic class, spectrum of X-ray diffraction and prevailing use. On the basis of this classification, the codes EINECS and CAS were subsequently allocated to each colorant, making the identification of the products easier from a commodity knowledge and toxicological point of view.

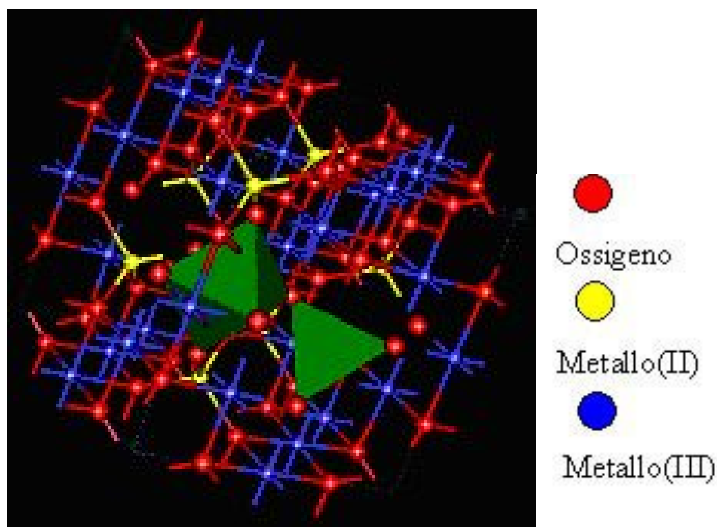


Figure 2. An exemplum of an idiochromatic pigments: cubic spinel structure of CoAl_2O_4

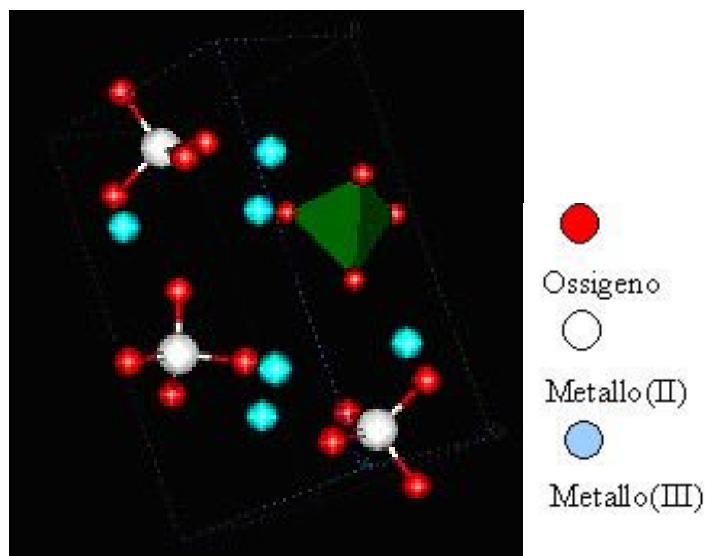


Figure 3. An exemplum of an allochromatic pigment: the zircon structure of $(\text{Zr,Pr})\text{SiO}_4$.

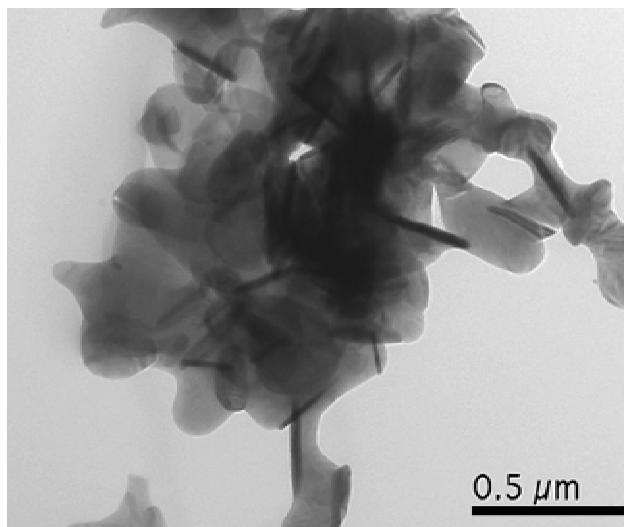


Figure 4. An exemplum of an inclusion pigment: acicular Fe_2O_3 crystals in SiO_2 matrix.

Finally, among all possible methods of classifying inorganic pigments, the one historically used but by no means satisfactory, is that of sub-dividing these pigments into natural and synthetic. Natural pigments are available in nature and for a very long time were the only pigments known and used. For thousands of years, in fact, humankind has beautified its world and expressed its feelings through colour. The first known graffiti date back over 30,000 years to the Palaeolithic: pigments used for colouring the caves at Chauvet-Pont-d'Arc, in South-Eastern France, were black, red and yellow (Figure 5). The pigments based on iron oxides were, and in some cases still are (e.g. the typical red hue of bricks, *brick red*), the most widely used of all the natural pigments. Red, associated with the colour of blood, was indeed the appropriate colour for symbolizing the meaning of life and death. The word "hematite" (the mineral from which many iron-based pigments are derived) comes from the Greek *hema* meaning "blood". Pigments based on iron oxides provided the basic colours for ancient artists, from Egypt to India to China.



Figure 5. Graffiti found in the caves at Chauvet-Pont-d'Arc (France).

Simple natural oxides and spinels are still widely used in industry, displaying excellent colouring properties and being available at a low cost [11]. One of the main drawbacks to their use in mass production is the difficulty in reproducing them if they come from different locations. In fact, they can have a different genesis and, therefore, prove to be poorly homogeneous and generally contain different types and quantities of impurities.

In conclusion, synthetic pigments for ceramic material must show the following characteristics:

- they can be produced at a higher degree of chemical purity and uniformity;
- they can be studied and formulated to obtain colourings that are difficult to obtain using natural inorganic pigments;
- they show greater thermal and chemical stability that allows them to be used in the coloration of materials obtained at high temperatures;
- they are obviously more expensive than natural inorganic pigments since they require different steps of preparation (selection of raw materials at a high level of purity, thermal process of calcination, grinding, quality control, corrections....).

The most common industrial method is based, in fact, on the calcinations of well controlled precursors containing chromophore elements. In such cases, the reaction at the solid state provides for the use of different types and amounts of mineralisers (up to 10% in weight) with the aim of reducing the temperature of synthesis, that varies from 500 to 1400°C according to the system used.

In a ceramic dictionary, mineraliser is a substance that acts in such a way as to lower the temperature of synthesis of the final product and/or promote the sinterisation. In the field of pigments, these substances can essentially be subdivided into two classes:

1. *promoting mineralisers*: increase the solid state reactivity by the formation of a fluid phase (molybdates, borates, halogenides), by the formation of a volatile phase (fluorures with pigments containing silica), by superficial activation or through the control and stabilisation of the oxidation conditions (nitrates);
2. *structural mineralisers*: are those that contain ions that are capable of structurally integrating themselves in the pigment crystal structure producing a cell distortion. This change can cause either an increase in the solubility of the chromophore or a modification of the intensity of the crystalline field on the ion and therefore, leading to a variation in the coloration of the structure.

For exemplum the formation mechanism of praseodymium-doped zircon [12], a market leader ceramic pigment in the high temperature color range, were defined in presence of mineralizers as a two steps mechanism. At lower temperature (Figure 6a), the silicate formation is facilitate by a viscous phase, which is constituted by the mixture of mineralizers (NaF and NaCl mixture which melts at 726°C), while increasing temperature, the reaction occurs between SiO₂ and mineralizers to produce a volatile halide (SiX₄, where X is a halide element) that successively reacts with ZrO₂ and praseodymium oxide (Pr₆O₁₁) at the ZrO₂ sites (Figure 6b).

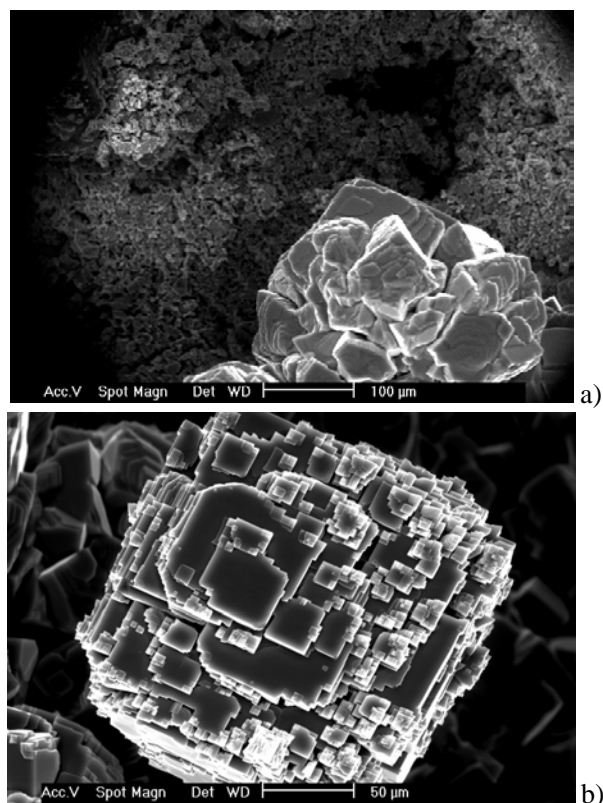


Figure 6. Reaction mechanism of $(\text{Zr,Pr})\text{SiO}_4$ yellow pigment formation determined by ESEM analysis at high temperature. 866 (a) and 900°C (b).

The role of mineralizers in the solid state synthesis to promote or induce selectively the formation of certain species is not however well understood. As a matter of fact different mineralizers seem to have different effects and in many case more than one mechanism is involved in their action. Is therefore necessary to examine processes that occur at very high and wide temperature range.

PIGMENT PROPERTIES AND APPLICATIONS

Aside from the pigment's structure and classification, the value of a ceramic pigment result from its physical-optical properties. These are primarily determined by pigments crystal structure, physical characteristics (particle size and distribution, particle shape, agglomeration, etc.) and chemical properties (composition, purity, stability, etc.). However, the two most important physical-optical properties of pigments to be considered are the ability to color the environment in which they are dispersed and to make it opaque.

Otherwise, a significant limitation on the selection of ceramic pigments is the predefinition of processing parameters imposed during coating application and firing. An engobe or body stain must be stable during tile firing, usually between 1200-1300°C. An underglaze color, or a coloured glaze, must be stable during glost firing, usually between

1000-1200°C, and to corrosion by molten glaze ingredients. An overglaze or glass color needs to be stable during decorative firing applied to it, usually between 625-775°C. A more important factor here is corrosion by the molten flux in the application (generally lead oxides).

Physical Properties

Particle size and particle size distribution are the most fundamental measured properties of powders. Those properties impact a number of ceramic pigment characteristics. Those affected the most are color, color strength and rheological properties. For inorganic pigments to be useful in most applications, they must have an average particle size between 0.1 and 10 µm. Selecting an optimum particle size distribution is a compromise between considerations of dissolution rate, agglomeration of the pigment, loss of strength on milling, uneven surface smoothness and pigment strength. The optimum particle size is the largest size that gives adequate dispersion and adequate strength in letdowns.

Optical Properties

The opacity of a pigment lies in its ability to prevent the transmission of light through the medium. The opacity of a pigments is a function of the pigment particle size and of the difference between the pigments refractive index and that of the media in which the pigment particles are dispersed.

For ceramic pigments to be effective as scattering, the discrete substance must have a refractive index that differs appreciably from that of the glassy phase, because the greater the difference in refraction index between the matrix and the scattering phase, the greater the degree of opacity. Because generally the refraction index of glazes is 1.5-1.6, the refraction index of opacifiers must be significantly higher or lower of this value. Some possibilities are reported in Table I. In the opacifier choice are important also other factors; i.e. titanium dioxide, in the anatase form, has a very high refraction index and is the most used for applications below 1000°C. At around 850°C, in fact, anatase transforms in rutile that absorbs in the visible region developing a cream color.

Regarding the particle size, a pigment with particles size approaching that of the wavelength of light provides the maximum scattering of light. However, excessive fineness leads to increase the solubility in the glaze and glassy phases and difficulties in dispersion.

The pigment color is uniquely described by its spectral reflectance curve (Figure 7). This curve shows the fraction of light reflected at each wavelength from a material. Obviously, the colour of an object is entirely characterised by its spectral behaviour, that is from knowing which wavelengths of light it absorbs, which it reflects and which it diffuses. It is not practical, however, that every time one wants to characterise or reproduce a colour, one has to measure and refer to the spectral-photometric curves on graphs, or rather the transmission and reflection in all its visible ranges.

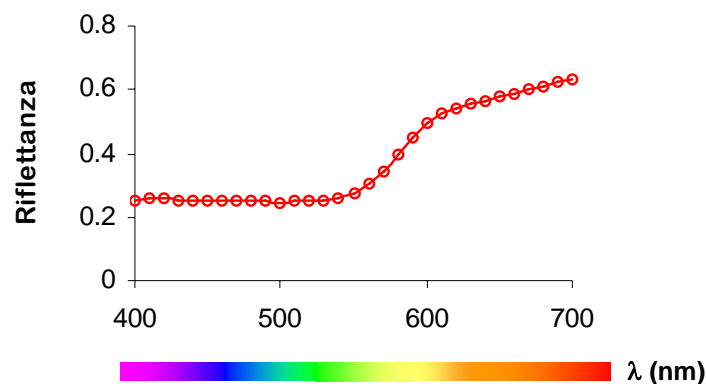


Figure 7. The reflectance curve of a red pigment.

In the industrial practice, however, to exclude the particular conditions of illumination and the physio-psychological response of the observer, a color is defined using the CIELab method (L^*, a^*, b^* system) that measures the absorption intensity in the visible [13]. The formulation, as well as the adjustment of glazes color in the ceramic tile industry, however, is still empirical, making its control difficult. Moreover a common problem is the hue variation between the products that not only impairs the product appearance but also increases stock management costs, and is prejudicial to product competitiveness. This hue variations can be caused by process variables as i.e. pigment and opacifier preparation conditions that affect the pigments and opacifiers physical and chemical properties.

The control of these color problems is generally made using the CIELab system, through the measure of L^* , a^* , b^* parameters, obtained by the analysis of the reflectance curves provided by a spectrophotometer. But despite this system have some limitations. In fact there isn't a systematic relation between the L^* , a^* , b^* values and the concentration of added pigments. The L^*, a^*, b^* coordinates of glazes prepared with different percentages of black pigment (spinel Ni-Fe-Cr) and opacifier ($ZrSiO_4$) are showed in Figure 8 [14]. The L^* parameter (lightness) reduces as the pigment concentration is increased, as expected due to the major quantity of particles pigment that absorbs the light. The a^* and b^* parameters, instead, have aleatoric changes with difficult interpretation underlining the difficulty to use these parameters for the formulations of colors.

The model developed by Kubelka-Munk (1931) [15] supported in reflectance data can be instead very helpful to explain the color variation. This model relates the reflectance (R) for every wavelength to the absorption (K) and scattering (S) of light by pigment particles. This means that for every frequency of the visible spectrum, every component of a formulation possesses a coefficient of absorption, K , and a coefficient of scatter, S . In particular, when the layer of the absorbing scattering material is so thick that no light penetrates through the layer (opaque surfaces), the relationship described the Kubelka–Munk theory, taking into account also the Saunderson correction [16], is given by:

$$\frac{K_{\lambda}}{S_{\lambda}} = \frac{(1 - r_{\lambda})^2}{2r_{\lambda}} \quad (1)$$

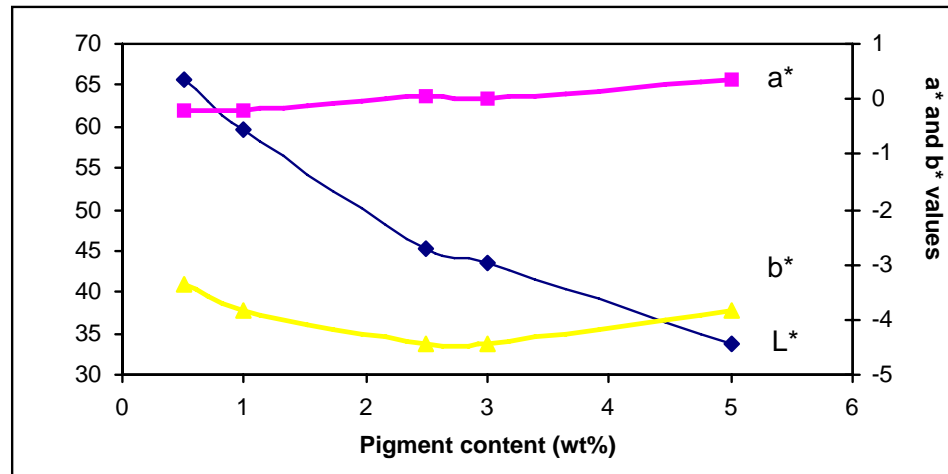


Figure 8. L^* , a^* , b^* parameters as a function of the percentage of black pigment (spinel Ni-Fe-Cr) in the glazes.

where r_λ is the decimal fractional reflectance ($0 < r < 1$) measured at the wavelength λ with the specular component excluded. Another important equation for color matching, developed by Duncan [17], demonstrates the additivity in a mixture M of the absorption and diffusion contributions of each component:

$$\frac{K_\lambda}{S_\lambda} = \frac{\sum c_n K_{n(\lambda)}}{\sum c_n S_{n(\lambda)}} \quad (2)$$

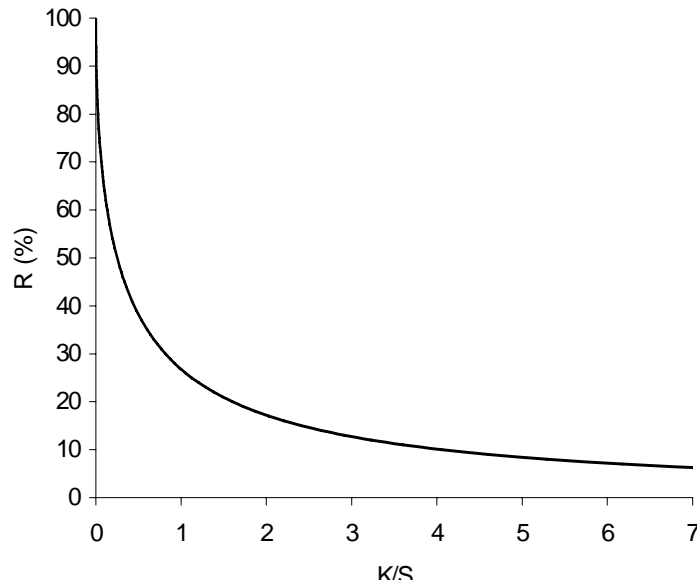


Figure 9. Graph showing the relationship of reflectance, R_∞ , and the ratio K/S according to Eq 1. [Patton, 1973]

where c_n is the fractional concentration ($0 < c_n < 1$) of the n th pigment in the mixture; $K_n(\lambda)$ the absorption coefficient of the n -th pigment in the mixture at the wavelength λ ; and $S_n(\lambda)$ the scattering coefficient of the n -th pigment in the mixture at the wavelength λ . To make use of this theory, one needs a straightforward way to obtain these coefficients from measurable reflectance data. In particular knowing these coefficients for all the components of a mixture it is possible to obtain the reflectance value, and thus the color, that it can be developed by a mixture, changing the components concentration. In fact:



$$(3)$$

where for the Saunderson correction for an opaque glaze surface, $R_\lambda = r_\lambda / (0.576 + 0.4r_\lambda)$ with r_λ decimal fractional reflectance ($0 < r < 1$) measured at the wavelength λ with the specular component excluded.

The simple equation 1 tells that if the absorption, K , is increased and the scattering, S , is kept constant, the reflectance is decreased. Thus adding a strongly absorbing pigment, such as black, to a system its reflectance decreases; while if S is increased keeping K constant, the reflectance is increased. Thus adding a strongly scattering pigment, such as white, to a system the reflectance increases; if both the absorption and scattering are changed by the same quantity, this will not affect the resulting reflectance or the color (Figure 9). Thus changing the amount of pigment in a system the reflectance does not change when hiding is complete. Remembering that the nature of the color is described by its spectrophotometric curve and that at each wavelength the Kubelka-Munk model describes how the reflectance is determined, one can visualize how the curve may be modified in a desired way.

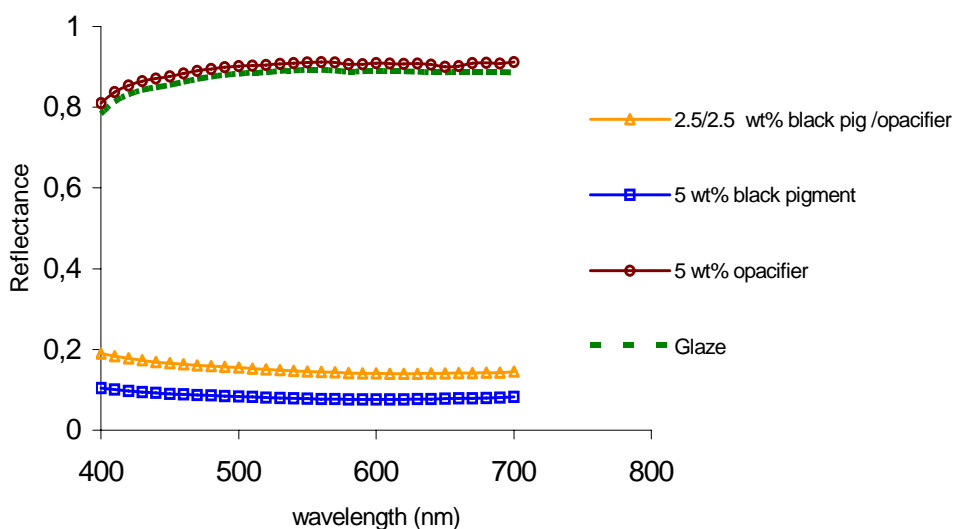


Figure 10. Reflectance curves of the four glazes samples prepared to calculate the Kubelka-Munk coefficients.

In the spinel black pigment exemplum, from equation 1 and with the reflectance curves of the prepared glazes (Figure 10) is possible to calculate the values of the K/S (absorption light caused for the pigment) at each wavelength of visible region as a function of the concentration of pigment added (Figure 11). The Figure shows that the K/S value increases as the quantity of the pigment is increased with a small exponential tendency starting from 3.0% of pigment. This indicate that with the Kubelka-Munk model is possible to relate systematically the color with the quantity of pigment added.

The reflectance curves predict by Kubelka-Munk model are showed in Figure 12. An excellent agreement between the experimental curves and the model curves was observed. The deviations are lesser that 2.0%.

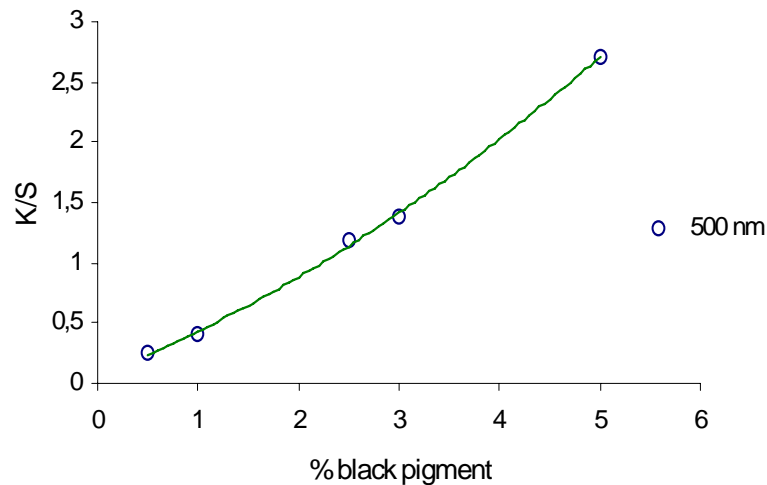


Figure 11. Kubelka-Munk absorption as a function of the black pigment (spinel Ni-Fe-Cr) concentration in the glaze.

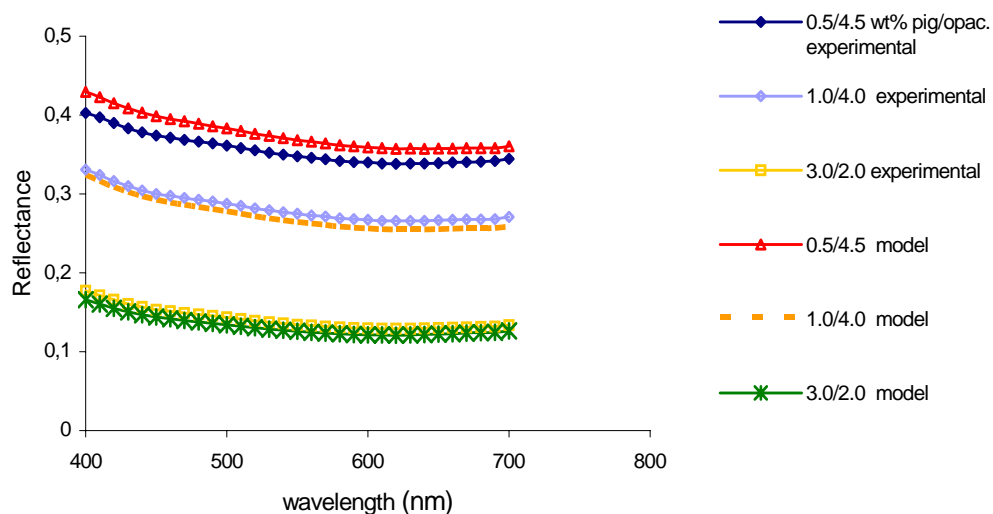


Figure 12. Reflectance curves obtained experimentally in comparison with that determined by the Kubelka-Munk model for same glazes prepared.

Algorithms in the formulation of colors is not a new idea in the industry [18-21]. It has been approximately 50 years since the first colorant formulation algorithm was reported introducing the color matching concept. With color matching, we mean the ability to reproduce, through mixing few fundamental pigments, whatever type of color experimentally measured by using algorithms of calculus. In activities such as printing, the textile industry, plastics or cold paints, this technique represents a working tool, long consolidated and efficient in supplying rapid solutions to many of the chromatic problems of the production process, both those of a formulating and qualitative nature. The advantages are a lot: the possibility to have an elevated number of colors using a low number of pigments; the rejects elimination in the pigment production because the color matching equipment can prepare in real time the required volume of mixtures; the possibility to replicate colors also if it is not available the pigment with the target color; the possibility to adjust errors in the preparation of the color; etc. These aspects should be certainly advantageous also in the ceramic field where many producers now use different typology of applicators (flat, drum, rotary with photoincisive rollers serigraphic machines, ink jet printing) that, in many plants, frequently cohabit. All these factors normally leads to use a wide range of decorating materials (often a question of hundreds of colored products) that make up a complex system to manage both at a warehouse and production level. However, despite various attempts (studies intended to predict the color of a ceramic glaze can be found with interesting results in literature), in ceramic tiles sector the technology of colorant formulation via software has not found a fertile field. For the final result, in fact, some specific limitations, characteristics of a ceramic material that develops its color during firing, have to be considered. The most important is connected with the thermal and chemical stability that pigments must have towards the molten glass (frits or sintering aids) developed during the firing cycle at high temperatures: the same pigment, in fact, can develop slightly different colors depending on both firing temperature and chemical composition of glaze or ceramic body to color. Aspects such as the grain size distribution, the chemical and physical interaction between pigments and glazes, variations during the firing process, the final appearance of the ceramic tile surface, make up a series of elements that influence in a determining way not easily controllable the development of colors. All the most modern formulation softwares are essentially based on the application of the Kubelka–Munk theory, the most widely used in industrial sectors, in the form used for opaque surface coatings. However, in order to determine the coefficient of absorption, K , and the coefficient of scatter, S , for all the components in a mixture it is necessary to introduce a series of approximations.

Artificial neural networks (ANN) are computational models based on biological neural networks. They can be used to represent complex relationships between inputs and outputs or to find patterns in data. ANN are applied within a large number of cases, both in science and industrial fields, thank to their highly mathematical flexibility. The models can be used to carry out simulation in a very quickly and inexpensive way. Finally, they can be used to optimize one or more independent parameters in the same time so reducing costs in a very efficient way, if the model was correctly built. Samples were prepared using thirty industrial pigments and one frit for wall tiles. Mixing the pigments, seventy nine samples were prepared in a fast ball mill and applied as water suspension on fired wall tiles. After drying, the samples were fired in an industrial firing cycle. The color data were analyzed using the open source software JOONE (Java Object Oriented Neural Engine) [22], in order to verify if ANN is an available method to carry out colour matching in ceramic tile production. Efficiency of a

neural network architecture depends by a number of factors. Among the most important ones: architecture of the network; number of hidden layer; number of neurons for each hidden layer; number of epochs; activation function used; learning parameters etc. The validity is restricted to the conditions used to produce the experimental data. When the fixed parameter are changed, the network is not able to predict the right mix of pigments, but if they are respected the results are very interesting. A important advantage is the possibility to avoid the time consuming step of determination of K and S parameters in Kubelka-Munk method, because of it is possible to use directly the data obtainable by the production database to built the neural model.

Chemical Reactivities

Selecting the right pigments for ceramic decoration requires a basic understanding of pigment characteristics and their reactivity with other constituents of the ceramic material.

The most important glaze consideration is probably the presence or absence of ZnO in the glaze. The pink $(Al,Mn)_2O_3$, green-black $(Fe,Cr)_2O_3$, Victoria-green garnet, orchid chrome-tin cassiterite and pink chrome-tin sphene are not stable in the presence of zinc oxide mainly due to the formation of spinels. The brown iron ematite, pink chrome-alumina spinel, brown iron-chromite spinel, brown zinc-ferrite spinel and brown zinc-iron chromite spinel requie high ZnO concentration. High calciumoxide concentration is required for adequate stability of Victoria-green carnet and chrome-tin splene. CaO should be avoided when using pink chrome-alimuna spinel, brown zinc-ferrite spinel and brown zinc-iron-chromite spinel. Pigments containing chromium(III) oxide are incompatibile with pigments containing tin oxide.

The presence or absence of PbO in a glaze affects some pigments. Victoria-green and cobalt-black pigments are stronger in a high PbO glaze. Blue zircon-vanadium, yellow zircon-praseodymium and pink gray zircon pigments are stronger in low PbO and lead-free glazes.

FUTURE TREND

To contribute to the innovation process in the traditional ceramic field and to maintain a high level of competitiveness and market penetration, the research has to be directed to both the transfer and the application of the scientific knowledge to the industrial practice. This has to be realized by means of the critical revision of the different production steps allowing the design, realization, development and industrial application of new materials, essentially of ceramic or glassy nature, with higher aesthetical and functional performances.

A strong distinctive element of the scientific and technological development of the last ten years is represented by the increasing interest and by the remarkable research dedicated to nanomaterials. In fact it has been observed that, when a material is constituted by nanometric component, different properties, interesting from a technological point of view, are also considerably changed with respect to the materials science laws. This evidence starts up the development of completely innovative materials and applications. This is therefore an area

that, using a multidisciplinary approach, looks to revolutionize all the most important technological and productive fields.

The most important exemplum is the application of innovative technology solutions such as the digital printing to the ceramic field. The research is mainly devoted to the optimisation of the ink-jet printer for ceramic tiles already present on the market but also to the formulation of specific ceramic inks. In fact, the emerging field of digital printing onto ceramic bodies requires a four color set of pigments to produce process color. The way to obtain such colors are different but the research is mainly devoted to innovative nanosized pigments with improved aesthetical properties. The objective is pursued through the development of synthesis methods capable to limit or eliminate the problems belonging to this specific technology when applied to the ceramic industrial process, i.e. high wear of the printing heads. From these considerations the optimal solution of these problems can be identified in the nanopowders technology allowing to obtain the complete range of colour with the right hue and grain size distribution narrower with respect to the micro powders.

It is thus clear that the correct running of the synthesis method and the knowledge of the parameters that influence the dimensions, the grain size distributions and the morphologies of nanoparticles become strategically important. There are a very high number of production techniques to obtain nanostructured powders. In particular, two approaches can be individualized:

- Top down that is based on the successively granulometric refinement of a micrometric powder mainly by milling, lithography or etching;
- Bottom up. In this field the methods can be subdivided in three categories:
 - condensation from vapour phase;
 - wet chemical methods (Figure 13);
 - solid state process.

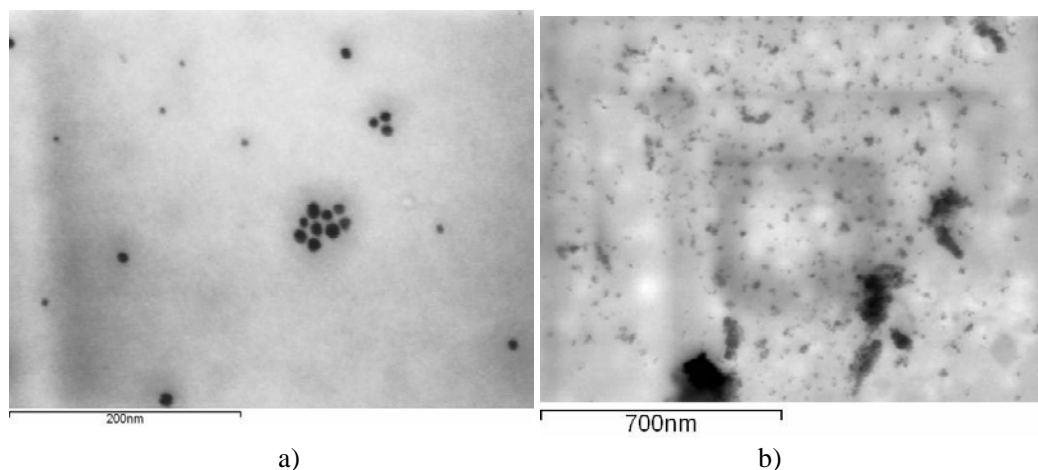


Figure 13. Exempla of powders obtained by chemical method (micrographs courtesely given by Colorobbia Italia, ParNaSos Products: Au particle (a); titania particle (b))

The nanostructured pigments are characterized by a high thermal and chemical stability. In Figure 14 the mineralogical analysis on a Co-blu pigment both with a micro and nano grain size distribution. While the MICRO pigment was obtained by solid state reaction generally starting from Co_3O_4 and $\text{Al}(\text{OH})_3$, the NANO pigment was obtained by condensation from vapour phase. Mineralogically both the pigments are constituted by CoAl_2O_4 (ICDD #00-003-0896) with the spinel general formula AB_2O_4 . The NANO pigment has a minor crystallinity as underlined by both the lower peak intensity and the higher peak broadening. To evaluate the thermal and chemical stability, the NANO pigment were mixed (2 wt%) with two commercial frits for high temperature (a transparent gloss and a white gloss respectively) and the obtained mixture studied by a heating optical microscope. The obtained results show the stability of the nanoparticles in the used frits (Figure 15-17).

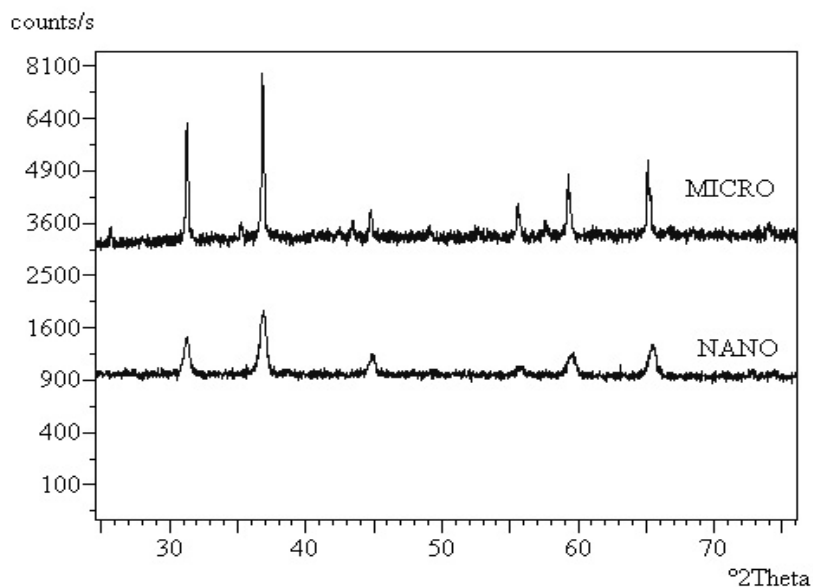


Figure 14. X-ray diffraction patterns of both NANO and MICRO Co-blu pigment.



Figure 15. Stability of the CoAl_2O_4 nanoparticles in two commercial frits for high temperature.

REFERENCES

- [1] Proven, A. *Interceram*, 1990, 39[7], 39-44.
- [2] Schoppe, K.H. *Interceram*, 1990, 39[3], 17-22.
- [3] Avallone, A. *Interceram*, 1995, 44[3], 186-188.
- [4] Sladek, R. *Interceram*, 1995, 44[3], 176-179.
- [5] *Pigment Handbook*, Ed. by P.A. Lewis, J. Wiley & Sons, New York, Vol. 1, p. VII (1988).
- [6] Ferrari, A.M.; Leonelli, C.; Manfredini, T.; Miselli, P.; Monari, G.; Pellacani, G.C. In *Advances in Science and Technology 3A*; Vincenzini, P.; Ed.; Techna: Faenza, IT; 1995; pp 83-90.
- [7] Eppler, R.A. *Am. Ceram. Soc. Bull.* 1987, 56[2], 213-217.
- [8] Lambies, V.; Rincòn, J.M. *Trans. J. Br. Ceram Soc.* 1981, 80, 105-108.
- [9] Berry, F.J.; Eadon, D.; Holloway, J.; Smart, L.E.; *J. Mat. Sci.* 1999, 34, 3631-38.
- [10] Bondioli, F.; Ferrari, A.M.; Leonelli, C.; Manfredini, T. *Mat. Res. Bull.* 1998, 33[5], 723-729.
- [11] Bondioli, F.; Ferrari, A.M.; Leonelli, C.; Manfredini, T. *Ceram. Eng. Sci. Proc.* 1997, 18[2], 44-58.
- [12] Bondioli, F.; Corradi, A.; Ferrari, A.M.; Manfredini, T.; Baldi, G. *J. Am. Ceram. Soc.* 2000, 83[6], 1518-1520.
- [13] Johnston, R.M. in *Pigment Handbook*; Putton. T.C.; Ed.; Wiley-Interscience Publication; New York (NY) 1973; Vol. 3, pp 229-88.
- [14] Schabbach, L.M.; Bondiola, F.; Ferrari, A.M.; Manfredini, T.; Setter, C.O.; Fredel, M.C. *J. Euro. Ceram. Soc.* 2007, 27, 179-184.
- [15] Kubelka P., Munk F., Ein Beitrag zur Optik der Farbanstriche, *Z. Tech. Phys.* 1931, 12, 593-601.
- [16] Saunderson, J.L. *J. Opt. Soc. Am.*, 1942, 32[12], 727-732.
- [17] Duncan, D.R. *J. Oil Colour Chem. Assoc.*, 1962, 45, 300-304.
- [18] Murdock, S.H.; Wise, T.D.; Eppler, R.A. *Am. Ceram. Soc. Bull.*, 1990, 69[2], 228-231.
- [19] Murdock, S.H.; Wise, T.D.; Eppler, R.A. *Ceram. Eng. Sci. Proc.* 1990, 11[3-4], 270-277.
- [20] Eppler, D.R.; Eppler, R.A. *Cer. Eng. Sci. Proc.*, 1998, 19[2], 17-22.
- [21] Bondioli, F.; Manfredini, T.; Romagnoli, M. *J. Euro. Ceram. Soc.*, 2006, 26[3], 311-316.
- [22] Available at <http://www.joone.org>

Chapter 14

**SYNTHESIS AND CHARACTERIZATION
OF SEVERAL SERIES OF
SUBSTITUTED METALLOPHthalOCYANINES**

Fangdi Cong^{a,b}, Xiguang Du^{a,b,}, Jianxin Li^a,
Dongliang Tian^b and Wenjuan Duan^b*

^aCollege of Material Science & Engineering, Nanjing University of Aeronautics and
Astronautics, Nanjing, Jiangsu, 210016, China

^bFaculty of Chemistry, Northeast Normal University, Changchun 130024, China

ABSTRACT

The twenty-four substituted metallophthalocyanines were synthesized, in two steps, from 4-nitrophthalonitrile or 3-nitrophthalonitrile, and characterized by MS, ¹H NMR, UV-vis, IR and element analysis. The results showed that they all were consistent with proposed structures. They behaved excellent solubility in some organic solvents, but the stability of them in solution was not good as in solid state. According to the scopes of red shift, the impact of metals, substituents and substitution positions on Q-bands could be displayed as follow: Mn > Zn ≈ Cu > Ni ≈ Co; 2-isopropyl-5-methylphenoxy ≥ 4-tert-butylphenoxy ≥ quinolin-8-yloxy ≥ 2-methoxyethoxy; non-periphery > periphery. The research displayed that the alternative ways to control the Q bands of Pc compounds to have a big change were to alter the chemical value of metal in the center of Pc ring, replace the atom banding directly with Pc ring or its chemical circumstance, and change the substitution position of substituent on Pc ring (periphery or non-periphery).

Key words: Phthalocyanine, Synthesis, UV-vis spectra, Q band, solubility, stability

* Corresponding author: Tel: +86-0431-85098720; E-mail: xgdu@yahoo.cn

1. INTRODUCTION

Pc compounds have extensive applications in the area of material science, such as liquid crystal [1], catalysis [2], nonlinear optics [3], Photodynamic therapy [4], film [5] and semiconductor [6], etc. The various functions are associated with their aromatic 18- π electron system [7], which cause them all have the special Q band absorption (around 700 nm). So almost of all the investigations on Pcs were paid attention to the properties [8] and changes [9] of Q bands, which might present the significant information implying the potential application of Pcs.

In order to obtain more spectral data of Pc complexes, a number of substituted metal and metal-free Pcs were synthesized by diversified methods [10-12]. But many Pc compounds were practically insoluble in common organic solvents due to the intermolecular interactions between the macrocycles, which limited the investigations on them as well as the applications of them [13]. Hence a considerable effort was made to generate novel soluble substituted Pcs by introduction of the suitable substituents on the periphery that, to some extent, increases the distance of 18- π electron conjugated systems of Pcs and facilitates the solubility [14,15].

In our previous works on the synthesis of soluble substituted Pc compounds [16-18], we prepared some Pc derivatives with enhanced solubility in common organic solvents, which derived from the steric bulk and solvent affinity of the substituents preventing aggregation [19]. We also found that the coordinated metals in the center of Pc ring, substituents around Pc ring and substitution positions (periphery and non-periphery) had different impacts on the UV-vis of Pcs [20,21]. In order to systemically understand the impact of above three factors on UV-vis spectra, a series of soluble substituted metal Pcs, $1a_1\sim 1e_4$ and $2a_1\sim 2b_2$, were synthesized according to the modified strategy based on the literature [16]. The orders of Q-band wavelength derived from different metals, substituents and substitution positions were obtained, respectively. The potential ways to availably change the Q-band wavelength were suggested in this paper.

2. EXPERIMENTAL

2.1. Materials and Methods

Pentan-1-ol was distilled from Na prior to use. DMSO was predried over BaO and distilled under reduced pressure. Column chromatography purifications were performed on silica gel. All other reagents and solvents are commercial available and used without further purification. Petroleum ether used had bp 60–90 °C.

^1H NMR spectra were recorded on a Bruker AV 500 spectrometer. IR spectra were measured on a Magna 560 FT-IR spectrometer. UV/Vis spectra were taken on a Cary 500 UV-VIS-NIR spectrophotometer. MS spectra were obtained on a LDI-1700-TOF mass spectrometer. Elemental analyses were performed on a Perkin-Elmer 2400 Elemental Analyzer.

2.2. Synthesis of Several Substrates

4-(2-isopropyl-5-methylphenoxy)phthalonitrile; typical procedure:

4-nitrophthalonitrile (6.92 g, 40.0 mmol) and 2-isopropyl-5-methylphenol (6.00g, 40.0 mmol) was added to 80 mL DMSO at r.t. The reaction mixture was stirred and LiOH (2.4 g, 100 mmol) was added over 2 h, and then the mixture was stirred for 2 days. The reaction progress was monitored by TLC analysis. The mixture was then poured into 10% NaCl (400 mL). The product was collected by vacuum filtration. The crude product was purified by column chromatography with petroleum ether–anhyd Et₂O (1:1) as the mobile phase to afford yellow crystal of 4-(2-isopropyl-5-methylphenoxy)phthalonitrile; yield: 9.88 g (89%), m.p. 106~108°C. ¹H NMR (500 MHz, CDCl₃) δ = 7.708 (d, 1 H, *J* = 8.5 Hz, ArH), 7.295 (d, 1 H, *J* = 8.5 Hz, ArH), 7.219 (s, 1 H, ArH), 7.189 (d, 1 H, *J* = 8 Hz, ArH), 7.109 (d, 1 H, *J* = 8 Hz, ArH), 6.745 (s, 1 H, ArH), 2.958 (m, 1 H CH), 2.331 (s, 3 H, ArCH₃), 1.154 (d, 6 H, *J* = 6.5 Hz, CH(CH₃)₂). MS (QUSTAR-TOF): *m/z* calcd for [M]: 276.1; found: 299.1 (an isotopic cluster peak) [M +Na⁺], 314.9 (an isotopic cluster peak) [M +K⁺]. UV/Vis (CHCl₃): λ_{max} = 264, 306 nm. IR (KBr): 2230 cm⁻¹ (C≡N), 1246 cm⁻¹ (C-O-C).

4-(4-tert-butylphenoxy)phthalonitrile

Yellow solid; yield: 10.20 g (92%), m.p. 116~118°C. ¹H NMR (500 MHz CDCl₃): δ = 7.711 (d, 1 H, *J* = 2 Hz, ArH), 7.477 (d, 1 H, *J* = 2 Hz, ArH), 7.464 (s, 1 H, ArH), 7.248 (q, 2 H, *J* = 2 Hz, ArH), 6.994 (q, 2 H, *J* = 2 Hz, ArH), 1.358 (s, 9 H, t-C₄H₉). MS (QUSTAR-TOF): *m/z* calcd for [M]: 276.1; found: 299.1 (an isotopic cluster peak) [M +Na⁺], 314.9 (an isotopic cluster peak) [M +K⁺]. UV/Vis (CHCl₃): λ_{max} = 264, 306 nm. IR (KBr): 2231 cm⁻¹ (C≡N), 1244 cm⁻¹ (C-O-C).

4-(quinolin-8-yloxy)phthalonitrile

White solid; yield: 8.78 g (81%). m.p. 176~178°C. ¹H NMR (500MHz, CDCl₃): δ = 9.031 (d, 1 H, ArH), 8.504 (d, 1 H, ArH), 7.925 (d, 1 H, ArH), 7.722 (m, 3 H, ArH), 7.584 (d, 1 H, ArH), 7.225 (d, 2 H, ArH). MS (QUSTAR-TOF): *m/z* calcd for [M]: 273.0; found: 271.8 (an isotopic cluster peak) [M +Na⁺]. UV/Vis (CHCl₃): λ_{max} = 263, 296 nm. IR (KBr): 2230 cm⁻¹ (C≡N), 1246 cm⁻¹ (C-O-C).

4-(2-methoxyethoxy)phthalonitrile

Yellow solid; yield: 6.63 g (82%). m.p. 80~82°C. ¹H NMR (500MHz, CDCl₃): δ = 7.711 (dd, 1 H, *J* = 8.7 Hz, ArH), 7.309 (d, 1 H, *J* = 2.52 Hz, ArH), 7.239 (m, 1 H, *J* = 8.8 Hz, ArH), 4.217 (m, 2 H, ArOCH₂), 3.784 (m, 2 H, CH₂O), 3.449 (s, 3 H, OCH₃). MS (QUSTAR-TOF): *m/z* calcd for [M]: 202.1; found: 225.4 (an isotopic cluster peak) [M +Na⁺]. UV/Vis (CHCl₃): λ_{max} = 264, 297, 305 nm. IR (KBr): 2230 cm⁻¹ (C≡N), 1240 cm⁻¹ (C-O-C).

3-(2-isopropyl-5-methylphenoxy)phthalonitrile and 3-(4-tert-butylphenoxy)phthalonitrile can be obtained by the similar sythesis method after 4-nitrophthalonitrile was replaced with 3-nitrophthalonitrile.

3-(2-isopropyl-5-methylphenoxy)phthalonitrile

Yellow solid; yield: 9.18 g (83%). m.p. 84~86°C. ¹H NMR (500 MHz, CDCl₃): δ = 7.543 (dd, 1 H, *J* = 8 Hz, ArH), 7.425 (d, 1 H, *J* = 8 Hz, ArH), 7.286 (d, 1 H, *J* = 8 Hz, ArH), 7.091 (d, 1 H, *J* = 9 Hz, ArH), 6.971 (d, 1 H, *J* = 9 Hz, ArH), 6.769 (s, 1 H, ArH), 3.023 (m, 1 H, CH), 2.320 (s, 3 H, ArCH₃), 1.182 (d, 6 H, *J* = 6.5 Hz, CH(CH₃)₂). MS (QUSTAR-TOF): *m/z* calcd for [M]: 276.1; found: 299.1 (an isotopic cluster peak) [M +Na⁺], 314.9 (an isotopic cluster peak) [M +K⁺]. UV/Vis (CHCl₃): λ_{max} = 219, 321 nm. IR (KBr): 2233 cm⁻¹ (C≡N), 1240 cm⁻¹ (C-O-C).

3-(4-tert-butylphenoxy)phthalonitrile

Yellow solid; yield: 9.52g (86%). m.p. 104~106°C. ^1H NMR (500 MHz, CDCl_3): δ = 7.551 (dd, 1 H, J = 8 Hz, ArH), 7.451 (d, 2 H, J = 9 Hz, ArH), 7.427 (d, 1 H, J = 8 Hz, ArH), 7.093 (d, 1 H, J = 8 Hz, ArH), 7.022 (d, 2 H, J = 9 Hz, ArH), 1.342 (s, 9 H, t- C_4H_9). MS (QUSTAR-TOF): m/z calcd for [M]: 276.1; found: 299.1 (an isotopic cluster peak) [M + Na^+], 314.9 (an isotopic cluster peak) [M + K^+]. UV/Vis (CHCl_3): λ_{max} = 214, 321 nm. IR (KBr): 2235 cm^{-1} (C \equiv N), 1247 cm^{-1} (C-O-C).

2.3. Synthesis of MPcs 1a₁~1e₄ and 2a₁~2b₂

Synthesis of 1a₁; typical procedure: 4-(2-isopropyl-5-methylphenoxy)phthalonitrile (1.04 g, 4.0 mmol) and $\text{Zn}(\text{OAc})_2 \cdot 2\text{H}_2\text{O}$ (0.22g, 1.0 mmol) were added under stirring to pentan-1-ol (10 mL) in a 25 mL oneneck round-bottomed flask equipped with an air condenser. Then, a catalytic amount of DBU was added, and the mixture was stirred and heated at 135 °C under N_2 over 24 h. After cooling under N_2 , pentan-1-ol was removed under reduced pressure. The collected solid was purified by column chromatography with a mixture of CHCl_3 -MeOH (20:1) as eluents to afford 1a₁; yield: 0.68 g (53%). m.p. > 320°C. ^1H NMR (500 MHz, CDCl_3): δ = 7.340 (br s, 12 H, ArH), 7.044 (br s, 12 H, ArH), 3.452 (br s, 4H, 4CH), 2.300 (br s, 12H, 4ArCH₃), 1.394 (br s, 24 H, 4CH(CH₃)₂). MS (LDI-1700-TOF): m/z calcd for [M + H^+]: 1169.4; found: 1169.6 [M + H^+]. IR (KBr) 1247 cm^{-1} (C-O-C). Anal. Calcd for $\text{C}_{72}\text{H}_{64}\text{N}_8\text{O}_4\text{Zn}$ (1168.4): C, 73.87; H, 5.51; N, 9.57. Found: 72.85; H, 5.86; N, 9.43.

1b₁; yield 0.65 g (51%). m.p. > 320°C. MS (LDI-1700-TOF): m/z calcd for [M + H^+]: 1168.4; found: 1168.3 [M + H^+]. IR (KBr) 1248 cm^{-1} (C-O-C). Anal. Calcd for $\text{C}_{72}\text{H}_{64}\text{N}_8\text{O}_4\text{Cu}$ (1167.4): C, 73.98; H, 5.52; N, 9.59. Found: 72.64; H, 5.87; N, 9.24.

1c₁; yield: 0.56 g (49%). m.p. > 320°C. MS (LDI-1700-TOF): m/z calcd for [M + H^+]: 1163.4; found: 1163.9 [M + H^+]. IR (KBr) 1249 cm^{-1} (C-O-C). Anal. Calcd for $\text{C}_{72}\text{H}_{64}\text{N}_8\text{O}_4\text{Ni}$ (1162.4): C, 74.29; H, 5.54; N, 9.63. Found: 73.68; H, 5.73; N, 9.48.

1d₁; yield: 0.52 g (44%). m.p. > 320°C. MS (LDI-1700-TOF): m/z calcd for [M + H^+]: 1164.4; found: 1164.9 [M + H^+]. IR (KBr) 1248 cm^{-1} (C-O-C). Anal. Calcd for $\text{C}_{72}\text{H}_{64}\text{N}_8\text{O}_4\text{Co}$ (1163.4): C, 74.28; H, 5.54; N, 9.62. Found: 73.55; H, 5.76; N, 9.45.

1e₁; yield: 0.50 g (43%). m.p. > 320°C. MS (LDI-1700-TOF): m/z calcd for [M + H^+]: 1160.4; found: 1160.8 [M + H^+]. IR (KBr) 1246 cm^{-1} (C-O-C). Anal. Calcd for $\text{C}_{72}\text{H}_{64}\text{N}_8\text{O}_4\text{Mn}$ (1159.4): C, 74.53; H, 5.56; N, 9.66. Found: 73.66; H, 5.82; N, 9.45.

1a₂; yield: 0.64 g (50%). m.p. > 320°C. ^1H NMR (500 MHz, CDCl_3), δ = 7.359-7.469 (m, 12 H, ArH), 7.139-7.243 (m, 16 H, ArH), 1.361-1.555 (m, 36 H, 4t- C_4H_9). MS (LDI-1700-TOF): m/z calcd for [M + H^+]: 1169.4; found: 1169.0 [M + H^+]. IR (KBr) 1235 cm^{-1} (C-O-C). Anal. Calcd for $\text{C}_{72}\text{H}_{64}\text{N}_8\text{O}_4\text{Zn}$ (1168.4): C, 73.87; H, 5.51; N, 9.57. Found: 72.85; H, 5.86; N, 9.43.

1b₂; yield: 0.68 g (53%). m.p. > 320°C. MS (LDI-1700-TOF): m/z calcd for [M + H^+]: 1168.4; found: 1168.0 [M + H^+]. IR (KBr) 1238 cm^{-1} (C-O-C). Anal. Calcd for $\text{C}_{72}\text{H}_{64}\text{N}_8\text{O}_4\text{Cu}$ (1167.4): C, 73.98; H, 5.52; N, 9.59. Found: 72.64; H, 5.87; N, 9.24.

1c₂; yield: 0.58 g (50%). m.p. > 320°C. MS (LDI-1700-TOF): m/z calcd for [M + H^+]: 1163.4; found: 1163.9 [M + H^+]. IR (KBr) 1238 cm^{-1} (C-O-C). Anal. Calcd for $\text{C}_{72}\text{H}_{64}\text{N}_8\text{O}_4\text{Ni}$ (1162.4): C, 74.29; H, 5.54; N, 9.63. Found: 73.68; H, 5.73; N, 9.48.

*Id*₂; yield: 0.54 g (46%). m.p. > 320°C. MS (LDI-1700-TOF): *m/z* calcd for [M + H⁺]: 1164.4; found: 1164.8 [M + H⁺]. IR (KBr) 1238 cm⁻¹ (C-O-C). Anal. Calcd for C₇₂H₆₄N₈O₄Co (1163.4): C, 74.28; H, 5.54; N, 9.62. Found: 73.55; H, 5.76; N, 9.45.

*Ie*₂; yield: 0.50 g (43%). m.p. > 320°C. MS (LDI-1700-TOF): *m/z* calcd for [M + H⁺]: 1160.4; found: 1160.8 [M + H⁺]. IR (KBr) 1236 cm⁻¹ (C-O-C). Anal. Calcd for C₇₂H₆₄N₈O₄Mn (1159.4): C, 74.53; H, 5.56; N, 9.66. Found: 73.66; H, 5.82; N, 9.45.

*Ia*₃; yield: 0.68 g (59%). m.p. > 320°C. ¹H NMR (500 MHz, CDCl₃): δ = 10.24-7.43 (m, 24 H, ArH), 7.04-4.78 (m, 12 H, ArH). MS (LDI-1700-TOF): *m/z* calcd for [M + H⁺]: 1149.2; found: 1149.6 [M + H⁺]. IR (KBr) 1247 cm⁻¹ (C-O-C). Anal. Calcd for C₆₈H₃₆N₁₂O₄Zn (1148.2): C, 70.99; H, 3.15; N, 14.61. Found: 70.78; H, 3.25; N, 14.23.

*Ib*₃; yield: 0.58 g (51%). m.p. > 320°C. MS (LDI-1700-TOF): *m/z* calcd for [M + H⁺]: 1148.2; found: 1148.1 [M + H⁺]. IR (KBr) 1248 cm⁻¹ (C-O-C). Anal. Calcd for C₆₈H₃₆N₁₂O₄Cu (1147.2): C, 70.10; H, 3.16; N, 14.63. Found: 69.89; H, 3.33; N, 14.46.

*Ic*₃; yield: 0.55 g (48%). m.p. > 320°C. MS (LDI-1700-TOF): *m/z* calcd for [M + H⁺]: 1143.2; found: 1143.5 [M + H⁺]. IR (KBr) 1248 cm⁻¹ (C-O-C). Anal. Calcd for C₆₈H₃₆N₁₂O₄Ni (1142.2): C, 71.41; H, 3.17; N, 14.70. Found: 71.51; H, 3.36; N, 14.45.

*Id*₃; yield: 0.60 g (53%). m.p. > 320°C. MS (LDI-1700-TOF): *m/z* calcd for [M + H⁺]: 1144.2; found: 1144.5 [M + H⁺]. IR (KBr) 1248 cm⁻¹ (C-O-C). Anal. Calcd for C₆₈H₃₆N₁₂O₄Co (1143.2): C, 71.39; H, 3.17; N, 14.69. Found: 71.63; H, 3.35; N, 14.43.

*Ie*₃; yield: 0.48 g (42%). m.p. > 320°C. MS (LDI-1700-TOF): *m/z* calcd for [M + H⁺]: 1140.2; found: 1140.4 [M + H⁺]. IR (KBr) 1247 cm⁻¹ (C-O-C). Anal. Calcd for C₆₈H₃₆N₁₂O₄Mn (1139.2): C, 71.64; H, 3.18; N, 14.74. Found: 71.83; H, 3.35; N, 14.57.

*Ia*₄; yield: 0.52 g (59%). m.p. > 320°C. ¹H NMR (500MHz, CDCl₃): δ = 7.714-7.301 (m, 4 H, ArH), 7.181-6.257 (m, 8 H, ArH), 3.409 (m, 12 H, 4OCH₃), 3.190 (m, 16 H, 4OCH₂CH₂O). MS (LDI-1700-TOF): *m/z* calcd for [M + H⁺]: 873.2; found: 873.2 [M + H⁺]. IR (KBr) 1240 cm⁻¹ (C-O-C). Anal. Calcd for C₄₄H₄₀N₁₂O₄Zn (872.2): C, 60.45; H, 4.61; N, 12.82. Found: 61.05; H, 4.63; N, 12.85.

*Ib*₄; yield: 0.56 g (44%). m.p. > 320°C. MS (LDI-1700-TOF): *m/z* calcd for [M + H⁺]: 872.2; found: 872.4 [M + H⁺]. IR (KBr) 1241 cm⁻¹ (C-O-C). Anal. Calcd for C₄₄H₄₀N₁₂O₄Cu (871.2): C, 60.58; H, 4.62; N, 12.84. Found: 60.29; H, 4.47; N, 12.26.

*Ic*₄; yield: 0.44 g (35%). m.p. > 320°C. MS (LDI-1700-TOF): *m/z* calcd for [M + H⁺]: 867.2; found: 866.8 [M + H⁺]. IR (KBr) 1244 cm⁻¹ (C-O-C). Anal. Calcd for C₄₄H₄₀N₁₂O₄Ni (866.2): C, 60.92; H, 4.65; N, 12.92. Found: 60.69; H, 4.48; N, 12.60.

*Id*₄; yield: 0.48 g (38%). m.p. > 320°C. MS (LDI-1700-TOF): *m/z* calcd for [M + H⁺]: 868.7; found: 868.8 [M + H⁺]. IR (KBr) 1242 cm⁻¹ (C-O-C). Anal. Calcd for C₄₄H₄₀N₁₂O₄Co (867.2): C, 60.90; H, 4.65; N, 12.91. Found: 60.89; H, 4.57; N, 12.83.

*Ie*₄; yield: 0.47 g (38%). m.p. > 320°C. MS (LDI-1700-TOF): *m/z* calcd for [M + H⁺]: 864.2; found: 864.8 [M + H⁺]. IR (KBr) 1245 cm⁻¹ (C-O-C). Anal. Calcd for C₄₄H₄₀N₁₂O₄Mn (867.2): C, 61.18; H, 4.67; N, 12.97. Found: 60.55; H, 4.92; N, 12.83.

*2a*₁; yield: 0.68 g (53%). m.p. > 320°C. ¹H NMR (500 MHz, CDCl₃): δ = 7.309-7.622 (m, 12 H, ArH), 6.912-7.065 (m, 12 H, ArH), 3.538 (br s, 4 H, 4CH), 2.145-2.227 (m, 12 H, 4ArCH₃), 1.187-1.340 (m, 24 H, 4CH(CH₃)₂). MS (LDI-1700-TOF): *m/z* calcd for [M + H⁺]: 1169.4; found: 1169.0 [M + H⁺]. IR (KBr) 1251 cm⁻¹ (C-O-C). Anal. Calcd for C₇₂H₆₄N₈O₄Zn (1168.4): C, 73.87; H, 5.51; N, 9.57. Found: 72.95; H, 5.66; N, 9.53.

$2b_1$; yield: 0.65 g (51%). m.p. > 320°C. MS (LDI-1700-TOF): m/z calcd for $[M + H]^+$: 1168.4; found: 1168.0 $[M + H]^+$. IR (KBr) 1252 cm^{-1} (C-O-C). Anal. Calcd for $\text{C}_{72}\text{H}_{64}\text{N}_8\text{O}_4\text{Zn}$ (1168.4): C, 73.98; H, 5.52; N, 9.59. Found: 72.64; H, 5.87; N, 9.24.

$2a_2$; yield: 0.64 g (50%). m.p. > 320°C. $^1\text{H NMR}$ (500 MHz, CDCl_3), δ = 7.305-7.389 (m, 12 H, ArH), 6.857-7.031 (m, 16 H, ArH), 1.290-1.347 (m, 36 H, 4t- C_4H_9). MS (LDI-1700-TOF): m/z calcd for $[M + H]^+$: 1169.4; found: 1169.0 $[M + H]^+$. IR (KBr) 1251 cm^{-1} (C-O-C). Anal. Calcd for $\text{C}_{72}\text{H}_{64}\text{N}_8\text{O}_4\text{Zn}$ (1168.4): C, 73.87; H, 5.51; N, 9.57. Found: 72.85; H, 5.86; N, 9.43.

$2b_2$; yield: 0.68 g (53%). m.p. > 320°C. MS (LDI-1700-TOF): m/z calcd for $[M + H]^+$: 1168.4; found: 1168.0 $[M + H]^+$. IR (KBr) 1253 cm^{-1} (C-O-C). Anal. Calcd for $\text{C}_{72}\text{H}_{64}\text{N}_8\text{O}_4\text{Cu}$ (1167.4): C, 73.98; H, 5.52; N, 9.59. Found: 72.64; H, 5.87; N, 9.24.

3. RESULTS AND DISCUSSION

3.1. Synthesis and Characterization

According to literature [16], a modified method was used to synthesize twenty-four Pc compounds $1a_1\sim 1e_4$ and $2a_1\sim 2b_2$ in two steps from 4-nitro-phthalonitrile or 3-nitro-phthalonitrile. The synthetic route involves the aromatic nucleophilic substitution reaction between nitrophthalonitriles and a suitable oxygen nucleophile followed by cyclotetramerization of the resultant phthalonitrile derivatives. First, we chose two kinds of nitrophthalonitriles and four kinds of oxygen nucleophiles as starting materials to synthesize phthalonitrile derivatives with good yield in the presence of LiOH and anhydrous DMSO at room temperature. Upon treatment with inorganic salts in refluxing pentan-1-ol with DBU as catalyst under nitrogen, MPcs $1a_1\sim 1e_4$ and $2a_1\sim 2b_2$ were synthesized from the aforementioned phthalonitrile derivatives, which could be purified by column chromatography. Their synthesized route and molecular structures were displayed in Figure 1.

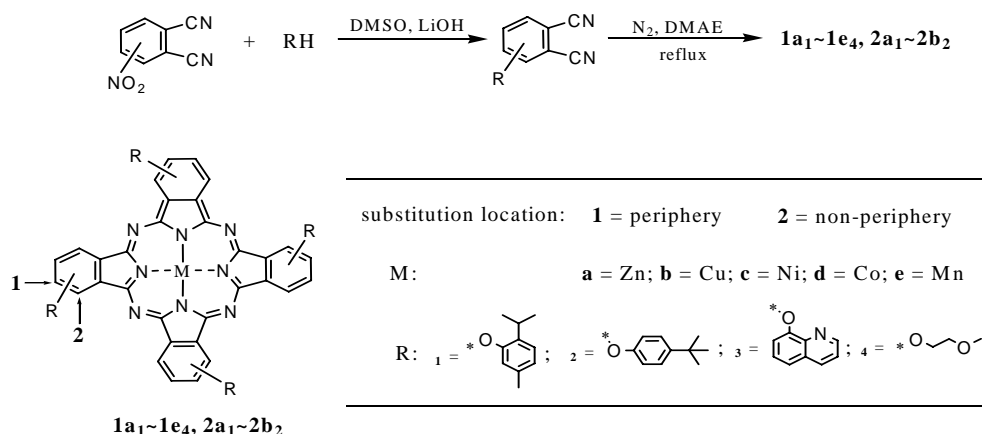


Figure 1. Synthesis and molecular structures of $1a_1\sim 1e_4$ and $2a_1\sim 2b_2$.

The obtained twenty-four Pc compounds were characterized by methods of ^1H NMR, TOF-MS, UV-vis, IR and elemental analysis (Section 2.3), which were consistent with the proposed structures. The ^1H NMR spectra of the Pc compounds without zinc were precluded for that the paramagnetic nature of them in a square planar environment, which phenomenon can be seen in our previous investigations [21].

3.2. Solubility and Stability of $1a_1\sim 1e_4$ and $2a_1\sim 2b_2$

The Pcs $1a_1\sim 1e_4$ and $2a_1\sim 2b_2$, all presented excellent solubility in CHCl_3 , CH_2Cl_2 , pyridine and quinoline (10^{-1} mol/L), but they were hardly soluble in acetone and methanol ($\leq 10^{-5}$ mol/L). Only the Pcs processing Zn, $1a_1\sim 1a_4$ and $2a_1\sim 2a_2$, could slightly dissolve in acetone (10^{-5} mol/L). The Pcs with Zn, Co and Mn, $1a(d,e)_1\sim 1a(d,e)_4$ and $2a_1\sim 2a_2$, could dissolve in DMF and DMSO (10^{-1} mol/L), but in which the solubility of Pcs with another two metals Cu and Ni, $1b(c)_1\sim 1b(c)_4$ and $2b_1\sim 2b_2$, was poor ($< 10^{-5}$ mol/L). The good solubility facilitated the structural characterization and property investigation of them.

However, the stability of them in solution was not as good as in solid state. It was found that they could be quickly degraded by sunlight in HCCl_3 , especially $1a_1\sim 1a_4$ and $2a_1\sim 2a_2$. The color of their solutions converted from blue-green to slight yellow under midday sunlight for 30 min, and accordingly the UV-vis spectra occurred obvious change, e.g. the UV-vis spectrum of $1a_4$ in chloroform (Figure 2). The solutions of $1b_1\sim 1b_4$ and $2b_1\sim 2b_2$ in chloroform displayed color change after two days, and the solutions of other Pcs in chloroform didn't occur remarkable color difference even if one week had past. According to the views of the literatures [22,23], the poor stability of their solutions might be ascribed to the photocatalysis of Pcs containing non-transition metals, especially Zn (II), which monomer in solution is efficient photocatalyst for phenols and itself. As a photosensitizer, it is excited to its triplet state, and then transfers the energy to ground-state triplet oxygen O_2 ($^3\Sigma_g$) forming the excited-state singlet oxygen, O_2 ($^1\Delta_g$), through the so called Type II mechanism. The aforementioned photodegrade of $1a_4$ in solution occurs via attack by singlet oxygen generated by it.

3.3. Impact of Metals on UV-vis Spectra

The UV-vis spectral data of twenty-four Pcs $1a_1\sim 1e_4$ and $2a_1\sim 2b_2$ were given in Table 1, from which the impact of metals, substituents and substitution positions on the UV-vis spectra of them could be seen clearly. When the substituent and the substitution position of Pcs were same, the coordinated metals in the center of Pc ring caused an uneven red-shifted impact on the Q bands and followed an order: $\text{Mn} > \text{Zn} \approx \text{Cu} > \text{Ni} \approx \text{Co}$. The Q band wavelength of the Pcs with Zn (Ni) and the Pcs with Cu (Co) are almost equal, and the Q band wavelength of the Pcs with Zn (Cu) red shifted no more than 10 nm comparing with that of the Pcs with Ni (Co). But the Q bands of the Pcs with Mn red shifted approximate 50 nm relative to that of the Pcs with other metals. The phenomenon could also be clearly showed in the UV-vis spectra of $1a_1\sim 1e_1$ (Figure 3). To refer to the previously reported results [21,24,25], the Q band difference of the Pcs with Co, Ni, Cu and Zn derived from different d electron number in the several metals. The reason that the Q band of Pcs with Mn markedly

shifted 50 nm towards red region relative to the others, should be that there is a Mn^{III} , not Mn^{II} , in the center of Pc ring like the common manganese Pc complexes [26,27]. Moreover, comparing with the Pc compounds with common M^{II} , the distinctly higher B bands and the additional bands near 520 nm in the UV-vis were also the characters of Pc compounds with Mn^{III} (e.g. $1e_1\sim 1e_4$ Figure 3) [28]. This implied that it might be a way to cause the Q band to shift largely by altering the value of center metal.

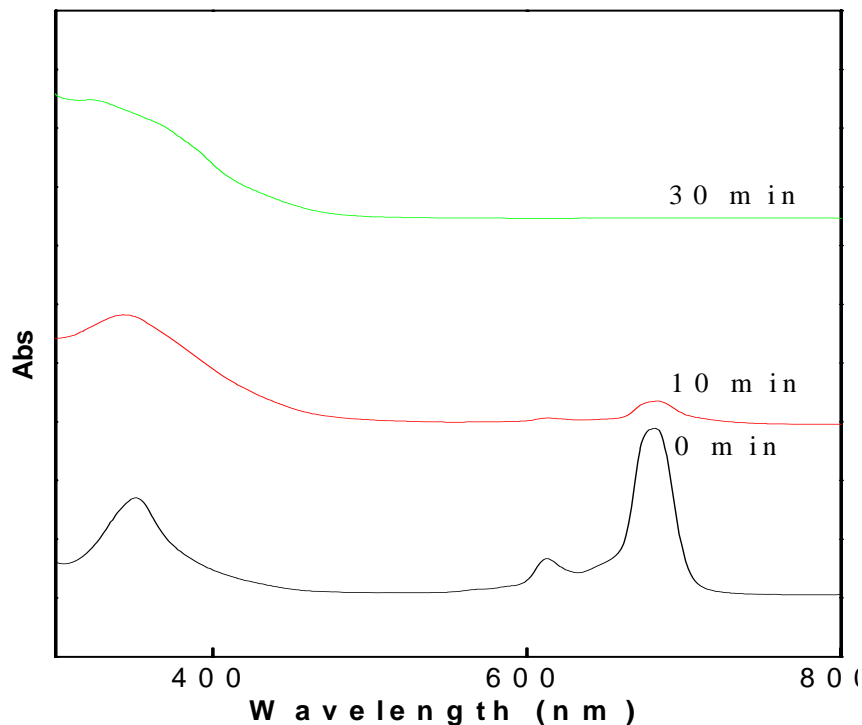


Figure 2. UV-vis spectral changes of MPC $1a_4$ in chloroform (2.0×10^{-4} mol/L) under midday sunlight for 0 min (1), 10 min (2) and 30 min (3): showing the poor stability of $1a_4$ in chloroform.

Table 1. Parameters on UV-Vis spectra of $1a_1\sim 1e_4$ and $2a_1\sim 2b_2$ in chloroform (2.0×10^{-4} mol/L)

Sample	λ (nm) / Q (B) band				
	Zn	Cu	Ni	Co	Mn
$1a_1\sim 1e_1$	684 (353)	684 (340)	675 (332)	676 (327)	737 (391)
$1a_2\sim 1e_2$	682 (352)	683 (340)	674 (331)	674 (325)	734 (390)
$1a_3\sim 1e_3$	682 (358)	681 (340)	674 (331)	673 (326)	733 (388)
$1a_4\sim 1e_4$	682 (351)	680 (338)	672 (328)	673 (326)	732 (388)
$2a_1\sim 2b_1$	705 (331)	707 (327)			
$2a_2\sim 2b_2$	702 (332)	703 (336)			

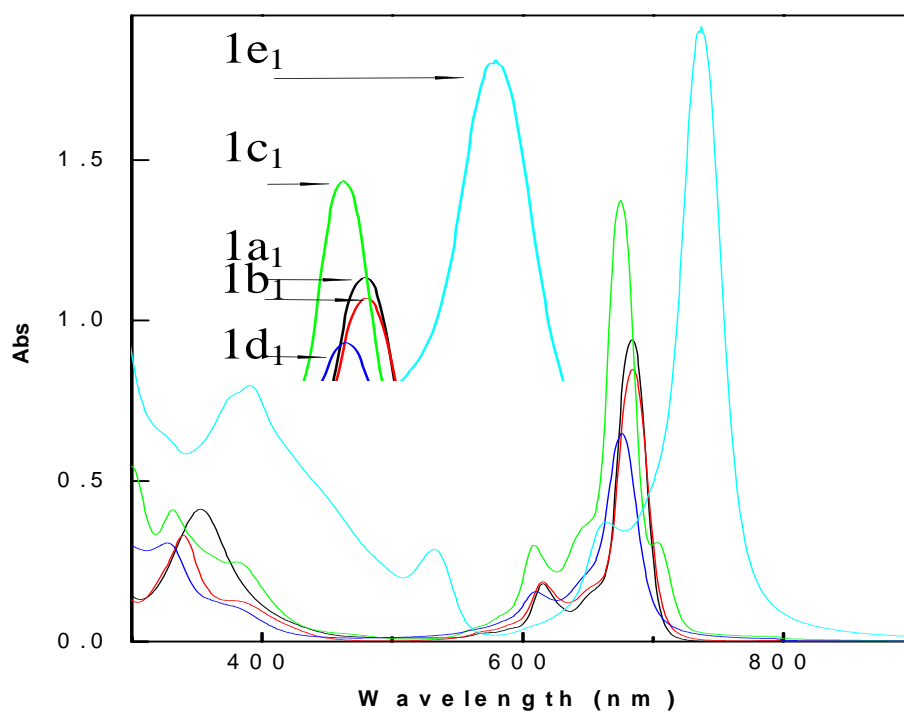


Figure 3. UV-vis spectra of $1a_1 \sim 1e_1$ in chloroform (2.0×10^{-4} mol/L): showing the impact of metals on Q bands.

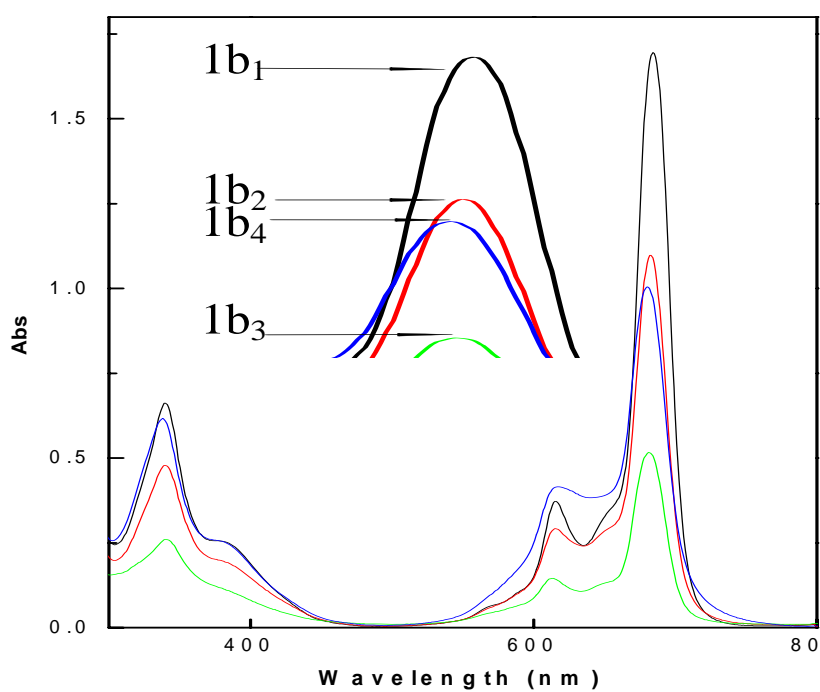


Figure 4. UV-vis spectra of $1b_1 \sim 1b_4$ in chloroform (2.0×10^{-4} mol/L): showing the impact of substituents on Q bands.

3.4. Impact of Substituents on UV-vis Spectra

When the metal and the substitution position of Pcs were uniform, from table 1 it is found that the impact of four substituents on the red shift of Q band followed a tendency: 2-isopropyl-5-methylphenoxy \geq 4-tert-butylphenoxy \geq quinolin-8-yloxy \geq 2-methoxyethoxy. But the difference is not great. Comparing one substituent with its neighboring one in the above order, the gaps between the two Q bands of the two corresponding Pcs were no more than 2 nm. This might be attributed to that the atoms bonding directly with Pc ring all were oxygen in the four substituents and the other part of four substituents had less distinction in terms of pushing or pulling electrons. Here, the tendency of Q band depending on substituents could be directly indicated by the UV-vis spectra, e.g. that of $1b_1 \sim 1b_4$ (Figure 4). It suggested that the shift of Q band wouldn't be obvious if the atoms banding directly with Pc ring were same and their chemical circumstances were similar in different substituents. Namely, it must be change the atom banding directly with Pc ring or its chemical circumstance in substituent if a large Q band shift is demanded.

3.5. Impact of Substitution Positions on UV-vis Spectra

When the Pcs had same metal and substituent, from table 1 it was found that the substitution positions (periphery and non-periphery) gave a large impact on the Q bands of Pcs, which was non-periphery $>$ periphery. The Q band of non-peripherally substituted Pcs red shifted more than 20 nm relative to that of peripherally substituted Pcs, which could be seen in their UV-vis spectra, e.g. that of $1a_2$ and $2a_2$ (Figure 5). According to our previous investigation [20], the substituent at the non-peripheral substitution position of Pc ring help to enlarge the conjugate structure of Pc ring. The enlarged conjugate area was in favor of electron cloud delocalizing from substituents to 18- π electron system of Pc ring, which could lead to a red shift of Q band [36,37]. This meant that the two substitution positions, non-periphery and periphery, could give a largely different impact on the Q band of substituted Pc compounds.

4. CONCLUSION

Twenty-four Pcs, $1a_1 \sim 1e_4$ and $2a_1 \sim 2b_2$, were synthesized in two steps from 4-nitro-phthalonitrile or 3-nitro-phthalonitrile. They had excellent solubility in some organic solvents, but poor stability in solution. Their UV-vis spectra showed that the coordinated metals (Zn^{II} , Cu^{II} , Co^{II} and Ni^{II}) with II value had not obvious differences in terms of the impact on the Q bands. Analogously, the four substituents around Pc ring also generated a little distinction. But the substituent on the non-peripheral position of Pc ring offered a great red shift of Q band comparing with that on the peripheral position. The impacts of three aspects on the Q bands were concisely described as follows: $Mn > Zn \approx Cu > Ni \approx Co$; 2-isopropyl-5-methylphenoxy $>$ 4-tert-butylphenoxy $>$ quinolin-8-yloxy $>$ 2-methoxyethoxy; non-periphery $>$ periphery. The alternative ways to cause the Q band of Pc to have a big change were to alter the chemical value of metal in the center of Pc ring, replace the atom banding

directly with Pc ring or its chemical circumstance, and change the substitution position of substituent on Pc ring (periphery or non-periphery).

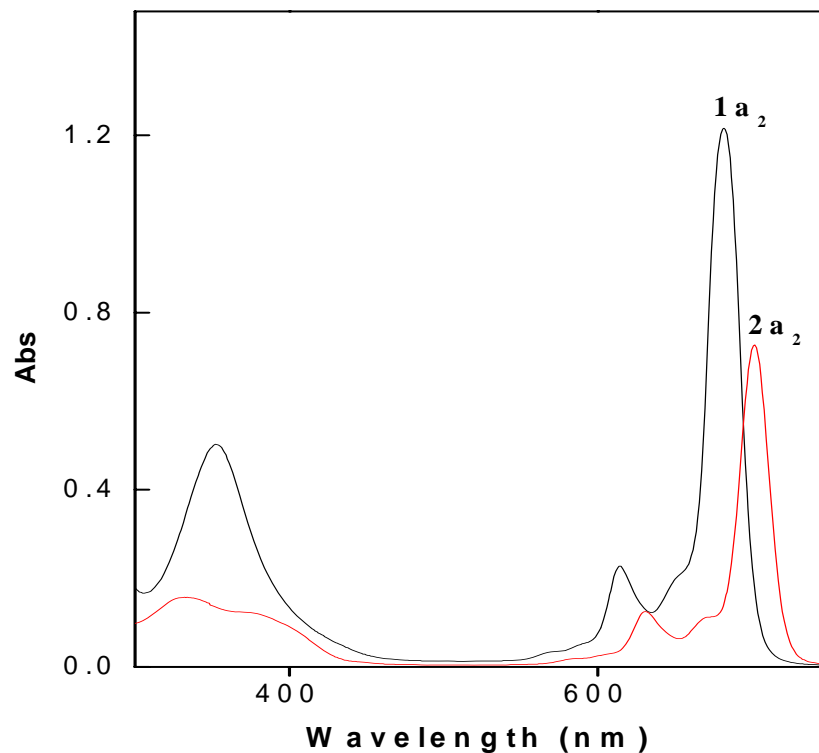


Figure 5. UV-vis spectra of $1a_2$ and $2a_2$ in chloroform (2.0×10^{-4} mol/L): showing the impact of substitution positions on Q bands.

ACKNOWLEDGEMENTS

Financial support of this project was provided by National Science Foundation of China (NSFC 20472014) and Jiang Su Science Foundation of China (JSSFC BK2005126). This project was supported by the 41th China Postdoctoral Science Foundation.

REFERENCES

- [1] N. Kobayashi, *Coordin. Chem. Rev.* 219-221 (2001) 99-123.
- [2] S. Griveau, J. Pavez, J.H. Zagal, F. Bedioui, *J. Electroanal. Chem.* 497 (2001) 75-83.
- [3] M.F. Joseph, J.K. Thomas, V.E. Sven, V. Thierry, K. Martti, P. André, T. Tienthong, K. Todd, B. Louis, *J. Am. Chem. Soc.* 121 (1999) 3453-3459.
- [4] C. Fabris, G. Jori, F. Giuntini, G. Roncucci, *J. Photoch. Photobiol. B* 64 (2001) 1-7.
- [5] M.P. Srinivasan, Y. Gu, R. Begum, *Colloid. Surf. A* 198-200 (2002) 527-534.
- [6] G. Liu, A. Klein, A. Thissen, W. Jaegermann, *Surf. Sci.* 539 (2003) 37-48.

- [7] J.H. Burroughes, C.A. Jones, R.H. Friend, *Nature* 335 (1998) 137-139.
- [8] N.B. McKeown, *Phthalocyanine Materials—Synthesis, Structure and Function*, Cambridge University Press, Cambridge, 1998.
- [9] P.M. Burnham, M.J. Cook, L.A. Gerrard, M.J. Heeney, D.L. Hughes, *Chem. Commun.* (2003) 2064-2065.
- [10] N. Ishikawa, Y. Kaizu, *Coordin. Chem. Rev.* 226 (2002) 93-101.
- [11] H. Kantekin, M. Rakap, Y. Gök, H.Z. Şahinbas, *Dyes Pigments* 74 (2007) 21-25.
- [12] C. Rager, G. Schmid, M. Hanack, *Chem. Eur. J.* 5 (1999) 280-288.
- [13] J. Rusanova, M. Pilkington, S. Decurtins, *Chem. Commun.* (2002) 2236-2237.
- [14] M. Brewis, N.B. McKeown, *Chem. Eur. J.* 4 (1998) 1633-1640.
- [15] M. Hanack, A. Beck, H. Lehmann, *Synthesis-Stuttgart.* (1987) 703-705.
- [16] C. Ma, D. Tian, X. Hou, Y. Chang, F. Cong, H. Yu, X. Du, G. Du, *Synthesis-Stuttgart.* 5 (2005) 741-748.
- [17] C. Ma, G. Du, Y. Cao, S. Yu, C. Cheng, W. Jiang, Y. Chang, X. Wang, F. Cong, H. Yu, *Dyes Pigments* 72 (2007) 267-270.
- [18] C. Ma, K. Ye, S. Yu, G. Du, Y. Zhao, F. Cong, Y. Chang, W. Jiang, C. Cheng, Z. Fan, H. Yu, W. Li, *Dyes Pigments* 74 (2007) 141-147.
- [19] C.C. Leznoff, S.M. Marcuccio, S. Greenberg, A.B. P. Lever, K. B. Tomer, *Can. J. Chem.* 63 (1985) 623-632.
- [20] F.D. Cong, B. Ning, H.F. Yu, X.H. Cui, B. Chen, S.G. Cao, C.Yu. Ma, *Spectrochim. Acta Part A* 62 (2005) 394-397.
- [21] F.D. Cong, B. Ning, X.G. Du, C.Yu. Ma, H.F. Yu, B. Chen, *Dyes Pigments* 66 (2005) 149-154.
- [22] E. Marais, R. Klein, E. Antunes, T. Nyokong, *Journal of Molecular Catalysis A: Chemical* 261 (2007) 36-42.
- [23] A. Ogunsipe, T. Nyokong, *Journal of Molecular Structure* 689 (2004) 89-97.
- [24] K.R. Venugopala Reddy, J. Keshavayya, J. Seetharamappa, *Dyes Pigments* 59 (2003) 237-244.
- [25] S. Sasmaz, E. Agar, A. Agar, *Dyes Pigments* 42 (1999) 137-142.
- [26] C.C. Leznoff, L.S. Black, A. Hiebert, P.W. Causey, D. Christendat, A.B.P. Lever, *Inorg. Chim. Acta* 359 (2006) 2690-2699.
- [27] J. Obirai, T. Nyokong, *Electrochim. Acta* 50 (2005) 5427-5434.
- [28] M.J. Stillman, T. Nyokong, in: C.C. Leznoff, A.B.P. Lever (Eds.), *Phthalocyanines: Properties and Applications*, vol. 1, VCH, New York, 1989 (Chapter 3).
- [29] S. Qu, Y. Gao, C. Zhao, Y. Wang, S. Fu, Y. Song, D. Wang, J. Qiu, C. Zhu, *Chem. Phys. Lett.* 367 (2003) 767-770.
- [30] A. Grofcsik, P. Baranyai, I. Bitter, V. Csokai, M. Kubinyi, K. Szegletes, J. Tatai, T. Vido'czy, *J. Mol. Struct.* 704 (2004) 11-15.
- [31] M. Durmusx, T. Nyokong, *Tetrahedron* 63 (2007) 1385-1394.
- [32] D. Wróbel, A. Boguta, *J. Photoch. Photobio. A* 150 (2002) 67-76.
- [33] M. Durmusx, C. Lebrun, V. Ahsen, *J. Porphyr. Phthalocya.* 8 (2004) 1175-1186.
- [34] G. Cheng, X. Peng, G. Hao, V. O. Kennedy, I. N. Ivanov, K. Knappenberger, J. J. Hill, M. A. J. Rodgers, M. E. Kenney, *J. Phys. Chem. A* 107 (2003) 3503-3514.
- [35] M. Aoudia, G. Cheng, V. O. Kennedy, M. E. Kenney, M. A. J. Rodgers, *J. Am. Chem. Soc.* 119 (1997) 6029-6039.

-
- [36] K.P. Unnikrishnan, J. Thomas, V.P.N.Nampoori, C.P.G. Vallabhan, *Synth. Met.* 139 (2003) 371-375.
- [37] S.N. Hari, H. Michael, P. Georg, K.E. Michael, *Chem. Phys.* 245 (1999) 17-26.

Chapter 15

DYES AND PIGMENTS WITH ECOLOGICALLY MORE TOLERANT APPLICATION

T. N. Konstantinova and P. P. Miladinova*

Organic Synthesis Department, University of Chemical Technology & Metallurgy,
8 Ohridsky str., Sofia 1756, Bulgaria

ABSTRACT

A review of the basic ecological problems related to the application of dyes and pigments for textile, foods and polymers is presented. A modern approach for solving the problems is shown. Along with a review of the synthesis and application of functional dyes and pigments already reported, in this paper we present a synthesis of 20 new bifunctional azo- and anthraquinone dyes-triazine derivatives. Six of them are metallized (Cu, Cr^{III} and Co^{III}) dyes and two of them contain a tetramethylpiperidine (TMP) stabilizer fragment in their molecule. In a color assessment of the new dyes, the percentage of exhaustion and fixation to cotton was found to be with 10-15 % higher compared to those of the model ones.

The photo degradation of 10 fluorescent naphthalimide dyes, synthesized before, was investigated and the structure-stability dependence was determined.

The copolymers of acryl amide and five fluorescent 9-phenylxanthene dyes derivatives, allylic ether-esters were obtained. The percentage of the chemical bound in the polymer dye was found to be 45-80, providing an intensive, stable to wet treatment and solvent's color and fluorescence, thus making the dyes suitable for ecologically tolerant application in food and cosmetics.

The photo stability of the triazine azodyes with a TMP fragment in the molecule was 25-30 % higher than those of the similar bifunctional azodyes without TMP. Their polymers of acrylonitrile were obtained and it was found that they have a good stabilizing effect on the photo degradation of the copolymer thus making these dyes suitable for "one-step" coloration and stabilization of materials with more tolerant ecological behavior.

* Corresponding author; E mail address : temekonstantinova@abv.bg

INTRODUCTION

Dyes and pigments are among the most widespread products applied in human life. We can not even imagine our life without colors and colored materials. The important influence of color on humans was determined a long time ago. Nowadays, there are no places in our lives without the application of dyes and pigments. At the same time, their application has caused various ecological problems. In spite of this, no one proposed their prohibition, because the most important principle in modern ecology is the principle of prevention but not of prohibition [1].

In the present paper we will try, while describing the main ecological problems in the application of dyes and pigments, to concentrate on the possibilities for the synthesis of products with more tolerant behavior and application.

Nowadays, depending on their nature and properties, the dyes and pigments are applied in the following areas:

1. Coloration of textile materials;
2. Coloration of polymers;
3. Dyes and pigments for foodstuffs and cosmetics; and
4. Dyes and pigments in high technologies (most recent application).

We will focus on these areas of application consecutively to express the kind of ecological problems presented and what approaches to take for their solution.

1. COLORATION OF TEXTILE MATERIALS

1.1. Ecological Problems

Ecological problems resulting from the coloration of textile materials arise at three different times: during the dyeing of the respective material, during the use of the colored material, and at the time of its washing and cleaning.

- *Ecological problems arising during the dyeing process*

Textile materials of natural origin are colored with different dyes [2, 3]. No matter what the conditions of coloration are, some quantity of the dye remains in the bath. First of all it is an important economical problem, because a part of the dye is lost with the waste water. But also as important, it is an ecological problem. Furthermore, the water undergoes a physical, chemical and biological purification, so the organic products can be destroyed or made harmless.

- *Problems arising at the time of the application*

Dyes, which are used for coloration of textile materials, are fixed to the material forming hydrogen, ion and/or van der Waals bonds with it. It is known that these bonds are not stable and during the application, due to different factors such as rubbing, light, heat, sweat and others, these bonds can be broken down. This releases the dye and its

molecules migrate and could fall onto human skin. This is a serious ecological problem because dyes, in many cases, could cause allergic or toxic reactions.

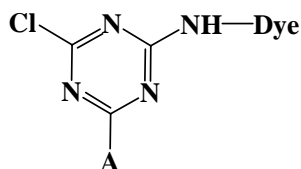
Another problem appeared when, during the application, the material was subjected to wet treatment or cleaning. During this procedure, a part of the dye was released into the wash water or into the solvents.

1.2. Approaches for Solving these Problems

One rather successful decision made to solve the ecological problems mentioned above was the synthesis of the reactive dyes [2, 3]. Nowadays almost all companies, working in organic synthesis, produce different brands of reactive dyes. In contrast to the other classes, the coloration by these dyes is due to the forming of covalent (chemical) bonds with the material, which guarantees durability of the color on physical factors. The most important part of the reactive dyes are the 1, 3, 5-triazine derivatives. In the dichlorotriazine dyes, the two chlorine atoms are the active groups.

The dichlorotriazine dyes showed one very serious disadvantage. During the coloration, because of its high reactivity, a part of the dye is lost in the bath. This additional problem was successfully solved with the synthesis of the monochlorotriazine dyes and especially the bifunctional ones [3]. The last ones contain two types of active groups in their molecule, which are able to react consecutively or simultaneously with the material. With the contemporary brands of bifunctional dyes, it was possible to reach an over 80% degree of exhaustion of the dye from the bath and a more than 90% degree of fixation to the material. The most common combination of active groups is chlorotriazine and vinylsulfone ones.

Keeping in mind the above mentioned, we synthesized a group of bifunctional triazine dyes with a general formula 1, where the Dye is different azo- and anthraquinone chromophors, and A is an unsaturated group like allylamine or allyloxy [4].



Formula 1.

The novelty in these dyes was that the two active groups are chlorine and allylamino- or allyloxy ones. The difference between the traditionally applied active vinylsulfone or bromoacrylic groups is that they can easily be involved in the triazine ring [4]. We synthesized two yellow azotriazine dyes with formula 1. Our investigations showed that these groups had good activity and the dyes had a good ability for coloration of cotton with a high degree of exhaustion (70-79%) and of fixation (98%). On the other hand, they are bifunctional as well, because of their ability to take part in copolymerization with some monomers, thus self-colored polymers can be obtained. The copolymers of these dyes with acryl amide (ACA) and acrylonitrile (AN) were obtained with a color stable when exposed to

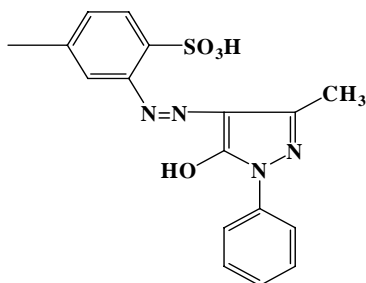
wet treatment and solvents. These results made those types of dyes suitable for coloration of materials of natural and synthetic origin and their blends as well.

The above-mentioned studies encouraged us to continue our investigations into the synthesis of other derivatives of that class.

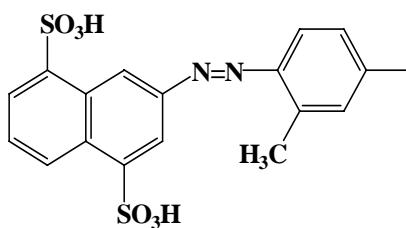
Synthesis of Bifunctional Reactive Triazine Dyes

The synthesis of 10 new triazine derivatives (yellow, orange, red, and blue in color) took place with formula 1, where the meanings of Dye are as follows:

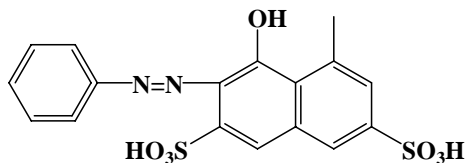
1.1



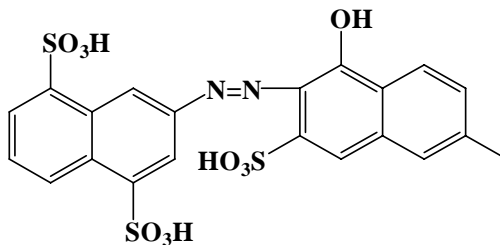
1.2



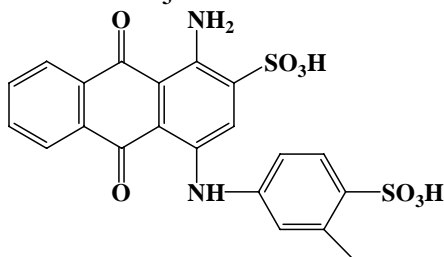
1.3



1.4

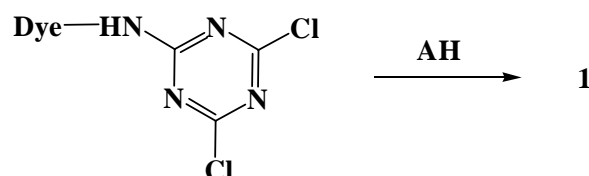


1.5



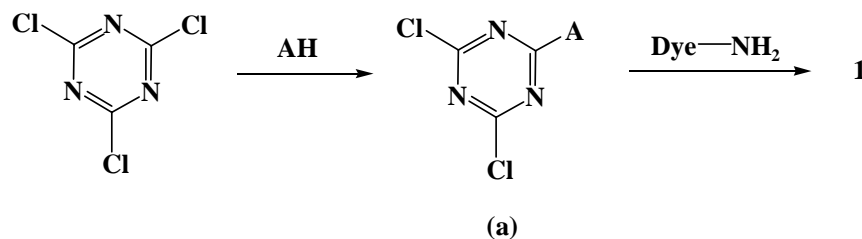
With each chromophore we obtained 3 sub-derivatives where the meanings of A are: 1.1^a A is $-\text{NHCH}_2\text{CH}=\text{CH}_2$, 1^b A is $-\text{OCH}_2\text{CH}=\text{CH}_2$ and 1^c A is $-\text{NH}_2$. The (c) derivatives were used as model ones in order to compare the properties of the new dyes. The synthesis of the derivatives with formula 1 was achieved experimenting with two different synthetic routes.

According to the first scheme (1) firstly the corresponding dichlorotriazine reactive dye was obtained, which at the second step reacted with allylamine (1^a derivatives), with allylic alcohol (1^b) and with ammonia (1^c derivatives).



Scheme 1.

According to the second route (Scheme 2) firstly the corresponding 2-monoallyl-4, 6-dichlorotriazine compound (a) was obtained, which at the next step reacted with the corresponding chromophore.

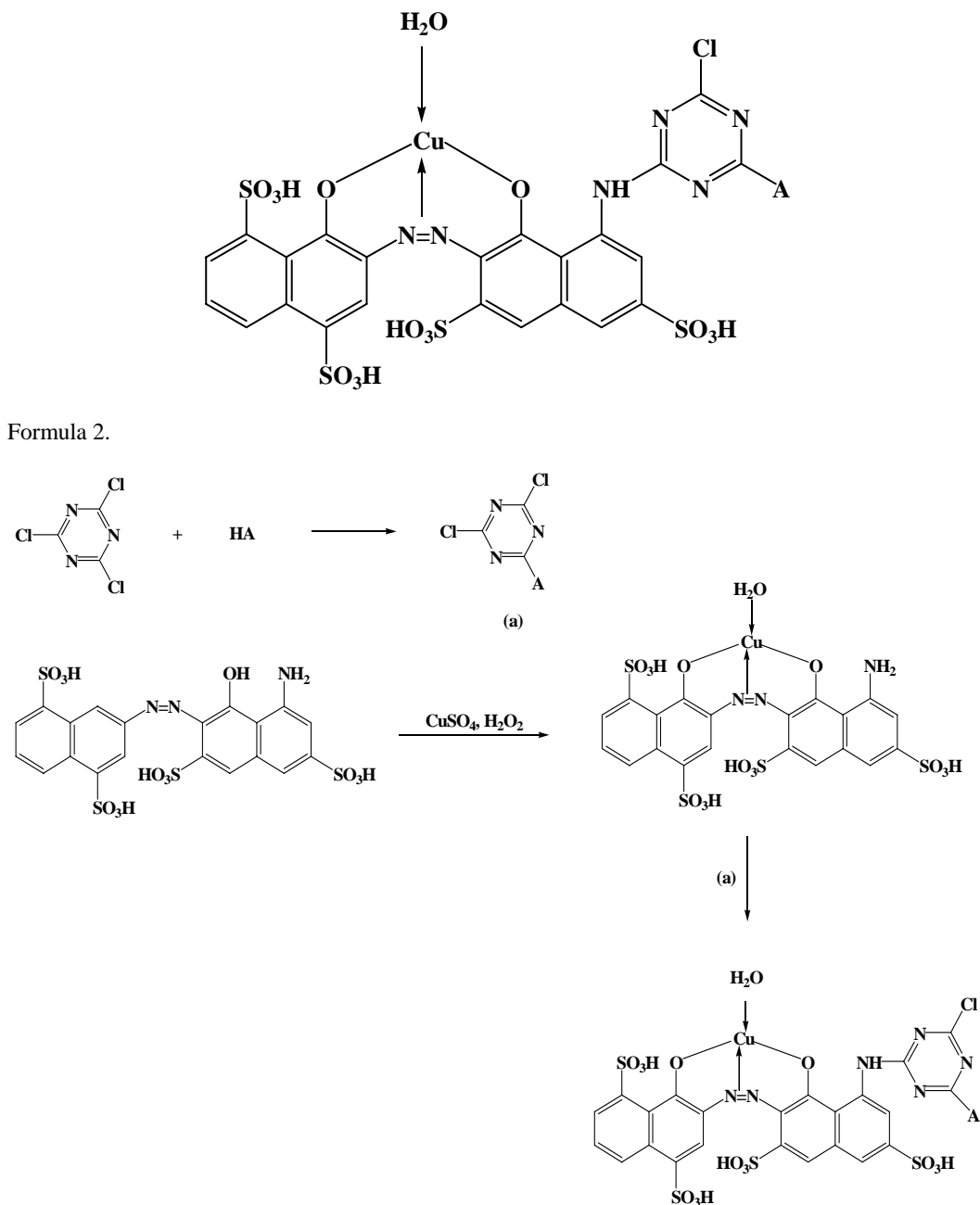


Scheme 2.

Table 1. Characteristic data for dyes with formula 1

Dye	$\lambda_{\text{max}}^{\text{abs}}$ (nm)*	R _f	Dye	$\lambda_{\text{max}}^{\text{abs}}$ (nm)	R _f
1.1 ^a	386	0.80 ¹	1.3 ^c	525	0.58 ²
1.1 ^b	392	0.83 ¹	1.4 ^a	498	0.50 ²
1.1 ^c	390	0.74 ¹	1.4 ^b	492	0.50 ²
1.2 ^a	382	0.64 ¹	1.4 ^c	496	0.52 ²
1.2 ^b	378	0.65 ¹	1.5 ^a	600	0.47 ³
1.2 ^c	374	0.63 ¹	1.5 ^b	596	0.47 ³
1.3 ^a	528	0.61 ²	1.5 ^c	598	0.44 ³
1.3 ^b	529	0.64 ²			

* Solution in water; ¹ - Silica gel plates 60F₂₅₄ eluent system n-propanol-ammonia (1:1, v/v); ² - Silica gel 60F₂₅₄ plates and eluent system n-propanol-ammonia (2:1, v/v) and ³ - Silica gel 60F₂₅₄ plates and eluent system n-butanol-acetic acid-H₂O (4: 1: 5,v/v).



Scheme 3.

The course of the synthesis was followed by a quantitative thin-layer chromatography (TLC) using a “Camag” system comprising of a TLC Linomat IV device for sample application, a Scanner II and a SP 4290 Integrator. TLC analysis was performed on 20x20 aluminium-backed ready-made plates precoated with 0.2mm layers (Silica gel 60F₂₅₄ products of Merck) following a procedure described before [5].

Scheme 1 was found to be more suitable for the synthesis of compounds 1.5, when for the rest of the dyes it was Scheme 2.

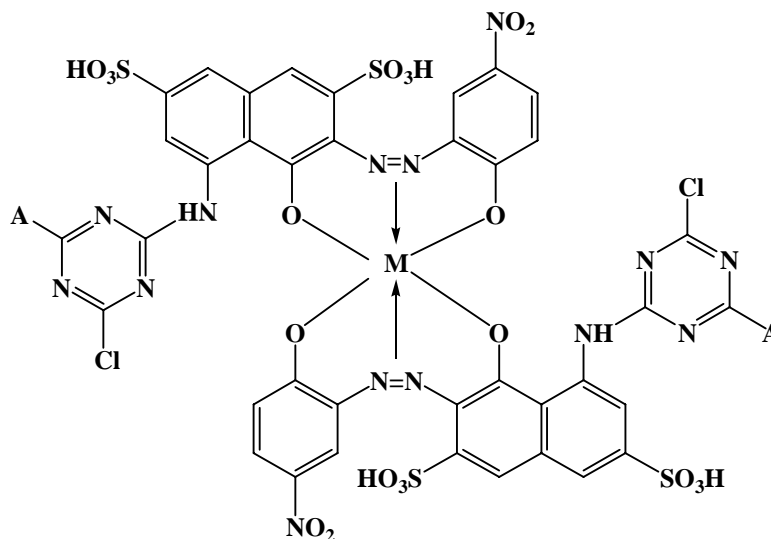
All the dyes were isolated in good yields, characterized and identified by TLC, UV/Vis, IR and $^1\text{H-NMR}$ spectra. The analytical data confirmed the structures. Some of these data are presented in Table 1.

The metallized dyes had their advantages and are of importance for the practice. The synthesis of more tolerant structures is of main importance as well. It was of interest to study the synthesis of structures similar to those shown above, where the basic chromophore is a metallized dye. Having in mind that among them the most applying are 1:1 copper (II) - azodye complexes, chromium (III) and cobalt (III) 2:1 -azo dye complexes, the dyes with such a structure were chosen. The first 3 derivatives (copper 1:1 complexes) are presented with formula 2, where A is - $\text{NHCH}_2\text{CH}=\text{CH}_2$ (dye 2.1), - $\text{OCH}_2\text{CH}=\text{CH}_2$ (dye 2.2) and - NH_2 (2.3 a model dye).

The synthesis of the dyes is presented by Scheme 3, where HA are allylamine, allylic alcohol or ammonia.

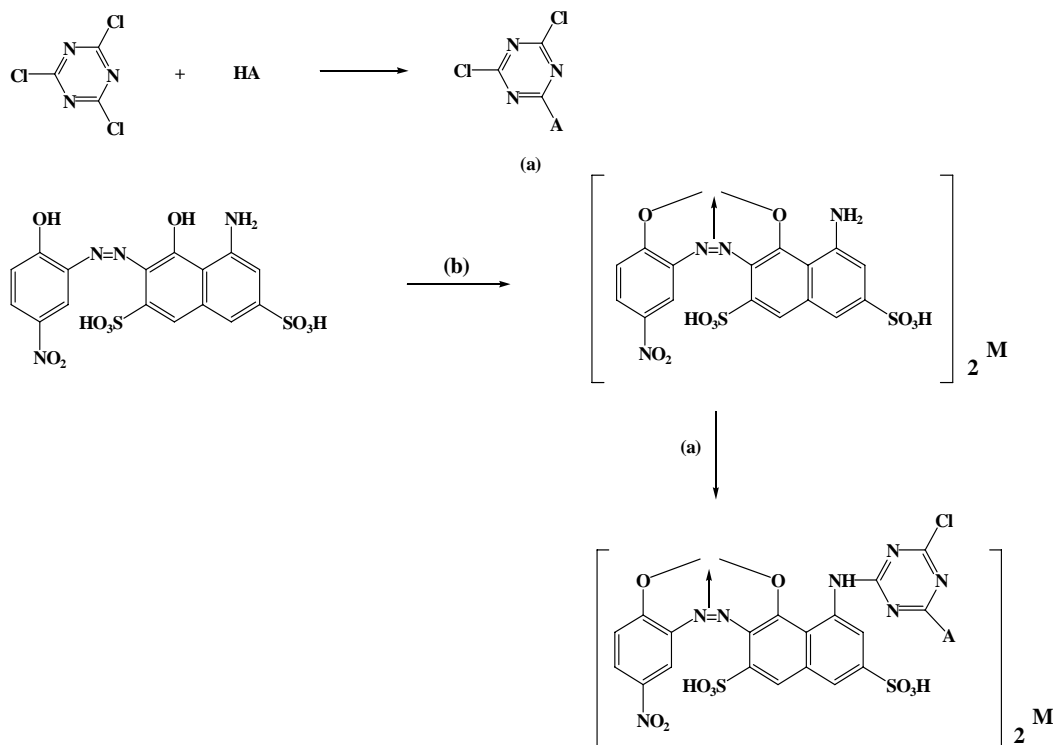
The synthesis was performed following the traditional procedure [4] and was monitored by a quantitative TLC [5]. The target compounds were obtained with good yields, they were characterized and identified by TLC, UV/Vis, IR and $^1\text{H-NMR}$ spectra. Some of the data are presented in Table 2.

The next 7 dyes have the general formula 3, where the meanings of the M (metal) and A are as follows:



Formula 3.

3.1 - M is Cr, A - $\text{NHCH}_2\text{CH}=\text{CH}_2$; 3.2 - M is Cr, A - $\text{OCH}_2\text{CH}=\text{CH}_2$; 3.3- M is Cr, A - NH_2 ; 3.4 - M is Co, A - $\text{NHCH}_2\text{CH}=\text{CH}_2$; 3.5 - M is Co, A - $\text{OCH}_2\text{CH}=\text{CH}_2$ and 3.6- M is Co, A - NH_2 . Their synthesis is presented by Scheme 4.



Scheme 4.

According to the scheme at the first stage by a reaction of cyanuric chloride with AH (allylamine, allylic alcohol or ammonia) the corresponding semi-products (a) were obtained. At the next stage, the products (a) thus obtained reacted with (b) - the corresponding complexes of Cr or Co with salicylic acid [3]. Four of the dyes (3.1, 3.2, 3.4 and 3.5) are new compounds, while 3.3 и 3.6 are model ones. The synthesis was monitored by a quantitative TLC [5]. The compounds were obtained with good yields, characterized and identified by the above-mentioned analytical methods. Some of the data are presented in Table 2.

Table 2. Characteristic data for dyes with formula 2 and 3

Dye	$\lambda_{\max}^{\text{abs}}$ (nm)	R_f
2.1	568	0.53 ¹
2.2	568	0.50 ¹
2.3	568	0.50 ¹
3.1	588	0.69 ¹
3.2	592	0.69 ¹
3.3	590	0.70 ¹
3.4	584	0.68 ²
3.5	584	0.70 ²
3.6	584	0.68 ²

¹Silica gel 60F₂₅₄ plates and eluent system n-propanol-ammonia (1:1, v/v); ²Silica gel 60F₂₅₄ plates, system n-butanol-acetic acid-H₂O (4: 1: 5, v/v).

Furthermore, by mixing dyes 3.1 and 3.4 in ratio 1:1 (dye 4.1), 3.2 and 3.5 (dye 4.2) and 3.3 and 3.6 (dye 4.3), 3 black dyes were obtained.

Color Assessment of the Synthesized Dyes

Cotton fabrics were dyed with dyes 1.1÷1.5 at 3 % depth o.w.f., according to the standard procedure [3, 6]. Materials with an intense color (yellow for dyes 1.1÷1.2, orange with 1.3, red with 1.4 or blue with 1.5) were obtained. Using the “Data color” technique and the associated software, the color characteristics of the dyes were recorded. From these data we saw some movement to the blue-reddish color for dyes 1.1^a, 1.2^a, 1.3^a, 1.4^a and 1.5^a in comparison to the corresponding model dyes 1.1^c ÷1.5^c. The similar movement but to the blue-greenish color was registered for the dyes 1.1^b÷1.5^b. The percentage of exhaustion and fixation of the dyes were determined applying the standard procedure. Data obtained are presented in Table 3.

One can see from these data that the dyes with two active groups (chloro- and allylic) in the triazine ring had approximately a 10- 15 % higher percent of exhaustion and fixation on the fabrics, which make them ecologically more tolerant and more suitable for application.

With dyes 2, 3 and 4, wool fabrics were dyed and intensively colored in blue, violet and black materials were obtained. Similar investigations to determine the color characteristics of the dyed materials (using Data Color technique) were performed and the percentage of exhaustion and fixation of the dyes was determined. It was found between 85 and 90 % of exhaustion and 99 - 100 % of fixation for all the dyes containing allylic active group(s). These data are higher compared to those for the model dyes (2.3, 3.3, 3.6 and 4.3). Wash fastness for all the dyed materials was determined to be 5 / 5 /5.

The electrochemical behavior of dyes with formula 1.1- 1.2 into aqueous solution was studied. It was found that the bifunctional dyes were reduced more easily in water than the model ones, which again is an indication for their ecologically more tolerant application.

Table 3. Exhaustion (%) and Fixation (%) of the dyes with formula 1 on cotton

Dye	1.1 ^a	1.1 ^b	1.1 ^c	1.2 ^a	1.2 ^b	1.2 ^c	1.3 ^a	1.3 ^b	1.3 ^c	1.4 ^a	1.4 ^b	1.4 ^c	1.5 ^a	1.5 ^b	1.5 ^c
Ex.* (%)	82	80	74	86	88	70	85	85	70	82	80	75	90	88	74
F** (%)	96	95	85	97	98	92	99	99	90	99	98	90	99	99	90

*Exhaustion; **Fixation.

2. DYES AND PIGMENTS FOR POLYMERS

2.1. Ecological Problems

Production of synthetic polymers and their application is extremely intensive. This sets the question for their qualitative and lasting coloration. There are several methods of polymer coloration [9].

- Method of textile coloration
- Method of surface coloration
- Method of coloration “in mass”

According to the first method, the polymers are dyed in the same way as the textile materials. The coloration is achieved by fixing of the respective dye by hydrogen, ionic or/and van der Waals bonds to the material. The disadvantages of this method and the ecological problems are the same as the ones for the dyeing of the textile materials. Furthermore, the polymer must have appropriate functional groups in its molecule with which the dye can form bonds. Considerable part of the polymers is not up to this requirement. Such widespread applied polymers like polyethylene (PE), polypropylene (PP) and polyvinylchloride (PVC) do not have such groups and cannot be dyed in this way. Other polymers such as polyesters and polyamides, even though they contain functional groups in the polymer chain, due to the higher density of the polymeric structure, these functional groups are inaccessible for the dyes.

The disadvantages of the second method are that only the surface layer of the polymer is colored, some of its properties can be broken during the coloration, and it is vulnerable on mechanical impact.

According to the third method, the dyeing can be achieved during or after the processing of the products, when the molecules of the dye or the pigment diffuse or dissolve into the mass of the polymer. To carry out a qualitative and uniform coloration in this way definite requirements are put on the dyes and the polymers. The dye must be in fine dispersing form, mixed with different additives. The main disadvantage of this method is that the colored polymer is a mixture of a higher molecular and a lower molecular substance. With time, the lower molecular substance (the dye) migrated to the surface of the polymer, damaging the quality of the color. This can change some of the properties of the polymer, too. Besides, if the polymers do not have amorphous areas in which the dye's molecule can diffuse, the coloration will not be possible.

2.2. Approaches for Solving the Problems-chemical Method

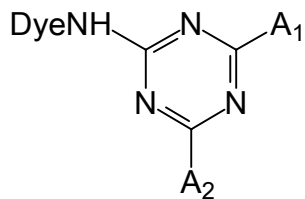
The first information about chemical coloration of polymers has appeared in 1960's. This method has economical and ecological advantages and can be realized in two ways: modification of polymers already synthesized or obtaining of self-colored polymers by copolymerization or polycondensation of a monomer with a color compound.

- *Modification of already synthesized polymer*

An example of coloration by this method is the obtaining of self-colored polystyrene described in [9]. Another example is when the colorless *Vinyon* fiber was passing through a solution of a dye, which contained aldehyde groups, which reacted with the hydroxyl groups of the polymer thus the self-colored polymer was obtained.

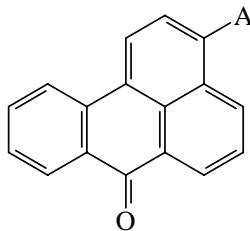
- *Synthesis of self-colored polymers by copolymerization*

To apply this method, the corresponding dye or pigment must have functional groups able to participate in copolymerization, to be stable during the process, to not prevent the polymerization. The first polymerizing dyes of this type were patented by BASF in 1962 and were obtained by acylation or vinylation of some anthraquinone dyes [10]. The corresponding self-colored copolymers were obtained by the copolymerization with styrene, methylmetacrylate and acrylonitril. During this period the information for the synthesis of self-colored polymers was summarized and published by Asquit [11], Mareshal [12], Guthrie [13] and others [14], including our earlier investigations on the synthesis and application of self-colored polymers [15-19]. For the first time, we demonstrated a principally new approach for introducing a polymerizing group in a dye molecule. As a base for the synthesis of such dyes, a proposal was made to use triazine reactive dyes with allylic- or acrylic group(s) as the substituents in the triazine ring. The dyes obtained had formula 4, where A_1 and A_2 are residues of allyl- or diallylamine, allylic alcohol, acryl- or methacrylamide.



Formula 4.

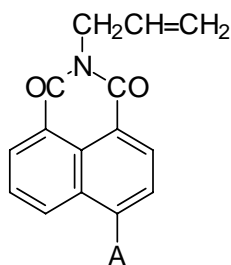
Firstly we studied two azo- and an anthraquinone chromophores only, and following the above mentioned idea, more than 30 polymerizable dyes and pigments were obtained. Later, the range of the chromophores was widened with benzanthrone (formula 5), whose derivatives were interesting with their bright colors, intensive fluorescence and good thermo- and light stability. Seven new polymerizing dyes with formula 5 were synthesized [20-25].



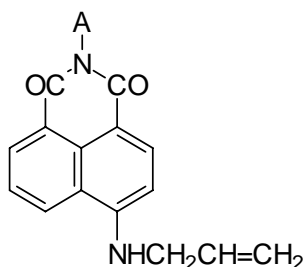
Formula 5.

The excellent color qualities and intensive fluorescence of the benzanthrone derivatives provoked our interest on the synthesis of some other polymerizing luminophores. Naphthalimide and 9-phenylxanthene dyes, which are among the most widely applied in different areas, were chosen.

Following this idea a group of polymerizing derivatives of naphthalimide with general formula 6 and 7, where A are residues of different aliphatic amines, were synthesized [26-31].



Formula 6.



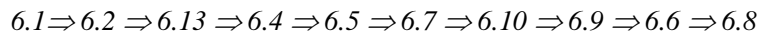
Formula 7.

Their spectral properties were studied [27]. With all synthesized dyes self-colored copolymers of styrene, MMA and AN, with a stable to solvents color and an intense fluorescence were obtained.

Having in mind how important for the application the photo stability of the dyes is, it was of interest to study the stability of the obtained functional naphthalimide dyes.

In this present paper, we reported our recent investigations on the photo degradation of 10 dyes with formula 6, where meanings of A are as follows: 6.1 – Br, 6.2- morpholino, 6.3- piperidino-, 6.4- piperazine, 6.5-dimethylamino-, 6.6- methyl amino-, 6.7- diethyl amino-, 6.8- ethyl amino-, 6.9- allylamino- and 6.10- NH₂.

To determine what the influence of the substituents on the photo stability of the dyes is, the solutions of the dyes in DMSO ($2 \cdot 10^{-4}$ g.mL⁻¹) were subjected to irradiation with UV light in a Suntest equipment (using a Xenon lamp 1.1 kW and $\lambda = 290$ nm). During the irradiation no change in the λ_{max} of absorption of the dyes was observed, which enable us to follow the kinetic of photo degradation spectrophotometrically by the method of the standard calibration curve. The data obtained at the end of the 2nd h are between 50 and 75 %, where the quantity of the dye in the solution before the irradiation was accepted 100 %. According to them we found that the photo stability of the compounds decreased in the order:



One can see from these data that the presence of an HN- fragment in the 4th position of the naphthalimide molecule (6.8, 6.6, 6.9 and 6.10) had a negative influence on the photo stability of the chromophore.

Table 4. Concentration of the dyes in copolymer (%)* during irradiation

Dye	6.1	6.2	6.3	6.4	6.5	6.6	6.7	6.8	6.9	6.10
Time 2h	97	93	95	95	92	90	91	87	90	90
Time 10 h	86	76	76	75	74	54	75	58	68	70

* The concentration of the dye in copolymer before irradiation was accepted 100 %.

Furthermore it was of interest to see the photo stability of the same dyes when they are incorporated into the polymer molecule. The copolymers of the above dyes with methyl methacrylate (MMA) were studied under the same conditions as the dyes- in solution of DMSO (2.10^{-3} g.mL⁻¹) and in films (plates with $d = 90$ mm and 2 mm thickness). The kinetics of photo degradation for 10 h was followed spectrophotometrically. The data obtained are presented in Table 4.

One can see from these data that:

- The photo stability of the dyes in copolymer is higher than that in solution and
- The structure- photo stability relationship followed the same order as in solution.

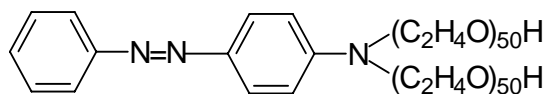
3. DYES FOR FOOD AND COSMETICS

3.1. Ecological Problems

It is well-known that for coloration of foods and cosmetics only a limited number of dyes and pigments is permitted. The ecological danger in this case is the most because the dyes and pigments get into the human organism directly, can undergo change and some toxic products can be obtained. In this connection looking for more tolerant dyes and pigments is of special interest.

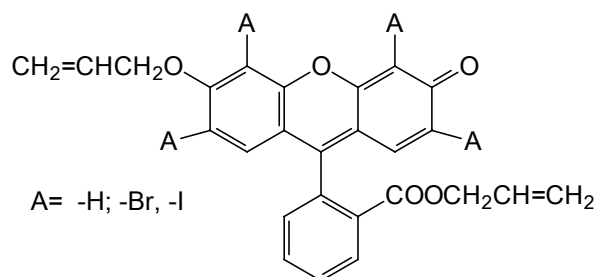
3.2. Approaches for Solving the Problems

It was established that if the molecular mass of an organic compound is over 1000, its penetration through the stomach walls and cells is very difficult or not possible [2, 32]. This fact has given a direction for synthesis of dyes with enlarged molecular mass. For example the Milliken dyes with a formula 8 were produced [2, 32].

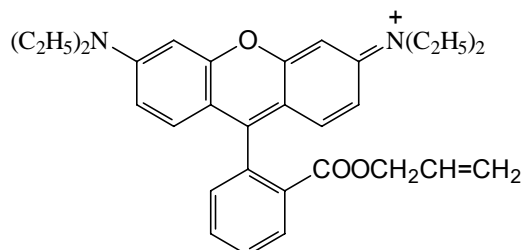


Milliken Yellow

Formula 8.



Formula 9.



Formula 10.

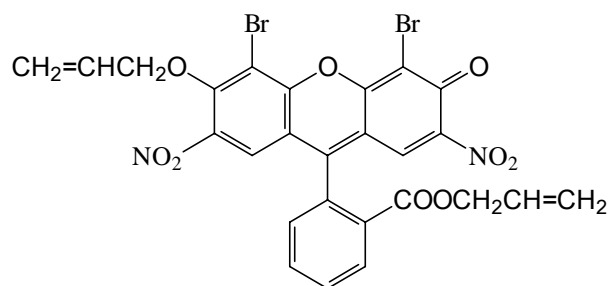
Derivatives of 9-phenylxanthene, due to their nice color and intense fluorescence have taken an important place among the dyes and pigments permitted and applied for coloration of food and cosmetics. In our earlier papers we demonstrated the synthesis of functional derivatives of 9-phenylxanthene [33-37]. They can be presented by formula 9 and 10.

The copolymers of these derivatives with MMA were obtained. Due to the chemical bonding of the dyes to the polymer chain, the copolymers thus obtained had an intensive color and fluorescence stable to solvents, which made them suitable for ecologically more tolerant application in some products like children's toys. Their spectral properties and photo stability were studied and it was found that the incorporation of the dyes into the polymer chain led to a considerable increasing of their photo stability [36, 37].

Polyacrylamide (PolyACA) is among the polymers widely applied in medicine, cosmetics, food processing industry and agriculture [38, 39]. It is well soluble in water which is important for the application. In a previous work of ours, the possibility of obtaining copolymers of acrylamide with some triazine herbicides and bactericides with more tolerant application, was established [40- 42].

Based on our experience, in the present paper we reported our study on the synthesis of copolymers of ACA with 5 dyes, derivatives of 9-phenylxanthene, with the view of their more tolerant application in the polymer form as food additives.

The dyes subject of the present study have the general formula 9, 10 and 11, where the meanings of A in formula 9 are: -H (dye 9.1); -Br (dye 9.2) and -I (dye 9.3).



Formula 11.

PolyACA is obtained easily by polymerization of acrylamide (ACA) in an aqueous medium, the polymer being water-soluble. That suggests a very good opportunity for application of the dyes in a water soluble polymer form. We performed the copolymerization at 50°C for 7 h in aqueous medium at two different concentrations of the corresponding dyes (0.1 wt. % and 0.2 wt %) in relation to ACA. The polymers thus obtained, brightly coloured and with an intense fluorescence are purified from unreacted monomers by three-fold reprecipitation from water solution with methanol. The latter is very good solvent for the dyes, but not for the polymer. After precipitation until a colourless filtrate was obtained, the polymers retained their color. This was an indication that the dyes were chemically bound to the polymer. The colored polymers thus purified were analysed.

The absorption UV/Vis spectra of all colored copolymers (solutions in formamide with concentration $2 \cdot 10^{-2} \text{ g.mL}^{-1}$) were recorded and compared to those of the pure dyes in the same solvent (concentration $2 \cdot 10^{-4} \text{ g.mL}^{-4}$). Neither hypso-, nor bathochromic shift in their absorption maxima was established, thus showing that the basic chromophore did not change, neither during the polymerization nor as a result of its bonding to the polymer molecule. These results enable us to determine spectrophotometrically the quantity of the chemically bound dye using the method of the standard calibration curve. The data obtained are presented in Table 5.

Considering these results one can see that the percentage of the dye chemically bound in the copolymer, except for the dye 11, is satisfactory. Taking into account the fact that during the reprecipitation of the polymers, lower-molecular fractions were removed as well, the real quantity of the dye reacted is higher and exceeds 50%. Thanks to the high color strength of the chromophores, the polymers reprecipitated were very intensely colored with bright fluorescence, and this intensity of theirs would be sufficient for the practice. The relatively lower activity (30 to 45% bound dye) of dye 11, could be due to the steric hinderence. More accurate conclusions however, could be possible after future investigations. The intrinsic viscosity $[\eta]$ of all precipitated colored copolymers was determined. The same measurements were performed for PACA, obtained under the same conditions, but without a dye. These data showed that the participation of the dyes in the copolymerization process did not affect the molecular mass of the copolymer. These results enable us to consider that the dyes under study will be suitable for application in polymer form as food or cosmetic additives.

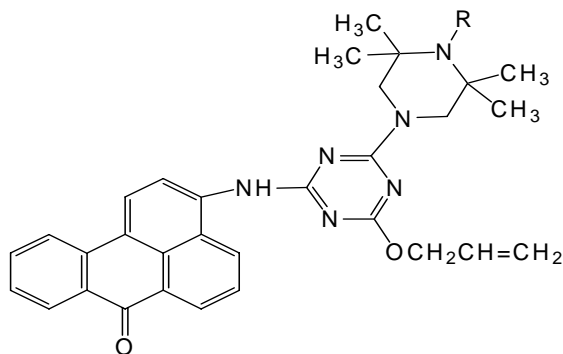
Table 5. Data for the chemically bonded in the copolymer dyes with formula 9, 10 and 11 (%)*

Copolymer with dye №	$\lambda_{\max}^{\text{abs}}$ (nm)	Chemically bounded dye at 0.1wt % initial concentration	Chemically bounded dye at 0.2 wt % initial concentration
9.1	460	56	74
9.2	534	57	80
9.3	542	52	65
10	570	72	72
11	538	30	45

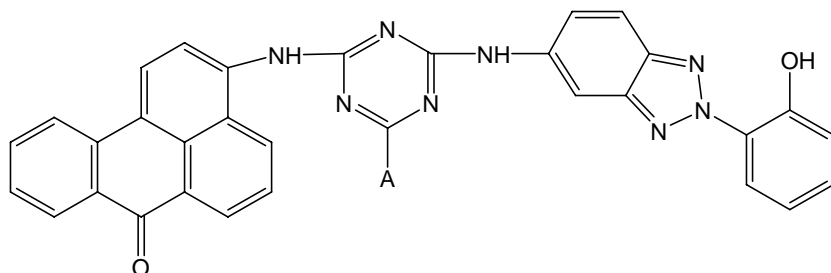
* initial concentration of the dye was accepted 100 %.

4. DYES AND PIGMENTS FOR “ONE-STEP” COLORATION AND STABILIZATION

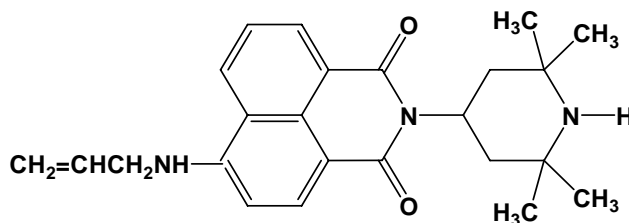
Along with the coloration, the photo stability of the materials is of great importance. Among different stabilizers used 2-hydroxyphenylbenzotriazole (HBT) and 2, 2, 6, 6-tetramethylpiperidine (TMP) derivatives are of interest [43]. Recently, the polymerizable stabilizers of different types were synthesized [44 - 48]. Their covalent bonding to the polymer chain provided stability towards solvents and a migration, both improving their environmental behavior, which is of importance for application in food and cosmetics. We reported before the possibility for “one-step” coloration and stabilization of polymethylmethacrylate (PMMA) and polystyrene (PSt), using polymerizable benzanthrone (formula 12 and 13) [24, 49] and naphthalimide (formula 14) [50] dyes, containing a polymerizable group and a stabilizer's fragment in the same molecule.



Formula 12.



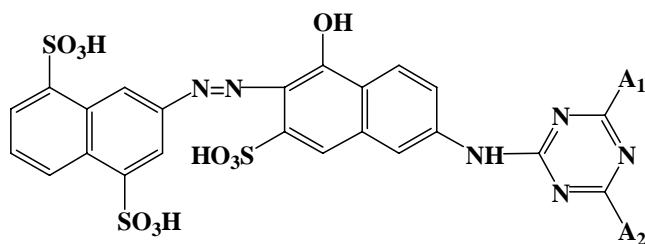
Formula 13. A is $\text{-NHCH}_2\text{CH}=\text{CH}_2$ or $\text{-OCH}_2\text{CH}=\text{CH}_2$ fragment.



Formula 14.

Bearing in mind these investigations and the fact that the azodyes are among the compounds with the lower photo stability, it was of interest to synthesize some azodyes, containing a TMP fragment in their molecule. To study the possibility for their application both for coloration and stabilization of polymers will be of interest as well.

The dyes reported in this paper have a general formula 15, where meanings of A are: A_1 -tetramethylpiperidinilamino, A_2 - $\text{NHCH}_2\text{CH}=\text{CH}_2$ (15.1); A_1 -tetramethylpiperidinilamino, A_2 - $\text{OCH}_2\text{CH}=\text{CH}_2$ (15.2); A_1 -Cl, A_2 - $\text{NHCH}_2\text{CH}=\text{CH}_2$ (15.3) and A_1 -Cl, A_2 - $\text{OCH}_2\text{CH}=\text{CH}_2$ (15.4).



Formula 15.

The synthesis of the dyes was achieved according to the procedure described before [4, 24]. Our idea was to see what the influence of a stabilizer's fragment on the photo stability of the dye is. In this connection the solutions of the dyes were subjected to irradiation with UV light (in a Suntest equipment) and the kinetic of their photo degradation spectrophotometrically was followed. The data obtained are presented in Figure 1, where the numbers of the curves are 1- dye 15.1; 2- dye 15.2; 3- dye 15.3 and 4- dye 15.4.

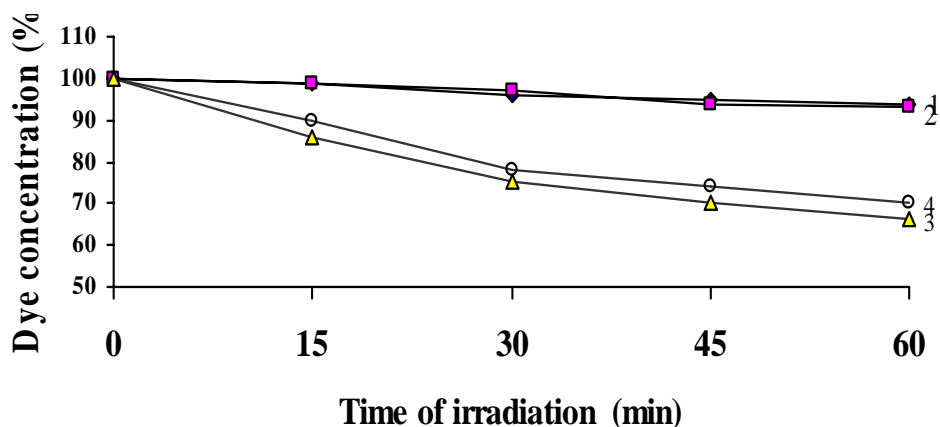


Figure 1. Dependence of dye's concentration (%) on the time of irradiation (min) 1- dye 15.1; 2- dye 15.2; 3- dye 15.3 and 4- dye 15.4.

One can see from these data that the presence of the TMP fragment in the dye's molecule led to the increasing of its photo stability by 25-30%.

Having in mind that the dyes had an unsaturated group in their molecule their ability to copolymerize with some monomers was studied. Polyacrylonitrile (PAN) is widely applied and its coloration and stabilization is of interest. Following the standard procedure the copolymerization of AN with the dyes with formula 15 (at 1% against AN) was performed in DMF solution at 70 °C. After 8h the orange-reddish colored polymers were obtained. After precipitation with hot water they retained their color, which was an indication for the covalent bonding of the dyes in the polymer. The influence of the dyes on the photo stability of the copolymers was studied, measuring the intrinsic viscosity $[\eta]$ of the polymers before and after the irradiation. The data for the molecular mass calculated presented in Table 6 showed that the dyes 15.1 and 15.2 with a TMP fragment in the molecule had a very good stabilizing effect on the photo degradation of the polymer.

Table 6. Data for molecular mass of the copolymers of AN with the dyes with formula 15 before and after irradiation of UV light

Copolymer with dye	$Mn_0 \times 10^3$ before irradiation	$Mn \times 10^3$ after 8h irradiation	S^*
15.1	310	284	0.09
15.2	247	231	0.07
15.3	157	122	0.28
15.4	192	153	0.25
PAN without dye	338	295	0.15

$S^* = Mn_0 / Mn - 1$ [48].

Based on the results obtained we can conclude that the dyes 15.1 and 15.2 having good photo stability and a stabilizing effect on the copolymers of AN can be applied successfully for one-step coloration and stabilization of these polymers with more tolerant behavior.

CONCLUSION

Based on this review and the results of our investigations, we can summarize that the polymer modifications of the dyes and pigments give definitely promising possibilities for their more tolerant and safe application, and the work in this direction is of great interest.

REFERENCES

- [1] Korte, F., *Lehrbuch der Okologischen Chemie*, Stuttgart: Thieme, 1992, p.1-24.
- [2] Zollinger, H., *Color Chemistry*, Weinheim: VCH, 1987, p.136-140; 215-233.
- [3] *The Chemistry and Application of Dyes*, D. Waring, G. Hallas, editors. London: Plenum Press, 1990, p. 50-60.
- [4] Konstantinova, T. N., Petrova, P. M., *Dyes & Pigments*, 2002, 52, 115-120.
- [5] Konstantinova, T. N., Lazarova, R. A., Miladinova, P. M., Venkova, A. Y., *J. of Planar Chromatography*, 2005, 17, 444-448.
- [6] ISO105CO6 (BDS), Bulgaria.
- [7] Zandoni, M. V., Carneiro, M. F., *Analytica Chimica Acta*, 1999, 385, (1-3), 385-392.
- [8] Gosser, D. K., *Cyclic Voltametry*, N.Y.: Wiley –VCH, 1993.
- [9] Vinogradova, C.V., Antipova, I. P. in *Progress polymernoy chimii* (in russian), Korshak, V. V. editor, Moskva: Nauka, 1969, 375-396.
- [10] Hans, W., Penning, E., *Patent BASF 1115925*, 1962.
- [11] Asquit, R., Blair, H., *J. Soc. Dyers & Col.*, 1977, 93, 9114-125.
- [12] Mareshal, E., *Progress in Org. Coatings*, 1982, 10, 251-263.
- [13] Guthrie, J. T., *Rev. Progress Coloration*, 1990, 20,120-126.
- [14] Patric, L. G., Whiting, A., *Dyes and Pigments*, 2002, 55, (2), 123-132.
- [15] Konstantinov, Hr. I., Konstantinova, T. N., Draganov, A. S., Kabaivanov, Vl. S., *J. Applied Polymer Sci*, 1972, 16, 725- 731.
- [16] Konstantinova, T. N., Draganov, A. S., *Angew. Makromol. Chemie*,1975, 43, 29-35
- [17] Draganov, A. S., Neitcheva, T. S., *Annual of VHTI*, (in bulg), 1968, XV, (3), 85-95.
- [18] Konstantinova, T. N., Konstantinov, Hr. I., Draganov, A. S., Kabaivanov, V. S., *Compt. rendus de l ' Acad. Bulg. des Sci.*,1975, 28, (5), 663-666.
- [19] Konstantinova, T. N., Konstantinov, Hr. I., Draganov, A. S., *Angew. Makromol. Chemie*, 1976, 50,1-8.
- [20] Konstantinova, T. N., *Dyes & Pigments*, 1988, 10, 63-67.
- [21] Konstantinova, T. N., Meallier, P., Konstantinov, H. I., Staneva, D. *Polymer Degradation & Stability*, 1995, 48, 161-166.
- [22] Bojinov, V. V., Konstantinova, T. N., *Dyes & Pigments*, 1996, 32, (3), 151-157.
- [23] Miloshev, S. M., Konstantinova, T. N., Novakov, K. N., Novakov, P. H., *J. Applied Polymer Sci*, 1997, 65, 91-97.
- [24] Bojinov, V. V., Konstantinova, T. N., *Polymer Degradation & Stability*, 2000, 68, 295.
- [25] Konstantinova, T. N., Lazarova, R. A., *Dyes & Pigments*, 2007, 74, 208-214.
- [26] Konstantinova, T. N., Meallier, P., Grabchev, I. K., *Dyes & Pigments*, 1993, 22,191-198.

- [27] Grabchev, I. K., Guittonneau, S., Konstantinova, T. N., Meallier, P., *Bull. Societe de Chemie de France*, 1994, 131, 828-830.
- [28] Grabchev, I. K., Meallier, P., Konstantinova, T. N., Popova, M. S., *Dyes & Pigments*, 1995, 28, (1), 41-46.
- [29] Konstantinova, T. N., Grabchev, I. K., *J. Applied Polymer Sci.*, 1996, 62, 447-449.
- [30] Konstantinova, T. N., Spirieva A. P., Petkova, T. I., *Dyes & Pigments*, 2000, 45, 125-129.
- [31] Konstantinova, T. N., Lazarova, R. A., Venkova, A. Y., Vassileva, V. N., *Polymer Degrad & Stability*, 2004, 84, 405-409.
- [32] Development in Food Color, J. Walford editor, vol. 95, London: *Appl. Sci. Publ.*, 1990, p.219-222.
- [33] Konstantinova, T. N., Kirkova, G. C., Betcheva, R. P., *Dyes & Pigments*, 1998, 38,(1-3),11-18.
- [34] Meallier, P., Guittonneau, S., Emmelin, C., Konstantinova, T. N., *Dyes & Pigments*, 1999, 40, 95-98.
- [35] Konstantinova, T. N., Bojinov, V. V., *Dyes & Pigments*, 1998, 39, (2), 69-75.
- [36] Konstantinova, T. N., Cheshmedjieva, G. K., Konstantinov, H. I., *Polymer Degrad & Stability*, 1999, 65, 249-252.
- [37] Konstantinova, T. N., Cheshmedjieva, G. K., *Polymer Degrad & Stability*, 2000, 70, 77-80.
- [38] Pesticide Formulation, Innovation & Development, editor Cross, B., N. Orleans: *Am. Chem. Soc.*, 1987, 1-16.
- [39] Applied Bioactive Polymeric Materials, editors Gebelein, C. G., Carraher, Ch. E., Foster, V.R., *NY: Plenum Press*, 1989, 5-20.
- [40] Konstantinova, T. N., Bogatzevska, N. S., *Compt. rendus de l'Acad. Bulg. des Sci.*, 1989, 42, (3), 113-116.
- [41] Konstantinova, T. N., *Compt. rendus de l'Acad. Bulg. des Sci.*, 1988, 41, (10), 69-71.
- [42] Konstantinova, T. N., Metzova, L. P., Konstantinov, H. I., *J. Applied Polymer Sci.*, 1994, 54, 2187-2190.
- [43] *Aspects of Degradation and Stabilization of Polymers*, editor Jellinek H., Amsterdam: Elsevier; 1978. p. 195-218.
- [44] Shuhaibar K, Rasoul F, Pasch H, Mobasher A., *Angew Macromol Chemie 1991*; 193:147-158.
- [45] Bojinov, V. B., *Polymer Degrad. Stability*, 2006, 91, 128-135.
- [46] Malik, J., Ligner, G., Avar, L. *Polymer Degrad Stabilit*, 1998, 60, 205-213.
- [47] Danko, M., Chmela, St., Hrdlovic, P., *Polymer Degrad Stability*, 2006, 91, 1045-1051.
- [48] Bojinov, V. B., *J. Appl. Polymer Sci.*, 2006, 102, 2408-2415.
- [49] Konstantinova, T. N., Lazarova, R. A., *Polymer Degrad Stability*, 2007, 92, 239-243.
- [50] Konstantinova, T. N., Lazarova, R. A., Bojinov, V. V., *Polymer Degrad & Stability*, 2003, 82, 115-118.

Reviewed by: *Prof. Dr. Sci. Kolio Troev*, Bulgarian Academy of Science, Acad. G. Bonchev str., Sofia 1113, Bulgaria, E mail address: ktroev@polymer-bas.bg

Chapter 16

**ENHANCED ANTHRAQUINONE DYE PRODUCTION IN
PLANT CELL CULTURES OF *RUBIACEAE* SPECIES:
EMERGING ROLE OF SIGNALING PATHWAYS**

Norbert Orbán*, Imre Boldizsár and Károly Bóka

Eötvös University, Department of Plant Anatomy, Pázmány Péter sétány 1/C,
Budapest, 1117 Hungary

ABSTRACT

Synthetic and natural analogues of 9,10-anthracenedione are well-known and widely used substances in the food and dye industries. Beyond their dyeing ability some anthraquinones are used as medicines as they exhibit beneficial effects in mammals and humans; moreover, anthracycline antibiotics have been applied therapeutically in the case of several malignant diseases. Total synthesis of anthraquinone derivatives using organic chemical methods is common; however, sophisticated biotechnological techniques provide alternatives for synthesis and overcome some environmental and economical concerns. The most frequently studied plant cell culture systems originate from members of the *Rubiaceae* family because these cell cultures are capable of producing high amounts of anthraquinone derivatives. Several methods to enhance the dye yield in order to obtain the best results have been and are still being used on a small-scale prior to applying them in large-scale industrial production. Numerous factors regulate the biosynthesis of anthraquinones in cell cultures like compartmentation, environmental stimuli (e.g. light, precursors) and endogenous (metabolic and developmental) factors. Since major points of the anthraquinone biosynthesis regulation are known in the *Rubiaceae* family, various possibilities have been raised to exploit these findings. Formation of hairy root and other transgenic cell cultures have proved to be useful tools to increase the anthraquinone production capacity; moreover, newer approaches (DNA and protein microarrays, proteomics) are promising techniques to define biosynthetic pathways to elucidate the unknown and rate limiting steps. Another effective approach to dye production enhancement in plant cell cultures is elicitation: exogenous stimuli induced gene activation. Various elicitors have been introduced during the past two

d) * E-mail address: norbiorban@gmail.com; Tel: +3613812165, Fax: +3613812166

decades affecting anthraquinone yields of measured cell cultures; however, the background of the influence on physiological events caused by elicitors is not fully understood. Elicitors are recognized by plant receptor(s) localized in the plasma membrane or cytoplasm. After elicitor signal perception, plant receptors activate effectors and signal transduction leads to the modulation of genes via second messengers. Altered gene expression might manifest itself in heightened production of anthraquinone derivatives. An increasing knowledge of plant signal transduction enables us to choose a suitable elicitor, which activates/modulates the desired pathways for anthraquinone production leading to a more selective production of the needed compounds. This commentary summarizes results of the latest studies on elicitor induced signal transduction leading to anthraquinone production in plant cell cultures and discusses other relevant techniques on a comparative basis. Furthermore, major problems and a future outlook are also debated.

INTRODUCTION

Plants are unique sources of a wide range of metabolites including important natural dyes such as indigo, betalains, anthocyanins, flavonoids and anthraquinones. These specific molecules are produced by secondary metabolism of plant cells and, among other roles, they are important in survival of the plants amidst unfavorable environmental factors. Due to the genetic diversity of the plant kingdom, these specific compounds are produced by well-defined taxonomic groups, although molecules with similar chemical structure may be present in several non-related groups, also. Unfortunately, the majority of the secondary metabolites are not produced in all parts of the plants and are not produced in all developmental stages. Synthesis of the desired compounds often does not start until the plants are several years old. If the metabolites are accumulated in underground organs (e.g. rhizomes, roots), harvesting results in destruction of the whole plant; therefore, isolation of the valuable components is not always economic or acceptable from the ecological point of view.

To overcome the problems above, several efforts have been made in the past decades to establish plant cell cultures in order to produce secondary metabolites [1-2].

In spite of intensive research and its results, only a few secondary metabolites are produced industrially in large scale by plant cell cultures: the naphthoquinone pigment shikonin (by *Lithospermum erythrorhizon* cells, Mitsui Petrochemical Industry, Co. Ltd., Japan), the antitumor diterpene derivative taxol (by *Taxus cuspidata* cells, Bristol-Myers-Squibb Co., USA) and the 9,10-anthracenedione derivative pigment purpurin (by *Rubia akane* cells, Nitto Denko Co., Japan) [3]. Production of quinoid pigments seems to be the most successful application of plant cell cultures.

Anthraquinones (derivatives of 9,10-anthracenedione) are widely distributed molecules in living organisms, they are present in bacteria, fungi, lichens and several families of higher plants, such as *Rubiaceae*, *Rhamnaceae*, *Polygonaceae*, and *Leguminosae* [4] (Figure 1.)

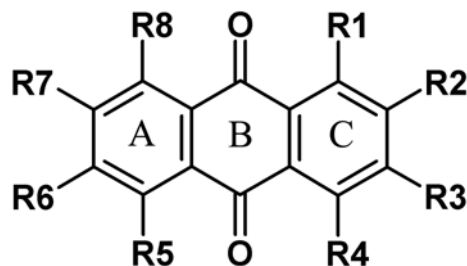


Figure 1. Chemical structure of anthraquinones.

Natural derivatives of 9,10-anthracenedione are well known and widely used chemicals to dye textiles in many regions of the world since ancient times (the oldest evidence is from 1350 B.C.) [5-6]. Extracts of *Rubiaceae* plants have been used for dyeing silk, cotton, jute, and other textiles, and to tint cosmetics and foods [5]. For better dyeing results and color modification of anthraquinones, numerous mordants have been applied as pre- or post-mordating agents, such as alum, copper sulfate, stannous chloride, ferrous sulphate, and potassium dichromate [5-6]. Recently, a wide range of synthetic anthraquinone derivatives has become available for dyeing purposes [7-8].

Beyond their dyeing ability, anthraquinones exhibit some valuable biological activities: their antimicrobial [9-10], antifungal [11], antimalarial [9], antithrombotic [12], antitumor [13], renal calculus eliminative [5], mutagenic and DNA binding [14], and antioxidant [15] features have been described. Moreover, some anthraquinone derivatives, called anthracycline antibiotics, are applied in the therapy of different malignant diseases (doxorubicin and its derivatives, and mitoxantrone and its derivatives). Unfortunately, they have some dangerous side effects, like congestive heart failure [16]. In the case of human malignant disease chemotherapy, one of the critical points is the selection of multidrug resistant tumor (MDR) cell lines in the organism, which are not responding to the applied drugs. To overcome the problems associated with anthracycline MDR cell lines, some new anthraquinone derivatives have been synthesized in the past decade [16-17].

Due to the diversified application of anthraquinones, their synthesis by organic chemical methods is common, although emission of toxic byproducts is unavoidable. Anthraquinone production by plant cell cultures is a more environmentally friendly method. Albeit this technology is suitable to generate only a few derivatives, its products are useful as basic molecules for further semi-synthetic processes of anticancer compounds [18]. One of the crucial factors of fermentation methods is the relatively high energy demand. As a consequence, several sub-methods have been developed in the past decades to increase the anthraquinone yield of plant cell cultures.

A number of plant cell cultures have been established in the past two decades from plant species of the *Rubiaceae* family with high capability of anthraquinone production: *Cinchona robusta* [19]; *Galium verum* [20], *M. citrifolia* [21], *M. elliptica* [22], *Ophiorrhiza pumila* [23], *R. akane* [24], *Rubia cordifolia* [25], *Rubia tinctorum* [2,26]. Moreover, some cell cultures produce anthraquinones also in bioreactors [27-30] offering the possibility of efficient production of these dyes in higher volumes (Table 1.).

Table 1. Examples of isolated anthraquinone derivatives from the *Rubiaceae* family

Compound	Source plant cell culture	R1	R2	R3	R4	R5	R6	R7	R8
Robustaquinone A	<i>Cinchona robusta</i>	OH	CH ₃	H	OH	H	OCH ₃	OH	OCH ₃
Robustaquinone B	<i>Cinchona robusta</i>	OH	CH ₃	H	H	H	OCH ₃	OCH ₃	H
1,3-dimethoxy-2-hydroxy-AQ	<i>Galium verum</i>	OCH ₃	OH	OCH ₃	H	H	H	H	H
Rubiadin	<i>Galium verum</i> <i>Morinda elliptica</i> <i>Ophiorrhiza pumila</i> <i>Rubia tinctorum</i>	OH	CH ₃	OH	H	H	H	H	H
1,6-dihydroxy-2-methyl-AQ	<i>Galium verum</i>	OH	CH ₃	H	H	H	OH	H	H
Alizarin	<i>Rubia akane</i> <i>Rubia cordifolia</i> <i>Rubia peregrina</i> <i>Rubia tinctorum</i>	OH	OH	H	H	H	H	H	H
Lucidin	<i>Ophiorrhiza pumila</i> <i>Rubia cordifolia</i> <i>Rubia tinctorum</i>	OH	CH ₂ OH	OH	H	H	H	H	H
Purpurin	<i>Rubia akane</i> <i>Rubia cordifolia</i> <i>Rubia tinctorum</i>	OH	OH	H	OH	H	H	H	H
Lucidin- ω -methyl ether	<i>Morinda citrifolia</i> <i>Morinda elliptica</i> <i>Rubia tinctorum</i>	OH	CH ₂ OCH ₃	OH	H	H	H	H	H
Nordamnacanthal	<i>Morinda citrifolia</i> <i>Morinda elliptica</i> <i>Rubia tinctorum</i>	OH	CHO	OH	H	H	H	H	H
Lucidin-primveroside	<i>Morinda citrifolia</i> <i>Rubia tinctorum</i>	OH	CH ₂ OH	O-Pr*	H	H	H	H	H
Alizarin primveroside	<i>Morinda citrifolia</i> <i>Rubia tinctorum</i>	OH	O-Pr*	H	H	H	H	H	H
Munjistin	<i>Rubia cordifolia</i>	OH	COOH	OH	H	H	H	H	H
2-methyl-1,3,6-trihydroxy-AQ	<i>Rubia akane</i>	OH	CH ₃	OH	H	H	OH	H	H
Pseudopurpurin	<i>Rubia tinctorum</i>	OH	COOH	OH	OH	H	H	H	H
1,6-dihydroxy-2-methyl-AQ	<i>Galium verum</i>	OH	CH ₃	H	H	H	OH	H	H
1,3,8-trihydroxy-2-methoxy-AQ	<i>Cinchona robusta</i>	OH	OCH ₃	OH	H	H	H	H	OH

*=primverose (6-*O*- β -D-xylopyranosyl- β -D-glucose); AQ=anthraquinone.

See also Figure 1.

SOME FEATURES OF BIOSYNTHESIS OF ANTHRAQUINONES IN THE *RUBIACEAE* FAMILY

To understand the secondary product formation of plant cell cultures in the *Rubiaceae* plants, a short overview is given here on their anthraquinone biosynthesis (for more details see [4]).

Essentially two basic biosynthetic pathways exist leading to anthraquinones in plants: the polyketide pathway and the chorismate/*o*-succinylbenzoic acid pathway [4,31]. The polyketide pathway is not involved in the anthraquinone formation in the *Rubiaceae* family.

The speciality of the anthraquinone biosynthesis in *Rubiaceae* plants is that A and B rings are formed via *o*-succinyl benzoic acid (OSB) whereas ring C is formed from isopentenyl diphosphate (IPP) via the terpenoid pathway [31].

Initial molecules of A and B ring synthesis are phosphoenol-pyruvate and erythrose 4-phosphate. From these substances, the chorismic acid (its intermediary molecule is the sikimic acid) is formed via several steps. Isochorismate synthase (ICS) produces isochorismate from chorismic acid [32] and isochorismate in its turn is converted into OSB by OSB synthase in the presence of α -ketoglutarate and thiamine diphosphate. The OSB-CoA ligase activates the OSB by forming OSB-CoA ester and subsequently this ester goes through ring closure resulting in the formation of 1,4-dihydroxy-2-naphthoic acid, which gives the A and B rings of anthraquinones [33].

Formation of the C ring in the anthraquinones results from the cyclization via C-C bond formation between the aromatic ring of the naphthoquinone and isoprene unit IPP or 3,3-dimethylallyl diphosphate (DMAPP) [4]. IPP can be formed via two independent pathways: the mevalonic acid (MVA) or the 2-C-methyl-D-erythritol 4-phosphate (MEP) pathways [34].

In the MVA pathway's first reaction, acetyl-CoA is converted into 3-hydroxy-3-methylglutaryl-CoA (HMG-CoA) via several steps. HMG-CoA is converted into MVA, and next in a few steps the isopentenyl diphosphate is synthesized from the MVA [4,35].

In the MEP pathway, the initial step is the formation of 1-deoxy-D-xylulose-5-phosphate (DOXP) by the condensation of glyceraldehyde 3-phosphate and pyruvate [36]. The reaction is catalyzed by 1-deoxy-D-xylulose-5-phosphate synthase (DXS) [37]. In the next reaction, DOXP is converted into MEP by the enzyme DOXP reductoisomerase (DXR). Then MEP is transformed into 4-cytidil diphospho-2C-methyl-D-erythritol (CDP-ME), and the CDP-ME is further changed into 2-C-methyl-D-erythritol 2,4-cyclophosphate (MEC). This molecule forms the IPP.

After its formation, IPP is converted by the enzyme IPP isomerase in both pathways into DMAPP, the activated monomer unit of isoprenoids [38 and references therein].

Most of the anthraquinones of the *Rubiaceae* family have substitutions in ring C and/or in ring A (Table 1). These substitutions might be introduced in late stages of anthraquinone biosynthesis and some anthraquinones are stored in their glycoside forms, due to the glycosylation processes [4,39].

FACTORS AND METHODS LEADING TO ENHANCED ANTHRAQUINONE BIOSYNTHESIS AND YIELDS

Screening, Medium Optimization

The most common approach to enhance secondary metabolite production of plant cell cultures is selection of appropriate plants/cell strains [40]. This screening process may involve the selection of different organs/plants/biochemical variants/cultivars/species or *in vitro* cultured cell lines [40]. The latter approach has recently been applied to select *R. tinctorum* populations for optimal (e. g. low-level of genotoxic lucidin) anthraquinone composition [41]. In the case of anthraquinone derivatives, selection of high-producing cell lines is simple because of their color attribute, and lines could be selected by visual examination for cell aggregate cloning [42].

Another general technique is optimization of the culture medium composition [43]. Several studies have shown the positive effects of plant growth regulators on the anthraquinone production, e. g. an increase of 1-naphthaleneacetic acid (NAA) level promoted the anthraquinone production in cell cultures of *Morinda*, *Galium*, *Cinchona*, *Rubia* [44-47]. Naturally, the developmental stage of cell cultures must be taken into consideration. Hagendoorn et al. [48] showed that the growth phase and the production phase could be affected distinctly with different concentrations of 2,4-dichlorophenoxyacetic acid (2,4-D). Abdullah and co-workers [27-28] described remarkable differences in anthraquinone production of *M. elliptica* cell cultures grown in “maintenance”, “production” and “growth” media. The “production” medium strategy enabled 5-fold anthraquinone yield in comparison to the “growth” medium.

The type and quantity of carbon source is also an important regulating factor of anthraquinone production. Generally sucrose has priority in use but not in all cases. Actually, in *R. cordifolia* culture glucose has a better effect [49]. The effect of sucrose is influenced by the phytohormone composition of the medium [46].

There are no general formulas for media because of the various demands of the different cultures; therefore it is advisable that the medium should be optimized according to their needs [43,45,50].

Medium optimization is the most essential step during establishment of plant cell suspension cultures. Combining it with the approaches above productivity might reach a 20-30 times higher rate in the case of compounds which were present in the initial cultures [51].

Techniques to Enhance Yields of Secreted Compounds into the Medium

Due to the chemical characteristics of anthraquinone derivatives, several cells secrete them (mainly in glycosidic form) into the culture medium [21,52]. This phenomenon could be utilized either by application of permeabilizing agents [53-54] resulting in 14-170-fold higher release of anthraquinones or by using a two-phase medium system facilitating the collection of less water-soluble anthraquinone derivatives into a non-polar phase [21,55]. Besides the two-phase liquid method, some authors have also applied adsorbents (eg. XAD resins) to ameliorate the separation of the released anthraquinone derivatives [54,56]. Immobilization of

cells is also an adequate method to enhance the production of secondary metabolites. Immobilization of *Cruciata glabra* cells resulted in a 5.6-fold increase in anthraquinone production and 34-fold higher anthraquinone release to the medium [57-58].

Direct Influence on the Biosynthetic Capacity

Our knowledge on the biosynthetic pathways gives several opportunities to enhance the anthraquinone production of plant cell cultures [4]. A simple method is the precursor feeding to the cultures as intermediary molecules of the metabolic pathways such as chorismate, OSB (added to *Morinda* cell cultures) or pyruvate (precursor of the MEP pathway). Supplying them resulted in up to 4-fold increased anthraquinone production [4,59-61]. A further technique is the application of stimulators of different pathways such as proline (stimulator of pentose phosphate pathway leading to erythrose phosphate, a basic molecule of the shikimate pathway) or blocking competitive pathway's activity with specific inhibitors (like aminoindan-2-phosphonic acid an inhibitor of phenylalanine ammonia liase, the key enzyme of cinnamate biosynthetic pathway). Applying these methods, anthraquinone production of *R. tinctorum* cells was increased by around 50 percent [62]. Glyphosate, a partial inhibitor of chorismate biosynthesis, behaved controversially: in *M. citrifolia* cell culture it decreased the anthraquinone biosynthesis, while in *R. tinctorum* culture it enhanced the anthraquinone production [63].

Environmental Factors and Compartmentation

Taking into consideration the environmental factors of cell cultures (light, temperature, shaking, aeration etc.) their effect is obvious on culture metabolite production. Light intensity may have a principal role in association with anthraquinone production. Generally, illumination of the cell cultures reduces anthraquinone yield [22,64]; however, high-producing cell cultures are maintained for several years at dimmed natural light [65].

For anthraquinone production the compartmentation of cells is an important reality, at least four intracellular compartments are essential: plastids, endoplasmic reticulum, cytosol, and vacuolar system (e. g. for storage). All influences on differentiation status of the above compartments alter the secondary metabolite production ability of the cells. This fact should be considered during the process of designing the culture medium and engineering the fermentation strategy [4,66].

Plant Genetic Engineering

Plant genetic engineering approaches and techniques have made great progress during the past two decades and their use has led to the commercial introduction of several transgenic plants (e.g. various crops) in agriculture [51,67]. In the past years, tremendous advances have also been attained in metabolic engineering of plant secondary metabolism [4,68]. The major approaches of plant genetic engineering are summarized in Table 2. (for more details see [68-70] and references therein).

Table 2. Approaches of plant genetic engineering

Approach	Applied techniques	Reference
Discovery of new enzymes and genes of plant natural product biosyntheses	Enzyme purification, Peptide microsequencing, Screening of cDNA libraries, Establishment of expressed sequence tag, Whole genome sequencing, PCR	[68,69]
Identification and application of transcription factors involved in plant secondary metabolism	RT-PCR, cDNA isolation, Dnase footprint analysis, Recombinant protein isolation	[70-73]
Inhibition and overexpression of biosynthetic enzymes	RNA interference, Overexpression of different genes, Overexpression of transcription factors	[69,74-76]
Investigation of enzymes involved in plant secondary metabolism	Protein crystallization, X-ray diffraction, Mass spectrometry	[68,77-78]
Combinational biosynthesis of plant natural products	Ligation of cDNA into plasmids and transfer into foreign organisms (bacteria, fungi, plants)	[79-81]

To enhance production of anthraquinone derivatives ICS gene (*ics*) was introduced into *M. citrifolia* and the cell line containing the *ics* gene in sense orientation showed higher ICS activity [4]. A DXS gene encoding cDNA was cloned from *M. citrifolia*, and its transcript level correlated with the anthraquinone accumulation of the culture suggesting DXS small gene family regulation at the transcriptional level [82]. Unfortunately, there are only some relevant molecular biological works published in this field from *Rubiaceae*. This fact may be a result of the relatively low price of anthraquinone derivatives in comparison with other plant-derived compounds, e.g. taxol.

Among the extremely organized and genetically modified cultures, hairy root cultures are the best-studied. The hairy root development is based on the transfer of *Agrobacterium rhizogenes* T-DNA into the genome of infected plants. This T-DNA carries a set of genes encoding enzymes to regulate auxin and cytokinin biosynthesis. The altered balance of the hormones induces extraordinary root proliferation, called hairy roots (for details see [83] and references therein).

Several authors have demonstrated that anthraquinone derivatives are produced by hairy root systems from plants of the *Rubiaceae* family and the main compounds are very similar to the native roots. However, the yield of these compounds is often lower in the artificial root system than the measured amount in the native roots [29,46,84-85]. Other authors have established anthraquinone producing transformed *Rubia* calli. They are good subjects for the investigation of the transferred cells' behavior under different stresses [86-88].

Elicitor Induced Anthraquinone Accumulation and Signal Transduction

The connection between plant secondary metabolism and plant defense mechanism is well-known, plants in reaction to unfavorable biotic/abiotic signals developed a set of defense

responses involving the production of secondary metabolites (phytoalexins, e.g. anthraquinones) [3,89]. For the plant defense response induction, the whole biotic/abiotic environment is not necessary but the presence of a special part of it is enough. Keen was the first person to use the term “elicitor” for substances, which can generate responses manifesting in phytoalexin production [90]. Nowadays, elicitors can be defined as substances of which small amounts induce or enhance the production of specific metabolites in a living cell system [91]. During the last decades, several elicitors were found; accordingly the classification of elicitors became necessary and they were classified on the basis of different approaches, such as molecular structure, specificity, origin etc. We can also include among elicitors some abiotic stress factors, such as shearing stress or temperature stress, in spite of the fact that no substances are added to the cell system [30]. Table 3 shows a classification of elicitors based on the papers of [3,89,91].

The first step in triggering elicitor induced defense reactions is the recognition of the elicitor by the plant cell “receptors”. This highly specific recognition process is essential in response generation [92]. The physical/chemical linkage between the elicitor and its receptor causes conformational changes in the receptor’s structure [3]. This structural alteration enables it to activate the effector molecules and via signal transduction pathways the appearance of the elicitor is transformed into particular signals expounded by the cell’s metabolic and genetic apparatus. Receptors can be located in the plasma membrane, apoplast and cytoplasm, according to the molecular structures, which they recognize. The elicitor-receptor recognition is specific and characterized by high affinity, showing reversible and saturable binding. The above-mentioned specificity may manifest itself in altered anthraquinone production (both qualitatively and quantitatively) giving a key approach to influence the anthraquinone composition of cultured cells. Elicitors, jasmonic acid (JA) and salicylic acid (SA) act at particular sites of the signaling network regulating the formation of final outcome. Apart from the specific elicitor-receptor recognition, interactions of second messengers diversify also the induced responses in the cells [3,89].

Table 3. Classification of elicitors

Elicitor					
Abiotic	Physical	Wounding, Shearing stress, Temperature stress, UV irradiation			
	Chemical	Metal ions (europium, calcium, vanadium)			
Biotic	Chemical	Complex composition	Fungal cell wall extracts, Fungal spores, Bacterial culture extracts, Bacterial/Fungal homogenates		
		Defined composition	Polysaccharide	Alginate, Chitosan, Pectin, Chitin	
			Oligosaccharide	Galacturonides	
			Peptides	Glutathion, Systemin	
			Proteins	Cellulase, Elicitins	
			Lipids	Lipopolisaccharides, Syringolide	
			Glicoproteins	Cryptogeins	
			Volatiles	Volicitin	

Activation of particular sections of the signal transduction and types of the plant defense phenomena differ in accordance to the elicitor types and the nature of their perception (e.g. the type and localization of receptors). However, elicitor induced signal transduction is a multi-component network involving several junctions and cross-talking points; accordingly the parts of this signaling system are not separated from each other but appearing side by side. Generally, they amplify/attenuate/modulate the other processes and finally this determines the induced gene expression patterns and the redistribution of metabolic fluxes [89].

The major parts and known key molecules of the signal transduction leading to increased production of secondary metabolites are indicated in Table 4. [3,89].

Table 4. Most important signaling components and some examples of their roles

Signaling event	Known roles
(receptor-induced) GTP binding protein (G-protein) activation	NADPH oxidase activation, Ion channel activation, Phospholipase activation, Anthraquinone pigment production
Ion fluxes/ Ca^{2+} signal	Gene expression alteration, NADPH oxidase activation, Anthraquinone pigment production, Activation of calcium/calmodulin dependent molecules (protein kinases/phosphatases), Transcription factor activation/synthesis, Regulation/alteration/integration of other signaling events and transfers signals to downstream events
Cytoplasmic acidification	PAL and HMGC _o A gene transcription enhancement, Formation of oxidative stress
Oxidative burst	Direct antimicrobial effect, Cell wall reinforcement, enhancement of the synthesis of phytoalexins, Second signal messenger role –modulates/amplify other signaling events, Expression enhancement of defense genes (PAL)
Inositol phosphates/cyclic nucleotides	Calcium ion mobilization from intracellular stores, Regulation of plasmamebrane positive ion channels
Salicylic acid/Nitric-oxide	Hypersensitive response formation, Systemic acquired resistance formation, Gene expression modification, Influence on the synthesis of several secondary metabolites (e.g. anthraquinones)
Jasmonic acid	Gene expression alteration, Elicitor signal transduction, Second messenger of the different signaling pathways (modulator molecule)
MAP and other kinases/phosphatases	Regulation of different molecules (e.g. ion channels, transcription factors) via phosphorylation/dephosphorylation
Abscisic acid /ethylene	Alteration of gene expression
Lipid signaling (oxylipins, phospholipases, and other lipid messengers)	Wound healing, Protein kinase and kinase cascade activation, Oxidative burst generation

GTP-Guanosine 5'-triphosphate; NADPH-Nicotinamide adenine dinucleotide phosphate (reduced form); PAL-Penylalanine ammonia-lyase; HMGC_oA-3-hydroxy-3-methylglutaryl Coenzyme A; MAP-Mitogen-activated protein kinase.

Elicitation of plant cell systems is a simple and relatively cheap method to enhance production of desired compounds. In the cell cultures of plants belonging to the *Rubiaceae* family, several authors have applied elicitors to enhance the anthraquinone biosynthesis, such as fungal elicitors [26,65,93], chitosan [94-95], and signaling molecules such as JA

[26,86,96-97] or SA [26,86]. Elicitation with fungal elicitors and JA seems to be the most effective on anthraquinone yields and elicitation methods generally enable high anthraquinone production of the cells (up to 30-fold increase in the case of particular compounds). Our recent results have shown that fungal elicitors mainly increased production of glycosides while signaling compounds, like JA and SA, caused higher synthesis rates of aglycons. These findings may facilitate further advantages of selective dye turnout [26].

Other recently published data have also proved that several signaling events take part in elicitor induced anthraquinone production of *R. tinctorum* cell cultures, such as G-protein activation, oxidative burst, lipid signaling, calcium mobilization [95,98-101]. Understanding the above in connection with the biosynthetic routes is crucial in the conscious engineering of anthraquinone dye production. Exploration of the key reactions and rate limiting steps of signaling and biosynthesis, as well as using the regulator/modifier molecules, would give us the chance to obtain more effective, selective and economic processes in production of 9,10-anthracenedione analogue dyes. A new breakthrough can be expected from proteomic and metabolomic investigations. Detailed observation of protein content changes and metabolite composition after stresses or elicitor exposition may help to understand the role of regulators and interactions among the different signal transduction pathways.

CONCLUSION

Taking into consideration the valuable results in the enhancement of anthraquinone production, we can pronounce that the synthesis of 9,10-anthracenedione derivatives by plant cell cultures is successful and in several cases has economical and environmental advantages. Our main problem recently has been that production is not specific enough and several undesired derivatives are also produced in line with the other valuable ones. Tools to control the biosynthetic routes are not effective enough yet to narrow the turnout of the cells to one, maximum two main compounds, which might reduce the costs of the expensive separation procedures. Fortunately, new analytical methods provide fast scan, high selectivity and good productivity possibilities, so identification and quantification of the proper derivatives is a routine process even at a higher number of samples [102-103]. In the future, dye production by application of plant cell cultures should be a more prudential process and engineering should be more efficient once you know the target product and the affected key steps. The most relevant and progressive methods are genetic engineering and exploitation of elicitor-induced gene activation. The first method has small advantages in the case of anthraquinone production, the latter one has the benefits of several new advances, but the relationship between the elicitor type and the produced molecule has not yet been fully clarified. Based on our current knowledge, beyond the fully optimized culturing circumstances and application of the key precursors, over-expression of the key enzymes of the proper biosynthetic pathway(s) on its own is not enough to obtain optimal yields of cultures. This approach should be supplemented with the extinction of the capacity of competitive pathways by genetic modification or by applying specific inhibitors and/or by further stimulation of the over-expressed pathways with the proper elicitor. If the previous optimization steps were realized depending on the target molecule, further yield enhancing techniques (two-phase medium, immobilization) would be applied. A new approach in the additional processing of the

synthesized glycosidic molecules is the enzymatic hydrolysis with the native enzymes of plant cultures allowing the step of the additional hydrolysis to be replaced by the plant cultures, resulting in further cost reduction (Boldizsár et al. *in manuscript*).

Our hope is that in the coming years the above mentioned techniques will give the full possibility of producing more selectively the desired specific anthraquinone derivatives economically by using plant cell cultures.

REFERENCES

- [1] Yeoman, M. M., Holden, M. A., Corchet, P., Holden, P. R., Goy, J. G. & Hobbs, M. C. (1990). Exploitation of disorganized plant cultures for the production of secondary metabolites. In B. V. Charlwood, & M. J. C. Rhodes (Eds.), *Secondary Products from Plant Tissue Culture* (pp. 139-166). Oxford, UK: Clarendon Press.
- [2] László, M., Kretovics, J., Dános, B., Szókán, Gy., Liszt, K., Hollósi, F., Tóth, Z. & Gyurján, I. (1992). The production of secondary metabolites by plant cells of *Rubia tinctorum* cultivated in bioreactors. *Planta Medica*, *47*, 613.
- [3] Vasconsuelo, A. & Boland, R. (2007). Molecular aspects of the early stages of elicitation of secondary metabolites in plants. *Plant Science*, *172*, 861-875.
- [4] Han, Y. S., Van der Heijden, R. & Verpoorte, R. (2001). Biosynthesis of anthraquinones in cell cultures of the Rubiaceae. *Plant Cell, Tissue Organ Culture*, *67*, 201-220.
- [5] Singh, R., Geetnajali, S. & Chauhan, S. M. S. (2004). 9,10-Anthraquinones and other biologically active compounds from the genus *Rubia*. *Chemistry & Biodiversity*, *1*, 1241-1264.
- [6] Derksen, G. C. H. & van Beek, T. A. (2002). *Rubia tinctorum* L. In Atta-ur-Rahman (Ed.), *Studies in Natural Products Chemistry* (vol 26., pp. 629-673). Amsterdam, The Netherlands: Elsevier Science B.V.
- [7] Yavari, Y., Albrozi, A. R. & Mohtat, B. (2006). Synthesis of highly functionalized 9,10-anthraquinones. *Dyes and Pigments*, *68*, 85-88.
- [8] Yavari, I. & Kowsari, E. (2008). Synthesis, spectral and thermal properties of some phosphorus-containing 9,10-anthraquinoid, thermally stable dyes. *Dyes and Pigments*, *77*, 103-110.
- [9] Sittie, A. A., Lemmich, E., Olsen, C. E., Hviid, L., Kharazmi, A., Nkrumah, F. K. & Christensen, S. B. (1999). Structure-activity studies: *In vitro* antileishmanial and antimalarial activities of anthraquinones from *Morinda lucida*. *Planta Medica*, *65*, 259-261.
- [10] Ogzen, U., Houghton, P. J., Ogundipe, Y. & Coskun, M. (2003). Antioxidant and antimicrobial activities of *Onosma argentatum* and *Rubia peregrina*. *Fitoterapia*, *74*, 682-685.
- [11] Manojlovic, N. T., Solujic, S., Sukdolak, S. & Milosev, M. (2005). Antifungal activity of *Rubia tinctorum*, *Rhamnus frangula*, and *Caloplaca cerina*. *Fitoterapia*, *76*, 244-246.
- [12] Chung, M. I., Jou, S. J., Cheng, T. H., Lin, C. N., Ko, F. N. & Teng, C. M. (1994). Antiplatelet constituents of formosan *Rubia akane*. *Journal of Natural Products*, *57*, 313-316.

- [13] Chang, P. & Cheng, C. (1995). Isolation and characterization of antitumor anthraquinones from *Morinda umbellata*. *Chinese Pharmaceutical Journal*, 47, 347-353.
- [14] Jager, I., Hafner, C., Welsch, C., Schneider, K., Iznaguen, H. & Westendorf, J. (2006). The mutagenic potential of madder root in dyeing processes in the textile industry. *Mutation Research-Genetic Toxicology and Environmental Mutagenesis*, 605, 22-29.
- [15] Tipathi, Y. B., Sharma, M. & Manickam, M. (1997). Rubiadin a new antioxidant from *Rubia cordifolia*. *Indian Journal of Biochemistry & Biophysics*, 34, 302-306.
- [16] Dzierzbicka, K. & Kołodziejczyk, A. M. (2005). Anthracenedione analogues – synthesis and biological activity. *Polish Journal of Chemistry*, 79, 1-29.
- [17] Dzierzbicka, K., Sowinski, P. & Kołodziejczyk, A. M. (2006). Synthesis of analogues of anthraquinones linked to tuftsin or retro-tuftsin residues as potential topoisomerase inhibitors. *Journal of Peptide Science*, 12, 670-678.
- [18] Schenk, L. W., Kuna, K., Frank, W., Albert, A., Asche, C. & Kucklaender, U. (2006). 1,4,9,10-Anthradiquinone as precursor for antitumor compounds. *Bioorganic & Medical Chemistry*, 14, 3599-3614.
- [19] Schripsema, J., Ramos-Valdivia, A. C. & Verpoorte, R. (1999). Robustaquinones, novel anthraquinones from an elicited *Cinchona robusta* suspension culture. *Phytochemistry*, 51, 55-60.
- [20] Banthorpe, D. V. & White, J. J. (1995). Novel anthraquinones from undifferentiated cell cultures of *Galium verum*. *Phytochemistry*, 38, 107-111.
- [21] Bassetti, L., Pijnenburg, J. & Tramper, J. (1996). Silicone-stimulated anthraquinone production and release by *Morinda citrifolia* in a two-liquid-phase system. *Biotechnology Letters*, 18, 377-382.
- [22] Abdullah, M. A., Ali, A. M., Marziah, M., Lajis, N. H. & Ariff, A. B. (1998). Establishment of cell suspension cultures of *Morinda elliptica* for the production of anthraquinones. *Plant Cell Tissue and Organ Culture*, 54, 173-182.
- [23] Kitajima, M., Fischer, U., Nakamura, M., Oshawa, M., Ueno, M., Takayama, H., Unger, M., Stöckigt, J. & Aimi, N. (1998). Anthraquinones from *Ophiorrhiza pumila* tissue and cell cultures. *Phytochemistry*, 48, 107-111.
- [24] Endo, M., Skakata, K. & Katayama, A. (1997). The pigments in the callus of *Rubia akane* and their dyeing properties. *Nippon Sanshigaku Zasshi*, 66, 107-112.
- [25] Mischenko, N. P., Fedoreyev, S. A., Glazunov, V. P., Chernoded, G. K., Bulgakov, V. P. & Zhuravlev, Y. N. (1999). Anthraquinone production by callus cultures of *Rubia cordifolia*. *Fitoterapia*, 70, 552-557.
- [26] Orbán, N., Boldizsár, I., Szűcs, Z. & Dános, B. (2008). Influence of different elicitors on the synthesis of anthraquinone derivatives in *Rubia tinctorum* L. cell suspension culture. *Dyes and Pigments*, 77, 249-257.
- [27] Abdullah, M. A., Arbakariya, B. A., Marziah, M., Ali, A. M. & Lajis, N. H. (2000a). Growth and anthraquinone production of *Morinda elliptica* cell suspension cultures in a stirred-tank bioreactor. *Journal of Agricultural and Food Chemistry*, 48, 4432-4438.
- [28] Abdullah, M. A., Ariff, A. B., Marziah, M., Ali, A. M. & Lajis, N. H. (2000b). Strategies to overcome foaming and wall-growth during the cultivation of *Morinda elliptica* cell suspension culture in a stirred-tank bioreactor. *Plant Cell, Tissue and Organ Culture*, 60, 205-212.

- [29] Bányai, P., Kuzovkina, I. N., Kursinszki, L. & Szőke, E. (2006). HPLC analysis of alizarin and purpurin produced by *Rubia tinctorum* L. hairy root cultures. *Chromatographia*, *63*, 111-114.
- [30] Busto, V. D., Talou, J. R., Giulietti, A. M. & Merchuk, J. C. (2008). Effect of shear stress on anthraquinones production by *Rubia tinctorum* suspension cultures. *Biotechnology Progress*, *24*, 175-181.
- [31] Leistner, E. (1985). Biosynthesis of chorismate-derived quinones in plant cell cultures. In K. H Neumann, W. Barz, & E. Reinhard (Eds), *Primary and Secondary Metabolism of Plant Cell Cultures* (pp. 215-224), New York, USA: Springer-Verlag.
- [32] Poulsen, C. & Verpoorte, R. (1991). Roles of chorismate mutase, isochorismate synthase and anthranile synthase in plants. *Phytochemistry*, *30*, 377-386.
- [33] Sieweke, H. J. & Leistner, E. (1992). *O*-succinylbenzoate: coenzyme A ligase from anthraquinone producing cell suspension cultures of *Galium mollugo*. *Phytochemistry*, *31*, 2329-2335.
- [34] Eisenreich, W., Rohdich, F. & Bacher, A. (2001). Deoxyxylulose phosphate pathway to terpenoids. *Trends in Plant Science*, *6*, 78-84.
- [35] Leistner, E. & Zenk M. H. (1968). Mevalonic acid a precursor of the substituted benzenoid ring of Rubiaceae anthraquinones. *Tetrahedron Letters*, 1395-1396.
- [36] Eichinger, D., Bacher, A., Zenk, M. H. & Eisenreich, W. (1999). Quantitative assessment of metabolic flux by ¹³CNMR analysis. Biosynthesis of anthraquinones in *Rubia tinctorum*. *Journal of the American Chemical Society*, *121*, 7469-7475.
- [37] Lois, L. M., Campos, N., Putra, S. R., Danielsen, K., Rohmer, M. & Boronat, A. (1998). Cloning and characterization of a gene from *Escherichia coli* encoding a transketolase-like enzyme that catalyses the synthesis of 1-deoxy-D-xylulose-5-phosphate, a common precursor for isoprenoid, thiamin, and pyridoxol biosynthesis. *Proceedings of the National Academy of Sciences of the United States of America*, *95*, 2105-2110.
- [38] Ramos-Valdivia, A. C., Van der Heijden, R. & Verpoorte, R. (1997). Isopentenyl diphosphate isomerase: A core enzyme in isoprenoid biosynthesis. A review of its biochemistry and function. *Natural Product Reports*, *14*, 591-603.
- [39] Van der Plas, L. H. W., Hagendoorn, M. J. M. & Jamar, D. C. L. (1998). Anthraquinones glycosylation and hydrolysis in *Morinda citrifolia* cell suspensions: regulation and function. *Journal of Plant Physiology*, *152*, 235-241.
- [40] Berlin, J. (1990). Screening and selection for variant cell lines with increased levels of secondary metabolites. In B. V. Charlwood, & M. J. C. Rhodes (Eds.), *Secondary Products from Plant Tissue Culture* (pp. 119-137). Oxford, UK: Clarendon Press.
- [41] Boldizsár, I., László-Bencsik, Á., Szűcs, Z. & Dános, B. (2004). Examination of the anthraquinone composition in root-stock and root samples of *Rubia tinctorum* L. plants of different origins [In Hung]. *Acta Pharmaceutica Hungarica*, *74*, 142-148.
- [42] Van den Berg, A. J. J., Radema, M. H. & Labadie, R. P. (1987). A high yielding callus culture of *Rhamnus purshiana* by visual selection. *Journal of Natural Products*, *50*, 940-943.
- [43] Becker, H., & Sauerwein, M. (1990). Manipulating the biosynthetic capacity of plant cell cultures. In B. V. Charlwood & M. J. C. Rhodes (Eds.), *Secondary Products from Plant Tissue Culture* (pp. 43-57). Oxford, UK: Clarendon Press.

- [44] Zenk, M. H., Schulte, U. & El-Shagi, H. (1984). Regulation of anthraquinone formation by phenoxyacetic acids in *Morinda cell* cultures. *Naturwissenschaften*, *71*, 266.
- [45] Khuori, H., Ibrahim, R. K. & Rideau, M. (1986). Effects of nutritional and hormonal factors on growth and production of anthraquinone glucosides in cell suspension cultures of *Cinchona succirubra*. *Plant cell reports*, *5*, 423-426.
- [46] Sato, K., Yamazaki, T., Okuyama, E., Yosishira, K. & Shimomura, K. (1991). Anthraquinones production by transformed root cultures of *Rubia tinctorum*: influence of phytohormones and sucrose concentration. *Phytochemistry*, *30*, 1507-1509.
- [47] Leistner, E. (1995). XVI *Morinda* species: Biosynthesis of quinones in cell cultures. In Y. P. S. Bajaj (Ed), *Biotechnology in Agriculture and Forestry, Medicinal and Aromatic Plants VIII* (vol.33, pp. 296-307). Berlin, Heidelberg, Germany, Springer-Verlag.
- [48] Hagendoorn, M. J. M., Jamar, D. C. L., Meykamp, B. & Van der Plas, L.H. W. (1997). Cell division versus secondary metabolite production in *Morinda citrifolia* cell suspensions. *Journal of Plant Physiology*, *150*, 325-330.
- [49] Suzuki, H., Matsumoto, T. & Mikami, Y. (1984). Effects of nutritional factors on the formation of anthraquinone by *Rubia cordifolia* plant cells in suspension culture. *Agricultural and Biological Chemistry*, *48*, 603-610.
- [50] Schulte, U., El-shagi, H. & Zenk, M. H. (1984). Optimization of 19 Rubiaceae species in cell suspension cultures of *Cincona ledgeriana*. *Plant Cell Reports*, *3*, 51-54.
- [51] Verpoorte, R., Contin, A. & Memelink, J. (2002). Biotechnology for the production of plant secondary metabolites. *Phytochemistry Reviews*, *1*, 13-25.
- [52] Kinooka, M., Mine, K., Taya, M., Tone, S. & Ichi, T. (1994). Production and release of anthraquinone pigments by hairy roots of madder (*Rubia tinctorum* L.) under improved culture conditions. *Journal of Fermentation and Bioengineering*, *77*, 103-106.
- [53] Bassetti, L., Hangendoorn, M. & Tramper, J. (1995). Surfactant-induced nonlethal release of anthraquinones from suspension-cultures of *Morinda citrifolia*. *Journal of Biotechnology*, *39*, 149-155.
- [54] Shim, J. J., Shin, J. H., Pai, T., Chung, I. S. & Lee, H. J. (1999). Permeabilization of elicited suspension culture of madder (*Rubia akane* Nakai) cells for release of anthraquinones. *Biotechnology Techniques*, *13*, 249-252.
- [55] Bassetti, L. & Tramper, J. (1995). Increased anthraquinone production by *Morinda citrifolia* in a 2-phase system with pluronic F-68. *Enzyme and Microbial Technology*, *17*, 353-358.
- [56] Chiang, L. & Abdullah, M. A. (2007). Enhanced anthraquinone production from adsorbent-treated *Morinda elliptica* cell suspension cultures in production medium strategy. *Process Biochemistry*, *42*, 757-763.
- [57] Dörnenburg, H. & Knorr, D. (1996). Semicontinuous processes for anthraquinone production with immobilized *Cruciata glabra* cell cultures in a three-phase system. *Journal of Biotechnology*, *50*, 55-62.
- [58] Dörnenburg, H. (2004). Evaluation of immobilization effects on metabolic activities and productivity in plant cell processes. *Process Biochemistry*, *39*, 1369-1375.
- [59] Zenk, M. H., El-Shagi, H. & Schulte, U. (1975). Anthraquinone production by cell suspension cultures of *Morinda citrifolia*. *Planta Medica, (Suppl)*, 79-101.

- [60] Bauch, H. J. & Leistner, E. (1978). Aromatic metabolites in cell suspension cultures of *Galium mollugo*. *Planta Medica*, *33*, 105-123.
- [61] Han, Y. S., Van der Heijden, R. & Verpoorte, R. (2002). Improved anthraquinone accumulation in cell cultures of *Cinchona* 'Robusta' by feeding of biosynthetic precursors and inhibitors. *Biotechnology Letters*, *24*, 705-710.
- [62] Perassolo, M., Quevedo, C., Busto, V., Ianone, F., Giulietti, A. M. & Rodríguez-Talou, J. (2007). Enhance of anthraquinone production by effect of proline and aminoindan-2-phosphonic acid in *Rubia tinctorum* suspension cultures. *Enzyme and Microbial Technology*, *41*, 181-185.
- [63] Stalman, M., Koskamp, A. M., Luderer, R., Vernooy, J. H. J., Wind, J. C., Wullems, G. J. & Croes, A. F. (2003). Regulation of anthraquinone biosynthesis in cell cultures of *Morinda citrifolia*. *Journal of Plant Physiology*, *160*, 607-614.
- [64] Suzuki, H., Matsumoto, T. & Mikami, Y. (1985). Effects of physical factors and surface active agents on the formation of anthraquinone by *Rubia cordifolia* cells in suspension culture. *Agricultural and Biological Chemistry*, *48*, 519-520.
- [65] Bóka, K., Jakab, J. & Király, I. (2002). Comparison of the effect of fungal elicitors on *Rubia tinctorum* L. suspension culture. *Biologia Plantarum*, *45*, 281-290.
- [66] Yamamoto, H., Tabata, M. & Leistner, E. (1987). Cytological changes associated with induction of anthraquinone synthesis in photoautotrophic cell suspension cultures of *Morinda lucida*. *Plant Cell Reports*, *6*, 187-190.
- [67] Verpoorte, R., Van der Heijden, R., Ten Hoorpen, H. J. G. & Memelink, J. (1999). Metabolic engineering of plant secondary metabolite pathways for the production of fine chemicals. *Biotechnology Letters*, *21*, 467-479.
- [68] Petersen, M. (2007). Current status of metabolic phytochemistry. *Phytochemistry*, *68*, 2847-2860.
- [69] Dixon, R. A. (2005). Engineering of plant natural product pathways. *Current Opinion in Plant Biology*, *8*, 329-336.
- [70] Fridman, E. & Pichersky, E. (2005). Metabolomics, genomics, proteomics, and the identification of enzymes and their substrates and products. *Current Opinion in Plant Biology*, *8*, 242-248.
- [71] Van der Fits, L., Zhang, H., Menke, F. L. H., Deneka, M. & Memelink, J. (2000). A *Catharanthus roseus* BPF-1 homologue interacts with an elicitor-responsive region of the secondary metabolite gene *Str* and is induced by elicitor via JA-independent signal transduction pathway. *Plant Molecular Biology*, *44*, 675-685.
- [72] Grotewold, E., Chamberlin, M., Snook, M., Siame, B., Butler, L., Swenson, J., Maddock, S., Clair, G. S. & Bowen, B. (2000). Engineering secondary metabolism in maize cells by ectopic expression of transcription factors. *The Plant Cell*, *10*, 721-740.
- [73] Vom Endt, D., e Silva, M. S., Kijne, J. W., Pasquali, G. & Memelink, J. (2007). Identification of a bipartite jasmonate-responsive promoter element in the *Catharanthus roseus* *ORCA3* transcription factor gene that interacts specifically with AT-Hook DNA-binding proteins. *Plant Physiology*, *144*, 1680-1689.
- [74] Ogita, S., Oefuji, H., Morimoto, M. & Sano, H. (2004). Application of RNAi to confirm theobromine as the major intermediate for efficient biosynthesis in coffee plants with potential for construction of decaffeinated varieties. *Plant Molecular Biology*, *54*, 931-941.

- [75] Niggeweg, R., Michael, A. & Martin, C. (2004). Engineering plants with increased levels of the antioxidant chlorogenic acid. *Nature Biotechnology*, *22*, 746-754.
- [76] Mathews, H., Clendennen, S. K., Caldwell, C. G., Liu, X. L., Connors, K., Matheis, N., Schuster, D. K., Menasco, D. J., Wagoner, W., Lightner, J. & Wagner, D. R. (2003). Activation tagging in tomato identifies a transcriptional regulator of anthocyanin biosynthesis, modification, and transport. *Plant Cell*, *15*, 1689-1703.
- [77] Austin, M. B., Bowman, M. E., Ferrer, J.-L., Schröder, J. & Noel, J. P. (2004). An aldol switch discovered in stilbene synthases mediates cyclization specificity of type III polyketide synthases. *Chemistry & Biology*, *11*, 1179-1194.
- [78] Qureshi, M. I., Quadir, S. & Zolla L. (2007). Proteomics-based dissection of stress-responsive pathways in plants. *Journal of Plant Physiology*, *164*, 1239-1260.
- [79] Ye, X., Al-babili, S., Klott, A., Zhang, J., Lucca, P., Beyer, P. & Potrykus, I. (2000). Engineering provitamin A (β -carotene) biosynthetic pathway into (carotenoid-free) rice endosperm. *Science*, *287*, 303-305.
- [80] Jennewein, S., Wildung, M. R., Chau, M., Walker, K. & Croteau, R. (2004). Random sequencing of an induced *Taxus* cell cDNA library for identification of clones involved in taxol biosynthesis. *Proceedings of the National Academy of Sciences of the United States of America*, *101*, 9149-9154.
- [81] Ro, D. K., Paradise, E. M., Ouellet, M., Fisher, K. J., Newman, K. L., Ndungu, J. M., Ho, K. A., Eachus, R. A., Ham, T. S., Kirby, J., Chang, M. C. Y., Withers, S. T., Shiba, Y., Sarpong, R. & Keasling, J. D. (2006). Production of the antimalarial drug precursor artemisinic acid in engineered yeast. *Nature*, *440*, 940-943.
- [82] Han, Y. S., Roytrakul, S., Verberne, M. C., Van der Heijden, R., Linthorst, H. J. M. & Verpoorte, R. (2003). Cloning of a cDNA encoding 1-deoxy-D-xylulose 5-phosphate synthase from *Morinda citrifolia* and analysis of its expression in relation to anthraquinone accumulation. *Plant Science*, *164*, 911-917.
- [83] Guillon, S., Trémouillaux-Gullier, J., Pati, P. K., Rideau, M. & Gantet, P. (2006). Hairy root research: recent scenario and exciting prospects. *Current Opinion in Plant Biology*, *9*, 341-346.
- [84] Van der Heijden, R., Verpoorte, R., Hoekstra, S. S. & Hoge, J. H. C. (1994). Nordamnacanthal, a major anthraquinone from an *Agrobacterium-rhizogenes*-induced root culture of *Rubia tinctorum*. *Plant Physiology and Biochemistry*, *32*, 399-404.
- [85] Kuzovkina, I. N., Mantrova, O. V., Alterman, I. E. & Yakimov, S. A. (1996). Culture of genetically transformed hairy roots derived from anthraquinone-producing European madder plants. *Russian Journal of Plant Physiology*, *43*, 252-258.
- [86] Bulgakov, V. P., Tchernoded, G. K., Mischenkol, N. P., Khodakovskaya, M., Glazunov, V. P., Radchenko, S. V., Zvereva, E. V., Fedoreyev, S. A. & Zhuravlev, Y. N. (2002). Effect of salicylic acid, methyl jasmonate, etephon, and cantharidin on anthraquinone production by *Rubia cordifolia* callus cultures transformed with the rolB and rolC genes. *Journal of Biotechnology*, *97*, 213-221.
- [87] Bulgakov, V. P., Tchernoded, G. K., Mischenkol, N. P., Shkryl, Y. N., Glazunov, V. P., Fedoreyev, S. A. & Zhuravlev, Y. N. (2003). Effects of Ca^{2+} , channel blockers and protein kinase/phosphatase inhibitors on growth and anthraquinone production in *Rubia cordifolia* callus cultures transformed by the rolB and rolC genes. *Planta*, *217*, 349-355.

- [88] Bulgakov, V. P., Tchernoded, G. K., Mischenkol, N. P., Shkryl, Y. N., Fedoreyev, S. A. & Zhuravlev, Y. N. (2004). The rolB and rolC genes activate synthesis of anthraquinones in *Rubia cordifolia* cells by mechanism independent of octadecanoid signaling pathway. *Plant Science*, 166, 1069-1075.
- [89] Zhao, J., Davis, L. C. & Verpoorte, R. (2005). Elicitor signal transduction leading to production of plant secondary metabolites. *Biotechnology Advances*, 23, 283-333.
- [90] Keen, N. T. (1975). Specific elicitors of plant phytoalexin production – determinants of race specificity in pathogens? *Science*, 187, 74-75.
- [91] Radman, R., Saez, T., Bucke, C. & Keshavarz, T. (2003). Elicitation of plants and microbial cell systems. *Biotechnology and Applied Biochemistry*, 37, 91-102.
- [92] Nürnberger, T. & Brunner F. (2002). Innate immunity in plants and animals: emerging parallels between the recognition of general elicitors and pathogen associated molecular patterns. *Current Opinion in Plant Biology*, 5, 318-324.
- [93] Van Tegelen, L. J. P., Bongaerts, R. J. M., Croes, A. F., Verpoorte, R. & Wullems, G. J. (1999). Isochorismate synthase isoforms from elicited cell cultures of *Rubia tinctorum*. *Phytochemistry*, 51, 263-269.
- [94] Dörnenburg, H. & Knorr, D. (1994). Elicitation of chitinases and anthraquinones in *Morinda citrifolia* cell cultures. *Food Biotechnology*, 8, 57-65.
- [95] Vasconsuelo, A., Giulietti, A. M., Picotto, G. & Talou, J. R. (2003). Involvement of the PLC/PKC pathway in chitosan-induced anthraquinone production by *Rubia tinctorum* L. cell cultures. *Plant Science*, 165, 429-436.
- [96] Gundlach, H., Muller, M. J., Kutchan, T. M. & Zenk, M. H. (1992). Jasmonic acid is a signal transducer in elicitor-induced plant cell cultures. *Proceedings of the National Academy of Sciences of the United States of America*, 1992, 89, 2389-2393.
- [97] Chong, T. M., Abdullah, M. A., Fadzillah, N. M., Lai, O. M. & Lajis, N. H. (2005). Jasmonic acid elicitation of anthraquinones with some associated enzymic and non-enzymic antioxidant responses in *Morinda elliptica*. *Enzyme and Microbial Technology*, 36, 469-477.
- [98] Vasconsuelo, A., Giulietti, A.M. & Boland, R. (2004). Signal transduction events mediating chitosan stimulation of anthraquinone synthesis in *Rubia tinctorum*. *Plant Science*, 166, 405-413.
- [99] Vasconsuelo, A., Morelli, S., Picotto, G., Giulietti, A. M. & Boland, R. (2005). Intracellular calcium mobilization: a key step for chitosan-induced anthraquinone production in *Rubia tinctorum* L. *Plant Science*, 169, 712-720.
- [100] Vasconsuelo, A., Picotto, G., Giulietti, A. M. & Boland, R. (2006). Involvement of G-proteins in chitosan-induced anthraquinone synthesis in *Rubia tinctorum*. *Physiologia Plantarum*, 128, 29-37.
- [101] Bóka, K., Orbán, N., Kristóf, Z. (2007). Dynamics and localization of H₂O₂ production in elicited plant cells. *Protoplasma*, 230, 89-97.
- [102] Boldizsár, I., Szűcs, Z., Füzfa, Zs. & Molnár-Perl, I. (2006). Identification of the constituents of madder root by gas chromatography and high-performance liquid chromatography. *Journal of Chromatography A*, 1133, 259-274.
- [103] Rafaëly, L., Héron, S., Nowik, W. & Tchaplá, A. (2008). Optimisation of ESI-MS detection for the HPLC of anthraquinone dyes. *Dyes and Pigments*, 77, 191-203.

Short Commentary

THE USE OF SOLID MEDIA FOR BACTERIAL GROWTH IN DEGRADATION OF DYES

Carlos Costa^{1,}, Blanca E. Barragán² and M. Carmen Márquez¹*

¹Chemical Engineering Department, Faculty of Chemical Sciences, University of Salamanca, Plaza de la Merced s/n, 37008 Salamanca, Spain

²Environmental Systems Department. National School of Biological Sciences. National Polytechnic Institute. Carpio y Plan de Ayala. 11340 DF, México

ABSTRACT

Dyes are normally difficult to eliminate from effluents by conventional biological wastewater treatments. There are many references in which it is proven a poor removal by activated sludge or other systems in wastewater treatment plants. Their xenobiotic nature and their low concentration in residual streams (20 – 200 mg/l) make them to be difficult substrates for bacterial growth. Actually it is not clear the role they play in biological systems. Under anaerobic environment, it seems they act as electron acceptors in organic matter biodegradation. Under aerobic environment, it seems that a few number of microorganisms are able to use them as electron donors, in the presence of oxygen. Combined anaerobic-aerobic processes have efficiency on dye removal due to the first step in dye degradation, the breakdown of the azo bond, is assumed to be done under anaerobic conditions.

The use of solid supports for bacteria which utilize azo dyes is an attractive alternative for remove them from residual streams. These supports need to have two characteristics: an adequate texture for bacterial growth (particle and porous size) and affinity for dye. Under this situation, dye is adsorb and concentrated on solid surface and bacteria can grow and degrade it on the surface of the solid. The surface of the solid seems to be a good environment for dye degradation, because oxygen concentration can be low inside the porous structure and microaerophilic conditions can be established, therefore cleavage of the azo bond can be performed easily. Several solids can be used on this purpose: activated carbon, bentonite and kaolin, for example. The solid used has to

e) * Corresponding author: Tel: 34-923-294479, fax: 34-923-294574; E-mail address: ccosta@usal.es (Carlos Costa)

be investigated in terms of texture of the surface, growth of microorganisms and dye degradation.

INTRODUCTION

Actually it is assumed textile dyes to be degraded under a combined biological anaerobic-aerobic process (Panswad and Luangdilok, 2000; Tan et al., 2000; Coughlin et al., 2003; Van der Zee and Villaverde, 2005; Lodato et al., 2007). Most of the dyes used in textile industry are from the class azo dyes and they need firstly an anaerobic environment for performance of the reductive cleavage of the azo bond. The hydrolase (azoreductase) involved needs no oxygen present and reductive environment for hydrogenation of the $-N=N-$ bond. On the other hand, aromatic amines formed have to be degraded under aerobic oxidative conditions (Figure 1), otherwise the oxidation will not be complete and some toxic and carcinogenic intermediates can be generated (Coughlin et al., 1999).

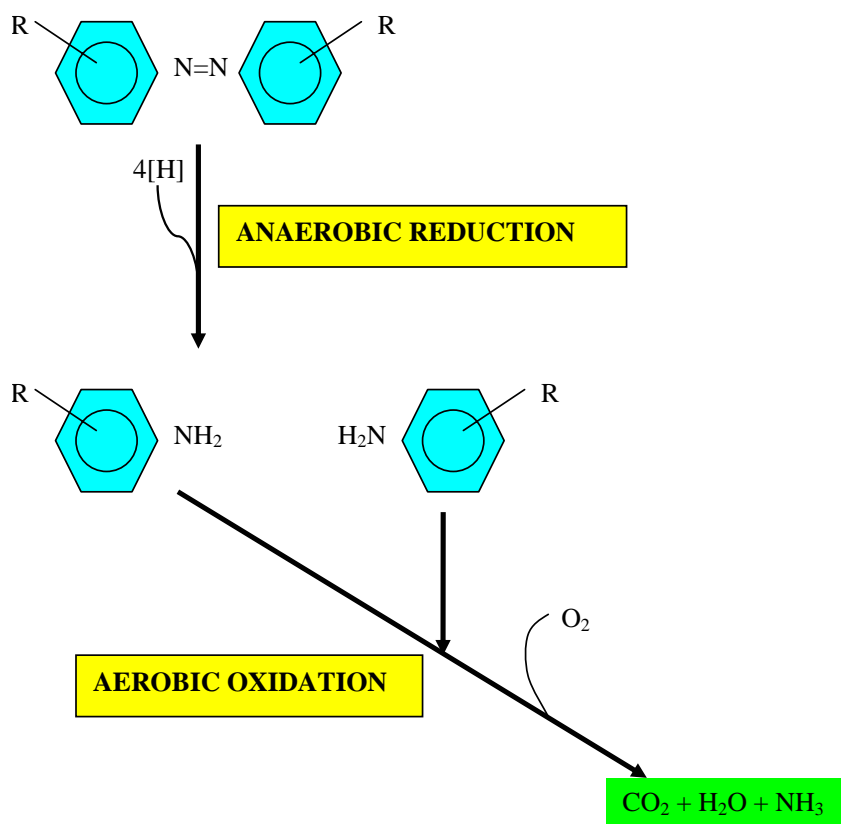


Figure 1. Scheme of azo dye degradation showing the two steps for two environments, anaerobic and aerobic.

Some authors describe azo dyes degradation under aerobic conditions (Coughlin et al., 1997; Coughlin et al., 2002; Coughlin et al., 2003; Buitrón et al., 2004; Davies et al., 2006).

In this case, a high substrate specificity is expected which reduces industrial application of the process.

If oxygen tension can inhibit hydrogenation of the azo bond it does not mean rejection of aerobic degradation of azo dyes. The solution can be a solid support in which azo dye is adsorbed and concentrated under low oxygen concentration. In this “environment” bacteria can grow and degrade it.

In this case the election of the support has to be affected by the property of having two environments for dye degradation. Firstly, dye molecule has to be fixed in a zone in which oxygen concentration is low, promoting bacterial growth on this region. Secondly the products from dye degradation (aromatic amines) have to emigrate to a region with high oxygen concentration, giving the possibility for bacterial degradation of these substrates.

These conditions can be reproduced using a support with a porous structure and with the ability for dye adsorption. Dye is adsorbed and fixed inside the porous structure, where oxygen concentration is low and products formed after bacterial activity are desorbed and conducted to the surface of the solid, where oxygen concentration is much higher (Figure 2).

For the solid selected an adequate relation between particle size and the porous structure is needed because inside the porous structure colonization of bacteria has to be achieved. If it is assumed bacterial size about 1-3 μm , porous size has to be bigger and particle size has to be high enough for supporting a good number of cells.

Finally, the solid used has to be able to adsorb the dye or dyes and conduct them to a low oxygen region, then the support needs high specific surface and porous depth.

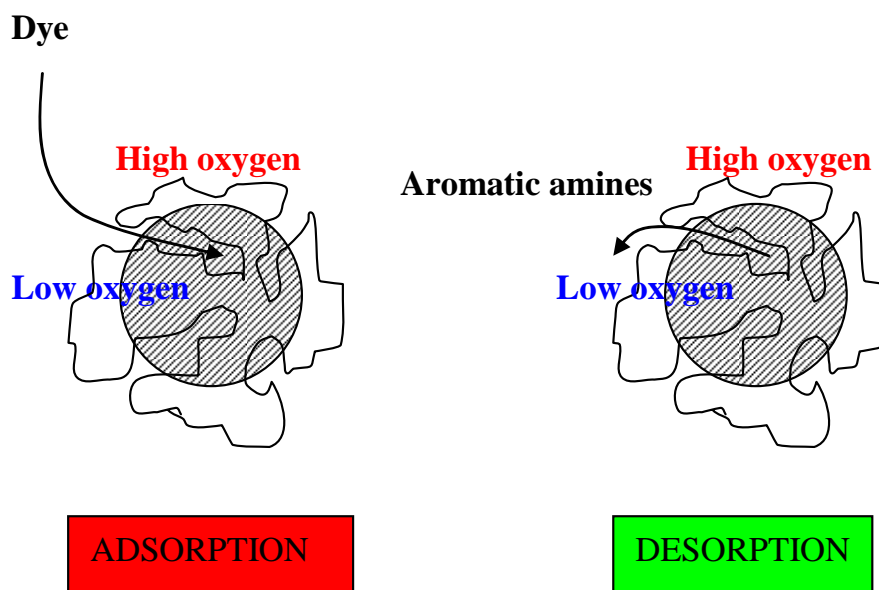


Figure 2. Picture of the support and adsorption of the dye inside the porous structure (low oxygen environment). Products from dye degradation are released out of the porous to the external surface of the solid (high oxygen environment).

SOLID STUDY

Different solids can be studied as supports for azo dyes degradation, natural or artificial made. The best way for investigating texture and porous structure is SEM (Scanning Electron Microscopy), which permits a view of the relief of the solid showing porous structure in high detail. Comparing bacterial size, porous structure and particle size, the best “microniche” for bacterial growth and dye degradation can be selected.

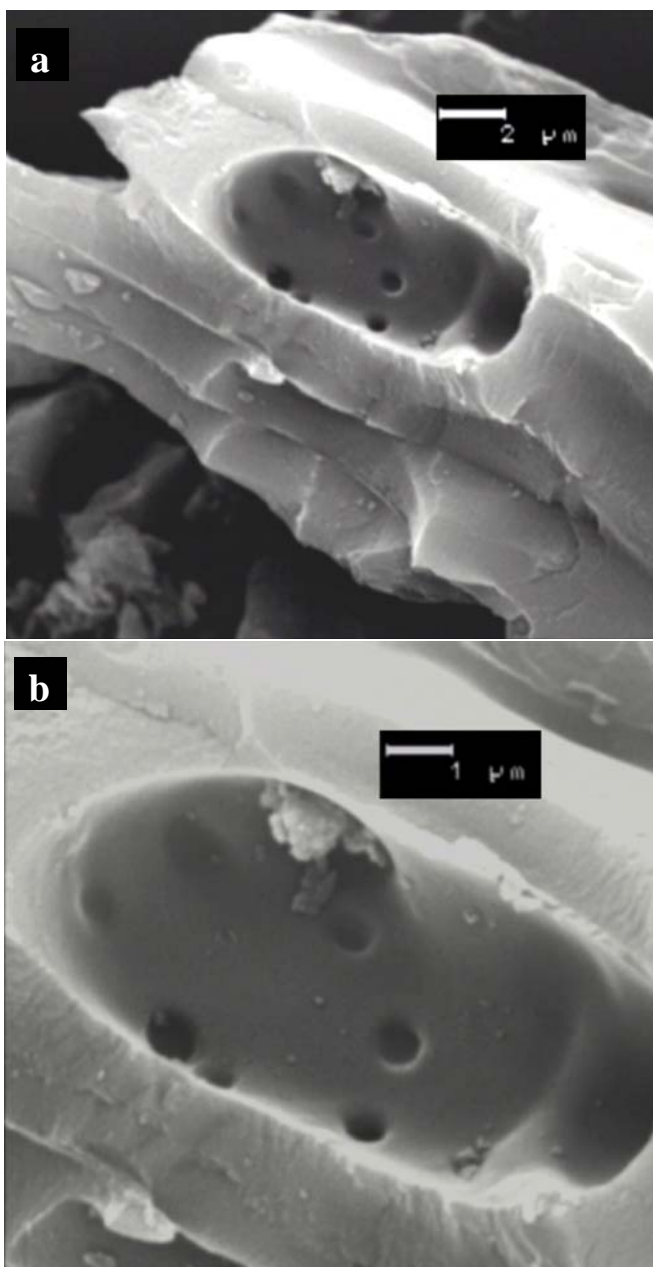


Figure 3. SEM microphotograph of activated carbon. Magnification: 5 000 in *a* and 10 000 in *b*.

In Figure 3 a particle of *activated carbon* is shown by SEM in which porous structure can be observed clearly. In the center of the microphotograph a macroporous with some microporous indicates how can be the microniche for bacteria. Comparing porous size with size bar (2 μm and 1 μm), one can conclude that microporous can not be colonized by bacteria and macroporous have the adequate size and texture for been colonized by bacteria.

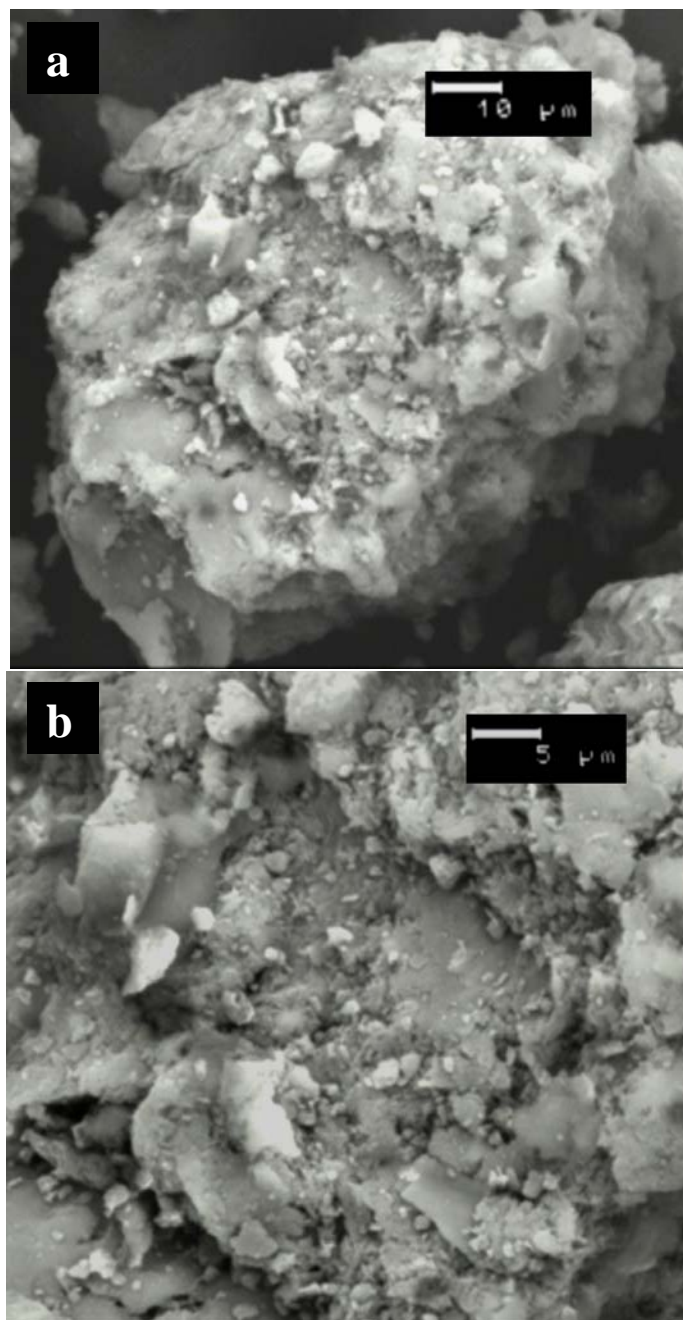


Figure 4. SEM microphotograph of bentonite. Magnification: 1 000 in *a* and 2 000 in *b*.

In Figure 4 a particle of *bentonite* can be observed by SEM. This particle has an adequate size for been colonized by bacteria, but texture of the surface has not a good porous structure for generating a microenvironment with low oxygen concentration. The porous structure is not deep enough for having a lack of oxygen in the inner structure.

Figure 5 is the microscopic study of *kaolin* as a support for microorganisms. In comparison with activated carbon and bentonite, kaolin has a much lower particle size which reduces availability of space for bacterial colonization. The scaly texture of kaolin does not seem to be a good environment for bacteria and porous structure needed for low oxygen ambient is not present.

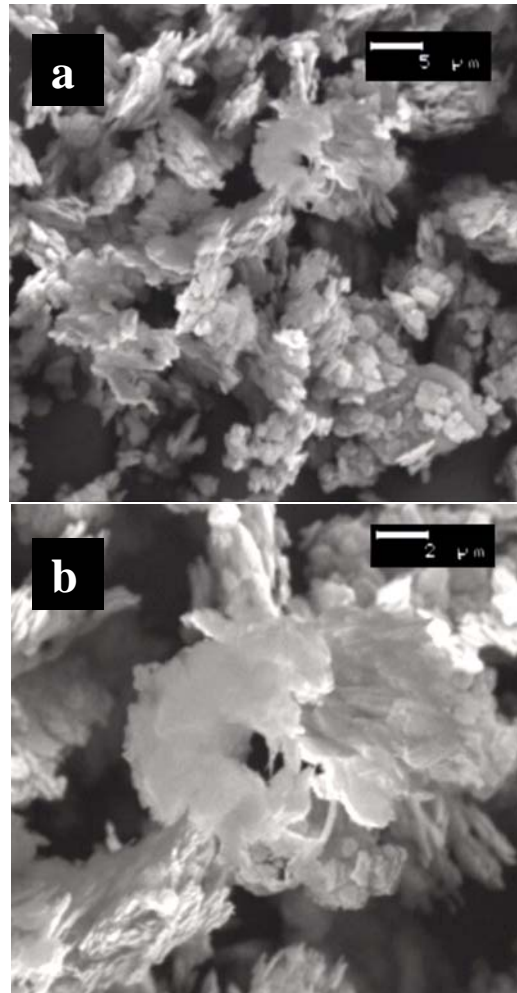


Figure 5. SEM microphotograph of kaolin. Magnification: 2 000 in *a* and 5 000 in *b*.

In view of these results and comparing the three solids studied: *activated carbon*, *bentonite* and *kaolin*, it can be concluded that the adequate solid for bacterial colonization seems to be activated carbon. Particle size is in the range desired (a good number of cells can be “living” in a particle) and macroporous structure of activated carbon seems to be an

adequate microniche for supplying both environments, low and high oxygen, for biodegradation of azo dyes.

BACTERIAL COLONIZATION

Once the support has been selected for the assays, bacterial colonization has to be achieved on the surface of the solid. For this purpose strains that show azo dye degradation activity have to be collected from textile wastewaters or obtained from other sources, for example, enrichments from soil or water which show biodegradation power on azo dyes.

These strains are inoculated on the solid by culture them in liquid media under agitation conditions with the solid and azo dye present. The best way for promoting bacterial growth is using batch cultures (erlenmeyers for example) with a moderate dye concentration (similar to textile wastewaters, 20-200 mg/l, Van der Zee & Villaverde, 2005). The solid used is saturated by azo dye in a continuous system and placed in the medium in which bacteria is inoculated. Saturation of the solid takes two advantages: dye is strongly concentrated in the inner structure of the adsorbent, where oxygen concentration is low and the concentration of dye in the bulk liquid is not been affected by adsorption and biodegradation can be followed by measuring dye concentration in the bulk liquid. The high concentration of the azo dye inside the porous structure promotes bacterial growth and dye degradation. If the environment is adequate and adaptation of bacteria is achieved, a spectacular growth can be observed (Figures 6 and 7).

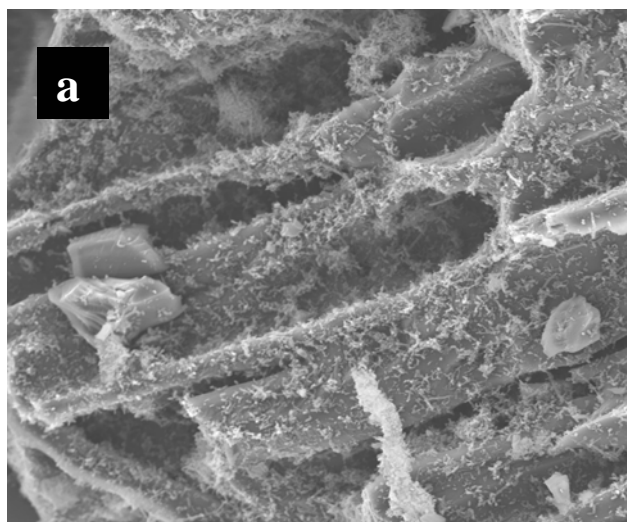


Figure 6. (Continued)

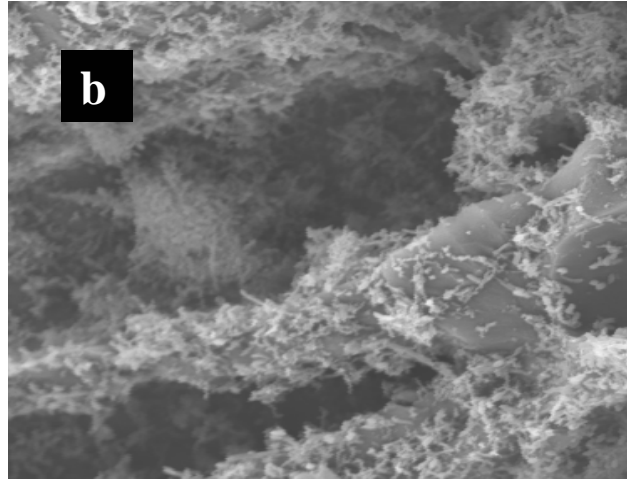


Figure 6. SEM microphotograph of activated carbon colonized by bacteria in a medium in which a textile dye is present (Acid Orange 7, CI 15510). In microphotograph *a* bacteria can be observed fixed on the surface of the adsorbent. In more detail, microphotograph *b* shows bacteria inside the porous structure.

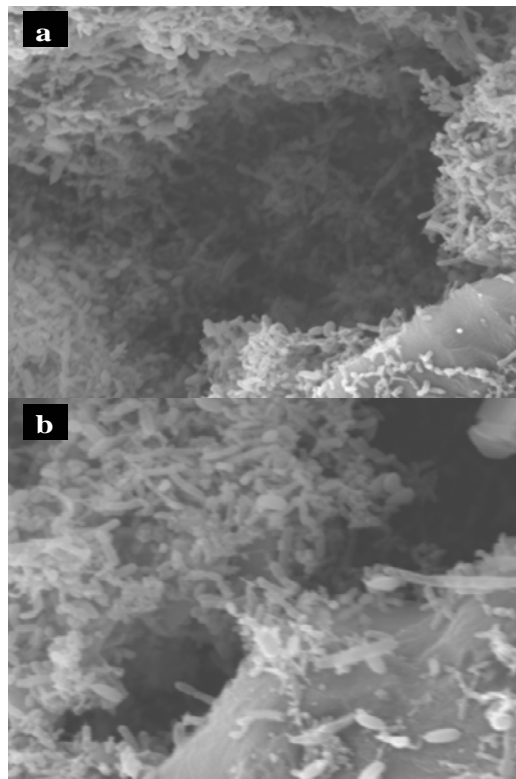


Figure 7. SEM microphotograph of microniches occupied by bacteria in activated carbon structure in a medium in which a textile dye is present (Acid Orange 7, CI 15510). Cells are present in the border of the porous structure (*a* and *b*) and they can be visualized inside the porous structure (*a*), where oxygen concentration is low and the first step in dye degradation can be performed.

DYE DEGRADATION

Visual observation of cells on the surface of the solid is not a proof of a dye degrading population of microorganisms. These microorganisms can prosper by the presence of several carbon sources and dye degradation has to be proven by measuring dye concentration in the medium.

In the next figure, two strains (E and P) isolated from textile wastewaters and inoculated on activated carbon, were tested to degrade Acid Orange 7 (CI: 15510):

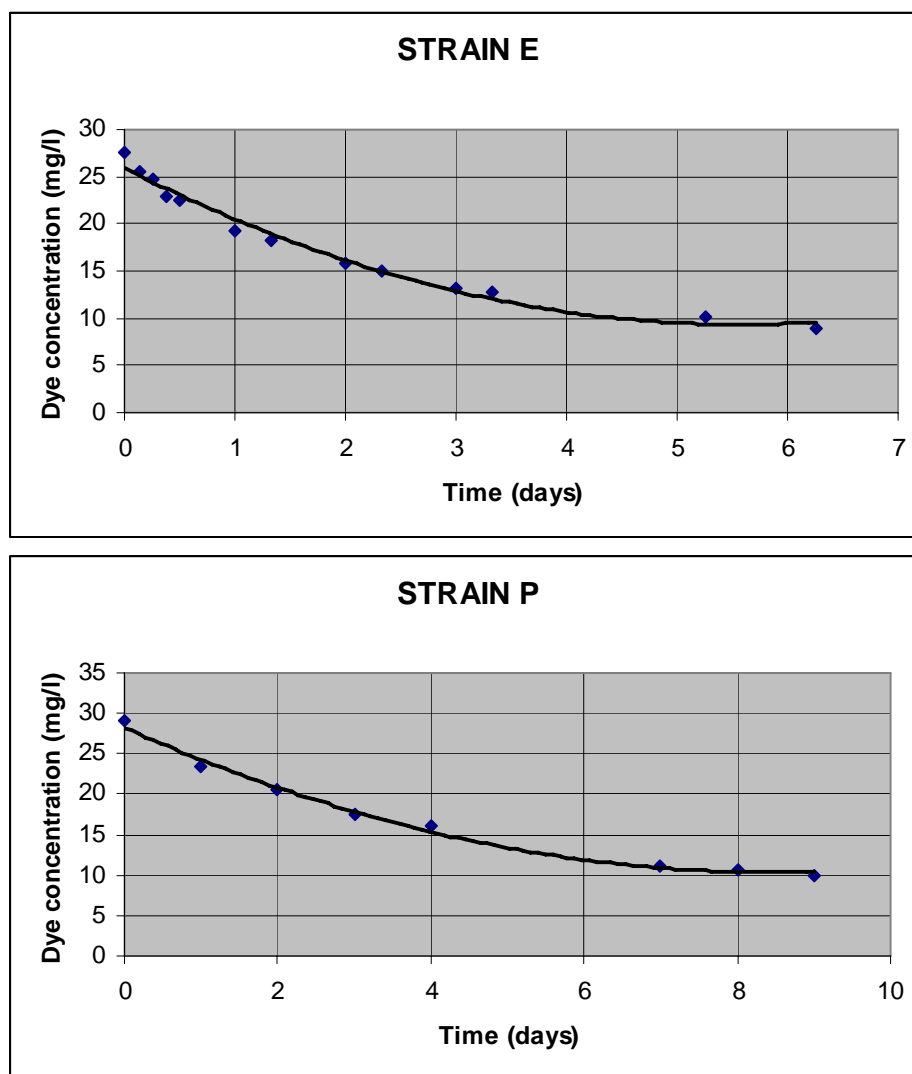


Figure 8. Degradation of Acid Orange 7 (CI: 15510) by two strains isolated from textile wastewaters and inoculated on activated carbon. Experiments were performed by saturation of activated carbon in continuous system and inoculation of the strains on saturated activated carbon in the liquid medium. Time for dye degradation is counted in batch culture.

In a batch system, dye variation in time is only due to substrate utilization rate (dye degradation), because there is not incoming or effluent substrate:

$$\frac{dS}{dt} = r_{su} \quad (1)$$

r_{su} is the substrate utilization rate, S substrate concentration and t is the time. Kinetics of dye degradation is often a second order kinetics:

$$r_{su} = -kS^2 \quad (2)$$

k is the kinetic coefficient and mathematical expression for dye degradation can be written:

$$\frac{dS}{dt} = -kS^2 \quad (3)$$

$$\frac{dS}{S^2} = -kdt \quad (4)$$

Integrating the differential equation (4), it can be obtained:

$$\frac{1}{S} = \frac{1}{S_o} + kt \quad (5)$$

Kinetic coefficients can be calculated by linearization of curves in Figure 8 (Barragán *et al.*, 2007):

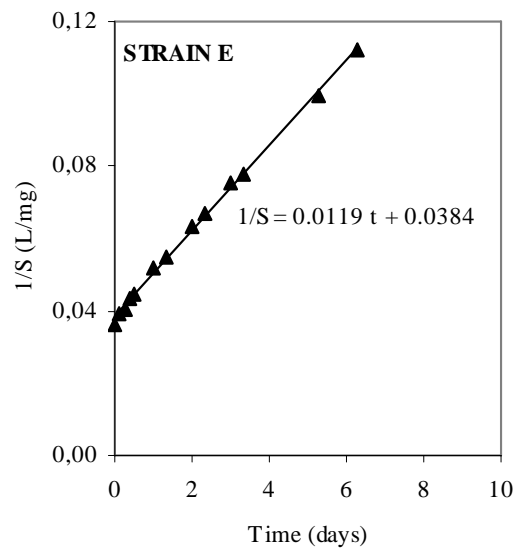


Figure 9. (Continued)

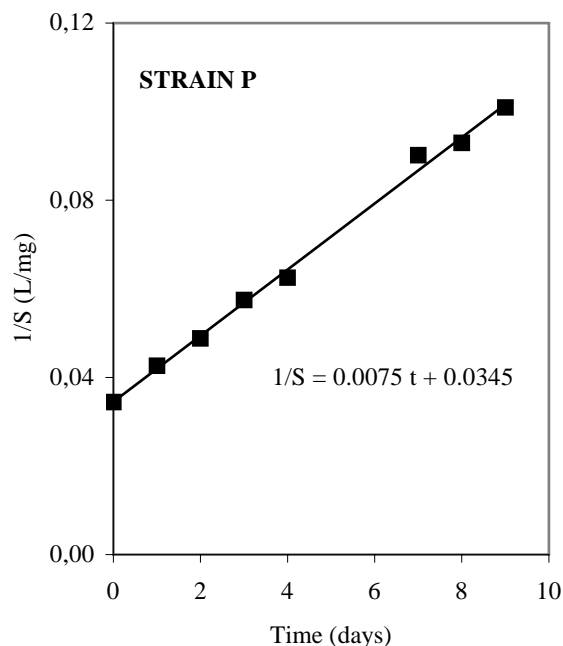


Figure 9. Graphical presentation of dye degradation for strains E and P for a second order kinetics.

STRAIN E $k_E = 0.0119$ L/(mg days)

STRAIN P $k_P = 0.0075$ L/(mg days)

k is the kinetic coefficient for strains E (k_E) and P (k_P). In view of these results, dye degradation is much faster for strain E than for strain P and it can be a reason for selecting strain E in this environment. Kinetic study has to be done under these conditions because changing bacterial environment can be a motive for modifying kinetics.

CONCLUSIONS

A new technique for dye removal from textile wastewaters is presented in this work. The idea is to inoculate bacteria on an adequate solid which has to play the role of a support for microorganisms and an environment of low-high oxygen. Activated carbon has both characteristics because macroporous structure represents a microniche with low oxygen concentration inside the porous and high oxygen concentration outside, in the outer surface of the adsorbent. By this way, the dye can be adsorb to the inner structure and degraded under low oxygen conditions, needed for the cleavage of the azo bond. Aromatic amines formed, with much lower molecular weight, are desorbed to the outer structure and degraded aerobically.

Kinetics of dye degradation can be studied by a second order model with regards to substrate concentration and kinetic coefficients can be used for selecting the adequate strain for dye degradation.

REFERENCES

- Barragán, B.E., Costa, C. & Márquez, M.C. (2007). Biodegradation of azo dyes by bacteria inoculated on solid media. *Dyes and Pigments*, 75, 73-81.
- Buitrón, G., Quezada, M. & Moreno, G. (2004). Aerobic degradation of the azo dye acid red 151 in a sequencing batch biofilter. *Bioresource Technology*, 92, 143-149.
- Coughlin, M.F., Kinkle, B.K., Tepper, A. & Bishop, P.L. (1997). Characterization of aerobic azo dye-degrading bacteria and their activity in biofilms. *Water Science and Technology*, 36 (1), 215-220.
- Coughlin, M.F., Kinkle, B.K. & Bishop, P.L. (1999). Degradation of azo dyes containing aminonaphthol by *Sphingomonas* sp. strain 1CX. *Journal of Industrial Microbiology and Biotechnology*, 23, 341-346.
- Coughlin, M.F., Kinkle, B.K. & Bishop, P.L. (2002). Degradation of acid orange 7 in an aerobic biofilm. *Chemosphere*, 46, 11-19.
- Coughlin, M.F., Kinkle, B.K. & Bishop, P.L. (2003). High performance degradation of azo dye Acid Orange 7 and sulfanilic acid in a laboratory scale reactor after seeding with cultured bacterial strains. *Water Research*, 37, 2757-2763.
- Davies, L.C., Pedro, I.S., Novais, J.M. & Martins-Dias (2006). Aerobic degradation of acid orange 7 in a vertical-flow constructed wetland. *Water Research*, 40, 2055-2063.
- Lodato, A., Alfieri, F., Olivieri, G., Di Donato, A., Marzocchella, A. & Salatino, P. (2007). Azo-dye conversion by means of *Pseudomonas* sp. OX1. *Enzyme and Microbial Technology*, 41, 646-652.
- Panswad, T. & Luangdilok, W. (2000). Decolorization of reactive dyes with different molecular structures under different environmental conditions. *Water Research*, 34 (17), 4177-4184.
- Tan, N.C.G., Borger, A., Sienders, P., Svitelskaya, A., Lettinga, G. & Field, J.A. (2000). Degradation of azo dye Mordant Yellow 10 in a sequential anaerobic and bioaugmented aerobic bioreactor. *Water Science and Technology*, 42 (5-6), 337-344.
- Van der Zee, F.P. & Villaverde, S. (2005). Combined anaerobic-aerobic treatment of azo dyes- A short review of bioreactor studies. *Water Research*, 39, 1425-1440.

INDEX

A

- Abdullah, 142, 281, 283, 408, 415, 417, 420
abiotic, 180, 410, 411
absorbents, 265
absorption coefficient, 186, 230, 361
absorption spectra, viii, 12, 26, 89, 111, 112, 132, 134, 135, 138, 231, 232, 233, 243, 247, 250, 337, 343
absorption spectroscopy, 52
accelerator, 229, 252, 253
acceptor, 116, 178
acceptors, xiii, 421
accessibility, 312, 316
accidental, 2
accuracy, 100
acetaminophen, 110
acetate, 24, 26, 31, 104, 190, 329
acetic acid, 13, 23, 183, 387, 390
acetone, 83, 262, 375
acetonitrile, 75
acetylation, 13, 211
acidic, viii, 26, 29, 143, 159, 183, 204, 211, 214, 250, 265, 272, 286, 317, 319, 320, 333, 338
acidification, 319, 412
acidity, xi, 331, 333, 338, 339, 340
acne, 16, 45
acne vulgaris, 45
acoustic, 144, 194
acrylic acid, 23
acrylonitrile, xii, 383, 385
actinic keratosis, 16
activated carbon, ix, xi, xiv, 143, 144, 146, 147, 164, 165, 167, 169, 171, 173, 201, 202, 203, 206, 208, 209, 213, 215, 216, 217, 218, 220, 221, 222, 223, 226, 264, 282, 289, 309, 310, 311, 320, 322, 323, 324, 421, 424, 425, 426, 428, 429
activation, vii, xiii, 1, 8, 9, 33, 37, 41, 57, 59, 203, 204, 216, 321, 323, 356, 364, 403, 412, 413
active centers, 275
active oxygen, 50
active site, 207, 214, 276
active transport, 18
actuators, 113
acute, 8, 176
acylation, 393
adaptation, 190, 427
additives, x, 101, 225, 250, 268, 277, 290, 303, 347, 392, 398
adducts, 345
adenine, 412
adenocarcinoma, 18, 32, 47
adenocarcinomas, 50
adhesion, 303
adjustment, 305, 359
administration, 13, 16, 18, 21, 23, 24, 26, 27, 33, 35, 45, 48, 49
adriamycin, 36, 59, 60
adsorption, ix, xi, 132, 144, 146, 147, 163, 164, 165, 171, 173, 178, 179, 180, 201, 202, 204, 205, 206, 207, 208, 209, 211, 212, 213, 214, 216, 217, 218, 219, 220, 221, 222, 223, 261, 264, 276, 279, 281, 285, 288, 309, 310, 312, 315, 316, 319, 320, 321, 322, 323, 324, 325, 326, 327, 328, 423, 427
adsorption isotherms, 211, 214, 218, 219, 320, 324
aerobic, xiii, 179, 189, 190, 226, 421, 422, 423, 432
aerobic bacteria, 189
aerodigestive tract, 27
aerogels, 287, 288
AFM, 133
Ag, 23, 75, 91, 277, 279, 289
age, 8, 20, 48, 103, 304
ageing, 334
agent, 3, 22, 23, 35, 39, 51, 84, 87, 103, 182, 183, 191, 202, 278

- agents, 2, 3, 48, 54, 83, 84, 92, 98, 101, 181, 182, 186, 191, 250, 329, 405, 408, 418
- age-related macular degeneration, 9, 20, 48
- age-related macular degeneration (AMD), 9, 20
- aggregates, 215, 315, 319, 324, 326
- aggregation, 27, 28, 34, 52, 53, 64, 79, 81, 84, 296, 297, 299, 300, 320, 370
- agricultural, 220
- agriculture, xi, 175, 203, 309, 396, 409
- aid, 104, 209, 214
- air, 31, 60, 78, 145, 180, 203, 232, 249, 278, 372
- alanine, 18
- alcohol, 77, 286, 387, 389, 390, 393
- alcohols, 206, 276
- aldehydes, x, 206, 225, 242, 253
- algae, 14, 176, 272, 315
- algal, 208
- alginate, 411
- algorithm, 363
- alicyclic, 17
- aliphatic amines, 394
- alkali, 33, 191, 208, 319, 320, 327
- alkaline, 18, 150, 183, 185, 204, 228, 241, 264, 265, 272, 320, 347
- alkaline media, 241, 272
- alkylating agents, 36
- allergic, 177, 385
- allergic reaction, 177
- allylamine, 385, 387, 389, 390
- alpha, 22
- alternative, ix, xii, xiii, 56, 101, 144, 180, 201, 202, 203, 206, 209, 270, 369, 378, 421
- alternatives, xiii, 403
- aluminium, 10, 27, 35, 67, 181, 301, 313, 321, 343, 388
- aluminosilicate, 314, 321, 327
- aluminosilicates, 204
- aluminum, 41, 64, 301, 313, 316, 334, 365
- AMD, 20, 23
- amide, xii, 17, 383, 385
- amine, 177, 202, 205, 236, 237
- amines, 188, 189, 190, 205, 226, 290, 321, 422, 423, 431
- amino, 14, 17, 18, 19, 30, 46, 47, 53, 178, 235, 237, 238, 241, 244, 250, 315, 394
- amino acid, 18, 46, 47
- amino acids, 18
- amino groups, 250, 315
- AML, 286
- ammonia, 208, 387, 389, 390, 409, 412
- ammonium, 27, 122, 205, 217
- amorphous, 315, 392
- amphiphilic compounds, vii, 63
- amylase, 56
- anaerobic, xiii, 179, 189, 190, 217, 421, 422, 432
- anaerobic bacteria, 189
- anaerobic sludge, 190
- analytical techniques, 334
- anatase, 285, 288, 290, 358
- aniline, 189, 289
- animal models, 22, 24, 26, 52
- animals, 304, 332, 420
- anion, 6, 33, 165, 228, 241, 250, 274, 328, 339
- anionic surfactant, 222, 325
- anions, 202, 239, 250, 264, 271, 320, 338, 339
- ANN, 363
- anoxia, 8
- anoxic, 7
- anthocyanin, 419
- antiangiogenic, 20
- antibiotics, xiii, 36, 403, 405
- anticancer, 36, 58, 59, 405
- anticancer drug, 36, 59
- anti-inflammatory, 60, 332
- anti-inflammatory drugs, 60
- antimicrobial, 29, 405, 412, 414
- antioxidant, 332, 405, 415, 419, 420
- antioxidants, 332
- antitumor, 36, 37, 43, 48, 50, 59, 60, 61, 404, 405, 415
- apoptosis, 8, 23, 32, 37, 41, 42, 50
- apoptotic, 8
- aquatic, 144, 188, 315
- aqueous solution, ix, x, 16, 61, 79, 131, 144, 151, 153, 160, 161, 172, 173, 201, 202, 203, 204, 206, 207, 208, 210, 211, 212, 216, 217, 218, 219, 220, 221, 222, 223, 225, 235, 250, 263, 280, 282, 283, 284, 285, 286, 287, 288, 289, 299, 319, 320, 322, 323, 324, 325, 326, 327, 328, 347, 391
- aqueous solutions, ix, x, 61, 144, 153, 161, 172, 201, 202, 204, 207, 208, 210, 211, 216, 217, 219, 220, 221, 222, 225, 250, 263, 280, 283, 284, 285, 289, 322, 323, 324, 325, 326, 328
- aqueous suspension, 287, 288, 289, 290
- aromatic, x, 11, 12, 17, 29, 32, 72, 73, 177, 179, 181, 182, 183, 188, 189, 190, 206, 212, 225, 226, 234, 237, 241, 242, 243, 244, 245, 247, 248, 287, 290, 298, 300, 324, 370, 374, 407, 422, 423
- aromatic compounds, 182, 241
- aromatic hydrocarbons, 183
- aromatic rings, x, 72, 179, 183, 206, 212, 225, 234, 242, 243, 247, 248
- aromatics, 294
- arsenic, 324
- artificial, 410, 424
- artistic, 332, 333, 334

- ascorbic, 26, 33, 58, 110
 ascorbic acid, 26, 33, 58, 110
 ash, ix, 201, 206, 210, 211, 213, 215, 217, 218, 219,
 220, 222, 223, 313, 323, 324, 328
 assessment, xii, 383, 416
 assignment, 72, 73, 79
 associations, 294
 asymptotically, 214
 atherosclerosis, 32
 atherosclerotic plaque, 31
 ATM, 324
 atmosphere, 78, 203
 atoms, 5, 16, 26, 27, 64, 114, 115, 178, 202, 204,
 209, 227, 240, 245, 248, 250, 294, 301, 302, 305,
 314, 321, 378, 385
 ATP, 8, 329
 ATRP, 329
 attachment, 91
 attacks, 183, 239
 attention, x, xi, 3, 20, 27, 64, 123, 130, 133, 208,
 259, 292, 293, 294, 303, 309, 310, 312, 320, 321,
 322, 334, 370
 autophagy, 41
 availability, 15, 16, 28, 156, 206, 209, 426
 azo dye, x, xiii, 98, 99, 100, 105, 106, 107, 108, 109,
 145, 148, 153, 159, 169, 172, 173, 176, 177, 178,
 185, 187, 188, 189, 190, 191, 192, 197, 216, 217,
 220, 221, 223, 225, 226, 233, 235, 236, 237, 244,
 281, 282, 283, 284, 285, 287, 288, 289, 290, 321,
 323, 389, 421, 422, 423, 424, 427, 432
 azo groups, 186
 azobenzene, 234, 235, 239, 240
- B**
- bacteria, xiii, 14, 25, 30, 177, 189, 190, 194, 404,
 410, 421, 423, 425, 426, 427, 428, 431, 432
 bacterial, xiii, xiv, 272, 421, 423, 424, 426, 427, 431,
 432
 bacterial strains, 432
 bactericides, 396
 band gap, 126, 276
 bandgap, 276
 barium, 300
 barium sulphate, 300
 barley, 222
 barrier, 341
 barriers, 29, 302
 BAS, 75
 basal cell carcinoma, 16, 21, 29, 32, 49, 58
 basic research, 298
 basis set, 126
 baths, 191
 beams, 144
 behavior, xii, 21, 53, 76, 99, 108, 109, 113, 114, 115,
 117, 119, 121, 123, 124, 127, 134, 135, 136, 216,
 245, 246, 310, 316, 317, 319, 320, 321, 323, 325,
 333, 337, 340, 346, 347, 383, 384, 391, 398, 400,
 410
 beneficial effect, xiii, 332, 403
 benefits, x, 9, 225, 413
 benign, viii, 21, 49, 97, 223
 benign prostatic hyperplasia, 49
 benzene, 11, 12, 24, 26, 28, 35, 67, 70, 72, 92, 235,
 236, 301
 beta, 22, 57, 58, 204
 bevacizumab, 20, 48
 bias, 191
 biliary tract, 49
 binding, 180, 206, 208, 213, 215, 346, 347, 405, 411,
 412, 418
 bioaccumulation, 176, 208
 bioavailability, 64, 65
 biochemical, 408
 biochemistry, 416
 biodegradability, 176
 biodegradability, x, xi, 202, 259, 271, 280, 281, 282,
 309
 biodegradable, ix, 201, 252
 biodegradation, xiii, 179, 188, 189, 190, 226, 254,
 261, 310, 421, 427
 biofilms, 432
 biological, vii, xi, xiii, 1, 6, 9, 17, 28, 29, 34, 35, 53,
 101, 176, 179, 181, 182, 189, 195, 202, 248, 252,
 253, 281, 282, 310, 331, 332, 346, 363, 384, 405,
 410, 415, 421, 422
 biological activity, xi, 17, 331, 332, 415
 biological media, 6, 34, 35
 biological systems, xiii, 421
 biologically, 18, 19, 34, 44, 303, 414
 biologically active compounds, 414
 biomass, 180, 189, 204, 208, 217, 220, 223
 biopolymer, 204
 bioreactor, 415, 432
 bioreactors, 405, 414
 biosorption, 208, 215, 216, 218, 219, 221
 biosynthesis, xiii, 14, 15, 16, 17, 18, 19, 403, 407,
 409, 410, 412, 413, 416, 418, 419
 biosynthetic pathways, xiii, 403, 407, 409
 biotechnological, xiii, 202, 403
 biotechnology, 126, 217
 biotic, 410
 BIS, 134, 135, 136, 137
 bisphenol, 280
 black, viii, 143, 146, 172, 217, 221, 285, 289, 294,
 305, 319, 320, 353, 355, 359, 360, 361, 362, 364,
 391

- Blacks, 301
 bladder, 18, 48, 50
 bladder cancer, 18
 bleaching, 145, 181, 322, 328, 333
 blends, 103, 108, 386
 blind spot, 20
 blocks, xi, 277, 291, 294, 295, 301
 blood, 2, 7, 8, 12, 13, 20, 29, 31, 35, 55, 355
 blood stream, 35
 blood vessels, 8, 20
 body fluid, 18
 body weight, 27
 bonding, xi, 116, 293, 294, 313, 314, 331, 347, 378, 396, 397
 bonds, x, xi, 2, 13, 177, 178, 234, 246, 291, 293, 294, 295, 297, 300, 301, 302, 305, 316, 384, 385, 392
 borderline, 294, 298, 301
 boron, 289
 bottleneck, 15
 BPD, 19
 brain, 3, 14, 21, 23, 43, 49
 brain tumor, 3, 21, 23, 43, 49
 breakdown, xiii, 176, 188, 262, 421
 breast, 27, 31, 32, 50, 54, 56, 57
 Breast, 51
 breast cancer, 27, 31, 32, 50, 54, 56, 57
 breast carcinoma, 31
 brick, 210, 218, 355
 bromine, 5
 bubble, 187, 262
 bubbles, 36, 187, 237
 building blocks, x, xi, 121, 291, 292, 293, 294, 295, 299, 300, 301, 305
 burning, 302
 butyl ether, 172, 283, 289
 by-products, 203, 206, 249, 290, 311
- C**
- Ca²⁺, 300, 316, 342, 343, 345, 412, 419
 cadmium, 219, 327
 calcium, 181, 206, 207, 217, 313, 314, 343, 411, 412, 413, 420
 calculus, 363
 calibration, 146, 148, 394, 397
 calmodulin, 412
 cancer, vii, 1, 3, 5, 7, 14, 16, 18, 20, 21, 23, 24, 25, 27, 28, 31, 32, 33, 39, 40, 41, 42, 43, 44, 45, 46, 47, 49, 50, 51, 52, 53, 54, 55, 57, 58, 59, 61, 63, 64, 67, 78, 93
 cancer cells, 5, 7, 16, 32, 78
 cancer treatment, vii, 1, 5, 14, 20, 32, 33, 55, 58
 cancers, 23, 32, 176
 candidates, viii, 32, 111, 295
 CAP, 323
 capacity, xiii, 15, 146, 165, 180, 181, 204, 205, 206, 207, 208, 209, 210, 211, 214, 218, 228, 229, 253, 311, 312, 313, 316, 319, 320, 321, 403, 409, 413, 416
 capillary, 325
 carbazole, 118, 120
 carbon, viii, x, 11, 26, 97, 98, 99, 100, 101, 103, 106, 107, 108, 126, 146, 148, 164, 165, 167, 171, 177, 179, 180, 188, 189, 202, 203, 205, 206, 209, 210, 211, 217, 222, 223, 225, 226, 235, 236, 237, 242, 245, 247, 248, 253, 262, 282, 288, 294, 301, 302, 305, 324, 325, 328, 408, 426, 429, 431
 carbon atoms, 26, 205, 245
 carbon dioxide, viii, 97, 98, 99, 100, 101, 103, 106, 107, 108, 188, 203, 262
 carbon nanotubes, 126, 324
 carbonyl groups, 17, 18, 296
 carboxyl, 102, 107, 190, 202
 carboxylic, x, 17, 46, 206, 214, 225, 242, 253
 carboxylic acids, x, 225, 242, 253
 carcinogenic, 144, 176, 190, 226, 261, 310, 422
 carcinoma, 23, 37, 41, 59
 carotene, 419
 carotenoids, 178
 carpets, xi, 331, 332
 CAS, 354
 case study, 287
 casein, 332
 caspase, 37, 41
 catalysis, ix, 133, 143, 261, 370
 catalyst, ix, x, 33, 67, 71, 143, 165, 173, 208, 259, 262, 269, 274, 275, 276, 277, 279, 281, 282, 290, 374
 catalysts, 173, 181, 203, 281, 282, 285, 288, 289, 321
 catalytic, vii, 1, 33, 58, 67, 146, 165, 173, 183, 249, 250, 253, 263, 264, 268, 276, 281, 282, 372
 cation, 6, 91, 92, 205, 215, 237, 313, 316, 319, 320, 321
 cations, 202, 204, 205, 207, 215, 217, 250, 271, 313, 316, 319, 321, 346
 cavitation, 144, 187, 280
 cavities, 144
 C-C, 13, 67, 71, 83, 88, 407
 cDNA, 410, 419
 CEC, 316, 321
 cell, vii, xiii, 2, 3, 7, 8, 9, 14, 17, 18, 21, 29, 30, 32, 36, 40, 41, 42, 47, 49, 57, 58, 59, 60, 61, 63, 67, 76, 77, 91, 92, 114, 115, 116, 136, 229, 230, 263, 313, 356, 403, 404, 405, 406, 407, 408, 409, 410, 411, 412, 413, 414, 415, 416, 417, 418, 419, 420

- cell culture, vii, xiii, 30, 63, 67, 92, 403, 404, 405, 406, 407, 408, 409, 412, 413, 414, 415, 416, 417, 418, 420
- cell death, 2, 8, 32, 42
- cell killing, 7, 36, 61
- cell line, 18, 29, 47, 49, 58, 405, 408, 410, 416
- cell lines, 29, 49, 58, 405, 408, 416
- cell membranes, 17, 29
- cell metabolism, 42
- cell surface, 21
- cellulose, 103, 108, 177, 204, 206, 207, 216, 228, 250, 288, 295, 296, 297
- cellulose fibre, 108, 295, 296
- cement, 326
- central nervous system, 14
- ceramic, xii, 305, 324, 351, 352, 353, 356, 357, 358, 359, 363, 364, 365
- ceramics, xii, 302, 351
- cervical, 14
- cervical cancer, 14
- channel blocker, 419
- channels, 316, 321
- charcoal, 324
- charge density, 320
- chelates, 347
- chelating agents, 347
- chemical bonds, 263, 300
- chemical composition, 181, 310, 315, 363
- chemical industry, 295
- chemical oxidation, 145, 151, 181, 263, 280, 323
- chemical properties, 46, 208, 357, 359
- chemical reactions, 87, 179, 230, 233, 239, 253, 277
- chemical stability, xii, 78, 202, 209, 351, 352, 356, 363, 366
- chemical structures, 260, 317
- chemicals, x, xi, 2, 146, 175, 179, 183, 187, 191, 192, 193, 259, 260, 268, 309, 311, 405, 418
- chemisorption, 207, 211, 275
- chemistry, viii, xi, 111, 113, 140, 214, 226, 229, 278, 285, 292, 293, 294, 295, 298, 299, 301, 304, 305, 348
- chemotherapy, 60, 405
- children, 301, 396
- China, 13, 14, 43, 44, 103, 108, 111, 287, 355, 369, 379
- Chinese, 2, 60, 107, 282, 415
- chirality, 304
- chitin, 180, 204, 411
- chitosan, 204, 209, 211, 217, 219, 220, 223, 320, 325, 326, 327, 412, 420
- chitosan nanoparticles, 219
- chloride, 27, 29, 30, 51, 56, 67, 70, 75, 145, 172, 173, 181, 192, 205, 207, 217, 262, 299, 319, 390, 405
- chlorinated hydrocarbons, 183
- chlorine, 290, 296, 385
- chloroform, 70, 375, 376, 377, 379
- chlorogenic, 419
- chlorogenic acid, 419
- chlorophenol, 173, 282
- chlorophenols, 276, 286, 289
- chlorophyll, 1, 22, 303
- cholangiocarcinoma, 14, 44
- choroidal neovascularization, 48, 51
- chromatographic technique, 335
- chromatography, 67, 248, 262, 310, 334, 348, 370, 371, 372, 374, 388
- chromium, 250, 252, 289, 294, 325, 334, 364, 389
- chronic, 176
- circadian, 2
- circadian rhythm, 2
- classes, xi, 182, 186, 202, 204, 206, 260, 291, 298, 310, 312, 314, 353, 356, 385
- classical, 298, 300, 305
- classification, x, xi, 113, 178, 214, 218, 291, 292, 293, 294, 298, 303, 313, 353, 354, 357, 411
- classified, 177, 178, 202, 209, 260, 297, 310, 312, 315, 411
- clay, xi, 204, 205, 206, 207, 209, 210, 219, 220, 223, 309, 312, 313, 315, 316, 319, 320, 321, 322, 324, 325, 326, 327, 328, 329
- clays, ix, xi, 201, 204, 205, 209, 217, 309, 310, 311, 312, 313, 317, 319, 322, 326, 327
- cleaning, 176, 264, 384, 385
- cleanup, 324
- cleavage, xiv, 34, 112, 118, 179, 185, 190, 235, 421, 422, 431
- clinical, 3, 7, 10, 12, 13, 14, 16, 17, 19, 20, 21, 23, 26, 27, 28, 29, 30, 31, 37, 43, 44, 47, 50, 53, 54, 55, 57
- clinical trial, 12, 14, 20, 21, 23, 26, 27, 28, 31, 54
- clinical trials, 12, 14, 20, 21, 23, 26, 27, 28
- clones, 419
- cloning, 408
- closure, 51, 407
- clusters, 295
- C-N, 248
- CO₂, viii, x, 97, 98, 99, 100, 101, 102, 103, 105, 106, 107, 108, 109, 110, 225, 226, 242, 245, 249, 250, 253, 263, 265, 273, 276
- coagulation, xi, 179, 181, 202, 203, 226, 261, 280, 282, 309, 310, 323
- coagulation process, 282
- coal, 203, 206, 207, 210, 211, 218, 220, 223

- coatings, 77, 79, 81, 92, 301, 363
cobalt, 33, 58, 324, 364, 389
codes, 354
coenzyme, 416
coffee, 418
cohesion, 301, 303
collagen, 56
collisions, 5
colon, 3, 37, 47, 59
colonization, 423, 426, 427
colorectal, 23, 50
colorectal cancer, 50
colors, 315, 332, 334, 353, 359, 363, 365, 384, 393
combination therapy, 20
combined effect, 152, 160, 287
combustion, 205, 206
combustion processes, 206
commercial, 145, 180, 182, 185, 203, 263, 281, 286, 287, 299, 315, 319, 366, 370, 409
commodity, 64, 354
communication, 257
competition, 215, 240, 242, 248
competitive process, 5
competitiveness, 359, 364
compilation, 44
complementary, 335
complexity, ix, 175
components, xi, 6, 9, 36, 331, 333, 334, 339, 340, 361, 363, 404, 412
composite, 205, 207, 209, 220, 223, 285, 320, 325, 326, 327
composites, 209
composition, ix, 10, 13, 33, 175, 186, 191, 195, 357, 408, 411, 413, 416
compositions, 352
composting, 284
compression, 187
computer, 230
concentrates, 28
concrete, 230, 326
condensation, 11, 17, 31, 67, 365, 366, 407
conductance, 124
conduction, 274
conductive, viii, 111
conductivity, viii, 111, 112, 123, 124, 125, 126
configuration, 244
conformational, 121, 122, 411
confusion, 313
congestive heart failure, 405
Congress, 38, 47
conjugation, 73, 112, 240, 244, 245, 246, 248, 301, 338, 347
conservation, 257, 332
constitutional, 32
constraints, 311
construction, 253, 298, 418
consumers, 175
consumption, x, 7, 165, 175, 226, 252, 311
contact dermatitis, 177
contact time, 180
contaminant, 226, 263
contaminants, 144, 145, 173, 176, 179, 226, 261, 263, 264, 310
contaminated soils, 98, 268, 280, 284, 323
contamination, 102
control, vii, viii, ix, xii, 1, 7, 8, 9, 15, 97, 121, 127, 130, 175, 206, 223, 259, 356, 359, 369, 413
controlled, viii, 46, 97, 102, 111, 146, 209, 212, 213, 234, 239, 242, 302, 313, 356
convective, 213
conversion, x, 4, 5, 15, 16, 179, 225, 226, 242, 244, 261, 263, 432
convex, 214
cooking, 173
cooling, 67, 71, 129, 130, 138, 372
coordination, 285, 294, 301, 316
COP, 298, 305
copolymer, xii, 119, 120, 121, 134, 135, 136, 137, 138, 139, 383, 395, 397, 398
copolymerization, 385, 392, 393, 397, 398, 400
copolymers, xii, 284, 383, 385, 393, 394, 395, 396, 397, 400
copper, 181, 219, 250, 251, 252, 301, 325, 334, 389, 405
coral, 136
corona, 144
coronary artery disease, 31, 57
correlation, 100, 106, 107, 108, 191, 293
correlations, 99, 106, 293
corrosion, 358
Corynebacterium, 210, 223
cosmetics, xii, 38, 383, 384, 395, 396, 398, 405
cost-effective, ix, 175, 254
costs, 102, 181, 189, 194, 202, 209, 351, 359, 363, 413
cotton, xii, 102, 103, 106, 108, 109, 110, 177, 180, 207, 222, 290, 383, 385, 391, 405
couples, 76, 86, 87, 89
coupling, 145, 283, 285, 286
covalent, 177, 205, 293, 295, 297, 298, 301, 303, 305, 385, 398, 400
covalent bond, 177, 295, 297, 298, 303, 398, 400
covalent bonding, 398, 400
CRC, 254
critical points, 405
critical temperature, 98, 136

- crops, 409
 cross-linked, 217, 299, 302
 crosslinking, 204
 cross-linking, 293
 cross-linking, 300
 cross-sectional, 133
 cross-talk, 412
 crustaceans, 204
 cryosurgery, 53
 crystal, viii, xi, 22, 57, 111, 112, 113, 114, 115, 127, 128, 129, 130, 139, 222, 291, 294, 296, 298, 299, 300, 303, 304, 314, 316, 323, 353, 356, 357, 370, 371
 crystal lattice, xi, 114, 291, 300
 crystal structure, 57, 115, 298, 304, 314, 356, 357
 crystal structures, 298
 crystalline, 113, 115, 127, 130, 204, 294, 303, 316, 353, 354, 356
 crystallinity, 127, 366
 crystallisation, 296, 299
 crystallization, 118, 295, 296, 297, 298, 410
 crystallographic, 298, 354
 crystals, 113, 291, 294, 296, 298, 301, 313, 315, 316, 319, 355
 cultivation, 415
 culture, 47, 91, 408, 409, 410, 411, 415, 416, 417, 418, 419, 427, 429
 culture conditions, 417
 cycles, 115, 119, 120, 122, 132, 136, 187
 cyclic voltammetry, 67
 cycling, 120
 cyclodextrin, 204, 217, 221, 323
 cyclodextrins, 204, 329
 cyclohexanone, 77
 cyclooxygenase, 8
 cysteine, 6
 cystic fibrosis, 30, 55
 cystoscopy, 40
 cytokine, 21
 cytokines, 9
 cytoplasm, xiii, 8, 404, 411
 cytosol, 8, 35, 58, 59, 409
 cytotoxic, 3, 4, 5, 39
 cytotoxicity, 35, 36, 37, 55
- D**
- damping, 209
 danger, 176, 183, 395
 data set, 100
 database, 58, 364
 death, 5, 7, 9, 41, 355
 decay, 4, 78, 228, 229, 231, 273, 275, 340
 decoloration, v, 175, 179, 180, 184, 186, 187, 188, 190, 191, 192, 193, 194, 195, 243, 244
 decomposition, x, 61, 144, 165, 172, 173, 181, 183, 185, 190, 225, 226, 228, 236, 237, 241, 245, 250, 251, 252, 268, 270, 272, 273, 283, 285, 287
 decomposition reactions, 144
 decontamination, xi, 165, 173, 289, 309, 310, 312
 defects, 17, 275, 276, 303
 defense, 332, 410, 411, 412
 definition, 293, 303, 353
 degenerative disease, 332
 degradation mechanism, 229
 degradation pathway, x, 259
 degradation process, 179, 202, 333, 334
 degradation rate, 150, 153, 159, 161, 164, 170, 185, 250
 degrading, 274, 429, 432
 degree, 10, 73, 81, 89, 104, 203, 204, 215, 245, 249, 253, 313, 339, 356, 358, 385
 delays, 190
 delivery, 8, 24, 34, 35, 47, 49, 54, 59
 delocalization, 11, 126
 delta, 45, 46, 47, 48
 demand, ix, 98, 104, 143, 179, 183, 248, 253, 260, 269, 302, 309, 405
 density, 99, 100, 101, 104, 106, 109, 112, 117, 126, 140, 233, 235, 293, 392
 density functional theory, 126, 235
 deposition, 131, 132, 182, 289
 deposits, 315
 derivatives, vii, xi, xii, xiii, 3, 10, 16, 17, 18, 19, 23, 28, 31, 32, 36, 43, 46, 47, 48, 51, 53, 55, 57, 63, 64, 65, 67, 72, 75, 76, 78, 79, 81, 89, 106, 220, 260, 262, 282, 288, 289, 290, 325, 331, 332, 370, 374, 383, 385, 386, 387, 389, 393, 394, 396, 397, 398, 403, 404, 405, 406, 408, 410, 413, 414, 415
 dermatologic, 17
 dermatologist, 2
 dermatology, 2, 16, 20, 28, 39, 45
 desorption, 220
 destruction, vii, x, 1, 3, 5, 7, 8, 9, 43, 187, 203, 206, 225, 240, 244, 245, 248, 249, 253, 254, 262, 263, 273, 404
 detection, 4, 6, 18, 44, 229, 230, 334, 346, 420
 detergents, 183
 detoxification, 276, 281, 282
 detoxifying, 285
 deviation, 115
 dexamethasone, 20
 dextrose, 25
 diagnostic, 4, 16, 35, 40, 334, 347
 diatoms, 315
 dichotomy, xi, 291, 293

- dielectric, 112
 dielectric constant, 112
 diesel, 325
 differential scanning, 327
 differential scanning calorimetry, 327
 differentiation, 409
 diffusion, 8, 102, 212, 213, 216, 220, 234, 239, 242, 296, 300, 321, 346, 360
 diffusion mechanisms, 212
 diffusion process, 220, 321
 dimer, 18, 115, 240
 dimeric, 27
 dimerization, 18
 dimethylformamide, 70
 dimethylsulfoxide, 70
 diode laser, 50
 diodes, 48
 dipole, 121
 dipole moment, 121
 discharges, 101
 diseases, 2, 23, 37, 177, 405
 disinfection, x, 30, 56, 183, 225, 272
 dispersion, 104, 110, 358
 dissociation, ix, xi, 201, 211, 214, 228, 244, 272, 331, 338, 339
 dissolved oxygen, 241, 249, 250, 279
 distillation, 283
 distilled water, 250
 distribution, viii, 4, 32, 47, 54, 61, 64, 65, 97, 104, 108, 126, 127, 213, 324, 352, 357, 358, 363, 365, 366
 distribution function, 213
 diversity, 209, 212
 division, 417
 DMF, 70, 80, 83, 86, 87, 375, 400
 DNA, xiii, 8, 40, 286, 403, 405, 410, 418
 dogs, 26, 27, 48, 54
 donor, 116, 178, 189, 190
 donors, xiii, 421
 dopant, 276
 doped, 118, 276, 289, 356
 doping, 276
 dosage, 24, 144, 171
 dose-response relationship, 10
 dosimetry, 57
 dosing, 24, 43
 double bonds, 11, 19, 26, 126, 178, 246
 DPP, 300
 drainage, 209, 223
 drinking, 272, 280
 drinking water, 272, 280
 drug delivery, 34, 46, 109, 133
 drugs, vii, 1, 9, 12, 20, 37, 59, 298, 405
 dry, 20, 98, 101, 249, 332
 drying, 98, 284, 312, 363
 DSC, 129
 DSS, 282
 durability, 209, 385
 duration, 103, 180, 263
 DWI, 106
 dyeing, iv, viii, xi, xiii, 97, 98, 100, 101, 102, 103, 105, 106, 107, 108, 109, 110, 144, 172, 175, 176, 177, 178, 190, 191, 193, 252, 284, 290, 292, 295, 297, 300, 302, 303, 331, 333, 334, 342, 384, 392, 403, 405, 415
- E**
- earth, 216, 315, 320, 322, 327, 328
 ecological, xii, 179, 191, 192, 383, 384, 385, 392, 395, 404
 ecology, 195, 384
 economic, 98, 102, 253, 404, 413
 ecosystems, ix, 175, 188, 189
 efficacy, vii, 9, 16, 21, 23, 25, 26, 42, 49, 55, 61, 63, 67, 189
 effluent, 102, 176, 187, 195, 221, 222, 252, 261, 277, 282, 285, 288, 310, 311, 430
 effluents, ix, xiii, 173, 176, 181, 190, 195, 201, 202, 204, 208, 209, 216, 220, 222, 226, 250, 261, 280, 281, 282, 287, 310, 323, 326, 327, 421
 egg, 24, 332
 eicosanoids, 8
 elderly, 20
 election, 120, 423
 electric current, 303
 electric field, 124, 133
 electrical, viii, 111, 112, 113, 123, 139, 144, 313
 electrical conductivity, viii, 111, 112, 113, 139
 electrical properties, 123
 electricity, 112, 203
 electrochemical, 27, 52, 75, 112, 144, 222, 290, 391
 electrodes, 75
 electrolysis, 188
 electromagnetic, 230
 electron, x, xiii, 5, 6, 27, 29, 72, 73, 75, 76, 87, 89, 90, 91, 92, 112, 126, 165, 178, 190, 202, 225, 227, 229, 230, 231, 233, 234, 235, 236, 237, 239, 240, 242, 244, 245, 251, 252, 256, 274, 275, 278, 303, 338, 370, 375, 378, 421
 electron beam, x, 225, 230, 251
 electron density, 76, 90, 233, 234, 239
 electron pairs, 278
 electronegativity, 304
 electronic, viii, x, 34, 53, 111, 112, 123, 126, 133, 144, 225, 301, 335
 electronic structure, viii, 111, 112, 123

- electronics, viii, 111
 electrons, 4, 5, 11, 75, 89, 126, 178, 226, 229, 231, 240, 271, 274, 275, 276, 278, 300, 378
 electron-transfer, 112, 165
 electrophoresis, 325
 electroplating, 216
 electrostatic, 205, 208, 211, 317, 320
 electrostatic force, 211
 embryonic, 39
 emission, xi, 4, 5, 89, 118, 119, 120, 185, 331, 333, 339, 340, 341, 342, 343, 344, 345, 347, 405
 employees, 252, 302
 employment, 16, 28
 emulsifier, 252
 emulsifying, 23
 emulsion polymerization, 329
 emulsions, viii, 97, 299
 encapsulation, 353
 encoding, 410, 416, 419
 endobronchial, 51
 endocytosis, 8, 34
 endogenous, xiii, 3, 15, 16, 17, 403
 endoplasmic reticulum, 8, 41, 409
 endosperm, 419
 endothermic, 321
 energy, vii, x, 1, 2, 4, 5, 6, 8, 9, 34, 56, 76, 81, 87, 126, 127, 144, 178, 189, 225, 227, 229, 230, 232, 252, 264, 297, 311, 335, 336, 337, 341, 352, 375, 405
 energy consumption, 352
 energy transfer, 5, 6, 87, 178
 engineering, 113, 223, 294, 409, 410, 413, 418
 enhancement, 59, 60, 61, 285
 entropy, 304
 environment, ix, xi, xiii, xiv, 5, 6, 8, 27, 29, 34, 73, 76, 90, 144, 146, 175, 176, 179, 189, 202, 257, 259, 310, 311, 319, 322, 331, 333, 347, 357, 375, 411, 421, 422, 423, 426, 427, 431
 environmental, viii, ix, xiii, 97, 101, 133, 143, 144, 176, 177, 194, 195, 201, 202, 214, 223, 226, 231, 259, 261, 281, 310, 322, 328, 398, 403, 404, 409, 413, 432
 environmental advantage, 413
 environmental conditions, 133, 432
 environmental contamination, 101
 environmental factors, 404, 409
 environmental issues, 259
 environmental stimuli, xiii, 403
 enzymatic, 17, 28, 189, 414
 enzyme, 14, 15, 18, 26, 32, 407, 409, 416
 enzymes, 6, 42, 410, 413, 418
 EPA, 195
 EPR, 61
 equilibrium, xi, 98, 99, 100, 102, 156, 171, 211, 212, 213, 217, 218, 219, 220, 221, 228, 275, 309, 310, 320, 322, 324, 325
 equipment, 188, 363, 394, 399
 Erk, 293, 306
 erythrocyte, 59
 erythrocytes, 62
 Escherichia coli, 53, 290, 416
 ESI, 420
 esophageal, 3, 14, 25, 39
 esophageal cancer, 14
 esophagus, 14, 44
 ESR, 59
 ester, 13, 16, 17, 18, 19, 24, 31, 41, 47, 127, 324, 407
 esterases, 18
 esterification, 17, 18, 20, 208, 211
 esters, xii, 17, 18, 26, 46, 47, 48, 383
 etching, 365
 ethanol, 21, 25, 99, 100, 101, 105, 107, 278, 339
 ethylene, 11, 17, 20, 48, 52, 412
 ethylene glycol, 17, 20, 48
 ethylene oxide, 52
 ethylenediamine, 207, 221
 eucalyptus, 110
 eukaryotic, 14, 15
 eukaryotic cell, 14, 15
 European, 47, 48, 175, 176, 197, 198, 280, 323, 419
 European Union, 176
 europium, 411
 evaporation, 67, 71
 evidence, 18, 58, 236, 364, 405
 evolution, 295, 338, 345
 excitation, 9, 11, 34, 76, 79, 80, 88, 120, 127, 178, 335, 342
 excretion, 25
 exogenous, xiii, 15, 16, 403
 exoskeleton, 204
 experimental condition, viii, 81, 143, 227
 experimental design, 192
 experts, 294
 exploitation, 413
 exponential, 362
 exposure, 2, 3, 76, 176, 333
 expressed sequence tag, 410
 extinction, 10, 11, 26, 273, 413
 extracellular, 36, 190
 extraction, 5, 98, 222, 237, 262, 284
 extraction process, 98
-
- F**
-
- fabric, 102, 107, 296, 297
 factorial, 191

- family, xiii, 11, 19, 25, 26, 313, 403, 405, 406, 407, 410, 412
- fatigue, 113, 115, 120, 122, 134
- fatty acid, 6
- fatty acids, 6
- fax, 1, 421
- FDA, 23
- feedback, 15, 279
- feeding, 112, 409, 418
- feelings, 355
- fermentation, 204, 405, 409
- ferric ion, 273
- ferrite, 364
- ferrous ion, 173, 182, 267, 268, 269, 271, 281
- fertilizer, 206
- fetal, 91
- fiber, 204, 222, 325, 392
- fiber membranes, 325
- fibers, 316
- fillers, 315
- film, 76, 77, 78, 92, 113, 118, 119, 120, 130, 131, 132, 136, 187, 212, 213, 299, 370
- films, 77, 78, 105, 109, 110, 114, 118, 131, 133, 222, 287, 289, 299, 395
- filters, 98, 104, 229
- filtration, xi, 84, 179, 181, 202, 203, 262, 309, 371
- first generation, 10
- fixation, xii, 383, 385, 391
- flame, 232
- flat panel displays, 303
- flavone, xi, 331, 332, 333, 336
- flavonoids, xi, 331, 332, 333, 346, 404
- flexibility, 352, 363
- flocculation, 179, 181, 182, 320, 322
- flow, 99, 105, 110, 185, 190, 351, 432
- flow rate, 185
- fluid, 98, 99, 100, 101, 102, 103, 104, 105, 106, 108, 109, 110, 353, 356
- fluid extract, 110
- fluorescence, vii, viii, xi, xii, 2, 3, 4, 18, 30, 40, 41, 48, 63, 73, 76, 79, 80, 85, 88, 89, 91, 92, 111, 112, 113, 118, 119, 120, 139, 331, 333, 334, 335, 338, 339, 340, 342, 343, 344, 345, 346, 347, 383, 393, 394, 396, 397
- fluorinated, 60
- fluorine, 286
- fluorogenic, 346
- fluorometric, 338
- fluorophores, 347
- focusing, xii, 351
- folding, 316
- food, xii, xiii, 176, 333, 383, 396, 397, 398, 403
- food additives, 397
- food processing industry, 396
- foodstuffs, 384
- foreign organisms, 410
- forestry, 417
- formaldehyde, 237, 267
- formamide, 397
- fouling, 181, 264
- Fourier, 232
- fractionation, 98
- fragmentation, x, 8, 225, 242
- free radical, 36, 165, 183, 204, 263, 346
- free radical scavenger, 263
- free radicals, 36, 165, 346
- freedom, 122
- freezing, 136
- frequency distribution, 302
- fresh water, 175, 221, 315
- Freundlich isotherm, 214
- fruits, 332, 333
- FTIR, 232
- FT-IR, 128, 129
- FT-IR, 370
- fuel, 204
- fungal, 16, 30, 45, 55, 208, 222, 412, 418
- fungus infection, 16, 30, 45, 55
- fungi, 220, 404, 410
- fungus, 215
- furniture, 302

G

- gadolinium, 32
- gallium, 36, 52, 59, 61
- garbage, 204
- gas, 98, 144, 187, 203, 232, 237, 248, 262, 264, 420
- gas chromatograph, 232, 420
- gas phase, 237
- gases, viii, 97, 220
- gasoline, 284
- gastric, 14
- gastrointestinal, 14, 44
- gastrointestinal tract, 14, 44
- gel, viii, 13, 31, 67, 111, 113, 134, 135, 136, 138, 139, 288, 370, 387, 388, 390
- gel permeation chromatography, 13
- gelatin, 284
- gels, 135, 136
- gene, xiii, 35, 59, 403, 410, 412, 413, 416, 418
- gene expression, xiii, 404, 412
- gene therapy, 35, 59
- generation, 10, 33, 36, 37, 50, 54, 64, 65, 125, 126, 144, 182, 185, 203, 236, 263, 346, 411, 412
- genes, xiii, 404, 410, 412, 419, 420
- genetic, 404, 409, 410, 411, 413

- genetic diversity, 404
genome, 410
genome sequencing, 410
genomics, 418
genotoxic, 408
glass, 118, 133, 220, 243, 262, 263, 299, 300, 303, 314, 325, 353, 358
glasses, 136
glioma, 3, 23
gliomas, 14, 44
glucose, 190, 406, 408
glutamate, 14
glutamic acid, 14
glycine, 14
glycol, 20, 46, 48, 54, 104
glycoside, 407
glycosides, 332, 413
glycosylation, 407, 416
gold, 287, 288
government, iv
GPO, 143
G-protein, 412, 413, 420
grades, 300
graffiti, 355
grafting, 205
grain, 363, 365, 366
grains, 211, 222
graphite, 52, 173, 282, 301
Greeks, 2
Ground state, 5
groundwater, 259, 324
group work, 296
groups, vii, ix, 1, 12, 13, 22, 31, 53, 64, 91, 92, 116, 118, 121, 177, 201, 202, 205, 206, 208, 211, 214, 222, 233, 237, 245, 248, 266, 272, 287, 295, 298, 299, 300, 302, 304, 314, 320, 321, 337, 338, 346, 385, 391, 392, 393, 404
growth, xiii, xiv, 43, 131, 132, 144, 189, 303, 408, 415, 417, 419, 421, 423, 424, 427
guanine, 6
GVHD, 31
- H**
- H₂, 188, 207, 227, 248
half-life, 13, 19, 21, 24, 26, 31, 176, 183, 188, 203
halogen, 91
halogenated, 17
halogenation, 29, 30, 31
handling, 188, 202, 310, 311
hands, 164
hardness, 180, 304
harmful, 176, 181, 261, 272, 310
harmful effects, 176
harvesting, 404
hazards, 176, 332
H-bonding, 338
head, 14, 17, 21, 25, 53, 59, 76, 114
head and neck cancer, 14, 21
healing, 412
health, 2, 176
heat, 5, 34, 187, 216, 352, 384
heating, 34, 128, 129, 130, 229, 352, 366
heating rate, 352
heavy metal, 202, 207, 212, 216, 217, 220, 221, 223, 226, 264
heavy metals, 202, 207, 212, 216, 217, 220, 223, 226
height, 133
hematite, 305, 325, 355
heme, 3, 15, 16
hemoglobin, 9, 14
hepatoma, 23
herbicides, 313, 396
heterogeneity, 212, 214
heterogeneous, viii, xii, 143, 165, 211, 214, 219, 262, 270, 273, 275, 276, 283, 288, 289, 351, 352
heterogeneous catalysis, viii, 143
hexane, 114
high fat, viii, 111, 112
high pressure, 102, 237, 334
high tech, 92, 384
high temperature, xii, 100, 151, 159, 205, 270, 351, 356, 357, 363, 366
high-performance liquid chromatography, 420
histology, 29
histone, 52
histoplasmosis, 20
HIV, 28
HOMO, 73, 76, 87, 126, 127, 233, 235, 240
homogeneity, 118, 146, 209
homogeneous, viii, 104, 136, 143, 146, 165, 213, 229, 270, 356
homogeneous catalyst, 270
hormones, 410
host, viii, 40, 43, 111, 204
hot water, 400
HPLC, 13, 232, 235, 246, 248, 262, 310, 334, 416, 420
hue, 296, 355, 359, 365
human, ix, 3, 6, 7, 9, 16, 17, 18, 19, 26, 27, 29, 30, 32, 34, 39, 41, 46, 47, 48, 49, 56, 58, 59, 175, 312, 332, 384, 385, 395, 405
human leukemia cells, 59
humans, xiii, 26, 45, 183, 384, 403
humate, 207, 219, 223
humic acid, 206, 320, 325, 327
humic substances, 206

- Hungarian, 225, 254
 Hungary, 225, 403
 hybrid, 223, 282, 285
 hybrids, 329
 hydration, 319
 hydro, 10, 64, 101, 206, 299, 319
 hydrodynamic, 36
 hydrogels, 136, 220, 223
 hydrogen, x, 5, 6, 33, 56, 70, 116, 141, 146, 150, 165, 169, 172, 173, 181, 182, 183, 185, 186, 187, 191, 225, 226, 227, 228, 245, 250, 254, 259, 264, 265, 266, 267, 268, 269, 270, 271, 273, 281, 282, 283, 284, 285, 313, 314, 338, 347, 384, 392
 hydrogen atoms, 70, 226, 245
 hydrogen bonds, 116
 hydrogen peroxide, x, 6, 33, 56, 146, 150, 165, 169, 172, 173, 181, 182, 183, 185, 186, 191, 228, 250, 254, 259, 264, 265, 266, 267, 268, 269, 270, 271, 273, 281, 282, 283, 284, 285
 hydrogenation, 422, 423
 hydrolysis, 13, 17, 19, 26, 47, 150, 169, 414, 416
 hydrolyzed, 13, 24, 26, 190, 290
 hydrophilic, 10, 64, 101, 206, 299, 319
 Hydrophilic, 187
 hydrophilic groups, 64
 hydrophilicity, 17, 18, 321
 hydrophobic, 8, 23, 24, 34, 51, 101, 103, 187, 204, 299, 317
 Hydrophobic, 54
 hydrophobic properties, 299
 hydrophobicity, 25, 205
 hydroquinone, 285
 hydroxide, 146, 165, 180, 210, 221, 313
 hydroxyl, x, 6, 33, 56, 59, 144, 150, 151, 152, 160, 165, 170, 181, 182, 183, 185, 186, 187, 190, 202, 225, 227, 234, 236, 237, 239, 244, 250, 261, 266, 267, 270, 271, 272, 277, 278, 282, 285, 286, 333, 336, 337, 338, 339, 347, 392
 hydroxyl groups, 165, 333, 336, 337, 338, 347, 392
 hyperplasia, 21
 hyperthermia, 60
 hypothesis, 3, 344, 347
 hypoxia, 7, 8, 40
 hypoxic, 6, 7
-
- identification, 38, 176, 190, 229, 232, 233, 244, 248, 334, 348, 354, 413, 418, 419
 illumination, 4, 7, 8, 9, 10, 31, 136, 229, 359, 409
 images, 76, 136, 137, 139
 imaging, 118, 136, 137
 immersion, 299
 immobilization, 413, 417
 immune response, vii, 1, 7, 9
 immunity, 9, 43, 420
 immunodeficient, 9
 immunomodulatory, 21
 immunotherapy, 43
 implementation, 188
 impurities, 182, 356
 in situ, 290, 334, 335
 in vitro, 4, 16, 23, 25, 32, 34, 35, 37, 42, 46, 58, 62, 408
 in vivo, 4, 13, 25, 26, 32, 34, 35, 37, 40, 46, 51, 52, 56, 64, 65
 inactivation, 16, 29, 30, 42, 53, 55
 inactive, 13, 19, 28, 250
 incineration, 249
 inclusion, 204, 353, 355
 incubation, 8, 91
 India, 108, 176, 355
 Indian, 2, 107, 255, 415
 indication, 23, 391, 397, 400
 indium, 8, 24, 51, 282
 indium tin oxide, 282
 indomethacin, 8
 induction, 8, 411, 418
 industrial, ix, x, xi, xii, xiii, 26, 64, 104, 176, 189, 201, 202, 204, 205, 206, 208, 219, 221, 225, 226, 227, 250, 252, 253, 254, 259, 260, 261, 267, 271, 277, 281, 289, 293, 297, 298, 299, 300, 301, 309, 312, 314, 351, 356, 359, 363, 364, 365, 403, 423
 industrial application, 26, 104, 364, 423
 industrial production, xiii, 403
 industrial sectors, 363
 industrial wastes, ix, 201, 202, 267
 industry, xi, 175, 188, 202, 203, 204, 207, 226, 285, 288, 290, 294, 295, 309, 356, 359, 363
 inert, xii, 351
 infarction, 7
 infection, 29, 55
 infinite, 294, 300, 312
 inflammatory, 9
 infrared, 26, 67, 179
 inhibition, 277
 inhibitor, 8, 409
 inhibitors, 409, 413, 415, 418, 419
 inhibitory, 146, 189
 inhibitory effect, 146, 189
 initial state, 138
 initiation, 183, 237
 injection, 8, 16, 22, 28, 51, 127
 injections, 13
 innovation, 364, 402
 inoculation, 429

- inorganic, ix, x, 176, 179, 188, 201, 202, 203, 205, 207, 209, 211, 215, 249, 253, 284, 291, 292, 293, 294, 295, 299, 301, 302, 303, 305, 353, 354, 355, 356, 358, 374
 inorganic salts, ix, 201, 207, 211, 215, 284, 374
 insects, 304
 insertion, 23
 insight, 134, 138
 instability, 17, 19, 28, 48, 304, 353
 institutions, 64
 integration, 121, 153, 412
 intensity, 66, 76, 112, 119, 120, 186, 191, 192, 229, 244, 265, 271, 335, 339, 342, 347, 356, 359, 366, 397, 409
 interaction, 2, 5, 42, 46, 60, 75, 76, 89, 90, 112, 116, 121, 138, 165, 173, 180, 208, 262, 271, 340, 342, 344, 346
 interactions, 4, 35, 36, 81, 84, 121, 180, 204, 212, 317, 334, 342, 344, 411, 413
 intercalation, 205, 319
 interface, 180, 207, 212, 219, 237
 interference, 230, 263, 301, 410
 intermolecular, x, 115, 116, 291, 293, 294, 295, 296, 297, 300, 302, 304, 370
 intermolecular interactions, 370
 internalization, 33, 34, 35, 59
 international, 12, 354
 International Atomic Energy Agency (IAEA), 254, 257
 interpretation, 297, 359
 interstitial, 57
 intervention, 57
 intravenous, 37, 39
 intrinsic, 338, 397, 400
 intrinsic viscosity, 397, 400
 invasive, 217
 inversion, 346
 investigations, 55, 98, 105, 110
 investment, 102, 181, 194
 ion channels, 412
 ion exchangers, 180
 ion-exchange, 311
 ionic, 28, 124, 125, 133, 202, 205, 206, 211, 214, 215, 216, 220, 242, 272, 277, 294, 295, 297, 317, 319, 321, 392
 ionic polymers, 124
 ionic-covalent, 294
 ionization, 232, 338
 ionizing radiation, x, 2, 225, 226
 ions, 64, 145, 150, 151, 159, 160, 165, 172, 173, 188, 208, 209, 219, 221, 222, 250, 251, 252, 253, 264, 268, 269, 270, 271, 272, 277, 278, 279, 293, 299, 300, 301, 305, 316, 319, 320, 321, 323, 325, 328, 342, 343, 344, 345, 346, 347, 353, 356, 411
 IR, xii, 9, 67, 71, 83, 84, 88, 129, 310, 369, 370, 371, 372, 373, 374, 375, 389
 IR spectra, 129, 370
 iron, ix, 2, 15, 16, 33, 145, 146, 150, 153, 159, 172, 182, 201, 206, 209, 219, 220, 223, 250, 251, 268, 269, 270, 281, 285, 287, 288, 294, 313, 315, 323, 324, 325, 334, 355, 364
 irradiation, viii, 9, 10, 13, 16, 19, 21, 23, 26, 28, 33, 35, 60, 111, 115, 117, 118, 119, 120, 121, 123, 125, 126, 127, 134, 135, 136, 138, 139, 144, 172, 181, 187, 192, 194, 226, 229, 231, 232, 241, 243, 244, 245, 249, 250, 252, 253, 254, 263, 264, 279, 285, 394, 395, 399, 400
 irritation, 177
 isoforms, 420
 isolation, 12, 43, 404, 410
 isomerization, 113, 117, 121, 126, 134
 isomers, vii, 14, 21, 32, 63, 70, 71, 72, 73, 74, 75, 76, 79, 81, 87, 88, 90, 91, 92, 112, 118, 120, 244
 isoprene, 407
 isoprenoid, 416
 isotherms, 214, 316
 isotropic, 129
- K**
- K^+ , 316, 371, 372
 kaolinite, xi, 204, 309, 312, 313, 314, 315, 319, 325, 326
 KBr, 67, 71, 83, 84, 88, 371, 372, 373, 374
 kernel, 207, 210, 215, 219, 221
 ketimine, 18
 ketones, x, 18, 225, 242, 253
 kidney, 61, 176
 kinase, 412, 419
 kinetic constants, 212, 271, 339, 340
 kinetic curves, 153, 161, 231
 kinetic model, 161, 167, 212, 220, 221, 283
 kinetic parameters, 104, 153, 161, 169
 kinetic studies, 171, 319
 kinetics, ix, x, 47, 58, 110, 143, 145, 146, 153, 155, 159, 161, 162, 166, 167, 171, 172, 183, 211, 218, 219, 220, 222, 223, 225, 226, 245, 246, 270, 272, 281, 283, 284, 287, 304, 320, 323, 324, 326, 395, 430, 431
- L**
- lactic acid, 105, 204
 lakes, 259, 332, 343
 lamellar, 296
 Langmuir, 142, 213, 214, 220, 275, 320

language, 302
 lanthanide, 32
 large-scale, ix, xiii, 201, 202, 252, 403
 laryngeal cancer, 49
 laser, 34, 51, 64, 76, 77, 78, 79, 81, 92
 lattice, 204, 315
 lattices, 300
 law, 192, 213, 230
 laws, 364
 leachate, 284
 lead, 8, 12, 13, 138, 181, 226, 241, 242, 268, 294, 358, 364, 378
 leakage, 8, 42
 learning, 364
 leather, 290
 legislation, 177
 Leguminosae, 404
 lens, 229, 230
 lenses, 230
 lesions, 3, 28, 31, 44, 55
 leukemia, 42, 56
 leukemia cells, 42
 leukocyte, 42
 lifetime, 6, 8, 27, 40, 64, 65, 77, 78, 79, 81, 82, 92, 339
 ligand, 31, 32, 53
 lignin, 206
 lignocellulose, 180
 limitation, 9, 204, 313, 357
 limitations, xii, 33, 118, 181, 351, 359, 363
 linear, 130, 191, 213, 219, 230, 245, 249, 268
 linear dependence, 268
 linkage, 121, 127, 129, 189, 235, 236, 250, 411
 lipid, 59, 412, 413
 lipid peroxidation, 59
 lipids, 6, 36
 lipophilic, 6, 24, 29, 41, 46, 64
 lipoproteins, 31
 liposomes, 24
 liquid chromatography, 232, 334
 liquid crystal displays, 98, 104
 liquid crystals, viii, 111, 127, 295, 297, 298, 303
 liquid film, 212
 liquid phase, 101, 212
 liquids, viii, 97, 98, 102, 187, 220, 313
 literature, xi, 19, 66, 67, 102, 107, 213, 271, 275, 296, 299, 309, 310, 313, 319, 320, 321, 322, 338, 363, 370, 374
 lithography, 365
 liver, 23, 176
 liver cancer, 23
 localization, 3, 8, 16, 41, 42, 43, 58, 412, 420
 location, 144

long-term, vii, 1, 8, 9, 10, 13, 57, 118
 losses, 180
 low molecular weight, 102, 261, 273
 low-level, 408
 LTD, 257
 luminescence, 117, 118, 120
 LUMO, 73, 76, 87, 126, 127, 233, 235, 239, 240
 lung, 3, 14, 23, 25, 41, 50, 51
 lung cancer, 14, 25, 51
 lutetium, 31, 32, 57
 lymphatic, 39
 lymphocytes, 56
 lymphoid, 43
 lymphoma, 41
 lysis, 59
 lysosomal enzymes, 16
 lysosomes, 8, 16, 35, 59
 lysozyme, 325

M

M and A, 288
 machinery, 102
 machines, 363
 macromolecules, 34
 macrophages, 9
 Madison, 255
 magnesium, 206, 313, 316
 magnet, 209
 magnetic, 32, 112, 179, 208, 217, 220, 222, 223
 magnetic properties, 112, 209
 magnetic resonance, 32
 magnetic resonance imaging, 32
 magnetism, viii, 111, 112
 magnetite, 209, 223
 maintenance, 263, 264, 311, 342, 408
 maize, 180, 418
 malignant, xiii, 28, 44, 49, 54, 403, 405
 mammals, xiii, 14, 403
 management, 38, 50, 195, 359
 management practices, 195
 manganese, 285, 376
 mango, 219
 man-made, 293, 302
 manufacturer, 33, 297
 manufacturing, 202
 market, 299, 356, 364, 365
 market penetration, 364
 mask, 118, 136
 mass spectrometry, 334
 mass transfer, viii, 97, 104, 105, 212, 213
 mass transfer process, 212
 mast cells, 9
 materials science, 112, 304, 364

- mathematical, 212, 363, 430
matrix, xii, 8, 56, 263, 277, 351, 352, 353, 355, 358
maximum sorption, 207, 214
MDR, 405
meanings, 386, 387, 389, 394, 397, 399
measurement, 107, 121, 124, 147, 246, 249, 253
measures, 359
mechanical, iv, 34, 35, 98, 104, 126, 209, 252, 320, 392
mechanical properties, 209
media, viii, xii, 64, 65, 84, 97, 104, 109, 113, 114, 120, 133, 136, 190, 204, 217, 272, 289, 320, 322, 351, 358, 408, 427, 432
medicinal, 3, 17
medicine, xi, 2, 46, 53, 331, 396
medium composition, 408
melanin, 9
melanoma, 20, 29, 31, 32, 47, 54, 55, 58
melting, 99, 352
melts, 356
membranes, 8, 17, 28, 35, 270, 285, 324, 325
memory, viii, 111, 113, 117, 120, 136
mental health, 2
Merck, 388
mercury, 185, 263
mesoscopic, 133
messengers, xiii, 404, 411, 412
metabolic, xiii, 17, 28, 208, 403, 409, 411, 412, 416, 417, 418
metabolic pathways, 409
metabolism, 3, 16, 32, 208, 404, 409, 410, 418
metabolite, 16, 408, 409, 413, 417, 418
metabolites, 404, 409, 411, 412, 414, 416, 417, 418, 420
metal ions, xi, 64, 146, 165, 204, 208, 302, 331, 333, 342, 344, 345, 346, 347
metal oxide, 305
metal oxides, 305
metal salts, 33
metallophthalocyanines, xii, 369
metalloporphyrins, 39
metals, xi, xii, 23, 32, 250, 264, 270, 276, 301, 331, 369, 370, 375, 377, 378
metastases, 27, 37
metastasis, 23
metastatic, 23, 31, 50
metastatic cancer, 23
methanol, 24, 31, 101, 121, 122, 336, 337, 339, 341, 342, 343, 344, 346, 347, 375, 397
methionine, 18
methyl group, 237
methyl groups, 237
methyl methacrylate, 395
methylation, 55, 211
methylene, 24, 30, 55, 72, 145, 146, 148, 150, 151, 169, 171, 172, 173, 216, 217, 218, 219, 220, 221, 222, 223, 288, 319, 320, 321, 322, 323, 324, 326, 327, 328
methylene group, 24
metric, 104
Mg²⁺, 316
m-hydroxyphenyl, 21
mica, 204, 220, 301, 305, 312
mice, 9, 16, 20, 23, 37, 47, 52, 56, 58
micelles, 296
microaerophilic, xiv, 421
microbial, 190, 282, 417, 418, 420, 432
microenvironment, 426
micrometer, 118
microorganism, 226
microorganisms, xiii, xiv, 55, 182, 188, 190, 311, 421, 422, 426, 429, 431
micro-organisms, 190
microscope, 91, 130, 366
microscopy, 41, 296
microstructures, 136, 289
microwave, 110
migration, 187, 319, 398
mineralization, x, 172, 182, 183, 188, 189, 190, 225, 226, 234, 242, 245, 248, 249, 253, 254, 263, 273, 274, 281, 283, 285, 286, 288, 289
mineralized, 183
minerals, 204, 209, 221, 222, 313, 315, 316, 321, 323, 328, 332
Ministry of Education, 92
mirror, 76, 88
mitochondria, 8, 16, 41
mitochondrial, 8, 41
mixing, 363, 391
MMA, 394, 395, 396
MMT, 320
mobility, 126
modality, 33
modeling, 106, 216, 324, 327
models, 24, 40, 54, 100, 153, 212, 214, 216, 218, 219, 296, 304, 324, 363
modulation, xiii, 404
moieties, 10, 17, 27, 65, 118, 121, 206, 212, 335
mold, 313
mole, 70, 99
molecular biology, 31
molecular mass, x, 225, 229, 233, 242, 248, 395, 398, 400
molecular orientation, 130
molecular oxygen, 290

- molecular structure, viii, 67, 70, 73, 77, 79, 81, 111, 112, 116, 123, 126, 127, 204, 341, 374, 411, 432
 molecular weight, 101, 282, 431
 molecular weight distribution, 282
 molten glass, xii, 351, 363
 monochromator, 230
 monoclonal, 10
 monoclonal antibodies, 10
 monocytes, 9
 monograph, 292, 294, 296, 298, 303
 monolayer, 205, 213, 320
 monomer, 375, 392, 407
 monomeric, 118
 monomers, 12, 293, 319, 385, 397, 400
 montmorillonite, 204, 205, 209, 223, 312, 313, 315, 319, 320, 325, 326, 327
 morphological, 102, 106, 113
 morphology, 133, 136, 321
 mouse, 26, 41, 43, 60
 mouse model, 26
 mouth, 30, 55
 movement, 313, 391
 MRI, 32
 mucous membrane, 177
 mucus, 55
 multidisciplinary, 365
 multilayer films, 131, 132
 multiple myeloma, 56
 multiplicity, 5
 multivariate, 191
 muscle, 21, 26
 mutagenic, 144, 176, 202, 333, 405, 415
 MVA, 407
 myopia, 20

N

- Na⁺, 18, 277, 316, 321, 327, 371, 372
 NAA, 408
 NaCl, 191, 192, 207, 215, 356, 371
 NADH, 6
 Nafion, 270
 nanocomposites, 320
 nanocrystal, 25, 51
 nanocrystals, 289
 nanomaterials, 209, 364
 nanoparticles, 35, 108, 209, 220, 223, 289, 365, 366
 nanotechnology, 300
 nanotube, 290
 naphthalene, 127, 235, 240
 National Academy of Sciences, 416, 419, 420
 National Gallery, 349
 National Science Foundation, 379
 NATO, 254
 natural, ix, xi, xii, xiii, 1, 16, 33, 102, 103, 106, 109, 110, 175, 189, 201, 202, 204, 205, 208, 211, 220, 221, 222, 271, 280, 295, 309, 315, 320, 321, 324, 325, 328, 334, 348, 351, 352, 355, 356, 384, 386, 403, 404, 409, 410, 418, 424
 natural environment, 315
 neck, 25, 53, 59
 necrosis, 23, 50
 needles, 296
 nematic, 129
 neoplastic, 31, 32, 39
 neoplastic cells, 31
 neoplastic tissue, 31
 neovascularization, 20, 24, 26, 31
 network, 294, 300, 316, 353, 364, 411, 412
 networking, 293, 294, 302
 neural network, 191, 216, 363
 neural networks, 191, 363
 neurologist, 2
 neurons, 364
 neutralization, 13, 202
 next generation, 53
 nickel (Ni), xii, 23, 34, 58, 282, 324, 359, 360, 362, 369, 375, 376, 378
 Nielsen, 59
 NIPA, 135
 NIR, 370
 nitrate, 145, 173, 188, 190
 nitrates, 356
 nitric oxide, 5
 nitrobenzene, 287
 nitrogen, vii, 26, 63, 64, 65, 177, 179, 237, 250, 374
 nitrous oxide, 100, 108
 nitroxide, 37
 NMR, xii, 22, 67, 70, 71, 72, 79, 83, 84, 88, 139, 232, 369, 370, 371, 372, 373, 374, 375, 389
 Nobel Prize, 2, 3
 non-biological, 202, 203
 non-destructive, 35, 311, 334, 335
 non-enzymatic, 189
 non-hazardous, 203
 nonionic, 109, 319, 327, 329
 nonlinear, 130, 370
 non-linear, ix, 144, 219, 246
 nonlinear optics, 370
 non-steroidal anti-inflammatory drugs, 36
 nontoxic, 304
 normal, ix, 9, 16, 18, 21, 30, 31, 52, 143, 181, 314, 347
 normal conditions, 314
 novelty, 385
 nuclear, 67
 nuclear magnetic resonance, 67

nucleation, 105
nuclei, 297
nucleic acid, 6
nucleophiles, 374
nucleophilicity, 304
nucleoprotein, 52
nucleotides, 10, 412
nucleus, 8
nutrients, 8
nutrition, 311
nylon, 103

O

observations, 3, 76, 150
occlusion, 52
oil, 204, 222, 264, 324, 332
oil spill, 324
oils, 38, 207, 315
oligomer, 13
oligomeric, 12, 13, 27
oligomers, 10, 12, 14
oligonucleotides, 35
oligosaccharide, 204
olive, 207, 217, 323, 334
oncological, 48
oncology, 23, 43, 50, 54
online, 43, 46, 48, 50, 53, 56, 57, 58, 59, 325
onychomycosis, 29
opacity, 358
ophthalmic, 20
optical, viii, 9, 43, 76, 111, 112, 113, 117, 118, 127, 130, 133, 136, 137, 140, 230, 276, 283, 299, 357, 366
optical fiber, 76, 283
optical properties, 43, 127, 130, 357
optical storage, 136, 137
optimization, 106, 171, 191, 217, 281, 408, 413
optoelectronic, 112, 113
optoelectronic devices, 112, 113
oral, 27, 30, 43, 45, 49, 54
oral cavity, 27, 43
organ, 222
organelle, 8
organelles, 8, 32
organic compounds, 159, 165, 166, 173, 175, 181, 183, 185, 262, 263, 267, 273, 274, 280, 281, 282
organic matter, xiii, 185, 285, 288, 324, 421
organic solvent, xii, 6, 27, 64, 65, 70, 100, 104, 262, 295, 297, 369, 370, 378
organic solvents, xii, 6, 27, 64, 65, 70, 104, 295, 297, 369, 370, 378
organism, 395, 405
organoclay, 222

organoclays, 209
orientation, 70, 130, 313, 410
oropharynx, 54
oscillator, 336
osmosis, xi, 179, 181, 309
oxalate, 188, 285
oxalic, 183, 250
oxidants, 181, 226, 237, 263
oxidation rate, 169
oxidative, 5, 187, 196, 235, 281, 283, 346, 412, 413, 422
oxidative damage, 5
oxidative stress, 346, 412
oxide, 78, 209, 220, 282, 287, 288, 294, 301, 302, 305, 315, 316, 324, 326, 356, 364, 412
oxide nanoparticles, 209
oxides, 206, 285, 301, 303, 315, 353, 355, 356, 358
oxygen consumption, 55
oxygen saturation, 249
oxygenation, 40
oxyhemoglobin, 9
ozonation, 144, 145, 153, 161, 172, 183, 185, 261, 262, 272, 273, 274, 279, 282, 287, 290
ozone, x, 145, 181, 183, 185, 187, 188, 194, 203, 241, 254, 259, 262, 264, 272, 273, 280, 282, 285, 286, 287, 323
ozone degradation, 286
ozonolysis, 272, 274, 286

P

p53, 59
pain, 18
paints, viii, 97, 294, 363
pairing, 101, 108
palladium, 25, 26, 43, 51
PAN, 400
pancreatic, 46, 56
paper, xi, xii, 38, 92, 99, 100, 102, 103, 104, 146, 214, 217, 219, 288, 291, 292, 293, 301, 302, 304, 310, 331, 370, 383, 384, 394, 397, 399
paramagnetic, 32, 375
parameter, 130, 169, 210, 213, 214, 219, 266, 359, 364
parsley, 333
particle shape, 357
particles, viii, 35, 97, 98, 104, 106, 110, 188, 213, 223, 276, 313, 323, 325, 358, 359
partition, 100, 102, 109, 237
passive, 8, 208
patents, 292
pathogenic, 313
pathogens, 29, 56, 420

- pathways, xiii, 32, 187, 226, 227, 271, 275, 290, 335, 404, 407, 409, 411, 413, 418, 419
- patients, 3, 10, 16, 25, 26, 31, 32, 35, 44, 50, 51, 52, 57
- Pb, 222, 328
- PBC, 300
- PCR, 410
- peat, 180, 206, 216, 218, 219, 222, 310, 323, 324
- pectin, 411
- peptide, 17, 41, 47, 59, 287, 410, 415
- perception, xiii, 177, 404, 412
- perchlorate, 75
- performance, 103, 113, 134, 138, 150, 220, 232, 284, 289, 300, 302, 305, 311, 327, 422, 432
- periodic, 300
- periodontal, 56
- periodontitis, 56
- peripheral, 45, 51, 57
- peritoneal, 16
- permeabilization, 43
- permeation, 78
- peroxidation, 36, 284
- peroxide, viii, 6, 143, 150, 156, 165, 169, 172, 182, 183, 186, 191, 261, 264, 266, 267, 268, 269, 271
- peroxide radical, 267
- pesticides, 183, 208, 241, 267, 280, 281, 313
- PET, 100, 101, 102, 105, 109, 110, 120, 136, 204
- petroleum, 281, 325, 371
- Petroleum, 370
- PF, 280, 281
- pH, viii, ix, xi, 17, 18, 19, 133, 143, 146, 147, 148, 149, 150, 155, 157, 158, 160, 169, 170, 171, 176, 179, 180, 182, 183, 185, 186, 189, 195, 201, 205, 208, 210, 211, 214, 216, 217, 220, 226, 227, 234, 239, 240, 250, 264, 265, 268, 272, 276, 277, 287, 311, 314, 319, 320, 321, 331, 333, 335, 336, 337, 338, 339, 340, 347
- pH values, 150, 183, 211, 265, 268, 272, 336, 337, 340
- pharmaceutical, 109
- pharmacokinetic, 4, 9, 20, 22, 25, 37, 54, 58
- pharmacokinetics, 43, 47, 49, 51, 54
- phenol, 221, 237, 250, 289, 324
- phenolic, 206, 208, 283
- phenolic compounds, 208, 283
- phenothiazines, 55
- phenotype, 41
- phenoxyl radicals, 238
- phenylalanine, 6
- phosphatases, 412
- phosphate, 91, 323, 325, 407, 409, 412, 416, 419
- phosphates, 412
- phosphorescence, 5
- phosphorus, 414
- photobleaching, 9
- photocatalysis, x, 144, 172, 259, 261, 263, 275, 276, 280, 281, 283, 285, 287, 288, 375
- photocatalysts, 281
- photocatalytic, 274, 275, 278, 281, 282, 283, 285, 287, 288, 289, 290
- photochemical, vii, 1, 28, 29, 33, 35, 37, 54, 59, 87, 112, 117, 134, 144, 222, 262, 263, 283, 323, 347
- photochemical degradation, 347
- photoconductivity, 123
- photodegradation, 273, 276, 278, 288, 289
- photodestruction, 289
- photodissociation, 283
- photodynamic therapy, vii, 1, 2, 41, 43, 44, 45, 46, 47, 48, 49, 50, 51, 53, 54, 370
- photoexcitation, 81, 275
- photoirradiation, 112, 121
- photoluminescence, 119, 120
- photolysis, x, 76, 77, 78, 79, 81, 92, 144, 229, 259, 262, 263, 264, 265, 266, 267, 283
- photon, 4, 5, 120, 185, 264
- photonic, 112
- photonic devices, 112
- photons, 232, 277
- photooxidation, 78, 79
- Photooxidative, 283
- photosensitivity, 3, 10, 14, 16, 19, 20, 21, 22, 25, 26, 51, 52
- photosynthetic, 176
- phototransformation, viii, 111
- photovoltaic, 64
- photovoltaic cells, 64
- phthalocyanines, vii, 1, 8, 11, 12, 27, 34, 37, 40, 41, 52, 53, 62, 65, 66, 70, 303
- phyllosilicates, 312, 313
- physical factors, 385, 418
- physical force, 179
- physical interaction, 207, 363
- physical properties, 112
- physico-chemical properties, viii, 97
- physics, 297
- physiological, xiii, 15, 17, 47, 404
- pigments, viii, xii, 97, 98, 178, 182, 187, 292, 293, 294, 295, 296, 297, 298, 300, 301, 302, 303, 305, 332, 334, 351, 352, 353, 354, 355, 356, 357, 358, 359, 363, 364, 365, 366, 383, 384, 393, 395, 396, 401, 404, 415, 417
- pitch, 207
- pith, 180
- PKC, 420
- planar, 294, 338, 375
- planning, 32

- plantar, 45
plants, ix, xi, xiii, 14, 102, 177, 189, 201, 202, 206, 252, 304, 315, 331, 332, 363, 404, 405, 407, 408, 410, 412, 414, 416, 418, 419, 420, 421
plaque, 30, 32, 45
plaques, 56
plasma, xiii, 6, 8, 19, 21, 22, 24, 25, 26, 41, 404, 411
plasma levels, 22
plasma membrane, xiii, 6, 8, 41, 404, 411
plasmids, 410
plastic, 268, 294, 299, 303, 305
plasticity, 312
plastics, 293, 294, 295, 299, 302, 363
platelets, 301, 305
platinum, 75, 220
play, xiii, 18, 146, 150, 165, 206, 211, 226, 228, 300, 332, 421, 431
PLC, 420
PMMA, 77, 78, 79, 92, 110, 118, 119, 120, 134, 398
PNA, 59
poisonous, 182
polarity, 5, 18
polarizability, viii, 111, 112
polarization, 126
polarized, 113
polarized light, 113
political, 259
pollutant, 267, 272, 287, 310, 321
pollutants, 175, 188, 202, 203, 204, 206, 207, 208, 209, 212, 216, 252, 256, 259, 262, 263, 264, 271, 281, 285, 290, 310, 312, 316, 322, 333
pollution, ix, 175, 185, 194, 195, 206, 223, 333
poly(ethylene terephthalate), 100, 106, 107
poly(methyl methacrylate), 77
polyacrylamide, 207, 223
polyamide, 325
polyamides, 103, 392
polycondensation, 392
polycyclic aromatic hydrocarbon, 284
polyelectrolyte, 181
polyelectrolytes, 131
polyester, 100, 101, 102, 103, 105, 106, 107, 108, 109, 110, 177, 250, 297
polyesters, 103, 296, 392
polyethylene, 103, 392
polyethylene terephthalate, 103
polymer, viii, xii, 100, 111, 113, 114, 118, 121, 122, 123, 124, 125, 131, 137, 139, 204, 217, 224, 299, 320, 323, 325, 328, 383, 391, 392, 395, 396, 397, 398, 400, 401, 402
polymer films, 114, 118
polymer materials, viii, 111, 113, 139
polymer matrix, 118
polymer molecule, 395, 397
polymer systems, 121
polymeric materials, xi, 309
polymerization, 204, 205, 393, 397
polymers, viii, xii, 111, 118, 123, 181, 215, 221, 299, 323, 383, 384, 385, 392, 393, 396, 397, 399, 400
polymethylmethacrylate, 398
polyolefins, 178
polyoxometalates, 282
polypropylene, 101, 103, 107, 108, 392
polysaccharides, 325
polystyrene, 103, 392, 398
polystyrenesulfonate, 131
polyvinylchloride, 392
pomace, 207, 217
poor, xiii, 176, 202, 375, 376, 378, 421
population, 104, 429
pore, 213, 296, 297, 321, 324
pores, 212, 296, 305, 316
porosity, 181, 203, 312, 321
porous, xiv, 136, 206, 312, 313, 315, 316, 324, 421, 423, 424, 425, 426, 427, 428, 431
porphyria, 3, 16
porphyrins, vii, 1, 3, 12, 16, 17, 23, 32, 33, 34, 36, 39, 52, 58, 64
port-wine stain, 14, 20
potassium, 24, 405
potential energy, 341
powder, 17, 173, 210, 219, 221, 223, 270, 282, 365
powders, xii, 98, 106, 351, 352, 358, 365
power, 16, 104, 182, 194, 206, 252, 427
power plant, 206
power plants, 206
PPA, 234, 240, 246, 247
pragmatic, 103
praseodymium, 356, 364
praxis, 30
precipitation, viii, 97, 98, 104, 108, 109, 146, 179, 208, 209, 300, 352, 397, 400
preclinical, 52
prediction, 100, 109
preference, 315
preparation, iv, 3, 17, 25, 67, 106, 126, 208, 209, 217, 218, 356, 359, 363
preservatives, 268
pressure, viii, 97, 98, 99, 100, 102, 105, 110, 185, 187, 263, 297, 370, 372
prevention, 31, 195, 384
prices, ix, 201, 202, 209
primary products, 246
primate, 51
printing, 175, 294, 302, 322, 328, 363, 365
pristine, 327

probability, 5, 114, 115
 probe, 117, 140, 194, 347
 procedures, ix, 175, 207, 208, 262, 295, 335, 413
 process control, 352
 prodrugs, 18
 producers, 302, 363
 production, viii, x, xiii, 5, 6, 8, 9, 10, 28, 29, 30, 31, 33, 34, 53, 59, 64, 97, 98, 105, 159, 176, 181, 183, 185, 188, 202, 203, 225, 252, 264, 266, 269, 271, 272, 275, 286, 290, 294, 299, 300, 301, 311, 351, 353, 356, 363, 364, 365, 403, 405, 408, 409, 410, 411, 412, 413, 414, 415, 416, 417, 418, 419, 420
 productivity, 103, 351, 408, 413, 417
 progenitor cells, 31
 program, 92, 123, 126, 127
 progressive, 413
 proliferation, 410
 promote, 38, 165, 171, 356, 357
 promoter, 32, 418
 propagation, 264, 271, 273
 property, viii, 9, 24, 64, 84, 92, 111, 112, 208, 315, 317, 375, 423
 propylene, 104
 prostate, 21, 23, 26, 31, 32, 43, 49, 50, 52, 57
 prostate cancer, 21, 26, 31, 43, 49, 52, 57
 prostate gland, 52
 protection, 332
 protective coating, xii, 351, 352, 353
 protein, xiii, 35, 403, 410, 412, 413, 419
 protein kinases, 412
 proteins, 8, 59, 177, 411, 418
 proteomics, xiii, 403, 418
 protocol, 21
 protocols, 335
 protons, 72, 268
 PSD, 104
 pseudo, ix, 144, 153, 161, 167, 212, 270, 271, 272, 319, 320
 Pseudomonas, 55, 190, 290, 432
 Pseudomonas aeruginosa, 55
 psoriasis, 2, 16, 31, 38, 45
 PSS, 131, 132, 133
 psychiatry, 2
 psychological, 359
 PTT, 34
 pulp, 282
 pulp mill, 282
 pulse, x, 76, 225, 226, 229, 230, 233, 235, 242, 253
 pulses, 34, 229
 pupa, 207
 pure water, 227

purification, 27, 69, 70, 144, 176, 222, 253, 254, 257, 259, 322, 324, 370, 384, 410
 PVA, 77, 78, 79, 81, 92
 PVC, 392
 pyridine ring, vii, 63, 65, 67, 70, 79
 pyrrole, 64
 pyruvate, 407, 409

Q

quality control, 356
 quantum, 3, 5, 6, 10, 15, 26, 29, 30, 31, 64, 113, 120, 126, 235, 339, 342, 344, 346, 347
 quantum chemical calculations, 346
 quantum yields, 5, 10, 30, 64, 113
 quartz, 243, 263, 264, 315, 352
 quaternary ammonium, 205, 215, 217
 quaternary ammonium salts, 215
 quinone, 242
 quinones, 416, 417

R

race, 420
 radiation, x, 1, 2, 9, 40, 43, 186, 191, 202, 223, 225, 226, 227, 229, 243, 253, 254, 255, 256, 257, 262, 263, 265, 266, 271, 286, 287, 302, 325, 332
 radiation therapy, 43
 radical, x, 6, 33, 36, 59, 144, 156, 182, 183, 186, 187, 194, 225, 227, 228, 233, 234, 235, 236, 237, 238, 239, 241, 242, 244, 247, 248, 250, 255, 263, 266, 267, 273, 274, 275, 277
 radical reactions, 183, 187, 234, 248, 250
 radiotherapy, 49
 radius, 8
 Raman, 53, 346
 Raman spectroscopy, 53
 range, 4, 5, 6, 9, 17, 29, 32, 64, 98, 100, 101, 120, 150, 159, 160, 177, 187, 190, 203, 204, 206, 209, 215, 226, 227, 231, 241, 243, 245, 246, 248, 253, 267, 269, 272, 276, 303, 304, 320, 334, 344, 356, 357, 363, 365, 393, 404, 405, 426
 rat, 50, 51, 56
 rats, 36, 56
 raw material, 67, 70, 203, 301, 356
 reactant, 262, 275
 reactants, ix, 143, 151
 reaction mechanism, 227, 233, 253, 271
 reaction rate, 145, 148, 153, 155, 159, 160, 161, 165, 167, 183, 275, 276, 279
 reaction rate constants, 161, 167, 183
 reaction temperature, 151, 157
 reaction time, 146, 159, 188
 reactive oxygen, vii, 1, 6, 33

- reactive oxygen species, 6, 33
reactive oxygen species (ROS), 6, 33
reactivity, 6, 22, 113, 150, 159, 203, 228, 234, 240, 241, 245, 246, 249, 268, 304, 321, 356, 364, 385
reading, 292, 293
reagent, 144, 145, 146, 153, 159, 171, 172, 173, 182, 262, 267, 269, 271, 273, 274, 280, 281, 283, 284, 285, 290
reagents, 112, 160, 164, 165, 261, 263, 267, 271, 370
real time, 363
reality, 409
receptors, xiii, 404, 411, 412
reclamation, 280
recognition, 411, 420
recombination, 275, 276, 278
recovery, 120, 122, 127, 208, 209, 216, 311
recovery processes, 311
recrystallization, 114
recurrence, 49
recycling, x, 176, 181, 226, 253, 282
red blood cell, 28
red blood cells, 28
red light, 2, 3, 28, 48, 57
red shift, xii, 138, 369, 375, 378
redistribution, 55, 412
redox, 32, 53, 55, 76, 86, 87, 89, 90, 91, 146, 189, 274
reduction, x, 6, 10, 11, 21, 28, 75, 76, 86, 87, 89, 90, 91, 102, 104, 150, 159, 169, 172, 179, 182, 188, 189, 190, 191, 202, 215, 225, 226, 241, 242, 249, 252, 262, 269, 304, 352, 414
reflection, 76, 176, 358
refraction index, 358
refractive index, viii, 111, 112, 358
refractory, xii, 351
regenerate, 209
regeneration, 165, 180, 182, 185, 202, 203, 205, 209, 223, 311, 328
regression, ix, 7, 144, 153, 161
regular, 344
regulation, xiii, 2, 403, 410, 416
regulations, 144, 259
regulators, 408, 413
reinforcement, 412
rejection, 423
relationship, 24, 42, 73, 79, 266, 298, 359, 360, 395, 413
relationships, 81, 100, 105, 340, 363
relaxation, 5, 335, 339, 340, 344, 347
reliability, 253
remediation, 188, 226, 256, 280, 284, 323
renal, 47, 405
renal calculus, 405
reputation, 300
research, viii, xii, 12, 44, 92, 102, 107, 111, 113, 148, 188, 195, 226, 232, 241, 259, 298, 351, 364, 365, 369, 404, 419
research and development, xii, 351
researchers, 298, 310, 319, 320, 322
residues, 122, 222, 393, 394, 415
resin, 305, 324
resins, 180, 203, 305, 310, 324, 408
resistance, viii, 37, 111, 112, 120, 125, 126, 134, 209, 297, 299, 412
resolution, 118
respiratory, 177
response format, 412
response time, 229
restoration, 332
retention, x, 190, 204, 205, 207, 211, 226, 252
reticulum, 41
returns, 121
rheological properties, 358
rhodopsin, 178
rice, 180, 207, 219, 221, 223, 419
rice husk, 180, 207, 219, 221, 223
rings, vii, 11, 12, 19, 26, 28, 31, 35, 63, 65, 70, 72, 75, 76, 84, 89, 90, 92, 177, 235, 247, 248, 253, 312, 407
risk, 48, 284
risk assessment, 48
rivers, 259
RMS, 133
RNA, 410
RNAi, 418
rods, 299
room temperature, x, 75, 83, 118, 119, 135, 138, 225, 227, 228, 241, 374
ROS, 7
roughness, 133
rubber, 252, 268
rutile, 302, 358
- S**
- safety, 23, 26, 43, 49, 50, 264
saline, 91
salt, 22, 33, 145, 188, 191, 215, 315, 323, 325
salt formation, 188
salts, 27, 29, 55, 145, 173, 183, 189, 190, 207, 215, 217, 250, 264, 290, 302, 311, 325, 334, 343
sample, 76, 117, 205, 229, 262, 388
sampling, 334, 335
sand, 310, 323, 325, 329
sapphire, 76, 77
SAS, 104
satellite, 72

- saturation, 145, 227, 245, 248, 249, 429
sawdust, 180, 207, 210, 217, 218, 222
scaffold, 299
scaling, 56
scalp, 17
Scanning Electron Microscopy (SEM), 136, 424, 425, 426, 428
scar tissue, 20
scatter, 359, 363
scattering, 295, 352, 358, 359, 361
scavenger, 148, 156, 169, 182, 186, 194, 278
Schmid, 48, 380
science, 260, 309, 320, 363, 370
scientific, xi, 17, 227, 292, 296, 322, 331, 332, 364
scientific community, 17, 322
scientific knowledge, 364
scientists, 2, 3, 204
SDT, 35, 36
searching, 37, 104, 303
seaweed, 208, 210, 217, 223
second generation, 10, 25
secrete, 408
sediment, 226, 284
sedimentation, xi, 179, 181, 309
sediments, 303
seed, 210, 219
seeding, 432
selecting, 431
selectivity, 3, 8, 9, 10, 12, 14, 16, 18, 21, 24, 33, 49, 64, 209, 234, 239, 304, 311, 413
self-assembly, 121, 131, 132, 141, 299
self-destruction, 9
semiconductor, 226, 276, 278, 287, 370
semiconductors, 274, 276
sensing, 123, 222
sensitivity, 229, 332
sensitization, 58, 64, 299
sensors, 346
sentences, 295, 304
separation, xi, 19, 75, 76, 86, 90, 116, 118, 135, 188, 190, 209, 229, 232, 235, 246, 248, 276, 309, 310, 408, 413
sequencing, 286, 419, 432
series, 21, 24, 55, 130, 144, 226, 271, 363, 370
serum, 91
services, iv
sewage, 280, 323, 325
SFD, 103, 109
shape, 31, 76, 122, 231, 245, 302, 304, 315
shear, 36, 299, 416
shellfish, 204
shock, 34
shortage, 18
short-term, 9
shoulder, 243, 344
side effects, 9, 37, 405
sign, 2
signal transduction, xiii, 404, 411, 412, 413, 418, 420
signaling, 42, 332, 411, 412, 413, 420
signaling pathway, 412, 420
signaling pathways, 412
signals, 9, 118, 410, 411, 412
signs, 294
silanol groups, 327
silica, xi, 206, 210, 216, 282, 288, 301, 309, 314, 315, 316, 325, 356, 370
silicate, 305, 312, 313, 316, 319, 320, 321, 353, 356
silicates, 316
silicon, 28, 40, 53, 54, 316
silk, 103, 334, 405
silkworm, 207
silver, 75, 288, 299
similarity, 298, 300
simulation, 167, 222, 363
single crystals, 114, 300
sintering, xii, 351, 352, 363
SiO₂, 206, 301, 314, 353, 355, 356
sites, 27, 41, 211, 213, 215, 233, 234, 279, 314, 319, 320, 346, 353, 356, 411
skeleton, 2, 254, 335, 337
skin, 2, 3, 10, 13, 14, 16, 17, 18, 19, 20, 21, 22, 25, 26, 27, 28, 29, 45, 46, 47, 48, 50, 51, 53, 54, 58, 177, 282, 385
skin cancer, 20, 25, 46, 48, 53
skin diseases, 2
skin disorders, 2, 16, 17
slag, ix, 201, 206
sludge, xiii, 144, 180, 181, 182, 183, 185, 188, 190, 194, 203, 208, 210, 217, 219, 268, 280, 284, 286, 311, 323, 421
smallpox, 2
smart materials, 121, 133
smoothness, 358
social, 259
society, 2
sodium, 8, 10, 12, 13, 14, 22, 23, 24, 27, 33, 36, 38, 50, 61, 75, 114, 146, 172, 192, 223, 313, 314, 325
sodium hydroxide, 146, 192
SOFC, 117, 118
software, 74, 363, 391
soil, 189, 226, 271, 281, 284, 287, 310, 427
soils, 261, 322
solar, 47, 182, 280, 281, 282, 283, 284, 285, 286, 302
solid phase, 213, 218

- solid solutions, 353
solid state, xii, 113, 294, 356, 357, 365, 366, 369, 375
solid tumors, 7
solid waste, 204, 206, 221, 226
solubility, viii, xi, xii, 21, 24, 25, 27, 28, 64, 65, 70, 79, 84, 97, 98, 99, 100, 101, 102, 103, 104, 105, 106, 107, 110, 144, 159, 183, 185, 202, 204, 291, 292, 293, 295, 329, 356, 358, 369, 370, 375, 378
solutions, 17, 19, 27, 29, 60, 76, 110, 144, 145, 146, 183, 208, 217, 221, 227, 228, 230, 235, 237, 242, 243, 244, 245, 246, 247, 250, 254, 266, 283, 286, 288, 326, 334, 337, 342, 343, 344, 345, 352, 363, 365, 375, 394, 397, 399
solvent, viii, xii, 5, 27, 67, 71, 72, 83, 87, 97, 98, 101, 102, 103, 104, 105, 107, 110, 231, 297, 347, 370, 383, 397
solvent molecules, 5
solvents, 64, 78, 81, 84, 101, 102, 303, 370, 385, 386, 394, 396, 398
sonodynamic therapy, vii, 1, 23, 33, 36
sorbents, ix, xi, 201, 202, 204, 205, 206, 207, 209, 210, 211, 212, 213, 214, 215, 217, 222, 309, 310, 319, 324, 327
sorption, ix, 166, 201, 204, 205, 206, 207, 208, 209, 210, 211, 212, 213, 214, 215, 216, 217, 218, 219, 220, 221, 222, 223, 312, 316, 319, 323, 325, 327
sorption isotherms, ix, 201, 214
sorption kinetics, 212
sorption process, ix, 201, 209, 211, 212, 213, 214, 325
soybean, 208, 218
spatial, 190, 338
specialists, 292, 294
species, vii, viii, 1, 4, 5, 6, 8, 10, 22, 27, 34, 111, 139, 150, 181, 187, 189, 204, 208, 211, 214, 227, 228, 230, 239, 241, 242, 245, 248, 253, 256, 262, 267, 268, 269, 271, 272, 274, 275, 278, 312, 313, 314, 315, 321, 337, 338, 339, 344, 345, 357, 405, 408, 417
specific surface, 206, 222, 316, 321, 423
specificity, 411, 419, 420, 423
spectra, viii, xi, 67, 72, 73, 76, 79, 80, 83, 84, 88, 89, 111, 117, 119, 120, 128, 129, 130, 132, 138, 231, 243, 296, 331, 333, 336, 337, 340, 343, 344, 345, 347, 369, 370, 375, 376, 377, 378, 379, 389, 397
spectrophotometric, 138, 146, 147, 246, 310, 337, 338, 361
spectrophotometry, 229, 235, 243, 262, 334
spectroscopy, x, 67, 132, 225, 232, 310, 326, 334
spectrum, 1, 2, 3, 9, 80, 138, 177, 179, 231, 232, 243, 244, 245, 246, 248, 253, 315, 335, 337, 338, 342, 343, 344, 347, 354, 359, 375
speed, 19, 147
spheres, 301, 305
spin, 4, 5, 61, 76, 77, 118
squamous cell, 23, 27, 32, 50, 58, 59
squamous cell carcinoma, 23, 27, 32, 50, 58, 59
stability, xi, xii, 9, 18, 28, 31, 48, 73, 113, 176, 183, 226, 268, 291, 294, 298, 300, 301, 302, 304, 305, 357, 364, 366, 369, 375, 376, 378, 383, 393, 394, 395, 396, 398, 399, 400
stabilization, xi, xii, 297, 331, 383, 398, 399, 400
stabilize, 19, 236, 237, 334, 338, 342
stabilizers, 25, 398
stages, 244, 249, 404, 407, 414
standards, 259, 293
starch, 190, 215, 221, 323
stasis, 42
steady state, 334, 335
steel, 206
stem cells, 31
stent, 57
steric, 237, 370, 397
sterile, 25
sterilization, 272
steroids, 10, 20
stock, 359, 416
stoichiometry, 345, 346, 347
stomach, 27, 395
storage, 64, 112, 118, 127, 133, 135, 136, 140, 264, 409
strain, 431, 432
strains, 408, 427, 429, 431
strategies, 202, 209
streams, xiii, 145, 181, 421
strength, 36, 104, 133, 216, 220, 242, 300, 303, 319, 321, 336, 397
streptomyces, 210
stress, 36, 56, 411, 416, 419
stress factors, 411
stretching, 129
structural changes, 113, 122, 129, 130, 316
structural characteristics, 312
students, xi, 292, 295
styrene, 324, 393, 394
subcellular, 41, 42, 44
substances, x, xiii, 98, 144, 175, 176, 177, 180, 206, 207, 209, 215, 259, 272, 277, 303, 310, 312, 356, 403, 407, 411
substitutes, 313
substitution, xii, 11, 12, 27, 41, 236, 314, 316, 369, 370, 374, 375, 378, 379
substitution reaction, 374
substrates, xiii, 4, 6, 118, 280, 299, 302, 303, 418, 421, 423

- sucrose, 408, 417
 sugar, 332
 sulfate, vii, 63, 83, 145, 146, 173, 190, 250, 325, 405
 sulfur, 260, 294
 sulfuric acid, 24
 sulphate, 146, 181, 188, 190, 278, 405
 sulphur, 177, 181, 189, 206
 sunlight, 10, 33, 176, 375, 376
 supercritical, viii, 97, 98, 99, 100, 101, 102, 103, 104, 105, 106, 107, 108, 109, 110
 supercritical carbon dioxide, viii, 97, 98, 99, 100, 101, 102, 103, 105, 106, 107, 108, 109, 110
 supercritical fluids, viii, 97, 98, 99, 102, 103, 104, 107, 108, 110
 superficial bladder cancer, 14, 40
 superoxide, 6, 33, 228, 241
 superposition, 313
 supply, 7, 8, 15, 189, 246, 262
 supramolecular, 121, 299
 surface area, 180, 203, 208, 312, 316, 319
 surface layer, 392
 surface modification, 206
 surface properties, 205, 215, 276, 310
 surface reactions, 212
 surface roughness, 133
 surface structure, 133
 surface tension, 102
 surface water, 189
 surface-initiated atom transfer radical polymerization, 329
 surfactant, 60, 107, 109, 205, 216, 217, 289, 319, 326, 329
 surfactants, ix, 101, 201, 205, 211, 215, 219, 226, 326
 surplus, 280, 323
 survival, 404
 suspensions, 220, 284, 289, 326, 416, 417
 sweat, 384
 swelling, 316
 switching, viii, 111, 112, 114, 115, 119, 123, 135, 136, 137, 138, 139
 symmetry, 32, 73, 74, 79, 92, 313
 symptoms, 49
 synergistic, 20, 34, 59, 297
 synergistic effect, 20, 59, 297
 synthesis, xii, xiii, 3, 14, 15, 16, 17, 18, 24, 47, 51, 54, 57, 298, 324, 356, 357, 365, 370, 383, 384, 385, 386, 387, 388, 389, 390, 393, 395, 396, 397, 399, 403, 405, 407, 412, 413, 415, 416, 418, 420
 synthetic, xii, 11, 21, 26, 31, 32, 67, 103, 109, 114, 115, 125, 128, 173, 176, 177, 180, 188, 189, 202, 203, 205, 207, 209, 218, 252, 260, 280, 284, 288, 322, 323, 332, 351, 352, 354, 355, 356, 374, 386, 387, 391, 405
 synthetic polymers, 391
 systematic, 130, 145, 176, 359
 systems, x, xii, xiii, 24, 64, 98, 112, 123, 126, 127, 133, 145, 160, 181, 187, 189, 190, 209, 212, 214, 217, 218, 225, 226, 227, 228, 273, 284, 293, 303, 323, 324, 351, 352, 370, 403, 410, 412, 420, 421
- T**
- T lymphocytes, 48
 talc, 204, 312
 targets, 8, 29, 34, 37, 41, 42, 346
 taxonomic, 404
 T_c, 129, 130, 420
 tea, 333
 technicians, 298, 303
 technological, 17, 127, 178, 294, 298, 304, 334, 364
 technological developments, 334
 technology, x, 12, 13, 23, 34, 50, 98, 103, 105, 108, 109, 144, 181, 195, 225, 226, 254, 260, 274, 299, 309, 352, 363, 365, 405
 temperature, viii, 5, 18, 34, 97, 99, 100, 101, 102, 110, 130, 133, 135, 136, 139, 143, 146, 148, 150, 151, 155, 159, 171, 179, 180, 181, 183, 185, 187, 189, 205, 216, 221, 223, 226, 270, 316, 319, 352, 356, 357, 363, 409, 411
 tension, 423
 textbooks, 292, 293
 textile, viii, ix, x, xii, 97, 98, 101, 102, 103, 105, 107, 110, 144, 145, 172, 173, 175, 176, 177, 181, 187, 188, 190, 191, 195, 202, 205, 208, 215, 216, 217, 222, 225, 226, 235, 250, 252, 255, 282, 283, 284, 285, 286, 287, 289, 290, 295, 296, 297, 321, 326, 327, 363, 383, 384, 392, 415, 422, 427, 428, 429, 431
 textile industry, viii, 97, 101, 102, 144, 175, 176, 181, 191, 195, 296, 363, 415, 422
 textiles, xi, 101, 102, 103, 105, 106, 109, 307, 331, 332, 333, 334, 342, 347, 405
 theoretical, 22, 74, 123, 126, 127, 130, 216, 235
 theory, 73, 79, 104, 233, 239, 294, 307, 359, 361, 363
 therapeutic, 2, 10, 13, 16, 17, 32, 34, 43, 49, 58, 333
 therapeutic agents, 34, 49
 therapeutics, 53
 therapy, vii, 1, 2, 5, 9, 16, 20, 27, 29, 31, 33, 34, 35, 37, 38, 39, 40, 41, 42, 43, 44, 45, 46, 47, 48, 49, 50, 51, 52, 53, 54, 55, 56, 57, 58, 59, 61, 63, 64, 405
 thermal, xii, 25, 135, 136, 138, 139, 151, 159, 176, 180, 206, 293, 316, 327, 351, 352, 353, 356, 363, 366, 414

- thermal analysis, 327
thermal decomposition, 151, 159
thermal properties, 414
thermal stability, xii, 293, 351, 352
thermodynamics, 100, 218, 304, 323
thiamin, 416
thin film, 126, 130, 131, 281, 282, 288, 289, 326
thin films, 130, 131, 282, 288, 289, 326
thin-film deposition, 131
thinking, 295, 298
thioredoxin, 32
three-dimensional, 293
threshold, 269
thrombocytopenia, 42
thrombosis, 42
thrombus, 8
timber, 207
time, x, 2, 5, 6, 8, 13, 14, 21, 23, 31, 37, 50, 77, 78, 79, 102, 121, 134, 144, 147, 153, 159, 164, 167, 176, 180, 183, 189, 191, 192, 193, 194, 208, 212, 226, 227, 229, 230, 231, 245, 246, 249, 251, 252, 253, 254, 264, 279, 292, 293, 298, 300, 302, 334, 335, 355, 358, 363, 384, 392, 393, 400, 430
time consuming, 364
tin, 23, 50, 334, 364
tin oxide, 364
TiO₂, 52, 144, 181, 226, 261, 276, 277, 279, 280, 281, 282, 283, 284, 285, 286, 287, 288, 289, 290, 301, 302, 323
tissue, 3, 7, 16, 18, 21, 22, 24, 28, 36, 39, 47, 52, 54, 61, 64, 91, 305, 415
titania, 281, 365
titanium, 194, 281, 282, 283, 288, 289, 294, 301, 305, 358
Titanium, 276, 290
titanium dioxide, 281, 283, 288, 289, 301, 305, 358
titration, 138, 337, 338
T-lymphocytes, 21
TMP, xii, 383, 398, 399, 400
TOC, x, 182, 191, 192, 193, 194, 226, 248, 249, 274, 322
toluene, 67, 70, 71, 72, 77, 83, 84, 85, 87, 88
tomato, 419
torus, 204
total organic carbon, 179, 183, 248, 322
total organic carbon (TOC), 179, 183, 322
toxic, 8, 10, 35, 36, 98, 176, 181, 182, 183, 189, 194, 202, 207, 217, 248, 253, 254, 261, 273, 304, 310, 311, 332, 333, 385, 395, 405, 422
toxic effect, 311
toxic products, 395
toxicity, x, xi, 10, 14, 16, 29, 31, 36, 59, 172, 176, 182, 194, 248, 254, 259, 269, 271, 282, 285, 309
toxicological, 354
toxins, 35, 313
toys, 332, 396
trade, 176, 292, 294
training, 102
transcript, 410
transcription, 410, 418
transcription factor, 410, 418
Transcription factor, 412
transcription factors, 410, 418
transcriptional, 410, 419
transducer, 194, 420
transduction, xiii, 404, 412, 420
transfer, 2, 4, 5, 6, 67, 76, 87, 90, 91, 92, 120, 213, 219, 226, 245, 304, 335, 340, 341, 352, 364, 410
transformation, 248, 250
transformation product, 248, 250
transformations, x, 225, 248
transgenic, xiii, 403, 409
transgenic plants, 409
transition, 70, 72, 73, 76, 78, 129, 228, 250, 251, 276, 333, 335, 336, 352, 353, 375
transition metal, 78, 228, 250, 251, 276, 333, 352, 375
transition metal ions, 228, 251, 352
transitions, 5, 293, 301, 335, 336
translation, 197
transmission, 230, 263, 358
transparency, 144, 243
transparent, 366
transplantation, 31
transport, 13, 36, 47, 102, 208, 212, 419
transportation, 209
treatable, 37
treatment methods, 179
trees, 304
trend, 99, 344, 346
trial, 31, 57
trifluoroacetic acid, 25
trout, 286
tryptophan, 18
tuberculosis, 2
tumor, vii, 1, 3, 7, 8, 9, 10, 12, 13, 14, 16, 21, 22, 24, 29, 30, 32, 34, 35, 36, 37, 39, 41, 42, 43, 46, 48, 49, 50, 54, 61, 64, 65, 405
tumor cells, 7, 9, 16, 30, 34, 41, 46
tumor growth, 32
tumor progression, 50
tumors, 2, 3, 9, 14, 16, 22, 24, 32, 33, 37, 50, 53, 54, 64, 78
tumour, 40, 41, 46, 52, 54, 58, 62
tumours, 47, 48, 58
turnout, 413

typology, 363
Tyrosine, 287

U

UAE, 259, 309
ultra-fine, 98
ultrasound, 23, 35, 36, 37, 59, 60, 61, 62, 144, 145,
153, 161, 172, 188, 194, 195, 287
ultraviolet, 2, 67, 76, 179, 332
Ultraviolet, 38, 197
ultraviolet light, 2, 76
undifferentiated, 415
uniform, 3, 104, 299, 378, 392
uniformity, 103, 356
United Arab Emirates, 259
United States, 49, 51, 416, 419, 420
upper respiratory tract, 177
urea, 192, 208
urinary, 49, 176
urinary bladder, 176
urinary tract, 49
users, 175
UV irradiation, 116, 121, 122, 125, 126, 127, 130,
132, 145, 192, 282, 287, 288, 289, 411
UV light, 119, 120, 135, 136, 137, 138, 139, 185,
226, 262, 263, 264, 266, 273, 394, 399, 400
UV radiation, 185, 186, 263, 273, 274, 277, 281,
285, 287

V

vaccination, 9
vaccines, 43
vacuum, 371
valence, 274
validity, 364
values, 5, 6, 72, 73, 76, 81, 90, 100, 130, 146, 150,
167, 191, 192, 194, 206, 210, 248, 249, 268, 272,
337, 338, 359, 362
van der Waals, 305, 384, 392
vanadium, 289, 364, 411
vapor, 185, 263
variable, 45, 56, 192, 226, 313, 315
variables, 191, 192, 359
variation, viii, 32, 76, 90, 97, 148, 153, 156, 160,
276, 344, 356, 359, 430
vascular, vii, 1, 7, 8, 18, 20, 24, 26, 42, 43, 52
vasculature, 8, 24
vasoconstriction, 8
vegetable oil, 315
vegetables, 333
vehicles, 47, 332
vermiculite, 204, 312

versatility, 130
vessels, 42, 50, 262, 263
vibrational, 347
viral, 16, 45
viral infection, 16, 45
virus, 56
virus infection, 56
viruses, 28, 30, 313
viscose, 177
viscosity, viii, 111, 112, 113, 121, 122, 139, 299
visible, 1, 2, 67, 112, 118, 120, 135, 138, 139, 146,
176, 177, 179, 243, 244, 245, 246, 248, 253, 285,
290, 301, 302, 332, 346, 352, 358, 359, 362
vision, 20
visual, 136, 408, 416
visualization, 32
vitamin A, 5
vitamin C, 6
vitiligo, 2
vitreous, 353
vitrification, 352
voltammetric, 75

W

warts, 16, 29, 45
Washington, 256
waste, xi, 101, 145, 176, 180, 181, 188, 204, 206,
207, 209, 210, 215, 218, 220, 221, 222, 252, 271,
281, 282, 284, 285, 309, 324, 326, 384
waste water, 101, 176, 271, 281, 282, 285, 326, 384
wastes, 203, 208, 216, 221
wastewater, ix, x, xiii, 98, 101, 102, 144, 145, 169,
171, 172, 173, 175, 176, 177, 179, 180, 181, 182,
183, 185, 189, 190, 195, 196, 197, 201, 202, 203,
205, 208, 215, 216, 217, 219, 221, 223, 225, 226,
251, 252, 253, 254, 257, 269, 271, 273, 277, 280,
282, 283, 285, 290, 310, 322, 323, 324, 325, 327,
328, 421
wastewater treatment, ix, xiii, 98, 175, 177, 180, 181,
189, 195, 196, 197, 201, 202, 203, 209, 215, 219,
221, 223, 253, 273, 290, 310, 328, 421
wastewaters, ix, 171, 175, 179, 181, 182, 195, 201,
202, 205, 206, 208, 209, 215, 217, 218, 220, 222,
226, 235, 250, 259, 268, 288, 320, 321, 427, 429,
431
water quality, 177, 259
water-soluble, 22, 53, 64, 315, 324, 397, 408
wavelengths, 9, 10, 12, 28, 29, 32, 76, 185, 231, 246,
253, 264, 336, 337, 344, 345, 358
wavelet, 109
wavelet neural network, 109
wealth, 304
wear, 365

weathering, 285, 313
wet, xii, 20, 23, 102, 144, 290, 296, 299, 365, 383,
385, 386
wetting, 250
wheat, 222, 333
WHO, 12, 22
wine, 48
wires, 75
wood, 180, 203, 207, 218, 220, 222, 267, 323, 325,
334
wool, 103, 106, 107, 110, 180, 334, 391
workers, 65, 176, 177, 236, 237, 242, 259, 408
writing, 136, 137

X

xenobiotic, xiii, 421
xenografts, 59
xenon, 76, 263
X-ray, 22, 114, 295, 296, 354, 366, 410
X-ray diffraction, 22, 354, 366, 410
XRD, 130, 352

xylene, 281

Y

yeast, 190, 419
yield, xiii, 3, 5, 6, 13, 15, 24, 26, 29, 30, 31, 67, 71,
83, 84, 88, 104, 151, 160, 185, 236, 337, 339,
342, 344, 347, 371, 372, 373, 374, 403, 405, 408,
409, 410, 413
yolk, 24

Z

zeolites, ix, xi, 180, 201, 204, 205, 309, 316, 321,
328
zinc (Zn), vii, 23, 26, 27, 37, 41, 42, 53, 54, 63, 64,
65, 66, 67, 70, 81, 92, 276, 277, 301, 323, 325,
364, 369, 372, 375, 376, 378
zinc oxide (ZnO), 276, 286, 288, 364
zirconium, 353
zwitterions, 122, 125